

## REDOX REACTIONS OF SODIUM TETRAHYDROBORATE AND TRANSITION METAL IONS. II. FORMATION OF ZIRCONIUM(III)

M. DASGUPTA, S. DASGUPTA, M. K. MAHANTI\*

*Department of Chemistry, North-Eastern Hill University, 793 022 Shillong, India  
E-mail: mkmahanti@gmail.com*

### ABSTRACT

A novel protocol is suggested for the reaction between zirconium(IV) and sodium tetrahydroborate, in aqueous acidic medium, resulting in the formation of zirconium(III), which has been supported by chemical and spectral analyses.

*Keywords:* zirconium(IV), zirconium(III), sodium tetrahydroborate, acidic medium.

### AIMS AND BACKGROUND

The common oxidation state of zirconium is  $Zr^{4+}$ . Aqua ions of lower valency states of zirconium are not well defined. The reduction of zirconium(IV) to a lower oxidation state is difficult even when carried out in the presence of appropriate ligands like CO, phosphines and cyclopentadienyl<sup>1</sup>. There has been some evidence to show that zirconium could form metal–metal bonds, as characterised by several diamagnetic dimeric zirconium(III) complexes<sup>2</sup>. The present communication focuses attention on the redox reaction between zirconium(IV) and  $NaBH_4$ , and establishes the simplicity associated with the formation of zirconium(III).

### EXPERIMENTAL

*Materials.* Sodium tetrahydroborate ( $NaBH_4$ , Loba Chemical Co.) was kept under vacuum. The purity of  $NaBH_4$  was checked by infrared analysis (FT-IR spectrophotometer). Two sharp peaks were obtained at 2290 and 1120  $cm^{-1}$ , both being characteristic for  $NaBH_4$ . These peaks have been assigned<sup>3</sup> as follows: (i) 2290  $cm^{-1}$ :  $(B-H)_{asym}$  stretching; (ii) 1120  $cm^{-1}$ :  $BH_2$  deformation.

The  $(B-H)_{asym}$  stretching mode was further split (2380 and 2290  $cm^{-1}$ ). It was suggested that the splitting was a consequence of the inability of the tetrahedral anion to rotate freely in the crystal lattice<sup>4</sup>. Sulphuric acid (E. Merck) was used after check

---

\* For correspondence.

of its physical constants. The zirconium(IV)–alizarin-S complex in solution was used as a source of zirconium(IV). Zirconyl chloride,  $\text{ZrOCl}_2$  (4.86 g) was dissolved in HCl ( $1.0 \text{ mol dm}^{-3}$ ), and 1 drop of an aqueous solution of alizarin-S was added. A pink coloured solution was obtained ( $\lambda_{\text{max}}$  at 515 nm) (Ref. 5).

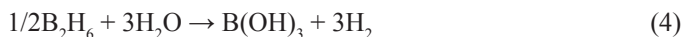
*Product analysis.* A known weight of the precipitate (0.307 g  $\text{ZrOCl}_2$ , corresponding to 0.087 g  $\text{Zr}^{4+}$ ) was dissolved in HCl ( $0.2 \text{ mol dm}^{-3}$ ), and a drop of alizarin-S was added. This mixture was allowed to react with  $\text{NaBH}_4$  ( $1.0 \text{ mol dm}^{-3}$ , taken in  $1.0 \text{ mol dm}^{-3}$  HCl). When the initial reaction had subsided and the product became colourless, 2 ml of concentrated  $\text{H}_2\text{SO}_4$  were added, and an inert atmosphere was maintained by the addition of 5 ml of  $\text{Na}_2\text{CO}_3$  solution ( $0.1 \text{ mol dm}^{-3}$ ). The reaction mixture was heated to  $70^\circ\text{C}$ , and a solution of  $\text{KMnO}_4$  ( $0.1 \text{ mol dm}^{-3}$ ) was gradually added in order to re-oxidise zirconium (in the reduced state) back to the  $\text{Zr}^{4+}$  state. In this process, 7.5 ml of  $\text{KMnO}_4$  were consumed (corresponding to 0.022 g of  $\text{KMnO}_4$  or 0.008 g of manganese). On the basis of an one-electron transfer with respect to zirconium, and a 5-electron transfer with respect to manganese, this corresponded to 0.074 g of zirconium, as against 0.087 g  $\text{Zr}^{4+}$  originally taken. This value compared favourably (85.1%), within the limits of experimental error, with the theoretical percentage of zirconium present in  $\text{ZrOCl}_2$ . This confirmed that the oxidation state of zirconium in the final product was +3 ( $\text{Zr}^{3+}$ ).

The solution containing the zirconium(IV)–alizarin-S complex ( $0.01 \text{ mol dm}^{-3}$ , taken in  $0.2 \text{ mol dm}^{-3}$  HCl), was mixed with a solution of  $\text{NaBH}_4$  ( $0.1 \text{ mol dm}^{-3}$ , taken in  $0.2 \text{ mol dm}^{-3}$  HCl), and allowed to stand at  $30^\circ\text{C}$  for 24 h. A spectral analysis of the product, over the range 300–850 nm, did not reveal any characteristic peak. Further, the esr signal showed lower paramagnetic character than that expected of a zirconium(III) species. This was due to dimerisation and Zr–Zr bond formation<sup>6,7</sup>, an observation that finds support from the lower magnetic moment value (of the order 1.4 to 1.5 BM (Bohr Magneton)) than the expected value of 1.73 BM for 1 electron per atom<sup>8</sup>.

*Mechanism.* The first step of the reaction could be represented as follows:



The mechanistic process could be represented as follows:



The overall stoichiometric reaction was:



Earlier reports had suggested the formation of the intermediate boron compound,  $\text{BH}_3\text{OH}^-$ , during the reaction of ketones with  $\text{NaBH}_4$  (Refs 9 and 10). We have already

established that such an intermediate,  $\text{BH}_3\text{OH}^-$ , was indeed formed during the reaction of sodium tetrahydroborate with sodium bismuthate<sup>11</sup>. Further hydrolysis would yield species such as  $\text{BH}(\text{OH})_2^-$ ,  $\text{BH}_2\text{OH}$ ,  $\text{BH}(\text{OH})_2$  and  $\text{H}_3\text{BO}_3$  (boric acid).

## CONCLUSIONS

The redox reaction between zirconium(IV) and sodium tetrahydroborate, in aqueous acidic medium, resulted in the facile formation of zirconium (III).

## ACKNOWLEDGEMENT

Financial support from the University Grants Commission, New Delhi, as part of the Special Assistance Programme, is gratefully acknowledged.

## REFERENCES

1. A. F. REID, J. S. SHANNON, J. M. SWAN, P. C. WAILES: Characterization of Bis [chloridodi(cyclopentadienyl) zirconium] Oxide, a Compound Containing the Zr–O–Zr Linkage. *Aust J Chem*, **18**, 173 (1965).
2. J. H. WENGROVIUS, P. R. SCHROCK: Attempts to Prepare Alkylidene Zirconium Complexes by  $\alpha$ -hydrogen Atom Abstraction. *J. Organomet Chem*, **205**, 319 (1981); J. H. WENGROVIUS, P. R. SCHROCK, C. S. DAY: Preparation and Reaction of  $[\text{ZrCl}_3(\text{PR}_3)_2]$  (R = Ethyl, Propyl, Butyl) and the X-ray Structure of  $[\text{ZrCl}_3(\text{PBU}_3)_2]$ . *Inorg Chem*, **20**, 1844 (1981).
3. W. C. PRICE, H. C. LONGUETT-HIGGINS, B. RICE, T. F. YOUNG: The Vibrational Spectra of Some Metal Borohydrides. *J Chem Phys*, **17**, 217 (1949).
4. T. C. WADDINGTON: Infrared Spectra of Metal Tetrahydroborates. *J Chem Soc*, 4783 (1958).
5. G. CHARLOT: Colorimetric Determination of Elements: Principles and Methods. Elsevier, Amsterdam, 1964, p. 439.
6. J. W. LAUHER, R. HOFFMAN: Structure and Chemistry of Bis(cyclopentadienyl)- $\text{ML}_n$  Complexes. *J Am Chem Soc*, **98**, 1729 (1976).
7. G. FOCHI, G. GUIDI, C. FLORIANI: Bis (cyclopentadienyl)–Zirconium (III) Complexes Containing a Metal–Metal Bond: Synthesis And Properties of Zr (II) and Zr (III) Complexes. *J Chem Soc Dalton*, 1253 (1984).
8. A. MAHAJAN, A. RANGWALA: Electricity and Magnetism. John Wiley, New York, 1989, p. 419.
9. J. GOUBEAU, H. KALFASS: Die Reaktion Natriumborhydrid und Wasser. *Z Anorg Allgem Chem*, **299**, 160 (1959).
10. J. A. GARDINER, J. W. COLLATT: Kinetics of the Stepwise Hydrolysis of Tetrahydroborate Ion. *J Am Chem Soc*, **87**, 1692 (1965).
11. S. DASGUPTA, M. K. MAHANTI: Evidence for the Boron Intermediate  $\text{BH}_3\text{OH}^-$ , in the Oxidation of Sodium Tetrahydroborate by Sodium Bismuthate. *Oxid Commun*, **29**, 618 (2006).

*Received 12 March 2010*

*Revised 12 April 2010*

## PHENOLIC COMPOSITION AND ANTIOXIDANT ACTIVITY OF FRESH FRUIT EXTRACTS OF MULBERRIES FROM SERBIA

D. A. KOSTIC, D. S. DIMITRIJEVIC\*, G. S. STOJANOVIC, S. S. MITIC, M. N. MITIC

*Department of Chemistry, Faculty of Natural Sciences and Mathematics, University of Nis, 33 Visegradska Street, 18 000 Nis, Serbia  
E-mail: danicadimitrijevic7@gmail.com*

### ABSTRACT

The aim of this research was determination of total phenolic, flavonoid and anthocyanin contents as well as measuring antioxidant activity in 3 types of mulberry (black, *Morus nigra* L.; red, *Morus rubra* L. and white, *Morus alba* L.) in 3 solvents (acetone, acetone–water (50/50, v/v%) and water) grown in south-east Serbia. The total phenolic content was determined using the Folin–Ciocalteu assay. The content of total flavonoids was measured spectrophotometrically using the aluminum chloride assay. The content of monomeric anthocyanins was measuring also spectrophotometrically using the pH differential method. Antioxidant assay was based on the measurement of DPPH absorbance at 517 nm caused by the reaction of DPPH with the test sample.

The results showed that the highest total phenolic, flavonoid and anthocyanin contents were displayed by the water extract of *Morus rubra* L. The highest antioxidant capacity in the DPPH assays showed the acetone–water (50/50, v/v%) extract of *Morus rubra* L. Due to the high degree of antioxidant activity, extracts of the fresh fruit of *Morus* species can serve well as natural antioxidants in pharmaceutical products and supplements.

*Keywords:* *Morus* species, natural phenolic compounds, antioxidant activity.

### AIMS AND BACKGROUND

The mulberry belongs to the genus *Morus* of the family Moraceae. Mulberry is found from temperate to sub-tropical regions of the Northern hemisphere to the tropics of the Southern hemisphere and they can grow in a wide range of climatic, topographical and soil conditions. These are widely spread throughout all regions from the tropics to the sub-arctic areas. Genus *Morus* is widespread in Asia, Europe, North and South America and Africa as well.

---

\* For correspondence.

*Morus* species are deciduous and in a period of low temperatures during the winter require to break dormancy. Mulberry fruit may be coloured white, red or black when they are ripe. Deep-coloured fruits are good sources of phenolics, including flavonoids, anthocyanins and carotenoids<sup>1-4</sup>, and mulberries are rich in phenolics<sup>5</sup>. Mulberry has an unique delicious fruit, sour and refreshing taste. It has been used as a folk remedy to treat oral and dental diseases, diabetes, hypertension, arthritis and anemia<sup>6</sup>. The bright black and purple mulberry fruits, which have a very pleasant taste when eaten fresh, are also used in jams, juices, liquors, natural dyes as well as in the cosmetics industry<sup>7</sup>.

The plant has high level of anthocyanins, hence it has a very important role in the food industry. It is considered that the fresh fruit colour comes from anthocyanins present in the fruit. This has contributed to the positive effects of fruit on the people health. The mulberry is found to be especially rich in anthocyanins, flavonoid and phenol compounds. The total content and the yield (percentage) of these compounds is dependent on geographic location and soil on which the mulberry tree grows. Despite the previous research on this plant, there is no information about its contents. Accordingly, the results obtained in this study differ from the results of *Morus* species found in other countries.

With the aim of finding new sources of natural antioxidants, a lot of plants, fruits, vegetables and other plant materials, that are known to possess antioxidant activity, have been investigated<sup>8</sup>. Many studies have investigated the contents of phenolics, flavonoids and anthocyanins<sup>7,9,10</sup>. Along with these compounds, black mulberry has been found to contain carotenoids<sup>2,11</sup>. Several studies have previously reported that anthocyanins display significant antioxidant activity<sup>12,13</sup>. There is growing interest for natural antioxidants, which prevent oxidation disorders in humans, rather than synthetic antioxidants, which are identified as carcinogens<sup>14</sup>.

## EXPERIMENTAL

*Preparation of the fresh fruit extracts.* Plant material was collected in the south-east Serbia in early July 2011. Fresh fruit maturity was estimated on the basis of the colour. Samples were stored in plastic bags and kept frozen until extraction. The frozen fresh fruit material homogenised using a blender. Black, red and white mulberry fresh fruits (10 g) were extracted with water, acetone–water (50/50, v/v%) and acetone. All solvents were acidified with 1 ml conc. HCl. The extraction was performed with 100 ml of solvents using ultrasonic bath for 30 min. The suspension was gravity filtered through a Buchner funnel and Whatman No 1 filter paper. Extracts were stored in the fridge until their analysis.

*Chemicals and reagents.* 1,1-Diphenyl-2-picrylhydrazyl (DPPH), catechin and AlCl<sub>3</sub> were purchased from Sigma Chemical Co. (St. Louis, MO, USA). The 6-hydroxy-2,5,7,8-tetramethylchroman-2-carboxylic acid (Trolox) was purchased from Acros Organics (New Jersey, USA). The Folin–Ciocalteu phenol reagent and sodium

carbonate were purchased from Merck Chemical Suppliers (Darmstadt, Germany). Sodium chlorate buffer (pH 1.0) and acetate buffer (pH 4.5) were purchased from the same producer.

The other used chemicals including solvents were of analytical grade. An Agilent 8453 UV-vis. spectrophotometer was used for absorbance measurements and spectra recording, using an optical or quartz cuvettes of 1-cm optical path. The pH measurements were made with Hanna Instruments pH-meter equipped with glass electrode.

*Determination of total phenolics.* Total phenol contents of the extracts were determined by the modified Folin–Ciocalteu method<sup>15</sup>. An aliquot of the extracts (1 ml) was mixed with 0.5 ml Folin–Ciocalteu reagent and 2 ml of sodium carbonate (20%). Absorbance was measured after 10-min incubation at room temperature at 760 nm. Total phenolic content was expressed as mg/100 g gallic acid equivalent (GAE). The result of each one assay was obtained from 3 parallel determinations.

*Determination of total flavonoid content.* Total flavonoid content was determined using a spectrophotometric method based on formation of flavonoid complex with aluminum<sup>16</sup>. Black, red and white mulberry extract (1 ml) was mixed with 3 ml deionised water and 0.3 ml NaNO<sub>2</sub>. After standing at room temperature for 5 min, 3 ml AlCl<sub>3</sub> were added to the solution, followed by the addition of 2 ml of NaOH after another 5-min standing. The solution was then filled up to the line with deionised water in a 10-ml flask. The absorbance of the prepared solution was measured at 510 nm. Total flavonoid content was calculated as catechin (mg CE/100 g) using the equation based on the calibration curve.

*Determination of total monomeric anthocyanins.* The total monomeric anthocyanin content in the plant extracts was determined using the pH-differential method previously described<sup>17</sup>. Anthocyanins demonstrate maximum of absorbance at 520 nm at pH 1.0. The coloured oxonium form predominates at pH 1.0, and the colourless hemiketal form – at pH 4.5. The pH-differential method is based on reaction producing oxonium forms and permits accurate and rapid measurement of the total monomeric anthocyanins. The result, considered as the monomeric anthocyanin pigment, was expressed as mg of cyanidin 3-O-glucoside, by using molar absorptivity ( $\epsilon$ ) of 26.900 dm<sup>3</sup> mol<sup>-1</sup> cm<sup>-1</sup> and molecular weight of 449.2. For this method, 1 ml of the black, red and white mulberry extract was poured into 2 separate 10-ml volumetric flasks. Then, one was filled up to the line with solution of KCl (pH=1), and the second with CH<sub>3</sub>COON<sub>a</sub> (pH=4.5). The two diluted solutions were left to stand for 15 min at room temperature. Finally, the absorbance of both samples was measured at  $\lambda_{\max}$  520 and 700 nm. Absorbances ( $A$ ) of the investigated extracts were calculated by equation (1):

$$A = (A_{\lambda_{\text{vis-max}}} - A_{700})_{\text{pH } 1.0} - (A_{\lambda_{\text{vis-max}}} - A_{700})_{\text{pH } 4.5} \quad (1)$$

The content of the monomeric anthocyanin pigment (MAP) was calculated using the following equation:

$$\text{MAP (mg dm}^{-3}\text{)} = (A \times \text{MW} \times \text{DF} \times 1000) / (\epsilon l) \quad (2)$$

where  $A$  is absorbance were calculated by equation (1);  $\epsilon$  – the molar absorptivity ( $26.900 \text{ dm}^3 \text{ mol}^{-1} \text{ cm}^{-1}$ ); MW – the molecular weight (449.2); DF – the dilution factor, and  $l$  – the path length ( $\text{cm}^{-1}$ ). The result, taken as the monomeric anthocyanin pigment (MAP), was expressed as mg of cyaniding 3-O-glucoside per  $\text{dm}^3$ .

*Free radical scavenging activity.* The free radical scavenging activity of the plant extracts was analysed by using the 2,2-diphenyl-1-picrylhydrazyl (DPPH) assay<sup>18–22</sup>. The antioxidant assay is based on the measurement of the loss of colour of DPPH solution by the change of absorbance at 517 nm caused by the reaction of DPPH with the tested sample. The reaction was monitored using UV-vis. spectrophotometer. Plant extracts (1 ml), 5 ml of freshly prepared DPPH in methanol and 4 ml of water were put into a cuvette at room temperature. After 30 min of incubation period at room temperature, the absorbance was read against a blank at 517 nm. All measurements were performed in triplicate at a final concentration. The ability of extracts to inhibit DPPH in percents (RSC %) was calculated from the decrease of absorbance according to the relationship (equation (3)):

$$\text{RSC (\%)} = (1 - A_{\text{sample}} / A_{\text{blank}}) \times 100 \quad (3)$$

where  $A_{\text{blank}}$  is the absorbance of control ( $1 \times 10^{-4} \text{ mol dm}^{-3}$  DPPH methanol solution), and  $A_{\text{sample}}$  – the absorbance of the test sample.

The final results were expressed as mg of Trolox equivalents (TE) per 100 g of fresh sample (mg TE/100 g).

*Statistical analysis.* The experimental results were expressed as mean value  $\pm$  standard error of mean value of 3 replicates. In order to estimate statistically any significant differences among mean values, where it was applicable, the data were subjected to a one-way analysis of variance (ANOVA test), and differences among samples were determined by the Duncan Multiple Range test using the Statistical Analysis System (SAS, 1999) software<sup>23</sup>.

## RESULTS AND DISCUSSION

The results show that the content of total phenols in the investigated extracts of *Morus nigra* L. was ranging from 103.90 to 120.78 mg GAE/100 g for the acetone and acetone–water (50/50 v/v%) extract of fresh fruit, respectively. The content of total phenols of *Morus rubra* L. was found to be 71.40 to 210.39 mg GAE/100 g for the acetone and water extract, respectively. The highest content of phenols of *Morus alba* L. extract was in the water extract (146.11 mg GAE/100 g) and the lowest amount was identified in the acetone–water (50/50 v/v%) extract (62.97 mg GAE/100 g) (Fig. 1).

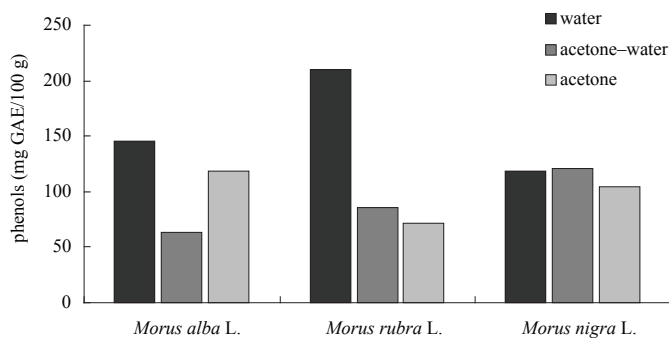


**Fig. 1.** Total phenol contents in water, acetone–water (50/50 v/v %) and acetone extracts of *Morus* spp.

Many studies have shown that the physiological functions of natural ingredients have been usually attributed to the antioxidant activity of phenolic compounds<sup>24–26</sup>.

In a previous work, methanol was used usually as a solvent to determine the content of phenolic compounds. In this paper, all the solvents (water, acetone–water (50/50 v/v%) and acetone) were acidified. Three analysed extracts gave different values for phenols, flavonoids and anthocyanins contents and different antioxidant activity as well. The difference in contents of phenolic compounds is a consequence of different solvent polarity and solubility of oxidant compounds in a given solvent.

Previous studies examined the total content of phenols, flavonoids, anthocyanins and antioxidant activity of *Morus nigra* L. from different countries and regions. For example, Kutlu et al.<sup>10</sup> used acidified methanol, acidified water and non-acidified methanol–water (70/30 v/v%) for the extraction of phenolic compounds in *Morus nigra* L. fruit. The highest content of phenolic compounds was found in non-acidified methanol–water (70/30 v/v%) (580 mg GAE/100 g) extract, while water extract exhibited the lowest amount of phenols (330 mg GAE/100 g). The methanol extract had 440 mg GAE/100 g fresh fruit. The authors concluded that the increase of acidity does not increase the amount of extracted phenols<sup>10</sup>. Ercisli et al.<sup>27</sup> analysed the phenolic content using the Folin–Ciocalteu method from the black and red mulberry collected in Turkey. Their results indicated that the plant contained phenols 215 mg GAE/100 g (*Morus nigra* L.) and 169 mg GAE/100 g (*Morus rubra* L.), which was more than the contents of phenolics from a black and red mulberry tree from south-east Serbia.

Also, Ozgen et al.<sup>6</sup> found higher the phenol content (270 mg GAE/100 g fruit of *Morus nigra* L. acetone extract and 160 mg GAE/100 g fresh fruit of *Morus rubra* L. than the content found in this work. Ercisli et al.<sup>28</sup> discovered significantly higher values of total phenol content in the plant of 1422 mg GAE/100 g fruit of *Morus nigra* L. extract, 1035 mg GAE/100 g for *Morus rubra* L. and 181 mg GAE/100 g fresh fruit of *Morus alba* L. methanol extract. The phenol content of *Morus nigra* L. was high using the extraction with methanol in Soxhlet, 1943–2237 mg GAE/100 g fruit<sup>7</sup>. *Morus alba* L. from Korea had 152–257 mg GAE/100 g in ethanol extract<sup>29</sup>.



The ethanol extract of black mulberry from Korea gave 867 mg GAE/100 g (Ref. 30). *Morus nigra* L. from Pakistan had 661 mg GAE/100 g and *Morus alba* L. showed 775 mg GAE/100 g (Ref. 31). *Morus alba* L. from Taiwan gave 1515 mg GAE/100 g fresh fruit<sup>5</sup>. *Morus rubra* L. grown in Brasil had 373 mg GAE/100g of fresh fruit<sup>32</sup> (Table 1).

**Table 1.** Comparison of levels of phenolic compounds from black, red and white mulberry grown in other regions

Sample	Country	Solvent	Total phenols content (mg GAE/100 g)	References
<i>Morus alba</i> L.	Taiwan	water	1515	5
<i>Morus rubra</i> L.	Turkey	acetone	160	6
<i>Morus nigra</i> L.	Turkey	acetone	270	6
<i>Morus nigra</i> L.	Turkey	methanol	1943–2237	7
<i>Morus nigra</i> L.	Turkey	methanol	330–580	10
<i>Morus nigra</i> L.	Turkey	ethanol	215	27
<i>Morus rubra</i> L.	Turkey	ethanol	169	27
<i>Morus nigra</i> L.	Turkey	methanol	1422	28
<i>Morus rubra</i> L.	Turkey	methanol	1035	28
<i>Morus alba</i> L.	Turkey	methanol	181	28
<i>Morus alba</i> L.	Korea	ethanol	2570	29
<i>Morus nigra</i> L.	Korea	ethanol	867	30
<i>Morus nigra</i> L.	Pakistan	methanol	661	31
<i>Morus alba</i> L.	Pakistan	methanol	775	31
<i>Morus rubra</i> L.	Brasil	methanol	373	32

The differences in total phenol content have been found to be dependent on the extraction medium used and polarity of the organic solvents used for the extraction. The extraction duration, method and the plant material condition attribute to the content of phenols.

Total flavonoid contents of the extracts of *Morus nigra* L. fresh fruit were ranging from 141.70 mg (water extract) to 191.91 mg CE/100 g (acetone–water extract (50/50 v/v%)), while in *Morus rubra* L. – from 44.95 mg CE/100 g (acetone extract) to 192.07 mg CE/100 g fresh fruit (water extract), and in extracts of *Morus alba* L. – from 52.73 (water extract) to 100.80 mg CE/100 g (acetone extract) (Fig. 2).

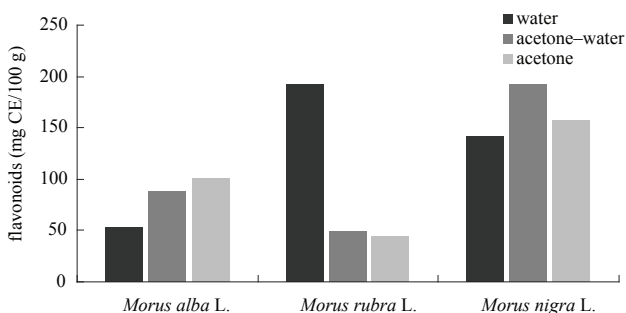


**Fig. 2.** Total flavonoid contents in water, acetone–water (50/50 v/v%) and acetone extracts of *Morus* spp.

In previous studies, flavonoids content ranged from 0.56 to 6.54 mg CE/100 g (Ref. 30) of *Morus alba* L. which is found to be much less compared to our findings.

Anthocyanins contents of *Morus nigra* L. were between 74.72 mg cyanidin (Cy) 3-O-glucoside/100 g for acetone–water extract (50/50 v/v%) and 114.83 mg cyanidin-3-O-glucoside/100g for water extract. The extracts of *Morus rubra* L. showed the anthocyanins content from 1.77 to 5.28 mg cyanidin 3-O-glucoside/100 g for the acetone–water extract (50/50 v/v%) and acetone extract, respectively. The extracts of white mulberry did not show the anthocyanin content (Fig. 3).

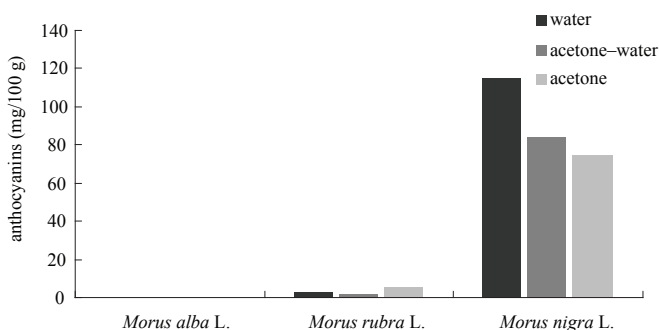


**Fig. 3.** Total anthocyanins contents in water, acetone–water (50/50 v/v%) and acetone extracts of *Morus* spp.

The anthocyanins analysis of black mulberry from Turkey had 720 mg Cy-3-O-glucoside per 100 g fruit and 109 mg Cy-3-O-glucoside per 100 g fruit for *Morus rubra* L. (Ref. 27). Our analysis showed that black mulberry contains less value of anthocyanins ranged from 74.72 to 114.83 mg Cy-3-O glucoside per 100 g of fruit for black mulberry and from 1.77 to 5.28 mg Cy-3-O glucoside per 100 g of fruit for red mulberry. Black mulberry from Korea contained 571 mg Cy-3-O-glucoside per 100 g dry fruit<sup>6</sup>.

All the extracts exhibited good scavenging activity against DPPH radicals from 44.50% (*Morus alba* L., water extract) to 89.41% (*Morus rubra* L., acetone–water extract (50/50 v/v%)) (Fig. 4). Methanol extract of black mulberry from Turkey had an antioxidant activity of 95%, aqueous 80% and methanol–water (70/30, v/v%) 85% (Ref. 10). Other studies have shown that the activity, expressed as Trolox equivalent, was 748 and 442 mg TE/100 g for black and red mulberry which was considerably higher than our results<sup>27</sup>.

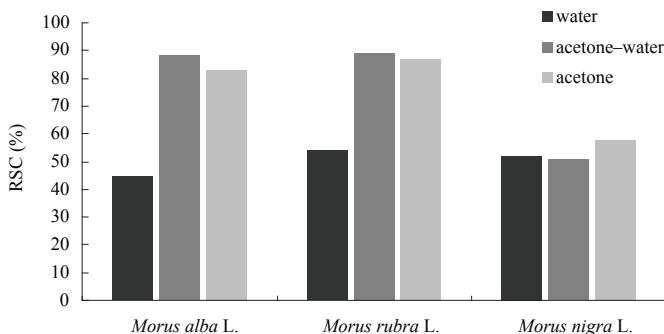


**Fig. 4.** DPPH radical scavenging power of water, acetone–water (50/50 v/v%) and acetone extracts of *Morus* spp.

Kinetic-spectrophotometric monitoring of disappearance of DPPH in the presence of 3 different mulberries in acetone extracts is shown in Fig. 5.

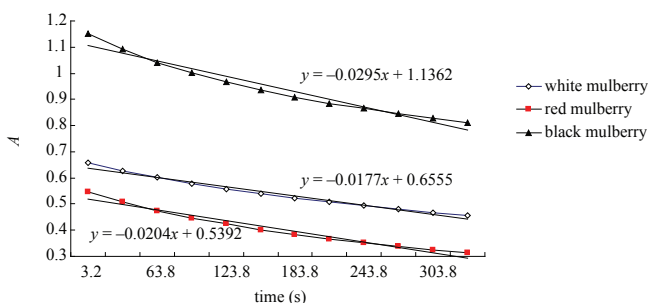


**Fig. 5.** Disappearance of absorbance of DPPH solution in the presence of 3 acetone extracts (1 ml) of different mulberries

The rate constants of tarnish of DPPH are 0.0295, 0.0204 and 0.0177 ( $\text{mol dm}^{-3} \text{s}^{-1}$ ) of black, red and white mulberry extract, respectively, which is consistent with increasing antioxidant activity of extracts.

The correlation coefficients between the results are shown in Table 2. The correlation can be very high ( $0.9 < |r| \leq 1$ ), high ( $0.7 < |r| \leq 0.9$ ), substantial ( $0.5 < |r| \leq 0.7$ ), insignificant ( $0.2 < |r| \leq 0.5$ ) and low ( $|r| \leq 0.2$ ).

**Table 2.** Correlation of total phenol, flavonoid and anthocyanins contents, and their correlation with antioxidant activity of black, red and white mulberry fresh fruit

Sample	Total phenols content	Flavonoid content	Monomeric anthocyanin	RSC (%)
<i>Morus alba</i> L.	total phenols content	1	0.2999	–
	flavonoid content		1	–
	monomeric anthocyanin			1
	RSC (%)			–
<i>Morus rubra</i> L.	total phenols content	1	0.9956	0.1470
	flavonoid content		1	0.1033
	monomeric anthocyanin			1
	RSC (%)			0.0529
<i>Morus nigra</i> L.	total phenols content	1	0.1018	0.0720
	flavonoid content		1	0.9972
	monomeric anthocyanin			1
	RSC (%)			0.9522

As Table 2 shows there was a very high coefficient of correlation between the content of flavonoids and anthocyanins (0.9972), between flavonoids and RSC (%) (0.9723) and between the content of anthocyanins and RSC (%) (0.9522) (*Morus nigra* L.). A very high coefficient of correlation was found between the content of total phenols and flavonoids (0.9956) (*Morus rubra* L.). A high coefficient of correlation was observed between flavonoids and RSC (%) (0.8637) (*Morus alba* L.), a substantial coefficient of correlation is between the total phenols and RSC (%) (0.6689) (*Morus alba* L.). There is a slight correlation of total phenols and RSC (%) (0.2188) (*Morus nigra* L.), total phenols and RSC (%) (0.4849), flavonoids and RSC (%) (0.4190) (*Morus rubra* L.) and between the total phenols and flavonoids (0.2999) (*Morus alba* L.). In other cases the correlation is found to be low.

## CONCLUSIONS

In this study, we compared phenolic, anthocyanin, flavonoids content and antioxidant activity of different extracts of *Morus nigra* L., *Morus rubra* L. and *Morus alba* L. fresh fruit from Serbia. High phenolic content and high antioxidant activity increase mulberry nutritive and phytomedicinal potentials.

Thus, the fruit of mulberry is of significant biological importance for its antioxidant properties. This study suggested the use of mulberry as potential healthy foods, or important antioxidant carrier in food and pharmaceutical industries.

## ACKNOWLEDGEMENTS

Financial support of this work by the Serbian Ministry of Education and Science, Project No ON 172047 is highly acknowledged.

## REFERENCES

1. E. CIESLIK, A. GRADA, W. ADAMUS: Contents of Polyphenols in Fruit and Vegetables. *Food Chem*, **94**, 135 (2003).
2. A. SASS-KISS, J. KISS, P. MILOTAY, M. M. KEREK, M. TOTH-MARKUS: Differences in Anthocyanin and Carotenoid Content of Fruits and Vegetables. *Food Res Inter*, **38**, 1023 (2005).
3. J. Y. QUIAN, D. LIU, A. G. HUANG: The Efficiency of Flavonoids in Polar Extracts of *Lycium chinense* Mill Fruits as Free Radical Scavenger. *Food Chem*, **87**, 283 (2004).
4. A. II TRAPPEY, A. H. BAWADI, R. R. BANSODE, N. J. LOSSO: Anthocyanin Profile of Mayhaw (*Cretaeus opaca*). *Food Chem*, **91**, 665 (2005).
5. J. Y. LIN, C. Y. TANG: Determination of Total Phenolic and Flavonoid Contents in Selected Fruits and Vegetables as well as Their Stimulatory Effects on Mouse Splenocyte Proliferation. *Food Chem*, **101**, 140 (2007).
6. M. OZGEN, S. SERCE, K. KAYA: Phytochemical and Antioxidant Properties of Anthocyanin-rich *Morus nigra* and *Morus rubra* Fruits. *Sci Hortic*, **119**, 275 (2009).
7. S. ERCISLI, E. ORHAN: Some Physico-chemical Characteristics of Black Mulberry (*Morus nigra* L.) Genotypes from Northeast Anatolia Region of Turkey. *Sci Hortic*, **116**, 41 (2008).
8. G. MILIAUSKAS, P. R. VENSKUTONIS, T. A. BEEK: Screening of Radical Scavenging Activity of Some Medicinal and Aromatic Plant Extracts. *Food Chem*, **85**, 231 (2004).
9. D. GERASOPOULOS, G. STAVROULAKIS: Quality Characteristics of Four Mulberry (*Morus* sp.) Cultivars in the Area Of Chania, Greece. *J Sci Food Agric*, **73**, 261 (1997).
10. T. KUTLU, G. DURMAZ, B. ATEŞ, I. YILMAZ, M. S. CETIN: Antioxidant Properties of Different Extracts of Black Mulberry (*Morus nigra* L.). *Turk J Biol*, **35**, 103 (2011).
11. R. ZADERNOWSKI, M. NACZK, J. NESTEROWICZ: Phenolic Acid Profiles in Some Small Berries. *J Agric Food Chem*, **53**, 2118 (2005).
12. F. C. STINZING, A. S. STINZING, R. CARLE, B. FREI, R. E. WROLSTAD: Color and Antioxidant Properties of Cyanidin-based Anthocyanin Pigments. *J Agric Food Chem*, **50**, 6172 (2002).
13. H. WANG, G. CAO, R. L. PRIOR: Oxygen Radical Absorbing Capacity of Anthocyanin. *J Agric Food Chem*, **45**, 304 (1997).
14. N. ITO, S. FUKUSHIMA, A. HASEGAWA, M. SHIBATA, T. OGISO: Carcinogenicity of Butylated Hydroxy Anisole in F344 Rats. *J Natl Cancer Inst*, **70**, 343 (1983).
15. V. L. SINGLETON, J. A. ROSSI: Colorimetry of Total Phenolics with Phosphomolybdic-phosphotungstic Acid Reagents. *Am J Enol Viticult*, **16**, 144 (1965).
16. A. A. L. ORDON, J. D. GOMEZ, M. A. ATTUONE, M. L. ISLA: Antioxidant Activities of *Sechium edule* (Jacq.) Swart Extracts. *Food Chem*, **97**, 452 (2006).
17. M. GUISTI, R. WROLSTAD: Characterization and Measurement of Anthocyanins by UV Visible Spectroscopy. *Current Protocols in Food Analytical Chemistry*. John Wiley and Sons, New York, 2003.
18. B. FUHRMAN, N. VOLKOVA, A. SURASKI, M. AVIRAM: White Wine with Red Wine-like Properties: Increased Extraction of Grape Skin Polyphenols Improves the Antioxidant Capacity of the Derived White Wine. *J Agric Food Chem*, **49**, 3164 (2001).
19. J. LACHMAN, M. SULC, M. SCHILLA: Comparison of the Total Antioxidant Status of Bohemian Wines during the Wine-making Process. *Food Chem*, **103**, 802 (2007).
20. J. SANCHEZ-MORENO, J. A. LARRAURI, F. SAURA-CALIXTO: Free Radical Scavenging Capacity of Selected Red, Rose and White Wines. *J Agric Food Chem*, **79**, 1301 (1999).

21. A. TURKOGLU, M. E. DURU, N. MERCAN, I. KIVRAK, K. GEZER: Antioxidant and Antimicrobial Activities of *Laetiporus sulphureus* (Bull.) Murrill. *Food Chem*, **101**, 267 (2007).
22. D. VILLANO, M. S. FERNANDEZ-PACHON, A. M. TRONCOSO, M. C. GARCIA-PARRILLA: Influence of Enological Practices on the Antioxidant Activity of Wines. *Food Chem*, **95**, 394 (2006).
23. Statistical Analysis and Reporting System. ser Guide, version 1.0, 1MB, 1999.
24. N. GOUGOULIAS: Comparative Study on the Antioxidant Activity and Polyphenol Content of Some *Salvia* Species (*Salvia* L.). *Oxid Commun*, **35** (2), 404 (2012).
25. V. YANEVA, D. BABRIKOV, N. MASHEV: Study on Polyphenols Content and Antioxidant Activity of Selected Seedless Grape Varieties (*V. vinifera*). *Oxid Commun*, **33** (3), 661 (2010).
26. N. GOUGOULIAS: Comparative Study on the Polyphenol Composition and Antioxidant Potential of Peloponnese Wines. *Oxid Commun*, **32** (2), 473 (2009).
27. S. ERCISLI, M. TOSUN, B. DURALIJA, S. VOĆA, M. SENGUL, M. TURAD: Phytochemical Content of Some Black (*Morus nigra* L.) and Purple (*Morus rubra* L.) Mulberry Genotypes. *Food Technol Biotechnol*, **48**, 102 (2010).
28. S. ERCISLI, E. ORHAN: Chemical Composition of White (*Morus alba*), Red (*Morus rubra*) and Black (*Morus nigra*) Mulberry Fruits. *Food Chem*, **103**, 1380 (2007).
29. S. H. BAE, H. J. SUH: Antioxidant Activities of Five Different Mulberry Cultivars in Korea. *LWT*, **40**, 955 (2007).
30. W. CHUN, X. LI, W. YUANCHANG, C. HU, H. XIANZHI: Determination of Total Polyphenol Content and Antityrosinase Capacity of Mulberry Medicine (*Morus nigra* L.) Extract. *A J Biotech*, **10**, 16175 (2011).
31. A. A. MEMON, N. MEMON, L. D. LUTHRIA, I. M. BHANGER, A. A. PITAFI: Phenolic Acids Profiling and Antioxidant Potential of Mulberry (*Morus leavigata* W., *Morus nigra* L., *Morus alba* L.). *J Food Nutr Sci*, **60**, 25 (2010).
32. N. M. A. HASSIMOTTO, M. I. S. GENOVESE, F. M. LAJOLO: Antioxidant Activity of Dietary Fruits, Vegetables and Commercial Frozen Fruit Pulps. *J Agric Food Chem*, **53**, 2928 (2005).

*Received 4 June 2012*  
*Revised 18 August 2012*

## ANTIOXIDANT POTENTIAL OF MUNGBEAN CULTIVARS COMMONLY CONSUMED IN PAKISTAN

M. ZIA-UL-HAQ<sup>a</sup>, R. AMAROWICZ<sup>b</sup>, S. AHMAD<sup>c</sup>, M. QAYUM<sup>d</sup>, S. ERCISLI<sup>e\*</sup>

<sup>a</sup>Department of Pharmacognosy, University of Karachi, 75 270 Karachi, Pakistan

<sup>b</sup>Institute of Animal Reproduction and Food Research, Polish Academy of Sciences, 10 Tuwima Street, 10 747 Olsztyn, Poland

<sup>c</sup>Department of Agronomy, Bahauddin Zakariya University, 60 800 Multan, Pakistan

<sup>d</sup>Department of Pharmacy, Kohat University of Science and Technology, 2600 Kohat, Pakistan

<sup>e</sup>Department of Horticulture, Ataturk University, 25 240 Erzurum, Turkey  
E-mail: sercisli@gmail.com

### ABSTRACT

Antioxidant potential of 4 mungbean (*Vigna radiata* (L.) W i l c z e k) varieties indigenous to Pakistan, namely Mung 88, NM 51, NM 54 and AEM 96, was evaluated. The content of total phenolics in the seeds ranged from 51.9 mg/100 g (AEM 96) to 74.2 mg/100 g (NM 54). The antioxidant activities of the mungbean extracts were tested using DPPH (18.97–19.33  $\mu\text{mol Trolox/g}$ ), ORAC (56.4–72.3  $\mu\text{mol Trolox/g}$ ), and ABTS (21.2–31.1  $\mu\text{mol Trolox/g}$ ) assays. All the extracts exhibited also antioxidant activity in linoleic acid system as well reducing power and chelation activity. The results of the present study showed mungbean, indigenous to Pakistan, to be a potentially valuable legume crop with high antioxidant potential.

*Keywords:* mungbean, antioxidant activity, free radicals, phenolic compounds.

### AIMS AND BACKGROUND

The antioxidant properties of the phenolic compounds in legumes are associated with the health benefits of legume products. Antioxidants play an important role in chronic disease prevention, because they can protect the organism against oxidative damage caused by reactive oxidant species (ROS) to vital biomolecules such as DNA, lipids, and proteins<sup>1</sup>. Many phenolic compounds found in legumes can help preserve vascular health. Direct antioxidant activity may mediate much of this benefit<sup>2</sup>.

---

\* For correspondence.

Phenolic compounds are secondary metabolites commonly found in legume seeds. Evaluation of their antioxidant activity has been of interest in recent years. Antioxidant activity has been reported for extracts of legumes such as pea, white, green, red, and navy beans; beach pea; lentils, everlasting pea; broad bean; faba bean; lima bean; Jack bean; vetch; adzuki bean; cowpea, chickpea and lentil<sup>3-17</sup>. Antioxidative and antiradical activity of leguminous extracts were investigated using methods like the storage studies<sup>18</sup>, a  $\beta$ -carotene–linoleate model system<sup>3-4,10,11,19</sup>, enhanced chemiluminescence and photoluminescence<sup>5</sup>, scavenging of AMVN (2,2'-azo-bis (2,4-dimethylvaleronitrile) radical<sup>20</sup>, ABAP (2,2'-azo-bis(2-amidinopropane) radical<sup>21</sup>, DPPH radical<sup>15,16,22</sup>, ABTS cation radical<sup>17,22-24</sup>, superoxide anion radical<sup>22</sup>, peroxy radical<sup>22</sup>, reducing power<sup>9</sup>, LDL cholesterol oxidation<sup>18</sup> and Fe<sup>2+</sup> chelating capacity<sup>18,22</sup>.

Pakistan due to its climatic conditions is conducive for cultivation of legumes and many legume crops are grown throughout country. However, majority of these legume species have not been evaluated for their nutritional and antioxidant potential. As part of our continuous studies on exploring biological activities and antioxidant potential of various crops and plants of Pakistan<sup>23-33</sup>, the present study is an attempt for screening the antioxidant potential of mungbean (*Vigna radiata* (L.) Wilczek) cultivars of Pakistan.

## EXPERIMENTAL

All solvents used were of analytical grade. Methanol, acetone, ethanol, ferrous chloride, linoleic acid, vanillin, gallic acid, the Folin–Ciocalteu phenol reagent, 2,2-diphenyl-1-picrylhydrazyl radical (DPPH•), 2,2'-azino-bis-(3-ethylbenzothiazoline-6-sulphonic acid) (ABTS), 2,4,6-tri(2-pyridyl)-s-triazine (TPTS) and 6-hydroxy-2,5,7,8-tetramethyl-chroman-2-carboxylic acid (Trolox) were obtained from Sigma (St Louis, MO). The seeds of 4 mungbean (*Vigna radiata* (L.) Wilczek), cultivars namely Mung 88, NM 51, NM 54 and AEM-96 were procured from Nuclear Institute for Agriculture and Biology (NIAB), Faisalabad (Pakistan). Seeds of all the cultivars were divided into groups for storage in stainless-steel containers at 4°C prior to analysis.

The mungbean samples were ground to flour with an IKA®all basic mill (IKA Works Inc., Wilmington, N.C., U.S.A.) and were passed through a 60-mesh sieve. The flour (0.5 g each) was accurately weighed into a set of centrifuge tubes and 5 ml 50% acetone (v/v) were added. Then the capped tubes were placed horizontally and shaken at 300 rpm at room temperature on an orbital shaker for 3 h. The mixture was extracted for another 12 h by keeping them in the dark overnight. The extracts were centrifuged at 2000 g for 10 min. Residue was re-extracted with 5 ml of the respective extraction solvents. Two extracts were combined and stored at 4°C in the dark. The extractions were conducted in triplicates for each individual variety.

The total phenolic contents in extracts were estimated using the Folin–Ciocalteu phenol reagent<sup>34</sup>. Gallic acid was used as a standard in this work.



DPPH• scavenging capacity of mungbean extracts was evaluated according to the method described in Ref. 35. The absorbance of the sample ( $A_{\text{sample}}$ ) was measured using a Hitachi UV-vis. Model U-2000 spectrophotometer at 517 nm against ethanol blank. A negative control ( $A_{\text{control}}$ ) was taken after adding DPPH• solution to 0.2 ml of the respective extraction solvent.

Antiradical activity was calculated by the following equation:

$$\text{antiradical activity \%} = \left(1 - \frac{A_{\text{sample}}}{A_{\text{control}}}\right) \times 100.$$

The calibration curve of Trolox standard was plotted. Results were expressed as micromoles of Trolox equivalent per gram of extract ( $\mu\text{mol Trolox/g}$ ).

ABTS<sup>+</sup> scavenging assay was carried out following the reported modified method<sup>36</sup>. ABTS radical cation was prepared by passing a 5 mM ABTS aqueous solution through the oxidising reagent, manganese dioxide, on a Fisher Brand P8 filter paper. Excess manganese dioxide was removed from the filtrate by passing the solution through a 0.2 mm Fisher Brand membrane. The extracts were diluted in 5 mM phosphate buffered saline (PBS, pH 7.4), to an absorbance of about 0.700 ( $\pm 0.020$ ) at 734 nm in a 1-cm cell. 1.0 ml of each of the extracts was added to 5 ml ABTS<sup>+</sup> solution and the absorbance reading were taken 10 min after the initial mixing at room temperature. PBS was used as the blank. The calibration curve of Trolox standard was plotted. The antioxidant activities of mungbean extracts were expressed as Trolox equivalent content in 1.0 g of extract.

Reducing power of phenolics was determined as described earlier<sup>37</sup>. Extracts (0.2, 0.4, 0.6, 0.8, 1.0, 1.2 mg) were mixed with phosphate buffer (5.0 ml, 2.0 M, pH 6.6) and 1% potassium ferricyanide (5 ml), and the mixtures were incubated at 50°C for 20 min. About 5 ml of 10% trichloroacetic acid were added and the mixture was centrifuged at 650 g for 10 min. The upper layer of the solution (5 ml) was mixed with distilled water (5 ml) and 0.1% ferric chloride (1 ml) and absorbance was measured at 700 nm.

Hydrophilic ORAC assay was carried out on a Gemini EM Microplate Spectrofluorometer (Molecular Devices, Sunnyvale, CA, U.S.A.), which was equipped with an incubator and wavelength adjustable fluorescence filters. The procedures were based on the previous reports<sup>38,39</sup>. The kinetic of the fluorescence was recorded immediately by the software SoftMax Pro (Molecular Devices, Sunnyvale, CA, USA). The final ORAC values were calculated using a linear equation between the Trolox standards or sample concentration and net area under the fluorescein decay curve. The data were analysed using Microsoft Excel (Microsoft, Roselle, IL, USA). The area under curve (AUC) was calculated as:  $\text{AUC} = 0.5 + (R_2/R_1 + R_3/R_1 + R_3/R_1 + \dots + 0.5 R_n/R_1)$ , where  $R_1$  was the fluorescence reading at the initiation of the reaction and  $R_n$  – the last measurement. The net AUC was obtained by subtracting the AUC of the blank from that of a sample or standard. The ORAC value was calculated and expressed as micromoles of Trolox equivalent per g legume ( $\mu\text{mol of TE/g legume}$ )

using the calibration curve of Trolox. Linearity range of the calibration curve was 5.0 to 50  $\mu\text{M}$  ( $r = 0.99$ ). For each specific sample, triplicate extractions were analysed.

The antioxidant activity of sample extracts was determined following a reported method<sup>40</sup>. Sample extracts were added to a solution mixture of linoleic acid (0.13 ml), 99.8% ethanol (10 ml), and 0.2 M sodium phosphate buffer (pH 7.0, 10 ml). The total volume was adjusted to 25 ml with distilled water. The solution was incubated at 40°C and the degree of oxidation was measured according to the thiocyanate method (Yen and Duh, 1993) with 10 ml of ethanol (75%), 0.2 ml of an aqueous solution of ammonium thiocyanate (30%), 0.2 ml sample solution and 0.2 ml of ferrous chloride ( $\text{FeCl}_2$ ) solution (20 mM in 3.5% HCl) being added sequentially. After 3 min of stirring, the absorption values of mixtures measured at 500 nm were taken as peroxide contents. A control was performed with linoleic acid but without the extracts. Synthetic antioxidants, BHT (butylated hydroxytoluene) and  $\alpha$ -tocopherol were used as positive control. The percent inhibition of linoleic acid peroxidation to express antioxidative activity was calculated using the following equation:

$$\text{antioxidant activity (\%)} = 100 - \frac{\Delta A_{\text{sample}} \text{ after 360 h}}{\Delta A_{\text{control}} \text{ after 360 h}} \times 100.$$

$\text{Fe}^{2+}$  chelating activity was measured by a 2,2'-bipyridyl competition assay<sup>41</sup>. The reaction mixture contained 0.25 ml of 1 mM  $\text{FeSO}_4$ , 1 ml of Tris-HCl buffer (pH 7.4), 0.25 ml of extract, 0.4 ml of 10% hydroxylamine-HCl, 1 ml of 2, 2'-bipyridyl solution (0.1% in 0.2 M HCl) and 2.5 ml of ethanol. The final volume was made up to 6.0 ml with water. The absorbance at 522 nm was measured and used to evaluate  $\text{Fe}^{2+}$  chelating activity using disodium ethylenediaminetetraacetate ( $\text{Na}_2\text{EDTA}$ ) as a standard.

Analyses of variance and the Tukey Student test were performed at level of  $P < 0.05$  to evaluate the significance of differences among mean values. Data were analysed by using the 'MSTATC' statistical computer package.

## RESULTS AND DISCUSSION

Mungbean is an important legume crop of Pakistan and is consumed as a whole seed and in processed form. It can be used as a main dish, side dish or in salads. Whole seeds are used as ingredient in soup mixes or to produce bean sprouts for salads. They are almost free from flatulence-causing factors; because of this, they are preferred for feeding babies and convalescents. Sprouted mungbean seeds are rich in proteins, mineral compounds, and vitamins.

Polyphenolic compounds are one of the most effective antioxidative constituents in plant foods including fruit, vegetables, and grains hence it is important to quantify polyphenolic contents and to assess their contribution to antioxidant activity. The polyphenolic contents of mungbean were expressed as mg gallic acid equivalents per 100 g of sample (Fig. 1). A wide variation was observed for the TPC (total phenolic

contents) and the cultivars differed significantly with respect to this parameter. The highest TPC was obtained in the case of NM54 (74 mg GAE/g), which was followed by NM51 (62 mg GAE/g), whereas the lowest TPC was obtained in the case of AEM 96 (52 mg GAE/g). Our values are in partial agreement with those reported by other authors<sup>42,43</sup>. The differences between current results and previous report may be attributed to the differences in the sources of the samples.

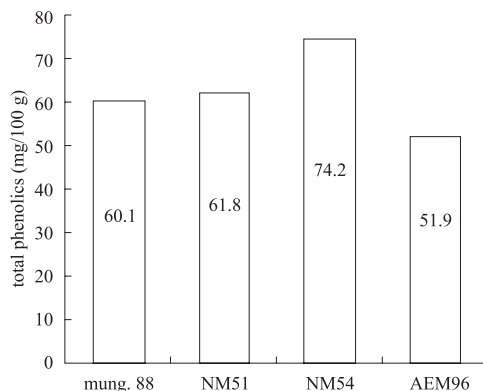


**Fig. 1.** Total phenolic contents of mungbean cultivars

The scavenging activity of mung beans was determined by DPPH<sup>•</sup> and ABTS<sup>•+</sup> assays as shown in Figs 2 and 3. The stable DPPH radical, which has a maximum absorption at 515 nm, is widely used to evaluate the free radical scavenging activity of hydrogen donating antioxidants in many plant extracts. Both of these radicals are commonly used for assessment of antioxidant activity *in vitro* and are foreign to biological systems. H-atom-donating capacity of polyphenols is an important biologically significant property, in line with the ability of the plant antioxidants to convert potentially damaging reactive oxygen species into nontoxic species. In particular, DPPH<sup>•</sup> is increasingly used for quickly assessing the ability of antioxidants to transfer the labile H atom to radicals. All the cultivars exhibited appreciable scavenging activity against both the radicals and the same order of scavenging was observed by both the assays. Maximum scavenging activity was observed for NM54 followed by NM51. Maximum difference among the cultivars was observed at 5 min of reaction and the remaining amount (%) of DPPH radical at 5 min after initiation of reaction, as shown in Fig. 2. Differences between our results and previous reports may be attributed partly to the differences in the sources of materials and in expressions based on dry weight or fresh weight basic calculation. Although the DPPH<sup>•</sup> free radical is ubiquitously used to estimate the potential free radical scavenging activity of natural products, the ABTS<sup>•+</sup> cation radical is commonly used when issues of solubility or interference arise and the use of DPPH<sup>•</sup>-based assays becomes inappropriate. The ABTS<sup>•+</sup> scavenging data (Fig. 3) suggest that the components within the extracts are capable of scavenging free radicals via a mechanism of electron/hydrogen donation

and should be able to protect susceptible matrices from free radical mediated oxidative degradation. All cultivars exhibited appreciable scavenging activity against both the radicals and the same order of scavenging was observed by both assays. The antiradical activity of phenolic compounds present in the extracts of mungbean seeds against DPPH<sup>•</sup> and ABTS<sup>•+</sup> were close to reported earlier<sup>42</sup>.

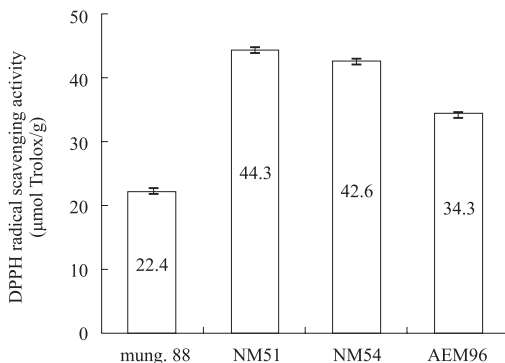


**Fig. 2.** DPPH<sup>•</sup> radical scavenging activity of mungbean cultivars

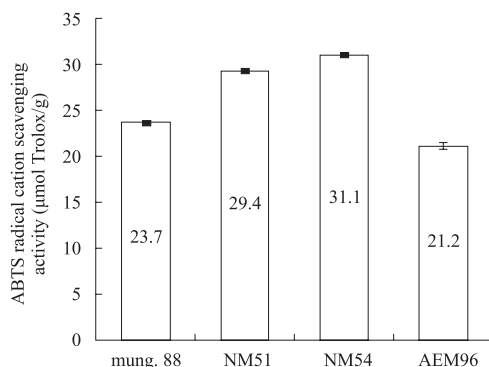


**Fig. 3.** ABTS<sup>•+</sup> radical scavenging activity of mungbean cultivars

The reducing power of phenolic compounds is associated with antioxidant activity. Thus, a relation should be located between reducing power and the antioxidant effect. The reducing power of methanolic extracts was measured and found to increase with increasing amount of extracts. BHA was used to compare the reducing power of these extracts (Fig. 4). The highest reducing power was observed for NM54 followed by NM51. The results were close to reported earlier<sup>42</sup>. The highest reducing power out of these cultivars observed was in agreement with TPC, radical and radical cation scavenging ability. However, for all the cultivars the reducing power was less than that for BHA. As results for all the cultivars were in agreement with TPC and scavenging activities. Therefore, reducing power evaluation may be taken as an important parameter for the assessment of antioxidant activity. A large variation in reducing power was observed among the cultivars but this difference went on decreas-

ing with the increase in the dose of extracts. The results can be exploited in terms that cultivars with long growth period and demanding less quantity of water have greater reducing power and vice versa.

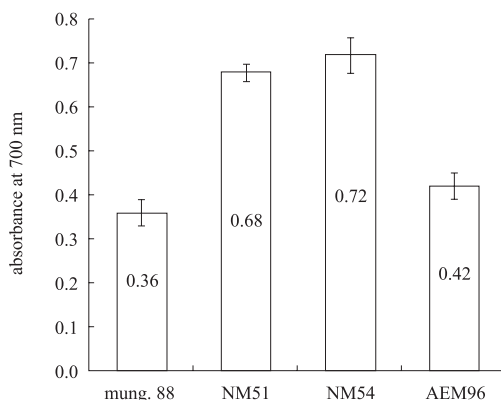


**Fig. 4.** Reducing power of mungbean cultivars

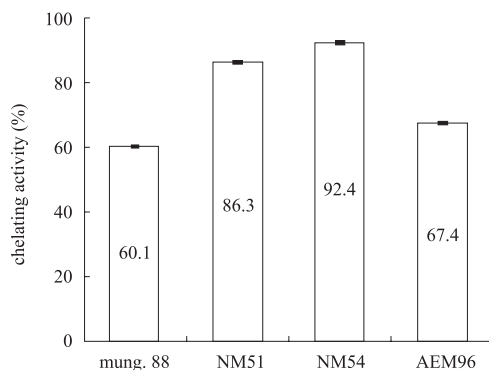


**Fig. 5.** Chelating activity of mungbean cultivars

Chelation is an important parameter in the sense that iron is essential for life because it is required for oxygen transport, respiration and the activity of many enzymes. However, iron is an extremely reactive metal and will catalyse oxidative changes in lipids, proteins and other cellular components. The chelating activity was measured against  $\text{Fe}^{2+}$  and reported as EDTA equivalents (Fig. 5). A large difference in chelating activity was observed among the species. The highest chelating activity was observed for NM 54 followed by NM51. The results were close to reported earlier<sup>42</sup>.

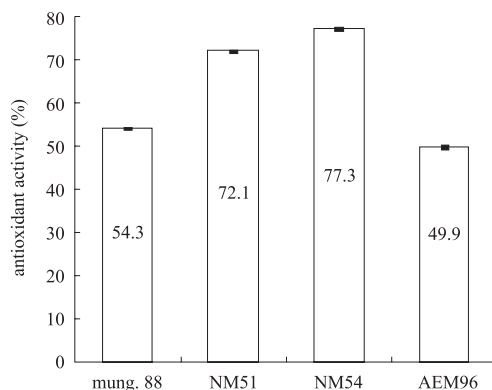


**Fig. 6.** Antioxidant activity of linoleic acid model system of mungbean cultivars

All the extracts of mungbean exhibited good antioxidant activity in the linoleic acid peroxidation system (Fig. 6); the highest antioxidant activity was observed for NM54, whereas the lowest value was for AEM96. At a concentration of 0.2 mg/ml of linoleic acid solution, the mungbean inhibited 49.90–77.30% peroxidation of linoleic acid after incubation for 360 h (15 days). The results obtained in this study are in agreement with literature data. Antioxidant activity of the extracts of leguminous seeds (pea, bean, lentil, faba bean, broad bean, everlasting bean) in a  $\beta$ -carotene–linoleate model system has been reported in several studies<sup>3,4,7–10</sup>. These results suggest that mungbean may be used for a possible treatment of cardiovascular diseases, for cholesterol lowering and other lipid peroxidation processes, being a more powerful antioxidant complex than tocopherol.

**Table 1.** Antioxidant capacity of mungbean cultivars

Antioxidant parameters	Mung. 88	NM51	NM54	AEM96
ORAC ( $\mu$ mol Trolox/g)	57.3 $\pm$ 0.13 <sup>c</sup>	69.7 $\pm$ 0.16 <sup>b</sup>	72.3 $\pm$ 0.14 <sup>a</sup>	56.4 $\pm$ 0.12 <sup>c</sup>

Means with the same letters are not significantly different ( $P < 0.05$ ).

The ORAC method is usually employed to estimate antioxidant activity of foods and to evaluate *in vivo* responses to dietary antioxidant manipulation. The ORAC is the only method so far that combines both inhibition time and degree of inhibition into a single quantity<sup>44</sup>. The food and nutraceutical industries have accepted the method to the point that some manufacturers now include ORAC values on product labels. All mungbean extracts exhibited significant ORAC values and results were expressed as TE (Table 1). Significant differences ( $P < 0.05$ ) in ORAC existed among mungbean cultivars with values ranging from 56.4 mmol of Trolox/g (AEM96) to 72.3 mmol Trolox/g (NM54).

## CONCLUSIONS

Many colourful and attractive, raw and processed, food and nutraceutical products are prepared from mungbean for local consumption besides its use in traditional folklore medicines. Mungbean may contribute to the significant supply of antioxidant to prevent oxidative stress as people from all income groups are consuming mungbean. Our results could have a direct impact on mungbean consumption by increasing consumer awareness of the health benefits of mungbean and its demand is expected to rise if consumers are informed about the important micronutrients and nutraceutical properties in mungbean. It can contribute towards improving the economy through industrial processing and value addition for export.

## REFERENCES

1. P. C. H. HOLLMAN: Evidence for Health Benefits of Plant Phenols: Local or Systemic Effects? *J Sci Food Agri*, **81**, 842 (2001).
2. M. McCARTY: Proposal for a Dietary 'Phytochemical Index'. *Med Hypo*, **63**, 813 (2004).
3. R. AMAROWICZ, A. TROSZYNSKA, M. KARAMAC, H. KOZLOWSKA: Antioxidative Properties of Legume Seed Extracts. In: *Agri-Food Quality. An Interdisciplinary Approach* (Eds G. R. Fenwick, C. Hedley, R. L. Richards, S. Khokahr). The Royal Society of Chemistry, Cambridge, UK, 1996, 376–379.
4. R. AMAROWICZ, M. KARAMAC, H. KMITA-GLAZEWSKA, A. TROSZYNSKA, H. KOZLOWSKA: Antioxidant Activity of Phenolic Fractions of Everlasting Pea, Faba Bean and Broad Bean. *J Food Lipid*, **3**, 199 (1996).
5. R. AMAROWICZ, B. RAAB: Antioxidative Activity of Leguminous Seed Extracts Evaluated by Chemiluminescence Methods. *Z. Naturforsch C*, **52**, 709 (1997).
6. R. AMAROWICZ, M. NACZK, R. ZADERNOWSKI, F. SHAHIDI: Antioxidative Activity of Condensed Tannins of Beach Pea, Canola Hulls, Evening Primrose, and Faba Bean. *J Food Lipids*, **7**, 195 (2000).
7. R. AMAROWICZ, M. KARAMAC, U. CHAVAN: Influence of the Extraction Procedure on the Antioxidative Activity of Lentil Seed Extracts in a  $\beta$ -Carotene–Linoleate Model System. *Grasas Aceites*, **52**, 89 (2001).
8. R. AMAROWICZ, M. KARAMAC, S. WEIDNER: Antioxidative Activity of Phenolic Fractions of Pea (*Pisum sativum*). *Czech J Food Sci*, **19**, 139 (2001).
9. R. AMAROWICZ, M. KARAMAC, F. SHAHIDI: Antioxidant Activity of Phenolic Fractions of Lentil (*Lens culinaris* L.). *J Food Lipids*, **10**, 1 (2003).
10. R. AMAROWICZ, A. TROSZYNSKA: Antioxidant Activity of Extract of Pea and Its Fractions of Low Molecular Phenolics and Tannins. *Polish J Food Nut Sci*, **1**, 10 (2003).
11. R. AMAROWICZ, M. KARAMAC, S. WEIDNER, F. SHAHIDI: Antioxidative Activity of Phenolic Fractions of White Bean (*Phaseolus vulgaris* L.). *J Food Lipids*, **11**, 165 (2004).
12. R. AMAROWICZ, A. TROSZYNSKA, N. BARYLKO-PIKIELNA, F. SHAHIDI: Extracts of Polyphenolics from Legume Seeds – Correlation between Their Total Antioxidant Activity, Total Phenolics Content, Tannins Content and Astringency. *J Food Lipids*, **11**, 278 (2004).
13. R. AMAROWICZ, A. TROSZYNSKA, R. B. PEGG: Antioxidative and Radical Scavenging Effects of Phenolics from *Vicia sativum*. *Fitoterapia*, **79**, 121 (2008).
14. R. AMAROWICZ, I. ESTRELLA, T. HERNANDEZ, A. TROSZYNSKA: Antioxidant Activity of Extract of Adzuki Bean and Its Fractions. *J Food Lipids*, **15**, 119 (2008).

15. M. ZIA-UL-HAQ, S. IQBAL, S. AHMAD, M. I. BHANGER, W. WICZKOWSKI, R. AMAROWICZ: Antioxidant Potential of Desi Chickpea Varieties Commonly Consumed in Pakistan. *J Food Lipids*, **15**, 326 (2008).
16. M. ZIA-UL-HAQ, S. AHMAD, S. IQBAL, D. L. LUTHRIA, R. AMAROWICZ: Antioxidant Potential of Lentil Cultivars Commonly Consumed in Pakistan. *Oxid Commun*, **34**, 819 (2011).
17. M. ZIA-UL-HAQ, S. A. SHAHID, S. AHMAD, M. QAYUM, N. RASOOL: Mineral Contents and Antioxidant Potential of Selected Legumes of Pakistan. *J Med Plants Res*, **32**, 4735 (2012).
18. T. MADHUJITH, F. SHAHIDI: Antioxidant Potential of Pea Beans (*Phaseolus vulgaris* L.). *J Food Sci*, **70**, S85 (2005).
19. T. MADHUJITH, R. AMAROWICZ, F. SHAHIDI: Phenolic Compounds in Beans and Their Effects on Inhibition of Radical-induced DNA Damage. *J Am Oil Chem Soc*, **81**, 691 (2004).
20. T. ARIGA, M. HAMANO: Radical Scavenging Action and Its Mode in Procyanidins B1 and B-3 from Adzuki Beans to Peroxyl Radicals. *Agri Bio Chem*, **54**, 2499 (1990).
21. H. ZIELINSKI: Peroxyl Radical-trapping Capacity of Germinated Legume Seeds. *Nahrung*, **46**, 100 (2002).
22. K. ZHOU, L. YU: Total Phenolic Contents and Its Antioxidant Properties of Commonly Consumed Vegetables Grown in Colorado. *LWT – Food Sci Tech*, **39**, 1155 (2006).
23. M. ZIA-UL-HAQ, S. CAVAR, M. QAYUM, I. KHAN, S. AHMAD: Compositional Studies and Antioxidant Potential of *Acacia leucophloea* R o x b. *Acta Bot Croat*, (2013) (in press).
24. M. ZIA-UL-HAQ, S. AHMAD, M. QAYUM, S. ERCISLI: Compositional Studies and Antioxidant Potential of *Albizia lebbek* (L.) B e n t h. *Tur J Bio*, **36**, 1 (2012).
25. M. ZIA-UL-HAQ, S. IQBAL, M. AHMAD: Characteristics of Oil from Seeds of 4 Mungbean (*Vigna radiata* (L.) Wilczek] Cultivars Grown in Pakistan. *J Am Oil Chem Soc*, **85**, 851 (2008).
26. M. ZIA-UL-HAQ, S. AHMAD, E. CHIAVARO, MEHJABEEN, S. AHMED: Studies of Oil from Cowpea (*Vigna unguiculata* (L.) W a l p.) Cultivars Commonly Grown in Pakistan. *Pak J Bot*, **42**, 1333 (2010).
27. M. ZIA-UL-HAQ, S. AHMAD, M. A. SHAD, S. IQBAL, M. QAYUM, A. AHMAD, D. L. LUTHRIA, R. AMAROWICZ: Compositional Studies of Some of Lentil Cultivars Commonly Consumed in Pakistan. *Pak J Bot*, **43**, 1563 (2011).
28. M. ZIA-UL-HAQ, S. CAVAR, M. QAYUM, I. IMRAN, V. DEFEO. Compositional Studies, Antioxidant and Antidiabetic Activities of *Capparis decidua* (F o r s k.) E d g e w. *Int J Mol Sci*, **12**, 8846 (2011).
29. M. ZIA-UL-HAQ, M. NISAR, M. R. SHAH, M. AKHTER, M. QAYUM, S. AHMAD, S. A. SHAHID, M. HASANUZZAMAN: Toxicological Screening of Some Selected Legumes Seed Extracts. *Legume Res*, **34**, 242 (2011).
30. M. ZIA-UL-HAQ, S. A. SHAHID, S. AHMAD, M. QAYUM, I. KHAN: Antioxidant Potential of Various Parts of *Ferula assafoetida* L. *J Med Plants Res*, **16**, 3254 (2012).
31. M. ZIA-UL-HAQ, S. AHMAD, L. CALANI, T. MAZZEO, D. D. RIO, N. PELLEGRINI, V. DEFEO. Compositional Study and Antioxidant Potential of *Ipomoea hederacea* J a c q. and *Lepidium sativum* L. Seeds. *Molecules*, **17**, 10306 (2012).
32. M. ZIA-UL-HAQ, B. A. KHAN, P. LANDA, Z. KUTIL, S. AHMED, M. QAYUM, S. AHMAD: Platelet Aggregation and Anti-inflammatory Effects of Garden Pea, Desi Chickpea and Kabuli Chickpea. *Acta Poloniae Pharm*, **69**, 707 (2012).
33. M. ZIA-UL-HAQ, P. LANDA, Z. KUTIL, M. QAYUM, S. AHMAD: Evaluation of Anti-inflammatory Activity of Selected Legumes from Pakistan: *In vitro* Inhibition of Cyclooxygenase-2. *Pak J Pharm Sci*, (2013) (in press).
34. V. L. SINGLETON, J. A. ROSSI: Colorimetry of Total Phenolic with Phosphomolybdic-Phosphotungstic Acid Reagents. *Am J Enol Viticult*, **16**, 144 (1965).
35. C. W. CHEN, C. T. HO: Antioxidant Properties of Polyphenols Extracted from Green and Black Teas. *J Food Lipids*, **2**, 35 (1995).



36. D. D. REO, N. PELLEGRINI, A. PROTEGGENTE, A. PANNALA, M. YANG, C. RICE-EVANS: Antioxidant Activity Applying an Improved ABTS<sup>•+</sup> Radical Cation Decolourisation Assay. *Free Rad Bio Med*, **26**, 1231(1999).
37. M. OYAIZU: Studies on Products of Browning Reaction: Antioxidative Activities of Products of Browning Reaction Prepared from Glucosamine. *Japan J Nut*, **44**, 307(1986).
38. R. L. PRIOR, H. HOANG, L. W. GU, X. L. WU, M. BACCHIOCCA, L. HOWARD, M. HAMPSCHEWOODILL, D. J. HUANG, B. X. OU, R. JACOB: Assay for Hydrophilic and Lipophilic Antioxidant Capacity (Oxygen Radical Absorbance Capacity (ORACFL)) of Plasma and Other Biological and Food Samples. *J Agr Food Chem*, **51**, 3273 (2003).
39. X. L. WU, G. R. BEECHER, J. M. HOLDEN, D. B. HAYTOWITZ, S. E. GEBHARDT, R. PRIOR: Lipophilic and Hydrophilic Antioxidant Capacities of Common Foods in the United States. *J Agr Food Chem*, **52**, 4026 (2004).
40. T. OSAWA, M. NAMIKI: A Novel Type of Antioxidant Isolated from Leaf Wax of Eucalyptus Leaves. *Agri Bio Chem*, **45**, 735 (1981).
41. F. YAMAGUCHI, T. ARIGA, Y. YOSHIMURA, K. NAKAZAWA: Antioxidative and Antiglycation Activity of Garcinol from *Garcinia indica* Fruit Rind. *J Agr Food Chem*, **48**, 180 (2000).
42. Y. CHOI, H. S. JEONG, J. LEE: Antioxidant Activity of Methanolic Extracts from Some Grains Consumed in Korea. *Food Chem*, **103**, 130 (2007).
43. R. FERNANDEZ-OROZCO, J. FRIAS, H. ZIELINSKI, M. K. PISKULA, H. KOZLOWSKA, C. VIDAL-VALVERDE: Kinetic Study of the Antioxidant Compounds and Antioxidant Capacity during Germination of *Vigna radiata* cv. Emerald, *Glycine max* cv. Jutro and *Glycine max* cv. Merit. *Food Chem*, **111**, 622 (2008).
44. G. H. CAO, R. L. PRIOR: Measurement of Oxygen Radical Absorbance Capacity in Biological Samples. *Method Enzymol*, **299**, 50 (1999).

*Received 25 August 2012*

*Revised 23 October 2012*

## **ANTIOXIDANT CHARACTERISTICS OF SELECTED PLANT SPECIES GROWING UNDER POST-FIRE ENVIRONMENTAL CONDITIONS**

G. S. STOJANOVIC\*, V. D. MITIC, V. P. STANKOV-JOVANOVIC, M. D. ILIC, O. P. JOVANOVIC, G. M. PETROVIC

*Department of Chemistry, Faculty of Science and Mathematics, University of Nis, 33 Visegradska Street, 18 000 Nis, Serbia*

*E-mail: stgocaus@yahoo.com; gocast@pmf.ni.ac.rs*

### **ABSTRACT**

The flavonoid content (TFC), total phenols (TPC), DPPH radical scavenging activity (RSA) and, Fe(III) to Fe(II) reducing power (RP) of methanol extracts from 13 plant species that have been grown under non-disturbed environmental conditions (NDEC) and post-fire environmental conditions (PFEC) were investigated. The impact of wild-fire on examined properties depends on plant species. Although there are significant differences for most pairs of individual samples (PFEC and NEC) it could not be said for investigated characteristics when all thirteen NEC samples considered as one group and PFEC samples as another group ( $p > 0.05$ ). Some extracts expressed  $EC_{50}$  value close to the value of  $EC_{50}$  for BHT, proving themselves as excellent antioxidants. The content of flavonoids shows moderate correlation with Mo(VI) to Mo(V) and Fe(III) to Fe(II) reducing power and DPPH scavenging capacity. To the best authors knowledge, there were no reports on the impact of wild fire on the above-mentioned plant characteristics.

*Keywords:* methanol plant extracts, total phenols and flavonoids, radical scavenging capacity, total reducing power.

### **AIMS AND BACKGROUND**

A 10-day large-scale wildfire occurred in the summer of 2007 on the Vidlic mountain (Serbia, 43°10'16.7"N; 22°39'06.0"E). The fire affected more than 2500 ha of forest, grassland and low vegetation. It is known that fire, depending on the intensity and duration, affects soil physical, chemical and biological characteristics<sup>1</sup>. Our studies have shown that there were differences in soil characteristics on the Vidlic mountain

---

\* For correspondence.

such as: acidity, redox potential, conductivity, content of heavy metals, organic matter and chloride<sup>2</sup>. The changes caused by fire in the soil and atmosphere affect the vegetation, too<sup>3</sup>. Soil is a good insulator, buds underground are well protected, and plants can survive fires by re-sprouting from basal stems, and also from roots and horizontal rhizomes.

As a part of our study of the impact of wildfire on plants chemical and biological properties herein we report the examination of total flavonoid content (based on flavonoid affinity to form complex with  $\text{AlCl}_3$ ), total phenols (by the Folin–Ciocalteu reagent based on reduction of Mo(VI) to Mo(V)), DPPH radical scavenging activity and reducing power assay of Fe(III) to Fe(II) for methanol extracts of 13 plant species (Table 1) that have been grown under non-disturbed environmental conditions (NDEC) and post-fire environmental conditions (PFEC). To the best of our knowledge, there is no published data concerning this topic<sup>2,4</sup>.

## EXPERIMENTAL

*Instrumentation and chemicals.* The following substances were used: 1%  $\text{K}_3[\text{Fe}(\text{CN})_6]$  (Merck, Germany), buffer  $\text{NaH}_2\text{PO}_4$ – $\text{Na}_2\text{HPO}_4$  (pH 6.6) (Zorka, Serbia), 10%  $\text{CCl}_3$ – $\text{COOH}$  (Merck, Germany), 0.1%  $\text{FeCl}_3$  (Merck, Germany), ascorbic acid (vitamin C) (Seharlau, Germany), 3,5-di-*tert*-butyl-4-hydroxytoluene (BHT) (Zorka, Serbia), 2,2-diphenyl-1-picrylhydrazyl (DPPH) (La Chema, German),  $\text{AlCl}_3$  (Merck, German), rutin (Fluka, Germany), 20%  $\text{Na}_2\text{CO}_3$  (Merck, Germany), gallic acid (Mallinckrodt, Germany), the Folin–Ciocalteu reagent (Sigma Chemicals Co. (St. Louis, MO, USA), methanol (VWR International S.A.S., France), ethylacetate (Zorka, Serbia), acetone (Zorka, Serbia), ether (99.9%, VWR International S.A.S., Belgium), hexane (96.6%, VWR International S.A.S., France). Ultraviolet spectra were recorded on a Perkin-Elmer Lambda 15 spectrophotometer.

*Plant material.* *Geranium macrorrhizum* L. (Geraniaceae) and *Doronicum columnae* (Asteraceae) were collected in July 2008. Besides the above 2 species, another 11 species (Table 1) were collected in July 2009. All plant samples were collected in the flowering stage from normal environmental conditions (NEC) and post-fire environmental conditions (PFEC). The species were collected and identified by Marija Markovic, Department of Biology and Ecology, Faculty of Science and Mathematics, University of Nis, and the voucher specimens were deposited in the Herbarium of the above-mentioned Faculty. The plant material was air-dried for 10 days at  $25 \pm 2^\circ\text{C}$  without exposure to direct sunlight source. The air-dried powdered plant materials (10 g) were extracted with methanol (250 ml) at room temperature for a period of 24 h. The extracts were filtered and methanol was evaporated in vacuum at  $40^\circ\text{C}$ . The solutions of extracts were prepared in methanol to a final concentration of 1 mg of dry residue per ml.

Total flavonoid content and DPPH<sup>•</sup> assay. The above-mentioned experiments were performed as described before<sup>5</sup>.

Total phenolic content by the Folin–Ciocalteu method and reducing power assay Fe(III) to Fe(II). These parameters were determined as described previously<sup>6</sup>.

*Statistical analysis.* Results were presented as mean  $\pm$  SD. Significant differences between the groups were analysed with the Student *t*-test. Statistical difference was considered significant at  $p < 0.05$  (Ref. 7).

## RESULTS AND DISCUSSION

Table 1 shows an overview of the examined species, as well as their extraction yields.

**Table 1.** Extraction yields of the examined species under normal environmental conditions (NEC) and post-fire environmental conditions (PFEC)

Plant species	Family	Extraction yields (%)	
		NEC	PFEC
<i>Lathyrus venetus</i> *	Fabaceae	5.5 $\pm$ 0.3	5.7 $\pm$ 0.4
<i>Hypericum perforatum</i>	Hypericaceae	7.5 $\pm$ 0.4	12.4 $\pm$ 0.6
<i>Ajuga chamaepitys</i>	Lamiaceae	6.6 $\pm$ 0.2	8.5 $\pm$ 0.3
<i>Calamintha nepeta</i>	Lamiaceae	2.7 $\pm$ 0.1	4.4 $\pm$ 0.2
<i>Glehoma hirsuta</i>	Lamiaceae	5.1 $\pm$ 0.3	10.9 $\pm$ 0.5
<i>Hyssopus officinalis</i>	Lamiaceae	6.9 $\pm$ 0.4	5.9 $\pm$ 0.3
<i>Satureja montana</i>	Lamiaceae	3.0 $\pm$ 0.1	2.6 $\pm$ 0.1
<i>Epilobium angustifolium</i> *	Onagraceae	8.8 $\pm$ 0.5	6.1 $\pm$ 0.4
<i>Primula veris</i>	Primulaceae	4.4 $\pm$ 0.2	9.9 $\pm$ 0.5
<i>Fragaria vesca</i>	Rosaceae	5.4 $\pm$ 0.3	6.4 $\pm$ 0.3
<i>Viola odorata</i>	Violaceae	3.2 $\pm$ 0.1	5.4 $\pm$ 0.2
<i>Geranium macrorrhizum</i> 2008	Geraniaceae	3.6 $\pm$ 0.1	12.2 $\pm$ 0.6
<i>Geranium macrorrhizum</i> 2009	Geraniaceae	6.1 $\pm$ 0.3	7.9 $\pm$ 0.3
<i>Doronicum columnae</i> 2008	Asteraceae	10.7 $\pm$ 0.5	15.6 $\pm$ 0.6
<i>Doronicum columnae</i> 2009	Asteraceae	6.3 $\pm$ 0.2	7.9 $\pm$ 0.4

Results are presented as mean percentage  $\pm$  SD; \*  $p > 0.05$ .

The extraction yields range from 2.7 to 10.7% (samples from NEC) and from 2.6 to 15.6% (samples from PFEC). Differences in yields for *L. venetus* and *E. angustifolium* were without statistical significance ( $p > 0.05$ ). 9 samples have higher yields from areas affected by fire. Only *H. officinalis* and *S. montana* that grew in the area affected by fire have a lower percentage of methanol extractable substances than the respective plant species that grew in the area not affected by fire.

The results for total flavonoid content (based on flavonoid affinity to form complex with  $AlCl_3$ ), total phenols (by the Folin–Ciocalteu reagent based on reduction of Mo(VI) to Mo(V)), DPPH radical scavenging activity and reducing power assay of Fe(III) to Fe(II) are presented in Fig. 1a–d and Fig. 2a–d).

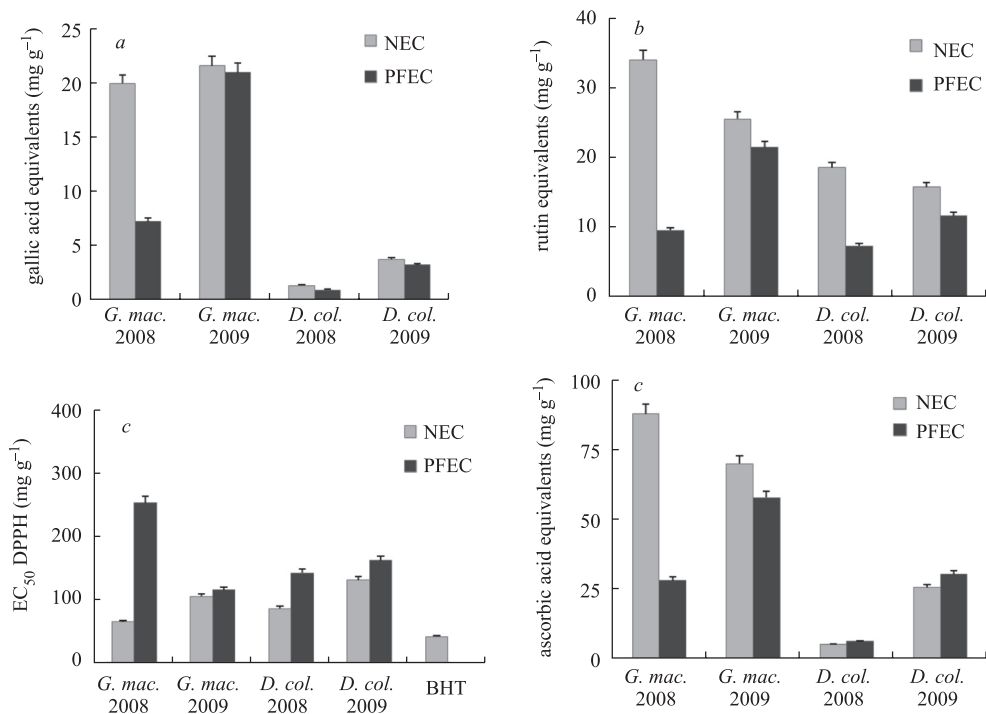


**Fig. 1.** Total phenols content (a), total flavonoids content (b), EC<sub>50</sub> DPPH (c), and reducing power Fe(III) to Fe(II) (d) for *G. macrorrhizum* (*G. mac.*) and *D. columnae* (*D. col.*) grown under NEC and PFEC in 2008 and 2009 year

Without statistical significance ( $p > 0.05$ ) where the differences in the values of the following properties: TPC (*G. macrorrhizum* 2009, *D. columnae* 2009, *G. hirsuta* and *V. odorata*), TFC (*S. montana*), RP (*D. columnae* 2008, *A. chamaepitys*, *C. nepeta* and *V. odorata*), and DPPH (*G. macrorrhizum* 2009 and *S. montana*).

For *D. columnae* and *G. macrorrhizum*, values of TPC, TPF and RP were higher for NEC samples collected in both years, 2008 and 2009, with the exception of RP for *D. columnae* 2009. Also, DPPH values were better for NEC samples. Furthermore, differences in the examined characteristics for both, NEC and PFEC samples were significantly higher for extracts obtained from plants harvested one year after the fire comparing with the corresponding extracts of plants harvested 2 years after the fire (Fig. 1a–d).

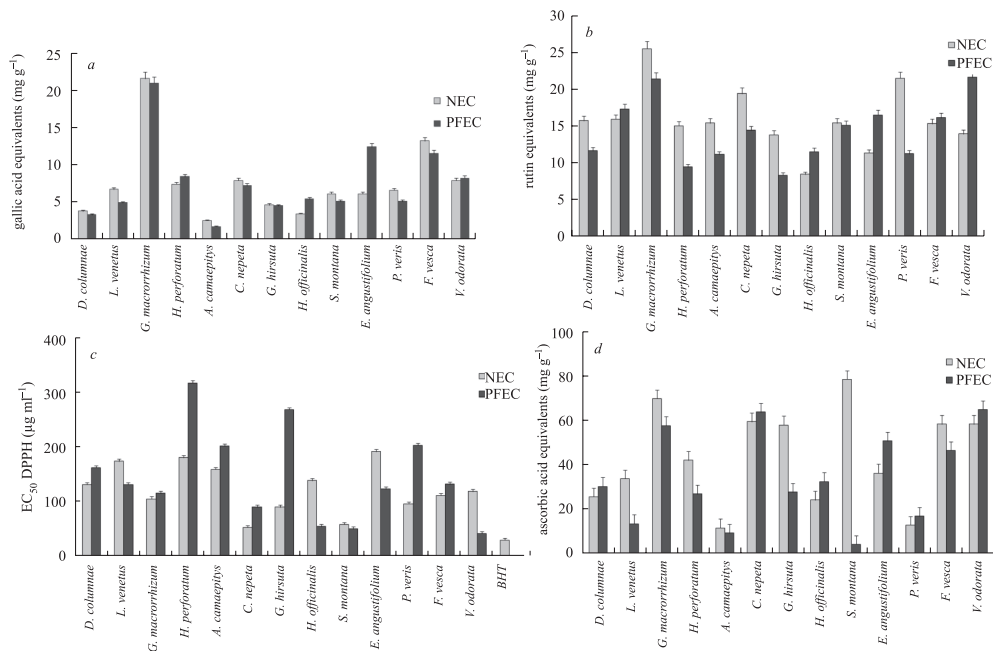


**Fig. 2.** Total phenols content (a), total flavonoids content (b), EC<sub>50</sub> DPPH (c), and reducing power Fe(III) to Fe(II) (d) for examined species grown under NEC and PFEC

From the presented results (Fig. 2a–d) it can be assumed that the impact of wildfire on flavonoid and phenol content, DPPH scavenging capacity and Fe(III) to Fe(II) reducing power depends on plant species. Although there are significant differences for most pairs of individual samples (PFEC and NEC) it could not be said for investigated characteristics when all 13 NEC samples considered as one group and PFEC samples as another group ( $p > 0.05$ ).

A similar observation was reported in the previous study about the chemical composition of essential oils of the aerial parts of the *A. chamaepitys* and their antioxidant capacity. Namely, examined NEC and PFEC essential oils had a qualitative similar composition. Both oil samples had approximately equal and moderate activity in reducing Fe(III) to Fe(II) and Mo(VI) to Mo(V) and, weak radical scavenging activity<sup>4</sup>.

It is noteworthy that both extracts of *S. montana*, and extracts of *V. odorata* and *H. officinalis* from the burned area as well as extract of *G. macrorrhizum* 2008 and *C. nepeta* from the unburned area expressed EC<sub>50</sub> value close to the value of EC<sub>50</sub> for BHT, proving themselves as excellent antioxidants, while the others have larger values, and consequently, weaker scavenging capacity. The correlation of examined properties of plants extracts is shown in Table 2.

**Table 2.** Correlation coefficients (*r*) between assays

	Total flavonoid content	DPPH <sup>•</sup>	Mo(VI) to Mo(V)	Fe(III) to Fe(II)
Total flavonoid content		0.57	0.65	0.45
DPPH <sup>•</sup>	0.57		0.18	0.57
Mo(VI) to Mo(V)	0.65	0.18		0.27
Fe(III) to Fe(II)	0.45	0.57	0.27	

The content of flavonoids shows moderate correlation with Mo(VI) to Mo(V) and Fe(III) to Fe(II) reducing power and DPPH scavenging capacity. There was weak correlation between Mo(VI) to Mo(V) and Fe(III) to Fe(II) reducing power although both methods are related to transfer of electron to metal ions probably due to different values of the solutions pH and the different standard potential of the observed ion pairs. No correlation was found between Mo(VI) to Mo(V) and DPPH scavenging capacity. This can be explained by different nature of the electron acceptor: metal ion against sterically protected DPPH radical.

## CONCLUSIONS

The flavonoid content (TFC), total phenols (TPC), DPPH radical scavenging activity (RSA) and, Fe(III) to Fe(II) reducing power (RP) of methanol extracts from 13 plant species grown under non-disturbed environmental conditions and post-fire environmental conditions were determined. There were significant differences for most pairs of examined extracts properties for individual samples (PFEC and NEC), but when all thirteen NEC samples were considered as one group and PFEC samples as another group no statistically significant differences ( $p > 0.05$ ) between groups on studied characteristics were found. These results may be helpful in directing future research in two ways. First, plant material should be harvested first year after fire if circumstances allow. It seems that the impact of fire on the investigated characteristics after 2 years is negligible. Second, it should be collected as many species as possible of the same genus. Perhaps, the impact of fire on the studied characteristics within the same genus may show a causal dependence.

## ACKNOWLEDGEMENTS

The research was supported by the Serbian Ministry of Education and Science (Grant No 172047). Part of the results was presented at the 10th Indo-Italian workshop on chemistry and biology of antioxidants, Sapienza University, Rome, Italy, Book of Abstracts, 2011, p. 63.

## REFERENCES

1. G. CERTINI: Effects of Fire on Properties of Forest Soils: A Review. *Oecologia*, **143**, 1 (2005).

2. V. STANKOV-JOVANOVIC, M. ILIC, M. MARKOVIC, V. MITIC, S. NIKOLIC-MANDIC, G. STOJANOVIC: Wild Fire Impact on Copper, Zinc, Lead and Cadmium Distribution in Soil and Relation with Abundance in Selected Plants of Lamiaceae Family from Vidlic Mountain (Serbia). *Chemosphere*, **84**, 1584 (2011).
3. R. KOKALY, B. ROCKWELL, S. HAIRE, T. V. KING: Characterization of Post-fire Surface Cover, Soils, and Burn Severity at the Cerro Grande Fire, New Mexico, Using Hyperspectral and Multi-spectral Remote Sensing. *Remote Sens Environ*, **106**, 305 (2007).
4. V. MITIC, V. STANKOV-JOVANOVIC, O. JOVANOVIĆ, I. PALIC, A. DJORDJEVIC, G. STOJANOVIC: Composition and Antioxidant Activity of Hydrodistilled Essential Oil of Serbian *Ajuga chamaepitys* (L.) Schreber ssp. Chia (Schreber) Arcan geli. *J Essent Oil Res*, **23**, 70 (2011).
5. N. MIMICA-DUKIC, N. SIMIN, J. CVEJIC, E. JOVIN, D. ORCIC, B. BOZIN: Phenolic Compounds in Field Horsetail (*Equisetum arvense* L.) as Natural Antioxidants. *Molecules*, **13**, 1455 (2008.)
6. G. STOJANOVIC, I. STOJANOVIC, V. STANKOV-JOVANOVIC, V. MITIC, D. KOSTIC: Reducing Power and Radical Scavenging Activity of Four Parmeliaceae Species. *Cent Eur J Biol*, **5**, 808 (2010).
7. J. N. MILLER, J. C. MILLER: *Statistics and Chemometrics for Analytical Chemistry*. Pearson Education Ltd., Edinburgh Gate Harlow, England, 2005, 39–47.

*Received 28 September 2012*

*Revised 27 October 2012*



## OXIDATION KINETICS AND MECHANISM OF NORFLOXACIN BY CHLORAMINE-B IN ACIDIC CHLORIDE SOLUTION

N. NANDA\*, S. M. MAYANNA

Department of Chemistry, B.M.S. College for Women, Basavanagudi,  
560 004 Bangalore, Karnataka, India  
E-mail: n\_nandashankar@yahoo.com

### ABSTRACT

The kinetics of oxidation of norfloxacin (NRF) by sodium N-chlorobenzene sulphonamide (Chloramine-B, CAB) has been studied in aqueous hydrochloric acid medium at 303 K. The reaction is first order with respect to [CAB] and [HCl], fractional order on [NRF]. Activation parameters were evaluated from the kinetic data at different temperatures. A negative entropy of activation indicated the involvement of a rigid complex in the activated state. The dielectric constant of the medium has a small effect on the rate. Ionic strength and the reaction product benzenesulphonamide have no effect on the reaction rate. The solvent isotope effect is studied. The reaction products are identified by spectral (IR and NMR) data. Rate equation is derived to account for the observed kinetic data and a probable mechanism has been proposed.

*Keywords:* kinetics, oxidation, norfloxacin, Chloramine-B.

### AIMS AND BACKGROUND

The chemistry of N-halo-N-sodium sulphonamides in aqueous solution has received considerable attention and the existing literature on the subject has been reviewed<sup>1-3</sup>. These compounds in aqueous solution give several oxidising species and the concentration of each species depends on the pH and nature of the medium<sup>4,5</sup>. Chloramine-B, one such compound, has been used to understand the mechanism of oxidation of few medicinal compounds<sup>6-8</sup>.

Norfloxacin, (NRF)[1-ethyl-6-fluoro-4-oxo-7-(piperazin-1-yl)-1,4-dihydroquinoline-3-carboxylic acid] is a synthetic broad-spectrum fluoroquinolone antibacterial agent for oral administration, which has *in vitro* activity against gram-positive and gram-negative aerobic bacteria. It inhibits deoxyribonucleic acid (DNA) synthesis and is bactericidal<sup>9,10</sup>.

---

\* For correspondence.

The kinetics and mechanism of oxidation of NRF in aqueous acetic acid containing  $\text{HClO}_4$  and also in  $\text{NaOH}$  has been studied<sup>11,12</sup>. These investigations revealed the considerable influence of the reaction medium on the oxidation kinetics. In order to have a comprehensive understanding of the oxidation mechanism of NRF under different experimental conditions, it was felt to investigate the influence of chloride ions on the kinetics of oxidation of NRF by Chloramines-B in acidic medium.

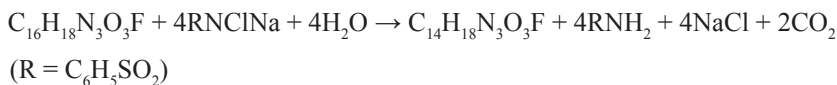
## EXPERIMENTAL

Preparation of CAB and its purification have been reported in earlier communication<sup>13</sup>. Aqueous solution of CAB was standardised iodometrically and preserved in brown bottle. NRF (Plama lab, India) was purified by  $\text{CH}_2\text{Cl}_2/\text{MeOH}$  (m.p. 227–228°C) and used. All other chemicals were of analytical grade. Doubly distilled water was used to prepare the solutions.

*Kinetics measurements.* The pseudo-first order condition was maintained by keeping  $[\text{NRF}] \gg [\text{CAB}]$ . The reaction was carried out in glass-stoppered pyrex boiling tubes whose outer surface was coated black to eliminate photochemical effects. Requisite amounts of CAB,  $\text{HCl}$  and water (to keep the total volume constant for all the runs) were taken in the tube and thermostated at 303 K for thermal equilibrium.

A measured amount of NRF solution was also thermostated at the same temperature and rapidly added to a mixture in the boiling tube. The progress of the reaction was monitored up to two and a half-lives by iodometric determination of unreacted CAB in measured aliquot of the reaction mixture withdrawn at different time intervals. The pseudo-first order rate constants ( $k'$ ) calculated were reproducible within  $\pm 3\%$ . Regression analysis of the experimental data was carried out.

*Stoichiometry and product analysis.* Reaction mixtures under conditions  $[\text{CAB}] \gg [\text{NRF}]$  were equilibrated at 303 K in  $1 \times 10^{-1} \text{ mol dm}^{-3}$   $\text{HCl}$  solution for 24 h. The results showed the consumption of 4 mol of CAB per 1 mol of NRF. On the basis of analysis of the reaction products, the following stoichiometric equations are proposed:



The reaction product of oxidant, benzenesulphonamide, was detected by TLC (Ref. 14).  $\text{CO}_2$  was identified by the lime-water test. The oxidation product of NRF (3-fluoro-4-piperazinyl-6-N-ethylaminophenylglyoxylic acid) was isolated and characterised by IR (Nicolet Impact 400D, FTIR) and NMR (Bruker, drx 500, FTNMR, SF = 125.75 MHz) spectral studies.

IR (KBr)  $\nu_{\text{max}}$   $\text{cm}^{-1}$ : 1621s(C=O), 1729s(C=O)acid, 3059s(NH), 3400s(OH)  
 $^1\text{H}$  NMR(DMSO) ppm: 1.51 (ethyl protons), 8.03(1H,m), 7.58(1H,m), 4.79 (piperazinyl protons), 9.23 (OH,s), 8.28 (1H, NH, s).

## RESULTS

The oxidation of NRF under different experimental conditions was investigated at various initial concentrations of the reactants in acidic medium.

Kinetics of oxidation of NRF ( $2.00 \times 10^{-3} \text{ mol dm}^{-3}$ ) by the oxidant at constant concentration ( $1 \times 10^{-1} \text{ mol dm}^{-3}$ ) of HCl was studied at various initial concentrations ( $[2-15] \times 10^{-4} \text{ mol dm}^{-3}$ ) of CAB at 303 K. Plots of  $\lg [\text{CAB}]$  versus time are linear indicating a first order dependence of the rate on  $[\text{oxidant}]$ . The constancy of rate constant ( $k_{\text{obs}}$ ) at different concentrations of oxidant evaluated from the integrated first order rate equation (Table 1) is a further evidence for the pseudo-first order dependence of the rate on  $[\text{oxidant}]$ . The order of the reaction with respect of  $[\text{CAB}]$  was found to be  $1.00 \pm 0.03$ . The oxidation was carried out with various concentrations ( $[0.5 - 3.0] \times 10^{-3} \text{ mol dm}^{-3}$ ) of NRF by using  $2 \times 10^{-4} \text{ mol dm}^{-3}$  CAB in  $1 \times 10^{-1} \text{ mol dm}^{-3}$  HCl. The rate of reaction increased with increasing  $[\text{NRF}]$  (Table 1). Plots of  $\lg k_{\text{obs}}$  versus  $[\text{NRF}]_0$  were linear with a slope of 0.60, indicating a fractional-order dependence on  $[\text{NRF}]$ .

**Table 1.** Effect of varying oxidant, substrate and HCl concentrations on the reaction rate at 303 K

$[\text{CAB}] \times 10^4$ ( $\text{mol dm}^{-3}$ )	$[\text{NRF}] \times 10^3$ ( $\text{mol dm}^{-3}$ )	$[\text{HCl}] \times 10$ ( $\text{mol dm}^{-3}$ )	$k' \times 10^4$ ( $\text{s}^{-1}$ )
2.00	2.00	1.00	9.33
5.00	2.00	1.00	9.32
7.50	2.00	1.00	9.34
10.00	2.00	1.00	9.30
15.00	2.00	1.00	9.31
2.00	0.50	1.00	3.55
2.00	0.75	1.00	4.75
2.00	1.00	1.00	5.92
2.00	2.00	1.00	9.33
2.00	3.00	1.00	11.65
2.00	2.00	0.25	2.06
2.00	2.00	0.50	3.45
2.00	2.00	0.75	6.85
2.00	2.00	1.00	9.33
2.00	2.00	1.50	13.91

The reaction was carried out with  $2 \times 10^{-4} \text{ mol dm}^{-3}$  oxidant and  $2 \times 10^{-3} \text{ mol dm}^{-3}$  of NRF in the presence of various concentrations ( $[0.25 - 1.50] \times 10^{-1} \text{ mol dm}^{-3}$ ) of HCl at 303 K. The rate increased with increase in  $[\text{HCl}]$  (Table 1). The reaction was first order with respect to  $[\text{HCl}]$ . At fixed  $[\text{H}^+]$ , addition of NaCl did not affect the rate significantly. Hence the dependence of the rate on  $[\text{HCl}]$  reflected the effect of  $[\text{H}^+]$  only on the reaction. Therefore, the rate of reaction is directly proportional to

[H<sup>+</sup>] when the overall acid concentration was varied and the ratio  $k'/[H^+]$  is nearly a constant.

The reaction of CAB ( $2 \times 10^{-4}$  mol dm<sup>-3</sup>) and NRF ( $2 \times 10^{-3}$  mol dm<sup>-3</sup>) was carried out in the mixtures of methanol and water of various compositions (% v/v) containing HCl ( $1 \times 10^{-1}$  mol dm<sup>-3</sup>) at 303 K. The reaction rate increased with increase in MeOH content in the medium (Table 2).

**Table 2.** Effect of varying dielectric constant of medium on the reaction rate at 303 K  
[CAB] =  $2.0 \times 10^{-4}$  mol dm<sup>-3</sup>; [NRF] =  $2.0 \times 10^{-3}$  mol dm<sup>-3</sup>; [HCl] = 0.10 mol dm<sup>-3</sup>

% MeOH (v/v)	$D$	$k' \times 10^4$ (s <sup>-1</sup> )
0	76.73	12.06
5	74.55	15.11
10	72.37	16.31
20	67.48	19.61

The ionic strength of the medium was varied by adding sodium perchlorate ( $\mu = 0.01 - 0.1$  mol dm<sup>-3</sup>), but this had negligible effect on the rate of the reaction. Hence, no attempt was made to keep it constant for kinetic runs. Addition of the reaction product, benzenesulfonamide ( $1 \times 10^{-3} - 1 \times 10^{-2}$  mol dm<sup>-3</sup>) had no significant effect on the rate. The reaction rates were studied at different temperatures (283–323 K). From the linear Arrhenius plot of  $\lg k'$  versus  $1/T$ , values of composite activation parameters, energy of activation ( $E_a$ ), enthalpy of activation ( $\Delta H^*$ ), entropy of activation ( $\Delta S^*$ ), free energy of activation ( $\Delta G^*$ ) and  $\lg A$  were computed. These results are compiled in Table 3.

**Table 3.** Temperature dependence on the reaction rate and activation parameters for the oxidation of NRF by CAB in acid medium

[CAB] =  $2.0 \times 10^{-4}$  mol dm<sup>-3</sup>; [NRF] =  $2.0 \times 10^{-3}$  mol dm<sup>-3</sup>; [HCl] = 0.1 mol dm<sup>-3</sup>

Temperature (K)	$k' \times 10^4$ (s <sup>-1</sup> )	Activation parameters	
283	3.01	$E_a$ (kJ mol <sup>-1</sup> )	43.7
293	5.65	$\Delta H^*$ (kJ mol <sup>-1</sup> )	41.2
303	9.31	$\Delta G^*$ (kJ mol <sup>-1</sup> )	91.7
313	17.27	$\Delta S^*$ (J K <sup>-1</sup> mol <sup>-1</sup> )	-166.7
323	30.61	$\lg A$	6.6

Addition of acrylamide solution to the reaction mixture in an inert atmosphere did not initiate polymerisation of the latter, indicating the absence of free radical formation in the reaction sequence.

## DISCUSSION

Bishop and Jennings<sup>15</sup>, Morris et al.<sup>16</sup> and Higuchi et al.<sup>17</sup> have established the presence of several equilibria in acidified Chloramines-T (CAT) solutions. The work of

Zilberg<sup>18</sup>, Mogilevski et al.<sup>19</sup> and Mahadevappa et al.<sup>20</sup> have indicated the operation of similar equilibria in acidified CAB solutions. Chloramine-B ionises in aqueous solution, as follows:

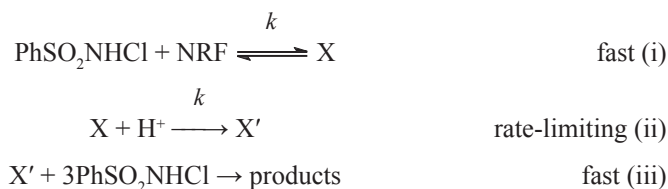


The anion picks up a proton in acid solution to give monochloramine ( $\text{PhSO}_2\text{NHCl}$ ), which can undergo disproportion and/or hydrolysis, to give the dichloramine, benzenesulphonamide and HOCl. Hence, the probable oxidising species are  $\text{PhSO}_2\text{NHCl}$ ,  $\text{PhSO}_2\text{NCl}_2$  and HOCl.  $\text{PhSO}_2\text{NCl}_2$  can be ruled out as the oxidising species in view of the strict first order dependence of rate on [CAB]. Similarly, a first order retardation of rate by benzenesulphonamide is expected, if HOCl is the reactive species. Since, these are not observed, the effective oxidising species in the rate-determining step could be conjugate acid ( $\text{PhSO}_2\text{NHCl}$ ) in acid solution of CAB in the present system.

In the present investigations, oxidation of NRF by CAB in acid medium shows a fractional-order dependence on [NRF] and clearly indicated complex formation between the substrate and oxidant in an equilibrium step prior to the rate-limiting step. However, the rate dependence on  $[\text{H}^+]$  indicates the involvement of a neutral species in the rate-determining step (rds). The reaction product of CAB, benzenesulphonamide had no effect on the rate thus indicating that it was not involved in pre-equilibrium with oxidant.

Based on the above facts, the mechanism of oxidation of NRF by CAB in acid medium is best explained by scheme 1 to account all the observed kinetic data.

Scheme 1



Assuming total concentration of CAB as  $[\text{CAB}]_T = [\text{RNHCl}] + [\text{X}]$  with  $[\text{H}^+]_T \gg [\text{CAB}]_T$ , one could obtain:

$$[\text{X}] = \frac{K [\text{CAB}]_T [\text{NRF}]}{1 + K [\text{NRF}]} \quad (1)$$

Since,

$$\text{rate} = k[\text{H}^+] [\text{X}]$$

substituting the value of [X], one gets

$$\text{rate} = \frac{kK [\text{CAB}]_T [\text{H}^+] [\text{NRF}]}{1 + K [\text{NRF}]} \quad (2)$$

Since,  $\text{rate} = k_{\text{obs}} [\text{CAB}]$ , after re-arrangement we get,

$$\frac{1}{k_{\text{obs}}} = \frac{1 + K[\text{NRF}]}{kK [\text{NRF}]} \frac{1}{[\text{H}^+]} \quad (3)$$

Further, equation (3) can be re-arranged

$$\frac{1}{k_{\text{obs}}} = \frac{1}{kK [\text{H}^+] [\text{S}]} + \frac{1}{k[\text{H}^+]} \quad (4)$$

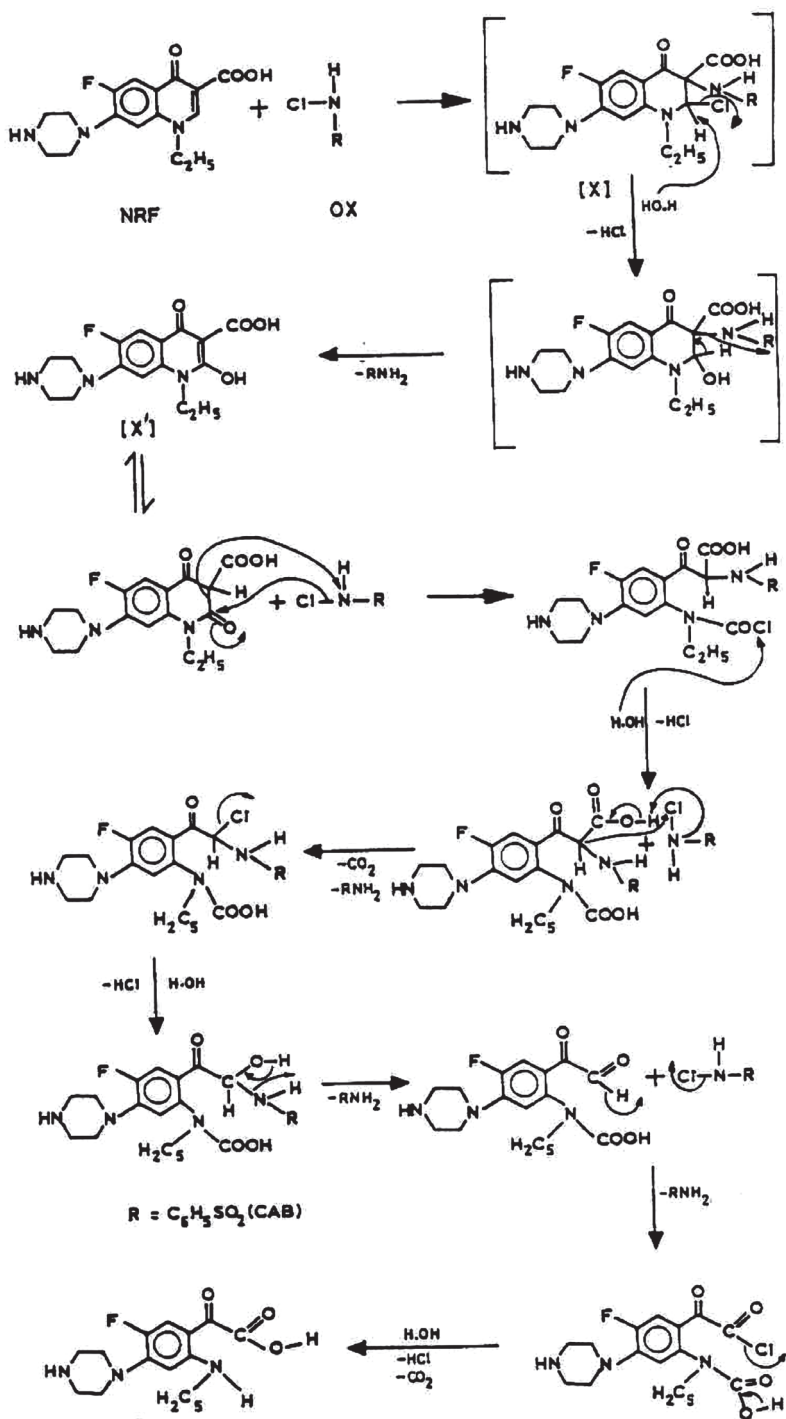
Based on equation (4), a double reciprocal plot of  $k_{\text{obs}}$  versus  $[\text{NRF}]$  at constant  $\text{HCl}$  was found to be linear and the value of  $(kK)$  was calculated from the intercept. From equation (3), plot of  $1/k_{\text{obs}}$  versus  $1/[\text{H}^+]$  was found to be straight line passing through the origin. The value of  $(kK)$  was calculated from the slope of the plots and the 2 values were found to be same. The constancy of  $(kK)$  values indirectly supports the proposed mechanism for the oxidation of NRF.

The effect of varying solvent composition on the reaction kinetics has been described in detail in the well-known monographs<sup>21,22</sup>. For the limiting case of zero angle of approach between 2 dipoles or an ion-dipole system, Amis<sup>22</sup> has shown that a plot of  $\lg k'$  versus  $1/D$  gives a straight line with a negative slope for a reaction between a negative ion and a dipole or between 2 dipoles, while a positive slope results for a positive ion and dipole interaction. The positive dielectric effect observed in the present studies clearly supports the positive ion and a dipole interaction reported. The slight increase in the rate with decrease in dielectric constant (i.e. increase in MeOH content) suggests a charge dispersal in the transition state.

The proposed mechanism is also supported by the moderate values of energy of activation. The fairly high positive values of  $\Delta G^*$  and  $\Delta H^*$  indicate that the transition state is highly solvated, while the negative  $\Delta S^*$  suggests that the transition state is fairly rigid with less degree of freedom.

Electron flow during the oxidation of NRF by CAB is depicted in reaction scheme 2. Electrophilic attack by the oxidant (RNHCl of CAB) on NRF results in the formation of X which on further hydrolysis, gives intermediate X'. Then X' reacts stepwise with 3 mol of oxidant. A total of 4 mol of the oxidant is consumed to yield the final products. The proposed mechanism is in conformity with the observed kinetic data.

Scheme 2



## REFERENCES

1. M. M. CAMPBELL, G. JOHNSON: Chloramine-T and Related N-halogen-N-metallo Reagents. *Chem Rev*, **78** (1), 65 (1978).
2. K. K. BANERJI, B. JAYARAM, D. S. MAHADEVAPPA: Mechanistic Aspects of Oxidations by N-metallo-N-haloaryl Sulfonamides. *J Sci Ind Res*, **46** (2), 65 (1987).
3. M. P. RAGHAVENDRA, D. S. MAHADEVAPPA, K. M. L. RAI, K. S. RANGAPPA: Mechanistic Investigations of Oxidation of Aminosugars by N-chloro-*p*-toluenesulfonamide in Alkaline Medium. *J Carbohyd Chem*, **16** (3), 343 (1997).
4. PUTTASWAMY, N. VAZ: Kinetic Analysis of Oxidation of Dipeptides by Sodium N-bromobenzenesulfonamide in Acidic Medium: A Mechanistic Approach. *B Chem Soc Jpn*, **76**, 73 (2003).
5. S. K. REVATHI, S. ANANDA, K. N. MOHANA, RANGAPPA: Palladium(II)-catalyzed Oxidation of  $\alpha$ -hydroxy Acids with Sodium N-chlorobenzenesulfonamide in Perchloric Acid Solution: A Kinetic and Mechanistic Study. *Collect Czech Chem Commun*, **69**, 1577 (2004).
6. K. N. MOHAN, N. PRASAD: Ruthenium(III)-catalyzed Oxidation of 2-phenylethylamine with Sodium N-chlorobenzenesulfonamide in Hydrochloric Acid Solution: A Kinetic and Mechanistic Study. *J Mol Catal A-Chem*, **266** (1–2), 267 (2007).
7. N. NANDA, S. DAKSHAYANI: Kinetic Analysis of Oxidation of Ofloxacin by Sodium N-chlorobenzenesulfonamide in Acid Medium: A Mechanistic Approach. *J Pharm Chem*, **3** (2), 60 (2009).
8. PUTTASWAMY, T. M. ANURADHA, K. L. MAHADEVAPPA: Kinetics Analysis of Oxidation of Dopamine by Sodium N-chlorobenzenesulfonamide in Perchloric Acid Medium. *Indian J Chem A*, **40A**, 514 (2001).
9. B. HOLMES, R. H. BROGDEN, D. M. RICHARDS: Norfloxacin: A Review of Its Antibacterial Activity, Pharmacokinetic Properties and Therapeutic Use. *Drugs*, **30**, 482 (1985).
10. J. B. LIPPIONCOTT, TORONTO: Drug Facts and Comparisons. Philadelphia, 1988, p. 1610.
11. N. NANDA, S. M. MAYANNA: Kinetics of Oxidation of Sulfamethoxazole by Sodium N-chlorobenzenesulfonamide and 1-chlorobenzotriazole. *Oxid Commun*, **22** (1), 107 (1999).
12. N. NANDA, S. M. MAYANNA, N. M. MADEGOWDA: Mechanism of Oxidation of Diazepam by Chloramine-B: A Kinetic Approach. *Int J Chem Kinet*, **30** (9), 605 (1998).
13. A. CHRZASZCZEWSKA: Chemistry of N-chloramides, III. *B Soc Lett Lodz Cl.III*, **3**, 5 (1952); *Chem Abstr*, **49**, 212 (1955).
14. D. S. MAHADEVAPPA, M. B. MADEGOWDA, K. S. RANGAPPA: Oxidation of Methionine by Chloramine-B in Aqueous Solution. A Kinetic Study. *Oxid Commun*, **7** (1–2), 167 (1984).
15. E. BISHOP, V. J. JENNINGS: Titrimetric Analysis with Chloramine-T. The Status of Chloramine-T as a Titrimetric Reagent. *Talanta*, **1**, 197 (1958).
16. J. C. MORRIS, J. A. SALAZAR, M. A. WINEMANN: Equilibrium Studies on N-chloro Compounds: The Ionization Constant of N-chloro-*p*-toluenesulfonamide. *J Am Chem Soc*, **70**, 2036 (1948).
17. T. HIGUCHI, A. HUSSAIN: Mechanism and Thermodynamics of Chlorine Transfer among Organochlorinating Agents: Part II. Reversible Disproportionation of Chloramine-T. *J Chem Soc B*, 549 (1967).
18. I. G. ZILBERG: Preparation and Certain Properties of *m*-benzenedisulfonamide. *Chem Abstr*, **42**, 144 (1948).
19. M. S. MOGILEVSKI, V. I. MALCHEVSKAYA, E. P. VOINAROVSKAYA: Mechanism of the Activation of Chloramine in Aqueous Solutions. *Chem Abstr*, **53**, 22749 (1959).
20. D. S. MAHADEVAPPA, RANGASWAMY: Physico-chemical Properties of Chloramine-B. Conductometric Study of the Interaction of Chloramine-B with Cr(III), Al(III) and Fe(III) Solutions. *Rev Roum Chim*, **22**, 1233 (1977).
21. E. A. MOELWYN, J. HUGHES: Kinetics of Reactions in Solutions. Oxford University Press, London, 1947, p. 279.
22. E. S. AMIS: Solvent Effects on Reaction Rates and Mechanisms. Academic Press, New York, 1966.

Received 30 December 2009

Revised 3 July 2010



**MECHANISTIC STUDIES OF OXIDATION OF D-SORBITOL AND D-MANNITOL BY AN ALKALINE SOLUTION OF POTASSIUM BROMATE IN THE PRESENCE OF CHLORO COMPLEX OF Ru(III) AS HOMOGENEOUS CATALYST**

SH. SRIVASTAVA\*, A. L. SINGH

*Chemical Laboratories, Feroze Gandhi College, Rae Bareli, 229 001 U.P., India*

*E-mail: she\_ila72@yahoo.com; anooplata.singh@gmail.com*

**ABSTRACT**

The present paper deals with the kinetics and mechanism of Ru(III)-catalysed oxidation of D-sorbitol and D-mannitol in an alkaline solution of  $\text{KBrO}_3$  carried out in the temperature range 30–45°C. Mercuric acetate was used as a scavenger for  $\text{Br}^-$  ion formed in the reaction mixture to prevent parallel oxidation by bromine. First order kinetics with respect to each  $[\text{KBrO}_3]$  and  $[\text{Ru(III) chloride}]$  was observed in the oxidation both of D-sorbitol and D-mannitol. The reactions show zero order with respect both to alcohols and  $[\text{OH}^-]$ , whereas a negative effect is observed for  $[\text{Cl}^-]$ . Negligible effect of mercuric acetate and ionic strength of the medium was observed. The reactive species of Ru(III) in alkaline medium is  $[\text{RuCl}_2(\text{H}_2\text{O})_3(\text{OH})]$ . A suitable mechanism in conformity with the kinetic observation has been proposed. The various activation parameters such as energy of activation ( $\Delta E^*$ ), the Arrhenius factor ( $A$ ), entropy of activation ( $\Delta S^*$ ) were calculated from the rate measurements at 30, 35, 40 and 45°C. The rate law has been derived on the basis of obtained data.

*Keywords:* kinetics, mechanism, oxidation, polyhydric alcohol, potassium bromate, Ru(III) catalyst.

**AIMS AND BACKGROUND**

Oxidants like potassium bromate, N-bromoacetamide<sup>1,2</sup>, N-bromosuccinimide<sup>3,4</sup> and sodium periodate<sup>5,6</sup> have been earlier used in oxidation of various compounds. The kinetics of redox reaction incorporating certain transition metal ion like osmium(VIII) (Refs 7 and 8), Rh(III) (Refs 9 and 10), Ir(III) (Refs 11 and 12), Ru(VIII) (Refs 6 and 13) and palladous ions<sup>1,13</sup> as homogeneous catalyst has been extremely investigated.

---

\* For correspondence.

Potassium bromate ( $\text{KBrO}_3$ ) (Refs 14–18) has been used to oxidise various compounds in acidic medium both catalysed and uncatalysed<sup>15,19</sup>. Scant attention has been paid to the activity of potassium bromate in the presence of catalyst in alkaline medium. The use of Ru(III) as non-toxic and homogeneous catalyst has been reported by several researchers in acidic medium. This prompted us to undertake the present investigation, which is focused on the kinetics and mechanism of Ru(III)-catalysed oxidation of polyhydric alcohols by bromate in alkaline medium with mercuric acetate as a scavenger.

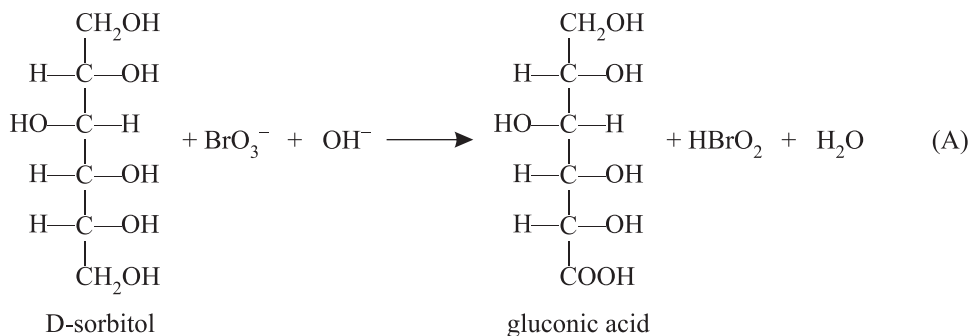
## EXPERIMENTAL

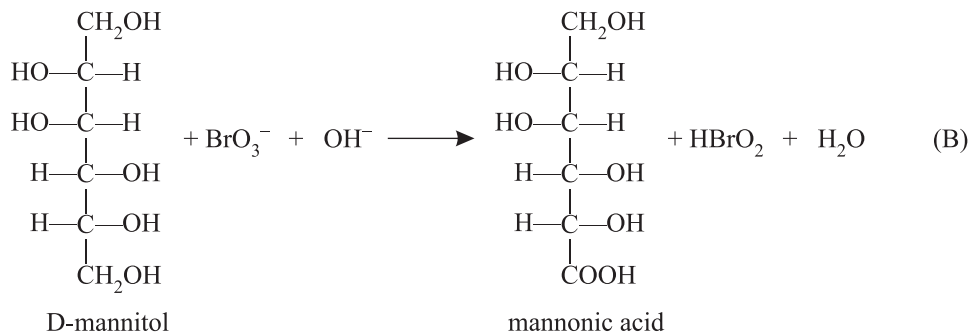
*Materials.* An aqueous solution of polyhydric alcohols (Thomas Baker), potassium bromate (BDH, AR),  $\text{NaClO}_4$  and mercuric acetate (E. Merck) were prepared by dissolving the weighed amount of sample in triply distilled water. NaOH (S. D. fine) was used as a source of  $\text{OH}^-$  ions. Ru(III) chloride (Johnson Matthey) was prepared by dissolving the sample in HCl of known strength. The reaction stills were blackened from outside to prevent photochemical effects.

*Kinetics.* A thermostated water bath was used to maintain the desired temperature within  $\pm 0.1^\circ\text{C}$ . Requisite volume of reagents, including substrate was taken in a reaction vessel and thermostated as  $35 \pm 0.1^\circ\text{C}$  for thermal equilibrium. A measured volume of potassium bromate solution, which was also maintained separately at the same temperature, was rapidly poured into the reaction vessel. The kinetics was followed by examining desired portion of reaction mixture for  $\text{KBrO}_3$  iodometrically using starch as an indicator after suitable time intervals.

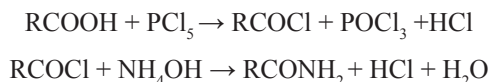
## RESULTS AND DISCUSSION

The stoichiometric analysis of the oxidation of D-sorbitol and D-mannitol with  $\text{KBrO}_3$  in alkaline medium indicates that 1 mol of substrate consumes 1 mol of bromate. This result showed 1:1 stoichiometry according to equation (A) and (B) for D-sorbitol and D-mannitol, respectively.





So the oxidation product of D-sorbitol and D-mannitol is the corresponding monocarboxylic acid, i.e. D-gluconic acid and D-mannonic acid, respectively, which were detected by measuring the m.p. of their amide derivatives as follows: keeping the reaction mixture for 48 h under kinetic conditions and then adding  $\text{PCl}_5$  to it; refluxing till the clear solution was obtained; cooling and adding 4–5 ml of concentrated ammonia solution, heating on water bath for 4–5 min, cooling and filtering the precipitated solid; washing with water, recrystallising it and determining its melting point.



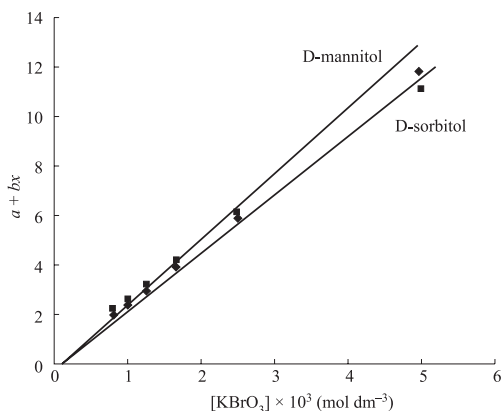
Melting point for amide derivatives of gluconic acid, i.e. gluconamide and mannonic acid, i.e. mannonamide were found to be  $120^\circ\text{C}$  as against the actual m.p. of  $119^\circ\text{C}$  and  $110^\circ\text{C}$  as against the actual m.p. of  $109^\circ\text{C}$ , respectively.

The kinetic results collected for various reactant concentrations (Table 1) exhibit first order kinetics with respect to oxidant, i.e. potassium bromate. This has also been confirmed by chi-square method (Fig. 1). Kinetics results obtained on varying hydroxide ion  $[\text{OH}^-]$  concentration show negligible effect. First order kinetics was observed in case of catalyst Ru(III) which was further confirmed by a plot of  $(-dc/dt)$  versus  $[\text{Ru(III)}]$  (Fig. 2). The curve obtained gives a slope value of  $2.50 \times 10^{-2} \text{ s}^{-1}$  for D-sorbitol and  $2.66 \times 10^{-2} \text{ s}^{-1}$  for D-mannitol, which is close to the average value of first order rate constant (i.e.  $k_1 = (-dc/dt)/[\text{Ru(III)}]$ ) equal to  $2.30 \times 10^{-2} \text{ s}^{-1}$  for D-sorbitol and  $2.70 \times 10^{-2} \text{ s}^{-1}$  for D-mannitol at  $35^\circ\text{C}$ . In both substrates a fair degree of closeness in the first order rate constant obtained graphically and obtained values of  $(-dc/dt)/[\text{Ru(III)}]$  clearly confirm the first order dependence on  $[\text{Ru(III)}]$ . Zero order kinetics was observed in case of polyhydric alcohols, i.e. D-sorbitol and D-mannitol.

**Table 1.** Effect of reactants on the reaction rate

$[\text{Hg}(\text{OAc})_2]=1.25 \times 10^{-3} \text{ mol dm}^{-3}$ ;  $[\text{NaOH}]=1.00 \times 10^{-3} \text{ mol dm}^{-3}$ ;  $[\text{Ru}(\text{III})]=9.6 \times 10^{-6} \text{ mol dm}^{-3}$ ;  
 $[\text{KCl}]=1.00 \times 10^{-3} \text{ mol dm}^{-3}$ ; temperature  $35^\circ\text{C}$

$[\text{BrO}_3^-] \times 10^3$ ( $\text{mol dm}^{-3}$ )	$[\text{S}] \times 10^2$ ( $\text{mol dm}^{-3}$ )	$[\text{NaOH}] \times 10^3$ ( $\text{mol dm}^{-3}$ )	$(-dc/dt) \times 10^7 (\text{mol dm}^{-3} \text{ s}^{-1})$	
			D-sorbitol	D-mannitol
0.83	2.00	1.00	1.80	1.95
1.00	2.00	1.00	2.28	2.50
1.25	2.00	1.00	2.90	3.15
1.66	2.00	1.00	3.65	3.98
2.50	2.00	1.00	5.86	6.30
5.00	2.00	1.00	11.65	12.65
1.00	0.33	1.00	2.30	2.90
1.00	0.40	1.00	2.50	2.40
1.00	0.50	1.00	2.45	3.00
1.00	0.66	1.00	2.30	2.60
1.00	1.00	1.00	2.40	2.75
1.00	2.00	1.00	2.28	2.50
1.00	2.00	0.83	2.50	2.50
1.00	2.00	1.00	2.28	2.50
1.00	2.00	1.25	2.00	2.18
1.00	2.00	1.66	2.50	2.00
1.00	2.00	2.50	2.00	2.00
1.00	2.00	5.00	2.30	1.80

**Fig. 1.** Plot of  $[\text{KBrO}_3]$  versus  $(a+bx)$  for oxidation of D-sorbitol and D-mannitol at  $35^\circ\text{C}$

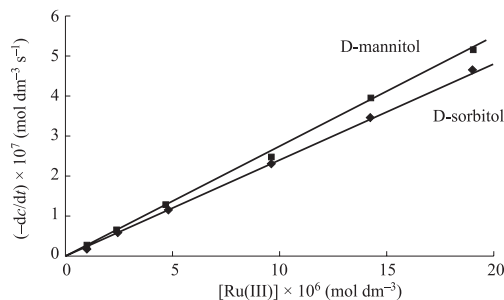


**Fig. 2.** Plot of [Ru(III)] versus  $(-dc/dt)$  for the oxidation of D-sorbitol and D-mannitol at 35°C

Variation of ionic strength of the medium and mercuric acetate showed negligible effect on the reaction rate. The negligible effect of mercuric acetate excludes the possibility of its involvement either as a catalyst or as an oxidant because it does not help the reaction proceeding without bromate. Hence the role of mercuric acetate here is to act as a scavenger for any bromide ion formed in the reaction and it helps to eliminate parallel oxidation by bromine which would have been formed as a result of the interaction between  $\text{Br}^-$  and  $\text{BrO}_3^-$  ions. Variation of chloride ion concentration shows negative effect (Table 2).

**Table 2.** Effect of variation of chloride ion, mercury(II) acetate and ionic strength ( $\mu$ )  
 $[\text{KBrO}_3]=1.00 \times 10^{-3} \text{ mol dm}^{-3}$ ;  $[\text{D-sorbitol}] = 5.00 \times 10^{-2} \text{ mol dm}^{-3}$ ;  $[\text{D-mannitol}] = 5.00 \times 10^{-3} \text{ mol dm}^{-3}$ ;  
 $[\text{NaOH}]=1.00 \times 10^{-3} \text{ mol dm}^{-3}$ ;  $[\text{Ru(III)}]=9.6 \times 10^{-6} \text{ mol dm}^{-3}$ ; temperature 35°C

[KCl] × 10 <sup>3</sup> (mol dm <sup>-3</sup> )	[Hg(OAc) <sub>2</sub> ] × 10 <sup>3</sup> (mol dm <sup>-3</sup> )	[NaClO <sub>4</sub> ] × 10 <sup>3</sup> (mol dm <sup>-3</sup> )	$(-dc/dt) \times 10^7 (\text{mol dm}^{-3} \text{ s}^{-1})$	
			D-sorbitol	D-mannitol
0.83	1.00	—	2.50	2.55
1.00	1.00	—	2.28	2.50
1.25	1.00	—	2.10	2.30
1.66	1.00	—	1.95	2.25
2.50	1.00	—	1.80	2.10
5.00	1.00	—	1.70	1.90
1.00	0.83	—	2.00	2.55
1.00	1.00	—	1.85	2.75
1.00	1.25	—	2.28	2.50
1.00	1.66	—	1.83	2.70
1.00	2.50	—	2.10	2.60
1.00	5.00	—	1.90	2.60
1.00	1.00	0.83	2.50	2.50
1.00	1.00	1.00	2.28	2.50
1.00	1.00	1.25	2.15	2.42
1.00	1.00	1.66	2.30	2.61
1.00	1.00	2.50	2.20	2.30
1.00	1.00	5.00	2.40	2.54

The kinetic studies were also made in the 30–45°C range and specific rate constants obtained were used to draw a plot between  $\lg k_r$  versus  $1/T$  (Fig. 3) which was linear. The values of activation parameters were calculated and presented in Table 3.

**Table 3.** Activation parameters for oxidation of D-sorbitol and D-mannitol

Parameters	Temperature (°C)	D-sorbitol	D-mannitol
$K_r \times 10^4$ (s <sup>-1</sup> )	30	1.60	1.70
$K_r \times 10^4$ (s <sup>-1</sup> )	35	2.28	2.50
$K_r \times 10^4$ (s <sup>-1</sup> )	40	3.25	3.45
$K_r \times 10^4$ (s <sup>-1</sup> )	45	4.50	5.10
$\lg A$	–	9.35	10.14
$\Delta E^*$ (kJ mol <sup>-1</sup> )	–	53.05	57.46
$\Delta G^*$ (kJ mol <sup>-1</sup> )	35	74.57	74.33
$\Delta H^*$ (kJ mol <sup>-1</sup> )	35	69.44	70.31
$\Delta S^*$ (J K <sup>-1</sup> mol <sup>-1</sup> )	35	-16.64	-13.04

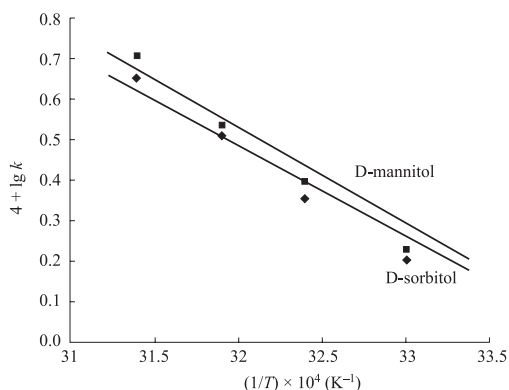


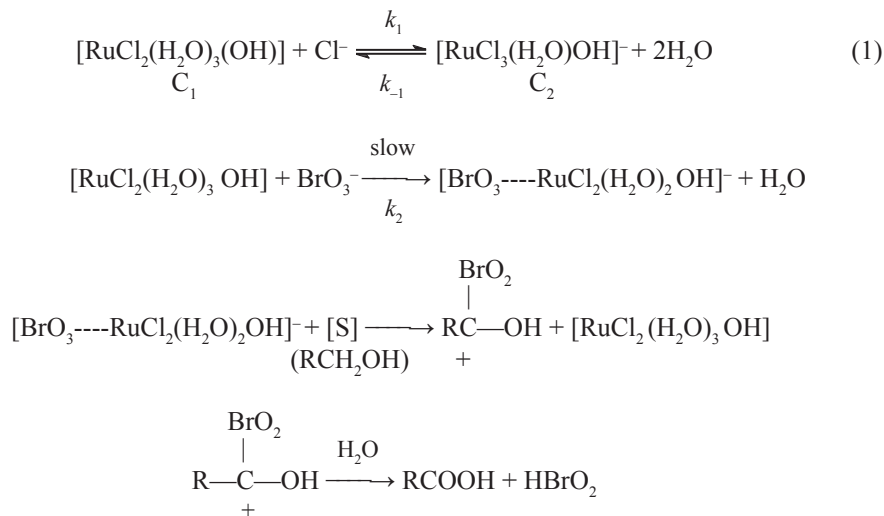
**Fig. 3.** Plot of  $4 + \lg k$  versus  $1/T$  for the oxidation of D-sorbitol and D-mannitol at 35°C  
 $[\text{Ru(III)}] = 9.60 \times 10^{-6} \text{ mol dm}^{-3}$ ;  $[\text{substrate}] = 2.00 \times 10^{-2} \text{ mol dm}^{-3}$ ;  $[\text{KBrO}_3] = 1.00 \times 10^{-3} \text{ mol dm}^{-3}$ ;  
 $[\text{NaOH}] = 1.00 \times 10^{-3} \text{ mol dm}^{-3}$ ;  $[\text{KCl}] = 1.00 \times 10^{-3} \text{ mol dm}^{-3}$ ;  $[\text{Hg(OAc)}_2] = 1.25 \times 10^{-3} \text{ mol dm}^{-3}$

The result of oxidation of D-sorbitol and D-mannitol shows that the reaction follows identical kinetics and thus appears to have a common mechanism. The following reaction steps are suggested on the basis of D-sorbitol and D-mannitol by potassium bromate in the presence of Ru(III) as catalyst.  $\text{Cl}^-$  exists in the following equilibrium in alkaline medium:



Negative effect with respect to  $\text{Cl}^-$  in the present investigation suggests that the equilibrium would shift to the left therefore  $[\text{RuCl}_2(\text{H}_2\text{O})_3\text{OH}]$  (Ref. 20) is the active species of  $\text{RuCl}_3$ .

The following reaction steps are suggested on the basis of the above discussion for the Ru(III)-catalysed oxidation of D-sorbitol and D-mannitol by  $\text{KBrO}_3$ :



Considering the above steps and applying the steady state treatment with a reasonable approximation the rate law may be written in terms of rate of consumption of  $[\text{BrO}_3^-]$  as the following equation:

$$\begin{aligned}
 - \frac{d[\text{BrO}_3^-]}{dt} &= k_2[\text{C}_1][\text{BrO}_3^-] \\
 - \frac{d[\text{BrO}_3^-]}{dt} &= \frac{k_2[\text{Ru(III)}]_{\text{T}}[\text{BrO}_3^-]}{(1+K_1[\text{Cl}^-])}
 \end{aligned}$$

where  $[\text{Ru(III)}]_{\text{T}} = [\text{C}_1] + [\text{C}_2]$

$$K_1 = \frac{k_1}{k_{-1}} .$$

The rate law is in agreement with the observed kinetics. The proposed mechanism is consistent with the activation parameters given in Table 3.

## CONCLUSIONS

The experimental results as shown reveal that the reaction rate doubles when the concentration of catalyst  $[\text{Ru(III)}]$  is doubled. The rate law is in conformity with all kinetic observations and the proposed mechanistic steps are supported by the negligible effect of ionic strength which indicates the involvement of an ion in a slow and rate-determining step. The high positive values of change in free energy of activation

( $\Delta G^*$ ) indicates highly solvated transition state, while clearly high negative values of change in entropy of activation ( $\Delta S^*$ ) suggest the formation of an activated complex with reduction in degree of freedom of molecules. From this investigation it is concluded that  $\text{BrO}_3^-$  and  $[\text{RuCl}_2(\text{H}_2\text{O})_3\text{OH}]$  are the reactive species of  $\text{KBrO}_3$  and  $\text{Ru(III)}$  chloride respectively in alkaline medium.

## REFERENCES

1. A. K. SINGH, J. SRIVASTAVA, Sh. RAHMANI, V. SINGH: Pd(II) Catalyzed and Hg(II) Co-catalyzed Oxidation of D-glucose and D-fructose by N-bromoacetamide in the Presence of Perchloric Acid. *Carbohydr Res*, **341** (3), 397 (2006).
2. A. K. SINGH, J. SRIVASTAVA, Sh. RAHMANI: Mechanistic Studies of Oxidation of D-arabinose and D-mannose by Acidic Solution of N-bromoacetamide in Presence of Chloro-complex of Ru(III) as Homogeneous Catalyst. *J Mol Catal*, **271** (1, 2), 151 (2007).
3. K. SUREKHA, MABALANG, M. NIRMAL, N. HALLIGUDI, S. T. NANDIBEWOOR: Ruthenium(III) Catalyzed Oxidation of Ethylenediaminetetraacetic Acid by N-bromosuccinimide in Aqueous Alkaline Medium – A Kinetic and Mechanistic Study. *Reac Kinet Catal L*, **72**, 391 (2001).
4. A. K. SINGH, D. CHOPRA, S. RAHMANI, B. SINGH: Kinetics and Mechanism of Pd(II) Catalysed Oxidation of D-arabinose, D-xylose and D-galactose by N-bromosuccinimide in Acidic Solution. *Carbohydr. Res*, **314**, 157 (1998).
5. Sh. SRIVASTAVA, Sh. SINGH: Kinetic Study of Rh(III) Catalyzed Oxidation of Sucrose by Sodium Periodate in Acidic Medium. *Asian J Chem*, **20** (2), 973 (2008).
6. Sh. SRIVASTAVA, S. SINGH, P. SRIVASTAVA: Ruthenium(VIII) Catalyzed Oxidation of Some Cyclic Alcohols by Sodium Periodate in Alkaline Medium. *Asian J Chem*, **20** (1), 317 (2008).
7. PUTTASWAMY, N. VAZ: Ruthenium(III)- and Osmium(VIII)-catalyzed Oxidation of 2-thiouracil by Bromamine-B in Acid and Alkaline Media: A Kinetic and Mechanistic Study. *Transit Metal Chem*, **28**, 409 (2003).
8. ASHISH, S. P. SINGH, A. K. SINGH, B. SINGH: Mechanistic Study of Osmium(VIII) Promoted Oxidation of Crotonic Acid by Aqueous Alkaline Solution of Potassium Bromate. *Transit Metal Chem*, **30**, 610 (2005).
9. A. K. SINGH, R. SINGH, J. SRIVASTAVA, Sh. RAHMANI, Sh. SRIVASTAVA: Mechanistic Studies of Oxidation of Maltose and Lactose by  $[\text{H}_2\text{OBr}]^+$  in Presence of Chloro-complex of Rh(III) as Homogeneous Catalyst. *J Organomet Chem*, **692**, 4270 (2007).
10. Sh. SRIVASTAVA, P. SRIVASTAVA, A. KUMAR, Sh. SINGH: Mechanism of Rhodium(III) Catalyzed Oxidation of Ethylene Glycol by Bromate in Acidic Medium. *Bull Catal Soc India*, **6**, 119 (2007).
11. Sh. SRIVASTAVA, V. SRIVASTAVA, V. GUPTA, L. CHAUDHARY: Mechanistic Study of Iridium(III) Catalysed Oxidation of Glycerol by N-bromoacetamide in Acidic Medium. *Oxid Commun*, **30** (3), 553 (2007).
12. Sh. SRIVASTAVA, V. SRIVASTAVA, A. AWASTHI: Kinetics and Mechanism Ir(III) Catalyzed Oxidation of Some Polyhydroxy Alcohols by N-bromoacetamide in Perchloric Acid Medium. *Oxid Commun*, **26** (3), 378 (2003).
13. B. SINGH, Sh. SRIVASTAVA: Kinetics and Mechanism of Ruthenium Tetroxide Catalysed Oxidation of Cyclic Alcohols by Bromate in a Base. *Transit Metal Chem*, **16**, 466 (1991).
14. A. K. SINGH, V. SINGH, Sh. RAHMANI, A. K. SINGH, B. SINGH: Mechanism of Pd (II) and Hg (II) Co-catalyzed Oxidation of D-mannose and Maltose by Acidic Solution of N-bromoacetamide. *J Mol Catal A-Chem*, **197** (2), 91 (2003).



15. S. M. DESAI, N. N. HOLLIGUDI, S. T. NANDIBEWOOR: Kinetics of Osmium(VIII) Catalyzed Oxidation of Allyl Alcohol by Potassium Bromate in Aqueous Acidic Medium – Autocatalysis in Catalysis. *Int J Chem Kinet*, **31** (8), 583 (1999).
16. K. RACZ, M. BURGER, Z. S. NAGY-UNGVARAI: Autocatalytic Oxidation of Hemin by Acidic Bromate. *Int J Chem Kinet*, **38** (8), 503 (2006).
17. Sh. SRIVASTAVA, Sh. SINGH: Kinetic Study of Rh(III) Catalyzed Oxidation of Sucrose by Sodium Periodate in Acidic Medium. *Asian J Chem*, **20** (2), 973 (2008).
18. Sh. SRIVASTAVA, P. SRIVASTAVA, A. KUMAR, Sh. SINGH: Mechanism of Rhodium(III) Catalyzed Oxidation of Ethylene Glycol by Bromate in Acidic Medium. *Bull Catal Soc India*, **6**, 119 (2007).
19. Sh. SRIVASTAVA, S. SINGH, R. K. SHARMA: Kinetics and Mechanism of Ruthenium(III) Catalyzed Oxidation of Some Polyhydric Alcohols by Acid Bromate. *J Indian Chem Soc*, **84**, 1109 (2007).
20. A. K. SINGH, N. CHAURASIA, S. RAHMANI, J. SRIVASTAVA, B. SINGH: Mechanism of Ruthenium(III) Catalysis of Periodate Oxidation of Aldoses in Aqueous Alkaline Medium. *Catal Lett*, **95**, 135 (2004).

*Received 27 May 2009*  
*Revised 23 August 2009*

## **KINETICS AND MECHANISTIC STUDY OF PHOSPHOTUNGSTIC ACID-CATALYSED OXIDATION OF BENZALDEHYDES BY N-BROMOPHTHALIMIDE**

J. V. BHARAD, B. R. MADJE, M. B. UBALE\*

*Department of Chemistry, Vasantrao Naik Mahavidyalaya, 431 003 Aurangabad (M.S.), India*

*E-mail: mbubale@yahoo.com*

### **ABSTRACT**

Kinetic investigations in the Keggin type phosphotungstic acid-catalysed oxidation of benzaldehyde and substituted benzaldehydes by N-bromophthalimide (NBP) in aqueous acetic acid medium in the presence of mercuric (II) acetate as a scavenger have been carried out. Oxidation kinetics of benzaldehyde by NBP in the presence of phosphotungstic acid (PTA) shows a first order dependence on NBP and fractional order on benzaldehydes and PTA. The variations of ionic strength,  $\text{Hg}(\text{OAc})_2$ ,  $\text{H}^+$  and phthalimide (reaction product) have insignificant effect on reaction rate. Activation parameters for the reaction have been evaluated from the Arrhenius plot by studying the reaction at different temperatures. The rate law has been derived on the basis of the obtained data.

*Keywords:* kinetics, benzaldehyde, N-bromophthalimide, phosphotungstic acid.

### **AIMS AND BACKGROUND**

In the recent years, studies on oxidation of various organic compounds by heteropoly acids and polyoxometalates, especially those with the Keggin type structure under homogeneous and heterogeneous reaction conditions<sup>1-9</sup> have attracted considerable attention of the researchers. Literature survey reveals that phosphotungstic acid (PTA), due to its thermal stability, makes it efficient and eco-friendly catalyst in oxidation of organic compounds such as aromatic amines<sup>10</sup>, aromatic alcohols<sup>11</sup>, cyclic alcohols<sup>12</sup>, allyl alcohols<sup>13</sup>, oximes<sup>14</sup>, styrene<sup>15</sup>, etc.

A number of reports on kinetic studies of oxidation of benzaldehyde and substituted benzaldehydes with variety of N-halo compounds such as N-bromosuccinimide<sup>16</sup>, N-bromoacetamide<sup>17</sup>, N-chloronicotinamide<sup>18</sup>, N-bromophthalimide<sup>19</sup>, chloramine-T<sup>20</sup>,

---

\* For correspondence.

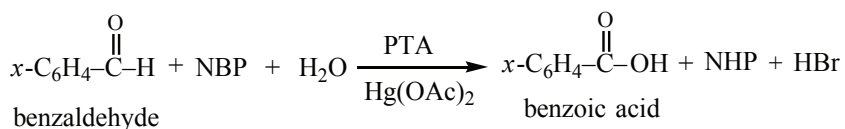
N-chlorosaccharin<sup>21</sup>, N-bromosaccharin<sup>22</sup>, and N-bromobenzamide<sup>23</sup> as oxidants have been reported. N-bromophthalimide (NBP) is a potential oxidising agent<sup>24</sup>, which has been extensively used in the oxidation of organic substrates. The present work reports kinetics and mechanism of PTA-catalysed oxidation of benzaldehydes by N-bromophthalimide in 30% acetic acid.

## EXPERIMENTAL

All benzaldehydes used were of AR grade. The oxidant NBP (Aldrich sample) was used. Acetic acid (A. R. grade) was purified by the literature procedure. The standard solutions of substituted benzaldehydes were prepared in acetic acid. Doubly distilled water was employed in all kinetic runs. To prevent photochemical effect, the freshly prepared solution of NBP was stored in an amber coloured bottle and its strength was checked iodometrically<sup>25</sup> using 1% solution of freshly prepared starch as an indicator.

*Kinetic measurements.* Kinetic measurements were performed under pseudo-first order conditions, by keeping large excess of benzaldehydes over oxidant. Mixture containing requisite amounts of solutions of benzaldehydes,  $\text{Hg}(\text{OAc})_2$  and PTA in 30% acetic acid were equilibrated at 303 K. To this mixture was added a measured amount of pre-equilibrated (303 K) standard solution of NBP. To maintain the desired temperature (within  $\pm 0.1^\circ\text{C}$ ) the reaction mixture was kept in a thermostatted water bath and the progress of the reaction was monitored iodometrically by withdrawing aliquots of the reaction mixture at regular time of intervals. The pseudo-first order rate constants  $k'$  were computed from linear least square plot of  $-\lg(a-x)$  versus time. Duplicate kinetic runs showed that the rate constants were reproducible to within  $\pm 4\%$ .

*Stoichiometry and product analysis.* Stoichiometry of the reaction was ascertained by equilibrating the reaction mixture containing an excess of NBP over benzaldehyde, mercuric(II) acetate and phosphotungstic acid in 30% acetic acid for 24 h at  $30^\circ\text{C}$ . The unreacted oxidant (NBP) was determined iodometrically. The estimated amount of unreacted NBP showed that 1 mol of benzaldehyde consumes 1 mol of NBP:



Benzaldehyde (0.2 mol) and NBP (0.4 mol) were mixed together with PTA (0.1 mol),  $\text{Hg}(\text{OAc})_2$  (0.5 mol) in 30% aqueous acetic acid (total volume 100 ml). The reaction mixture was set aside for about 24 h to ensure completion of the reaction. It was then evaporated and extracted with ether. The layer was separated and dried. The residue was confirmed as benzoic acid by m.p. ( $121^\circ\text{C}$ ), TLC and HPLC. Analysis by

TLC and HPLC confirmed the formation of benzoic acid in quantitative yield. The percentage yield calculated was 95%.

## RESULTS AND DISCUSSION

The kinetics of oxidation of benzaldehyde by NBP in 30% acetic acid in the presence of phosphotungstic acid ( $H_3PW_{12}O_{40}$ ) as a catalyst was carried out at 303 K. The concentration of  $Hg(OAc)_2$  was kept higher than NBP. The reactions were carried out under pseudo-first order conditions of  $[benzaldehyde] \gg [NBP]$ . The plot of  $\lg [NBP]$  versus time was found to be linear ( $R^2 > 0.9996$ ) indicating first order dependence of the reaction rate and from the slopes of such plots the pseudo-first order rates were evaluated (Table 1).

The rate constant ( $k'$ ) have been found to increase with increase in the concentration of benzaldehyde and plot of  $\lg k'$  versus  $\lg [benzaldehyde]$  was linear ( $R^2 = 0.998$ ) with slope less than unity for all the benzaldehyde indicating a fractional order (0.49) dependence on rate of benzaldehyde (Table 1).

**Table 1.** Effect of variation of reactants on pseudo-order rate constant  $k'$  at 303 K  
 $Hg(OAc)_2 = 2.00 \times 10^3$  (mol  $dm^{-3}$ ); 30%AcOH medium

[Benzaldehyde] $\times 10^2$ (mol $dm^{-3}$ )	[NBP] $\times 10^3$ (mol $dm^{-3}$ )	[PTA] $\times 10^4$ (mol $dm^{-3}$ )	$k' \times 10^4$ ( $s^{-1}$ )
1.00	1.00	5.00	1.46
2.00	1.00	5.00	2.86
3.00	1.00	5.00	4.32
4.00	1.00	5.00	5.84
5.00	1.00	5.00	7.12
6.00	1.00	5.00	8.86
1.00	1.00	5.00	1.46
1.00	2.00	5.00	2.04
1.00	3.00	5.00	2.46
1.00	4.00	5.00	2.82
1.00	5.00	5.00	3.26
1.00	6.00	5.00	3.58
1.00	1.00	2.50	1.19
1.00	1.00	5.00	1.46
1.00	1.00	7.50	1.98
1.00	1.00	10.00	2.28
1.00	1.00	15.00	2.63

The concentration of PTA was varied while the concentrations of benzaldehyde, [NBP] and  $Hg(OAc)_2$  were kept constant. The plot  $\lg k'$  versus  $\lg [PTA]$  shows slope less than unity indicating fractional order dependence of rate on [PTA] (Table 1).

The dependence of the reaction rate on hydrogen ion concentration has been investigated at different initial concentrations of H<sub>2</sub>SO<sub>4</sub> keeping the concentration of the other reactants constant. There was a slight increase in rate constant but not significant change in reaction rate was observed with variation of H<sup>+</sup> ion.

The ionic strength of the reaction was varied by the addition of NaClO<sub>4</sub> and the influence of ionic strength on the reaction rate was studied. It was found that the ionic strength of the reaction medium has negligible effect on the reaction rate. This may presumably be due to the attack of an ion on a neutral molecule in the rate-determining step<sup>26</sup>.

The concentration effect of mercury(II) acetate in our present study showed negligible effect on the reaction rate, but it was found its utility to fix bromide ion during the course of reaction and avoiding the oxidation of the latter to molecule bromine<sup>19</sup>.

Variation of phthalimide, one of the products of oxidation, had negligible effect on the rate of reaction. The reaction neither induces polymerisation nor retards the reaction rate by variation of acrylonitrile, which may be attributed to the inertness shown by free radicals.

*Effect of solvent composition.* The effect of changing solvent composition on the reaction rate was studied by varying concentration of acetic acid from 20–70%. The rate constants (Table 2) suggest that the rate of reaction decreases with increasing acetic acid content of the solvent mixture. The plot of lg *k'* versus 1/*D* was found to be linear with negative slope indicating the involvement of two dipoles or a negative ion–dipole reaction. This reveals that there is formation of a charge separated complex in the rate-limiting step which is in agreement with Amis<sup>26</sup>. A plot of lg *k'* versus (*D*–1/2*D*+1) has been found to be linear in accordance with the Kirkwood<sup>27</sup> theory of dipole–dipole type reaction.

**Table 2.** Effect of variation of dielectric constant of medium on reaction rate at 303 K

AcOH (%) (v/v)	Dielectric constant ( <i>D</i> )	10 <sup>3</sup> / <i>D</i>	( <i>D</i> – 1)/(2 <i>D</i> + 1) × 10 <sup>2</sup>	<i>k'</i> × 10 <sup>4</sup> (s <sup>-1</sup> )
20	58.2	17.18	48.7	1.54
30	52.2	19.16	48.6	1.46
40	45.5	21.98	48.4	1.36
50	39.0	25.64	48.1	1.27
60	32.4	30.86	47.7	1.15
70	26.1	38.31	47.2	1.01

*Effect of substituents.* The oxidation of benzaldehyde and substituted benzaldehyde by [NBP] was carried out in the temperature range 303–318 K. The observed rate constants were found to increase with temperature for all the compounds. All the substrates obey the same rate law as the parent substrate. Electron-donating groups

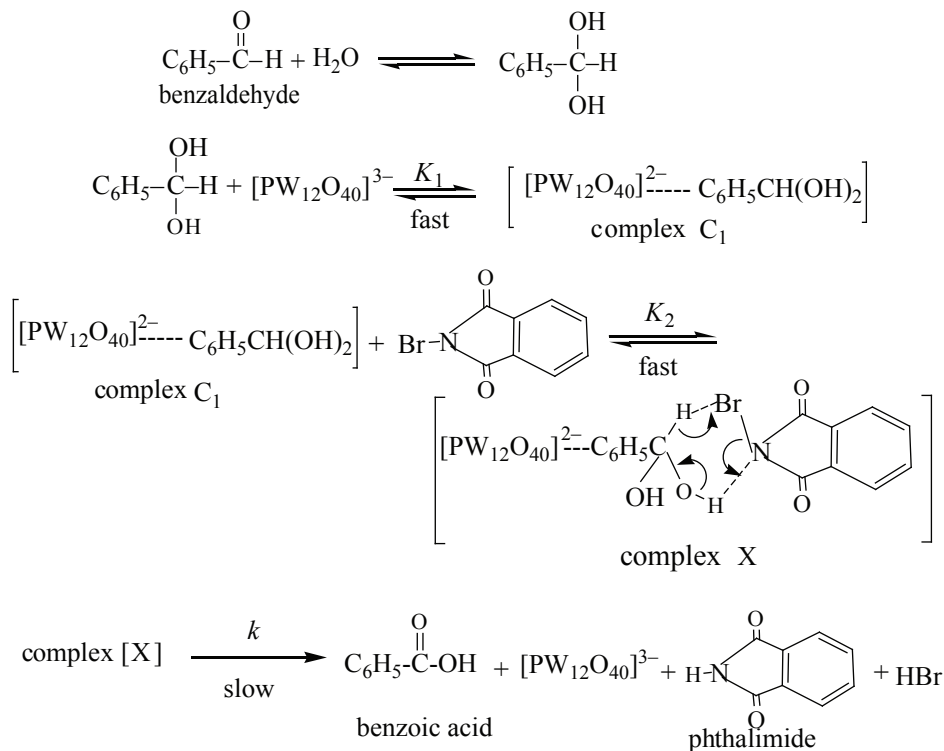
increase the rate while electron-withdrawing groups decrease the rate of oxidation. The order of reactivity of different benzaldehydes with [NBP] catalysed by [PTA] is:  $4\text{-OCH}_3 > 4\text{-CH}_3 > \text{H} > 3\text{-Cl} > 4\text{-Br} > 4\text{-Cl} > 3\text{-NO}_2 > 4\text{-NO}_2$ .

The Hammett plot of  $\lg k'$  versus  $\sigma$  is linear with a reaction constant  $\rho = -0.095$  and correlation coefficient of 0.90. The negative reaction constant  $\rho$  indicates the creation of carbonium ion in the transition state; this is in agreement with finding of Banerji<sup>23</sup>. Hence, the substituents, which can increase the magnitude of +ve charge on the carbonyl carbon of benzaldehyde would: (i) increase stability of diol, i.e. hydrated aldehyde formed; (ii) increase concentration of the diol, and (iii) stabilise the transition state and cause an increase in the rate. The negative reaction constant  $\rho$  also supports the loss of aldehyde hydrogen atom as a hydride in the slow step.

*Reactive species and mechanism.* In the present investigation and on the basis of experimental results the probable reactive oxidising species is free NBP which is in good agreement with the results reported by Amena Anjum<sup>19</sup>. The protons released during the reaction by PTA do not alter sufficient reaction rate but are responsible for protonation of NBP. Protonated NBP is not involved in the reaction mechanism which may be attributed to the negligible effect of variation of  $\text{H}_2\text{SO}_4$  on the reaction rate. The Keggin structure allows the molecule to hydrate and dehydrate without significant structural changes. Thus in aqueous solutions the heteropolyacids consist of solvate separated ion-pairs in which the protons are hydrated and linked to the anion as a whole and not to a specific centre in heteropolyanion<sup>28</sup>. Baker et al.<sup>29</sup> have shown that such water molecules can be replaced by other ligands. The heteropolyanion structure consists of a charged sphere with a large surface area where the acid protons are accommodated in the form of point charges<sup>30</sup>. In the present study the catalyst  $[\text{PW}_{12}\text{O}_{40}]^{3-}$  Keggin anion gets converted into the oxidised form and acts as an outer sphere reagent. Formation of an outer sphere complex by the replacement of one of the water molecules of hydration is more probable transition state. Since the probable transition state is less solvated and also in large size it will be more stabilised in the medium. Therefore, irrespective of the nature of benzaldehyde the transition state formed would be the same, making the rate of reaction independent on the nature of benzaldehyde. Oxidation of substrate by heteropolyanions occurred via overlap of the aromatic  $p$  system with the tungstate frame work<sup>31</sup>.

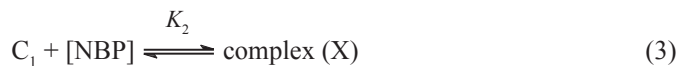
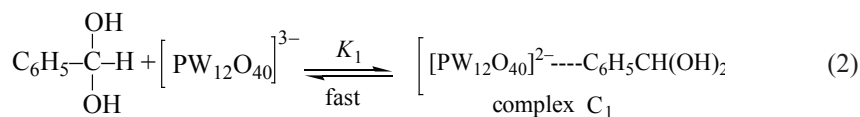
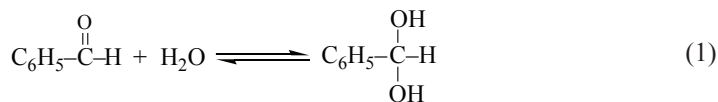
Based on the experimental observations, the most probable mechanism is shown in Scheme 1.

Scheme 1



RATE LAW

Based on kinetic results and the mechanism proposed, the following rate expression can be derived applying steady-state approximation:



The rate of the reaction may be expressed in terms of loss of [NBP] as follows:

$$-d[\text{NBP}]/dt = k[\text{X}]. \quad (5)$$

If  $[\text{NBP}]_T = \text{total concentration of } [\text{NBP}]$ , then  $[\text{NBP}]_T = [\text{NBP}] + [\text{X}]$

$$[\text{X}] = \frac{K_2[\text{C}_1][\text{NBP}]_T}{1 + K_2[\text{NBP}]} \quad (6)$$

But, rate =  $k[\text{X}]$  according to equation (5), substituting value of  $[\text{X}]$  in it, where  $[\text{S}]$  is substrate concentration, we have,

$$\text{rate} = \frac{k K_2[\text{C}_1][\text{NBP}]_T}{1 + K_2[\text{NBP}]} \quad (7)$$

$$\text{C}_1 = \frac{K_1[\text{PTA}][\text{S}]}{1 + K_1[\text{S}]} \quad (8)$$

$$\text{rate} = \frac{k K_2 K_1 [\text{PTA}][\text{NBP}]_T [\text{S}]}{(1 + K_1[\text{S}])(1 + K_2[\text{NBP}])} = \frac{k K_2 K_1 [\text{PTA}][\text{NBP}]_T [\text{S}]}{1 + K_1[\text{S}] + K_1 K_2 [\text{S}][\text{NBP}]} \quad (9)$$

The order with respect to  $[\text{NBP}]$  is one and fractional order with  $[\text{PTA}]$  and  $[\text{S}]$ . As  $[\text{S}] \gg [\text{NBP}]$  equation (9) further reduces to:

$$-\frac{d[\text{NBP}]}{dt} = \frac{k K_2 K_1 [\text{PTA}][\text{NBP}]_T [\text{S}]}{1 + K_1[\text{S}] + K_1 K_2 [\text{S}]} \quad (10)$$

rate =  $k'[\text{NBP}]_T$  and  $k' = \text{rate}/[\text{NBP}]_T$

$$k' = \frac{k K_2 K_1 [\text{PTA}][\text{S}]}{1 + K_1[\text{S}] + K_1 K_2 [\text{S}]} \quad (11)$$

$k'$  is the observed rate constant, and at constant  $[\text{PTA}]$ , double reciprocal of equation (11) results in:

$$\frac{1}{k'} = \frac{1}{k K_1 K_2 [\text{S}]} + \frac{1}{k K_2} + \frac{1}{k} \quad (12)$$

Equation (10) can be transformed into the rearranged equation (13) at fixed  $[\text{S}]$ :

$$\frac{[\text{PTA}]}{\text{rate} (k')} = \frac{1}{k K_1 K_2 [\text{S}]} + \frac{1}{k K_2} \quad (13)$$

The kinetic results suggest the possibility of formation of ternary complex involving oxidant, substrate and catalyst. However, such a ternary complex is of transient life-time due to fast interaction of catalyst and oxidant, and then former undergoes redox decomposition to the end of products intramolecularly. Such a mechanism, how-



ever, leads to the rate law equation (10) which is in a good agreement with the work reported by Binyahia et al.<sup>32</sup> The spectral evidence for complex formation between catalyst-substrate and oxidant was obtained from UV-vis. spectra of the mixture. One sharp intense peak for mixture indicates formation of complex. Such complex formation was also proved kinetically by the non-zero intercept of the double reciprocal plot of  $1/k'$  versus  $1/[S]$  and  $[PTA]/k'$  versus  $1/[S]$ . Evidence is also provided by the fractional order found in substrate. As per equation (12), double reciprocal plot of  $1/k'$  versus  $1/[S]$  (Fig. 1), decomposition rate constant  $k$  was found out from intercept and  $K_2$  was obtained by substituting  $1/k$  in intercept of plot  $[PTA]/k'$  versus  $1/[S]$  and also from equation (13), the value of  $K_1$  (formation constant) was determined (Table 3) from its slope,  $K_1$ ,  $K_2$  and  $k$  were found to be  $54.26 \text{ (dm}^3\text{mol}^{-1}\text{)}$ ,  $2 \times 10^3 \text{ (dm}^3\text{mol}^{-1}\text{)}$  and  $4.09 \times 10^4 \text{ (s}^{-1}\text{)}$ , respectively for benzaldehyde at 303 K.

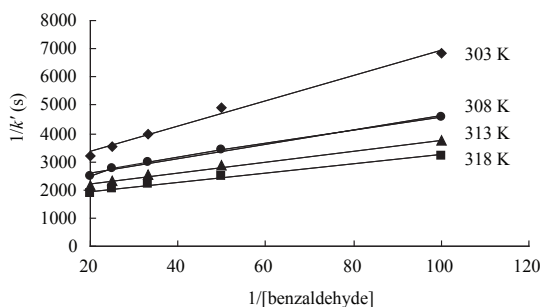


Fig. 1. Plot of  $1/[\text{substrate}]$  versus  $1/k'$  at different temperatures

*Effect of temperature and isokinetic phenomenon.* The rate of oxidation was determined at different temperatures and the Arrhenius plots of  $\lg k$  versus  $1/T$  were all linear (Fig. 2).

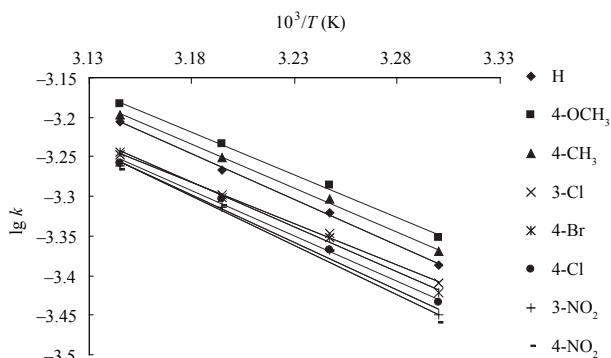


Fig. 2. The Arrhenius plot for oxidation of substituted benzaldehydes

**Table 3.** Decomposition rate constant ( $k$ ), formation constant ( $K_1$ ) and activation parameters for substituted benzaldehydes at 303 K

Substituent	$k \times 10^4$ (s <sup>-1</sup> )	$K_1$ (dm <sup>3</sup> mol <sup>-1</sup> )	$E_a$ (kJ mol <sup>-1</sup> )	$\Delta H^*$ (kJ mol <sup>-1</sup> )	$\Delta G^*$ (kJ mol <sup>-1</sup> )	$\Delta S^*$ (J K <sup>-1</sup> mol <sup>-1</sup> )	lg $A$
4-OCH <sub>3</sub>	4.45	68.08	20.61	18.09	75.31	-248.47	4.43
4-CH <sub>3</sub>	4.26	60.44	21.12	18.61	75.16	-248.49	4.47
H	4.09	54.26	22.02	19.50	75.32	-248.51	4.54
3-Cl	3.89	55.81	19.87	17.35	75.16	-248.53	4.45
4-Br	3.79	69.86	21.58	19.06	75.32	-248.54	4.55
4-Cl	3.68	57.12	21.81	19.29	75.33	-248.56	4.57
3-NO <sub>2</sub>	3.56	52.40	22.87	20.35	75.34	-248.57	4.64
4-NO <sub>2</sub>	3.47	51.10	23.62	21.10	75.34	-248.58	4.69

From these plots, the activation and thermodynamic parameter for equilibrium and rate-determining step of the scheme was evaluated (Table 3). The observed  $\Delta S^*$  values are large and negative. It may be interpreted that the fraction of collisions become more stringent and decomposition of activation complex is a quite slow process. The values of  $\Delta H^*$  indicate that the reactions are enthalpy-controlled. The validity of the isokinetic relation can be tested graphically by plotting the Exner plot  $\lg k_{303}$  versus  $\lg k_{313}$ . The isokinetic temperature  $\beta$  evaluated from the Exner criterion<sup>33</sup> was found to be 354.5 K (slope = 0.78 and  $R^2 = 0.94$ ), which is more than the experimental temperature, and implies that all the compounds are oxidised by the same mechanism<sup>34</sup>. Further the constancy in the calculated values of  $\Delta G^*$  for this oxidation reaction indicates that the same type of the reaction mechanism could be operative for the reaction.

## CONCLUSIONS

Kinetic studies demonstrate that the ternary complex of the Keggin anion, substrate and oxidant decomposes in a slow rate-determining step to give benzoic acid as the main product. The experimental stoichiometry is in a good agreement. First order to oxidant and fractional order to catalyst and substrate are supported by the derived rate law. The rate of oxidation of benzaldehydes was found to be in the order of 4-OCH<sub>3</sub> > 4CH<sub>3</sub> > H > 3-Cl > 4-Br > 4-Cl > 3-NO<sub>2</sub> > 4-NO<sub>2</sub>.

The Keggin type phosphotungstic acid catalyst is efficient homogeneous catalyst for oxidation of benzaldehydes and is participating in the reaction as the Keggin anion.

## ACKNOWLEDGEMENT

We are thankful to Principal, Vasantrao Naik Mahavidyalaya and Principal, Maulana Azad College, Aurangabad for providing the laboratory facilities.

## REFERENCES

1. M. CINDRIC, Z. VEKSLI, B. KAMENARA: Polyoxomolybdates and Polyoxomolybdovanadates – from Structure to Functions: Recent Results. *Croat Chem Acta*, **82** (2), 345 (2009).
2. J. SKRZPEK, T. WITCZAK, M. GRZESIK, M. WITCZAK: Kinetics of the Synthesis of Propyl and Butyl Acrylates in Presence of Some Heteropolyacids as Catalysts. *Int J Chem Kinet*, **41**, 12 (2009).
3. A. R. SUPALE, G. S. GOKAVI: 12-Tungstocobaltate (II) Catalyzed Selective Oxidation of Sulfides to Sulfoxides Using Aqueous Hydrogen Peroxide under Solvent Free Conditions. *React Kinet Catal L*, **96** (1), 83 (2009).
4. D. B. BOGDANOVIC, I. H. ANYUNOVIC, M. TODOROVIC, U. B. MIOC, J. ZAKRZEWSKA: A Study of 12-tungstosilicic and 12-molybdophosphoric Acids in Solution. *J Serb Chem Soc*, **73** (2), 197 (2008).
5. P. K. SAPATHY, G. C. DAS, P. MOHANTY: Oxidation of L-cystine by 12-tungstocobaltate (III) in Aqueous Perchlorate Medium: A Kinetic approach. *Indian J Chem*, **47A**, 1199 (2008).
6. D. S. RAJMANE, K. V. KAPSHIKAR, G. S. GOKAVI: Kinetics and Mechanism of Oxidation of Aliphatic Alcohols by Oxone Catalyzed by Keggin Type 12-tungstocobaltate (II). *Indian J Chem*, **45A**, 1626 (2006).
7. P. K. SATPATHY, G. C. DASH, S. ACHARYA, P. MOHANTY: Kinetics and Mechanism of Oxidation of DL-methionine by Keggin-type 12-tungstocobaltate (III) in Aqueous Acetic Acid Medium. *J Indian Chem Soc*, **83**, 891 (2006).
8. K. AMANI, F. MALEKI: Catalytic Effects of Some Keggin-type Heteropoly Acids and Polyoxometalates on Selective Nitration of Phenols. *J Iran Chem Soc*, **4**, 238 (2007).
9. S. P. MARADUR, G. S. GOKAVI: Poly(vinyl alcohol) Supported 12-tungstocobaltate (II) as a Novel Heterogeneous Catalyst for Oxidation of Benzyl Alcohols. *Bull Catal Soc India*, **6**, 42 (2007).
10. H. FIROUZABADI, N. IRANPOOR, K AMANI: Tungstophosphoric Acid Catalyzed Oxidation of Aromatic Amines to Nitro Compounds with Sodium Perborate in Micellar Media. *Green Chem*, **3**, 131 (2001).
11. H. FIROUZABADI, N. IRANPOOR, K AMANI: Solvent Free and Selective Oxidation of Hydroxy-groups to Their Corresponding Carbonyl Functions with  $\text{Fe}(\text{NO}_3)_3$  Activated by Heteropoly Acids. *Synthesis*, 408 (2003).
12. J. BHARAD, B. MADJE, F. CHAVAN, M. FAROOQUI, M. UBALE: Kinetic Study of Phosphotungstic Acid Catalyzed Oxidation of Cyclic Alcohols by N-bromophthalimide. *Bull Catal Soc India*, **7**, 168 (2008).
13. L. I. KUZNETSOVA, R. I. MAKSIMOVSKAYA, M. A. FEDOTOV: Oxidation of Allyl Alcohol by  $\text{H}_2\text{O}_2$  in Presence of Phosphotungstic Acid. *Inzvestiya Akademii Nauk SSSR*, **3**, 537 (1985).
14. N. JAIN, A. KUMAR, S. M. S. CHAUHAN: Metalloporphyrin and Heteropoly Acid Catalyzed Oxidation of Oximes in an Ionic Liquids. *Tetrahedron Lett*, **46**, 2599 (2005).
15. P. SHARMA, A. PATEL: Liquid Phase Non-solvent Selective Oxidation of Styrene Using Aqueous Hydrogen Peroxide with Supported 12-tungstophosphoric Acid. *Indian J Chem*, **48A**, 964 (2009).
16. P. S. RADHAKRISHNAMURTHY, B. SAHU: Kinetics and Mechanism of Oxidation of Aromatic Aldehydes by N-bromosuccinimide. *Indian J Chem*, **17 A**, 63 (1979).
17. V. SHARMA, K. K. BANERJI: Kinetics and Mechanism of Oxidation of Aldehydes by N-bromoacetamide. *J Chem Res (S)*, **234**, 2371 (1985).
18. N. MATHIYALAGAN, R. SRIDHARAN: Kinetics and Mechanism of Oxidation of Aromatic Aldehydes by N-chloronicotinamide in Aqueous Acetic Acid. *Indian J Chem*, **44 A**, 2044 (2007).
19. A. ANJUM, P. SRINIVAS: Analytical and Kinetic Behavior of N-bromoimide–Mercuric Acetate System towards Aromatic Aldehydes: A Mechanistic Study. *Asian J Chem*, **18**, 673 (2006).
20. P. S. RADHAKRISHNAMURTHY, B. SAHU: Kinetics and Mechanism of Oxidation of Benzaldehyde by Chloramine-T. *Indian J Chem*, **17 A**, 381 (1979).

21. S. K. NIGAM, M. U. KHAN, S. TIWARI, H. P. DWIVEDI, P. K. SINGH: Kinetics and Mechanism of Oxidation of Benzaldehyde and Substituted Benzaldehydes by N-chlorosaccharin. *Asian J Chem*, **16**, 761 (2004).
22. V. K. SHARMA, K. SHARMA, H. D. GUPTA, O. P. GUPTA: Kinetics and Oxidation of Benzaldehydes by N-bromosaccharin. *Oxid Commun*, **18**, 395 (1995).
23. K. K. BANERJI: Kinetics and Mechanism of Substituted Benzaldehydes by N-bromoacetamide. *J Org Chem*, **51**, 4764 (1986).
24. C. MOHAN DAS, P. INDRASENAN: N-bromophthalimide as an Oxidimetric Titrant, Some Direct Visual Titrations in Aqueous Acetic Acid Medium. *J Indian Chem Soc*, **64**, 382 (1987).
25. D. K. BHAT, B. S. SHERIGAR, B. T. GOWDA: Oxidation of a Dipeptide by Electrolytically Generated Manganese (III) in Aqueous Sulfuric Acid Medium: A Kinetic and Mechanistic Study. *B Chem Soc Jpn*, **69**, 41 (1996).
26. E. S. AMIS: In: *Solvent Effect on Reaction Rates and Mechanism*. Academic Press, New York, 1967, p. 42.
27. J. G. KIRKWOOD: The Theory of Strong Electrolyte Solutions. *J Chem Phys*, **2**, 354 (1934).
28. A. W. CHESTER: Oxidation of Alkyl Aromatic Hydrocarbons by Potassium 12-tungstocobaltate (III). *J Org Chem*, **35**, 1797 (1970).
29. L. C. BAKER, J. S. FIGGIS: A New Fundamental Type of Inorganic Complex: Hybrid between Heteropoly and Conventional Coordination Complexes. Possibilities for Geometrical Isomerisms in 11-, 12-, 17-, and 18-heteropoly Derivatives. *J Am Chem Soc*, **92**, 3974 (1970).
30. R. A. MARCUS, ANGREW: *Electron Transfer Reactions in Chemistry: Theory and Experiment*. *Pure Appl Chem*, **69** (1), 13 (1997).
31. C. KARUNAKARAN, P. N. PALANISAMY: Autocatalysis in the Sodium Perborate Oxidation of Anilines in Acetic Acid–Ethylene Glycol. *J Mol Cat-A*, **172**, 9 (2001).
32. A. R. BINYAHIA, S. DUBEY, P. D. SHARMA: Kinetics and Mechanism of Electron Transfer Reactions in Acid Perchlorate Medium. Hydrogen Ion Dependence on the Rate of Oxidation of Formic Acid by Thallium Perchlorate Catalysed by Ruthenium (III) Chloride in Acid Aqueous Medium. *Oxid Commun*, **24** (2), 246 (2000).
33. O. EXNER: The Inductive Effect: Theory and Quantitative Assessment. *Coll Chem Czech Comm*, **31**, 3222 (1966).
34. J. E. LEFFLER, E. GRUNWALD: *Rates and Equilibrium of Organic Reactions*. Wiley, New York, 1963.

*Received 9 March 2010*

*Revised 18 May 2010*

## **Ru(III) AND Ir(III) CATALYSIS IN OXIDATION OF BUTANOL BY QUINOLINIUM FLUOROCHROMATE. A COMPARATIVE STUDY**

SH. SRIVASTAVA\*, P. SRIVASTAVA

*Chemical Laboratories, Feroze Gandhi College, 229 001 Raebareli, U.P., India*

*E-mail: she\_ila72@yahoo.com; parul\_9880@yahoo.com*

### ABSTRACT

Kinetic investigation in Ru(III) and Ir(III)-catalysed oxidation of butanol in an acidified solution of quinolinium fluorochromate (QFC) has been carried out in the temperature range of 30–45°C. First order kinetics was observed in case of catalyst Ru(III) as well as oxidant substrate (butanol). The order of reaction with respect to QFC was found to be zero. Increase in  $[Cl^-]$  showed fractional positive order. The influence of  $[H^+]$  and ionic strength on the rate was found to be insignificant. The main product of oxidation of butanol for both Ru(III) and Ir(III)-catalysed reactions was identified as butanaldehyde. The reaction has been studied in 10 different solvents. The first order rate constant had not been affected by the decrease in the dielectric constant of the medium. The values of rate constants observed at 4 different temperatures (30, 35, 40 and 45°C) were utilised to calculate the activation parameters. A suitable mechanism in conformity with the kinetic observations has been proposed and the rate law has been derived on the basis of the obtained data. A transient complex, formed between catalyst and substrate in a slow and rate-determining step, further reacts with QFC to give the products in a series of fast steps.

*Keywords:* kinetics, oxidation, quinolinium fluorochromate, Ru(III)/Ir(III) chloride, butanol.

### AIMS AND BACKGROUND

Halochromates have been used as mild and selective oxidising reagent in synthetic organic chemistry<sup>1</sup>. Quinolinium fluorochromate<sup>2</sup> (QFC) is also one such compound. The kinetics of redox reactions involving homogeneous catalyst such as platinum group metals particularly osmium(VIII), iridium(III) and palladium(II) has been extensively investigated from mechanistic point of view. The use of Ru(III) chloride as a non-toxic and homogeneous catalyst has been reported by several workers<sup>3–6</sup>. The mechanism

---

\* For correspondence.

of reaction depends on the nature of the oxidant, nature of the substrate and the ways in which transition metal complex promote the reactant molecules to the activated state before changing into final products under experimental conditions. The kinetic and mechanistic aspects of the oxidation by halochromates, a chromium(VI) species like quinolinium bromochromate (QBC), quinolinium chlorochromate (QCC) and few reports on the mechanistic aspects of oxidation reactions of QFC are available in literature<sup>7-9</sup>. Nearly no explanation was forthcoming in trying to rationalise the difference in kinetic behaviour. It was thought worthwhile to study the kinetics and mechanism of Ru(III)-catalysed oxidation of unsaturated acid by QFC in acetone as a solvent, with a view to examine the kinetic features of the reaction and establish the mechanistic pathways for the oxidation processes in the presence of different solvents with aims to: (i) ascertain real reactive species of catalyst and oxidant; (ii) identify the oxidation products; (iii) elucidate a plausible reaction mechanism, and (iv) deduce rate law consistent with kinetic results and calculated activation parameters.

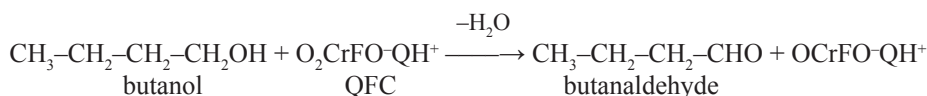
## EXPERIMENTAL

*Materials.* Butanol was commercial product and was used as obtained. QFC was prepared by the reported method<sup>2</sup> and its purity was ascertained by an iodometric method. Sodium perchlorate, quinolinium fluorochromate, perchloric acid, fumaric acid, crotonic acid (E.Merck) were used as supplied without further purification by their solutions in doubly distilled water. A stock solution of Ru(III) and Ir(III) chloride (Johnson Matthey) was prepared by dissolving the sample in hydrochloric acid of known strength. An allowance for the amount of hydrochloric acid present in the catalyst solution was made while preparing the reaction mixtures for kinetic studies. Sodium perchlorate was used to maintain the ionic strength of the medium. Perchloric acid (60%, S.d.fine) was used as a source of H<sup>+</sup> ion. Solvents were purified by the usual methods<sup>10</sup>. All other reagents were of AR grade and doubly distilled water was used throughout the work. The reaction vessels were coated black paint to prevent photochemical decomposition, if any.

*Kinetics.* A thermostatic water bath was used to maintain the desired temperature within  $\pm 0.1^\circ\text{C}$ . The appropriate volumes of substrate, perchloric acid, sodium perchlorate, Ru(III) chloride or Ir(III) chloride and water, except quinolinium fluorochromate were taken in a reaction vessel which was kept in a thermostatic water bath. After allowing sufficient time to attain the temperature of the experiment, requisite volume of quinolinium fluorochromate solution, also thermostated at the same temperature  $35 \pm 0.1^\circ\text{C}$ , was rapidly pipetted out and poured into the reaction vessel. The total volume of reaction mixture was 50 ml in each case. 5 ml aliquots of reaction mixture were pipetted out at different intervals of time and quenched with 4% acidified potassium iodide solution. The progress of reaction was monitored by iodometric estimation of unconsumed quinolinium fluorochromate using starch as an indicator after suitable time intervals. Each kinetic run was studied for 75% completion of the reaction. The

rate of reaction ( $-dc/dt$ ) was determined by the slope of the tangent drawn at a fixed [QFC] in each kinetic run. The order of reaction was calculated with the help of  $\lg(-dc/dt)$  versus  $\lg[\text{reactants}]$ .

*Stoichiometry and product analysis.* The kinetics and mechanism of Ru(III) and Ir(III)-catalysed oxidation of butanol by quinolinium fluorochromate have been studied in acidic medium in the temperature range 30–45°C. To determine the stoichiometric ratio of the reaction, sets of reaction mixture containing varying ratios of QFC and butanol were allowed separately to equilibrate at 35°C for about 24 h. The excess of QFC remaining in each set was estimated iodometrically. The estimation of unconsumed QFC showed that 1 mol of butanol consumed 1 mol of QFC (Table 1). Thus, stoichiometric determination indicated that the overall reaction can be written as follows:



Butanaldehyde was obtained as the end product of the oxidation of butanol catalysed both by Ru(III) and Ir(III) chlorides.

**Table 1.** Stoichiometric results for oxidation of butanol

[QFC] × 10 <sup>3</sup> (M)	[Substrate] × 10 <sup>3</sup> (M)	[QFC]* × 10 <sup>3</sup> (M) (residual)		[QFC] <sup>c</sup> /[Substrate]	
		Ru(III)	Ir(III)	Ru(III)	Ir(III)
12.50	1.00	11.55	11.65	0.95	0.85
10.00	1.00	8.85	8.90	1.15	1.10
5.00	1.00	3.90	4.00	1.10	1.00
2.50	1.00	1.65	1.45	0.85	1.05
12.50	2.00	10.35	10.55	1.07	0.97
12.50	3.00	9.60	9.75	0.96	0.92
12.50	4.00	8.70	8.35	0.95	1.04
12.50	5.00	7.30	7.70	1.04	0.96

[Ru(III)]-[Ir(III)] = 4.80 × 10<sup>-6</sup> M; [KCl] = 1.00 × 10<sup>3</sup> M; [S] = 2.00 × 10<sup>-2</sup> M; [HClO<sub>4</sub>] = 1.00 × 10<sup>-3</sup> M; temperature = 35°C, time = 48 h; [QFC]\* = [QFC] left unconsumed after 48 h; [QFC]<sup>c</sup> = [QFC]-[QFC]\*, i.e. oxidant consumed during the reaction.

QFC undergoes a 2-electron change. This is in accordance with earlier observations with other halochromates<sup>11-14</sup>.

Product analysis was carried out under kinetic conditions, i.e. with an excess of the reductant over QFC. In this experiment, butanol (0.2 mol) and QFC (6.18 g, 0.02 mol) were dissolved in 100 ml of acetone and allowed to stand for 24 h to ensure completion of the reaction. The solution was then treated with an excess of a saturated solution of 2,4-dinitrophenylhydrazine in 2 M HCl and kept overnight in a refrigerator. The precipitated 2,4-dinitrophenylhydrazone (DNP) was filtered off, dried, weighed, recrystallised from ethanol and weighed again. The yields of DNP before and after recrystallisation were 2.52 g (88%) and 2.26 g (79%), respectively. The DNP was

found identical (m.p. and mixed m.p.) with the DNP of pyruvic acid and acetone in the oxidation of fumaric and crotonic acids, respectively.

## RESULTS AND DISCUSSION

The kinetic results were collected at several initial concentrations of reactants (Table 2). Zero order kinetics was showed by QFC. The plots of  $\lg(-dc/dt)$  versus  $\lg[\text{substrate}]$  are linear indicating first order dependence on substrate (Fig. 1). The kinetic results recorded at various  $[\text{Ru(III)}]$ ,  $[\text{Ir(III)}]$ , ionic strength of the medium along with kinetics effects on successive addition of KCl,  $\text{HClO}_4$ , sodium perchlorate are given in Table 2.

**Table 2.** Effect of variation of reactants on the reaction rates for butanol at 35°C  
 $[\text{Ru(III)}] = 4.80 \times 10^{-6} \text{ M}$ ;  $[\text{substrate}] = 2.00 \times 10^{-2} \text{ M}$

$[\text{QFC}] \times 10^3$ (M)	$[\text{KCl}] \times 10^3$ (M)	$[\text{HClO}_4] \times 10^3$ (M)	$[\text{NaClO}_4] \times 10^3$ (M)	$(-dc/dt) \times 10^7 \text{ (M s}^{-1}\text{)}$	
				Ru(III)-cata- lysed	Ir(III)-cata- lysed
0.83	1.00	0.20	—	3.25	4.70
1.00	1.00	0.20	—	3.20	4.50
1.25	1.00	0.20	—	3.44	4.64
1.67	1.00	0.20	—	2.55	4.36
2.50	1.00	0.20	—	3.60	3.72
5.00	1.00	0.20	—	3.36	4.25
1.00	0.83	0.20	—	2.72	4.36
1.00	1.00	0.20	—	3.20	4.50
1.00	1.25	0.20	—	3.46	4.62
1.00	1.67	0.20	—	4.02	5.22
1.00	2.50	0.20	—	4.29	5.56
1.00	5.00	0.20	—	4.75	5.94
1.00	1.00	0.04	—	3.45	4.74
1.00	1.00	0.08	—	3.55	4.70
1.00	1.00	0.12	—	3.64	4.85
1.00	1.00	0.16	—	3.15	4.38
1.00	1.00	0.20	—	3.20	4.50
1.00	1.00	0.24	—	3.64	4.45
1.00	1.00	0.20	0.83	2.45	4.72
1.00	1.00	0.20	1.00	3.20	4.50
1.00	1.00	0.20	1.25	3.15	4.28
1.00	1.00	0.20	1.67	2.65	4.52
1.00	1.00	0.20	2.50	3.48	4.62
1.00	1.00	0.20	5.00	3.72	4.55



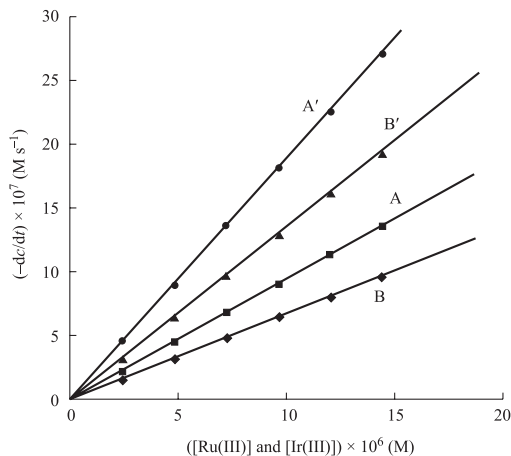


**Fig. 1.** Plot between  $(-dc/dt)$  and  $[\text{Ir(III)}]$  (A) and  $[\text{Ru(III)}]$  (B) for the oxidation of butanol in acidic medium at  $35^\circ\text{C}$

First order dependence of the reaction on Ru(III) is evident from the slope values ( $2.10 \times 10^{-2} \text{ s}^{-1}$  and  $4.00 \times 10^{-2} \text{ s}^{-1}$  at  $35$  and  $45^\circ\text{C}$ , respectively) and Ir(III) ( $3.26 \times 10^{-2} \text{ s}^{-1}$  and  $5.96 \times 10^{-2} \text{ s}^{-1}$  at  $35$  and  $45^\circ\text{C}$ , respectively) of straight lines obtained from plot of  $(-dc/dt)$  versus  $[\text{Ru(III)}]/[\text{Ir(III)}]$  (Fig. 2) and average  $k_1$  values ( $2.24 \times 10^{-2} \text{ s}^{-1}$  and  $4.35 \times 10^{-2} \text{ s}^{-1}$  for  $[\text{Ru(III)}]$  at  $35$  and  $45^\circ\text{C}$ , respectively, and  $3.25 \times 10^{-2} \text{ s}^{-1}$  and  $6.15 \times 10^{-2} \text{ s}^{-1}$  Ir(III) at  $35$  and  $45^\circ\text{C}$ , respectively). A positive effect of  $[\text{Cl}^-]$  is obvious from kinetic data in Table 2.

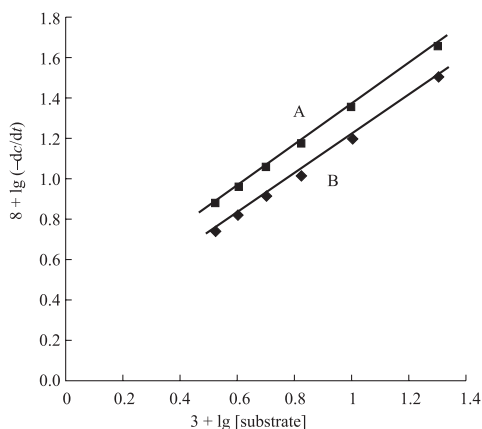


**Fig. 2.** Plot between  $\lg(-dc/dt)$  and  $\lg[\text{substrate}]$  in the presence of  $[\text{Ir(III)}]$  (A) and  $[\text{Ru(III)}]$  (B) for the oxidation of butanol in acidic medium at  $35^\circ\text{C}$

*Effect of solvents.* The rate of oxidation of butanol was obtained in 10 different organic solvents. The solubility of reagents and reaction of QFC with primary and secondary alcohols limited the choice of solvents. There was no reaction between QFC and the

solvents chosen. The kinetics observed was similar in all the solvents. The values of  $(-dc/dt)$  and  $k_1$  are presented in Table 3.

**Table 3.** Rate constants for the decomposition of catalyst-QFC complex in different solvents at 35°C

Solvents	$(-dc/dt) \times 10^7$ (M s <sup>-1</sup> )		$k_1 \times 10^4$ (s <sup>-1</sup> )	
	Ru(III)-catalysed	Ir(III)-catalysed	Ru(III)-catalysed	Ir(III)-catalysed
Acetone	3.20	4.50	4.32	5.29
Butanone	2.25	4.55	3.04	5.83
Benzene	3.60	4.16	3.55	4.20
Ethyl acetate	4.30	3.45	4.35	3.60
Nitrobenzene	2.28	5.80	3.00	5.75
Acetic acid	3.45	4.54	3.60	4.24
<i>t</i> -butyl alcohol	2.70	4.62	2.78	4.57
Acetophenone	3.15	3.40	3.25	3.44
Choloroform	3.00	4.20	3.25	4.38
Toluene	4.10	4.36	4.24	4.40

The rate constants,  $k_1$ , in 10 solvents were correlated in terms of linear salvation energy relationship of Kamlet et al.<sup>15</sup>:

$$\lg k_2 = A_0 + p\pi^* + b\beta + a\alpha \quad (\text{A})$$

where  $\pi^*$  is the solvents polarity;  $\beta$  – the hydrogen bond acceptor basicity;  $\alpha$  – the hydrogen bond donor acidity, and  $A_0$  – the intercept term. The results of correlation analyses in terms of equation (A), a biparametric equation involving  $\pi^*$  and  $\beta$  is given below:

$$\lg k_2 = -1.52 + 0.62(\pm 0.15) \pi^* + 3.20(\pm 0.12) \beta + 3.08(\pm 0.13) \alpha$$

$$R^2 = 0.80; \text{sd} = 0.45; n = 10.$$

The rate measurements were carried out at 30–45°C and specific rate constant were used to draw a plot of  $\lg k$  versus  $1/T$ , which was linear (Fig. 3). The values of energy of activation ( $\Delta E^*$ ), the Arrhenius factor ( $A$ ), entropy of activation ( $\Delta S^*$ ) and free energy of activation ( $\Delta G^*$ ) were calculated and given in Table 4.

**Table 4.** Rate constants and activation parameters of oxidation of butanol by QFC

Catalyst	$k_r \times 10^4$ (s <sup>-1</sup> ) at (°C)				$\Delta E^*$ (kJ mol <sup>-1</sup> )	$\Delta G^*$ (kJ mol <sup>-1</sup> )	$\Delta H^*$ (kJ mol <sup>-1</sup> )	$\Delta S^*$ (JK <sup>-1</sup> mol <sup>-1</sup> )	$\lg A$
	30	35	40	45					
Ru(III)-catalysed	2.25	3.20	4.48	6.58	53.63	75.29	52.31	-16.74	9.33
Ir(III)-catalysed	3.14	4.50	7.50	9.20	63.83	71.30	69.52	-5.77	11.74

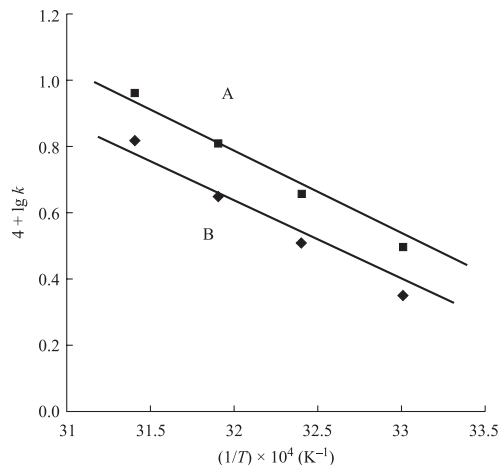


**Fig. 3.** Plot between  $\lg k$  and  $1/T$  in the presence of [Ir(III)] (A) / [Ru(III)] (B) for the oxidation of butanol in acidic medium at 35°C

[Substrate] =  $2.00 \times 10^{-2}$  M; [Ir(III)]–[Ru(III)] =  $4.80 \times 10^{-6}$  M; [KCl] =  $1.00 \times 10^{-3}$  M; [QFC] =  $1.00 \times 10^{-3}$  M; [HClO<sub>4</sub>] =  $1.00 \times 10^{-3}$  M; [NaClO<sub>4</sub>] =  $1.00 \times 10^{-3}$  M

*Test for free radical.* Addition of aqueous acrylamide monomer solution to the reaction mixture in the dark did not initiate polymerisation, indicating the absence of formation of free radical species in the reaction sequence. The control experiments were also performed under the same reaction conditions.

*Effect of dielectric constant and ionic strength of the medium.* In order to determine the effect of the dielectric constant ( $D$ ) or relative permittivity of the medium on the reaction rate, the reaction has been studied with different dielectric constants of the medium at constant concentration of all other reagents and at a constant temperature of 35°C. The change in dielectric constant of the medium has been affected by addition of acetic acid to the reaction mixture. Before conducting experiments for the study of the effect of dielectric constant of the medium on the reaction rate, we have performed experiments taking acetic acid as an organic substrate instead of unsaturated acid in usual manner and found that acetic acid is not oxidised by QFC in the presence of Ru(III) and Ir(III) as the homogeneous catalyst. Addition of acetic acid to the reaction mixture did not influence the rate of reaction. Therefore, the plot of  $\lg k$  versus  $1/D$  or the inverse of relative permittivity is not linear.

The ionic strength ( $\mu$ ) effect on the rate reaction has been described according to the theory of Bronsted and Bjerrum, which postulates the reaction occurring through the formation of an activated complex. According to this theory, the effect of ionic strength on the rate of reaction involving 2 ions is given by the relationship:

$$\lg k = \lg k_0 + 1.02 Z_A Z_B \mu^{1/2}$$

where  $Z_A$  and  $Z_B$  are the valencies of the ions A and B,  $k$  and  $k_0$  – the rate constant in the presence or absence of the added electrolyte, respectively. A plot of  $\lg k$  against



## CONCLUSIONS

The experimental results reveal that the reaction rate doubles when concentration of the catalyst is doubled. The rate law equation is in conformity with all kinetic observations and the proposed mechanistic steps are supported by the negligible effect of ionic strength. The high positive values of change in free energy of activation ( $\Delta G^*$ ) indicates highly solvated transition state, while fairly high negative values of change in entropy of activation ( $\Delta S^*$ ) suggest the formation of an activated complex with reduction in the degree of freedom of molecules. From this investigation it is concluded that  $[\text{RuCl}_6]^{-3}$ ,  $[\text{IrCl}_6]^{-3}$  and QFC are the reactive species of Ru(III) chloride<sup>16</sup>, Ir(III) chloride<sup>17</sup> and quinolinium fluorochromate<sup>18</sup> in acidic medium, respectively.

## ACKNOWLEDGEMENT

One of the authors, Parul Srivastava, thanks CST, U.P. for financial assistance.

## REFERENCES

1. E. J. COREY, W. J. SUGGS: Pyridinium Chlorochromate. An Efficient Reagent for Oxidation of Primary and Secondary Alcohols to Carbonyl Compound. *Tetrahedron L*, 2647 (1975).
2. V. MURUGESAN, A. PANDURANGAN: Quinolinium Fluorochromate: A New Reagent for the Oxidation of Organic Compounds. *Indian J Chem*, **B 31**, 377 (1992).
3. Sh. SRIVASTAVA, S. SINGH, R. K. SHARMA: Kinetics and Mechanism of Ruthenium(III) Catalyzed Oxidation of Some Polyhydric Alcohols by Acid Bromate. *J Indian Chem Soc*, **84**, 1109 (2007).
4. R. MULLA, G. HIREMATH, S. T. NANDIBEWOOR: Kinetic, Mechanistic and Spectral Investigation of Ruthenium (III)-catalysed Oxidation of Atenolol by Alkaline Permanganate (Stopped-flow Technique). *J. Chem. Sci.*, **117** (1), 33 (2005).
5. Sh. SRIVASTAVA, A. AWASTHI, K. SINGH: Ruthenium(III) Catalyzed Oxidation of Cyclopentanol and Cyclohexanol by N-bromoacetamide. *International J Chem Kinet*, **37** (5), 275 (2005).
6. Sh. SRIVASTAVA, P. SRIVASTAVA, L. CHAUDHARY, A. KUMAR, Sh. SINGH: A Kinetic Study of Ru(III) Catalyzed Oxidation of Galactose and Cyclopentanol by Potassium Bromate in Alkaline Medium. *J Indian Chem Soc*, **86**, 1 (2009).
7. R. KUMBHAT, V. SHARMA, K. K. BENERJI: Kinetics and Mechanism of Oxidation of Aliphatic Aldehydes by Quinolinium Bromochromate. *Oxid Commun*, **27** (2), 327 (2004).
8. K. G. SEKAR, M. RAVISHANKAR: Oxidation of Furfural by Quinolinium Chlorochromate. *Oxid Commun*, **24** (3), 368 (2001).
9. I. DAVE, V. SHARMA, K. K. BENERJI: Kinetics and Mechanism of the Oxidative Regeneration of Carbonyl Compounds from Oximes by Quinolinium Fluorochromate. *J Indian Chem Soc*, **79**, 347 (2002).
10. D. D. PERRIN, L. ARMAREGO, D. R. PERRIN: *Purification of Organic Compounds*. Pergamon, Oxford, 1966.
11. S. AGARWAL, K. CHOWDHARY, K. K. BENERJI: Kinetics and Mechanism of the Oxidation of Aromatic Aldehydes by Pyridinium Fluorochromate. *J Org Chem*, **56**, 5111 (1991).
12. K. LOONKER, P. K. SHARMA, K. K. BENERJI: Kinetics and Mechanism of the Oxidation of Organic Sulfides by Pyridinium Bromochromate. *J Chem Res*, (S) **194**, (M) 1262 (1997).
13. K. CHOWDHARY, P. K. SHARMA, K. K. BENERJI: Kinetics and Mechanism of the Oxidation of Aliphatic Alcohols by Quinolinium Fluorochromate. *Int J Chem Kinet*, **31**, 469 (1999).
14. A. BHANDARI, P. K. SHARMA, K. K. BENERJI: Kinetics and Mechanism of the Oxidative Regeneration of Carbonyl Compounds by Pyridinium Chlorochromate. *Indian J Chem Sect A*, **40**, 470 (2001).

15. M. J. KAMLET, J.-L. M. ABBOUD, M. H. ABRAHAM, R. W. TAFT: Linear Solvation Energy Relationships. 23. A Comprehensive Collection of the Solvatochromic Parameters,  $\pi^*$ ,  $\alpha$  and  $\beta$ , and Some Methods for Simplifying the Generalized Solvatochromic Equation. *J Org Chem*, **48**, 2877 (1983).
16. H. H. CADY, R. E. CONNICK: The Determination of the Formulas of Aqueous Ruthenium(III) Species by Means of Ion-exchange Resin:  $\text{Ru}^{+3}$ ,  $\text{RuCl}^{+2}$  and  $\text{RuCl}_2^+$ . *J Am Chem Soc*, **80**, 2646 (1958).
17. J. C. CHANG, C. S. GARNER: Kinetics of Aquation of Aquopentachloroiridate(III) and Chloride Anation of Diaquotetrachloroiridate(III) Anions. *Inorg Chem*, **4**, 209 (1965).
18. M. KHURANA, P. K. SHARMA, K. K. BENERJI: Kinetics and Mechanism of the Oxidation of Formic and Oxalic Acids by Quinolinium Fluorochromate. *Indian Academy of Sciences*, **112** (2), 73 (2000).

*Received 22 January 2009*

*Revised 15 March 2009*

## **A KINETIC STUDY ON OXIDATION OF 2-ARYL-*trans*-DECAHYDROQUINOLIN-4-ONES BY CERIUM(IV)**

N. SHARMILA, B. HARI BABU, P. V. V. SATYANARAYANA\*

*Department of Chemistry, Acharya Nagarjuna University, 522 510 Nnagar, Guntur, AP, India*

*E-mail: chemperuri@yahoo.co.in*

### **ABSTRACT**

The kinetics of oxidation of substituted 2-aryl-*trans*-decahydroquinolin-4-ones was studied at 35°C and in the presence of sulphuric acid by using cerium(IV) as oxidising agent. The order of the reaction was found to be each unity with respect to cerium(IV) and substrate. The substitution of methyl group at position 3 decreased the rate of oxidation of the ketones. The rate of oxidation of 3-methyl-2-aryl-*trans*-decahydroquinolin-4-ones was carried out under different reaction conditions. The rates of oxidations were found to increase with increase in concentration of sulphuric acid, acetic acid in the solvent composition.

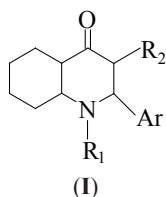
*Keywords:* 2-aryl-*trans*-decahydroquinolin-4-ones, kinetics, oxidation, cerium(IV).

### **AIMS AND BACKGROUND**

The kinetic studies on the oxidation of different aliphatic ketones<sup>1-6</sup>, alicyclic ketones<sup>7-9</sup>, aromatic ketones<sup>10-14</sup> and a series of 2,6-diaryl-4-piperidones<sup>15-21</sup> have been carried out extensively by various researchers and suitable mechanisms have been proposed. However, the kinetics of oxidation of 2-aryl-*trans*-decahydroquinolin-4-ones has received no attention though other studies like semicarbazone formation, stereochemistry of reduction, etc. have been performed. Hence, it is thought to take up kinetic studies on oxidation of 2-aryl-*trans*-decahydroquin-4-ones with a view to identify the possible product(s) formed in the oxidation and to suggest a suitable mechanism for the oxidation process. For this purpose the authors has prepared the said ketones (Fig. 1) by the method already reported by Baliah and Natarajan<sup>22</sup>.

---

\* For correspondence.



S. No	Ar	R <sub>1</sub>	R <sub>2</sub>
1	C <sub>6</sub> H <sub>5</sub>	H	H
2	<i>p</i> -Me-C <sub>6</sub> H <sub>4</sub>	H	H
3	<i>p</i> -OMe-C <sub>6</sub> H <sub>4</sub>	H	H
4	C <sub>6</sub> H <sub>5</sub>	H	Me
5	<i>p</i> -Me-C <sub>6</sub> H <sub>4</sub>	H	Me

**Fig. 1.** 2-aryl-*trans*-decahydroquinolin-4-ones

## EXPERIMENTAL

*Purification of materials.* The required ketones were purified by recrystallisation from suitable solvents to constant melting point. The samples were dried in vacuum before use. Glacial acetic acid (Excelar), supplied by Qualigens Fine Chemicals was refluxed with chromium trioxide and acetic anhydride for 6 h and fractionally distilled. The fraction boiling at 117–118°C was collected and used. Sulphuric acid (A.R), liquid ammonia (A.R) were used. Doubly distilled water was used for all purposes.

*Kinetic procedure.* All the kinetic runs were made under second order conditions by keeping the substrate and acid concentrations always in large excess over that of Ce(IV).

The required amount of cerium(IV) solution was prepared by dissolving the necessary amount of ceric sulphate in the solvent medium containing acid. The medium used was aqueous acetic acid (the ratio of acetic acid:water was 50:50 (v/v)). The concentration of cerium(IV) solution was determined by the Mohr salt solution. The solutions of the substrate (ketones) were prepared by dissolving the appropriate quantity of the compounds in the same solvent, so that the concentration of the ketones was always maintained higher than the concentration of cerium(IV).

The ketone solution and cerium(IV) solutions were thermally equilibrated. Equal volumes (10 ml) of these solutions were pipetted out into a conical flask kept in the thermostat. A stop watch was started when half of the second solution had been delivered. 2 ml aliquots were taken in a conical flask. To this 10 ml of 10N H<sub>2</sub>SO<sub>4</sub> and 20 ml of distilled water and 2 to 3 drops of ferroin indicator were added and titrated against the Mohr solutions. The appearance of pale blue is the end point of the titration. During the titration the acidity of the medium was maintained at 4.0 N. From the titre value, the amount of Ce(IV) reacted was calculated.



*Product analysis.* For oxidation of ketones by cerium(IV) the ketones were dissolved in 25 ml of 50% aqueous acetic acid and treated with cerium(IV) solution containing 4.0 N sulphuric acid. The concentration of cerium(IV) was maintained in excess over the concentration of ketone. The resulting mixture was kept aside at room temperature, neutralised with ammonia, extracted with ether and the combined ether extracts evaporated. A solid product was obtained.

*Stoichiometry.* The stoichiometry of the reaction was determined by allowing a known excess of the oxidant Ce(IV) to react with the substrate in the presence of H<sub>2</sub>SO<sub>4</sub> in aqueous 50% acetic acid medium and estimating the unreacted Ce(IV). The stoichiometry was found to be in a mol ratio of 2:1 for oxidant to substrate.



*Calculation of rate constants.* The rate constants of all the reactions were calculated by using the second order integrated rate equation.

$$k_2 = \frac{2.303}{t(a-b)} \lg \frac{b(a-x)}{a(b-x)},$$

where  $a$  is the initial concentration of ketone (mol/l);  $b$  – initial concentration of cerium(IV) (mol/l);  $x$  – amount of cerium(IV) reacted in time  $t$  (s).

## RESULTS AND DISCUSSION

The kinetics of oxidation of the ketones prepared (**1** to **5**) was carried out by using cerium(IV) as oxidant in aqueous acetic acid medium (50% (v/v)) in the presence of added sulphuric acid. The reaction was found to be almost negligible in the absence of added sulphuric acid. The reaction was found to take place smoothly in the presence of added sulphuric acid. Further the concentration of sulphuric acid was maintained constant in the reactions where comparison of the results was made. The reaction was found to follow overall second order; first order each in substrate and oxidant.

The rate constants for the different substrates are given in Table 1. An examination of the rate constants for the oxidation of 2-aryl-*trans*-decahydroquinolin-4-ones (**1** to **3** where there is no methyl group in 3-position) with those of corresponding 3-methyl-2-aryl-*trans*-decahydroquinolin-4-ones (**4** and **5**, where there is methyl group in 3-position) reveals that the latter series of compounds, i.e. **4** and **5** were oxidised at a much slower rate than former series of compounds **1** to **3**.

**Table 1.** Second order rate constants of the oxidation of substituted 2-aryl-*trans*-decahydroquinolin-4-ones by cerium(IV)AcOH/H<sub>2</sub>O = 50% (v/v); temperature 30°C; [H<sup>+</sup>] = 4.0N

Compound	$k_2 \times 10^3$ (dm <sup>3</sup> mol <sup>-1</sup> s <sup>-1</sup> )
<b>1</b> 2-ph-4-one	1.19 ± 0.04
<b>2</b> 2-( <i>p</i> -tolyl)-4-one	1.07 ± 0.02
<b>3</b> 2-( <i>p</i> -OMe)-4-one	1.23 ± 0.01
<b>4</b> 3-Me-2-ph-4-one	0.25 ± 0.02
<b>5</b> 3-Me-2- <i>p</i> -tolyl-4-one	0.03 ± 0.02

A similar trend was also reported, while studying the oxidation of 2,6-diaryl-4-piperidin-4-ones by using different oxidising agents like Cr(V) (Ref. 23), Mn(III) (Ref. 18), Pb(IV) (Ref. 24), Tl(III) (Ref. 25), V(V) (Ref. 17), etc.

The effect of 3-methyl substituent is attributed to the steric approach of the reagent in the transition state and further the hydrogen atom at 3-position being less acidic and hence the rates of oxidation of these compounds (**4** and **5**) are found to be lower than those of compounds **1** to **3**.

The introduction of electron-releasing and electron-withdrawing substituents in the aryl group at *ortho*- and *para*-positions was found to give better understanding of relation between structure and reactivity. Substitution at *ortho*- and *para*-positions of aryl ring is expected to produce little effect on the rate of oxidation, because aryl ring is far away from the reaction centre. However, it was observed that the substituents at *ortho*- and *para*-positions in benzene ring played a vital role on oxidation rates. This may be mainly due to the polar effect exerted by the substituents. The electron-releasing substituents increased the rate of oxidation. The rate of oxidation of *p*-OMe-ketone (**3**, Table 1) was higher than any of the other ketones under investigation.

The rate of oxidation of 2-(*p*-OMe)-2-phenyl-*trans*-decahydroquinolin-4-ones was found to be higher when compared with the rate of oxidation of compounds (**1** to **3**). This observation is quite similar to the observation made by Satyanarayana et al.<sup>25</sup> while studying the oxidation of 2-aryl-*trans*-decahydroquinolin-4-ones by thallium(III) (Table 2).

**Table 2.** Second order rate constants of the oxidation of substituted 2-aryl-*trans*-decahydroquinolin-4-ones by thallium(III)AcOH/H<sub>2</sub>O = 80% (v/v); temperature 35°C; [H<sup>+</sup>] = 4.0 N

S. No	Compound	$k_2 \times 10^3$ (dm <sup>3</sup> mol <sup>-1</sup> s <sup>-1</sup> )
<b>1</b>	2-ph-4-one	8.44 ± 0.09
<b>2</b>	2-( <i>p</i> -tolyl)-4-one	8.47 ± 0.13
<b>3</b>	2-( <i>p</i> -OMe)-4-one	11.22 ± 0.01
<b>4</b>	3-Me-2-ph-4-one	1.39 ± 0.04
<b>5</b>	3-Me-2- <i>p</i> -tolyl-4-one	1.44 ± 0.07

In product analysis, the reaction was carried out following the methods already given in the experimental part. The completion of the reaction was confirmed by comparison of TLC of starting material with reaction mixtures. It was found that the product is not confirming to any particular molecular mass and probably is a mixture along with the reactant. Attempts to isolate the product using different types of columns were not successful. Though a pure sample of the product could not be isolated experimental observations of the molecular mass were taken to predict the possible product obtained in these reactions.

The oxidation kinetics was carried out by varying the composition of solvent, sulphuric acid concentration. These values are given in Tables 3 and 4. With increasing the concentration of acid, the rate of oxidation was found to increase (Table 3). The increase in the oxidation potential of such reagents is probably responsible for increase in the rate of oxidation.

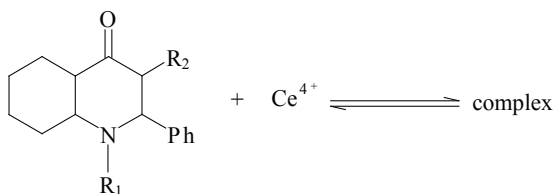
**Table 3.** Effect of  $[H^+]$  on rate of oxidation of 2-*p*-tolyl-*trans*-decahydroquinolin-4-one by cerium(IV) 50% AcOH; temperature = 35°C

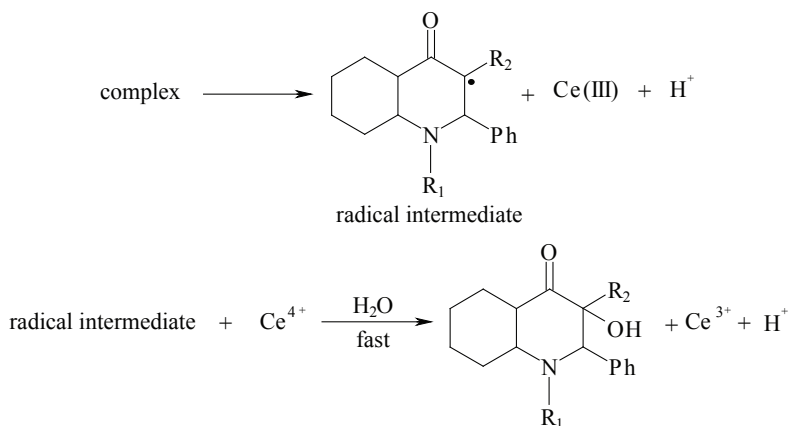
Variation in $[H^+]$	$k_2 \times 10^2$ ( $dm^3 mol^{-1} s^{-1}$ )
3.0 N	$7.36 \pm 0.07$
4.0 N	$10.46 \pm 0.01$
5.0 N	$15.08 \pm 0.07$

**Table 4.** Effect of variation in % of AcOH/H<sub>2</sub>O on the rate of oxidation of 2-*p*-tolyl-*trans*-decahydroquinolin-4-one by cerium(IV)  $[H^+] = 4.0N$ ; temperature 35°C

Variation in % of AcOH/H <sub>2</sub> O	$k_2 \times 10^2$ ( $dm^3 mol^{-1} s^{-1}$ )
40	$6.75 \pm 0.01$
50	$10.46 \pm 0.01$
60	$24.44 \pm 0.12$

The rate of oxidation was found to increase with increase in acetic acid concentration in the solvent medium (Table 4). This effect is attributed to the formation of enolic form which participated in the oxidation. Further as expected the rate of oxidation was found to increase with increase in temperature. Though the results reported in this investigation were not exhaustive the probable scheme of oxidation was given below.





The work in respect of these compounds is in progress to find more experimental evidence to confirm the mechanism of the oxidation.

## ACKNOWLEDGEMENTS

The authors are highly thankful to Acharya Nagarjuna University, Nagarjunanagar, Guntur, AP, for financial support.

## REFERENCES

1. B. SINGH, L. PANDEY, J. SHARMA, S. M. PANDAY: Mechanism of Oxidation of Some Aliphatic Ketones by N-bromosuccinimide in Acidic Media. *Tetrahedron*, **38**, 169 (1982).
2. D. S. MAHADEVAPPA, P. SWAMY: Kinetics of Oxidation of Aliphatic Ketones with Bromamine-T in Acid Medium. *Bull Chem Soc Jpn*, **61** (2), 543 (1988).
3. K. SINGH, J. N. TIWARI, S. P. MUSHRAN: Kinetics and Mechanism of Oxidation of Diethyl Ketone by N-bromosuccinimide. *Int J Chem Kinet*, **10**, 995 (1978).
4. T. CHIBA, H. SAKAGAMI, M. MURATA, M. OKIMOTO: Electrolytic Oxidation of Ketones in Ammoniacal Methanol in the Presence of Catalytic Amounts of KI. *J Org Chem*, **60**, 6764 (1995).
5. M. PECHAL, J. VOJTKO, J. KUBENA, M. HRUSOVSKY: Kinetics of the Oxidation of Aliphatic Ketones by Thallic Salts in Sulfuric Acid Medium. *React Kinet Catal L*, **20** (1-2), 151 (1982).
6. D. S. MAHADEVAPPA, K. MOHAN, S. ANANDA: Oxidation of Aliphatic Ketones by Bromamine-B: A Kinetic Study. *Tetrahedron*, **42** (17), 4857 (1986).
7. S. P. MUSHRAN, A. K. BOSE, J. N. TIWARI: Kinetic Study of Oxidation of Cycloheptanone by N-bromosuccinimide. *Monatsh Chem*, **107**, 1021 (1976).
8. K. SINGH, L. PANDEY, S. P. MUSHRAN: Kinetics of N-bromosuccinimide Oxidation of Cyclooctanone in Acid Media. *Indian J Chem*, **16A**, 875 (1978).
9. V. KARNOJITZKY: Oxidation of Ketones by Molecular Oxygen. *Russ Chem Rev*, **50**, 888 (1981).
10. Y. OGATA, Y. SAWAKI: Kinetics of the Baeyer-Villiger Reaction of Aromatic Ketones with Perbenzoic Acid. *J Org Chem*, **37** (19), 2953 (1972).
11. G. MANIVANNAN, P. MARUTHAMUTHU: Kinetics and Mechanism of Oxidation of Aliphatic and Aromatic Ketones by Peroxomonosulphate. *J Chem Soc Perk Trans*, **2**, 565(1986).
12. N. C. KHANDUAL, K. K. SATPATHY, P. L. NAYAK: Kinetics of Thallium (III) Oxidation of Aromatic Ketones. *P Math Sci*, **77** (4), 163 (1973).

13. S. R. ANNAPOORNA, M. PRASAD RAO, B. SETHURAM: Effect of Multiple Substituents on Oxidation of Phenyl Styryl Ketone and Its Substituted Analogs by V(V) in Acidic Medium: A Kinetic Study. *Indian J Chem*, **37B**, 868 (1998).
14. E. F. J. de VRIES, L. PLOEG, M. COLAO, J. BRUSSEE, A. VANDER GEN: Enantio Selective Oxidation of Aromatic Ketones by Molecular Oxygen, Catalysed by Chiral Monoaza-Crown Ethers. *Tetrahedron-Asymmetr*, **6** (5), 1123 (1995).
15. R. KUMABE, H. NISHINO, M. YASUTAKE, V. AN-HA NGUYEN, K. KURO SAWA: A Study of Conformational Effects on Oxidation Kinetics of N-H and N-methyl-4-piperidones with N-bromosuccinimide: A Comparative Analysis. *Tetrahedron Lett*, **42**, 691 (2001).
16. K. SELVARAJ, V. P. SENTHILNATHAN, K. RAMALINGAM: Kinetics of Oxidation of Some Substituted 4-piperidones by Vanadium(V). *Indian J Chem*, **17A**, 589 (1979).
17. K. SELVARAJ, K. RAMALINGAM: Kinetic Behaviour of Some Substituted 4-piperidones towards Oxidation by Vanadium(V). *Indian J Chem*, **23B**, 388 (1984).
18. M. KRISHNA PILLAY, A. THIRUNAVUKKARASU: Kinetics of Oxidation of Some Substituted Piperidones by Acid Permanganate. *Indian J Chem*, **20B**, 583 (1981).
19. K. SELVARAJ, S. SANKARAN, B. PREMA, K. RAMARAJAN: Kinetics of Oxidation of Some 4-piperidones by Cerium(IV), *J Indian Chem Soc*, **65**, 723 (1988).
20. R. K. DHAR, R. VARDARAJAN: Kinetics and Mechanism of Oxidation of Some Substituted 4-piperidones by Pyridinium Fluorochromate (PFC). *Indian J Chem*, **30A**, 936 (1991).
21. K. R. MEENAL, R. SELVAMEENA: Kinetics and Mechanism of Oxidation of 3-methyl-2,6-diphenylpiperidin-4-one by Pyridinium Fluorochromate. *J Indian Chem Soc*, **69**, 303 (1992).
22. V. BALIAH, A. NATARAJAN: Synthesis of 2-aryl and 2-aryl-3-methyl-decahydroquinolin-4-ones. *Indian J Chem*, **20B**, 830 (1981).
23. K. R. MEENAL, P. ROOPAKALYANI: Kinetic Behaviour of Some Substituted 4-piperidones towards Oxidation by Aqueous Acidic CrO<sub>3</sub>, *J Indian Chem Soc*, **65**, 624 (1988).
24. T. R. PADMINI: A Systematic Study on the Kinetics and Mechanism of Oxidation of Some Substituted 2,6-diarylpiperidin-4-ones by Pb(IV). Ph. D. Thesis, Bharathidasan University, 1988.
25. Ch. VIJAYASARADHI, R. S. C. RAO, B. HARI BABU, P. V. V. SATYANARAYANA: Kinetics of Oxidation of 2-aryl-*trans*-decahydroquinolin-4-ones by Thallium(III). *Oxid Commun*, **33** (2), 371 (2010).

*Received 26 May 2011*  
*Revised 18 August 2011*

**OXIDATION OF 2,5-di-*tert*-BUTYLHYDROQUINONE.  
INVESTIGATION OF ELECTROCHEMICALLY-INDUCED  
*para*-BENZOQUINHYDRONE FORMATION**

D. NEMATOLLAHI<sup>a\*</sup>, S. S. H. DAVARANI<sup>b</sup>, P. MIRAHMADPOUR<sup>c</sup>

<sup>a</sup>*Faculty of Chemistry, Bu-Ali Sina University, Hamedan, Zip Code 65178–38683, Iran*

*E-mail: nemat@basu.ac.ir*

<sup>b</sup>*Department of Chemistry, Shahid Beheshti University, Tehran, Iran*

<sup>c</sup>*Department of Chemistry, Faculty of Science, Arak Branch, Islamic Azad University, Arak, Iran*

**ABSTRACT**

Electrochemical oxidation of 2,5-di-*tert*-butylhydroquinone (**1**) has been studied in acetonitrile–water mixtures using cyclic voltammetry and controlled-potential coulometry. The results indicate that anodically generated 2,5-di-*tert*-1,4-benzoquinone (**1ox**) participates in non-covalently linked interactions with **1** converts to a new *para*-benzoquinhydrone (**2**). The structure of formed *para*-benzoquinhydrone (**2**) was characterised by <sup>1</sup>H NMR, <sup>13</sup>C NMR, MS and IR. In this work we derived a new *para*-benzoquinhydrone type complex (**2**) based on electrochemical oxidation of 2,5-di-*tert*-butylhydroquinone at carbon electrode in an undivided cell.

*Keywords:* cyclic voltammetry, electrochemical synthesis, controlled-potential coulometry, 2,5-di-*tert*-butylhydroquinone, *para*-benzoquinhydrone.

**AIMS AND BACKGROUND**

Electrochemistry provides a versatile means for the selective reduction and oxidation of organic compounds<sup>1,2</sup>. Unique selectivity due to *in situ* formation of an active species at the interface, green condition, inversion in polarity by transfer of an electron and variability, in product formation by the control of the electric potential are some of the advantages of electrosynthesis<sup>3–10</sup>. *para*-Quinhydrone, a 1:1 quinonehydroquinone, is a well-known molecular charge transfer complex<sup>11–15</sup>. In this complex, the charge transfer interactions between the electron donor (hydroquinone) and the electron acceptor (*p*-quinone) primarily stabilise the complex while the hydrogen bonds provide

---

\* For correspondence.

additional stability both in the solid state and in solution<sup>11–15</sup>. In this direction, recently, we have studied electrochemical oxidation of 3,5-di-*tert*-butylcatechol and derived a novel *ortho*-benzoquinhydrone complex<sup>16</sup>. In a continuation of our efforts to develop the synthesis of benzoquinhydrone complexes herein we wish to describe a simple protocol for the synthesis of a new *para*-benzoquinhydrone complex via electrochemical oxidation of 2,5-di-*tert*-butyl-1,4-hydroquinone (**1**). The major advantages of this paper is investigating the electrochemical oxidation of 2,5-di-*tert*-butyl-1,4-hydroquinone (**1**) in various acetonitrile–water mixtures using cyclic voltammetry and controlled-potential coulometry. The results show that the final oxidation product is dependent on the ratio of organic solvent in mixture. In water–acetonitrile (20:80 v/v) or %100 acetonitrile, the final product is 2,5-di-*tert*-butyl-1,4-benzoquinone (**1ox**) whereas in water–acetonitrile (80:20) or more, the main product is a *para*-benzoquinhydrone type complex (**2**).

## EXPERIMENTAL

*Apparatus.* Cyclic voltammetry and preparative electrolysis were performed using a  $\mu$ Autolab potentiostat/galvanostat type III. The working electrode which is used in the voltammetry experiment was a glassy carbon disk (1.8 mm diameter), and Pt wire was used as a counter electrode. The working electrode used in the voltammetry experiment was a glassy carbon disc (1.8 mm diameter) and platinum wire (2 mm diameter and 1.6 cm length) was used as the counter electrode. The working electrode potentials were measured versus the Ag/AgCl (3 M) as a reference electrode (all electrodes were obtained from Metrohm). The working electrode used in controlled-potential coulometry was a carbon rod (6 mm diameter and 4 cm length) and macroscale electrolysis was an assembly of 3 carbon rods (8 mm diameter and 6 cm length), and a Ag/AgCl (3 M) reference electrode. The pH was measured using a Metrohm pH meter 744 with a combined glass electrode.

*Reagents.* 2,5-Di-*tert*-butylhydroquinone was reagent-grade material from E. Merck. Phosphate salts, solvents, and reagents were of pro-analysis from E. Merck. These chemicals were used without further purification.

*Electroorganic synthesis of 1ox and 2.* For the synthesis of **2**, 100 ml mixture of water–acetonitrile (80:20 v/v) of phosphate buffer (pH = 7.2,  $c = 0.2$  M) containing 1 mmol of 2,5-di-*tert*-butyl-1,4-hydroquinone (**1**) {<sup>1</sup>H NMR (300 MHz, DMSO- $d_6$ ):  $\delta$  1.29 (s, *tert*-butyl, 18H), 6.60 (s, catecholic, 2H), 8.36 (s, OH, 2H)} was electrolysed at 0.35 V versus Ag/AgCl (3 M)), in an undivided cell. The electrolysis was stopped when the current reached a value that was less than 5% of the initial value. The process was interrupted during the electrolysis and the graphite anode was washed in acetone in order to reactivate it. At the end of electrolysis, the precipitated solid was collected by filtration and washed with a suitable mixture of water–acetonitrile (isolated yield 74%). IR (KBr,  $\text{cm}^{-1}$ ): 3422, 3064, 2961, 1648, 1596, 1531, 1481, 1409,

1369, 1260, 1183, 1124, 1077, 1018, 946, 878, 844, 793, 741, 601, 474;  $^1\text{H}$  NMR (300 MHz,  $\text{DMSO-}d_6$ ):  $\delta$  1.21 (s, *tert*-butyl of quinone ring) and 1.28 (s, *tert*-butyl of diol ring) (36H), 6.47 (s, quinonic) and 6.58 (s, catecholic) (4H), 8.32 (s, OH, about 2H);  $^{13}\text{C}$  NMR (75 MHz,  $\text{DMSO-}d_6$ ):  $\delta$  29.2, 29.8, 34.1, 34.7, 115.0, 133.1, 133.7, 147.9, 153.9, 188.5; MS (EI):  $m/z$  (relative intensity); 222 ( $\text{M}^+$ , 40), 207 (100), 137 (15), 115 (12), 91 (14), 57 (16).

For synthesis of **10x**, a solution (ca. 100 ml) of phosphate buffer (pH = 7.2,  $c = 0.2$  M) in water–acetonitrile (20:80 v/v) including 1 mmol of **1** was electrolysed. Other conditions are the same as previous case. IR (KBr,  $\text{cm}^{-1}$ ): 3064, 2991, 2973, 2869, 1649, 1597, 1481, 1459, 1390, 1367, 1349, 1259, 1183, 1076, 1018, 947, 842, 741, 633, 471;  $^1\text{H}$  NMR (300 MHz,  $\text{DMSO-}d_6$ ):  $\delta$  1.21 (s, *tert*-butyl of quinone ring, 18H), 6.47 (s, quinonic, 2H);  $^{13}\text{C}$  NMR (75 MHz,  $\text{DMSO-}d_6$ ):  $\delta$  29.3, 34.6, 133.6, 154.4, 188.4; MS (EI):  $m/z$  (relative intensity); 220 ( $\text{M}^+$ , 25), 205 (37), 177 (38), 163 (67), 135 (36), 91 (41), 67 (38), 41 (100).

## RESULTS AND DISCUSSION

Cyclic voltammetry of 1 mM of 2,5-di-*tert*-butylhydroquinone (**1**) in water (phosphate buffer, pH = 7.2,  $c = 0.2$  M)/acetonitrile (80:20 v/v) solution shows one anodic ( $A_1$ ) at 0.04 V and the corresponding cathodic peak ( $C_1$ ) at  $-0.23$  V versus Ag/AgCl (3 M), respectively, which is related to the transformation of 2,5-di-*tert*-butylhydroquinone (**1**) to 2,5-di-*tert*-butyl-1,4-benzoquinone (**10x**) and vice versa, within a quasi-reversible 2-electron process (Fig. 1). A peak current ratio ( $I_{\text{pC1}}/I_{\text{pA1}}$ ) of nearly unity can be considered as a criterion for the stability of **10x** produced at the surface of electrode under the experimental conditions. On the other hand, any hydroxylation<sup>17–19</sup> or dimerisation<sup>20,21</sup> reactions are too slow to be observed on the time scale of cyclic voltammetry.

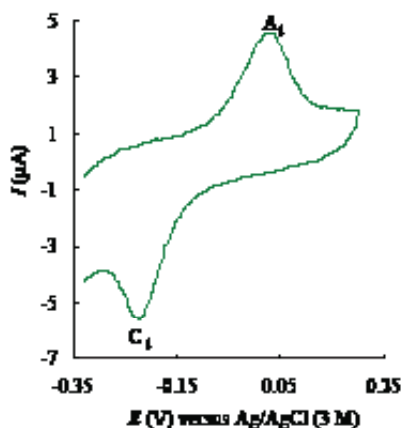


**Fig. 1.** Cyclic voltammogram of 1.0 mM 2,5-di-*tert*-butylhydroquinone (**1**), at glassy carbon electrode, in water (0.2 M phosphate buffer, pH = 7.2,  $c = 0.2$  M)/acetonitrile (80:20 v/v), scan rate: 100  $\text{mV s}^{-1}$ ,  $t = 25 \pm 1^\circ\text{C}$



Controlled-potential coulometry was performed in water (phosphate buffer, pH = 7.2,  $c = 0.2$  M)/acetonitrile (80:20 v/v) solution containing 0.25 mmol of **1** at 0.35 V versus Ag/AgCl (3 M) electrode. Monitoring of the progress of the electrolysis was carried out by cyclic voltammetry (Fig. 2). It is shown that, proportionally to the advancement of coulometry, the anodic and cathodic peaks ( $A_1$  and  $C_1$ ) decreases and disappears when the charge consumption becomes about  $1e^-$  per molecule of **1**. These observations allow us to propose the path way illustration in the Scheme.

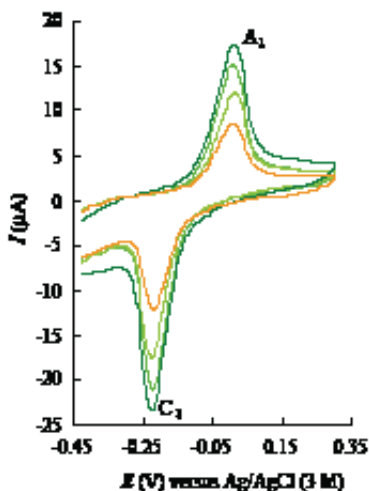
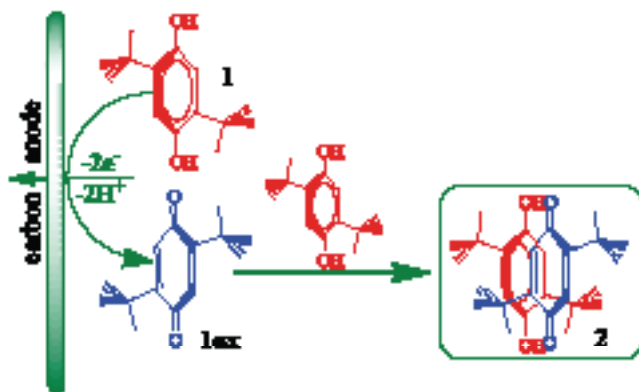


**Fig. 2.** Cyclic voltammograms of 0.25 mmol 2,5-di-*tert*-butylhydroquinone (**1**), in water (0.2 M phosphate buffer, pH = 7.2,  $c = 0.2$  M)/acetonitrile (80:20 v/v) during controlled-potential coulometry at 0.35 V versus SCE, scan rate;  $100 \text{ mV s}^{-1}$  and  $t = 25 \pm 1^\circ\text{C}$

Scheme  
Electrochemical oxidation of 2,5-di-*tert*-butylhydroquinone (**1**)



According to proposed pathway, in water–acetonitrile (80:20 v/v) solution the interaction of electrochemically generated **1ox** to **1**, leading to *para*-benzoquinhydrone **2**. While, in acetonitrile rich solutions (for example 20:80 v/v) final product of controlled potential coulometry of **1** is 2,5-di-*tert*-butyl-1,4-benzoquinone (**1ox**) that will be acquired after consumption of  $2e^-$  per molecule of **1**.

The quinhydrone electrode consists from a platinum dips into a solution saturated with quinhydrone. This electrode is a type of redox electrode which can be used to measure the pH of a solution in a chemical experiment. It provides an alternative to the commonly used glass electrode in a pH-meter. Here, in order to investigate the applicability of quinhydrone complex **2**, we have titrated HCl using  $\text{NH}_3$  in the presence of **2** (Fig. 3).

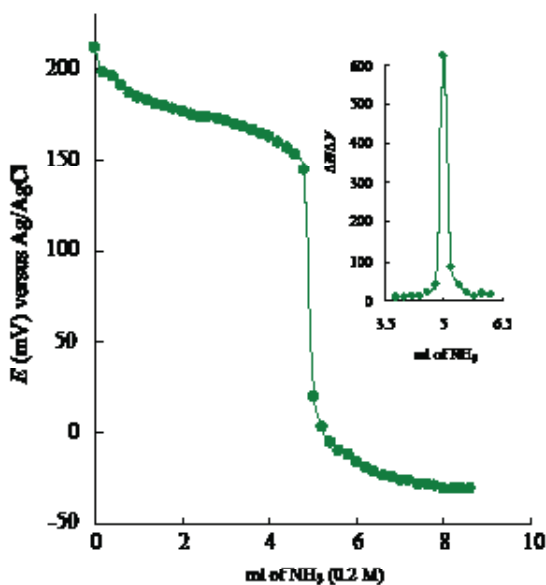


**Fig. 3.** Potentiometric titration curve of 5 ml, hydrochloric acid (0.2 M) with ammonia (0.2 M), using quinhydrone complex **2**

This confirms applicability of quinhydrone complex **2** as can be satisfactorily applied to the end-point determination of the titrations of bases or acids.

## CONCLUSIONS

The present results of this work show that 2,5-di-*tert*-butylhydroquinone (**1**) is oxidised in water–acetonitrile mixtures to its corresponding stable *p*-benzoquinone **1ox**. The non-covalently linked interactions of **1** with **1ox** lead to the formation of new

*para*-benzoquinhydrone (2). Also, this quinhydrone electrode can be used for the determination of the end point of acidimetric titrations of some acids and bases.

## ACKNOWLEDGEMENTS

The authors acknowledge the Bu-Ali Sina University Research Council and Center of Excellence in Development of Chemical Methods (CEDCM) for support of this work.

## REFERENCES

1. J. M. SAVEANT: Elements of Molecular and Biomolecular Electrochemistry. Willey-VCH, New Jersey, 2006.
2. H. LUND, O. HAMMERICH: Organic Electrochemistry. 4th ed. Marcel Dekker, New York, 2001.
3. T. SHONO: Electroorganic Synthesis. Academic Press, San Diego, 1991.
4. D. NEMATOLLAHI, A. AMANI, E. TAMMARI: Electrosynthesis of Symmetric and Highly Conjugated Benzofuran via a Unique ECECC Electrochemical Mechanism: Evidence for Predominance of Electrochemical Oxidation as against Intramolecular Cyclization. *J Org Chem*, **72**, 3646 (2007).
5. A. MALEKI, D. NEMATOLLAH: An Efficient Electrochemical Method for the Synthesis of Methylene Blue. *Electrochem Commun*, **11**, 2261 (2009).
6. D. NEMATOLLAHI, MALEKI: Electrochemical Oxidation of N,N-dialkyl-*p*-phenylenediamines in the Presence of Arylsulfonic Acids. An Efficient Method for the Synthesis of New Sulfonamide Derivatives. *Electrochem Commun*, **11**, 488 (2009).
7. D. NEMATOLLAHI, H. SHAYANI-JAM: Kinetic Study of Electrochemically Induced Michael Reactions of *o*-quinones with Meldrum's Acid Derivatives. Synthesis of Highly Oxygenated Catechols. *J Org Chem*, **73**, 3428 (2008).
8. D. NEMATOLLAHI, M. S. WORKENTIN, E. TAMMARI: Electrochemical Oxidation of Catechol in the Presence of Cyclopentadiene. Investigation of Electrochemically Induced Diels–Alder reactions. *Chem Commun*, 1631 (2006).
9. D. NEMATOLLAHI, M. RAFIEE: Diversity in Electrochemical Oxidation of Dihydroxybenzoic Acids in the Presence of Acetylacetone. A Green Method for Synthesis of New Benzofuran Derivatives. *Green Chem*, **7**, 638 (2005).
10. D. NEMATOLLAHI, M. RAFIEE, L. FOTOUHI: Mechanistic Study of Homogeneous Reactions Coupled with Electrochemical Oxidation of Catechols. *J Iran Chem Soc*, **6**, 448 (2009).
11. B. R. EGGINS, J. Q. CHAMBERS: Proton Effects in the Electrochemistry of the Quinone Hydroquinone System in Aprotic Solvents. *J Electrochem Soc*, **117**, 186 (1970).
12. R. E. MOSER, H. G. CASSIDY: Electron-Transfer Polymers. XXV. On 'Hydrophobic Bonding'. The Effect of Solvent on Quinhydrone. *J Am Chem Soc*, **87**, 3463 (1965).
13. F. FOSTER: Organic Charge–Transfer Complexes. Academic Press, New York, 1969.
14. M. A. SLIFKIN: Charge–Transfer Interactions of Biomolecules. Academic Press, New York, 1971.
15. F. GUTMANN, C. JOHNSON, H. KEYZER, J. MOLNAR: Charge–Transfer Complexes in Biological Systems. Marcel Dekker, New York, 1997.
16. D. NEMATOLLAHI, H. SHAYANI-JAM: Electrochemical Oxidation of 3,5-di-*tert*-butylcatechol: Synthesis and Characterization of the Formed *ortho*-Benzoquinhydrone Derivative. *Electrochim Acta*, **51**, 6388 (2006).

17. L. PAPOUCHADO, G. PETRIE, R. N. ADAMS: Anodic Oxidation Pathways of Phenolic Compounds: Part I. Anodic Hydroxylation Reactions. *J Electroanal Chem*, **38**, 389 (1972).
18. L. PAPOUCHADO, G. PETRIE, J. H. SHARP, R. N. ADAMS: Anodic Hydroxylation of Aromatic Compounds. *J Am Chem Soc*, **90**, 5620 (1968).
19. T. E. YOUNG, J. R. GRISWOLD, M. H. HULBERT: Melanin. I. Kinetics of the Oxidative Cyclization of Dopa to Dopakinone. *J Org Chem*, **39**, 1980 (1974).
20. D. RAYN, A. YUEH, C. WEN-YU: The Electrochemical Oxidation of Substituted Catechols. *J Electrochem Soc*, **127**, 1489 (1980).
21. D. NEMATOLLAHI, M. RAFIEE, A. SAMADI-MAYBODI: Mechanistic Study of Electrochemical Oxidation of 4-*tert*-butylcatechol. A Facile Electrochemical Method for the Synthesis of New Trimer of 4-*tert*-butylcatechol. *Electrochim Acta*, **49**, 2495 (2004).

*Received 15 November 2010*

*Revised 23 December 2010*

## STUDY AND CLASSIFICATION OF VEGETABLE OILS USING THE FOURIER TRANSFORM INFRARED SPECTROSCOPY

K. GEORGIEVA, P. PETKOV, Y. DENEV\*

*Prof. Asen Zlatarov University of Bourgas, 1 Prof. Yakimov Street, 8010 Bourgas, Bulgaria*

*E-mail: ydenev@abv.bg*

### ABSTRACT

Six commercial vegetable oils products of different origin and composition were studied. Using methods of the Fourier transform infrared spectroscopy (FTIR), spectra of oil samples were recorded in the mid-region 4000–400  $\text{cm}^{-1}$ . A detailed analysis of absorption bands in the spectra of vegetable oils was performed. A principal component analysis (PCA) as a statistical tool was used for exclusion of the unnecessary information in a studied spectrum. Using PCA 2 characteristic absorption bands, which can distinguish different studied edible oils (1377 and 1163  $\text{cm}^{-1}$ ) were observed. Using known methods values for free fatty acids content in the interval 1.5 to 5% were calculated for different oils. It is found that the analysed edible oils have high unsaturation degree (up to 90%) and this fact was proven by scientific computing methods using IR spectral data. Also *trans*-double bonds content in the vegetable oils was calculated using known equations and values from 20 to 80 % were obtained. The possibility of express analysis of vegetable oils and their derivatives avoiding the necessity of using expensive and slow chemical methods using only mid-infrared spectroscopy was proven.

*Keywords:* vegetable oils, the Fourier transform infrared spectroscopy (FTIR), unsaturation degree, *trans*-content, principal component analysis.

### AIMS AND BACKGROUND

The infrared region of the electromagnetic spectrum extends from 14 000 to 50  $\text{cm}^{-1}$  and is divided into 3 separate areas: the far-infrared from 400 to 50  $\text{cm}^{-1}$ , the mid-infrared region from 4000 to 400  $\text{cm}^{-1}$ , which is the most interesting region because the absorption bands are due to the vibration of functional groups in organic compounds, and near-infrared region from 14 000 to 4000  $\text{cm}^{-1}$  (Refs 1 and 2).

---

\* For correspondence.

An IR spectrum usually contains more information than is actually useful<sup>3</sup>. Often the entire spectrum is acquired in the interest of obtaining the position or absorbance values of a few peaks. The useful information from IR spectral data is not easy to identify. The variation in the IR spectra of different vegetable oils is subtle, and it is hard to classify different oils by visual comparison of these spectra. Using peak positions as variables in a principal component analysis (PCA), the different vegetable oils can be correctly classified<sup>3,4</sup>.

From literature<sup>5</sup> a method for simultaneous determination of *cis*- and *trans*-double bonds content in fats and oils using the FTIR is well known. The obtained mathematical model has great performance in a wide interval of *trans*-content from 0 to 15%. Some authors<sup>6</sup> have developed methods for determination of free fatty acids in fats and oils from IR spectroscopic data and this approach overlaps the concentration interval 0.2–8%.

It is known an application of principal component analysis methods in IR spectra processing for classification of fats and oils depending on their origin<sup>7</sup>. Mainly, these methods involve interest because are quick and do not need chemical reagent usage.

The overall unsaturation degree of vegetable oils is becoming very important in relation to their use as a renewable feedstock and biodiesel production. Most important aspect is the knowledge of the nature and amount of the unsaturation, which is the main reason for the differences in oxidative stability of the obtained esters used as biofuel.

The aim of present work is to study 6 different by their origin and composition vegetable oils and to determine overall unsaturation degree, free fatty acid content, *trans*-double bonds content and to assess differences between different samples. This was carried out using modern statistical techniques such as principal components analysis. The obtained complete description of the studied oils is made only by the methods of infrared spectroscopy and could be used as an express method for assessment of the quality and stability of vegetable oils and their derivatives.

## EXPERIMENTAL

Six commercial vegetable oils products were supplied from local supermarkets. The sample collection included: sunflower oil, designated (1); soybean oil (2); extra-virgin olive oil (3); palm oil (4); corn oil (5) and castor oil (6). Figure 1 shows the fatty acids composition of these samples as given by the manufacture industry. As it is clearly viewed the studied oils are constituted of fatty triglyceride esters with different substitution patterns, lengths and degrees of unsaturation of the chains.

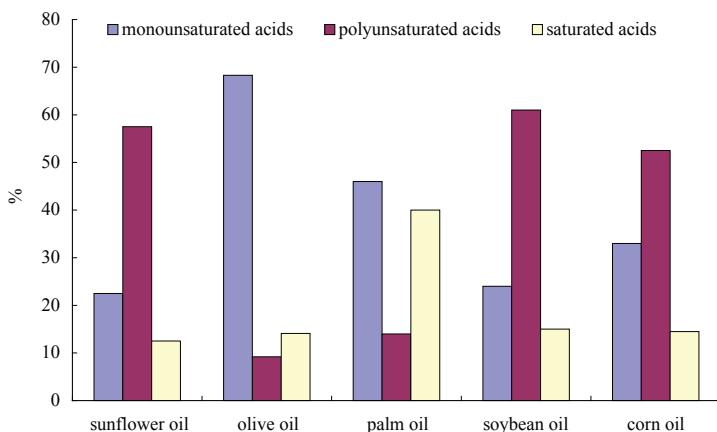


**Fig. 1.** Composition of the analysed vegetable oils given by the producers

The infrared spectra of the vegetable oils were recorded with a Fourier transform infrared spectrometer, Bruker Tensor 27, interfaced to a personal computer operating under Windows-based software OPUS 6.5. All spectra were recorded from 4000 to 400  $\text{cm}^{-1}$  with resolution better than 4  $\text{cm}^{-1}$ , co-adding 32 interferograms with frequency resolution better than 0.01  $\text{cm}^{-1}$ . A thin film of a small amount of each sample (approximately 2  $\mu\text{l}$ ) was deposited between 2 discs of KBr to avoiding the presence of air. The frequency of each band was obtained automatically using command of the instrumentation software OPUS 6.5.

The association of bands to specific functional groups was made by comparison of the peak frequencies with literature data for vibration mode in fats and oils<sup>8</sup>.

The absorption in some bands was automatically measured by building a base line from 3750 to 2472  $\text{cm}^{-1}$  to avoid experimental errors as is known from literature<sup>8</sup>.

The principal component analysis was carried out using Minitab Software 16.0. Our worksheet consists initially of 7 columns and 6 rows. Each column consists of the peak positions ( $\text{cm}^{-1}$ ) at which a specific peak appears. Each row corresponds to an individual spectrum.

## RESULTS AND DISCUSSION

In Fig. 2 the Fourier transform infrared spectra of the studied vegetable oils are shown.

All spectra except castor oil show small band at 3472  $\text{cm}^{-1}$  which is associated with the overtone of the glyceride ester carbonyl absorption (Fig. 2). Unlike the other edible oils in the spectrum of castor oil an absorption band at 3444  $\text{cm}^{-1}$  is detected. Similar peaks absent in the spectra of other oils and proves the presence of hydroperoxides<sup>6</sup>.

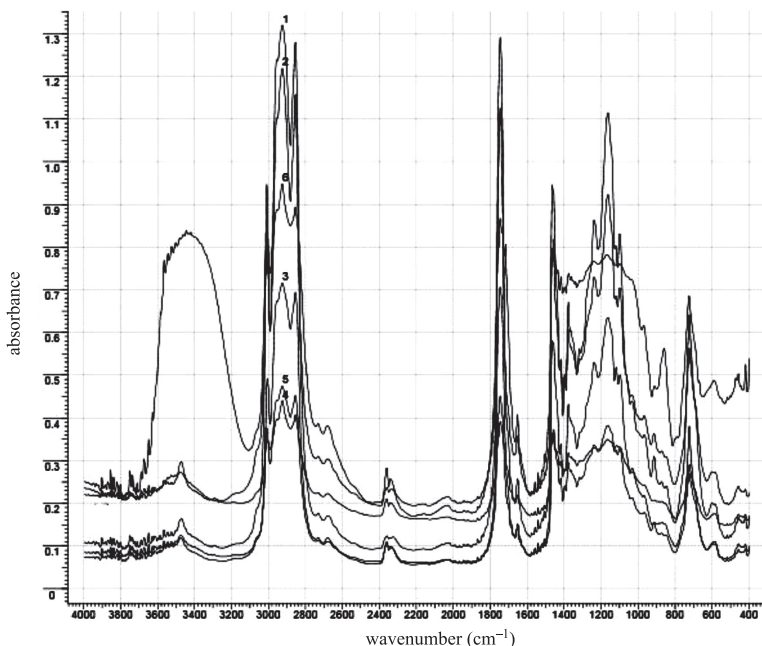


**Fig. 2.** Fourier transform infrared spectra of the analysed vegetable oils

Unlike animal fats in the spectra of the vegetable oils is absent a band at approximately  $3450\text{ cm}^{-1}$  which is described by the stretching vibration of OH-group of intermolecular-bonded water<sup>9</sup>.

Strong bands in the region  $3009\text{--}3006\text{ cm}^{-1}$  are observed in the spectra of all studied oil samples (Fig. 2). This absorption is due to the stretching vibration of the *cis*-olefinic double bonds<sup>10</sup>. Analysing the spectra of all studied vegetable oils a band at  $2925\text{ cm}^{-1}$  is observed. This band confirms methyl asymmetrical stretching vibration in samples. Simultaneously, a band at  $2853\text{ cm}^{-1}$  due to the methylene symmetrical stretching is present in all samples (Fig. 2). Two weak bands, probably due to the Fermi resonance of the carbonyl group, are observed at  $2731$  and  $2679\text{ cm}^{-1}$ . An interesting fact is the absence of band at  $2731\text{ cm}^{-1}$  in the extra-virgin olive oil sample (Fig. 2). In all samples C=O group of triglycerides shows a stretching vibration band at approximately  $1746\text{ cm}^{-1}$  and small shoulder at  $1711\text{ cm}^{-1}$ , which is assigned to free fatty acids<sup>11</sup>.

From literature<sup>6</sup> a deep analysis of the infrared spectra depending on free fatty acid (FFA) content is well known. Careful examination of the relation between absorption at  $1711\text{ cm}^{-1}$  and FFA content indicated that the relationship is not linear but has a slight curvature. The non-linear effect may be attributed to the monomer–dimer equilibrium, which is not accounted, because only the absorption by dimers is meas-



ured and related directly to the FFA content<sup>6</sup>. The calculation for the FFA content of the studied oils was made using equation (1).

$$\text{FFA} = -0.044 + 4.9594A + 1.5446A^{1/2} \quad (1)$$

where  $A$  (relative units) is absorption at  $1711 \text{ cm}^{-1}$ .

The calculated values of free fatty acids content are shown in Table 1.

**Table 1.** Calculated values of free fatty acids content

Vegetable oil	Absorption ( $1711 \text{ cm}^{-1}$ )	Free fatty acids content (%)
Sunflower oil	0.3871	2.83
Soybean oil	0.4434	3.18
Olive oil	0.2547	1.99
Palm oil	0.2840	2.18
Corn oil	0.2058	1.67
Castor oil	0.7094	4.77

In all samples, a small band at  $1654 \text{ cm}^{-1}$  can be detected. The C=C stretching mode of unconjugated olefins usually shows moderate to weak absorption at  $1667\text{--}1640 \text{ cm}^{-1}$  (Ref. 10). It is known that disubstituted *cis*-olefins absorb near  $1650 \text{ cm}^{-1}$ , and the absorption of this band is stronger than that of *trans*-olefins<sup>11</sup>. Some authors<sup>9</sup> explain the presence of peak at  $1650 \text{ cm}^{-1}$  by the deformation bands of OH group of water. The bands between  $1400$  and  $1000 \text{ cm}^{-1}$  are most difficult to assign. However, in this region, the differences to the eye in Fig. 2 are also the most significant<sup>10</sup>. At approximately  $1465 \text{ cm}^{-1}$ , all spectra show the scissoring band of the bending vibration of the methylene group. It is clear viewed that in the castor oil spectrum this absorption band is shifted to  $1457 \text{ cm}^{-1}$ . A strong band at  $1418 \text{ cm}^{-1}$  is observed in the spectra of extra-virgin olive oil, palm oil and castor oil. In the spectra of other vegetable oil such a band is absent. This band can be attributed to rocking vibrations of CH bonds of *cis*-disubstituted olefins. In the spectrum of sunflower oil a weak band at  $1400 \text{ cm}^{-1}$  is observed, which is difficult to assign, also a band at  $1377 \text{ cm}^{-1}$  could be due to symmetrical bending vibration of methyl group<sup>10</sup>.

In all samples twisting and wagging vibrations of the  $\text{CH}_2$  groups are observed in the region between  $1350$  and  $1150 \text{ cm}^{-1}$ , and these bands are generally appreciably weaker than those resulting from methylene scissoring.

Clearly viewed a band at  $1238 \text{ cm}^{-1}$  is observed in the spectra of all vegetable samples except the castor oil. At  $1163 \text{ cm}^{-1}$  band in all spectra are observed but in castor oil, this band is shifted to  $1171 \text{ cm}^{-1}$ . Peaks at  $1117 \text{ cm}^{-1}$  are recorded in the spectra of olive oil and palm oil while in the spectra of sunflower oil and olive oil, a band at  $1097 \text{ cm}^{-1}$  is observed. Some of them could be assigned to the stretching vibrations of the C–O group in esters<sup>11</sup>. This vibration consists of 2 asymmetric coupled vibrations C–C(=O)–O and O–C–, the former being more important. Some authors assign the band at  $1238 \text{ cm}^{-1}$  to bending vibration out-of-plane of a methylene group<sup>9</sup>.

In the spectra of soybean and castor oil 2 bands at 970 and 914  $\text{cm}^{-1}$  are observed, while in the spectra of sunflower and corn oil a single band at 914  $\text{cm}^{-1}$  occurs. The band at 970  $\text{cm}^{-1}$  is due to bending vibration out-of-plane of *trans*-disubstituted olefinic groups. Some authors<sup>12</sup> associate the band at 914  $\text{cm}^{-1}$  with bending vibration of *cis*-disubstituted olefinic groups, even though an olive oil and palm oil spectra do not show this band (Fig. 2).

Finally, at approximately 723  $\text{cm}^{-1}$  a strong band is observed as a result of the overlapping of the methylene rocking vibration and the out-of-plane bending vibrations of *cis*-disubstituted olefins<sup>11,13</sup>.

Using spectra of the 6 studied oils as a base 7 high intense bands are determined. They are used as variables in processing using principal components analysis (Table 2). The main goal of this task is to exclude the unnecessary information from the spectra of the vegetable oils.

**Table 2.** Values of characteristic bands frequencies used as variables in principal component analysis

Vegetable oil	Peak 1 ( $\text{cm}^{-1}$ )	Peak 2 ( $\text{cm}^{-1}$ )	Peak 3 ( $\text{cm}^{-1}$ )	Peak 4 ( $\text{cm}^{-1}$ )	Peak 5 ( $\text{cm}^{-1}$ )	Peak 6 ( $\text{cm}^{-1}$ )	Peak 7 ( $\text{cm}^{-1}$ )
Sunflower	3008.78	2923.92	2854.48	1463.89	1377.09	1163.01	723.26
Soybean	3008.78	2925.84	2854.48	1463.89	1377.09	1163.01	723.26
Olive	3004.92	2925.84	2854.48	1463.89	1377.09	1164.94	723.26
Palm	3006.85	2925.84	2854.48	1458.10	1363.50	1164.94	721.34
Corn	3008.78	2925.84	2854.48	1463.89	1396.38	1120.58	723.26
Castor	3008.78	2925.84	2854.48	1463.89	1396.38	1168.79	725.19

**Table 3.** Results of principal component analysis

Variables	Principal component 1	Principal component 2	Principal component 3
Peak 1	0.031	-0.048	-0.018
Peak 2	0.007	-0.003	-0.222
Peak 3	0	0	0
Peak 4	0.044	-0.140	0.956
Peak 5	0.463	-0.866	-0.150
Peak 6	-0.884	-0.464	-0.032
Peak 7	0.012	-0.114	0.111

From literature<sup>14-16</sup> methods for determination of unsaturation degree are well known. The first reference to the determination of the degree of unsaturation of fats and oils by means of infrared spectroscopy uses the ratio of absorbances of the olefinic (3020  $\text{cm}^{-1}$ ) and aliphatic (2857  $\text{cm}^{-1}$ ) CH-stretching vibration bands in the infrared spectra.

In Table 4 the frequencies of mentioned above characteristic bands and the absorbances at these bands are shown. The calculated value for the overall unsaturation degree shows good correlation between producer data and the obtained from spectral data results. The prove for the high degree of unsaturation in the 6 studied edible oils is the presence of very strong band at  $1746\text{ cm}^{-1}$ , which can be expressed by the stretching vibrations of C=O group in triglycerides. This band is one of best described in the vegetable oils with high unsaturation.

**Table 4.** Values of frequencies and absorption of bands at  $3010$  and  $2855\text{ cm}^{-1}$  and the calculated value of unsaturation degree

	Sunflower oil	Olive oil	Palm oil	Soybean oil	Corn oil	Castor oil
Band $3010\text{ cm}^{-1}$	3008.78	3004.92	3006.85	3008.78	3008.78	3008.78
Absorption ( $3010\text{ cm}^{-1}$ )	0.948	0.492	0.347	0.837	0.377	0.804
Band $2855\text{ cm}^{-1}$	2854.48	2854.48	2854.48	2854.48	2854.48	2854.48
Absorption ( $2855\text{ cm}^{-1}$ )	1.320	0.715	0.441	1.218	0.474	0.949
Calculated value of unsaturation (%)	0.74	0.71	0.85	0.72	0.83	0.90

The application of mid-infrared spectroscopy for determination of a *trans*-content in fats and oils is well known from literature<sup>17</sup>. This method is based on measurement of band absorption at  $970\text{ cm}^{-1}$ , which is associated with vibrations of isolated *trans*-bonds<sup>18</sup>.

The *trans*-content of studied vegetable oils was determined using one of the known from the literature methods<sup>18</sup>. The *trans*-absorption region is located at  $995\text{--}937\text{ cm}^{-1}$ . In this work two equations (2) and (3) for calculations of the *trans*-content were used measuring absorbances at  $966\text{ cm}^{-1}$  (Ref. 18).

$$\%trans = -3.917 + 131.276A_{966} \quad (2)$$

$$\%trans = -0.230 + 130.973A_{966} \quad (3)$$

where *%trans* is *trans*-content expressed as % trioleidin;  $A_{966}$  – the absorbance at  $966\text{ cm}^{-1}$ , relative to baseline drawn between  $995$  and  $937\text{ cm}^{-1}$ .

In Fig. 3, the calculated values of *trans*-content in the studied oil samples are presented. The oil with highest *trans*-content is castor oil and those with lowest – corn oil with values similar to these of extra-virgin olive oil.

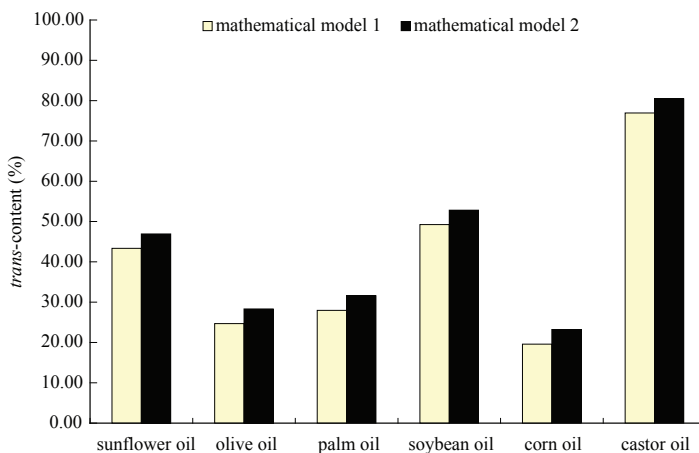


**Fig. 3.** Calculated values of *trans*-content in the studied vegetable oils

## CONCLUSIONS

The carried research clearly shows and proves the applicability of the Fourier transform infrared spectroscopy as a method for express analysis and detailed evaluation of the properties of different vegetable oils. The obtained data for the overall level of unsaturation, the content of free fatty acids and total *trans*-content correlate well with the data known from literature and those derived from the oil manufacture industry. Using advanced statistical methods such as principal components analysis a detailed analysis of spectral data and identification of the most informative and important bands for the classification of different vegetable oils were performed. Using principal component analysis 2 characteristic absorption bands which can distinguish different studied edible oils ( $1377$  and  $1163\text{ cm}^{-1}$ ) have been identified. This makes possible the classification of different vegetable oils and group the by certain sign of similarity.

The results clearly confirm the accuracy and the possibility of further assessment of other indicators of vegetable oils and their derivatives avoiding the necessity of using expensive and slow chemical methods.

## REFERENCES

1. B. STUART: Infrared Spectroscopy: Fundamentals and Applications. Wiley & Sons, Weinheim, 2004.
2. B. SMITH: Fundamentals of Fourier Transform Infrared Spectroscopy. CRC Press, New York, 2011.
3. D. RUSAK, L. BROWN, S. MARTIN: Classification of Vegetable Oils by Principal Component Analysis of FTIR Spectra. J Chem Educ, **80** (5), 541 (2003).
4. Y. LAI, E. KEMSLEY, R. WILSON: Potential of Fourier Transform Infrared Spectroscopy for the Authentication of Vegetable Oils. J Agric Food Chem, **42** (5), 1154 (1994).

5. H. LI, F. R. van der VOORT, J. SEDMAN, A. A. ISMAIL: Rapid Determination of *cis* and *trans* Content, Iodine Value, and Saponification Number of Edible Oils by Fourier Transform Near-infrared Spectroscopy. *J Am Oil Chem Soc*, **76** (4), 491 (1999).
6. A. A. ISMAIL, F. R. van der VOORT, G. EMO, J. SEDMAN: Rapid Quantitative Determination of Free Fatty Acids in Fats and Oils by Fourier Transform Infrared Spectroscopy. *J Am Oil Chem Soc*, **70** (4), 335 (1993).
7. N. DUPUY, L. DUPONCHEL, J. P. HUVENNE, B. SOMBRET, P. LEGRAND: Classification of Edible Fats and Oils by Principal Component Analysis by Fourier Transform Infrared Spectra. *Food Chem*, **57** (2), 245 (1996).
8. M. D. GUILLEN, N. CABO: Relationships between the Composition of Edible Oils and Lard and the Ratio of the Absorbance of Specific Bands of Their Fourier Transform Infrared Spectra. Role of Some Bands of the Fingerprint Region. *J Agric Food Chem*, **46**, 1788 (1998).
9. M. SAFAR, D. BERTRAND, P. ROBERT, M. F. DEVAUX, C. GENOT: Characterization of Edible Oils, Butters and Margarines by Fourier Transform Infrared Spectroscopy with Attenuated Total Reflectance. *J Am Oil Chem Soc*, **71**, 371 (1994).
10. M. D. GUILLEN, N. CABO: Characterization of Edible Oils and Lard by Fourier Transform Infrared Spectroscopy. Relationships between Composition and Frequency of Concrete Bands in the Fingerprint Region. *J Am Oil Chem Soc*, **74** (10), 1281 (1997).
11. R. M. SILVERSTEIN, F. X. WEBSTER, D. J. KIEMLE: *Spectrometric Identification of Organic Compounds*. Wiley & Sons, Weinheim, 2005.
12. F. R. van der VOORT, A. A. ISMAIL, J. SEDMAN: A Rapid Automated Method for the Determination of *cis* and *trans* Content of Fats and Oils by Fourier Transform Infrared Spectroscopy. *J Am Oil Chem Soc*, **72** (8), 873 (1995).
13. H. GUNZLER, H. BOCK: *IR-Spektroskopie. Eine Einführung*. Verlag Chemie, Weinheim, 1975.
14. M. D. GUILLEN, N. CABO: Infrared Spectroscopy in the Study of Edible Oils and Fats. *J Sci Food Agric*, **75**, 1 (1997).
15. A. AFRAN, E. J. NEWBERG: Analysis of the Degree of Unsaturation in Edible Oils by Fourier Transform Infrared Attenuated Total Reflectance Spectroscopy. *Spectrosc*, **6**, 31 (1991).
16. R. G. ARNOLD, T. E. HARTUNG: Infrared Spectroscopy Determination of the Degree of Unsaturation of Fats and Oils. *J Food Sci*, **36**, 166 (1971).
17. *Official Methods and Recommended Practices of the American Oil Chemists' Society*. 4th ed. American Oil Chemists' Society, Champaign, 1989.
18. J. SEDMAN, F. R. van der VOORT, A. A. ISMAIL, P. MAES: Industrial Validation of Fourier Transform Infrared *trans* and Iodine Value Analyses of Fats and Oils. *J Am Oil Chem Soc*, **75** (1), 33 (1998).

*Received 18 September 2012*

*Revised 24 October 2012*

## QUANTIFICATION OF TOTAL VITAMIN C IN *Potentilla anserina* L. ROOT

TING ZHANG<sup>a</sup>, LINGZHI LI<sup>b,c</sup>, YING CUI<sup>b,c\*</sup>

<sup>a</sup>Department of Pharmacy, Xiangya Hospital, Central South University, 410 008 Changsha, China

<sup>b</sup>Department of Medicine Chemistry, Logistics University of Chinese People Armed Police Forces, 300 162 Tianjin, China

<sup>c</sup>Tianjin Key Laboratory of Occupational and Environmental Hazards Biomarkers, 300 162 Tianjin, China

E-mail: flyingyting@yahoo.com.cn

### ABSTRACT

A high performance liquid chromatographic method was developed for the determination of total vitamin C in *Potentilla anserina* L. root. Trichloroacetic acid solution was used for the extraction of vitamin C in the presence of tris [2-carboxyethyl] phosphine which could transform dehydroascorbic acid to its reduced form ascorbic acid and protect the reduced form from oxidation. The separation was performed on a C<sub>18</sub> column with a sodium dihydrogen phosphate eluent (pH 5.75) containing tetrabutylammonium bromide as ion-pairing agent. The method showed adequate precision, with a relative standard derivation smaller than 3.5% and the recoveries were between 97.27–99.07% by standard addition procedure. The limits of detection and quantitation were estimated as 0.05 and 0.20 µg/ml, respectively. Application of the method to the analysis of 3 varieties of *Potentilla anserina* L., distributed in different geographic regions of Qinghai-Tibetan plateau, revealed relatively high content of vitamin C in *Potentilla anserina* L. root.

**Keywords:** *Potentilla anserina* L., total vitamin C, tris [2-carboxyethyl] phosphine, high performance liquid chromatography, tetrabutylammonium bromide.

### AIMS AND BACKGROUND

It is well known that vitamin C plays a paramount role as an antioxidant and a free radical scavenger to moderate the oxidative stress effects of various diseases<sup>1</sup>. L-ascorbic acid (AA) and L-dehydroascorbic acid (DHAA), which both contribute to vitamin C

---

\* For correspondence.

content, are the reduced and the oxidised forms, respectively. In humans, both forms are biologically active and the latter possesses biological activity approximately equal to that of the former<sup>2</sup>. Due to the lack of L-gulonolactone oxidase, humans must satisfy their vitamin C requirements through the diet. The main source of AA and DHAA in human nutrition is food of plant origin, especially fresh fruits and vegetables. Vitamin C deficiency has always been a major health problem<sup>3</sup>.

In the Qinghai-Tibetan plateau, fresh fruits and vegetables are deficient due to the special habitat. The Tibetan plant *Potentilla anserina* L., a kind of perennial herb, is widely distributed in the western areas of China. The root of *Potentilla anserina* L. grown in Qinghai-Tibetan plateau differs from those grown in low altitude area with characteristics of rounded shape, fleshy pulp, bright red colour and high yield. It is a type of traditional food in the Tibetan region, which contains various nutrients including vitamins, proteins and microelements, etc. A 2,4-dinitrophenylhydrazene (DNPH)-based method has been applied to the determination of total vitamin C in *Potentilla anserina* L. root<sup>4</sup>. However, the spectrophotometric method using DNPH is rather time-consuming and reported to produce errors<sup>5</sup>. For estimation of its nutrition value and further exploration of its value in vitamin C deficiency especially for high altitude residents, it is of particular importance to establish a suitable method to determine vitamin C in *Potentilla anserina* L. root.

HPLC is preferred over traditional techniques because it is more sensitive and permits more straightforward sample workup procedures<sup>2</sup>. In the present work, a chromatographic method with characteristics of ideal precision, accuracy and specificity had been developed for the quantification of total vitamin C in *Potentilla anserina* L. root. Trichloroacetic acid (TCA) solution was used for the extraction of vitamin C, and tris [2-carboxyethyl] phosphine (TCEP) was used as the reducing agent. Tetrabutylammonium bromide (TBAB) was added into the mobile phase as ion-pairing agent in order to improve the retention and resolution of AA on a C<sub>18</sub> column. Vitamin C content in 3 varieties of *Potentilla anserina* L. distributed in different geographic regions of the Qinghai-Tibetan plateau was determined with application of the method.

## EXPERIMENTAL

*Materials and reagents.* *Potentilla anserina* L. (var. *Anserina*, var. *Nuda Gaud* and var. *Serina Hayne*) plants, 3–5-year old, were grown outdoors at Jiangda, Haibei, Yushu and Guoluo, 4 different geographic regions in the Qinghai-Tibetan plateau. Roots were collected in autumn and stored in vacuum with temperature below –8°C till further processing.

L-ascorbic acid, tris [2-carboxyethyl] phosphine hydrochloride (TCEP·HCl) and trichloroacetic acid were obtained from Sigma-Aldrich. Tetrabutylammonium bromide and sodium dihydrogen phosphate were purchased from Damao reagent company (Tianjin, China). Ultrapure water was prepared using a Milli-Q filter system (Millipore, Bedford). HPLC-grade methanol was obtained from Merck.

*Sample preparation.* The stored root was dried under vacuum at  $50\pm 2^{\circ}\text{C}$  for 24 h, then mechanically powdered to pass through a 0.75-mm sieve. A portion of 1.0 g of powder was mixed with 10 ml TCEP solution (2 mM TCEP, 1% TCA). After sonication (20 min) and storage (20 min) in dark place, the extract was centrifuged at 10 000 rpm for 10 min. The supernatant was filtered through a 0.45- $\mu\text{m}$  filters prior to the injection into the HPLC system.

*Chromatographic conditions.* All experiments were performed with a Shimadzu LC 20A system. Samples were analysed on a reversed phase column (AQ-C<sub>18</sub>, 250 mm  $\times$  4.6 mm, 5  $\mu\text{m}$ , Welch materials). The flow rate was fixed at 1.0 ml/min at room temperature, and the detection wavelength was 266 nm. The mobile phase was prepared as follows: 900 ml of sodium dihydrogen phosphate solution (0.05 M) were mixed with 100 ml of methanol; then 1.25 g of TBAB were added to the solution and the pH of the solution was adjusted to pH 5.75 with phosphoric acid. Quantification was performed according to an external standard method.

*Validation of the chromatographic method.* The specificity of the method was verified by co-elution of authentic standards and by evaluation of the spectra of the peak of interest for assessing the separation of AA from the possible interferences in root extract. The linearity of the method was investigated with the use of a 5-point calibration curve with freshly prepared AA in TCEP solution at concentrations of 2.5, 5, 10, 20 and 40  $\mu\text{g/ml}$ , respectively. Three independent determinations were performed at each concentration. The limits of detection (LOD) and quantification (LOQ) were established with the use of a signal to noise ratio of 3:1 and 10:1, respectively.

In order to evaluate the precision of the proposed method, standard solutions containing 3 different concentrations of AA diluted in TCEP solution were prepared and analysed in 5 replicates. The percentage relative standard deviation (RSD, %) values were obtained within the same day to evaluate repeatability (intra-day precision), and over 5 different days to evaluate intermediate precision (inter-day precision). Recovery was tested by the standard addition procedure at 3 levels on *Potentilla anserina* L. (var. *Anserine*) roots collected in Jiangda. In each addition level, 5 determinations were carried out. For the stability study, the supernatant of homogenised sample was collected and filtered for injection at 20 min intervals for 8 h.

## RESULTS AND DISCUSSION

*Selection of mobile phase.* Due to the polar nature and small molecular weight, AA has little retention in regular reversed phase chromatographic conditions. In our work, initially a complete aqueous mobile phase was used for the resolution of AA in root extract. However, AA was poorly resolved under these conditions. Reversed phase ion pair HPLC procedures have been applied to the determination of AA to obtain increased retention<sup>6,7</sup>. In ion pair chromatography, the presence of ion pair agents in the mobile phase generally enhances the retention of oppositely charged molecules<sup>8</sup>.



In the present work, an ion pair reagent (TBAB) and organic modifier (10% methanol) were applied to maximise the resolution of AA and to minimise the retention of more hydrophobic compounds in root extract.

*Sample preparation.* Both AA oxidation and DHAA hydrolysis are further prevented to some extent by acidification. TCA and *meta*-phosphoric acid (MPA) have been used for the extraction and stabilisation of vitamin C (Refs 6, 7 and 9). Under the chromatographic condition mentioned above, MPA was co-eluted with AA. Thus the 1% TCA solution in the presence of TCEP was selected as the extraction solution. In our work, the content of AA decreased rapidly in extract without presence of reducer. It might be the degradation of AA derived from self-oxidation and protection to prevent unstable compounds in the root extract from oxidation. Reducing agents are frequently used to stabilise AA and convert DHAA into its reduced form<sup>2,10,11</sup>. TCEP could reduce DHAA to AA with higher efficiency at room temperature and low pH condition, and is less likely to interfere as it is not detected in the UV-chromatographic system<sup>11</sup>. With TCA as acidulant, TCEP was added to prevent AA from oxidation and reduce DHAA to AA in our work.

*Validation of the chromatographic method.* Under the chromatographic condition described above, AA was observed to be well resolved from the interference components in the root extract (Fig. 1). The identity of the peak was verified by time control and DAD spectra with an authentic standard.

The analytical curve for AA standard was constructed by plotting the area under the curve of the main peak versus drug concentration. Least square regression analysis was used to evaluate the concentration range data that showed excellent linearity over the interval studied, with  $r^2 > 0.999$ . The linear regression equation from the experimental results was found to be:  $y = 42543x - 1872$ . The determination of the limits was achieved by the estimation of the signal/noise ratios of 3:1 (LOD) and 10:1 (LOQ) by serial dilution of AA solutions. The LOD and LOQ values for this HPLC method were about 0.05 and 0.20 µg/ml, respectively.

The precision indicates the degree of dispersion within a series of determinations on the same sample. To calculate the precision, intra-day and inter-day tests were performed and the results are shown in Table 1. The low percentage values of relative standard deviation (RSD) were an evidence of the appropriate precision of this method.

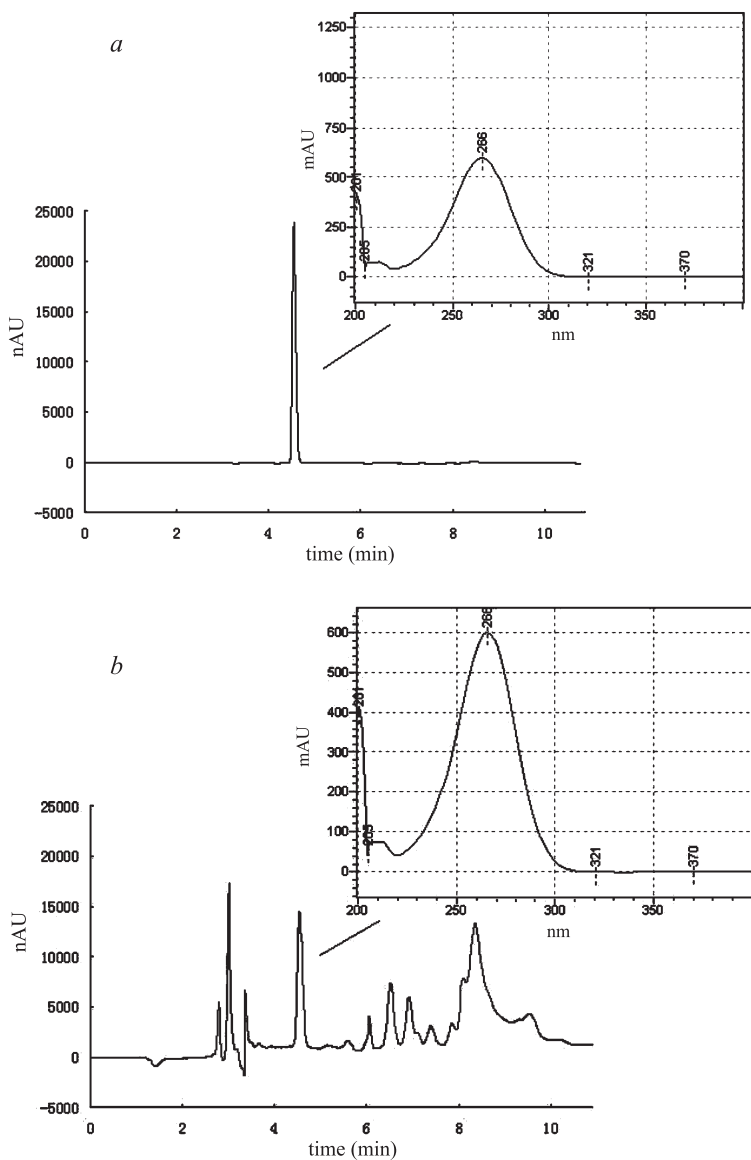


**Fig. 1.** HPLC-UV chromatograms of AA in standard solution (a) and in *Potentilla anserina* L. (b) root extract

Insets showed the absorbance spectra of the peak highlighted

**Table 1.** Precision of the evaluated method for AA determination ( $n=5$ )

Concentration of AA ( $\mu\text{g/ml}$ )	Intra-day precision (RSD, %)	Inter-day precision (RSD, %)
5	1.56	3.31
10	0.99	2.23
20	0.83	1.11

The recovery of the method was determined by a comparison between the theoretical concentrations of standard AA added to root extract and those obtained within the chromatographic analysis. The results, showed in Table 2, indicated an adequate accuracy of the HPLC method for the determination of total vitamin C in *Potentilla anserina* L. root.

**Table 2.** Recovery of the evaluated method for AA determination ( $n=5$ )

Added value ( $\mu\text{g/ml}$ )	Found value ( $\mu\text{g/ml}$ )	Recovery (%)	RSD (%)
7.5	7.37 $\pm$ 0.15	98.26	2.03
15	14.86 $\pm$ 0.22	99.07	1.51
30	29.18 $\pm$ 0.45	97.27	1.54

The stability of AA in root extract is presented in Fig. 2. AA was completely stable for a period of time about 140 min, after that, there was an apparent decline in its content. During the period of time about 140 min mentioned above, the degradation of AA derived from self-oxidation and protection to prevent unstable compounds in the root extract from oxidation was reversed by TCEP. As the reductant was exhausted, the content of AA began to decline. With the stability duration of about 140 min and a 10-min analysis time, these would allow the consecutive analysis of 8–10 samples in a single batch. Total vitamin C should be measured within 140 min after sample preparation in 1% TCA, 2 mM TCEP in our work.

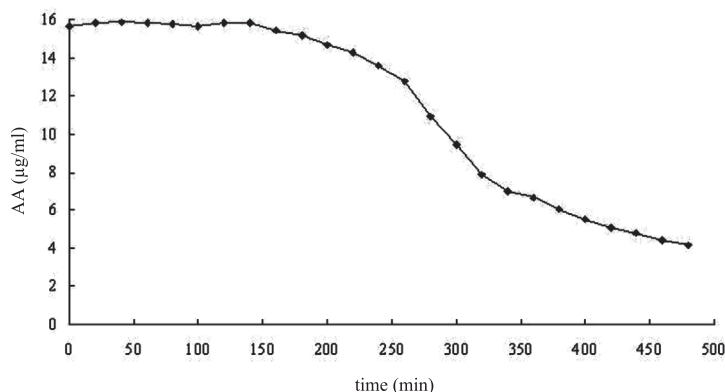


**Fig. 2.** Stability of AA in *Potentilla anserina* L. root extract

**Table 3.** Quantification of total vitamin C in *Potentilla anserina* L. root (n=5)

Geographic region	Variety	Total vitamin C content (mg/100g)	RSD (%)
Jiangda	<i>Potentilla anserina</i> L. var. <i>Anserina</i>	18.25	2.47
Haibei	<i>Potentilla anserina</i> L. var. <i>Anserina</i>	10.32	2.68
Yushu	<i>Potentilla anserina</i> L. var. <i>Anserina</i>	12.72	3.97
Guoluo	<i>Potentilla anserina</i> L. var. <i>Anserina</i>	13.45	2.43
Yushu	<i>Potentilla anserina</i> L. var. <i>Nuda Gaud</i>	12.90	1.96
Guoluo	<i>Potentilla anserina</i> L. var. <i>Nuda Gaud</i>	10.61	1.24
Yushu	<i>Potentilla anserina</i> L. var. <i>Serina Hayne</i>	7.61	2.65
Guoluo	<i>Potentilla anserina</i> L. var. <i>Serina Hayne</i>	15.35	2.77

*Quantification of total vitamin C in Potentilla anserina L. root.* The quantification of total vitamin C in 3 varieties of *Potentilla anserina* L. distributed in different geographic regions of the Qinghai-Tibetan plateau was carried out by means of an external calibration curve constructed right the day of sample determination. The results are shown in Table 3. Quoting from a FAO document reviewing worldwide vitamin C status, ‘... it is important to realise that the amount of vitamin C in a food is usually not the major determinant of a food importance for the supply, but rather regular intake’<sup>12</sup>. In spite of moderate content, consumption of the root of *Potentilla anserina* L. as daily diet may contribute to the supply of vitamin C for high altitude residents.

## CONCLUSIONS

A chromatographic method was developed for the determination of total vitamin C content in *Potentilla anserina* L. root for estimation of its nutrition value and further exploration of its value in vitamin C deficiency for high altitude residents. The established HPLC method showed excellent analytical specificity, linearity, precision, recovery and sensitivity during the validation study. Application of the method to the analysis of 3 varieties of *Potentilla anserina* L., distributed in different geographic regions of the Qinghai-Tibetan plateau, revealed that the variability of total vitamin C content ranged from 7.61 to 18.25 mg/100g.

## ACKNOWLEDGEMENT

The authors gratefully thank Qinghai hospital of Chinese People Armed Police Forces for the collection of *Potentilla anserina* L. roots.

## REFERENCES

1. B. HALLIWELL, J. M. GUTTERIDGE, C. E. CROSS: Free Radicals, Antioxidants, and Human Disease: Where Are We Now? *J Lab Clin Med*, **119**, 598 (1992).
2. H. S. LEE, G. A. COATES: Measurement of Total Vitamin C Activity in Citrus Products by HPLC: a Review. *J Liq Chromatogr R T*, **22**, 2367 (1999).
3. J. R. DELANGHE, M. R. LANGLOIS, M. L. de BUYZERE, N. NA, J. OUYANG, M. M. SPEECKAERT, M. A. TORCK: Vitamin C Deficiency: More than Just a Nutritional Disorder. *Genes Nutr*, **6**, 341 (2011).
4. D. SHANG, J. HUI, Q. LI: Analysis and Evaluation of Nutritional Components of *Potentilla anserina* in Xizang and Qinghai. *Acta Nutrimenta Sinica (China)*, **24**, 93 (2002).
5. F. TSUMURA, Y. OHSAKO, Y. HARAHUCHI, H. KUMAGAI, H. SAKURAI, K. ISHII: Rapid Enzymatic Assay for Ascorbic Acid in Various Foods Using Peroxidase. *J Food Sci*, **58**, 619 (1993).
6. A. KARLSEN, R. BLOMHOFF, T. E. GUNDERSEN: High-throughput Analysis of Vitamin C in Human Plasma with the Use of HPLC with Monolithic Column and UV-detection. *J Chromatogr B*, **824**, 132 (2005).
7. P. FONTANNAZ, T. KILINC, O. HEUDI: HPLC-UV Determination of Total Vitamin C in a Wide Range of Fortified Food Products. *Food Chem*, **94**, 626 (2006).
8. H. ZOU, Y. ZHANG, M. HONG, P. LU: Measurement of Partition Coefficients by Reversed-phase Ion-pair Liquid Chromatography. *J Chromatogr*, **625**, 169 (1992).
9. I. ODRIOZOLA-SERRANO, T. HERNANDEZ-JOVER, O. MARTIN-BELLOSO: Comparative Evaluation of UV-HPLC Methods and Reducing Agents to Determine Vitamin C in Fruits. *Food Chem*, **105**, 151 (2007).
10. A. R. BRAUSE, D. C. WOOLLARD, H. E. INDYK: Determination of Total Vitamin C in Fruit Juices and Related Products by Liquid Chromatography: Interlaboratory Study. *J AOAC Int*, **86**, 367 (2003).
11. J. LYKKESFELDT: Determination of Ascorbic Acid and Dehydroascorbic Acid in Biological Samples by High-performance Liquid Chromatography Using Subtraction Methods: Reliable Reduction with Tris [2-carboxyethyl] Phosphine Hydrochloride. *Anal Biochem*, **282**, 89 (2000).
12. FAO & WHO: Human Vitamin and Mineral Requirements. Report of a Joint FAO/WHO Expert Consultation. Bangkok, Thailand. Rome, FAO, 2002.

Received 8 August 2012  
Revised 19 September 2012

## TRANSFORMATION OF HIGH-ENERGY BONDS IN ATP

G. A. KORABLEV<sup>a\*</sup>, N. V. KHOKHRIAKOV<sup>a</sup>, G. E. ZAIKOV<sup>b</sup>,  
YU. G. VASILIEV<sup>a</sup>

<sup>a</sup>Basic Research and Educational Center of Chemical Physics and Mesoscopy,  
Izhevsk State Agricultural Academy, Udmurt Scientific Center, Ural Division,  
Russian Academy of Sciences, 426 000 Izhevsk, Russia

E-mail: biakaa@mail.ru; korablevga@mail.ru; khrv70@mail.ru; devugen@mail.ru

<sup>b</sup>N. M. Emanuel Institute of Biochemical Physics, Russian Academy of Sciences,  
4 Kosygin Street, 119 991 Moscow, Russia

E-mail: chembio@chph.ras.ru

### ABSTRACT

With the help of spatial-energy concept it is demonstrated that the formation and change of high-energy bonds in adenosine triphosphate (ATP) take place at the functional transitions of valence-active orbitals of the ‘phosphorus–oxygen’ system. These values of energy bonds are in accordance with experimental and quantum-mechanical data.

### SPATIAL-ENERGY PARAMETER

During the interaction of oppositely charged heterogeneous systems a certain compensation of volume energy of interacting structures takes place which leads to the decrease in the resulting energy (for example, during the hybridisation of atomic orbitals). But this is not the direct algebraic deduction of the corresponding energies. The comparison of multiple regularities of physical, chemical and biological processes allows assuming that in such and similar cases the principle of adding the reciprocals of volume energies or kinetic parameters of interacting structures is executed.

The Lagrangian equation for the relative movement of the system of 2 interacting material points with masses  $m_1$  and  $m_2$  in coordinate  $x$  is as follows:

$$m_{\text{red}} x'' = \partial U / \partial x, \quad (1)$$

where

$$1/m_{\text{red}} = 1/m_1 + 1/m_2, \quad (1a)$$

---

\* For correspondence.

where  $U$  is the mutual potential energy of material points;  $m_{\text{red}}$  – reduced mass, and  $x'' - a$  (system acceleration).

For the elementary areas of interactions  $\Delta x$  we can accept:  $\partial U/\partial x \approx \Delta U/\Delta x$ .

Then:

$$m_{\text{red}} a \Delta x = -\Delta U;$$

$$\frac{1}{1/(a \Delta x)} \frac{1}{1/m_1 + 1/m_2} \approx -\Delta U$$

or

$$\frac{1}{1/(m_1 a \Delta x) + 1/(m_2 a \Delta x)} \approx -\Delta U.$$

Since the product  $m_i a \Delta x$  by its physical sense equals the potential energy of each material point ( $-\Delta U_i$ ), then:

$$1/\Delta U \approx 1/\Delta U_1 + 1/\Delta U_2. \quad (2)$$

Thus, the resulting energy characteristic of the system of 2 interacting material points is found by the principle of adding the reciprocals of initial energies of interacting subsystems.

The electron with mass  $m$  moving about the proton with mass  $M$  is equivalent to the particle with the mass:  $m_{\text{red}} = mM/(m + M)$  (Ref. 1).

Therefore, modifying equation (2) we can assume that the energy of atom valence orbitals (responsible for interatomic interactions) can be calculated<sup>2</sup> by the principle of adding the reciprocals of some initial energy components based on the following equations:

$$1/(q^2/r_i) + 1/(W_i n_i) = 1/P_E \quad (3)$$

or

$$1/P_0 = 1/q^2 + 1/(W r n)_i; \quad (4)$$

$$P_E = P_0/r_i, \quad (5)$$

where  $W_i$  is the orbital energy of electrons<sup>3</sup>;  $r_i$  – orbital radius of  $i$  orbital<sup>4</sup>;  $q=Z^*/n^*$  ( $Z^*$  and  $n^*$  – nucleus effective charge and effective main quantum number, respectively) – according to Refs 5 and 6;  $n_i$  – number of electrons of the given orbital;  $r$  – bond dimensional characteristics.

$P_0$  is called a spatial-energy parameter (SEP), and  $P_E$  – effective  $P$ -parameter (effective SEP). Effective SEP has a physical sense of some averaged energy of valence orbitals in the atom and is measured in energy units, e.g. in electron-volts (eV).

The values of  $P_0$ -parameter are tabulated constants for electrons of the given atom orbital.

For SEP dimensionality:

$$[P_0] = [q^2] = [E][r] = [h][v] = kgm^3/S^2 = J m,$$

where  $[E]$ ,  $[h]$  and  $[v]$  – dimensionalities of energy, the Planck constant and velocity, respectively.

The introduction of  $P$ -parameter should be considered as further development of quasi-classical concepts with quantum-mechanical data on atom structure to obtain the criteria of phase-formation energy conditions. For the systems of similarly charged (e.g. orbitals in the given atom) homogeneous systems the principle of algebraic addition of such parameters is preserved:

$$\sum P_E = \sum (P_0/r_i); \quad (6)$$

$$\sum P_E = \sum P_0/r \quad (7)$$

or

$$\sum P_0 = P_0' + P_0'' + P_0''' + \dots \quad (8)$$

$$r \sum P_E = \sum P_0, \quad (9)$$

where  $P$  parameters are summed up by all atom valence orbitals.

To calculate the values of  $P_E$ -parameter at a given distance from the nucleus either the atomic radius ( $R$ ) or ionic radius ( $r_i$ ) can be used instead of  $r$  depending on the bond type.

Let us briefly explain the reliability of such an approach. As the calculations demonstrated the values of  $P_E$ -parameters are equal numerically (in the range of 2%) to the total energy of valence electrons ( $U$ ) by the atom statistic model. Using the known correlation between the electron density ( $\beta$ ) and intra-atomic potential by the atom statistic model<sup>7</sup>, we can obtain the direct dependence of  $P_E$ -parameter on the electron density at a distance  $r_i$  from the nucleus. The rationality of such a technique was proved by the calculation of electron density using wave functions by Clementi<sup>8</sup> and comparing it with the value of electron density calculated through the value of  $P_E$ -parameter.

The modules of maximum values of the radial part of  $\Psi$ -function were correlated with the values of  $P_0$ -parameter and a linear dependence between these values was found. Using some properties of wave function as applicable to  $P$ -parameter, a wave equation of  $P$ -parameter with the formal analogy with the equation of  $\Psi$ -function was obtained<sup>9</sup>.

## WAVE PROPERTIES OF $P$ -PARAMETERS AND PRINCIPLES OF THEIR ADDITION

Since  $P$ -parameter has wave properties (similar to  $\Psi'$ -function), the regularities of the interference of the corresponding waves should be mainly fulfilled at structural interactions.



The interference minimum weakening of oscillations (in antiphase) occurs if the difference of wave move ( $\Delta$ ) equals the odd number of semi-waves:

$$\Delta = (2n + 1)(\lambda/2) = \lambda(n + 1/2), \quad (10)$$

where  $n = 0, 1, 2, 3, \dots$

As applicable to  $P$ -parameters this rule means that the interaction minimum occurs if  $P$ -parameters of interacting structures are also ‘in antiphase’ – either oppositely charged or heterogeneous atoms (for example, during the formation of valence-active radicals  $\text{CH}$ ,  $\text{CH}_2$ ,  $\text{CH}_3$ ,  $\text{NO}_2$  ..., etc.) are interacting.

In this case  $P$ -parameters are summed by the principle of adding the reciprocals of  $P$ -parameters – equations (3) and (4).

The difference of wave move ( $\Delta$ ) for  $P$ -parameters can be evaluated via their relative value  $\gamma = P_2/P_1$  of relative difference of  $P$ -parameters (coefficient  $\alpha$ ) which at the interaction minimum produce an odd number:

$$\gamma = P_2/P_1 = n + 1/2 = 3/2; 5/2 \dots$$

When  $n = 0$  (main state)

$$P_2/P_1 = 1/2. \quad (11)$$

It should be pointed out that for stationary levels of one-dimensional harmonic oscillator the energy of these levels  $\varepsilon = h\nu(n+1/2)$ , therefore in quantum oscillator, in contrast to the classical one, the least possible energy value does not equal zero.

In this model the interaction minimum does not provide zero energy corresponding to the principle of adding reciprocals of  $P$ -parameters – equations (3) and (4).

The interference maximum, strengthening of oscillations (in phase) occurs if the difference of wave move equals the even number of semi-waves:

$$\Delta = 2n(\lambda/2) = \lambda n \text{ or } \Delta = \lambda(n + 1).$$

As applicable to  $P$ -parameters the maximum interaction intensification in the phase corresponds to the interactions of similarly charged systems or systems homogeneous by their properties and functions (for example, between the fragments or blocks of complex inorganic structures, such as  $\text{CH}_2$  and  $\text{NNO}_2$  in octogene).

And then:

$$\gamma = P_2/P_1 = n + 1. \quad (12)$$

By the analogy, for ‘degenerated’ systems (with similar values of functions) of 2-dimensional harmonic oscillator the energy of stationary states:

$$\varepsilon = h\nu(n + 1).$$

By this model the interaction maximum corresponds to the principle of algebraic addition of  $P$ -parameters – equations (6)–(8). When  $n=0$  (main state) we have  $P_2=P_1$ , or: the interaction maximum of structures occurs if their  $P$ -parameters are equal. This

concept was used<sup>2</sup> as the main condition for isomorphic replacements and formation of stable systems.

## EQUILIBRIUM-EXCHANGE SPATIAL-ENERGY INTERACTIONS

During the formation of solid solutions and in other structural equilibrium-exchange interactions the unified electron density should be established in the contact spots between atoms-components. This process is accompanied by the re-distribution of electron density between valence areas of both particles and transition of a part of electrons from some external spheres into the neighbouring ones.

It is obvious that with the proximity of electron densities in free atoms-components the transition processes between the boundary atoms of particles will be minimum thus contributing to the formation of a new structure. Thus the task of evaluating the degree of such structural interactions in many cases comes down to comparative assessment of electron density of valence electrons in free atoms (on the averaged orbitals) participating in the process.

Therefore, the maximum total solubility evaluated via the structural interaction coefficient  $\alpha$  is defined by the condition of minimum value of the coefficient  $\alpha$  which represents the relative difference of effective energies of external orbitals of interacting subsystems:

$$\alpha = \frac{P_0'/r_i' - P_0''/r_i''}{(P_0'/r_i' + P_0''/r_i'')/2} \times 100\% \quad (13)$$

or

$$\alpha = \frac{P_s' - P_s''}{P_s' + P_s''} \times 200\% \quad (14)$$

where  $P_s$  – the structural parameter is found by the following equation:

$$1/P_s = 1/(N_1 P_E') + 1/(N_2 P_E'') + \dots, \quad (15)$$

where  $N_1$  and  $N_2$  are number of the homogeneous atoms in the subsystems.

The nomogram of the dependence of structural interaction degree ( $\rho$ ) on the coefficient  $\alpha$ , the same for the wide range of structures, was prepared by the data obtained (the figure is not available).

Isomorphism as a phenomenon is usually considered as applicable to crystalline structures. But obviously the similar processes can also take place between molecular compounds where the bond energies can be assessed via the relative difference of electron densities of valence orbitals of interacting atoms. Therefore, the molecular electronegativity is rather easily calculated via the values of corresponding  $P$ -parameters.

In complex organic structures the main role in intermolecular and intramolecular interactions can be played by separate ‘blocks’ or fragments considered as ‘active’ areas

of the structures. Therefore it is necessary to identify these fragments and evaluate their spatial-energy parameters. Based on wave properties of  $P$ -parameter, the total  $P$ -parameter of each element should be found following the principle of adding the reciprocals of initial  $P$ -parameters of all the atoms. The resulting  $P$ -parameter of the fragment block or all the structure is calculated following the rule of algebraic addition of  $P$ -parameters of their constituent fragments.

Apparently, spatial-energy exchange interactions (SEI) based on levelling the electron densities of valence orbitals of atoms-components have in nature the same universal value as purely electrostatic Coulomb interactions and complement each other. Isomorphism known from the time of E. Mitscherlich (1820) and D. I. Mendeleev (1856) is only a special demonstration of this general natural phenomenon.

The quantitative side of evaluating the isomorphic replacements both in complex and simple systems rationally fits into  $P$ -parameter methodology. More complicated is the problem of evaluating the degree of structural SEI for molecular structures, including organic ones. Such structures and their fragments are often not completely isomorphic to each other. Nevertheless, SEI is going on between them and its degree can be evaluated either semi-quantitatively numerically or qualitatively. By the degree of isomorphic similarity all the systems can be divided into 3 types:

I. Systems mainly isomorphic to each other – systems with approximately the same number of heterogeneous atoms and cumulative similar geometric shapes of interacting orbitals;

II. Systems with organic isomorphic similarity – systems which either differ by the number of heterogeneous atoms but have cumulative similar geometric shapes of interacting orbitals or have certain differences in the geometric shape of orbitals but have the same number of interacting heterogeneous atoms;

III. Systems without isomorphic similarity – systems considerably different both by the number of heterogeneous atoms and geometric shape of their orbitals.

Taking into account the experimental data, all SEI types can be approximately classified as follows:

#### Systems I

1.  $\alpha < (0-6)\%$ ;  $\rho = 100\%$ . Complete isomorphism, there is complete isomorphic replacement of atoms-components;

2.  $6\% < \alpha < (25-30)\%$ ;  $\rho = 98 - (0-3)\%$ . There is wide or unlimited isomorphism;

3.  $\alpha > (25-30)\%$ ; no SEI.

#### Systems II

1.  $\alpha < (0-6)\%$ : (a) There is reconstruction of chemical bonds that can be accompanied by the formation of a new compound; (b) Cleavage of chemical bonds can be accompanied by a fragment separation from the initial structure but without adjoinings and replacements;

2.  $6\% < \alpha < (25-30)\%$ ; the limited internal reconstruction of chemical bonds is possible but without the formation of a new compound and replacements.

3.  $\alpha > (20-30)\%$ ; no SEI.

### Systems III

1.  $\alpha < (0-6)\%$ : (a) The limited change in the type of chemical bonds in the given fragment is possible, there is an internal re-grouping of atoms without the cleavage from the main molecule part and replacements; (b) The change in some dimensional characteristics of the bond is possible;

2.  $6\% < \alpha < (25-30)\%$ . A very limited internal re-grouping of atoms is possible.

$\alpha > (25-30)\%$ ; no SEI.

When considering the above systems, it should be pointed out that they can be found in all cellular and tissue structures in some form but are not isolated and are found in spatial-time combinations.

The values of  $\alpha$  and  $\rho$  calculated in such a way refer to a definite interaction type whose nomogram can be specified by fixed points of reference systems. If we take into account the universality of spatial-energy interactions in nature, such an evaluation can have the significant meaning for the analysis of structural shifts in complex bio-physical and chemical processes of biological systems.

Fermentative systems contribute a lot to the correlation of structural interaction degree. In this model the ferment role comes to the fact that active parts of its structure (fragments, atoms, ions) have such a value of  $P_E$ -parameter which equals the  $P_E$ -parameter of the reaction final product. That is the ferment is structurally 'tuned' via SEI to obtain the reaction final product, but it will not enter it due to the imperfect isomorphism of its structure (in accordance with III).

The important characteristics of atom-structural interactions (mutual solubility of components, chemical bond energy, energy of free radicals, etc.) for many systems were evaluated following this technique<sup>10,11</sup>.

## CALCULATION OF INITIAL DATA AND BOND ENERGIES

Based on equations (3)–(5) with the initial data calculated by quantum-mechanical methods<sup>3-6</sup> we calculate the values of  $P_0$ -parameters for the majority of elements being tabulated, constant values for each atom valence orbital. Mainly covalent radii – by the main type of the chemical bond of interaction considered were used as a dimensional characteristic for calculating  $P_E$ -parameter (Table 1). The value of the Bohr radius and the value of atomic ('metal') radius were also used for hydrogen atom.

**Table 1.** *P*-parameters of atoms calculated via the bond energy of electrons

Atom	Valence electrons	$W$ (eV)	$r_i$ (Å)	$q_0^2$ (eVÅ)	$P_0$ (eVÅ)	$R$ (Å)	$P_0/R$ (eV)
1	2	3	4	5	6	7	8
H	1s <sup>1</sup>	13.595	0.5295	14.394	4.7985	0.5292	9.0644
						0.28	17.1370
	2p <sup>1</sup>	11.792	0.596	35.395	5.8680	$R_1=1.36$	3.5250
						0.77	7.6208
						0.67	8.7582
						0.77	13.066
2p <sup>2</sup>	11.792	0.596	35.395	10.0610	0.67	15.016	
					0.77	18.862	
C	2s <sup>2</sup>				14.5240	0.77	18.862
	2s <sup>2</sup> +2p <sup>2</sup>				24.5850	0.77	31.929
					24.5850	0.67	36.694
	2p <sup>1</sup>	15.445	0.4875	52.912	6.5916	0.70	9.4166
	2p <sup>2</sup>				11.7230	0.70	16.747
	2p <sup>3</sup>				15.8300	0.70	22.614
					0.55	28.782	
N	2s <sup>2</sup>	25.724	0.521	53.283	17.833	0.70	25.476
	2s <sup>2</sup> +2p <sup>3</sup>				33.663	0.70	48.09
					6.4663	0.66	9.7979
	2p <sup>1</sup>	17.195	0.4135	71.383		$R_1=1.36$	4.7550
	2p <sup>1</sup>					$R_1=1.40$	4.6188
	2p <sup>2</sup>	17.195	0.4135	71.383	11.8580	0.66	17.967
					0.59	20.048	
O	2p <sup>4</sup>	17.195	0.4135	71.383	20.3380	$R_1=1.36$	8.7191
						$R_1=1.40$	8.4700
	2s <sup>2</sup>	33.859	0.450	72.620	21.4660	0.66	30.815
						0.59	34.471
						0.66	32.524
						0.66	63.339
2s <sup>2</sup> +2p <sup>4</sup>				41.8040	0.59	70.854	
Ca	4s <sup>1</sup>	5.3212	1.690	17.406	5.9290	1.97	3.0096
	4s <sup>2</sup>				8.8456	1.97	4.4902
	4s <sup>2</sup>					$R^{2+}=1.00$	8.8456
	4s <sup>2</sup>					$R^{2+}=1.26$	7.0203
P	3p <sup>1</sup>	10.659	0.9175	38.199	7.7864	1.10	7.0785
	3p <sup>1</sup>					$R^{3+}=1.86$	$P_9=4.1862$
	3p <sup>3</sup>	10.659	0.9175	38.199	16.594	1.10	15.085
	3p <sup>3</sup>					$R^{3+}=1.86$	8.9215
	3s <sup>2</sup> +3p <sup>3</sup>				35.644	1.10	32.403
Mg	3s <sup>1</sup>	6.8859	1.279	17.501	5.8568	1.60	3.6618
	3s <sup>2</sup>				8.7787	1.60	5.4867
						$R^{2+}=1.02$	8.6066

to be continued

Continuation of Table 1

1	2	3	4	5	6	7	8
Mn	4s <sup>1</sup>	6.7451	1.278	25.118	6.4180	1.30	4.9369
	4s <sup>1</sup> +3d <sup>1</sup>				12.9240	1.30	9.9414
	4s <sup>2</sup> +3d <sup>2</sup>				22.7740	1.30	17.518
Na	3s <sup>1</sup>	4.9552	1.713	10.058	4.6034	1.89	2.4357
						$R^+_{I}=1.18$	3.9010
						$R^+_{I}=0.98$	4.6973
K	4s <sup>1</sup>	4.0130	2.612	10.993	4.8490	2.36	2.0547
						$R^+_{I}=1.45$	3.3440

In some cases the bond repetition factor for carbon and oxygen atoms was taken into consideration<sup>10</sup>. For a number of elements the values of  $P_E$ -parameters were calculated using the ionic radii whose values are indicated in column 7. All the values of atomic, covalent and ionic radii were mainly taken by Belov-Bokiy, and crystalline ionic radii – by Batsanov<sup>12</sup>.

The results of calculating structural  $P_S$ -parameters of free radicals by equation (15) are given in Table 2. The calculations are done for the radicals contained in protein and amino acid molecules (CH, CH<sub>2</sub>, CH<sub>3</sub>, NH<sub>2</sub>, etc.), as well as for some free radicals formed in the process of radiolysis and dissociation of water molecules.

**Table 2.** Structural  $P_S$ -parameters calculated via the bond energy of electrons

Radicals, molecule fragments	$P'_i$ (eV)	$P''_i$ (eV)	$P_S$ (eV)	Orbitals
1	2	3	4	5
OH	9.7979	9.0644	4.7080	O (2p <sup>1</sup> )
	17.9670	17.1380	8.7712	O (2p <sup>2</sup> )
H <sub>2</sub> O	2×9.0644	17.9670	9.0227	O (2p <sup>2</sup> )
CH <sub>2</sub>	17.1600	2×9.0644	8.8156	C (2s <sup>1</sup> 2p <sup>3</sup> <sub>r</sub> )
	31.9290	2×17.1380	16.528	C (2s <sup>2</sup> 2p <sup>2</sup> )
CH <sub>3</sub>	15.0160	3×9.0644	9.6740	C (2p <sup>2</sup> )
	40.9750	3×9.0644	16.345	C (2s <sup>2</sup> 2p <sup>2</sup> )
CH	31.9290	12.7920	9.1330	C (2s <sup>2</sup> 2p <sup>2</sup> )
NH	16.7470	17.1380	8.4687	N(2p <sup>2</sup> )
	19.5380	17.1320	9.1281	N(2p <sup>2</sup> )
NH <sub>2</sub>	19.5380	2×9.0644	9.4036	N(2p <sup>2</sup> )
	28.7820	2×17.1320	18.450	N(2p <sup>3</sup> )
CO–OH	8.4405	8.7710	4.3013	C(2P <sup>2</sup> )
C=O	15.016	20.048	8.4405	C(2p <sup>2</sup> )
C=O	31.929	34.471	16.576	O(2P <sup>4</sup> )
CO=O	36.694	34.471	17.775	O(2P <sup>4</sup> )
C–CH <sub>3</sub>	17.435	19.694	9.2479	–

to be continued

Continuation of Table 2

1	2	3	4	5
C-NH <sub>2</sub>	17.4350	18.450	8.8844	–
CO-OH	12.3150	8.7712	5.1226	C(2s <sup>2</sup> 2p <sup>2</sup> ) O(2p <sup>2</sup> )
(HP)O <sub>3</sub>	23.1220	23.7160	11.7080	P(3s <sup>2</sup> 3p <sup>3</sup> ) O(2p <sup>1</sup> )
(H <sub>3</sub> P)O <sub>4</sub>	17.1850	17.2440	8.6072	P(3P <sup>1</sup> ) O(2p <sup>2</sup> )
(H <sub>3</sub> P)O <sub>4</sub>	31.8470	31.6120	15.8650	P(3s <sup>2</sup> 3p <sup>3</sup> ) O(2p <sup>2</sup> )
H <sub>2</sub> O	2×4.3623	8.71910	4.3609	r = 1.36 Å O(2P <sup>2</sup> )
H <sub>2</sub> O	2×4.3623	4.2350	2.8511	r = 1.40
C-H <sub>2</sub> O	2.9590	2.8511	1.4520	
(C-H <sub>2</sub> O) <sub>3</sub>			1.4520×3= 4.3563	–
Lactic acid (C-H <sub>2</sub> O) <sub>6</sub>	–	–	1.4520×6= 8.7121	–
Glucose	–	–		–

The technique previously tested<sup>10</sup> on 68 binary and more complex compounds was applied to calculate the energy of coupled bond of molecules by the following equations:

$$\frac{1}{E} = \frac{1}{P_s} = \frac{1}{\left(P_E \frac{n}{K}\right)_1} + \frac{1}{\left(P_E \frac{n}{K}\right)_2} \quad (16)$$

$$P_E(n/K) = P, \quad (17)$$

where  $n$  is the bond average repetition factor,  $K$  – hybridisation coefficient which usually equals the number of registered atom valence electrons.

Here the  $P$ -parameter of energy is characteristic of the given component structural interaction in the process of binary bond formation.

‘Non-valence, non-chemical weak forces act ... inside biological molecules and between them apart from strong interactions’<sup>13</sup>. At the same time, the orientation, induction and dispersion interactions are used to be called the Van der Waals forces. For the 3 main biological atoms (nitrogen, phosphorus and oxygen) the Van der Waals radii numerically are equal approximately to the corresponding ionic radii (Table 3).

Table 3. Ionic and the Van der Waals radii (Å)

Atom	Ionic radii		The Van der Waals radii			
	orbital	$R_i$	$P_E/K$ (eV)	$R_b$	orbital	$P_E/K$ (eV)
H	$1s^1$	$R^+ = 1.36$	3.525	1.10	$1s^1$	4.3623
		$r^- = 0.5292$	9.0644	1.32		3.6352
N	$2p^3$	$R^3 = 1.48$	10.696/3=3.5653	1.50	$2p^1$	4.3944/1
				1.50		10.553/3=3.5178
				1.50		22.442/5=4.4884
				1.90		4.0981/1
P	$3p^3$	$R^3 = 1.86$	8.9215/3=2.9738	1.90	$3p^1$	8.7337/3=2.9112
				1.90		18.760/5=3.752
				1.40		4.6188/1
				1.50		4.3109/1
O	$2p^2$	$R^2 = 1.36$	8.7191/2=4.3596	1.40	$2p^1$	8.470/2=4.2350
				1.40		7.9053/2=3.9527
				1.50		3.4518/1
				1.70		5.9182/2=2.9591
C	$2s^2 2p^2$	$d^*/2 = 3.2/2 = 1.6$	15.365/4=3.841	1.70	$2p^2$	14.462/4=3.6154
				1.70		$2s^2 2p^2$

$d^*$  – contact distance between C–C atoms in polypeptide chains<sup>13</sup>.



**Table 4.** Bond energy (eV)

Atoms, Bond structures, orbitals	Component 1		Component 2		Component 3		Calculation		$E$ (Refs 13, 14, 15)	$E$ (Refs 16 and 17)	Remarks
	$P_E$ (eV)	$n/K$	$P_E$ (eV)	$n/K$	$P_E$ (eV)	$n/K$	$E$	$E$			
1	2	3	4	5	6	7	8	9	10	11	12
P=O	cov.	32.403	1.5/5	70.854	1.5/6	6.14		6.2770	6.1385		PO free molecule
$3s^2 3p^3$				63.339	1.5/6			6.0240	6.14		
$2s^2 2p^4$								<6.15>			
H <sub>2</sub> O	cov.	2×9.0624	1/1	17.967	1/6			2.5700	2.476	10.04	decay of one molecule
$1s^1-2p^2$	cov.	2×9.0624	1/1	20.048	2/2			9.5200			
H <sub>3</sub> PO <sub>4</sub>	cov.	3×9.0624	1/1	32.405	1/5	4×17.967	1/2	4.8779	4.708		
C=O	cov.	7.6208	1.125/2	9.7979	1/1			4.2867			
( $2p^1-1s^1$ )											
C-N	cov.	7.6208	1/4	9.4166	1/5			0.9471			
$2p^1-2p^1$											
C=N	cov.	7.6208	1.125/4	9.4166	1.1667/5			1.0898	0.870		
$2p^1-2p^1$											
K-C-N	cov.	2.0547	1/1	7.6208	1/4	9.4166	1/5	0.648			
$4s^2-2p^1-$											
$2p^1$											
(C-H <sub>2</sub> O)-VdW		1.4520	1/1	1.4520	1/1			0.726			
(C-H <sub>2</sub> O)											
C=O	cov.	31.929	1.125/4	20.048	1/2			4.7367			
$2s^2 2p^2-2p^2$								4.4437			
N-H	cov.	9.4166	1.1667/1	9.0644	1/1			4.9654			
$2p^1-1s^1$								4.6186			

to be continued

Continuation of Table 4

1	2	3	4	5	6	7	8	9	10	11	12
C-H	cov.	13.066	1/2	9.0644	1/1			3.797	3.772		
$2p^1-1s^1$											
C-H		13.066	1/2	17.137	1/1			4.7295			
$2p^2-1s^1$											
N-H <sub>2</sub>	cov.	22.614	1/3	2×9.0644	1/1			5.3238			
$2p^3-1s^1$											
-H...O		3.525	3.525/ 17.037	4.6188	1/6			0.3730	0.3742		hydrogen bond
P=O	cov.	15.085	2/3	20.042	2/2			6.6970	6.504	6.1385	free mol- ecule $\Delta G$ ATP
$3p^3-2p^2$											
P-O	VdW	8.7337	1/5	8.470	1/6			0.781	0.670		
$3p^3-2p^2$											
P-O	cov.	7.0785	1/1	9.7979	1/1			4.1096	4.2059	4.2931	
$3p^1-2p^1$											
P-O	VdW	4.0981	1/5	4.6188	1/6			0.3970	0.34-0.35		phospho- lyration
$3p^1-2p^1$											

It is known that one of the reasons of the relative instability of phosphorus anhydride bonds in ATP is the strong repulsion of negatively charged oxygen atoms. Therefore, it is advisable to use the values of  $P$ -parameters calculated via Van der Waals radii as the energy characteristic of weak structural interactions of biomolecules (Table 3).

Bond energies for P and O atoms were calculated taking into account the Van der Waals distances for atomic orbitals:  $3p^1$  (phosphorus)- $2p^1$  (oxygen) and for  $3p^3$  (phosphorus)- $2p^2$  (oxygen). The values of  $E$  obtained slightly exceeded the experimental, literary data (Table 4). But for the actual energy physiological processes, e.g. during photosynthesis, the efficiency is below the theoretical one, being about 83%, in some cases<sup>14,15</sup>.

Perhaps the electrostatic component of the resulting interactions at anion-anionic distances is considered in such a way. Actually the calculated value of  $E - 0.83$  practically corresponds to the experimental values of bond energy during the phospholyration and free energy of ATP in chloroplasts.

Table 4 contains the calculations of bond energy following the same technique but for stronger interactions at covalent distances of atoms for the free molecule  $P \equiv O$  (sesquialteral bond) and for the molecule  $P=O$  (double bond).

The sesquialteral bond was evaluated by introducing the coefficient  $n = 1.5$  with the average value of oxygen  $P_E$ -parameter for single and double bonds.

The average breaking energy of the corresponding chemical bonds in ATP molecule obtained in the frameworks of semi-empirical method PM3 with the help of software GAMESS<sup>16</sup> are given in column 11 of Table 4 for comparison. The calculation technique is detailed in Ref. 17.

The calculated values of bond energies in the system  $K-C-N$  being close to the values of high-energy bond  $P \sim O$  in ATP demonstrate that such structure can prevent the ATP synthesis.

When evaluating the possibility of hydrogen bond formation, we take into account such value of  $n/K$  in which  $K = 1$ , and the value of  $n = 3.525/17.037$  characterises the change in the bond repetition factor when transiting from the covalent bond to the ionic one.

## FORMATION OF STABLE BIOSTRUCTURES

At equilibrium-exchange spatial-energy interactions similar to isomorphism the electrically neutral components do not repulse but approach each other and form a new composition whose  $\alpha$  is done in equations (13) and (14).

This is the first stage of stable system formation by the given interaction type which is carried out under the condition of approximate equality of component  $P$ -parameters:  $P_1 \approx P_2$ .

Hydrogen atom, element No 1 with the orbital  $1s^1$  determines the main criteria of possible structural interactions. Four main values of its  $P$ -parameters can be taken from Tables 1 and 3:

(1) for strong interactions:  $P_E'' = 9.0644$  eV with the orbital radius  $0.5292$  Å and  $P_E''' = 17.137$  eV with the covalent radius  $0.28$  Å.

(2) for weaker interactions:  $P_E' = 4.3623$  eV and  $P_E = 3.6352$  eV with the Van der Waals radii  $1.10$  Å and  $1.32$  Å. The values of  $P$ -parameters  $P':P'':P'''$  relates as  $1:2:4$ . In accordance with the concepts in the Section 'Wave properties of  $P$ -parameters and principles of their addition', such values of interaction  $P$ -parameters define the normative functional states of biosystems, and the intermediary can produce pathologic formations by their values.

The series with approximately similar values of  $P$ -parameters of atoms or radicals can be extracted from the large pool of possible combinations of structural interactions (Table 5). The deviations from the initial, primary values of  $P$ -parameters of hydrogen atom are in the range  $\pm 7\%$ . The values of  $P$ -parameters of atoms and radicals given in the Table define their approximate equality in the directions of interatomic bonds in polypeptide, polymeric and other multi-atom biological systems.

In ATP molecule these are phosphorus, oxygen and carbon atoms, polypeptide chains – CO, NH and CH radicals. In Table 5 you can also see the additional calculation of their bond energy taking into account the sesquialteral bond repetition factor in radicals  $C\cdots O$  and  $N\cdots H$ .

On the example of phosphorus acids it can be demonstrated that this approach is not in contradiction with the method of valence bonds which explains the formation of peculiarities of ordinary chemical compounds. It is demonstrated in Table 6 that this electrostatic equilibrium between the oppositely charged components of these acids can correspond to the structural interaction for  $H_3PO_4$   $3p^1$  orbitals of phosphorus and  $2p^1$  of oxygen, and for  $HPO_3$   $3s^23p^3$  orbitals of phosphorus and  $2p^2$  of oxygen. Here it is stated that  $P$ -parameters for phosphorus and hydrogen subsystems are added algebraically. It is also known that the ionised phosphate groups are transferred in the process of ATP formation that is apparently defined for phosphorus atoms by the transition from valence-active  $3p^1$  orbitals to  $3s^23p^3$  ones, i.e. 4 additional electrons will become valence-active. According to the experimental data the synthesis of 1 ATP mol is connected with the transition of 4 protons and when the 4th proton is being transited the energy accumulated by the ferment reaches its threshold<sup>18,19</sup>. It can be assumed that such proton transitions in ferments initiate similar changes in valence-active states in the system P–O. In the process of oxidating phosphorylation the transporting ATP-synthase uses the energy of gradient potential due to  $2H^+$ -protons which, in the given model for such a process, corresponds to the initiation of valence-active transitions of phosphorus atoms from  $3p^1$ - to  $3p^3$ -state.

**Table 5.** Bio-structural spatial-energy parameters (eV)

Series No	H	C	N	O	P	CH	CO	NH	Glucose	Lactic acid	OH	Remarks
I	9.0644 (1s <sup>1</sup> )	8.7582 (2p <sup>1</sup> ) 9.780 (2p <sup>1</sup> )	9.4166 (2p <sup>1</sup> )	9.7979 (2p <sup>1</sup> )	8.7337 (3p <sup>3</sup> )	9.1330 (2s <sup>2</sup> 2p <sup>2</sup> - 1s <sup>1</sup> )	8.4405 (2p <sup>2</sup> -2p <sup>2</sup> )	8.4687 (2p <sup>2</sup> -1s <sup>1</sup> ) 9.1281 (1s <sup>1</sup> -2p <sup>2</sup> )	8.7121		8.7710	strong interaction
II	17.132 (1s <sup>1</sup> )	17.435 (2s <sup>1</sup> 2p <sup>1</sup> )	16.747 (2p <sup>2</sup> )	17.967 (2p <sup>2</sup> )	18.760 (3s <sup>2</sup> 3p <sup>3</sup> )	C and H blocks	16.576 (2s <sup>2</sup> 2p <sup>2</sup> - 2p <sup>1</sup> )	N and H blocks				strong interaction
III	(4.3623) (1s <sup>1</sup> )	3.8696 (2p <sup>2</sup> )	4.3944 (2p <sup>1</sup> )	4.3109 (2p <sup>1</sup> ) 4.6188 (2p <sup>1</sup> )	4.0981 (3p <sup>1</sup> )	4.7295	4.4437 4.7367	4.6186 4.9654		4.3563 2p <sup>2</sup> - (1s <sup>1</sup> -2p <sup>2</sup> )	4.7084	weak interaction
IV	3.6352 (1s <sup>1</sup> )	3.4518 (2p <sup>1</sup> ) 3.6154 (2s <sup>2</sup> 2p <sup>2</sup> )	3.5178 (2p <sup>3</sup> )	4.2350 (2p <sup>2</sup> ) 3.6318 (2p <sup>1</sup> )	4.0981 (3p <sup>1</sup> ) 3.752 (3s <sup>2</sup> 3p <sup>3</sup> )	4.7295	4.4437 4.7367	4.6186 4.9654				effective bond energy

**Table 6.** Structural interactions in phosphorus acids

Molecule	Component 1			Component 2			$\alpha = (\Delta P / <P>) 100\%$
	Atom	Orbitals	$P = P_1 + P_2$ (eV)	Atom	Orbitals	P (eV)	
(H <sub>3</sub> P)O <sub>4</sub>	H <sub>3</sub> P	1s <sup>1</sup> - 3p <sup>1</sup>	4.3623×3+4.0981=17.185	O <sub>4</sub>	2p <sup>1</sup>	4.3109×4=17.244	0.34
		1s <sup>1</sup> - (3s <sup>2</sup> 3p <sup>3</sup> )	4.3623×3+18.760=31.847		2p <sup>2</sup>	7.9053×4=31.612	0.74
(HP)O <sub>3</sub>	HP	1s <sup>1</sup> - (3s <sup>2</sup> 3p <sup>3</sup> )	4.3623+18.760=23.122	O <sub>3</sub>	2p <sup>2</sup>	7.9053×3=23.716	2.54
					at r=1.50Å		

In accordance with equation (17) we can assume that in stable molecular structures the condition of the equality of corresponding effective interaction energies of the components by the couple bond line is fulfilled by the following equations:

$$(P_E(n/K))_1 \approx (P_E(n/K))_2 \rightarrow P_1 \approx P_2 \quad (18)$$

And for heterogeneous atoms (when  $n_1 = n_2$ ):

$$(P_E/K)_1 \approx (P_E/K)_2 \quad (18a)$$

In phosphate groups of ATP molecule the bond main line comprises phosphorus and oxygen molecules. The effective energies of these atoms by the bond line calculated by equation (18) are given in Tables 4 and 5, from which it is seen that the best equality of  $P_1$  and  $P_2$  parameters is fulfilled for the interactions P ( $3p^3$ ) – 8.7337 eV and O ( $2p^2$ ) – 8.470 eV that is defined by the transition from the covalent bond to Van der Waals ones in these structures.

The resulting bond energy of the system P–O for such valence orbitals and the weakest interactions (maximum values of coefficient  $K$ ) is 0.781 eV (Table 4). Similar calculations for the interactions P ( $2p^1$ ) – 4.0981 eV and O ( $2p^1$ ) – 4.6188 eV produce the resulting bond energy 0.397 eV.

The difference in these values of bond energies is defined by different functional states of phosphorous acids  $\text{HPO}_3$  and  $\text{H}_3\text{PO}_4$  in glycolysis processes and equals 0.384 eV that is close to the phosphorylation value (0.34–0.35 eV) obtained experimentally.

Such ATP synthesis is carried out in anaerobic conditions and is based on the transfer of phosphate residues onto ATP via the metabolite. For example: ATP formation from creatine phosphate is accompanied by the transition of its  $\text{NH}$ -group at ADP to  $\text{NH}_2$ -group of creatine at ATP.

From Table 4 it is seen that the change in the bond energy of these 2 main radicals of metabolite is  $5.3238 - 4.9654 = 0.3584$  eV – taking the sesquialteral bond  $\text{N}^{\text{---}}\text{H}$  into account (as in polypeptides) and  $5.3238 - 4.6186 = 0.7052$  eV – for the single bond  $\text{N}-\text{H}$ . This is one of the intermediary results of the high-energy bond transformation process in ATP through the metabolite. From Tables 4 and 6 we can conclude that the phosphorous acid  $\text{H}_3\text{PO}_4$  can have 2 stationary valence-active states during the interactions in the system P–O for the orbitals with the values of  $P$ -parameters of weak and strong interactions, respectively. This defines the possibility for the glycolysis process to flow in 2 stages. At the first stage, the glucose and  $\text{H}_3\text{PO}_4$  molecules approach each other due to similar values of their  $P$ -parameters of strong interactions (Table 2). At the second stage,  $\text{H}_3\text{PO}_4$   $P$ -parameter in weak interactions 4.8779 eV (Table 4) in the presence of ferments provokes the bond  $(\text{H}_2\text{O}-\text{C})-(\text{C}-\text{H}_2\text{O})$  breakage in the glucose molecule with the formation of 2 mol of lactic acid whose  $P$ -parameters are equal to 4.3563 eV. The energy of this bond breakage process equalled to 0.726 eV (Table 4) is realised as the energy of high-energy bond it ATP.

According to the reference data about 40% of the glycolysis total energy, i.e. about 0.83 eV, remain in ATP.

By the hydrolysis reaction in ATP in the presence of ferments ( $\text{HPO}_3 + \text{H}_2\text{O} \rightarrow \text{H}_3\text{PO}_4 + \text{E}$ ) for structural  $P_s$ -parameters (Table 2)  $E = 11.708 + 4.3609 - 15.865 = 0.276$  eV.

It is known that the change in the free energy ( $\Delta G$ ) of hydrolysis of phosphorous anhydrite bond of ATP at  $\text{pH} = 7$  under standard conditions is 0.311–0.363 eV. But in the cell the  $\Delta G$  value can be much higher as the ATP and ADP concentration in it is lower than under standard conditions. Besides, the  $\Delta G$  value is influenced by the concentration of magnesium ions which is the acting co-ferment in the complex with ATP. Actually  $\text{Mg}^{2+}$  ion has the  $P_E$ -parameter equalled to 8.6066 eV (Table 1) which is very similar to the corresponding values of  $P$ -parameters of phosphorous and oxygen atoms. The quantitative evaluation of this factor requires additional calculations.

## CONCLUSIONS

Bond energies of some biostructures have been calculated following  $P$ -parameter and quantum-mechanical techniques. High-energy bonds in ATP are formed in the system P–O under functional transitions of their valence-active states. The data obtained agree with the experimental ones.

## REFERENCES

1. H. EYRING, J. WALTER, G. E. KIMBALL: Quantum Chemistry. I. John Wiley, New York, 1948. 528 p.
2. G. A. KORABLEV: Spatial-energy Principles of Complex Structures Formation. Brill Academic Publishers and VSP, Netherlands, 2005. 426 p.
3. C. F. FISCHER: Average Energy of Configuration Hartree-Fock Results for the Atoms Helium to Radon. Atomic Data, (4), 301 (1972).
4. J. T. WABER, D. T. CROMER: Orbital Radii of Atoms and Ions. J Chem Phys, **42**, 4116 (1965).
5. E. CLEMENTI, D. L. RAIMONDI: Atomic Screening Constants from SCF Functions. J Chem Phys, **38**, 2686 (1963).
6. E. CLEMENTI, D. L. RAIMONDI, W. P. REINHARDT: Atomic Screening Constants from SCF Functions. II. Atoms with 37 to 86 Electrons. J Chem Phys, **47** (4), 1300 (1967).
7. P. GOMBASH: Atom Statistical Model and Its Application. M.: I. L., 1951. 398 p.
8. E. CLEMENTI: Tables of Atomic Functions. A Supplement to the paper IBM. J Res Developm, **9**, 2 (1965).
9. G. A. KORABLEV, G. E. ZAIKOV: Spatial-energy Parameter as a Materialised Analog of Wave Function. In: Progress on Chemistry and Biochemistry, Nova Science Publishers, Inc. New York, 2009, 355–376.
10. G. A. KORABLEV, G. E. ZAIKOV: Energy of Chemical Bond and Spatial-energy Principles of Hybridization of Atom Orbitals. J of Applied Polymer Science, **101** (3), 2101 (2006).
11. G. A. KORABLEV, G. E. ZAIKOV: Formation of Carbon Nanostructures and Spatial-energy Criterion of Stabilization. Mechanics of Composite Materials and Structures (RAS), **15** (1), 106 (2009).
12. S. S. BATSANOV: Structural Chemistry. Facts and Dependencies. Moscow State University, Moscow, 2009.
13. M. M. VOLKENSHTEIN: Biophysics. Nauka, Moscow, 1988. 598 p.

14. Photosynthesis (Ed. M. Govindzhi). Mir, Moscow, Vol. 1, 1987. 728 p; Vol. 2, 1987. 460 p.
15. R. CLAYTON: Photosynthesis. Physical Mechanisms and Chemical Models. Mir, Moscow, 1984, p. 350.
16. M. W. SCHMIDT, K. K. BALDRIDGE, J. A. BOATZ, S. T. ELBERT, M. S. GORDON, J. H. JENSEN, S. KOSEKI, N. MATSNAGA, K. A. NGUYEN, S. J. SU, T. L. WINDUS, M. DUPUIS, J. A. MONTGOMERY: General Atomic and Molecular Electronic Structure System. *J Comput Chem*, **14**, 1347 (1993).
17. N. V. KHOKHRIAKOV, V. I. KODOLOV: Influence of Active Nanoparticles on the Structure of Polar Liquids. *Chemical Physics and Mesoscopy*, **11** (3), 388 (2009).
18. B. A. FENIOUK: Study of the Conjugation Mechanism of ATP Synthesis and ATP Proton Transport. *Biology and Natural Science*, 1998. 108 p.
19. B. A. FENIOUK, W. JUNGE, A. MULKIDJANIAN: Tracking of Proton Flow across the Active ATP-synthase of *Rhodobacter capsulatus* in Response to a Series of Light Flashes. *EBEC Reports*, **10**, 112 (1998).

*Received 3 April 2012*

*Revised 14 May 2012*



## **KINETIC AND MECHANISTIC STUDIES ON THE OXIDATION OF CHLORAMPHENICOL DRUG BY MANGANESE(III) PYROPHOSPHATE IN PHOSPHORIC ACID–WATER MEDIUM**

B. L. HIRAN\*, N. SHORGAR, J. KHUNTWAL, S. JAIN, M. L. MEENA

*Chemical Kinetics and Polymer Research Laboratory, Department of Chemistry, University College of Science, Mohan Lal Sukhadia University, 313 001 Udaipur (Rajasthan), India*

*E-mail: hiranbl@rediffmail.com; jyoti\_khuantwal@rediffmail.com*

### **ABSTRACT**

Chloramphenicol (CAP) is an antibiotic drug having a wide spectrum of activity. Mechanistic studies on the oxidation of chloramphenicol (CAP) drug by manganese(III) pyrophosphate ( $\text{Mn(III)py}_3$ ) in phosphoric acid–water medium have been performed. The reaction exhibits complex formation, first order dependence on  $[\text{Mn(III)py}_3]$  and zero order dependence on  $[\text{CAP}]$ . The oxidation rate is positively influenced by acidity and the order with respect to  $\text{H}^+$  is fractional. The effects of  $[\text{MnSO}_4]$  and  $[\text{Na}_2\text{SO}_4]$  have been studied. The effects of the dielectric constant of the medium and the ionic strength indicate the reaction to be of ion–ion type. The stoichiometry of the reaction is 1:1 and the product of oxidation is an aldehyde. Activation energy and various thermodynamic parameters have been evaluated. A suitable mechanism has also been suggested.

*Keywords:* kinetics and mechanism, oxidation, chloramphenicol, manganese(III) pyrophosphate.

### **AIMS AND BACKGROUND**

The reaction dynamics of oxidative decomposition of the drugs aid in studying the process by which the drugs produce their therapeutic or toxic effects. These concepts are the building blocks on which the edifice of drug design is built. The drugs having both  $-\text{NR}_2$ - and  $-\text{OH}$ -groups as their functional moieties belong to varying categories such as antiparkinsonian<sup>1,2</sup>, cholinergic, antihypertensive, analgesic, antipyretic and antibiotic. Their derivatives also make valuable pharmacological preparations. Oxidation is the most significant pathway of drug decomposition as it involves a series of

---

\* For correspondence.

physiochemical reactions and includes metabolites, enzymes and coenzymes. Mn(III)py<sub>3</sub> is an efficient tool for studying the mode of action of isoniazid on the InhA protein of mycobacterium tuberculosis<sup>2</sup>. Adonitol is also oxidised to ribose by Mn(III)py<sub>3</sub> (Ref. 3). The oxidation of the iso-propyl mandelate by Mn(III)py<sub>3</sub> has been studied<sup>4</sup>.

The reaction kinetics of drug degradation is the key element in understanding the stability of drugs. Nandibewoor and co-workers<sup>5</sup> reported oxidation of gabapentin (neurontin) by diperiodatocuprate(III). Nandibewoor and co-workers<sup>6</sup> studied redox kinetics of PAM by diperiodatoargentato(III). Mulla et al.<sup>7</sup> investigated the Ru(III)-catalysed oxidation of atenolol (ATN) by alkaline permanganate using stopped flow technique. Oxidation of levodopa and methyl dopa<sup>8</sup> in pyrophosphate medium by Mn(III) was also established. Mayanna et al.<sup>9</sup> studied kinetics of oxidation of CAP in alkaline and HClO<sub>4</sub> medium by 1-chlorobenzotriazole. Nandibewoor et al.<sup>10</sup> studied oxidative degradation and deamination of ATN. Hiremath and co-workers<sup>11</sup> studied oxidation of atenolol by alkaline diperiodatonickelate(IV). Chandrashekar et al.<sup>12</sup> studied the electrochemical oxidation of dopamine drug. The oxidation of paracetamol by alkaline diperiodatoargentate (III) was investigated by Sirsalmath et al.<sup>13</sup>

CAP (Chloromycetin; D-(-)-threo-2-dichloroacetamido-1-*p*-nitrophenyl propane-1,3-diol) drug is an antibiotic and finds application in combating with wide range of infections. These medicines have been used to deal with various disorders but reports on their redox kinetics still require attention and further research. Oxidative method of assay of CAP drug in pharmaceutical formulations was developed<sup>14</sup> and an aldehyde was identified as the oxidation product of CAP with ozone-air mixture. These kinetic results emerge some interesting features, which may throw some light on the mechanism of metabolic conversion of these medicines in biological system and also to identify the probable reactive species of the oxidant in aqueous medium. There are few reports on the kinetics of oxidation of medicines compounds by Mn(III)py<sub>3</sub>. This prompted us to undertake the present investigation, i.e. the kinetics of oxidation of CAP drug by Mn(III)py<sub>3</sub> in an effort to probe into the mechanism of oxidation of this drug.

## EXPERIMENTAL

*Materials and method.* A cherry-red coloured complex Mn(III)py<sub>3</sub> was prepared by the method described by Lingane and Karplus<sup>15</sup> and its purity was checked by an iodometric method:



All the other chemicals and solvents used were of high purity analytical grade. CAP (Ranbaxy Laboratories Ltd., Delhi) was used as such without additional purification. The solution of HClO<sub>4</sub> in water was standardised by using NaOH and phenolphthalein as an indicator. Doubly distilled water was used as a medium. The solution

of CAP was prepared in minimum amount of  $H_3PO_4$  as it was water-insoluble. The stock solution of CAP was stored in refrigerator.

*Kinetic measurements.* The reaction was initiated by adding  $Mn(III)py_3$  to the CAP. Pseudo-first order conditions were attained by keeping excess of substrate upon oxidant, i.e.  $[oxidant] \ll [substrate]$ . Decrease in concentration of  $Mn(III)py_3$  was followed by taking absorbance at  $\lambda_{max}$  of 510 nm. At different time interval pH of the reaction mixture was adjusted by using phosphoric acid. The pseudo-first order constants  $k_{obs}$  were determined from the linear plots of  $\lg [Mn(III)py_3]$  versus time. The concentration of compounds of the reaction mixture was predetermined and they were kept at desired temperature in a thermostated Jasco model 7800 UV-vis. spectrophotometer and a digital pH-meter was used to adjust the pH. All the rate constants are average of 2 to 3 experiments. The kinetic runs were followed for more than 60–70% completion of the reaction and good first order kinetics was observed. The rate constants  $k_{obs}$  were reproducible within  $\pm 5\%$  error. The activation parameters were also calculated.

*Stoichiometry.* Stoichiometry was ascertained by treating excess concentration of  $Mn(III)py_3$  and CAP ( $Mn(III)py_3$  and substrate concentration was always kept in 10:1 ratio), at pH 1.5. Before and after completion of reaction, the concentration of residual  $Mn(III)py_3$  was determined spectrophotometrically. A calibration curve for  $Mn(III)py_3$  was prepared and concentration of  $Mn(III)$  was calculated. The results revealed that 1 mol of CAP consumes 1 mol of  $Mn(III)py_3$ .

*Product analysis.* Product analysis was carried out under kinetic conditions, i.e. with an excess of the reductant over of  $Mn(III)py_3$  (10:1). In the reaction mixture, large volumes (250–500 ml) of CAP and of  $Mn(III)py_3$  were taken and the concentrations of them were M/50 and M/500, respectively, and kept in dark for 24 h to ensure completion of the reaction. The solution was then treated with an excess of saturated solution of 2,4-dinitrophenyl hydrazine in 2M HCl and kept overnight in a refrigerator. The precipitated 2,4-dinitrophenyl hydrazone was filtered off, dried, weighted and recrystallised from ethanol. Further chemical analysis for the identification of aldehydic or ketonic group gave positive test for the former.

*Spectral evidence for Mn(III)-chloramphenicol complex.* The study of UV-vis. spectra of pure  $Mn(III)py_3$  and a mixture of  $Mn(III)$  and CAP shows a change in peak wavelength and absorbance. For instance, pure  $Mn(III)$  pyrophosphate has  $\lambda_{max}$  510 nm at pH 1.5 and when CAP is mixed with  $Mn(III)$ , it shifts to 503 nm leading to the conclusion that there is a complex formation between  $Mn(III)$  and the substrate (Figs 1 and 2).

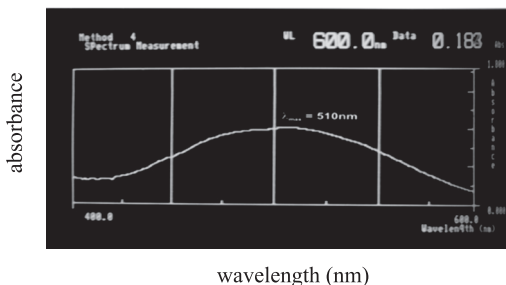


**Fig. 1.** Spectra of Mn(III) pyrophosphate without substrate (chloramphenicol) at pH 1.5 (spectra taken from a Jasco model 7800 UV-vis. spectrophotometer)

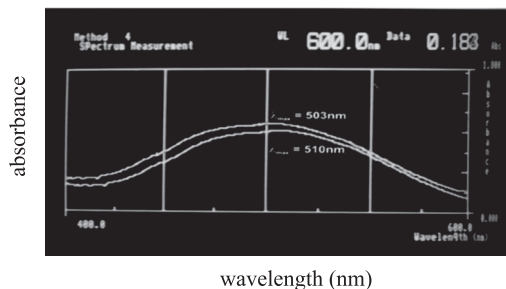


**Fig. 2.** Spectra of Mn(III) pyrophosphate at pH 1.5 with substrate (chloramphenicol) showing complex formation (spectra taken from a Jasco model 7800 UV-vis. spectrophotometer)

## RESULTS AND DISCUSSION

Oxidation of CAP drug by Mn(III)py<sub>3</sub> has been conducted in phosphoric acid–water medium (pH 1.5) at 318 K, under the pseudo–first order condition and the results will be discussed in the following pages.

*Stability of the oxidant (Mn(III)py<sub>3</sub>).* Solution of oxidant in phosphoric acid–water medium without substrate obeys the Beer–Lamberts law at  $\lambda_{\max} = 510$  nm. There was no change in the optical density of solution of Mn(III)py<sub>3</sub> in phosphoric acid–water mixture on long standing and heating upto 60–70°C. This indicated that Mn(III)py<sub>3</sub> is stable in phosphoric acid–water mixture.

*Effect of varying oxidant concentration.* The concentration of Mn(III)py<sub>3</sub> was varied in the range of 1.00 to 3.00×10<sup>-3</sup> mol dm<sup>-3</sup> at constant pH, [CAP], and at 318 K. The near constancy in the value of  $k_1$  irrespective of the concentration of Mn(III)py<sub>3</sub> confirmed the first order dependence (Table 1).

**Table 1.** Variation of rate with oxidant concentration, substrate concentration,  $[H^+]$ ,  $[MnSO_4]$ ,  $[Na_4P_2O_7]$ , acrylonitrile\* and temperature

$[Mn(III)py_3]$ $\times 10^3$ (mol dm <sup>-3</sup> )	$[Substrate]$ $\times 10^2$ (mol dm <sup>-3</sup> )	pH	$[MnSO_4]$ $\times 10^4$ (mol dm <sup>-3</sup> )	$[Na_4P_2O_7]$ $\times 10^3$ (mol dm <sup>-3</sup> )	Temperature (K)	$K_1 \times 10^5$ (s <sup>-1</sup> )
1	2	3	4	5	6	7
<b>1.00</b>	2.00	1.5	—	—	318	5.23
<b>1.85</b>	2.00	1.5	—	—	318	5.49
<b>1.92</b>	2.00	1.5	—	—	318	5.11
<b>2.00</b>	2.00	1.5	—	—	318	5.56
<b>2.08</b>	2.00	1.5	—	—	318	5.33
<b>2.17</b>	2.00	1.5	—	—	318	5.11
<b>2.27</b>	2.00	1.5	—	—	318	5.23
<b>3.00</b>	2.00	1.5	—	—	318	5.50
2.00	<b>1.53</b>	1.5	—	—	318	5.29
2.00	<b>1.66</b>	1.5	—	—	318	5.42
2.00	<b>1.81</b>	1.5	—	—	318	5.15
2.00	<b>2.00</b>	1.5	—	—	318	5.56
2.00	<b>2.22</b>	1.5	—	—	318	5.43
2.00	<b>2.50</b>	1.5	—	—	318	5.35
2.00	<b>2.85</b>	1.5	—	—	318	5.67
2.00	<b>3.33</b>	1.5	—	—	318	5.49
2.00	<b>4.00</b>	1.5	—	—	318	5.27
2.00	<b>5.00</b>	1.5	—	—	318	5.25
2.00	2.00	<b>1.2</b>	—	—	318	8.44
2.00	2.00	<b>1.3</b>	—	—	318	7.67
2.00	2.00	<b>1.5</b>	—	—	318	5.56
2.00	2.00	<b>1.6</b>	—	—	318	5.27
2.00	2.00	<b>1.7</b>	—	—	318	4.98
2.00	2.00	<b>1.9</b>	—	—	318	3.64
2.00	2.00	<b>2.1</b>	—	—	318	3.26
2.00	2.00	<b>2.3</b>	—	—	318	2.91
2.00	2.00	1.5	<b>0.00</b>	—	318	5.56
2.00	2.00	1.5	<b>0.66</b>	—	318	4.75
2.00	2.00	1.5	<b>1.33</b>	—	318	3.83
2.00	2.00	1.5	<b>2.00</b>	—	318	2.91
2.00	2.00	1.5	<b>2.66</b>	—	318	1.99
2.00	2.00	1.5	<b>3.33</b>	—	318	1.63
2.00	2.00	1.5	<b>4.00</b>	—	318	0.52
2.00	2.00	1.5	—	<b>0.0</b>	318	5.56
2.00	2.00	1.5	—	<b>1.2</b>	318	5.11
2.00	2.00	1.5	—	<b>2.4</b>	318	5.56
2.00	2.00	1.5	—	<b>3.6</b>	318	5.28

to be continued

Continuation of Table 1

1	2	3	4	5	6	7
2.00	2.00	1.5	–	<b>4.8</b>	318	5.39
2.00	2.00	1.5	–	<b>6.0</b>	318	5.35
2.00	2.00	1.5	–	<b>7.2</b>	318	5.11
2.00	2.00	1.5	–	–	<b>303</b>	1.48
2.00	2.00	1.5	–	–	<b>308</b>	2.30
2.00	2.00	1.5	–	–	<b>313</b>	4.09
2.00	2.00	1.5	–	–	<b>318</b>	5.56
2.00	2.00	1.5	–	–	<b>323</b>	8.82
2.00	2.00	1.5	–	–	<b>328</b>	10.55
2.00	2.00	1.5	–	–	318	5.56*

\* Contained 0.001 mol dm<sup>-3</sup> acrylonitrile.

*Effect of varying substrate concentration.* The substrate CAP was varied in the range of 1.53 to 5.00×10<sup>-2</sup> mol dm<sup>-3</sup> at 318 K, pH 1.5 and keeping all other reactant concentrations as constant and the rates were measured (Table 1). The results indicate that the rate of the reaction is independent with the change of substrate concentration, i.e. the reaction shows zero order dependence on CAP. This result is analogous with the oxidation of CAP (Ref. 9) in HClO<sub>4</sub> medium by 1-chlorobenzotriazole.

*Effect of varying pH.* The pH of the reaction mixture has been varied in the range 1.2 to 2.3 (Table 1). The results indicate that the rate of oxidation is positively influenced by acidity. The rate of oxidation increases with decrease in the pH of the medium. A plot of lg  $k_{\text{obs}}$  versus pH was linear with negative slope (Fig. 3) and the order with respect to H<sup>+</sup> is fractional. The pH of the medium has been altered by varying ortho-phosphoric acid concentration in reaction mixture at constant [CAP], [Mn(III)py<sub>3</sub>] and temperature. The pH corresponds to the final value achieved after adding the oxidant Mn(III)py<sub>3</sub>. Similar features were observed for the reaction of CAP in HClO<sub>4</sub> medium by 1-chlorobenzotriazole<sup>9</sup>.

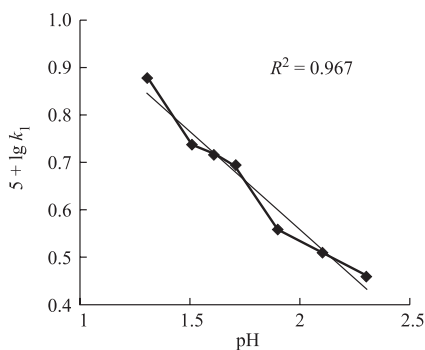


**Fig. 3.** Variation of rate with pH

*Effect of manganese sulphate concentration.* The rate of reaction decreases with increase in  $[\text{Mn(II)}]$  in the reaction mixture. The plot of  $k_{\text{obs}}$  versus  $[\text{Mn(II)}]$  (Fig. 4) is linear with negative slope. The rate reduced to almost 1/10 of the initial, as the concentration changes from  $0.66$  to  $4.00 \times 10^{-4} \text{ mol dm}^{-3}$  (Table 1). It may be due to the formation of organomanganous complex with the substrate which reduces the amount of free substrate for reaction with  $\text{Mn(III)py}_3$ .

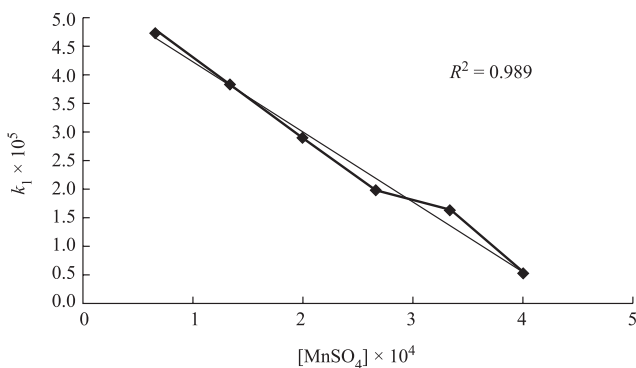


**Fig. 4.** Variation of rate with  $\text{MnSO}_4$

*Effect of sodium pyrophosphate concentration.* It has been observed that the rate of reaction remains unaltered with variation in  $\text{Na}_4\text{P}_2\text{O}_7$  concentration. The effect of  $\text{Na}_4\text{P}_2\text{O}_7$  has been studied in the range from  $1.2$  to  $7.2 \times 10^{-3} \text{ mol dm}^{-3}$  at constant  $[\text{CAP}]$ ,  $[\text{Mn(III)py}_3]$ , pH and temperature (Table 1).

*Induced polymerisation of acrylonitrile.* The oxidation of substrate CAP by  $\text{Mn(III)py}_3$ , in an atmosphere of  $\text{N}_2$  fails to induce the polymerisation of acrylonitrile. Then on dilution of the reaction mixture with methanol, no turbidity occurred, indicating the absence of free radical intervention (Table 1).

*Effect of ionic strength.* The concentration of salts such as  $\text{Na}_2\text{SO}_4$  and  $\text{CH}_3\text{COONa}$  has been varied to see the effect of salts on the rate of oxidation in the Debye–Hückel limit. The concentration has been varied in the range  $0.50$  to  $3.00 \times 10^{-2} \text{ mol dm}^{-3}$ , provided other conditions being constant (Table 2). It has been observed that the rate of oxidation is slightly inhibited by increasing ionic strength. It proves that the interaction in rate-determining step is of ion–ion type<sup>16</sup>.

**Table 2.** Variation of rate with ionic strength

$[\text{Na}_2\text{SO}_4] \times 10^2$ (mol dm <sup>-3</sup> )	$K_1 \times 10^5$ (s <sup>-1</sup> )	$[\text{CH}_3\text{COONa}] \times 10^2$ (mol dm <sup>-3</sup> )	$K_1 \times 10^5$ (s <sup>-1</sup> )
0.0	5.56	0.0	5.56
0.5	5.26	0.5	5.28
1.0	5.03	1.0	5.11
1.5	4.98	1.5	5.05
2.0	4.75	2.0	4.90
2.5	4.35	2.5	4.17
3.0	4.29	3.0	4.05

*Effect of solvent composition.* The influence of solvent polarity on the rate of oxidation has been studied in ethanol–water mixture. The ethanol % (v/v) has been varied from 0–40% at constant [CAP], [Mn(III)py<sub>3</sub>], pH and temperature (Table 3). Other solvents could not be used due to their reactivity with Mn(III)py<sub>3</sub>. The reaction rate increased with decrease in the dielectric constant of the medium, suggesting that a medium of low dielectric constant favours the oxidation process. Plot of  $\lg k_{\text{obs}}$  versus  $((D-1)/(2D+1))$  (Fig. 5) is a curvature indicating absence of dipole–dipole interaction in the rate-determining step. Plot of  $\lg k_1$  versus reciprocal of dielectric constant ( $1/D$ ) (Fig. 6) of the medium is linear with a positive slope, suggesting the presence of either ion–ion or ion–dipole type of interaction between the oxidant and the substrate<sup>17</sup>. But due to small change in the rate by the addition of ionic salts indicates the possibility of ion–ion type of interaction between the reactants. Therefore, the interaction in rate-determining step is of ion–ion type<sup>16</sup>. Positive slope indicating a reaction involving cation–anion interaction in the rate-determining step. This result is similar to KMnO<sub>4</sub> oxidation of ATN (Ref. 7) in alkaline medium.

**Table 3.** Variation of rate with ethanol composition

C <sub>2</sub> H <sub>5</sub> OH (% (v/v))	$(1/D) \times 10^2$	$((D-1)/(2D+1)) \times 10^2$	$k_1 \times 10^5$ (s <sup>-1</sup> )
0	1.27	49.05	5.56
5	1.28	49.04	6.14
10	1.30	49.03	7.06
15	1.32	49.01	9.32
20	1.34	49.00	14.05
25	1.36	48.98	16.78
30	1.38	48.97	20.37
35	1.41	48.94	31.75
40	1.44	48.92	46.65

\* Dielectric constant calculated by the law of mixtures.



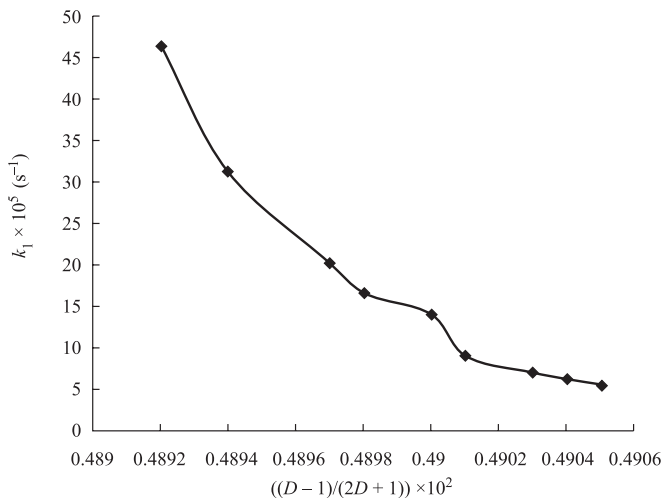


Fig. 5. Variation of rate with solvent composition

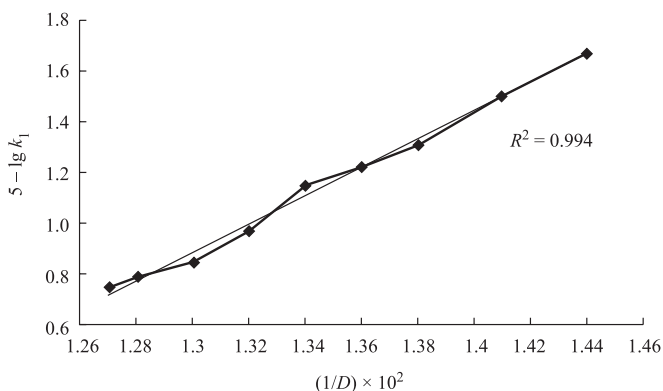
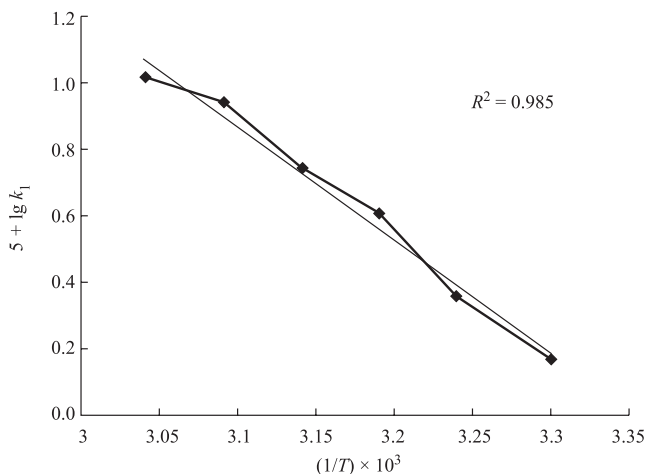


Fig. 6. Variation of rate with solvent composition

However, this result is contrary to the oxidation of levodopa and methyl dopa<sup>8</sup> where increase in ethanol percentage decreases the rate of reaction. In the oxidation of PAM by diperiodatoargentate<sup>6</sup> and CAP (Ref. 10) by 1-chlorobenzotriazole increase in the percentage of tertiary butanol decreases the rate of reaction.

*Effect of temperature.* The rate of oxidation increases with increase in the temperature. The reactions have been studied in the temperature range from 303 to 328 K (Table 1). Plot of  $\lg k_{\text{obs}}$  versus  $1/T$  (inverse of absolute temperature) (Fig. 7) is a straight line with negative slope. This shows that the Arrhenius equation is valid for this oxidation. Calculation of activation parameters for the rate-determining step showed that this reaction is not enthalpy-controlled (Table 4). Lowest energy of activation is not associated with highest rate or vice versa. According to Glasstone<sup>18</sup>, negative entropy suggests that the rate-determining step is a slow bimolecular reaction.



**Fig. 7.** Variation of rate with temperature

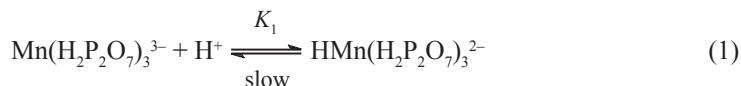
**Table 4.** Thermodynamic activation parameters

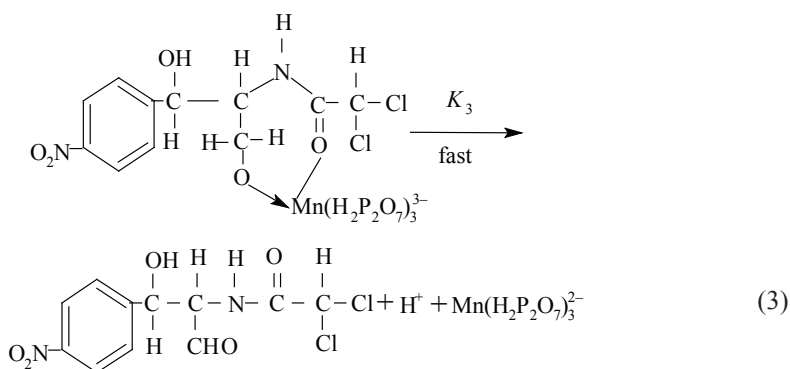
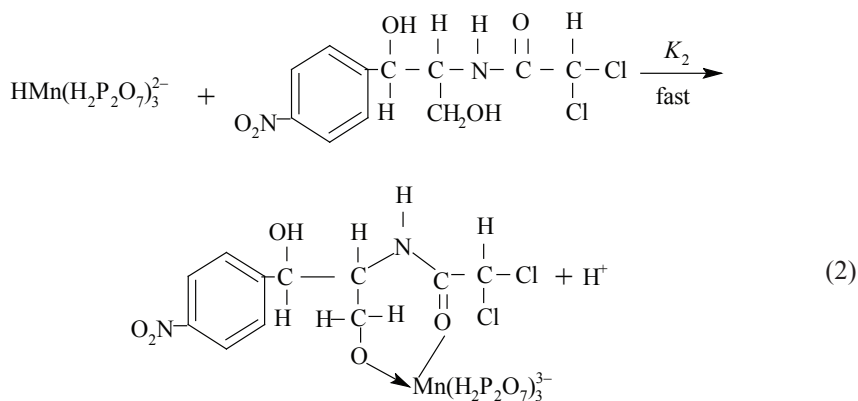
Activation parameters	Values
Energy of activation, $\Delta E_a^*$	62.59 kJ mol <sup>-1</sup>
Enthalpy of activation $\Delta H^*$	59.95 kJ mol <sup>-1</sup>
Entropy of activation $\Delta S^*$	-37.80 J K <sup>-1</sup> mol <sup>-1</sup>
Frequency factor pZ	$1.059 \times 10^{11}$
Free energy change $\Delta F^*$	71.97 kJ mol <sup>-1</sup>

#### MECHANISM

The lack of any effect of radical scavenger such as acrylonitrile on the reaction rate and failure to induce polymerisation of acrylonitrile point against the operation of a one-electron oxidation giving rise to free radicals. In the light of the observed experimental results and evidences from other investigations, a suitable scheme has been proposed and it is presented in the following Scheme.

#### Scheme





## CONCLUSIONS

The oxidation of chloramphenicol drug was carried out by manganese(III) pyrophosphate ( $\text{Mn(III)py}_3$ ) in phosphoric acid–water medium. The mechanism involves protonation of  $\text{Mn(III)py}_3$  which is the rate-determining step as it involves cation–anion interaction supported by the solvent effect and ionic strength results. This protonated species reacts with CAP to form a complex. This complex breaks to give the product D(-)-threo-2-dichloroacetamido-1-nitrophenyl-1-hydroxy-3-propanal and Mn(II).

## ACKNOWLEDGEMENT

The authors gratefully acknowledge CDRI, Lucknow and SICART Vallabh Vidhyanagar for analysis.

## REFERENCES

1. D. R. LAURENCE, P. N. BENNET: Chemical Pharmacology. 7th ed. ELBS Publication, 1993. 310 p.

2. M. NGUYEN, A. QUEMARD, S. BROUSSY, J. BERNADOU, B. MEUNIER: Mn(III) Pyrophosphate as an Efficient Tool for Studying the Mode of Action of Isoniazid on the InhA Protein of *Mycobacterium tuberculosis*. *Antimicrob Agents Chemother*, **46** (7), 2137 (2002).
3. A. G. FADNIS, S. K. KULSHRESTHA: Kinetics of Oxidation of Adonitol by Manganese (III) Pyrophosphate. *React Kinet Catal*, **19** (3–4), (1982).
4. R. K. MALKANI, K. S. SURESH, G. V. BAKORE: Kinetics and Mechanism of Oxidation of Isopropyl Mandelate by Manganese (III) Pyrophosphate. *J Inorg Nucl Chem*, **39** (4), 621 (1977).
5. S. A. CHIMATADAR, T. BASAVARAJ, K. A. THABAJ, S. T. NANDIBEWOOR: Ruthenium (III) Catalyzed Oxidation of Gabapentin (Neurontin) by Diperiodatocuprate (III) in Aqueous Alkaline Medium – A Kinetic and Mechanistic Study. *Asian J Chem*, **267** (1–2), 65 (2007).
6. D. C. HIREMATH, C. V. HIREMATH, S. T. NANDIBEWOOR: Oxidation of Paracetamol Drug by a New Oxidant Diperiodatoargentate (III) in Aqueous Alkaline Medium. *E-J Chem*, **3** (10), 13 (2006).
7. R. A. MULLA, G. C. HIREMATH, S. T. NANDIBEWOOR: Kinetic, Mechanistic and Spectral Investigation of Ruthenium (III)-catalyzed Oxidation of Atenolol by Alkaline Permanganate (Stopped-flow Technique). *J Chem Sci*, **117** (1), 33 (2005).
8. B. S. SHERIGARA, B. E. KUMARA SWAMY, E. V. S. SUBRAHMANYAM, K. I. BHAT: Oxidation of 3-(3,4-dihydroxy phenyl)-l-alanine (Levodopa) and 3-(3,4-dihydroxy phenyl)-2-methyl-l-alanine (Methyl dopa) by Manganese(III) in Pyrophosphate Media: Kinetic and Mechanistic Study. *Int J Chem Kinet*, **33** (8), 449 (2001).
9. R. C. HIREMATH, R. V. JAGDEESH, PUTTASWAMY, S. M. MAYANNA: Kinetics and Mechanism of Oxidation of Chloramphenicol by 1-chlorobenzotriazole in Acidic Medium. *J Chem Sci*, **117** (4), 333 (2005).
10. R. N. HEGDEA, N. P. SHETTIA, S. T. NANDIBEWOOR: Oxidative Degradation and Deamination of Atenolol by Diperiodatocuprate (III) in Aqueous Alkaline Medium: A Mechanistic Study. *Polyhedron*, **28** (16), 3499 (2009).
11. G. C. HIREMATH, R. M. MULLA, S. T. NANDIBEWOOR: Kinetic, Mechanistic and Spectral Investigation of Ruthenium (III) Catalyzed Oxidation of Atenolol by Alkaline Diperiodatonicckelate(IV) (Stopped Flow Technique). *Catal Lett*, **98** (1), (2004).
12. B. N. CHANDRASHEKAR, B. E. KUMARASWAMY, M. PANDURANGACHAR, S. S. SHANKAR, O. GILBERT, J. G. MANJUNATHA, B. S. SHERIGARA: Electrochemical Oxidation of Dopamine at Polyethylene Glycol Modified Carbon Paste Electrode: A Cyclic Voltammetric Study. *Int J Electrochem Sci*, **5**, 578 (2010).
13. K. T. SIRSALMATH, C. V. HIREMATH, S. T. NANDIBEWOOR: Kinetic, Mechanistic and Spectral Investigations of Ruthenium (III)/Osmium (VIII)-catalyzed Oxidation of Paracetamol by Alkaline Diperiodatoargentate (III) (Stopped Flow Technique). *Appl Catal A-Gen*, **305** (1), 79 (2006).
14. B. JAYARAM, S. M. MAYANNA: Oxidimetric Estimation of Chloramphenicol with Aromatic Sulphonyl Monohaloamines. *Talanta*, **30** (10), 798 (1983).
15. J. J. LINGANE, R. KARPLUS: New Methods for the Estimation of Manganese. *Ind Eng Chem Anal Ed*, **18**, 191 (1946).
16. K. J. LAIDLER: *Chemical Kinetics*. 3rd ed. Pearson Education, 2005. 198 p.
17. G. L. AGARWAL, SHAMI JHANE KHARE: Kinetics and Mechanism of Oxidation of 2, 3-butane Diol by Corey's Reagents (PCC) in Non-aqueous Medium. *J Ind Council Chem*, **X** (2), 26 (1994).
18. S. GLASSTONE, K. J. LAIDLER, H. ERYING: *The Theory of Rate Process*. McGraw–Hill, New York, 1947.

*Received 22 September 2010*

*Revised 10 November 2010*

## **EXPLORING QSAR ANALYSIS OF CYCLOHEXANAMINE CLASS OF HUMAN SEROTONIN TRANSPORTERS (HSERT) INHIBITORY ACTIVITIES USING PHYSICOCHEMICAL PARAMETERS**

N. SHUKLA\*, A. K. SRIVASTAVA

*QSAR Research Laboratory, Department of Chemistry, University of Allahabad, 211 002 Allahabad, India*

*E-mail: neerjashuklaau2007@rediffmail.com*

### **ABSTRACT**

QSAR studies have been made on a novel series of cyclohexanamine derivatives acting as potent and selective human serotonin transporters (HSERT). The HSERT inhibitory activities of these compounds were found to be dominantly controlled by steric and topological factors with inclusion of different indicator parameters such as  $I_1$ , and  $I_2$  at different positions. Cross-validation methodology was performed for ascertaining predictive power of the QSAR models.

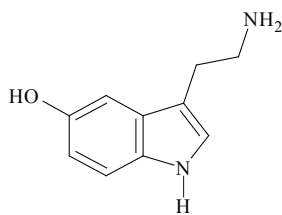
*Keywords:* QSAR, HSERT inhibitors, steric and topological parameters.

### **AIMS AND BACKGROUND**

The serotonin transporter (SERT) is a monoamine transporter protein. This protein is an integral membrane protein that transports the neurotransmitter serotonin from synaptic spaces into presynaptic neurons. This is a target of psychomotor stimulants such as amphetamine and cocaine and is a member of the sodium neurotransmitter symporter family. The transporter protein by recycling serotonin regulates its concentration in a gap or synapse and thus it affects a receiving neuron receptor. Any change in the serotonin transporter metabolism appears to be associated with different phenomena including alcoholism, clinical depression, obsessive-compulsive disorder (OCD), romantic love, hypertension and generalised social phobia. The current study represents the QSAR analysis of cyclohexanamine<sup>1</sup> derivatives using a number of structural parameters along with different indicator parameters at different substitution sites.

---

\* For correspondence.



serotonin

## EXPERIMENTAL

QSAR studies were performed on the series of cyclohexanamines. The 2D structures of the molecules were drawn using Chem. Sketch software<sup>2</sup>. Several physicochemical parameters were used in the present study: density ( $D$ ), polarisability (Pz), parachor (Pc). These are steric parameters calculated by ACD Lab Chem Sketch Software<sup>2</sup>. Density is related with the bulk and size of the substituents.

$$D = \frac{\text{Mw (molecular weight)}}{\text{Mv (molecular volume)}} .$$

Index of refraction (IOR) of a medium is the ratio of the speed of light in vacuum to its velocity in the medium<sup>2</sup>; surface tension (St) is the cohesive forces between liquid molecules responsible for the phenomenon called as surface tension<sup>2</sup>; molecular connectivity ( $\chi$ ) (Ref. 3) – the Randic index  ${}^1\chi = {}^1\chi(G)$  of  $G$  was introduced by Randic in 1975 as the connectivity index; partition coefficient ( $\lg P$ ) (Ref. 4) – the octanol-water partition coefficient,  $P$ , is a measure of the differential solubility of a neutral substance between the immiscible liquids and thereby, a descriptor of hydrophobicity (or lipophilicity) of a neutral substance. It is typically used in its logarithmic form,  $\lg P$ ; indicator variables<sup>5</sup>– these are not QSAR parameters but are used to indicate the significance of any particular group or species at a particular substitution site in a given series of drugs.

## RESULTS AND DISCUSSION

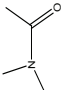
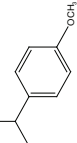
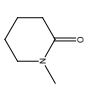
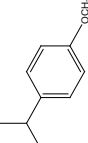
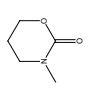
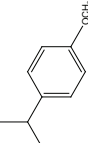
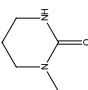
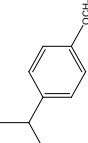
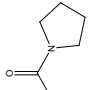
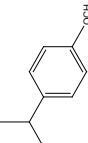
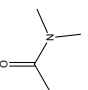
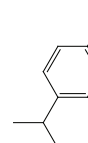
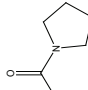
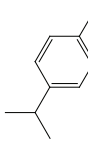
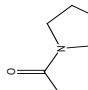
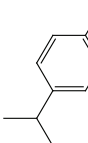
QSAR was performed on a series of 15 cyclohexanamine derivatives with the physicochemical parameters, which are listed in Table 1, where the biological activity ( $\text{pIC}_{50}$ ) is a measure of inhibitory activity. All the QSARs reported here were derived by us and were not reported with the original data set taken from literature as reference. We have used the Hansch analysis for developing these models. The QSAR multiple regression analyses were performed with SPSS (7.5) version program. Their activity data and the physicochemical parameters evaluated in the correlation are listed in Table 2. These parameters were found to be useful earlier in QSAR-based drug modelling<sup>6-15</sup>.

**Table 1.** Biological activity and physicochemical data for cyclohexanamine derivatives

S.No	R <sub>1</sub>	R <sub>2</sub>	pIC <sub>50</sub>	IOR	St	D	IgP	Pc	Pz	<sup>3</sup> χ	<sup>4</sup> χ	<sup>5</sup> χ	I <sub>1</sub>	I <sub>2</sub>
1	2	3	4	5	6	7	8	9	10	11	12	13	14	15
<b>1</b>			7.824	1.602	49.6	1.12	6.694	1238.2	63.48	14.859	12.400	9.670	1	0
<b>2</b>			7.770	1.603	52.0	1.14	5.665	1233.8	62.61	14.859	12.400	9.670	1	0
<b>3</b>			7.854	1.599	52.1	1.15	5.914	1292.4	65.13	15.678	12.868	9.977	1	0
<b>4</b>			8.097	1.609	53.4	1.19	5.878	1270.9	64.52	15.270	12.557	9.859	1	0
<b>5</b>			7.585	1.582	49.3	1.13	4.761	1178.0	58.85	13.373	11.239	8.563	1	0

to be continued

Continuation of Table 1

1	2	3	4	5	6	7	8	9	10	11	12	13	14	15
<b>6</b>			7.854	1.581	49.1	1.13	4.980	1216.1	60.78	14.348	11.472	8.643	1	0
<b>7</b>			7.959	1.594	51.5	1.15	5.411	1266.8	63.64	15.291	12.825	9.981	1	0
<b>8</b>			7.770	1.597	52.8	1.18	4.827	1247.0	62.49	15.291	12.825	9.981	1	0
<b>9</b>			7.620	1.603	53.4	1.17	4.827	1255.0	63.25	15.291	12.825	9.981	1	0
<b>10</b>			7.770	1.594	51.5	1.15	5.411	1266.8	63.64	15.454	12.735	9.317	1	0
<b>11</b>			7.420	1.581	49.1	1.13	4.980	1216.1	60.78	14.348	11.472	8.643	1	0
<b>12</b>			7.119	1.595	50.8	1.13	6.211	1246.4	62.95	15.046	12.424	9.207	0	0
<b>13</b>			7.229	1.604	52.8	1.19	6.211	245.3	63.03	15.046	12.424	9.207	0	0

to be continued



## Continuation of Table 1

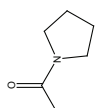
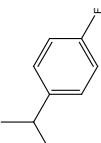
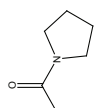
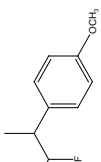
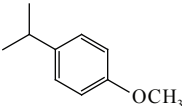
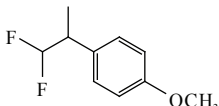
	1	2	3	4	5	6	7	8	9	10	11	12	13	14	15
				6.886	1.592	50.6	1.17	6.104	1215.5	61.16	15.046	12.424	9.207	0	0
<b>14</b>															
				5.319	1.580	49.7	1.20	5.623	1283.0	63.73	16.012	13.269	9.921	0	1
<b>15</b>															

Table 2. Correlation matrix between physicochemical parameters and indicator parameters

	pIC <sub>50</sub>	Pz	Pc	IOR	lg P	<sup>5</sup> χ	<sup>3</sup> χ	<sup>4</sup> χ	D	St	I <sub>1</sub>	I <sub>2</sub>
pIC <sub>50</sub>	1.000											
Pz	0.033	1.000										
Pc	-0.120	0.953	1.000									
IOR	0.462	0.630	0.414	1.000								
lg P	-0.139	0.483	0.297	0.468	1.000							
<sup>5</sup> χ	-0.007	0.822	0.800	0.594	0.219	1.000						
<sup>3</sup> χ	-0.314	0.871	0.926	0.372	0.341	0.805	1.000					
<sup>4</sup> χ	-0.282	0.838	0.867	0.464	0.322	0.901	0.949	1.000				
D	-0.431	0.400	0.493	0.261	0.030	0.505	0.611	0.618	1.000			
St	-0.082	0.083	0.167	-0.152	-0.039	-0.034	0.131	0.077	0.234	1.000		
I <sub>1</sub>	0.763	-0.018	-0.058	0.108	-0.487	0.082	-0.271	-0.241	-0.410	-0.153	1.000	
I <sub>2</sub>	-0.873	0.179	0.352	-0.419	0.026	0.244	0.438	0.409	0.473	0.040	-0.443	1.000

In order to study the role of different substituents at different positions indicator

parameters as  $I_1$  and  $I_2$  for  and  at  $R_2$  position,

were introduced and are also listed in Table 1. Multi-regression analysis of the data gave several regression models of which the following equations were found to be the significant.

$$\text{pIC}_{50} = 0.678 (\pm 0.412) I_1 - 1.853 (\pm 0.741) I_2 + 0.07 (\pm 0.105) \text{Pz} + 2.758 \quad (1)$$

$n = 15, R = 0.983, R^2 = 0.965, R^2_A = 0.956, \text{SE} = 0.143, F_{(3,11)} = 102.133, Q = 1.578;$

$$\text{pIC}_{50} = 0.667 (\pm 0.434) I_1 - 1.935 (\pm 0.821) I_2 + 0.004 (\pm 0.006) \text{Pc} + 2.473 \quad (2)$$

$n = 15, R = 0.981, R^2 = 0.962, R^2_A = 0.951, \text{SE} = 0.150, F_{(3,11)} = 92.339, Q = 1.656;$

$$\text{pIC}_{50} = 0.720 (\pm 0.444) I_1 - 1.562 (\pm 0.862) I_2 + 11.574 (\pm 21.107) \text{IOR} - 11.405 \quad (3)$$

$n = 15, R = 0.980, R^2 = 0.960, R^2_A = 0.949, \text{SE} = 0.154, F_{(3,11)} = 87.614, Q = 1.693;$

$$\text{pIC}_{50} = 0.826 (\pm 0.558) I_1 - 1.667 (\pm 0.864) I_2 + 0.166 (\pm 0.380) \lg P + 6.053 \quad (4)$$

$n = 15, R = 0.977, R^2 = 0.954, R^2_A = 0.942, \text{SE} = 0.165, F_{(3,11)} = 76.156, Q = 1.812;$

$$\text{pIC}_{50} = 0.651 (\pm 0.486) I_1 - 1.879 (\pm 0.885) I_2 + 0.169 (\pm 0.390) {}^5\chi + 5.525 \quad (5)$$

$n = 15, R = 0.977, R^2 = 0.954, R^2_A = 0.941, \text{SE} = 0.165, F_{(3,11)} = 75.671, Q = 1.820;$

$$\text{pIC}_{50} = 0.715 (\pm 0.485) I_1 - 1.895 (\pm 0.920) I_2 + 1.410 (\pm 0.351) {}^3\chi + 4.955 \quad (6)$$

$n = 15, R = 0.976, R^2 = 0.952, R^2_A = 0.939, \text{SE} = 0.168, F_{(3,11)} = 72.988, Q = 1.848;$

$$\text{pIC}_{50} = 0.711 (\pm 0.487) I_1 - 1.883 (\pm 0.919) I_2 + 0.146 (\pm 0.377) {}^4\chi + 5.260 \quad (7)$$

$n = 15, R = 0.975, R^2 = 0.951, R^2_A = 0.938, \text{SE} = 0.170, F_{(3,11)} = 71.825, Q = 1.864;$

$$\text{pIC}_{50} = 0.736 (\pm 0.527) I_1 - 1.859 (\pm 0.968) I_2 + 2.718 (\pm 9.395) D + 3.916 \quad (8)$$

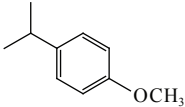
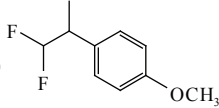
$n = 15, R = 0.973, R^2 = 0.946, R^2_A = 0.932, \text{SE} = 0.178, F_{(3,11)} = 64.804, Q = 1.960;$

$$\text{pIC}_{50} = 0.701 (\pm 0.552) I_1 - 1.758 (\pm 0.967) I_2 + 0.0009 (\pm 0.018) \text{ST} + 7.034 \quad (9)$$

$n = 15, R = 0.983, R^2 = 0.965, R^2_A = 0.956, \text{SE} = 0.143, F_{(3,11)} = 102.150, Q = 2.092$

where  $n$  is the number of data points;  $R$  – correlation coefficient of determination; SE – the standard error of estimate;  $R^2_A$  – represents adjusted  $R^2$ ;  $F$  – variance ratio<sup>16</sup> between observed and calculated activity;  $Q$  – the quality of fit<sup>17,18</sup>, and data within parenthesis are for the 95% confidence intervals.

The positive sign of coefficient of Pz, St, IOR, D, Pc,  $\lg P$ ,  ${}^3\chi$ ,  ${}^4\chi$ , and  ${}^5\chi$  indicates that more polar, more bulky, denser, more hydrophobic groups and groups with third, fourth and fifth orders of branching are preferable for the activity. The positive sign of

coefficient of  $I_1$  makes it that the group  at  $R_2$  position is beneficial for the activity, while negative coefficient of  $I_2$  explains that the group  at  $R_2$  position should be strictly avoided in the future drug modelling.

Predicted and residual values for the best model equation (1) are given in Table 3. In this equation the  $F$  ratio value is much higher than theoretical  $F$  value ( $F_{(3,11)} = 3.59$ ) indicating the statistical significance of this equation. Predicted values are the calculated activities of the equation and the residual values are the difference between the observed biological activities and the calculated activities and are found to be low.

**Table 3.** Comparison between observed and predicted activities and their residual values

S. No	Observed	Calculated	Residual
1	7.824	7.832	-0.008
2	7.770	7.772	-0.002
3	7.854	7.946	-0.092
4	8.097	7.904	0.193
5	7.585	7.512	0.073
6	7.854	7.645	0.209
7	7.959	7.843	0.116
8	7.770	7.764	0.006
9	7.620	7.816	-0.196
10	7.770	7.843	0.073
11	7.420	7.645	0.225
12	7.119	7.117	0.002
13	7.229	7.123	0.106
14	6.886	6.994	-0.108
15	5.319	5.319	0.000

The plot of observed  $pIC_{50}$  versus predicted  $pIC_{50}$  based on equation (1) is shown in Fig. 1 and the predicted  $R^2$  was found to be fairly large.

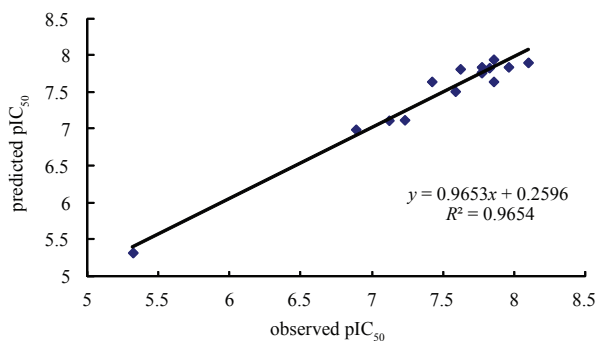


**Fig. 1.** Plot between observed and predicted pIC<sub>50</sub> values using model 1

#### CROSS-VALIDATION

The cross-validation analysis was performed using leave-one-out (LOO) method<sup>19</sup>, in which one compound is removed from the data set and the activity is correlated using the rest of the data set. The cross-validated  $R^2$  in each case was found to be very close to the value of  $R^2$  for the entire data set and hence these models can be termed as statistically significant.

Cross-validation provides the values of PRESS (predicted residual sum of squares), SSY (sum of the squares of the response) and  $R^2_{cv}$  (overall predicted ability) and PSE (predicted squares error) from which we can test the predictive power of the proposed model. It is argued that PRESS is a good estimate of the real predictive error of the model and if it is smaller than SSY the model predicts better than chance and can be considered statistically significant. Furthermore, the ratio PRESS/SSY can be used to calculate approximate confidence intervals of prediction of new compound. To be a reasonable QSAR model PRESS/SSY should be smaller than 0.4. Also, if PRESS value is transformed in a dimension less term by relating it to the initial sum of squares, we obtain  $R^2_{cv^2}$  i.e. the complement to the traces on of unexplained variance over the total variance. The PRESS and  $R^2_{cv}$  have good properties. However, for practical purposes of end users the use of square root of PRESS/N, which is called predictive square error (PSE), is more directly related to the uncertainty of the predictions. The PSE values also support our results. The calculated cross-validated parameters confirm the validity of the models. All the requirements for an ideal model have been fulfilled by model 1, that is why, we have considered as the best model.

$R^2_A$  takes into account the adjustment of  $R^2$  and is a measure of the percentage explained variation in the dependent variable that takes into account the relationship between the number of cases and the number of independent variables in the regression model. Whereas  $R^2$  will always increase when an independent variable is added,  $R^2_A$  will decrease if the added variable does not reduce the unexplained variable enough to offset the loss of decrease of freedom.

The predictive error of coefficient of correlation (PE) (Ref. 20) is yet another parameter used to decide the predictive power of the proposed models. We have calculated PE value of all the proposed models and they are reported in Table 4. It is argued that if

$R < PE$ , then correlation is not significant;

$R > PE$ ; several times (at least three times), then correlation is indicated; and if

$R > 6PE$ , then the correlation is definitely good.

For all the models developed the condition  $R > 6PE$  is satisfied and hence can be said they have a good predictive power.

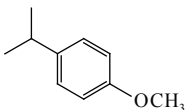
**Table 4.** Cross-validated parameters and predictive error of coefficient of correlation (PE) for the proposed model

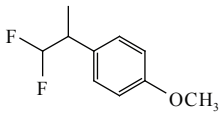
S. No	Parameters used	<i>n</i>	PRESS	SSY	PRESS/SSY	$R^2_{cv}$	PSE	<i>R</i>	$1 - R^2$	PE	6PE
1	$I_1 + I_2 + Pz$	15	0.226	6.284	0.036	0.964	0.123	0.983	0.035	0.006	0.036
2	$I_1 + I_2 + Pc$	15	0.249	6.261	0.040	0.960	0.129	0.981	0.038	0.007	0.042
3	$I_1 + I_2 + IOR$	15	0.261	6.248	0.042	0.958	0.132	0.980	0.040	0.007	0.042
4	$I_1 + I_2 + lg P$	15	0.299	6.211	0.048	0.952	0.141	0.977	0.046	0.008	0.048
5	$I_1 + I_2 + {}^5\chi$	15	0.301	6.209	0.048	0.952	0.142	0.977	0.046	0.008	0.048
6	$I_1 + I_2 + {}^3\chi$	15	0.311	6.198	0.050	0.950	0.144	0.976	0.048	0.008	0.048
7	$I_1 + I_2 + {}^4\chi$	15	0.316	6.194	0.051	0.949	0.145	0.975	0.049	0.008	0.048
8	$I_1 + I_2 + D$	15	0.349	6.161	0.057	0.943	0.153	0.973	0.054	0.009	0.054
9	$I_1 + I_2 + St$	15	0.398	6.111	0.065	0.935	0.163	0.969	0.061	0.011	0.066

## CONCLUSIONS

From the results and discussion made above, it may be concluded that:

- bulkier, denser and polar groups having more branching should be used;
- more hydrophobic groups are favourable for the activity;

– the group  at  $R_2$  position favours the inhibitory activity;

– the group  at  $R_2$  position should be avoided in future drug designing.

## REFERENCES

1. K. CHO, M. ANDO, K. KOBAYASHI, H. MIYAZOE, T. TSUJINO, S. ITO, T. SUZUKI, T. TANAKA, S. TOKITA, N. SATO: Design, Synthesis and Evaluation of a Novel Cyclohexanamine Class of Neuropeptide YY1. *Bioorg Med Chem Lett*, **19**, 4781 (2009).

2. ACD – LAB Software for Calculating the Referred Physiochemical Parameters. Chem Sketch. [www.acdlabs.com/acdlabs-rss-feed.xml](http://www.acdlabs.com/acdlabs-rss-feed.xml).
3. DRAGON Software for Calculation of Topological Indices: ([www.disat.unimib.it](http://www.disat.unimib.it)).
4. G. C. NYS, R. F. REKKER: Partition Coefficient. Chem Therap, **8**, 52 (1973).
5. M. RECONTANT, T. K. KLEIN, C. Z. YANG, J. McCLARIN, R. LANGRIDGE, C. HANSCH: Indicator Variables. Mol Pharmacol, **29**, 436 (1986).
6. A. K. SRIVASTAVA, N. SHUKLA, A. PANDEY, A. SRIVASTAVA: QSAR Based Modeling on a Series of Alpha-hydroxy Amides as a Novel Class of Bradykinin B1 Selective Antagonists. J Saudi Chem Soc, **15**, 215 (2011).
7. A. K. SRIVASTAVA, A. PANDEY, A. SRIVASTAVA, N. SHUKLA: QSAR Based Modeling of Hepatitis C Virus NS5B Inhibitors. J Saudi Chem Soc, **15**, 25 (2011).
8. A. K. SRIVASTAVA, N. SHUKLA, V. K. PATHAK: Quantitative Structure Activity Relationship (QSAR) Studies on a Series of Off-target Ion Channel Selective Diltiazem Sodium Derivatives. J Indian Chem Soc, **87**, 1 (2010).
9. A. K. SRIVASTAVA, N. SHUKLA: Quantitative Structure Activity Relationship (QSAR) Studies on a Series of Imidazole Derivatives as Novel ORL1 Receptor Antagonists. J Saudi Chem Soc, (2011).
10. A. K. SRIVASTAVA, N. SHUKLA, A. PANDEY: QSAR Based Modeling on a Novel Series of Pyrimidine-4-carboxamides as Antagonists of the Human A<sub>1</sub> Receptor. Oxid Commun (in press).
11. A. K. SRIVASTAVA, N. SHUKLA, A. PANDEY, A. SRIVASTAVA, V. K. PATHAK: QSAR Studies on a Novel Cyclohexanamine Class of Human Serotonin Transporter (HSERT) Inhibitory Activities. Oxid Commun (in press).
12. A. K. SRIVASTAVA, AKANCHHA SRIVASTAVA, N. SHUKLA: QSAR Study on TIE-2 Inhibitors: Dominating Role of Topological Parameters. Oxid Commun (in press).
13. A. K. SRIVASTAVA, N. SHUKLA: Quantitative Structure Activity Relationship(QSAR) Studies on a Series of Carbamate Appended N-alkylsulfonamides as Inhibitors of Peptide Amyloid- $\beta$  (A $\beta$ ). Oxid Commun (in press).
14. J. SINGH, V. K. DUBEY, V. K. AGARWAL, P. V. KHADIKAR: QSAR Study on Octanol–Water Partitioning: Dominating Role of Equalized Electronegativity. Oxid Commun, **31** (1), 27 (2008).
15. J. SINGH, V. K. AGARWAL, S. SINGH, P. V. KHADIKAR: Use of Topological as Well as Quantum Chemical Parameters in Modeling Antimalarial Activity of 2,4-diamino-6-quinazoline Sulphonamides. Oxid Commun, **31** (1), 17 (2008).
16. M. V. DIUDEA: SPR/QSAR Studies for Molecular Descriptors. Nova Science, Huntingtonclon, New York, 2000.
17. L. POGLIANI: Structural Property Relationships of Amine Acids and Some Peptides. Amino Acids, **6**, 141 (1994).
18. L. POGLIANI: Modeling with Special Descriptors Derived from a Medium Size Set of Connectivity Indices. J Phys Chem, **100**, 18065 (1996).
19. R. D. CRAMER, III, J. D. BUNCE, D. E. PATTERSON: Cross Validation, Boot Strapping, and Partial Least Squares Compared with Multiple Regression in Conventional QSAR Studies. Quant Struct-Act Rel, **1**, 18 (1988).
20. S. CHATTERJEE, A. S. HADI, B. PRICE: Regression Analysis by Example. 3rd ed. Wiley VCH, New York, 2000.

*Received 21 May 2010*

*Revised 18 June 2010*

## **QSAR STUDY ON TIE-2 INHIBITORS: DOMINATING ROLE OF TOPOLOGICAL PARAMETERS**

A. K. SRIVASTAVA, A. SRIVASTAVA\*, N. SHUKLA

*QSAR Research Laboratory, Department of Chemistry, University of Allahabad,  
211 002 Allahabad, India*

*E mail: akanchha\_au@rediffmail.com*

### **ABSTRACT**

QSAR studies on C-3 N-urea, amide and carbamate dihydroindazolo [5, 4- $\alpha$ ] pyrrolo [3, 4-c] carbazole analogues showing TIE-2 (tyrosine receptor kinase) inhibitory activity were performed. The TIE-2 inhibitory activity of these compounds was found to increase with branching. QSAR studies have been made on 32 compounds using distance-based topological indices along with indicator parameters. In multi-parametric regression topological indices play a dominating role in yielding a model with better statistics. The results are critically discussed using variety of statistical approaches.

*Keywords:* QSAR, TIE-2, topological indices, anti-angiogenic therapy.

### **AIMS AND BACKGROUND**

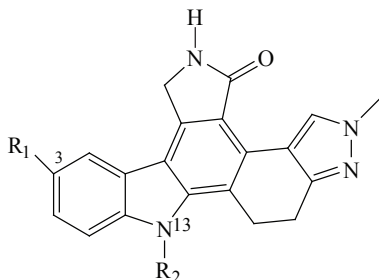
Anti-angiogenic therapies are trying to fight cancer and malignancies because tumors in general are nutrition- and oxygen-dependent, thus being in need of adequate blood supply. Vascular endothelial growth factor (VEGF) and its corresponding receptor tyrosine kinases play a key role in regulating vascular endothelial cells during embryonic development and tumor angiogenesis. VEGF primarily drives the formation of new capillaries. TIE-2 is an endothelial specific receptor tyrosine kinase required for normal blood vessel maturation. Endothelial receptor tyrosine kinase may play important roles in pathological vascular growth, particularly in tumors. TIE-2 signaling system works in the later steps of angiogenesis. Consistent with a central role for TIE-2 in angiogenesis germ line activating mutations in humans are associated with vascular dysmorphogenesis. Additionally the naturally occurring TIE-2 antagonist Ang-2 disrupts angiogenesis *in vivo*. Blocking TIE-2 activation with recombinant Ang-2 significantly inhibits tumor growth and is associated with activation of apoptosis. Hence studies aimed at better defining the regulation of TIE-2 expression are

---

\* For correspondence.

important in assessing anti-angiogenic therapeutic avenues. Becknell and co-workers<sup>1</sup> have described the modification of dihydroindazole core by the optimisation of the C-3 and N-13 positions and the identification of potent N-amide, urea and carbamate derivatives as potent dual inhibitors for VEGF-R<sub>2</sub>/TIE-2.

The leading compound is as follows:



The present QSAR studies with VEGF-R<sub>2</sub> inhibitory activity did not produce statistically sound models as compared to TIE-2 inhibitory activity and hence in the present paper we have included the QSAR results on TIE-2 inhibitory activity with an aim to obtain more potent drug compound from the present series.

## EXPERIMENTAL

QSAR was attempted with different parameters like first and fourth order of molecular connectivity (<sup>1</sup>χ, <sup>4</sup>χ) (Ref. 2), Balaban index (J) (Ref. 2) and mean Wiener index (WA) (Ref. 2) along with dummy parameters I<sub>1</sub>, I<sub>2</sub> and I<sub>3</sub>. The 2D structures of the molecules were drawn using Chem. Sketch software<sup>3</sup>. All the data on activity were taken from literature<sup>1</sup>.

*First order connectivity index* (<sup>1</sup>χ) (Ref. 2): The connectivity index  $\chi = \chi(G)$  of a graph  $G$  is defined by Randic as follows:

$${}^1\chi = {}^1\chi(G) = \sum_{ij} [\delta_i \delta_j]^{-0.5}$$

where  $\delta_i$  and  $\delta_j$  are the valence of a vertex  $i$  and  $j$ , equal to the number of bonds connected to the atoms  $i$  and  $j$ , in  $G$ . In the case of hetero systems the connectivity given in terms of valence delta values  $\delta_i^v$  and  $\delta_j^v$  of atoms  $i$  and  $j$  and is denoted by <sup>1</sup>χ<sup>v</sup>. This version of the connectivity index is called the valence connectivity index and is defined as follows:

$${}^1\chi^v = {}^1\chi^v(G) = \sum_{ij} [\delta_i^v \delta_j^v]^{-0.5}$$

*The Balaban index* (J) ((Ref. 2): The Balaban index (J) is the average distance sum connectivity index defined by:

$$J = J(G) \sum_{ij} (d_i d_j) \frac{M}{\mu + 1},$$



where  $M$  is the number of bonds in a graph  $G$ ;  $\mu$  – the cyclomatic number of  $G$ , and  $d_i$  ( $i = 1, 2, 3, N$ ) – the distance sums (distance degree) of atoms in  $G$  such that

$$d_i = \sum_{j=1}^N (D)_{ij}$$

The cycloatomic number  $\mu$  of  $G$  indicates the number of independent cycles in  $G$  and is equal to the minimum number of cuts necessary to convert a polycyclic structure into an acyclic structure.

$$\mu = M - N + 1.$$

One way to compute the Balaban index ( $J$ ) for hetero system is to modify the elements of the distance matrix for hetero system as follows:

*The diagonal elements*

$$(D)_{ij} = 1 - (Z_c/Z_i)$$

$Z_c = 6$ ;  $Z_i$  – atomic number of the given element.

*The off-diagonal elements*

$$(D)_{ij} d_i = \sum_r k_r$$

where the summation  $r$  is over all bonds. The bond parameter  $k_r$  is given by:

$$k_r = 1/b_r (Z_c^2/Z_i Z_j)$$

where  $b_r$  – the bond weight values 1 for single bond, 2 – for double bond, 1.5 – for aromatic bond, and 3 – for triple bond.

*Mean Wiener index (WA)* (Ref. 2). In chemical graph theory, the Wiener index (also Wiener number) is a topological index of a molecule, defined as the sum of the numbers of edges in the shortest paths in a chemical graph between all pairs of non-hydrogen atoms in a molecule. It was introduced by Wiener in 1947. The Wiener index may be calculated using the Floyd algorithm. Mohar and Pisanski presented an efficient algorithm for computing the Wiener index of a tree.

The Wiener index is the oldest topological index related to molecular branching. A tentative explanation of the relevance of the Wiener index in research of QSPR and QSAR is that it correlates with the van der Waals surface area of the molecule.

$$WA(G) = \frac{2W}{N(N-1)}.$$

## RESULTS AND DISCUSSION

The aim of current study is to discuss the role of different order of molecular connectivity indices such as  ${}^1\chi$ ,  ${}^4\chi$ , mean Wiener index (WA) and the Balaban distance

connectivity index (J) with different indicator variables. These parameters were found to be useful earlier in QSAR-based drug modelling<sup>4-11</sup>.

For the entire set of 32 compounds, their pIC<sub>50</sub> values and assumed indicator parameter I<sub>1</sub>, I<sub>2</sub> and I<sub>3</sub> are presented in Table 1. The dummy parameters, viz. indicator parameters, are used for accounting the presence or absence of 2-F-5-Me-phenylNHCO at R<sub>1</sub> as indicator I<sub>1</sub>, CH<sub>2</sub>CH<sub>2</sub>CH<sub>2</sub>CH<sub>3</sub> at R<sub>2</sub> as indicator I<sub>2</sub> and 2-furanylCO at R<sub>1</sub> as indicator I<sub>3</sub> in the series of 32 compounds. When present, the respective indicator parameter is taken as 1 otherwise 0. Intercorrelation of the topological descriptors and their correlation with pIC<sub>50</sub> are presented in correlation matrix (Table 2) which shows that indicator parameters I<sub>1</sub>, I<sub>2</sub>, and I<sub>3</sub> are useful in making multi-parametric regression analysis.

The step wise regression analysis has shown that for the set of 32 compounds we obtain significant results with improvement on each step.

*Linearly regressed models of anti-angiogenic activity TIE-2 with <sup>1</sup>χ, <sup>4</sup>χ, WA and J.* The linear models of first order of molecular connectivity (<sup>1</sup>χ), fourth order of molecular connectivity (<sup>4</sup>χ), mean Weiner index (WA) and the Balaban distance connectivity index (J) were found as below:

$$\text{pIC}_{50} = 0.241(\pm 0.071)^1\chi + 3.749 \quad (1)$$

$$n = 32, R = 0.786, R^2 = 0.618, R_A^2 = 0.605, \text{SE} = 0.311, F_{(1,30)} = 48.557, P = 2.911, S = 4.711, Q = 2.527;$$

$$\text{pIC}_{50} = 0.383(\pm 0.115)^4\chi + 2.665 \quad (2)$$

$$n = 32, R = 0.777, R^2 = 0.604, R_A^2 = 0.591, \text{SE} = 0.317, F_{(1,30)} = 45.765, P = 3.018, S = 4.604, Q = 2.451;$$

$$\text{pIC}_{50} = 0.587(\pm 0.166) \text{WA} + 4.518 \quad (3)$$

$$n = 32, R = 0.797, R^2 = 0.635, R_A^2 = 0.623, \text{SE} = 0.304, F_{(1,30)} = 52.173, P = 2.782, S = 4.839, Q = 2.621;$$

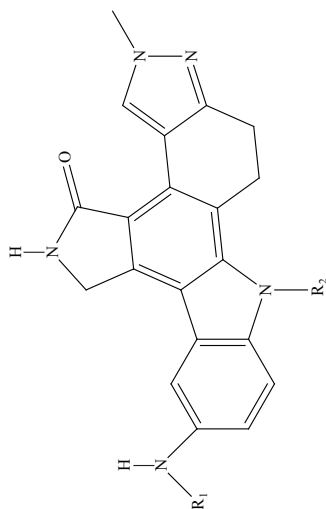
$$\text{pIC}_{50} = -3.734(\pm 1.149)J + 12.517 \quad (4)$$

$$n = 32, R = 0.771, R^2 = 0.595, R_A^2 = 0.581, \text{SE} = 0.320, F_{(1,30)} = 44.027, P = 3.089, S = 4.533, Q = 2.409,$$

where *n* is the number of compounds in the data set; *R* – the correlation coefficient; *R*<sup>2</sup> – the coefficient of determination; *R*<sub>A</sub><sup>2</sup> – the adjusted *R*<sup>2</sup>; *SE* – the standard error of estimate; *F* – the variance ratio<sup>12</sup>, and *Q* – the quality of fit<sup>13,14</sup>.

In all but one of the above models, the signs of the coefficient of parameters are positive which shows that bulky group with more branching should be preferred for modelling. All the statistical terms in the above given models shows that the models are significant. The negative coefficient of J in the above model is probably due to its high co-linearity with other parameter (<sup>1</sup>χ, <sup>4</sup>χ, WA).

**Table 1.** Biological activity and physicochemical data of TIE-2 inhibitors



S.No	R <sub>1</sub>	R <sub>2</sub>	WA	J	<sup>1</sup> χ	<sup>4</sup> χ	I <sub>1</sub>	I <sub>2</sub>	I <sub>3</sub>	pIC <sub>50</sub>
1	2	3	4	5	6	7	8	9	10	11
1	H	CH <sub>2</sub> CH <sub>2</sub> CH <sub>3</sub>	4.520	1.415	14.080	11.785	0	0	0	7.443
2	H	CH <sub>2</sub> CH(CH <sub>3</sub> ) <sub>2</sub>	4.628	1.416	14.436	11.922	0	0	0	7.318
3	H	CH <sub>2</sub> CH <sub>2</sub> CH <sub>2</sub> CH <sub>3</sub>	4.690	1.401	14.580	11.892	0	0	1	6.638
4	4-OMe-phenyl	INHCO	6.709	1.075	18.961	14.816	0	0	0	8.397
5	4-OMe-phenyl	INHCO	6.772	1.087	19.461	14.981	0	0	0	8.698
6	4-OMe-phenyl	INHCO	6.823	1.100	19.817	15.117	0	0	0	8.522
7	4-OMe-phenyl	INHCO	6.870	1.093	19.961	15.087	0	0	1	8.154
8	4-SMe-phenyl	INHCO	6.772	1.087	19.461	14.981	0	0	0	8.522
9*	4-NMe <sub>2</sub> -phenyl	INHCO	6.991	1.071	19.834	15.196	0	0	0	8.221
10	4-Me-phenyl	INHCO	6.522	1.108	18.923	14.670	0	0	0	8.522
11*	2-thienyl	INHCO	6.078	1.146	18.029	14.351	0	0	0	7.721
12	2-F-5-Me-phenyl	INHCO	6.605	1.110	19.334	15.032	1	0	0	9.000
13	2-F-5-CF <sub>3</sub> -phenyl	INHCO	7.117	1.081	20.545	15.583	0	0	0	8.397
14	phenyl	INHCO	6.292	1.127	18.529	14.528	0	0	0	8.301
15	phenyl(Me)	NCO	6.358	1.133	18.957	14.736	0	0	0	8.698

to be continued

Continuation of Table 1

1	2	3	4	5	6	7	8	9	10	11
16	3-OMe-phenylNHCO	CH <sub>2</sub> CH(CH <sub>3</sub> ) <sub>2</sub>	6.743	1.111	19.817	15.229	0	0	0	8.397
17	2-OMe-phenylNHCO	CH <sub>2</sub> CH(CH <sub>3</sub> ) <sub>2</sub>	6.662	1.122	19.834	15.321	0	0	0	8.096
18	4-F-phenylNHCO	CH <sub>2</sub> CH <sub>2</sub> CH <sub>3</sub>	6.522	1.108	18.923	14.670	0	0	0	8.698
19	3-F-phenylNHCO	CH <sub>2</sub> CH <sub>2</sub> CH <sub>3</sub>	6.479	1.114	18.923	14.879	0	0	0	8.698
20	2-F-phenylNHCO	CH <sub>2</sub> CH <sub>2</sub> CH <sub>3</sub>	6.436	1.120	18.940	14.796	0	0	0	8.698
21	4-Cl-phenylNHCO	CH <sub>2</sub> CH <sub>2</sub> CH <sub>3</sub>	6.522	1.108	18.923	14.670	0	0	0	8.221
22	2-Cl-phenylNHCO	CH <sub>2</sub> CH <sub>2</sub> CH <sub>3</sub>	6.436	1.120	18.940	14.796	0	0	0	8.522
23	2-Br-phenylNHCO	CH <sub>2</sub> CH <sub>2</sub> CH <sub>3</sub>	6.436	1.120	18.940	14.796	0	0	0	8.397
24	2-thienylCO	CH <sub>2</sub> CH <sub>2</sub> CH <sub>3</sub>	5.789	1.180	17.546	14.115	0	0	0	7.920
25	2-thienylCO	CH <sub>2</sub> CH(CH <sub>3</sub> ) <sub>2</sub>	5.856	1.190	17.902	14.252	0	0	0	8.000
26	2-furanylCO	CH <sub>2</sub> CH <sub>2</sub> CH <sub>3</sub>	5.789	1.180	17.546	14.115	0	1	0	7.537
27	2-furanylCO	CH <sub>2</sub> CH(CH <sub>3</sub> ) <sub>2</sub>	5.856	1.190	17.902	14.252	0	1	0	7.698
28	4-OMe-phenylOCO	CH <sub>2</sub> CH <sub>2</sub> CH <sub>3</sub>	6.772	1.087	19.461	14.981	0	0	0	8.301
29	4-F-phenylOCO	CH <sub>2</sub> CH <sub>2</sub> CH <sub>3</sub>	6.522	1.108	18.923	14.670	0	0	0	7.958
30	i-PrOCO	CH <sub>2</sub> CH <sub>2</sub> CH <sub>3</sub>	5.672	1.301	16.867	13.341	0	0	0	7.958
31	EtOCO	CH <sub>2</sub> CH <sub>2</sub> CH <sub>3</sub>	5.478	1.320	16.512	13.050	0	0	0	7.744
32	PrOCO	CH <sub>2</sub> CH <sub>2</sub> CH <sub>3</sub>	5.726	1.291	17.012	13.110	0	0	0	8.154

\* Compound taken as outlier.

*Biparametrically regressed models of anti-angiogenic activity TIE-2 with  ${}^1\chi$ ,  ${}^4\chi$ , WA and J.* Successive regression analysis has indicated that by the addition of indicator parameter  $I_1$  which signifies the presence of 2-F-5Me-phenylNHCO at position  $R_1$  shows improvement in the quality of regression model.

$$pIC_{50} = 0.234(\pm 0.068) {}^1\chi + 0.620(\pm 0.619) I_1 + 3.865 \quad (5)$$

$$n = 32, R=0.816, R^2=0.666, R^2_A=0.643, SE=0.296, F_{(2,29)} = 28.964, P=2.543, S=5.079, Q=2.756;$$

$$pIC_{50} = 0.371(\pm 0.112) {}^4\chi + 0.598(\pm 0.636) I_1 + 2.829 \quad (6)$$

$$n = 32, R=0.805, R^2=0.649, R^2_A=0.625, SE=0.303, F_{(2,29)} = 26.787, P=2.677, S=4.945, Q=2.656;$$

$$pIC_{50} = 0.570(\pm 0.158) WA + 0.634(\pm 0.601) I_1 + 4.603 \quad (7)$$

$$n = 32, R=0.828, R^2=0.685, R^2_A=0.664, SE=0.287, F_{(2,29)} = 31.592, P=2.398, S=5.224, Q=2.885;$$

$$pIC_{50} = -3.627(\pm 1.095) J + 0.654(\pm 0.635) I_1 + 12.372 \quad (8)$$

$$n = 32, R=0.805, R^2=0.649, R^2_A=0.624, SE=0.303, F_{(2,29)} = 26.760, P=2.678, S=4.943, Q=2.656.$$

The positive sign associated with  ${}^1\chi$ ,  ${}^4\chi$ , WA shows that first order branching and increasing number of atoms are favourable for the exhibition of  $pIC_{50}$  and the positive sign of  $I_1$  indicates that the presence of 2-F-5Me-phenylNHCO group at  $R_1$  is favourable for the anti-angiogenic activity. Values of other statistical terms have also improved as compared to equations (1)–(4).

*Triparametrically regressed models of anti-angiogenic activity TIE-2 with  ${}^1\chi$ ,  ${}^4\chi$ , WA and J.* Further regression analysis indicated that the quality of the above models increases further by the addition of yet another indicator parameter  $I_2$ . The resulting models are given as below:

$$pIC_{50} = 0.219(\pm 0.062) {}^1\chi + 0.599(\pm 0.558) I_1 - 0.553(\pm 0.405) I_2 + 4.170 \quad (9)$$

$$n= 32, R=0.860, R^2=0.739, R^2_A=0.711, SE=0.266, F_{(3,28)} = 26.449, P=1.988, S=5.634, Q=3.233;$$

$$pIC_{50} = 0.344(\pm 0.108) {}^4\chi + 0.585(\pm 0.595) I_1 - 0.488(\pm 0.436) I_2 + 3.249 \quad (10)$$

$$n= 32, R=0.839, R^2=0.704, R^2_A=0.673, SE=0.283, F_{(3,28)} = 22.241, P=2.253, S=5.369, Q=2.964;$$

$$pIC_{50} = 0.535 (\pm 0.143) WA + 0.611(\pm 0.537) I_1 - 0.551(\pm 0.390) I_2 + 4.855 \quad (11)$$

$$n= 32, R=0.870, R^2=0.758, R^2_A=0.732, SE=0.256, F_{(3,28)} = 29.178, P=1.847, S=5.774, Q=3.398;$$

$$\text{pIC}_{50} = -3.369(\pm 1.039)J + 0.635(\pm 0.589)I_1 - 0.507(\pm 0.431)I_2 + 12.104 \quad (12)$$

$n = 32, R = 0.842, R^2 = 0.709, R^2_A = 0.678, SE = 0.281, F_{(3,28)} = 22.718, P = 2.219, S = 5.402, Q = 2.996.$

The coefficient of the added parameter  $I_2$  is negative indicating that the presence of  $\text{CH}_2\text{CH}_2\text{CH}_2\text{CH}_3$  group at position  $R_2$  is not favourable for exhibition of  $\text{pIC}_{50}$ . The significance of other terms is the same as discussed earlier.

*Tetraparametrically regressed models of anti-angiogenic activity TIE-2 with  $^1\chi$ ,  $^4\chi$ , WA and J.* We observed that by the addition of third indicator parameter  $I_3$  which is 2-furanylCO at position  $R_1$  to the above model the statistics is still improved yielding the following models:

$$\text{pIC}_{50} = 0.211(\pm 0.057)^1\chi + 0.574(\pm 0.508)I_1 - 0.595(\pm 0.370)I_2 - 0.468(\pm 0.367)I_3 + 4.355 \quad (13)$$

$n = 32, R = 0.890, R^2 = 0.792, R^2_A = 0.761, SE = 0.242, F_{(4,27)} = 25.714, P = 1.585, S = 6.037, Q = 3.677;$

$$\text{pIC}_{50} = 0.335(\pm 0.095)^4\chi + 0.552(\pm 0.527)I_1 - 0.534(\pm 0.387)I_2 - 0.545(\pm 0.378)I_3 + 3.405 \quad (14)$$

$n = 32, R = 0.881, R^2 = 0.777, R^2_A = 0.744, SE = 0.251, F_{(4,27)} = 23.467, P = 1.702, S = 5.919, Q = 3.509;$

$$\text{pIC}_{50} = 0.510(\pm 0.137)WA + 0.593(\pm 0.506)I_1 - 0.589(\pm 0.370)I_2 - 0.389(\pm 0.369)I_3 + 5.036 \quad (15)$$

$n = 32, R = 0.891, R^2 = 0.794, R^2_A = 0.763, SE = 0.241, F_{(4,27)} = 25.949, P = 1.573, S = 6.048, Q = 3.697;$

$$\text{pIC}_{50} = -3.279(\pm 0.928)J + 0.603(\pm 0.525)I_1 - 0.551(\pm 0.386)I_2 - 0.533(\pm 0.377)I_3 + 12.037 \quad (16)$$

$n = 32, R = 0.882, R^2 = 0.778, R^2_A = 0.745, SE = 0.250, F_{(4,27)} = 23.641, P = 1.693, S = 5.929, Q = 3.528.$

The qualities of these models are improved by the addition of  $I_3$ , thus yielding tetraparametric models. Like  $I_2$ , the coefficient of  $I_3$  is also negative indicating that the presence of 2-furanylCO group is not favourable towards TIE-2 anti-angiogenic activity. The values of rest of the statistical terms are fairly improved.

On taking compounds **9** and **11** as outliers for the above tetraparametric models, we obtained the following models:

$$\text{pIC}_{50} = 0.214(\pm 0.054)^1\chi + 0.542(\pm 0.479)I_1 - 0.620(\pm 0.348)I_2 - 0.496(\pm 0.344)I_3 + 4.319 \quad (17)$$

$n = 30, R = 0.909, R^2 = 0.827, R^2_A = 0.799, SE = 0.226, F_{(4,25)} = 29.878, P = 1.282, S = 6.127, Q = 4.022;$

$$\text{pIC}_{50} = 0.343(\pm 0.090) {}^4\chi + 0.517(\pm 0.492) I_1 - 0.558(\pm 0.361) I_2 - 0.574(\pm 0.352) I_3 + 3.332 \quad (18)$$

$$n=30, R=0.904, R^2=0.818, R^2_A=0.789, SE=0.232, F_{(4,25)}=28.048, P=1.350, S=6.059, Q=3.896;$$

$$\text{pIC}_{50} = 0.526(\pm 0.128) \text{WA} + 0.556(\pm 0.467) I_1 - 0.613(\pm 0.341) I_2 - 0.414(\pm 0.340) I_3 + 4.968 \quad (19)$$

$$n=30, R=0.914, R^2=0.835, R^2_A=0.808, SE=0.221, F_{(4,25)}=31.543, P=1.225, S=6.183, Q=4.135;$$

$$\text{pIC}_{50} = -3.399(\pm 0.845) J + 0.562(\pm 0.472) I_1 - 0.576(\pm 0.346) I_2 - 0.565(\pm 0.339) I_3 + 12.211 \quad (20)$$

$$n=30, R=0.911, R^2=0.831, R^2_A=0.803, SE=0.224, F_{(4,25)}=30.632, P=1.255, S=6.153, Q=4.066.$$

The above four models which were found after taking outliers are the best tetra-parametric models. Equation (19) is the best suited model for future drug development as its statistical terms are better than other discussed models. Predicted and residual (difference between the observed biological activities and calculated activities) values for derived QSAR models are reported in Table 3. The small residues clearly show that model 19 is the most suitable model for predicting the inhibitory activity of present set of compounds. The calculated  $F$  value is greater than  $F$  theoretical value ( $F_{(4,25)} = 2.76$ ) for all the significant models.

**Table 2.** Correlation matrix between biological activity and physicochemical parameters and indicator variables

	A	WA	J	${}^1\chi$	${}^4\chi$	$I_1$	$I_2$	$I_3$
A	1.000							
WA	0.817	1.000						
J	-0.797	-0.965	1.000					
${}^1\chi$	0.800	0.991	-0.964	1.000				
${}^4\chi$	0.795	0.973	-0.977	0.990	1.000			
$I_1$	0.304	0.109	-0.103	-0.115	0.127	1.000		
$I_2$	-0.425	-0.173	0.209	-0.175	-0.225	-0.050	1.000	
$I_3$	-0.306	-0.156	0.047	-0.100	-0.041	-0.050	-0.071	1.000

**Table 3.** Comparison between observed and predicted activities and their residual values

S. No	pIC <sub>50</sub>	Predicted	Residual
1	7.443	7.346	0.096
2	7.318	7.403	-0.084
3	6.638	6.822	-0.184
4	8.397	8.498	-0.100
5	8.698	8.532	0.166
6	8.522	8.558	-0.036
7	8.154	7.970	0.184
8	8.522	8.532	-0.009
9	8.221	8.647	-
10	8.522	8.400	0.122
11	7.721	8.166	-
12	9.000	9.000	0.000
13	8.397	8.713	-0.315
14	8.301	8.279	0.021
15	8.698	8.314	0.384
16	8.397	8.516	-0.118
17	8.096	8.474	-0.377
18	8.698	8.400	0.298
19	8.698	8.377	0.321
20	8.698	8.355	0.343
21	8.221	8.400	-0.178
22	8.522	8.355	0.167
23	8.397	8.355	0.042
24	7.920	8.014	-0.093
25	8.000	8.049	-0.049
26	7.537	7.600	-0.063
27	7.698	7.635	0.063
28	8.301	8.532	-0.231
29	7.958	8.400	-0.441
30	7.958	7.953	0.005
31	7.744	7.851	-0.106
32	8.154	7.981	0.173

In order to examine the relative potential of the proposed models, we have further estimated their predictive correlation coefficients ( $R^2_{\text{pred}}$ ) by plotting graph between observed and calculated pIC<sub>50</sub> values using equation (19). Such a correlation is shown in Fig. 1. The values of  $R^2_{\text{pred}}$  determined by using equation (19) came out to be 0.8348 thus confirming our findings.



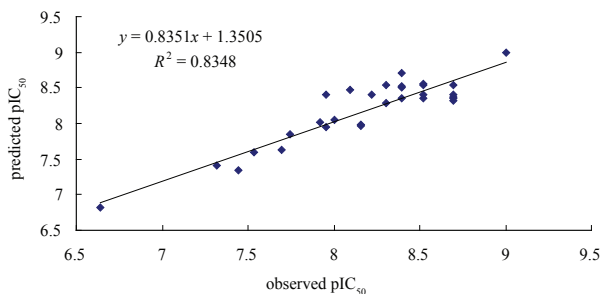


**Fig. 1.** Plot showing comparison between observed and predicted  $pIC_{50}$  values using equation (19)

#### CROSS-VALIDATION

The cross-validation analysis was performed using leave-one-out (LOO) method<sup>15</sup> in which one compound is removed from the data set and the activity is correlated using the rest of the data set. The cross-validated  $R^2$  in each case was found to be very close to the value of  $R^2$  for the entire data set and hence these models can be termed as statistically significant.

Cross-validation provides the values of PRESS (predicted residual sum of squares)<sup>15</sup>, SSY (sum of the squares of the response)<sup>15</sup> and  $R^2_{cv}$  (overall predicted ability) and PSE (predicted squares error)<sup>15</sup> from which we can test the predictive power of the proposed model. It is argued that PRESS is a good estimate of the real predictive error of the model and if it is smaller than SSY the model predicts better than chance and can be considered statistically significant. Furthermore, the ratio PRESS/SSY can be used to calculate approximate confidence intervals of prediction of new compound. To be a reasonable QSAR model PRESS/SSY should be smaller than 0.4. Also, if PRESS value is transformed in a dimension of less term by relating it to the initial sum of squares, we obtain  $R^2_{cv}$ , i.e. the complement to the traces on of unexplained variance over the total variance. The PRESS and  $R^2_{cv}$  have good properties. However, for practical purposes of end users the use of square root of PRESS/N, which is called predictive square error (PSE), is more directly related to the uncertainty of the predictions. The PSE values also support our results. The calculated cross-validated parameters confirm the validity of the models.

#### PREDICTIVE ERROR OF COEFFICIENT OF CORRELATION (PE)

The predictive error of coefficient of correlation (PE) (Ref. 16) is another parameter used to decide the predictive power of the proposed models. We have calculated PE value of all the proposed models and they are reported in Table 4. It is argued that if:

$R < PE$ , then correlation is not significant;

$R > PE$ ; several times (at least three times), then correlation is indicated; and if

$R > 6PE$ , then the correlation is definitely good.

For all the models developed the condition  $R > 6PE$  is satisfied and hence can be said they have a good predictive power.

**Table 4.** Predictive error of coefficient of correlation (PE) and cross-validation parameters for the proposed models

S. No	Model No	Parameter used	$n$	$R$	$1 - R^2$	PE	GPE	PRESS	SSY	PRESS/SSY	$R^2_{cv}$	PSE
1	1	$^1\chi$	32	0.786	0.382	0.045	0.270	2.911	4.711	0.617	0.383	0.301
2	2	$^4\chi$	32	0.777	0.396	0.046	0.280	3.018	4.604	0.655	0.345	0.307
3	3	WA	32	0.797	0.364	0.042	0.257	2.782	4.839	0.574	0.426	0.294
4	4	J	32	0.771	0.405	0.047	0.286	3.089	4.533	0.681	0.319	0.310
5	5	$^1\chi + I_1$	32	0.816	0.334	0.039	0.236	2.543	5.079	0.500	0.500	0.281
6	6	$^4\chi + I_1$	32	0.805	0.351	0.041	0.246	2.677	4.945	0.541	0.459	0.289
7	7	WA+ $I_1$	32	0.828	0.314	0.037	0.222	2.398	5.224	0.459	0.541	0.273
8	8	J+ $I_1$	32	0.805	0.351	0.041	0.246	2.678	4.943	0.541	0.459	0.289
9	9	$^1\chi + I_1 + I_2$	32	0.860	0.260	0.030	0.183	1.988	5.634	0.352	0.648	0.249
10	10	$^4\chi + I_1 + I_2$	32	0.839	0.296	0.034	0.209	2.253	5.369	0.419	0.581	0.265
11	11	WA+ $I_1 + I_2$	32	0.870	0.243	0.028	0.171	1.847	5.774	0.319	0.681	0.240
12	12	J+ $I_1 + I_2$	32	0.842	0.291	0.034	0.205	2.219	5.402	0.410	0.590	0.263
13	13	$^1\chi + I_1 + I_2 + I_3$	32	0.890	0.207	0.024	0.146	1.585	6.037	0.262	0.738	0.222
14	14	$^4\chi + I_1 + I_2 + I_3$	32	0.881	0.223	0.026	0.157	1.702	5.919	0.287	0.713	0.230
15	15	WA+ $I_1 + I_2 + I_3$	32	0.891	0.206	0.024	0.145	1.573	6.048	0.260	0.740	0.221
16	16	J+ $I_1 + I_2 + I_3$	32	0.882	0.222	0.026	0.156	1.693	5.929	0.285	0.715	0.230
17	17	$^1\chi + I_1 + I_2 + I_3$	30	0.909	0.173	0.021	0.126	1.282	6.127	0.209	0.791	0.206
18	18	$^4\chi + I_1 + I_2 + I_3$	30	0.904	0.182	0.022	0.132	1.350	6.059	0.222	0.778	0.212
19	19	WA+ $I_1 + I_2 + I_3$	30	0.914	0.164	0.019	0.114	1.225	6.183	0.198	0.802	0.202
20	20	J+ $I_1 + I_2 + I_3$	30	0.911	0.170	0.020	0.120	1.255	6.153	0.203	0.797	0.204

PRESS – predicted residual sum of squares; SSY – sum of the squares of the response;  $R^2_{cv}$  – overall predictive ability; PSE – predictive square error.

## CONCLUSIONS

From the results and discussion made above, we conclude that:

Out of the distance-based topological indices used the mean Weiner index WA is most appropriate for multiparametric regression analysis.

Bulky groups with more branching should be used in future modelling.

The group 2-F-5-Me phenylNHCO at R<sub>1</sub> favours the inhibitory activity.

Groups 2-furanylCO at R<sub>1</sub> position and CH<sub>2</sub>CH<sub>2</sub>CH<sub>2</sub>CH<sub>3</sub> at R<sub>2</sub> position are strictly avoided.

## REFERENCES

1. N. C. BECKNELL, A. L. ZULLI, T. S. ANGELES, S. YANG, M. S. ALBOM, L. D. AIMONE, C. ROBINSON, H. CHANG, R. L. HUDKINS: Novel C-3 N-urea, Amide, And Carbamate Dihydroindazolo [5,4- $\alpha$ ] pyrrolo [3,4-c] Carbazole Analogs as Potent TIE-2 and VEGF-R2 Dual Inhibitors. *Bioorganic Med Chem Lett*, **16**, 5368 (2006).
2. DRAGON Software for Calculation of Topological Indices: [www.disat.unimib.it](http://www.disat.unimib.it).
3. [www.acdlabs.com](http://www.acdlabs.com), Chem Sketch Program of ACD Labs Software.
4. A. K. SRIVASTAVA, M. JAISWAL, ARCHANA, A. SRIVASTAVA: QSAR Modelling of Selective CC Chemokine Receptor 3 (CCR3) Antagonists Using Physicochemical Parameters. *Oxid Commun*, **32**, 55 (2009).
5. A. K. SRIVASTAVA, A. SRIVASTAVA, ARCHANA, M. JAISWAL: Role of Physico-chemical parameters in Quantitative Structure–Activity Relationship-based Modeling of CYP26A1 Inhibitory Activity. *J Indian Chem Soc*, **85**, 721 (2008).
6. A. K. SRIVASTAVA, ARCHANA, M. JAISWAL: Quantitative Structure–Activity Relationship Studies of *p*-Arylthiocinnamides as Antagonists of Biochemical ICAM- 1/ LFA-1 Interaction in Relation to Antiinflammatory Activity. *Oxid Commun*, **31**, 44 (2008).
7. A. K. SRIVASTAVA, M. JAISWAL, ARCHANA: QSAR Studies on Indole Substituted Potent Human Histamine H<sub>4</sub> Antagonists: Role of Physicochemical and Statistical Parameters. *J Saudi Chem Soc*, **12**, 221 (2008).
8. A. K. SRIVASTAVA, ARCHANA, M. JAISWAL: Exploring QSAR of Selective PDE<sub>4</sub> Inhibitors as 8-substituted Analogues of 3-(3-cyclopentyloxy-4-methoxy-benzyl)-8 isopropyl Adenine. *J Saudi Chem Soc*, **12**, 227 (2008).
9. A. K. SRIVASTAVA, ARCHANA, M. JAISWAL, A. SRIVASTAVA: QSAR Modelling of Selective CC Chemokine Receptor 3 (CCR3) Antagonists Using Physicochemical Parameters. *Oxid Commun*, **32**, 55 (2009).
10. J. SINGH, V. K. DUBEY, V. K. AGARWAL, P. V. KHADIKAR: QSAR Study on Octanol–Water Partitioning: Dominating Role of Equalised Electronegativity. *Oxid Commun*, **31** (1), 27 (2008).
11. J. SINGH, V. K. AGARWAL, S. SINGH, P. V. KHADIKAR: Use of Topological as well as Quantum Chemical Parameters in Modeling Antimalarial Activity of 2,4- diamino-6-quinazoline Sulphonamides. *Oxid Commun*, **31** (1), 17 (2008).
12. M. V. DIUDEA (Ed.): *QSPR/QSAR Studies for Molecular Descriptors*. Nova Science, and Hunting Lon, New York, 2000.
13. L. POGLIANI: Structural Property Relationships of Amine Acids and Some Peptides. *Amino Acids*, **6**, 141 (1994).
14. L. POGLIANI: Modeling with Special Descriptors Derived from a Medium Size Set of Connectivity Indices. *J Phys Chem*, **100**, 18065 (1996).
15. R. D. CRAMER, III, J. D. BUNCE, D. E. PATTERSON: Cross-validation, Boot Strapping, and Partial Least Squares Compared with Multiple Regression in Conventional QSAR Studies. *Quant Struct-Act Rel*, **1**, 18 (1988).
16. S. CHATTERJEE, A. S. HADI, B. PRICE: *Regression Analysis by Example*. 3rd ed. Wiley VCH, New York, 2000.

*Received 8 January 2010*

*Revised 8 February 2010*

## EVALUATION OF ANTIMICROBIAL ACTIVITY AND QSAR STUDY OF A MOLECULE LIBRARY OF THE MANNICH BASES OF GLUTARIMIDES

A. DAS MANIKPURI<sup>a\*</sup>, SH. JOSHI<sup>b</sup>

<sup>a</sup>Resource Person – Chemistry Azimpremi Foundation, CG-492 773, Dhamtari, India

E-mail: [anju.dm@rediffmail.com](mailto:anju.dm@rediffmail.com); [anju.dm@gmail.com](mailto:anju.dm@gmail.com)

<sup>b</sup>School of Chemical Sciences, Devi Ahilya University, Takshashila Campus, Khandwa Road, 452 017 Indore, MP, India

E-mail: [spjoshi11@rediffmail.com](mailto:spjoshi11@rediffmail.com)

### ABSTRACT

Forty amino-alkylated Mannich bases of various glutarimides with intact imide moiety are synthesised for the first time from various sulphonamides and secondary amines. The structural characterisation is made using elemental and spectral studies. QSAR studies revealed that out of the large pool of topological indices and molecular descriptor used some topological indices are more useful for modelling antimicrobial activity against 6 bacteria: *B. subtilis*, *S. typhi*, *E. coli*, *S. aureus*, *K. pneumoniae* and *P. aeruginosa*. The Mannich bases are found more potent than their parent sulphonamides. The results are discussed critically using a variety of statistical parameters.

**Keywords:** glutarimides, sulphonamides, the Mannich bases, antimicrobial activity, QSAR.

### AIMS AND BACKGROUND

The increasing popularity of the Mannich reaction and utility of the Mannich bases has been provoked by the ubiquitous nature of nitrogen in them as well as by the potential of multi-component Mannich reaction to generate diversity. Interest in the Mannich bases has been quite attractive and wide ranged considering the enormous domain of the applications involving variant biological, pharmaceutical and industrial nature<sup>1</sup>. Glutarimide moiety with the intact imide group is acting as the carrier molecule (vector), which transports biologically active substituents (functional groups) through cell membranes<sup>2</sup>. It is also a component of newly synthesised antibiotics, which exert

---

\* For correspondence.

antiviral and antifungal activity<sup>3,4</sup>. Glutarimide (2,6-piperidinedione) has been found in a number of antibiotics with the antiviral and fungicidal activity<sup>5-8</sup>. In addition, the 2,6-piperidinedione moieties constitute an important center in several new anticancer drugs, which have recently been introduced into experimental chemotherapy<sup>9</sup>. It is also a structural part of a number of molecules with interesting biochemical activities<sup>10</sup>. Prompted by these observations, the aminoalkylation of various glutarimido-moieties with sulphonamides and secondary amines are presented in this paper.

## EXPERIMENTAL

*General information.* All the m.p. were determined using a Thomas Hoover capillary melting point apparatus. The purity of the Mannich bases was confirmed by TLC analysis in that the mobile phase was chloroform/methanol mixture (90:10) and stationary phase was silica gel-G (chromatographic grade). The antimicrobial screening was performed using paper disc method<sup>11</sup> and the results were statistically evaluated by analysis of variance<sup>12</sup>. The Mullar Hinton agar was taken as media for cultivation of bacteria. The inhibitory effect of the samples was measured against the bacteria after incubation for 24 h at 37°C. The experiments were run in triplicate and the mean of readings were recorded. The results were statistically analysed<sup>12</sup>.

*Synthesis of the Mannich bases from primary amines.* The Mannich bases of glutarimides were prepared by reacting various glutarimides (0.01 mol) dissolved in 20 ml of ethanol with sulphonamide (0.01 mol). 2.5 ml (0.01 mol) of formaldehyde solution (37%, v/v) were added slowly with constant stirring. The pH of the mixture was adjusted to 3.5 by adding 0.5 ml of 1 mol l<sup>-1</sup> HCl. The mixture was kept at efficient ice cooling for half an hour, and then refluxed on water bath. Reflux time varied with the sulphonamide used. The refluxed mixture was kept at 0°C for 4 days when crystalline product was obtained. The product was re-crystallised from dry distilled ethanol and dioxane-water (1:1). The compounds thus synthesised and their analytical data are presented in Table 1.

*Synthesis of the Mannich bases from secondary amines.* Secondary amine (0.01 mol) was added to an ethanol solution (50 ml) of glutarimide (0.01 mol) in a flat bottom flask. Amount of 0.4 ml (0.015 mol) of formaldehyde solution (37%, v/v) was added slowly with constant stirring. The reaction mixture was stirred at 70–75°C for 3.0 to 8.5 h, depending upon the secondary amine. The remaining portion of formaldehyde solution was added in 2 instalments after 1 and 2 h, respectively. The reaction mixture was kept overnight in the refrigerator. Next day, the excess of solvent was distilled off from the reaction mixture under reduced pressure. It was again kept for crystallisation in the refrigerator. The products obtained were purified by re-crystallisation from dry distilled ethanol. The compounds thus synthesised and their analytical data are presented in Table 1. For details see Schemes 1 and 2.

**Table1.** Physical data of the Mannich bases (1–40)

Com- pound No	Molecular formula	M.P. (°C)	Elemental analysis (%) found (calcd.)		
			C (%)	H (%)	N (%)
1	C <sub>16</sub> H <sub>17</sub> N <sub>5</sub> O <sub>4</sub> S	168	51.20 (51.19)	4.39 (4.56)	18.08 (18.66)
2	C <sub>16</sub> H <sub>18</sub> N <sub>4</sub> O <sub>5</sub> S	148–151	50.79 (50.78)	4.81 (4.79)	14.91 (14.81)
3	C <sub>12</sub> H <sub>15</sub> N <sub>3</sub> O <sub>4</sub> S	215–218	51.48 (48.47)	6.01 (5.08)	15.28 (14.130)
4	C <sub>14</sub> H <sub>17</sub> N <sub>3</sub> O <sub>5</sub> S	192–198	49.88 (49.55)	5.15 (5.05)	12.47 (12.38)
5	C <sub>13</sub> H <sub>17</sub> N <sub>5</sub> O <sub>4</sub> S	205–210	46.42 (46.01)	5.25 (5.05)	20.60 (20.64)
6	C <sub>10</sub> H <sub>18</sub> N <sub>2</sub> O <sub>4</sub>	200–206	52.60 (52.16)	7.98 (7.88)	12.60 (12.17)
7	C <sub>18</sub> H <sub>18</sub> N <sub>2</sub> O <sub>2</sub>	125–128	73.20 (73.45)	6.19 (6.16)	9.20 (9.52)
8	C <sub>8</sub> H <sub>14</sub> N <sub>2</sub> O <sub>2</sub>	110–115	56.20 (56.45)	8.20 (8.29)	16.52 (16.46)
9	C <sub>10</sub> H <sub>16</sub> N <sub>2</sub> O <sub>3</sub>	165–170	56.08 (56.59)	7.20 (7.60)	13.28 (13.20)
10	C <sub>10</sub> H <sub>17</sub> N <sub>3</sub> O <sub>2</sub>	165–170	56.20 (56.85)	8.08 (8.11)	19.90 (19.89)
11	C <sub>20</sub> H <sub>23</sub> N <sub>5</sub> O <sub>4</sub> S	206–210	55.20 (55.93)	5.30 (5.40)	16.30 (16.31)
12	C <sub>20</sub> H <sub>24</sub> N <sub>4</sub> O <sub>5</sub> S	146–150	55.60 (55.54)	5.62 (5.59)	12.92 (12.95)
13	C <sub>16</sub> H <sub>21</sub> N <sub>3</sub> O <sub>4</sub> S	210–212	54.64 (54.68)	6.10 (6.02)	11.88 (11.96)
14	C <sub>18</sub> H <sub>23</sub> N <sub>3</sub> O <sub>5</sub> S	188–192	54.08 (54.95)	5.80 (5.89)	10.80 (10.68)
15	C <sub>17</sub> H <sub>23</sub> N <sub>5</sub> O <sub>4</sub> S	208–214	51.80 (51.89)	5.86 (5.89)	17.60 (17.80)
16	C <sub>14</sub> H <sub>24</sub> N <sub>2</sub> O <sub>4</sub>	198–202	59.08 (59.13)	8.54 (8.51)	9.56 (9.85)
17	C <sub>22</sub> H <sub>24</sub> N <sub>2</sub> O <sub>2</sub>	120–125	75.88 (75.83)	6.98 (6.94)	8.08 (8.04)
18	C <sub>12</sub> H <sub>20</sub> N <sub>2</sub> O <sub>2</sub>	112–116	64.12 (64.26)	8.92 (8.99)	12.46 (12.49)
19	C <sub>14</sub> H <sub>22</sub> N <sub>2</sub> O <sub>3</sub>	168–172	63.12 (63.13)	8.64 (8.33)	10.42 (10.52)
20	C <sub>14</sub> H <sub>23</sub> N <sub>3</sub> O <sub>2</sub>	160–165	63.14 (63.37)	8.78 (8.74)	15.88 (15.84)
21	C <sub>21</sub> H <sub>25</sub> N <sub>5</sub> O <sub>4</sub> S	210–214	70.70 (56.87)	64.64 (56.87)	12.12 (15.79)
22	C <sub>21</sub> H <sub>26</sub> N <sub>4</sub> O <sub>5</sub> S	142–145	56.52 (56.49)	5.92 (5.87)	12.64 (12.55)
23	C <sub>17</sub> H <sub>23</sub> N <sub>3</sub> O <sub>4</sub> S	208–210	55.89 (55.87)	6.38 (6.34)	12.00 (11.50)
24	C <sub>19</sub> H <sub>25</sub> N <sub>3</sub> O <sub>5</sub> S	188–192	56.10 (56.00)	6.21 (6.18)	10.32 (10.31)
25	C <sub>18</sub> H <sub>25</sub> N <sub>5</sub> O <sub>4</sub> S	206–210	53.10 (53.05)	6.21 (6.18)	17.22 (17.19)
26	C <sub>15</sub> H <sub>26</sub> N <sub>2</sub> O <sub>4</sub>	198–204	60.41 (60.38)	8.82 (8.78)	9.42 (9.39)
27	C <sub>23</sub> H <sub>26</sub> N <sub>2</sub> O <sub>2</sub>	120–124	77.00 (76.21)	7.25 (7.23)	7.75 (7.73)
28	C <sub>13</sub> H <sub>22</sub> N <sub>2</sub> O <sub>2</sub>	110–115	65.55 (65.51)	9.32 (9.30)	11.78 (11.75)
29	C <sub>15</sub> H <sub>24</sub> N <sub>2</sub> O <sub>3</sub>	165–170	64.30 (64.26)	8.68 (8.63)	10.00 (9.99)
30	C <sub>15</sub> H <sub>25</sub> N <sub>3</sub> O <sub>2</sub>	165–170	64.52 (64.49)	9.06 (9.02)	15.06 (15.04)
31	C <sub>22</sub> H <sub>20</sub> N <sub>5</sub> O <sub>4</sub> SCl	210	54.36 (54.38)	4.20 (4.15)	14.46 (14.41)
32	C <sub>22</sub> H <sub>21</sub> N <sub>4</sub> O <sub>5</sub> SCl	146–149	54.10 (54.04)	4.38 (4.33)	11.49 (11.46)
33	C <sub>18</sub> H <sub>18</sub> N <sub>3</sub> O <sub>4</sub> SCl	210–214	53.06 (53.01)	4.49 (4.45)	10.36 (10.30)
34	C <sub>20</sub> H <sub>20</sub> N <sub>3</sub> O <sub>5</sub> SCl	188–192	53.41 (53.39)	4.50 (4.48)	53.42 (53.39)
35	C <sub>19</sub> H <sub>20</sub> ClN <sub>5</sub> O <sub>4</sub>	208–212	50.76 (50.72)	4.52 (4.48)	15.60 (15.57)
36	C <sub>16</sub> H <sub>21</sub> ClN <sub>2</sub> O <sub>4</sub>	200–204	56.42 (56.39)	6.24 (6.21)	8.30 (8.22)
37	C <sub>24</sub> H <sub>20</sub> N <sub>2</sub> O <sub>2</sub> Cl	122–127	71.24 (71.19)	5.26 (5.23)	7.00 (6.92)
38	C <sub>14</sub> H <sub>17</sub> N <sub>2</sub> O <sub>2</sub> Cl	112–117	59.92 (59.89)	6.12 (6.10)	10.00 (9.98)
39	C <sub>15</sub> H <sub>19</sub> ClN <sub>2</sub> O <sub>3</sub>	168–170	58.00 (57.97)	6.20 (6.16)	9.08 (9.01)
40	C <sub>15</sub> H <sub>20</sub> ClN <sub>3</sub> O <sub>2</sub>	168–172	58.19 (58.16)	6.56 (6.51)	13.58 (13.56)



*Spectral studies.* The  $^1\text{H}$  NMR spectra in DMSO and  $\text{CDCl}_3$  solvent (Table 2) were recorded on a Bruker DRX-300 FT NMR spectrometer. The IR spectra were recorded on a Shimadzu 820 IPC FTIR spectrophotometer using KBr pellets. The UV spectra were recorded on a Shimadzu UV-160A, UV-vis. spectrophotometer.

**Table 2.**  $^1\text{H}$  NMR spectral data of the Mannich bases (1–40)

Com- pounds	$\delta$ values (ppm)				
	$\text{CH}_2$ (d)	NH of sulphon- amide (s)	various ring proton	$\text{SO}_2\text{NH}$ (s)	CONH of ring (t)
1	2	3	4	5	6
1	2.50	6.80	6.70–6.75	10.68	8.00–8.12
2	2.48	6.40	6.80–6.84	11.04	8.00–8.10
3	2.60	5.70	6.95–6.98	10.58	8.10–8.12
4	2.68	5.60	6.67–6.82	11.20	7.82–8.00
5	2.64	6.40	6.90–6.94	11.54	8.00–8.12
6	2.56	–	6.82–6.87	–	8.00–8.12
7	2.65	–	6.60–6.65	–	8.00–8.12
8	2.66	–	6.50–6.55	–	8.00–8.12
9	2.64	–	6.82–6.83	–	8.10–8.12
10	2.68	–	6.92–6.93	–	8.00–8.12
11	2.46	6.30	6.86	11.08	7.84–8.00
12	2.48	6.32	6.86	11.04	7.88–8.00
13	2.50	6.88	6.60	10.62	7.86–8.00
14	2.52	6.32	6.88	11.12	7.82–8.00
15	2.64	6.34	6.82	11.12	7.80–8.00
16	2.66	–	6.80	–	7.92–8.00
17	2.66	–	6.86	–	7.94–8.00
18	2.62	–	6.88	–	7.96–8.00
19	2.60	–	6.90	–	8.00–8.12
20	2.66	–	6.94	–	7.94–8.10
21	2.54	6.24	7.84	10.62	7.98–8.00
22	2.50	6.22	7.82	10.52	7.96–8.00
23	2.52	6.22	7.86	10.22	7.92–8.10
24	2.50	6.20	7.84	10.42	7.90–8.00
25	2.56	6.22	7.86	10.40	7.92–8.00
26	2.60	–	7.72	–	7.94–8.00
27	2.62	–	7.70	–	7.96–8.00
28	2.64	–	7.74	–	7.84–8.00
29	2.58	–	7.70	–	7.88–8.00
30	2.64	–	6.92	–	7.86–8.00
31	2.56	5.62	7.42	10.34	8.00–8.10
32	2.57	5.96	7.40	10.28	8.10–8.20
33	2.54	6.02	7.42	10.26	8.10–8.30

to be continued



Continuation of Table 2

1	2	3	4	5	6
<b>34</b>	2.55	6.04	7.42	10.28	8.00–8.10
<b>35</b>	2.62	–	4.72	–	8.10–8.20
<b>36</b>	2.60	–	4.82	–	8.10–8.20
<b>37</b>	2.60	–	4.82	–	8.00–8.10
<b>38</b>	2.62	–	4.60	–	8.00–8.12
<b>39</b>	2.62	–	4.90	–	8.00–8.14
<b>40</b>	2.64	–	6.92	–	8.00–8.16

(d) – doublet; (s) – singlet; (t) – triplet.

*Antimicrobial activity.* The antibacterial activity of the newly synthesised Mannich bases are recorded in Table 3. The molecular parameters calculated using ACD Labs software<sup>13</sup> are summarised in Table 4, while the calculated values of topological indices using DRAGON software<sup>14</sup> are shown in Table 5.

**Table 3.** Antibacterial activity of the Mannich bases and NMR-chemical shift (1–40)

C.N.	$\sum$ NMR	<i>B.subtilis</i>	<i>S. typhi</i>	<i>E.coli</i>	<i>S. aureus</i>	<i>K. pneumo- niae</i>	<i>P. aurugi- nosa</i>
1	2	3	4	5	6	7	8
<b>1</b>	33.98	10.5	10.5	10.0	11.5	10.8	10.5
<b>2</b>	34.26	10.0	12.0	12.0	11.0	11.5	10.0
<b>3</b>	31.68	10.5	10.0	11.0	12.0	12.0	10.5
<b>4</b>	32.5	11.0	10;0	8.5	9.5	13.0	11.0
<b>5</b>	34.29	12.0	11.0	7.5	10.5	13.5	12.0
<b>6</b>	30.42	13.0	11.5	10.0	10.0	14.2	13.0
<b>7</b>	36.44	11.0	10.5	10.5	10.5	15.8	11.0
<b>8</b>	34.36	10.5	8.5	11.0	10.5	10.8	10.5
<b>9</b>	30.88	10.0	10.0	11.5	10.0	10.2	10.0
<b>10</b>	32.48	11.2	11.0	11.5	11.5	11.8	11.2
<b>11</b>	30.98	11.6	11.0	11.0	12.4	13.0	11.6
<b>12</b>	31.28	11.8	11.0	10.0	11.0	13.5	11.8
<b>13</b>	36.92	13.2	11.5	10.5	11.2	12.5	13.2
<b>14</b>	32.22	14.8	12.5	12.0	11.5	12.0	14.8
<b>15</b>	30.24	15.6	13.5	12.5	12.0	12.0	15.6
<b>16</b>	34.60	10.5	10.0	10.5	11.0	11.5	10.5
<b>17</b>	34.28	8.5	10.0	10.5	11.0	11.5	8.5
<b>18</b>	32.60	7.5	10.0	10.5	10.5	11.6	7.5
<b>19</b>	34.46	10.5	10.0	10.0	11.0	11.5	10.5
<b>20</b>	30.92	12.0	10.0	11.0	11.5	11.5	12.0
<b>21</b>	30.28	13.4	11.5	11.0	11.5	11.5	13.4
<b>22</b>	30.60	11.0	12.5	11.5	12.0	12.0	11.0

to be continued

Continuation of Table 3

1	2	3	4	5	6	7	8
23	32.42	15.5	13.5	12.5	12.5	11.5	15.5
24	32.72	14.8	12.5	11.5	11.0	11.0	14.8
25	27.04	–	–	–	–	–	–
26	34.42	12.0	13.5	12.5	12.0	12.5	12.0
27	30.90	12.5	12.5	10.0	12.5	12.0	12.5
28	34.90	11.5	10.5	11.0	12.5	12.5	11.5
29	32.48	11.0	10.5	10.5	11.5	12.5	11.0
30	36.50	10.0	10.0	10.5	14.5	12.5	10.0
31	30.26	10.8	10.8	12.2	13.5	11.5	10.5
32	34.62	10.4	13.8	11.2	12.5	10.5	15.5
33	34.42	10.6	11.8	13.2	16.5	12.0	12.5
34	30.24	10.8	12.8	12.2	17.5	12.5	11.5
35	32.40	10.9	13.8	13.2	12.5	12.5	11.5
36	30.92	10.6	11.8	14.2	11.5	11.5	11.5
37	30.24	10.4	14.8	15.2	10.5	10.5	11.5
38	30.20	10.4	13.8	11.2	13.5	13.0	11.5
39	34.92	10.0	12.8	10.2	12.5	13.5	11.5
40	34.90	10.0	11.8	12.2	13.5	11.5	11.5

**Table 4.** ACD Labs parameters for the Mannich bases used in the present study (1–40)

CN	FW	MR	MV	PC	$\eta$	SI	$d$	Pol	MM	NM
1	2	3	4	5	6	7	8	9	10	11
1	375.4	93.03	250.9	750.5	1.663	79.9	1.495	36.88	375.1	375
2	378.4	92.34	256.8	748.5	1.638	72.1	1.473	36.6	378.09	378
3	297.33	72.69	204.3	587	1.629	68	1.454	28.81	297.07	297
4	339.36	82.10	239.6	670.9	1.6	61.4	1.416	32.54	339.08	339
5	339.37	82.71	213.5	627.1	1.7	74.4	1.58	32.78	339.1	339
6	230.261	56.9	179.8	498	1.545	58.7	1.28	22.55	230.12	230
7	294.348	85.22	240.5	651.3	1.626	53.7	1.223	33.78	294.13	294
8	170.209	44.56	151.8	383.8	1.498	40.8	1.12	17.66	170.105	170
9	212.24	53.19	172.6	454.8	1.528	48.1	1.229	21.08	212.11	212
10	226.276	59.56	179.2	491	1.578	56.2	1.26	23.61	226.14	226
11	429.49	109.52	296	877.6	1.661	77.2	1.45	43.41	429.14	429
12	432.493	108.83	301.3	875.6	1.641	71.2	1.43	43.14	432.14	432
13	351.42	89.18	247.5	714.1	1.64	69.2	1.41	35.35	351.12	351
14	393.45	98.59	280.7	798	1.619	65.2	1.4	39.08	393.13	393
15	393.46	99.12	254.6	741.6	1.706	71.9	1.54	39.29	393.14	393
16	284.35	73.86	224.4	625.1	1.572	60.1	1.26	29.28	284.17	284
17	348.43	101.69	283	778.4	1.637	57.2	1.23	40.31	348.18	348
18	224.29	61.52	196.9	510.9	1.537	45.2	1.13	24.39	224.15	224
19	266.336	70.48	216.9	581.9	1.563	51.7	1.22	27.94	266.16	266

to be continued

Continuation of Table 4

1	2	3	4	5	6	7	8	9	10	11
<b>20</b>	265.35	72.39	218.4	589.8	1.577	53.1	1.21	28.7	265.17	265
<b>21</b>	443.51	114.15	312.1	917.7	1.652	74.6	1.42	45.25	443.16	443
<b>22</b>	446.51	113.46	317.4	915.6	1.633	69.2	1.4	44.98	446.16	446
<b>23</b>	365.44	93.81	263.7	754.2	1.629	66.9	1.38	37.19	365.1	365
<b>24</b>	407.48	103.22	296.8	838	1.612	63.4	1.37	40.92	407.15	407
<b>25</b>	407.48	103.73	270.6	780.2	1.692	69	1.5	41.12	407.16	407
<b>26</b>	298.378	78.49	240.6	665.1	1.565	58.3	1.23	31.11	298.18	298
<b>27</b>	362.46	106.32	299.2	818.5	1.628	56	1.21	42.14	362.19	362
<b>28</b>	238.326	66.15	213.3	550.9	1.532	44.5	1.11	26.22	238.16	238
<b>29</b>	280.36	75.12	233.2	622	1.55	50.5	1.2	29.78	280.1	280
<b>30</b>	279.37	77.03	234.6	629.9	1.57	51.8	1.19	30.53	279.19	279
<b>31</b>	473.93	118.78	310.6	929.8	1.69	80.2	1.52	47.09	473.09	473
<b>32</b>	476.93	118.09	315.9	927.7	1.67	74.3	1.5	46.81	476.09	476
<b>33</b>	395.86	98.44	262.2	766.3	1.674	72.8	1.5	39.02	395.07	395
<b>34</b>	437.89	107.85	295.4	850.1	1.65	68.5	1.48	42.75	437.08	437
<b>35</b>	437.9	108.33	279.9	809.1	1.701	69.7	1.56	42.94	437.09	437
<b>36</b>	328.79	83.12	239.3	677.2	1.611	64.1	1.37	32.95	328.11	328
<b>37</b>	392.87	110.95	297.7	830.6	1.667	60.5	1.31	43.98	392.12	392
<b>38</b>	268.739	70.78	212	563	1.582	49.7	1.26	28.06	268.09	268
<b>39</b>	310.77	79.75	231.8	634	1.6	55.9	1.34	31.61	310.1	310
<b>40</b>	313.60	76.31	263.80	628	1.5	70.1	1.5	30.51	270.20	270

FW – formular weight; MR – molar refractivity; MV – molar volume; PC – parachor;  $\eta$  – index of refraction (IR); SI – surface tension;  $d$  – density; Pol – polarisability; MM – monoisotopic mass; NM – nominal mass.

*QSAR study/correlation analysis.* Maximum  $R^2$  method<sup>15</sup> was used for obtaining statistically significant models (Tables 6–8). The predictive ability of the proposed models were judged by cross-validation method<sup>15</sup>.

**Table 5.** Topological indices for the Mannich bases used (1–40)

CN	ZM1	ZM2	Pol	SMT1	Xu	SP1	W	Har	$\% \chi$	${}^1 \chi$	${}^2 \chi$	${}^3 \chi$	${}^4 \chi$
1	2	3	4	5	6	7	8	9	10	11	12	13	14
1	134	154	39	8262	25.576	173.917	1929	47.659	18.571	12.454	11.541	9.18	7.283
2	136	157	38	8236	25.55	362.505	1928	47.798	18.734	12.348	11.821	9.259	7.402
3	102	116	29	3766	20.112	247.217	906	35.026	14.751	9.376	9.21	6.76	5.065
4	116	132	34	5572	22.859	896.61	1358	40.786	17.035	10.793	10.431	7.575	6.199
5	116	132	34	5572	22.859	896.61	1358	40.786	17.035	10.793	10.431	7.575	6.199
6	72	80	21	1794	16.098	60.861	456	25.853	11.966	7.685	6.228	4.78	3.797
7	112	130	33	4366	21.206	24.207	1006	40.661	15.364	10.754	11.43	7.836	6.424
8	56	62	15	782	11.932	34.756	194	18.832	9.138	5.609	5.179	3.524	2.76
9	74	84	20	1602	15.106	15.46	370	25.441	10.673	7.271	9.449	5.111	4.023
10	74	84	20	1602	15.106	15.46	370	25.441	10.673	7.271	9.449	5.111	4.023
11	162	190	47	12564	28.885	208.099	2866	57.421	21.192	14.369	13.726	11.03	9.378
12	164	193	46	12534	28.863	590.583	2865	57.56	21.355	14.262	14.006	11.11	9.497
13	130	152	37	6362	23.611	475.67	1483	44.679	17.372	11.29	11.395	8.616	7.161
14	144	168	42	8912	26.254	1899.56	2105	50.5	19.656	12.707	12.615	9.431	8.295
15	144	168	42	8912	26.254	1899.56	2105	50.5	19.656	12.707	12.615	9.431	8.295
16	100	116	29	3402	19.709	106.283	825	35.434	14.588	9.599	8.413	6.635	5.892
17	140	166	41	7118	24.621	25.846	1603	50.516	17.985	12.668	11.43	9.691	8.52
18	84	98	23	1770	15.776	7.305	419	28.212	11.759	7.523	7.363	5.38	4.855
19	102	120	28	3118	18.813	17.916	701	34.978	13.295	9.185	8.474	6.966	6.119
20	102	120	28	3118	18.813	17.916	701	34.978	13.295	9.185	8.474	6.966	6.119
21	166	194	50	13732	29.702	224.413	3146	59.428	21.899	14.869	14.079	11.28	9.555
22	168	197	49	13701	29.681	689.78	3145	59.567	22.062	14.762	14.359	11.36	9.674
23	134	156	40	7105	24.482	570.128	1664	46.664	18.079	11.79	11.748	8.866	7.337
24	148	172	45	9840	27.095	2326.94	2333	52.497	20.364	13.207	12.969	9.681	8.472
25	148	172	45	9840	27.095	2326.94	2333	52.497	20.364	13.207	12.969	9.681	8.472

to be continued

Continuation of Table 5

	1	2	3	4	5	6	7	8	9	10	11	12	13	14
<b>26</b>	104	120	32	3894	20.625	125.108	948	37.403	15.295	10.099	8.766	6.885	6.069	
<b>27</b>	148	174	45	9170	26.548	29.95	2081	53.954	19.399	13.665	12.125	10.23	8.958	
<b>28</b>	88	102	26	2098	16.762	94.297	500	30.145	12.466	8.023	7.717	5.63	5.032	
<b>29</b>	106	124	31	3588	19.749	18.894	813	36.938	14.002	9.685	8.827	7.216	12.10	
<b>30</b>	106	124	31	3588	19.749	18.894	813	36.938	14.002	9.685	8.827	7.216	12.10	
<b>31</b>	172	201	52	14990	30.516	712.792	3454	61.522	22.769	15.262	14.701	14.70	11.70	
<b>32</b>	174	204	51	14958	30.495	1475.95	3453	61.661	22.933	15.156	14.981	11.78	9.747	
<b>33</b>	140	163	42	7918	25.347	1034.17	1867	48.738	18.949	12.184	13.591	9.286	7.41	
<b>34</b>	154	179	47	10847	27.932	4090.63	2586	54.582	21.234	13.601	13.591	10.10	8.544	
<b>35</b>	154	179	47	10847	27.932	4090.63	2586	54.582	21.234	13.601	13.591	10.10	8.544	
<b>36</b>	110	127	34	4442	21.531	240.033	1089	39.463	16.165	10.493	9.388	7.306	6.142	
<b>37</b>	150	177	46	8788	26.338	82.662	2005	54.638	19.562	13.562	12.405	10.36	8.769	
<b>38</b>	94	109	28	2470	17.729	160.86	595	32.174	13.337	8.417	8.339	6.05	5.105	
<b>39</b>	112	131	33	4113	20.673	51.118	942	38.991	14.872	10.079	9.449	7.637	6.368	
<b>40</b>	112	131	33	4113	20.673	51.118	942	38.991	14.872	10.079	9.449	7.637	6.368	

ZM1 – first Zagreb index M1; W – the Wiener index; ZM2 – second Zagreb index M2; Har – the Harary index; Pol – polarity number;  $\chi^0$  – zero-order Randic connectivity index; SMT1 – the Schultz molecular topological index;  $\chi^1$  – first-order Randic connectivity index; Xu – Xu index;  $\chi^2$  – second-order Randic connectivity index; SP1 – superpendent index;  $\chi^3$  – third-order Randic connectivity index;  $\chi^4$  – fourth-order Randic connectivity index.

Table 6. Regression parameters and quality of correlation using NMR as molecular descriptor (1–40)

Bacteria	Model	Parameters used	$R^2$	R	SE	F
<i>B. subtilis</i>	1	$\sum \text{NMR}, \sum \text{NMR}^2, \sum \text{NMR}^3$	0.2821	0.2206	0.1343	4.555
<i>S. typhi</i>	2	$\sum \text{NMR}, \sum \text{NMR}^2, \sum \text{NMR}^3$	0.2821	0.2206	0.1343	4.585
<i>E. coli</i>	3	$\sum \text{NMR}, \sum \text{NMR}^2, \sum \text{NMR}^3$	0.1249	0.0499	0.1224	1.663
<i>S. aureus</i>	4	$\sum \text{NMR}, \sum \text{NMR}^2, \sum \text{NMR}^3$	0.4341	0.3855	0.1061	8.948
<i>K. pneumoniae</i>	5	$\sum \text{NMR}, \sum \text{NMR}^2, \sum \text{NMR}^3$	0.0017	0.0000	0.0936	0.020
<i>P. aeruginosa</i>	6	$\sum \text{NMR}, \sum \text{NMR}^2, \sum \text{NMR}^3$	0.2016	0.1332	0.1410	2.946

**Table 7.** Statistical models for modeling antibacterial activities of the Mannich bases using ACD labs parameters

<i>B. subtilis</i>			<i>S. typhi</i>			<i>E. coli</i>		
model	parameters used	R <sup>2</sup>	model	parameters used	R <sup>2</sup>	model	parameters used	R <sup>2</sup>
7	SI	0.01834	18	MV	0.0651	29	Mv	0.0106
8	IR, SI	0.0756	19	MV, Pol	0.0784	30	PC, IR	0.0402
9	MV, SI, Pol	0.1187	20	MR, MV, Pol	0.0983	31	FW, PC, MM	0.2599
10	MR, MV, SI, Pol	0.1327	21	MR, MV, Pol, IR	0.1085	32	FW, PC, MM, AM	0.3241
11	MR, PC, IR, SI, Pol	0.1458	22	FW, MV, <i>d</i> , Pol, MM	0.2794	33	FW, PC, MM, NM, AM	0.3657
12	PC, IR, SI, Pol, MM, NM	0.1624	23	FW, MV, <i>d</i> , Pol, MM, AM	0.3278	34	FW, PC, <i>d</i> , MM, NM, AM	0.3808
13	MR, PC, IR, SI, Pol, MM, NM	0.1832	24	FW, MV, <i>d</i> , Pol, MM, AM, IR	0.3485	35	FW, MR, PC, Pol, MM, NM, AM	0.3849
14	FW, PC, IR, SI, Pol, MM, NM, AM	0.2044	25	FW, MV, <i>d</i> , Pol, MM, AM, NM	0.3712	36	FW, MR, PC, IR, Pol, MM, NM, AM	0.3852
15	FW, PC, IR, SI, Pol, MM, NM, AM, PC	0.2234	26	FW, MV, PC, Pol, MM, AM, NM, SI	0.3816	37	FW, MR, PC, IR, <i>d</i> , Pol, MM, NM, AM	0.3906
16	FW, MR, IR, SI, <i>d</i> , Pol, MM, NM, AM, AM, PC	0.2250	27	FW, MV, MR, PC, Pol, MM, AM, NM, NM, SI	0.3825	38	FW, MR, MV, PC, IR, SI, Pol, MM, NM, AM	0.3996
17	FW, MR, IR, SI, <i>d</i> , Pol, MM, NM, NM, AM, PC, MV	0.2285	28	FW, MV, MR, <i>d</i> , PC, Pol, MM, AM, NM, SI	0.3825	39	FW, MR, MV, PC, IR, SI, <i>d</i> , Pol, MM, NM, AM	0.4001

to be continued

Continuation of Table 7

<i>S. aureus</i>			<i>K. pneumoniae</i>			<i>P. aeruginosa</i>		
model	parameters used	$R^2$	model	parameters used	$R^2$	model	parameters used	$R^2$
40	MV	0.0190	51	IR	0.0326	62	PC	0.0382
41	PC, Pol	0.0440	52	IR, SI	0.0413	63	PC, Pol	0.0922
42	MR, PC, Pol	0.0562	53	MR, PC, Pol	0.1214	64	MR, PC, Pol	0.1164
44	FW, PC, Pol, MM	0.3232	54	PC, <i>d</i> , MM, NM	0.21546	65	MR, PC, IR, Pol	0.1197
44	FW, MR, PC, Pol, MM	0.3630	55	MR, PC, Pol, NM, MM	0.2656	66	MR, PC, IR, SI, Pol	0.1328
45	FW, MR, PC, IR, Pol, MM	0.3926	56	MR, PC, IR, Pol, MM, NM	0.3000	67	MR, PC, IR, Pol, SI, MV	0.1340
46	FW, MR, PC, IR, <i>d</i> , Pol, MM	0.4282	57	MR, PC, IR, SI, Pol, MM, NM	0.3783	68	FW, MR, PC, IR, SI, Pol, AM	0.1951
47	MR, PC, IR, <i>d</i> , Pol, MM, NM, AM	0.4588	58	MR, PC, IR, , SI, <i>d</i> , Pol, MM, NM	0.4151	69	FW, PC, IR, SI, Pol, MM, NM, AM	0.2239
48	FW, MR, PC, IR, SI, <i>d</i> , Pol, MM, NM	0.4805	59	MR, MV, PC, IR, SI, <i>d</i> , Pol, MM, NM	0.4176	70	FW, MR, PC, IR, SI, Pol, MM, NM, AM	0.2603
49	FW, MR, PC, IR, SI, <i>d</i> , Pol, MM, NM, AM	0.4826	60	FW, MR, MV, PC, IR, SI, <i>d</i> , Pol, MM, NM	0.4617	71	FW, MR, MV, PC, IR, SI, Pol, MM, NM, AM	0.2629
50	FW, MR, MV, PC, IR, SI, <i>d</i> , Pol, MM, NM, AM	0.4827	61	FW, MR, MV, PC, IR, SI, <i>d</i> , Pol, MM, NM, AM	0.4629	72	FW, MR, MV, PC, IR, SI, <i>d</i> , Pol, MM, NM, AM	0.2629

**Table 8.** Stastical models for modelling antibacterial activities of Mannich bases using topological indices

<i>B. subtilis</i>			<i>S. typhi</i>			<i>E. coli</i>		
model	parameters used	$R^2$	model	parameters used	$R^2$	model	parameters used	$R^2$
73	${}^0\chi$	0.0904	83	Pol	0.2926	93	Pol	0.0759
74	Xu, ${}^3\chi$	0.1835	84	Pol, ${}^3\chi$	0.4605	94	Pol, Xu	0.2474
75	Xu, Har, ${}^3\chi$	0.2064	85	Pol, Har, ${}^3\chi$	0.5446	95	Pol, Xu, ${}^4\chi$	0.2925
76	Pol, Xu, Har, ${}^3\chi$	0.2222	86	Pol, Xu, ${}^3\chi$ , ${}^4\chi$	0.5304	96	Pol, Xu, ${}^0\chi$ , ${}^2\chi$	0.3290
77	${}^0\chi$ , Pol, Xu, Har, ${}^3\chi$	0.2285	87	Pol, Xu, Har, ${}^3\chi$ , ${}^4\chi$	0.5427	97	ZM1, ZM2, Pol, ${}^0\chi$ , ${}^2\chi$	0.3422
78	Pol, SMT1, Xu, W, Har, ${}^3\chi$	0.2392	88	Pol, Xu, Har ${}^2\chi$ , ${}^3\chi$ , ${}^4\chi$	0.5446	98	ZM1, ZM2, Pol, Xu, ${}^0\chi$ , ${}^2\chi$	0.3673
79	Pol, SMT1, Xu, W, SPI, Har, ${}^3\chi$	0.2461	89	Pol, Xu, Har, SMT1, ${}^2\chi$ , ${}^3\chi$ , ${}^4\chi$ , ${}^v\chi$	0.5450	99	ZM1, ZM2, Pol, ${}^0\chi$ , ${}^1\chi$ , ${}^2\chi$ , ${}^3\chi$	0.3723
80	Pol, SMT1, Xu, W, SPI, Har, ${}^3\chi$ , ${}^4\chi$	0.2487	90	Pol, Xu, Har, W, SMT1, ${}^2\chi$ , ${}^3\chi$ , ${}^4\chi$ , ${}^v\chi$	0.5455	100	ZM1, ZM2, Pol, ${}^0\chi$ , ${}^1\chi$ , ${}^2\chi$ , ${}^3\chi$ , ${}^4\chi$	0.3812
81	ZM1, ZM $_2$ , Pol, SMT1, Xu, W, ${}^1\chi$ , ${}^2\chi$ , ${}^4\chi$	0.2747	91	Pol, Xu, Har, W, SPI, SMT1, ${}^2\chi$ , ${}^3\chi$ , ${}^4\chi$ , ${}^v\chi$	0.5480	101	ZM1, ZM2, Pol, SMT1, SPI, W, ${}^0\chi$ , ${}^2\chi$ , ${}^4\chi$	0.4025
82	ZM1, ZM $_2$ , Pol, SMT1, Xu, SPI, W, ${}^1\chi$ , ${}^2\chi$ , ${}^3\chi$ , ${}^v\chi$	0.2830	92	Pol, Xu, Har, W, SPI, SMT1, ${}^0\chi$ , ${}^2\chi$ , ${}^3\chi$ , ${}^4\chi$ , ${}^v\chi$	0.5480	102	ZM1, ZM2, Pol, Xu, SMT1, SPI, W, ${}^0\chi$ , ${}^1\chi$ , ${}^2\chi$ , ${}^v\chi$	0.4143

to be continued



Continuation of Table 8

<i>S. aureus</i>			<i>K. pneumoniae</i>			<i>P. aeruginosa</i>		
model	parameters used	$R^2$	model	parameters used	$R^2$	model	parameters used	$R^2$
103	SPI	0.1670	113	SMT1	0.0154	123	$^0\chi$	0.1732
104	SPI <sup>4</sup> $\chi$	0.2270	114	Pol, SPI	0.0743	124	$^0\chi, ^3\chi$	0.2794
105	Pol, <sup>1</sup> $\chi, ^2\chi$	0.4340	115	$^0\chi, \text{Pol}, \text{W}$	0.0945	125	Pol, W, $^3\chi$	0.3013
106	Pol, <sup>1</sup> $\chi, ^2\chi, ^2\chi$	0.4566	116	$^0\chi, ^4\chi, \text{Pol}, \text{W}$	0.1127	126	Pol, Xu, <sup>1</sup> $\chi, ^3\chi$	0.3248
107	Pol, ZM2, Har, <sup>2</sup> $\chi$	0.4880	117	ZM2, SMT1, Sp1, W, <sup>0</sup> $\chi$	0.2100	127	Pol, SMT1, Xu, <sup>1</sup> $\chi$	0.3381
108	Pol, ZM2, Har, <sup>2</sup> $\chi$ , $^3\chi, ^4\chi$	0.4924	118	ZM1, SMT1, Sp1, W, Har, <sup>0</sup> $\chi$	0.2856	128	ZM2, Har, Pol, SMT1, <sup>1</sup> $\chi, ^3\chi$	0.3647
109	ZM1, Pol, Xu, SPI, Har, <sup>1</sup> $\chi, ^2\chi$	0.5218	119	ZM1, SMT1, Sp1, W, Har, <sup>0</sup> $\chi, ^3\chi$	0.3298	129	ZM2, Har, Pol, SMT1, <sup>1</sup> $\chi, ^3\chi, ^4\chi$	0.3783
110	ZM1, Pol, SMT1, W, SPI, Har, <sup>1</sup> $\chi, ^3\chi$	0.5312	120	ZM1, SMT1, Sp1, W, Har, <sup>0</sup> $\chi, ^2\chi, ^4\chi$	0.3680	130	ZM2, Har, Pol, SMT1, <sup>0</sup> $\chi, ^2\chi, ^3\chi, ^4\chi$	0.3844
111	ZM1, Pol, SMT1, W, SPI, Har, <sup>1</sup> $\chi, ^2\chi$ , $\chi, ^3\chi$	0.5551	121	ZM1, SMT1, Sp1, W, Har, <sup>0</sup> $\chi, ^2\chi, ^3\chi$ , $^4\chi$	0.3962	131	ZM2, Har, Pol, SMT1, W, <sup>1</sup> $\chi, ^2\chi$ , $^3\chi, ^4\chi$	0.3887
112	ZM1, ZM2, Pol, Xu, SMT1, W, SPI, Har, $^0\chi, ^1\chi$	0.5151	122	ZM1, ZM2, SMT1, Sp1, W, Har, <sup>0</sup> $\chi, ^2\chi$ , $^3\chi, ^4\chi$	0.4238	132	ZM2, Har, Pol, SMT1, W, <sup>0</sup> $\chi, ^1\chi, ^2\chi$ , $^3\chi, ^4\chi$	0.3906

## RESULTS AND DISCUSSION

*Antibacterial activity.* A perusal of Table 3 demonstrates the following sequence of activity:

*B. subtilis*

15 > 23 > 24 = 14 > 21 > 13 > 27 = 6 > 5 = 20 = 26 > 12 > 11 > 28 > 10 > 4 = 7  
= 22 = 29 > 35 > 31 = 34 > 36 > 33 > 3 = 8 = 16 = 19 > 32 = 37 = 38 > 2 = 9 = 30  
= 39 = 40 > 17 > 18

*S. typhi*

37 > 32 = 35 = 38 > 15 = 23 = 26 > 34 = 39 > 14 = 22 = 24 = 27 > 2 > 33 = 36 = 40 > 6 = 13  
= 21 > 5 = 10 = 11 = 12 > 31 > 1 = 7 = 28 = 29 > 3 = 4 = 9 = 16 = 17 = 18 = 19 = 20 = 30 > 8

*E. coli*

37 > 35 = 38 > 33 = 35 > 15 = 23 = 26 > 31 = 34 = 40 > 2 = 14 > 9 = 10 = 22 = 24 > 32  
= 38 > 3 = 8 = 10 = 20 = 21 = 28 > 7 = 13 = 16 = 17 = 18 = 29 = 30 > 39 > 1 = 6 = 12 = 19 = 27  
> 4 > 5

*S. aureus*

34 > 33 > 31 = 38 = 40 = 30 > 23 = 27 = 28 = 32 = 35 = 39 > 11 > 3 = 15 = 22 = 26 > 36  
= 1 = 10 = 14 = 20 = 21 = 29 > 13 > 2 = 12 = 16 = 17 = 19 = 24 > 5 = 7 = 8 = 18 = 37 > 6 = 9 > 4

*K. pneumoniae*

7 > 6 > 5 = 12 = 39 > 4 = 11 = 38 > 13 = 26 = 28 = 29 = 30 = 40 = 34 = 35 > 33 = 3 = 14 = 15  
= 22 = 27 > 10 = 31 = 36 > 18 > 2 = 16 = 17 = 19 = 20 = 21 = 23 > 24 > 1 = 8 > 32 = 37 > 9

*P. aeruginosa*

15 > 23 = 32 > 14 = 24 > 21 = 13 > 27 = 33 > 5 = 20 = 26 > 12 > 11 > 10 > 28 = 34 = 35  
= 36 = 37 = 38 = 39 = 40 > 4 = 7 = 22 = 29 = 31 = 1 = 3 = 8 = 16 = 19 > 2 = 9 = 30 > 17 > 18

The afore-mentioned results show that degeneracy in activity exists in each of the 6 bacteria used. Also, that the sequences are very different in each case. This clearly demonstrates that by considering referred sequences of activity alone no 1:1 correlation between structure and activity could be established. This has prompted us to examine structure–activity relationships using molecular descriptors and topological indices. Since  $\sum$ NMR chemical shifts are molecular structure dependent properties<sup>16,17</sup>, we thought of using  $\sum$ NMR chemical shifts and ACD (anemia of chronic disease) Lab parameters as molecular descriptors and examine their variance in terms of their antibacterial activity. Use of topological descriptors is well established<sup>12,18</sup>. Hence, our molecular modelling vis-à-vis drug designing in the present paper, will be carried out under following headings: (i) QSAR study based on using  $\sum$ NMR chemical shifts as molecular descriptor; (ii) QSAR study based on using ACD Lab parameters as molecular descriptor; (iii) QSAR study based on using topological indices as molecular descriptor, and (iv) QSAR study based on combinations of the afore-mentioned parameters.

The results obtained are discussed below:

*QSAR study based on using  $\sum$ NMR chemical shifts as molecular descriptor.* Recently Khadikar and co-workers<sup>16,17</sup> have suggested that sum of the  $\sum$ NMR chemical shifts

can be very successfully used as molecular descriptor. In the present study, we have, therefore, used  $\sum$ NMR chemical shifts as molecular descriptor and conducted molecular modelling using  $\sum$ NMR chemical shifts. Preliminary regression analysis has indicated that better results are obtained in non-linear regression analysis in that we have used  $\sum$ NMR and its second and third degree polynomials for modelling the antibacterial activity against the 6 bacteria used. The results obtained are presented in Table 6. The results recorded in this Table show that except for *S. aureus*, the proposed models are of very poor statistical quality. The failure of using  $\sum$ NMR as molecular descriptor prompted us to go for molecular modelling using ACD Lab parameters as molecular descriptors. Below we discussed the QSAR results obtained using ACD Labs parameters<sup>13</sup>.

*QSAR study based on using ACD Lab parameters as molecular descriptors.* The regression parameters and the quality of correlation for modelling antibacterial activity against the 6 bacteria using ACD Lab parameters<sup>13</sup> are given in Table 7. The results show that compared to  $\sum$ NMR chemical shifts better results are obtained using ACD Labs parameters. Best results are obtained for modelling antibacterial activity against *S. aureus*. Worse results are obtained in case of *B. subtilis* and *P. aeruginosa*.

At this stage, it is worthy mentioning that the parameters to be used in QSAR should follow the ‘rule of thumbs’<sup>19</sup>. According to this rule, the parameters to be used in multiple regression analysis should be 1/4 of the number of compounds under study. In our case we have used 40 Mannich bases, therefore, the optimum descriptors to be used are obviously 10. However, the lower the number of parameters used in the QSAR model, the better will be the proposed model. The data presented in Table 7 indicated that proposed 10-parameter model for modelling antibacterial activity against *S. aureus* is well justified in accordance with the famous rule of thumbs<sup>19</sup>. However, the results obtained using ACD Labs parameters are not that good. We have, therefore, carried out further molecular modelling Mannich bases using topological indices.

*QSAR study based on using topological indices as molecular descriptors.* The results as given in Table 8 show that using topological indices as the correlating parameters except for *B. subtilis* excellent results are obtained for modelling antibacterial activity against remaining 5 bacteria. Here also in all the cases 10-parametric model is found the most approximate model for modelling antibacterial activities of the Mannich bases against the bacteria used. Obviously, the models obtained are in accordance with the rule of thumb<sup>19</sup>.

(i) 10-parameter model for *B. subtilis*

The most appropriate 10-parameter model for modelling antibacterial Mannich bases against *B. subtilis* is found as below:

Antibacterial activity against *B. subtilis* =

$$5.9422 - 1.7055 (\pm 1.2085) ZM1 + 0.9964 (\pm 0.7748) ZM1 + 0.5643 (\pm 6.4062) Pol \\ + 0.0075 (\pm 0.7070) SMT1 + 4.9392 (\pm 2.4923) Xu + 0.0004 (\pm 0.0007) SP1 + 0.0313 \\ (\pm 0.0308) W - 4.6649 (\pm 2.6631) {}^1\chi + 0.3188 (\pm 0.4386) {}^2\chi - 0.6902 (\pm 0.6390) {}^3\chi$$

$$N=40, SE=0.1501, R^2 = 0.2830, R^2A= 0.0269, F= 1.105.$$

As stated earlier, the results obtained are not that good. The inferior QSAR model is due to the presence of large residues, i.e. difference between observed and calculated activity for compounds **14**, **16**, **24** and **25**. When we have deleted these compounds from the regression procedure no change in the quality of correlation is resulted. This means that compared to other Mannich bases, the Mannich bases **14**, **16**, **24** and **25** have possibly different type of mechanism and, therefore, their presence in the regression procedure could not result into better quality model.

(ii) 10-parameter model for *S. typhi*

The types of the topological indices used in the model given below are found quite useful for the modelling antibacterial activity of the Mannich bases against *S. typhi*.

Antibacterial activity against *S. typhi* =

$$10.7071 + 0.6240 (\pm 0.2979) \text{ Pol} + 0.0017 (\pm 0.0080) \text{ SMT1} - 0.4097 (\pm 6.9082) \text{ Xu} \\ - 0.0001 (\pm 0.0005) \text{ SP} + 0.0074 (\pm 0.0303) \text{ W} - 0.0743 (\pm 0.6492) \text{ Har} - 0.2087 (\pm 2.1486) {}^0\chi \\ + 0.1070 (\pm 0.2928) {}^2\chi + 0.6402 (\pm 0.4704) {}^3\chi - 0.1813 (\pm 0.1715) {}^4\chi$$

$$N=40, \text{ SE}=0.0.0994, R^2 = 0.5480, R^2A= 0.3866, F= 3.395.$$

This shows that the observed antibacterial activity against *S. typhi* is dependent of shape, size, and branching present in the Mannich bases.

(iii) 10-parameter model for *E. coli*

Comparatively lesser quality model is obtained for the exhibition of antibacterial activity of the Mannich bases against *S. coli*. The resulting model is as below:

Antibacterial activity against *E. coli* =

$$32.4337 - 1.8411 (\pm 0.6673) \text{ ZM1} - 0.0132 (\pm 0.0103) \text{ SMT1} + 3.0946 \\ (\pm 8.2830) \text{ Xu} - 0.0009 (\pm 0.0007) \text{ SP} + 0.0609 (\pm 0.0464) \text{ W} + 3.9806 (\pm 6.8050) \text{ Har} \\ - 2.8214 (\pm 3.7452) {}^0\chi - 10.8262 (\pm 21.3429) {}^1\chi + 0.5050 (\pm 0.3678) {}^2\chi$$

$$N=40, \text{ SE}=0.1140, R^2 = 0.4144, R^2A= 0.1757, F= 1.736.$$

Here we observed that compared to earlier two cases, the model does not involved connectivity indices of higher order. It means that higher order connectivity is not favourable for the exhibition of antibacterial activity of the Mannich bases against *E. coli*.

(iv) 10-parameter model for *S. aureus*

The statistically significant 10-parameter model for modelling antibacterial activity of the Mannich bases against *S. aureus* is found as below:

Antibacterial activity against *S. aureus* =

$$- 26.4408 + 3.7410 (+2.4508) \text{ ZM1} - 0.9703 (\pm 0.8211) \text{ ZM2} + 1.9021 (\pm 0.5418) \text{ Pol} \\ + 0.0093 (\pm 0.0095) \text{ SMT1} - 11.2560 (\pm 7.8966) \text{ Xu} + 0.0011 (\pm 0.0007) \text{ SP1} + 0.4571 \\ (\pm 0.0428) \text{ W} - 12.0492 (\pm 6.5854) \text{ Har} + 4.5639 (\pm 3.6310) {}^0\chi + 32.1220 (\pm 20.4818) {}^1\chi$$

$$N=40, R^2 = 0.5551, R^2A= 0.3963, F= 3.494.$$

The model shows that antibacterial activity of the Mannich bases against *S. aureus* is also independent of higher order connectivity.

(v) 10-parameter model for *K. pneumoniae*

The quality of correlation and statically significance of the model for modelling antibacterial activity of the Mannich bases against *K. pneumoniae* is found as below:

$$\begin{aligned} &\text{Antibacterial activity against } K. pneumoniae = \\ &-14.3219 - 0.8171 (\pm 0.4751) \text{ ZM1} + 0.3740 (\pm 0.3233) \text{ ZM2} + 0.0286 (\pm 0.0074) \text{ SMT1} \\ &+ 0.0016 (\pm 0.0005) \text{ SP1} - 0.1308 (\pm 0.0351) \text{ W} - 1.3528 (\pm 0.4552) \text{ Har} + 7.8314 \\ &(\pm 1.9883) {}^0\chi + 0.5311 (\pm 0.2782) {}^2\chi + 0.5446 (\pm 0.4049) {}^3\chi + 0.2120 (\pm 0.1344) {}^4\chi \\ &N=40, SE=0.0794, R^2 = 0.4238, R^2A= 0.2180, F= 2.059. \end{aligned}$$

This model appears to be most appropriate for the reason that here the coefficients of all the correlating parameters are considerably larger than their corresponding standard deviations. The involvement of  ${}^0\chi$ ,  ${}^2\chi$ ,  ${}^3\chi$  and  ${}^4\chi$  as having positive coefficients indicates that the antibacterial activity of the Mannich bases against *K. pneumoniae* is fraction of number of atoms and higher order of branching.

(vi) 10-parameter model for *P. aeruginosa*

Compared to the earlier models discussed above the model representing antibacterial activity of the Mannich bases against *P. aeruginosa* is of a lower quality. This is due to the fact that in the model the correlating parameters SMT1 and 2X have coefficients smaller than their respective standard deviation. The model is found as below:

$$\begin{aligned} &\text{Antibacterial activity against } P. aeruginosa = \\ &1.4288 + 0.3094 (\pm 0.2300) \text{ ZM2} + 0.9352 (\pm 0.4643) \text{ Pol} + 0.0032 (\pm 0.0066) \text{ SMT1} - 0.0132 \\ &(\pm 0.0296) \text{ W} - 0.28802 (\pm 1.7137) \text{ Har} + 0.5469 (\pm 1.8838) {}^0\chi + 4.8707 (\pm 4.1418) {}^1\chi \\ &+ 0.2629 (\pm 0.3907) {}^2\chi - 1.1125 (\pm 0.6138) {}^3\chi - 0.1395 (\pm 0.2350) {}^4\chi \\ &N=40, R^2 = 0.3906, R^2A= 0.1729, F= 1.794. \end{aligned}$$

The above model indicating the involvement of  ${}^0\chi$ ,  ${}^2\chi$ ,  ${}^3\chi$  and  ${}^4\chi$  as correlating parameters is favoured by the numbers of atoms and branching occurring in the Mannich bases. However, the coefficients of  ${}^3\chi$  and  ${}^4\chi$  both are negative. This indicates that decrease in higher order branching favours the exhibition of antibacterial activity of the Mannich bases against *P. aeruginosa*. The correlation of the observed against calculated antibacterial activity of the Mannich bases in all the 6 bacteria discussed (Figs 1–6) is in favour of models discussed above.

In order to confirm our findings we have calculated the antibacterial activity of the Mannich bases against all the 6 bacteria used and after correlation we observed antibacterial activity. The results obtained are demonstrated through regression equations. There equations are in support of our findings as discussed above.

## CONCLUSIONS

The newly synthesised Mannich bases appeared to be very potent and outstanding antibacterial agents with promising activity and are found safer. This shows that the newly prepared and novel Mannich bases could be used as useful drug. The results discussed herein will prove helpful to those who are engrossed in the synthesis of potential Mannich bases as drugs with minimum side effects and also having comparatively low cost. Thus our results are valuable in constructing pharmacologically imperative heterocyclic as a new exotic drug. Efforts are continuing to synthesise new amino methyl derivatives of various active hydrogen compounds, such that the derived compounds may have enhanced pharmacological activity.

## ACKNOWLEDGEMENTS

The authors are thankful to Director, CDRI, Lucknow, for recording elemental analysis.

## REFERENCES

1. M. TRAMONTINY, L. ANGIOLINI: Mannich Bases: Chemistry and Uses. CRC Press, Boca Raton, 1994.
2. K. SUGAWARA, Y. NISHIYAMA, S. TODA, N. KOMIYAMA, M. HATORI, T. MONYAMA, Y. SAWADA, H. KAMEI, M. KONISHI, T. OKI: Verucopeptin, a New Antitumor Antibiotic Active against B16. *J Antibiot*, **45**, 1433 (1992).
3. T. SONODA, H. OSADA, J. UZAWA, K. ISONO: Actiketol, a New Member of the Glutarimide. *J Antibiot*, **44**, 160 (1991).
4. T. SONODA, K. KOBAYASHI, M. UBUKATA, H. OSADA, K. ISONO: Absolute Configuration of Epiderstatin, a New Glutarimide Antibiotic Produced by *Streptomyces pulveraceus*. *J Antibiot*, **45**, 1963 (1992).
5. S. R. BURZYNSKI, T. T. HAI: Synthesis of Antineoplaston. *Drugs Fut*, **10**, 103 (1985).
6. S. R. BURZYNSKI: Toxicology Studies on Antineoplaston AS2-5 Injections in Cancer. *Adv Exp Chemother*, **6**, 45 (1988).
7. D. C. BIENKO, D. MICHALSKA, S. ROSZAK, W. WOJCIECHOWSKI : Infrared Matrix Isolation and Theoretical Studies on Glutarimide. *Phys Chem A*, **101**, 7834 (1997).
8. W. B. TAYLOR: Incomplete Block Designs with Row Balance and Recovery of Interblock Information. *Biometrics*, **13**, 1 (1957) .
9. N. SIDDIQUI, S. N. PANDEYA, S. A. KHAN, J. STABLE, A. RAN, M. ALAM, M. D. ARSHAD, M. A. BHAT: Synthesis and Anticonvulsant Activity of Sulfonamide Derivatives Hydrophobic Domain. *Bioorg Med Chem Lett*, **17**, 255 (2007).
10. S. JOSHI, N. KHOSLA, P. TIWARI: Synthesis and *in vitro* Study of Novel Mannich Bases as Antibacterial Agents. *Bioorg Med Chem*, **12**, 571 (2002).
11. A. D. MANIKPURI: Synthesis and Studies on Some Therapeutically Significant Mannich Bases. Ph.D. Thesis, D. A. University, Indore, 2009.
12. M. V. DIUDEA, M. S. FLORESCU, P. V. KHADIKAR: Molecular Topology and Its Applications. EFICON, Bucharest, 412 (2006).
13. ACD-Lab Software for Calculating the Referred Physicochemical Parameters; Chem Sketch 3.0, www.acdlabs.com.

14. The DRAGON Plus v 55 Program Is Available from Todeschini, R Taletè srl, via Pisani, 13-20124 Milano, Italy.
15. S. CHATERJEE, A. S. HADI, B. PRICE: Regression Analysis by Examples. 3rd Ed. Wiley, New York, 2000.
16. P. V. KHADIKAR, S. SINGH, M. JAISWAL, D. MANDOLI: Topological Estimation of Electronic Absorption Bands of Arene Absorption Spectra as a Tool for Modeling Their Toxicity and Environmental Pollution. *Bioorg Med Chem Lett*, **14**, 4795 (2004).
17. M. JAISWAL, P. V. KHADIKAR: Use of Distance-based Topological Indices for the Estimation of <sup>13</sup>C NMR Shifts: A Case of Benzene Derivatives. *J Indian Chem Soc*, **82**, 247 (2005).
18. J. DEVILLERS, A. T. BALABAN (Eds): Topological Indices and Related Descriptors in QSAR and QSPR. Gordon & Breach Science Pub., Amsterdam (The Netherlands), 1999.
19. M. S. TUTE: History and Objectives of Quantitative Drug Design in Advances in Drug Research (Eds N. J. Harter, A. B. Simmord). Academic Press, London, Vol. **6** 1971, p. 1.

*Received 3 March 2009*

*Revised 16 April 2009*

**QUANTITATIVE STRUCTURE–ACTIVITY RELATIONSHIP  
ANALYSIS OF SERIES OF SUBSTITUTED PIPERIDIN-2-ONE  
BIPHENYL TETRAZOLES ANALOGUES AS NOVEL  
ANGIOTENSIN II RECEPTOR ANTAGONISTS**

M. C. SHARMA\*, D. V. KOHLI

*Department of Pharmaceutical Sciences, Dr. Hari Singh Gaur University,  
470 003 Sagar (M.P.), India  
E-mail: mukeshcsharma@yahoo.com*

**ABSTRACT**

Predictive quantitative structure–activity relationship (QSAR) analysis was developed for a diverse series of substituted piperidin-2-one biphenyl tetrazoles with angiotensin II receptor antagonists in this study. Our attempt in correlating the derived physicochemical properties with the angiotensin II receptor activity resulted in some statistically significant QSAR models with good predictive ability. Multiple regression analysis coupled with stepwise variable selection method was applied to derive QSAR models which were further validated for statistical significance and predictive ability by internal and external validation. The best QSAR model was selected, having 0.8526 as the coefficient of determination ( $r^2$ ) was considered using the same molecules in the test and training sets. The model can explain 85.26% of the variance in the observed activity values. The model shows an internal predictive power ( $q^2=0.7784$ ) of 77% and predictivity for the external test set ( $\text{pred}_r^2 = 0.8101$ ) of about 81%. The  $F$ -test value of 54.3229 shows the overall statistical significance level for 99.99% of the model. These results should serve as a guideline in designing more potent and selective angiotensin II receptor antagonists.

*Keywords:* QSAR, angiotensin II, multiple regression analysis (MLR), piperidin-2-one antihypertensive activity.

**AIMS AND BACKGROUND**

The renin–angiotensin system (RAS) plays a key role in regulating cardiovascular homeostasis and electrolyte/ fluid balance in normotensive and hypertensive subjects<sup>1</sup>. Activation of the renin–angiotensin cascade begins with renin secretion from

---

\* For correspondence.



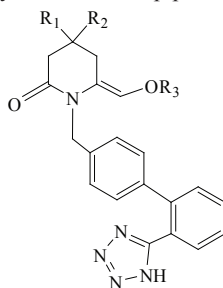
the juxtaglomerular apparatus of the kidney and culminates in the formation of the octapeptide angiotensin II (Ang II), which then interacts with specific receptors present in different tissues<sup>2</sup>. This directed many researchers towards the designing of drugs to block the effect of Ang II either by inhibiting the angiotensin-converting enzyme (ACE) or renin or by blocking the Ang II receptor<sup>3,4</sup>. Substantial effort has been made to find renin inhibitors, although orally active agents have only recently been reported<sup>5</sup>. Computational chemistry has developed as an important contributor to rational drug design. Quantitative structure–activity relationship (QSAR) modelling results in a quantitative correlation between chemical structure and biological activity. Rapid development of combinatorial chemistry and high throughput screening methods in recent years has significantly increased a bulk of experimental structure–activity relationship (SAR) datasets. QSAR has been traditionally perceived as a means of establishing correlations between trends in chemical structure modifications and respective changes of biological activity<sup>6</sup>. QSAR methodologies save resources and expedite the process of the development of new molecules and drugs<sup>7–10</sup>. The author of the article and his research team have developed a few QSAR models to predict biological activity of different group of compounds<sup>11–62</sup>.

To gain insight the structural and molecular requirement influencing the Ang II antagonistic activities, we herein describe the QSAR analysis of substituted piperidin-2-on biphenyl tetrazoles and a QSAR model has been obtained for Ang II AT<sub>1</sub> antagonistic activity. The relevance of the model for the design of novel derivatives should be assessed not only in terms of predictivity, but also in terms of their ability to provide a chemical and structural explanation of their binding interaction.

## EXPERIMENTAL

### DATA SET FOR ANALYSIS

The QSAR study was performed on a series of compounds substituted piperidin-2-one biphenyl tetrazoles, reported by Murray et al.<sup>63</sup> The series consists of well-defined biological activity values ( $IC_{50}$ ) for 16 compounds, ranging over a wide range with variation in substituent. The biological activity values [ $IC_{50}$  (nM)] reported in nanomolar units were converted to their molar units and then further to negative logarithmic scale ( $-\lg IC_{50}$ ) and subsequently used as the dependent variable for the QSAR analysis in Table 1.

**Table 1.** Structure and biological activity of substituted piperidin-2-one biphenyl tetrazoles

Compd.	R <sub>1</sub>	R <sub>2</sub>	R <sub>3</sub>	IC <sub>50</sub> (nM)	pIC <sub>50</sub>
<b>1</b>	Me	Me	OEt	5800	3.763
<b>2*</b>	Me	Et	OEt	250	2.397
<b>3</b>	Et	Et	OEt	20	1.301
<b>4</b>	Me	H	OEt	200	2.301
<b>5</b>	Me	<i>n</i> -butyl	OEt	470	2.672
<b>6*</b>	Et	<i>n</i> -butyl	OEt	180	2.255
<b>7</b>	<i>n</i> -propyl	<i>n</i> -propyl	OEt	330	2.518
<b>8</b>	Me	<i>n</i> -propyl	OEt	120	2.079
<b>9*</b>	Me	<i>i</i> -propyl	OEt	120	2.079
<b>10</b>	Et	<i>n</i> -propyl	OEt	90	1.954
<b>11</b>	Me	<i>n</i> -pentyl	OEt	680	2.832
<b>12*</b>	-cyclopentyl	H	OEt	540	2.732
<b>13</b>	-cyclohexyl	H	OEt	40	1.602
<b>14</b>	Et	Et	Me	3100	3.491
<b>15*</b>	Me	Et	OMe	320	2.505
<b>16</b>	Et	Et	OMe	210	2.322

\* Test compound.

## TWO-DIMENSIONAL MOLECULAR MODELLING

All the computational studies were performed on Compaq (Pentium-D) computer using the software VLife MDS (Ref. 64). Molecules were sketched using the same. Optimisations of the sketched compounds were done by batch minimisation process using force field computations of the VLife MDS. The molecular structures of all the 16 molecules were sketched using VLife MDS 3.5 software in the 2D builder module and then the structures were converted to 3D space for further analysis. All the compounds were batch-optimised for the minimisation of energies and geometry optimisation using Merck molecular force field (MMFF) followed by considering distance-dependent dielectric constant of 1.0, convergence criterion or root mean square (RMS) gradient at 0.01 kcal/mol Å and the iteration limit to 10 000 (Ref. 65). The energy-minimised geometry was used for the calculation of the various 2D descriptors (Individual, Chi, ChiV, Path count, ChiChain, ChiVChain, Chain path

count, Cluster, Path cluster, Kapa, Element Count, Estate number, Estate contribution, Semi-empirical, Hydrophilic-hydrophobic, Polar surface area and Alignment independent) and was considered as independent variables in the present study (Table 2). Alignment independent descriptors (AI) were calculated as discussed in the Baumann paper<sup>66</sup>. For calculation of AI descriptors every atom in the molecule was assigned at least one and at most three attributes. The first attribute is 'T-attribute' to thoroughly characterise the topology of the molecule. The second attribute is the atom type. The atom symbol is used here. The third attribute is assigned to atoms taking part in a double or triple bond. After all atoms have been assigned, their respective attributes, selective distance count statistics for all combinations of different attributes were computed. In this study to calculate AI descriptors, we have used the following attributes, 2 (double-bonded atom), 3 (triple-bonded atom), C, N, O, S, H, F, Cl, Br and I, and the distance range of 0–7. Dataset of 12 molecules (Table 1) was divided into training (9) and test (3) set compounds. Selection of the training set and the test set molecules was done manually by considering the fact that test set molecules represented a range of biological activity similar to that of the training set. Thus, the test set was a true representative of the training set. This was achieved by arbitrarily setting aside 4 compounds as a test set with a regularly distributed biological data. Sphere exclusion method was adopted for division of training and test set and creation of training and test set from the data. This is a rational selection method which takes into consideration both biological and chemical space for division of dataset. Dissimilarity value provides handle to vary train/test set size. It needs to be adjusted by trial and error until a desired division of train and test set is achieved. As a rule, increase in dissimilarity value will lead to increase in number of molecules in the test set<sup>67</sup>. The pre-processing of the independent variables (i.e. descriptors) was done by removing invariable (constant column), which resulted in total 241 descriptors to be used for QSAR analysis. A relationship between the independent and the dependent variables (physicochemical descriptors and biological activities, respectively) were determined using regression analysis. Linear regression was achieved by fitting a best-fit straight line to the data using the least square method. Descriptors included in a reasonable QSAR equation should exhibit low inter-correlation and thus behave as independent variables. Inter-correlation between the descriptors was used to select descriptors for the equation, and the quality of fit for a regression equation was assessed as relative to its correlation coefficient and standard deviation. The *F*-value represents the level of statistical significance of the regression. Quality of the selected models was further ascertained from cross-validated squared correlation coefficient ( $q^2$ ).

**Table 2.** Selected 2D descriptors used in best QSAR models for piperidin-2-one derivatives

T_C_O_3	T_2_Cl_2	T_2_C_3	Mom InertiaZ	T_T_O_1
4	5	9	6.7917	7
4	7	9	6.8220	8
4	8	9	6.8524	9
4	9	8	6.2488	7
4	2	9	7.3524	9
4	3	9	7.1327	10
4	4	9	7.4130	11
4	3	8	6.5292	9
4	6	8	6.2157	9
4	3	9	7.1327	10
4	9	8	6.8431	9
4	2	9	5.3216	10
4	6	9	8.3214	10
2	8	8	6.6778	5
2	9	9	6.6874	8
2	9	9	6.7178	9

#### MODEL QUALITY AND VALIDATION

The developed QSAR models are evaluated using the following statistical measures:  $n$  (the number of compounds in regression);  $k$  (number of variables); DF (degree of freedom); optimum component (number of optimum PLS components in the model);  $r^2$  (the squared correlation coefficient),  $F$ -test (the Fischer value) for statistical significance,  $q^2$  (cross-validated correlation coefficient);  $\text{pred}_r^2$  ( $r^2$  for external test set);  $Z_{\text{score}}$  ( $Z_{\text{score}}$  calculated by the randomisation test);  $\text{best\_ran\_}q^2$  (highest  $q^2$  value in the randomisation test);  $\text{best\_ran\_}r^2$  (highest  $r^2$  value in the randomisation test). The regression coefficient  $r^2$  is a relative measure of fit by the regression equation. It represents the part of the variation in the observed data that is explained by the regression. However, a QSAR model is considered to be predictive, if the following conditions are satisfied:  $r^2 > 0.6$ ,  $q^2 > 0.6$  and  $\text{pred}_r^2 > 0.5$ . The  $F$ -test reflects the ratio of the variance explained by the model and the variance due to the error in the regression. High values of the  $F$ -test indicate that the model is statistically significant. The low standard error of  $\text{pred}_r^2\text{se}$ ,  $q^2\text{se}$  and  $r^2\text{se}$  shows absolute quality of fitness of the model.

*Internal and external validation.* Internal validation is carried out using ‘leave-one-out’ (LOO) method<sup>68</sup>. The cross-validated coefficient,  $q^2$ , is calculated using the following equation:

$$q^2 = 1 - \frac{\sum(y_i - \hat{y}_i)^2}{\sum(y_i - y_{\text{mean}})^2},$$

where  $y_i$  and  $\hat{y}_i$  are the observed and predicted activity of the  $i$ -th molecule in the training set, respectively, and  $y_{\text{mean}}$  – the average activity of all molecules in the training set.

However, a high  $q^2$  value does not necessarily give a suitable representation of the real predictive power of the model for antihypertensive ligands. So, an external validation is also carried out in the present study. The external predictive power of the model is assessed by predicting  $\text{pIC}_{50}$  value of the 4 test set molecules, which are not included in the QSAR model development. The predictive ability of the selected model is also confirmed by  $\text{pred}_r^2$  or  $\text{rCVext}^2$ .

$$\text{pred}_r^2 = 1 - \frac{\sum(y_i - \hat{y}_i)^2}{\sum(y_i - y_{\text{mean}})^2},$$

where  $y_i$  and  $\hat{y}_i$  are the observed and predicted activity of the  $i$ -th molecule in the test set, respectively, and  $y_{\text{mean}}$  – the average activity of all molecules in the training set. The robustness of the selected model is checked by  $Y$ -randomisation test. The robustness of the models for training sets is examined by comparing these models to those derived for random datasets. Random sets are generated by rearranging the activities of the molecules in the training set. The significance of the models obtained is derived based on a calculated  $Z_{\text{score}}$ . The  $Z_{\text{score}}$  value is calculated by the following formula<sup>69</sup>:

$$Z_{\text{score}} = \frac{h - \mu}{\sigma},$$

where  $h$  is the  $q^2$  value calculated for the observed dataset;  $\mu$  – the average  $q^2$ , and  $\sigma$  – its standard deviation calculated for various iterations using models build by different random datasets. For example, a  $Z_{\text{score}}$  value greater than 3.10 indicates that there is a probability ( $\alpha$ ) of less than 0.001 that the QSAR model constructed for the real dataset is random. The randomisation test suggests that all the developed models have a probability of less than 1% that the model is generated by chance.

## RESULTS AND DISCUSSION

A QSAR analysis has been performed to study the quantitative effects of the molecular structure of the substituted piperidin-2-one biphenyl tetrazoles on their angiotensin II receptor antagonists. Although, generation of QSAR models with good statistical significance is of paramount importance, the models should also exhibit good predictive ability. The predictive ability of the models was gauged by a cross-validation procedure following a leave-one-out scheme. All the models exhibit high  $q^2$  and low  $r^2_{\text{se}}$  and  $q^2_{\text{se}}$  values confirm their excellent predictive potential. Furthermore, a comparison was made between the experimental activity values and predicted activity values calculated by using the obtained models in Table 3. Accurate mathematical models were developed for predicting the angiotensin II receptor activity. By taking all the calculated parameters and biological activity of compounds from the series

and subjected to stepwise and sequential multiple regression analysis the following models were generated.

**Table 3.** Comparison between observed and predicted activities (LOO) of substituted piperidin-2-one biphenyl tetrazoles

pIC <sub>50</sub>	Predicted activity			
	Model 1	Model 2	Model 3	Model 4
3.763	3.912	3.949	3.087	3.001
2.397	2.578	2.648	2.827	2.526
1.301	1.604	1.797	1.567	1.050
2.301	2.912	2.899	3.087	3.001
2.672	2.308	2.397	2.567	2.520
2.255	2.104	2.614	2.430	2.050
2.518	2.143	1.896	2.046	1.956
2.079	1.708	2.397	2.567	2.526
2.079	2.330	2.687	2.431	2.587
1.954	2.194	2.147	2.302	1.450
2.832	2.508	2.397	2.387	2.658
2.732	2.104	2.147	2.310	2.154
1.602	1.436	1.324	1.896	1.215
3.491	3.098	3.464	3.607	3.952
2.505	2.912	2.648	2.392	3.022
2.322	2.766	2.397	2.046	2.176

### Model 1

$$\lg(\text{IC}_{50}) = +0.3963 (\pm 0.0188) \text{T\_C\_O\_3} + 0.8543 (\pm 0.0165) \text{SssOE-index} \\ - 0.2669 (\pm 0.0215) \text{SssCH}_2\text{count} + 0.3297 (\pm 0.0510) \text{T\_C\_O\_7} + 0.1986$$

$n = 16$ , degree of freedom = 15,  $r^2 = 0.8526$ ,  $q^2 = 0.7784$ ,  $F\text{-test} = 54.3229$ ,  $r^2_{\text{se}} = 0.0851$ ,  $q^2_{\text{se}} = 0.1317$ ,  $\text{pred}_r^2 = 0.8101$ ,  $\text{pred}_r^2\text{se} = 0.4787$ .

The developed Model 1 has a correlation coefficient ( $r^2$ ) of 0.8526, significant cross-validated correlation coefficient ( $q^2$ ) of 0.7784,  $F$ -test of 54.3229,  $r^2$  for external test set ( $\text{pred}_r^2$ ) 0.8101, coefficient of correlation of predicted data set ( $\text{pred}_r^2\text{se}$ ) 0.4787 and degree of freedom 15. The developed model is validated by an external set of compounds with a predictive correlation of coefficient of 0.353. The model is validated by  $\alpha_{\text{ran}} r^2 = 0.00165$ ,  $\alpha_{\text{ran}} q^2 = 0.001$ ,  $\alpha_{\text{ran}} \text{pred}_r^2 = 0.0001$ ,  $\text{best}_{\text{ran}} r^2 = 0.215$ ,  $\text{best}_{\text{ran}} q^2 = 0.4322$ ,  $Z_{\text{score\_ran}} r^2 = 0.754$  and  $Z_{\text{score\_ran}} q^2 = 1.243$ . The randomisation test suggests that the developed model has a probability of less than 1% that the model is generated by chance. The major group of descriptors involved sub-groups like SssCH<sub>2</sub>count, T\_C\_O\_7, T\_C\_O\_3 alignment independent descriptors, and help in understanding the effect of substituent at different position of substituted piperidin-2-one biphenyl tetrazoles derivatives. The descriptor SssOE-index, which is an electrotopological state index for the number of oxygen atoms connected with two

single bonds, showed positive contribution of ~25%. Such a positive effect indicated that the antibacterial activity was increased with the presence of methoxy groups such as compounds **15** and **16**. The other descriptor SssCH<sub>2</sub>E-index, which signifies estate contributions defining electrotopologic state indices for the number of CH<sub>2</sub>-groups attached to two single bonds, also showed a negative contribution. The above study leads to the development of statistically significant QSAR model, which allows understanding of the molecular properties features that play an important role in governing the variation in the activities. In addition, this QSAR study allowed investigating influence of very simple and easy-to-compute descriptors in determining biological activities, which could shed light on the key factors that may aid in design of novel potent molecules. The observed versus predicted activity of both test set and training set are portrayed in Table 3. Graphical plot between observed and predicted activity values of training and test set compounds in QSAR model 1 is shown in Fig. 1.

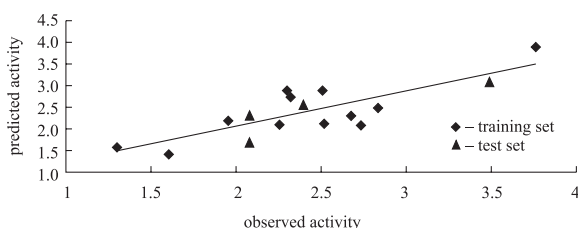


Fig. 1. Graph of observed versus predicted activities of the training and test set QSAR model 1

## Model 2

$$\lg(\text{IC}_{50}) = +0.5711(\pm 0.0836) \text{ T\_2\_Cl\_2} - 0.2548(\pm 0.0696) \text{ chiV3Cluster} + 0.3968(\pm 0.1544) \text{ polar surface area including P and S} + 0.0142$$

$n = 16$ , degree of freedom = 15,  $r^2 = 0.8225$ ,  $q^2 = 0.6777$ ,  $F\text{-test} = 37.7204$ ,  $r^2 \text{ se} = 0.2873$ ,  $q^2 \text{ s} = 0.3870$ ,  $\text{pred\_}r^2 = 0.6950$ ,  $\text{pred\_}r^2 \text{ se} = 0.3447$ .

Model 2 has correlation coefficient ( $r^2$ ) of 0.8225,  $F$ -test of 37.7204,  $r^2$  for external test set ( $\text{pred\_}r^2$ ) 0.6950, coefficient of correlation of predicted data set ( $\text{pred\_}r^2 \text{ se}$ ) 0.3447 and degree of freedom 15. The model is validated by  $\alpha_{\text{ran}} r^2 = 0.0001$ ,  $\alpha_{\text{ran}} q^2 = 0.00002$ ,  $\alpha_{\text{ran}} \text{pred\_}r^2 = 0.0016$ ,  $\text{best\_ran\_}r^2 = 0.3287$ ,  $\text{best\_ran\_}q^2 = 0.1543$ ,  $Z_{\text{score\_ran}} r^2 = 2.476$  and  $Z_{\text{score\_ran}} q^2 = 6.875$ . The randomisation test suggests that the developed model have a probability of less than 1% that the model is generated by chance. The major group of descriptors involved sub-groups like T\_2\_Cl\_2, chiV3Cluster, polar surface area including P and S. The descriptor polar surface area including P and S and the descriptor polar surface area excluding P and S (i.e. phosphorus and sulphur) play a most important role in determining activity in model. This descriptor signifies the total polar surface area excluding phosphorus and sulphur. This suggests that substituents such as -OH and -COOH, etc. would increase the activity. The influential descriptor chiV3Cluster signifies valence mo-

lecular connectivity index of 3rd order cluster. The descriptor T\_2\_Cl\_2 is positively contributed with activity (11%) which revealed the increased activity with the presence of chlorine atoms on piperidin-2-one moiety. Graphical plot between observed and predicted activity values of training and test set compounds in QSAR model 2 is shown in Fig. 2. The observed versus predicted activity of both test set and training set are portrayed in Table 3.

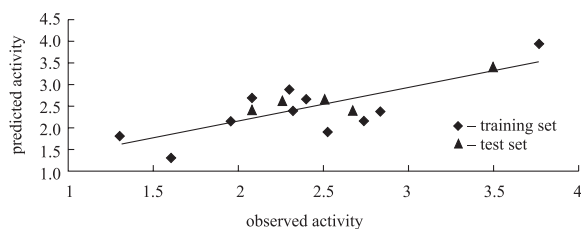


**Fig. 2.** Graph of observed and predicted activities of the training and test set QSAR model 2

### Model 3

$$\lg(\text{IC}_{50}) = +0.4621(\pm 0.1056) \text{ SaasCE-index} - 0.3383(\pm 0.0716) \text{ SdssCE-index} + 0.0720(\pm 0.0278) \text{ T\_2\_C\_3} - 0.6483(\pm 0.3177) \text{ SsssCHE-index} + 0.0008$$

$n = 16$ , degree of freedom = 14,  $r^2 = 0.7833$ ,  $q^2 = 0.6236$ ,  $F\text{-test} = 46.6404$ ,  $r^2 \text{ se} = 0.1840$ ,  $q^2 \text{ se} = 0.4311$ ,  $\text{pred}_r^2 = 0.6428$ ,  $\text{pred}_r^2 \text{ se} = 0.2873$ .

The developed model 3 developed has a correlation coefficient ( $r^2$ ) of 0.7833, significant cross-validated correlation coefficient ( $q^2$ ) of 0.6236,  $F$ -test of 46.6404,  $r^2$  for external test set ( $\text{pred}_r^2$ ) 0.6428, coefficient of correlation of predicted data set ( $\text{pred}_r^2 \text{ se}$ ) 0.4787 and degree of freedom 14. The model is validated by  $\alpha_{\text{ran}} r^2 = 0.00165$ ,  $\alpha_{\text{ran}} q^2 = 0.001$ ,  $\alpha_{\text{ran}} \text{pred}_r^2 = 0.0001$ ,  $\text{best}_{\text{ran}} r^2 = 0.215$ ,  $\text{best}_{\text{ran}} q^2 = 0.4322$ ,  $Z_{\text{score}_{\text{ran}} r^2} = 0.754$  and  $Z_{\text{score}_{\text{ran}} q^2} = 1.243$ . From the plot it can be seen that MLR model is able to predict the activity of training set quite well (all points are close to regression line) as well as external. Out of 4 descriptors selected in the above-mentioned model, 3 descriptors viz. SaasCE-index, SdssCE-index and SsssCHE-index are topological descriptors. These descriptors describe the overall topology of the molecules. The SaasCE-index is an electrotopological state index for the number of carbon atoms connected with 1 single bond along 2 aromatic bonds. The positive correlation of the descriptor in the model indicates that the electrotopological properties of the carbon atoms connected with aromatic rings and single bonds positively influence Ang II activity of the substituted piperidin-2-one biphenyl tetrazoles derivatives. The next SdssCE-index is an electrotopological parameter which can define the total number of carbon atoms connected with one double and two single bonds. The descriptor shows highest negative correlation among the parameters selected for the derived QSAR model. The negative coefficient suggests that inclusion of such carbon atoms in the molecules lead to decreased antihypertensive activity shown by



substituted piperidin-2-one derivatives. Lastly descriptor T\_2\_C\_3 is the count of number of double bounded atoms (i.e. any double bonded atom, T\_2) separated from any other double bonded atom by 3 bonds in a molecule. Graphical plot between observed and predicted activity values of training and test set compounds in QSAR model 3 is shown in Fig. 3. The observed versus predicted activity both of test set and training set are portrayed in Table 3.

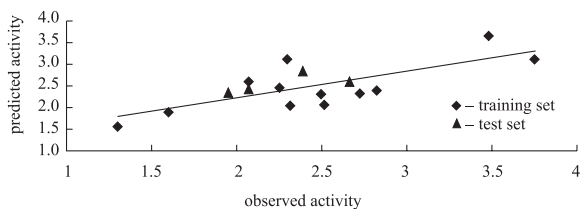


Fig. 3. Graph of observed and predicted activities of the training and test set QSAR model 3

#### Model 4

$$\lg(\text{IC}_{50}) = +0.4539(\pm 0.0664) \text{ T\_T\_O\_1} + 0.3323(\pm 0.0431) \text{ SssCH}_2\text{count} - 0.0001(\pm 0.0000) \text{ MomInertiaZ} - 2.6849(\pm 1.5266) \text{ XA MostHydrophobic} - 0.0004$$

$n = 12$ , degree of freedom = 4,  $r^2 = 0.7852$ ,  $q^2 = 0.7030$ ,  $F\text{-test} = 38.2280$ ,  $r^2 \text{ se} = 0.1435$ ,  $q^2 \text{ se} = 0.2311$ ,  $\text{pred}_r^2 = 0.6605$ ,  $\text{pred}_r^2 \text{ se} = 0.4133$ .

Model 4 generated using the multiple regression analysis method with 0.8852 as the coefficient of determination ( $r^2$ ) was considered using the same molecules in the test and training sets. The model can explain 78.52% of the variance in the observed activity values. The model shows an internal predictive power ( $q^2 = 0.7030$ ) of 70% and predictivity for the external test set ( $\text{pred}_r^2 = 0.6605$ ) of about 66%. The  $F$ -test value of 38.2280 shows the overall statistical significance level for 99.99% of the model. Model 4 also shows a positive correlation with T\_T\_O\_1, SssCH<sub>2</sub>count, and a negative correlation with Mom InertiaZ, XA Most Hydrophobic. The observed versus predicted activity of both test set and training set are portrayed in Table 3.

#### CONCLUSIONS

In the present investigation, all proposed QSAR models were statistically significant. However, model 1 could be considered as best one in terms of its excellent internal and external predictive abilities. According to model 1, the angiotensin II activity of substituted piperidin-2-one derivatives was positively contributed by the electrostatic parameters like T\_C\_O\_3, SssOE-index, SssCH<sub>2</sub>count, T\_C\_O\_7 of the molecule. Thus, from the above QSAR investigations it could be concluded that electrostatic and electronic properties of substituted piperidin-2-one derivatives are mainly involved in eliciting angiotensin II receptor activity.

## ACKNOWLEDGEMENT

The author wishes to express gratitude to V-life Science Technologies Pvt. Ltd. for providing the software for the study. Authors like to acknowledge Head, School of Pharmacy, Devi Ahilya Vishwavidyalaya Indore for providing facilities to carry out the study.

## REFERENCES

1. C. M. FERRARIO: The Renin–Angiotensin System: Importance in Physiology and Pathology. *J Cardiovasc Pharm*, **15** (Suppl. 3), 51 (1990).
2. M. B. VALLOTTON: The Renin-Angiotensin System Trends. *Pharmacol Sci*, **8**, 69 (1987).
3. A. BALI, Y. BANSAL, M. SUGUMARAN, J. S. SAGGU, P. BALAKUMAR, G. KAUR, G. BANSAL, A. SHARMA, M. SINGH: Design, Synthesis, and Evaluation of Novelty Substituted Benzimidazole Compounds as Angiotensin II Receptor Antagonists. *Bioorg Med Chem Lett*, **15**, 3962 (2005).
4. J. Y. XU, R. QIAN, Y. H. X. WEI, W. MING, J. W. QIU, Z. JING: Design and Synthesis of 2-alkyl-benzimidazole Derivatives as Novel Non-peptide Angiotensin II AT<sub>1</sub> Receptor Antagonists. *Chin Chem Lett*, **18**, 251 (2007).
5. H. D. KLEINERT: Recent Developments in Renin Inhibitors. *Exp Opin Invest Drugs*, **3**, 1087 (1994).
6. C. HANSCH, A. LEO: Substituent Constants for Correlation Analysis in Chemistry and Biology. Wiley Interscience, New York, 1979.
6. J. SINGH, V. K. DUBEY, V. K. AGARWAL, P. V. KHADIKAR: QSAR Study on Octanol–Water Partitioning: Dominating Role of Equalized Electronegativity. *Oxid Commun*, **31** (1), 27 (2008).
7. J. SINGH, V. K. AGARWAL, S. SINGH, P. V. KHADIKAR: Use of Topological as Well as Quantum Chemical Parameters in Modelling Antimalarial Activity of 2,4-diamino-6-quinazoline Sulphonamides. *Oxid Commun*, **31** (1), 17 (2008).
8. A. K. SRIVASTAVA, ARCHANA, M. JAISWAL: Quantitative Structure–Activity Relationship Studies of p-arylthiocinnamides as Antagonists of Biochemical ICAM-1/LFA-1 Interaction in Relation to Anti-inflammatory Activity. *Oxid Commun*, **31**, 44 (2008).
9. A. K. SRIVASTAVA, M. JAISWAL, ARCHANA, A. SRIVASTAVA: QSAR Modelling of Selective CC Chemokine Receptor 3 (CCR3) Antagonists Using Physicochemical Parameters. *Oxid Commun*, **32**, 55 (2009).
10. S. JOSHI, M. YADAV, L. PARADKAR, N. S. ANURAJ: A QSAR Study on Minimum Inhibitory Concentrations of Some Phenols: Predicting –log MIC Using Topological Indices. *Oxid Commun*, **35** (3), 684 (2012).
11. M. C. SHARMA, N. K. SAHU, D. V. KOHLI, S. C. CHATURVEDI, S. SHARMA: QSAR, Synthesis and Biological Activity Studies of Some Thiazolidinones Derivatives. *Digest J Nanomat Biostruct*, **4** (1), 223 (2009).
12. A. DHAKAD, M. C. SHARMA, S. C. CHATURVEDI, S. SHARMA: 3D-QSAR Studies, Biological Evaluation Studies on Some Substituted 3-chloro-1-[5-(5-chloro-2-phenyl-benzimidazole-1-ylmethyl)-[1,3,4] thiadiazole-2-yl]-azetid-2-one as Potential Antimicrobial Activity. *Digest J Nanomat Biostruct*, **4** (2), 275 (2009).
13. M. C. SHARMA, D. V. KOHLI, S. SHARMA, S. C. CHATURVEDI: Two-dimensional Quantitative Structure–Activity Relationships – 2,3-diarylthiophenes as Selective COX-1-2 Inhibitors. *Digest J Nanomat Biostruct*, **4** (3), 459 (2009).
14. M. C. SHARMA, D. V. KOHLI, N. K. SAHU, S. SHARMA, S. C. CHATURVEDI: 2D-QSAR Studies of Some 1, 3,4-thiadiazole-2yl azetid-2-one as Antimicrobial Activity. *Digest J Nanomat Biostruct*, **4** (2), 339 (2009).

15. M. C. SHARMA, S. SHARMA, D. V. KOHLI, S. C. CHATURVEDI: Three Dimensional Quantitative Structural–Activity Relationship (3D-QSAR) Studies of Some 3-{4-[3-(2-aryl-phenoxy) butoxy]-phenyl} Propionic Acids as Novel PPAR  $\gamma/\delta$  Agonists. *Der Pharma Chemica*, **2** (1), 82 (2010).
16. M. C. SHARMA, S. SHARMA, D. V. KOHLI, S. C. CHATURVEDI: Molecular Modelling Studies Atom Based of 3-bromo-4-(1-H-3-indolyl)-2, 5-dihydro-1H-2, 5-pyrroledione Derivatives Antibacterial Activity against *Staphylococcus aureus*. *Der Pharmacia Lettre*, **2** (1), 1 (2010).
17. M. C. SHARMA, S. SHARMA: Quantitative Structural–Activity Relationship (QSAR) Study for Antimycobacterial Activities of Pyrazine Containing Thiazoline and Thiazolidinone Derivatives. *Optoelect Advan Mater – Rapid Commun*, **4** (3), 415 (2010).
18. M. C. SHARMA, S. SHARMA: Quantitative Structure Activity Relationship Studies of a Novel Class of Dual PPAR  $\gamma/\delta$  Agonists. *Int J Pharm Tech Res*, **2** (2), 1376 (2010).
19. S. SHARMA, M. C. SHARMA, A. D. SHARMA: Quantitative Structure–Activity Relationship Analysis of a Series of Antibacterial 3-bromo-4-(1-H-3-indolyl)-2, 5-dihydro-1H-2,5-pyrroledione Derivatives. *J Chem Pharma Res*, **2** (2), 421 (2010).
20. N. K. SAHU, M. C. SHARMA, V. K. MOURYA, D. V. KOHLI: QSAR Studies of Some Side Chain Modified 7-chloro-4-aminoquinolines as Antimalarial Agents. *Arab J Chem*, 2011 (in press).
21. M. C. SHARMA, D. V. KOHLI, S. C. CHATURVEDI, S. SHARMA: Molecular Modeling Studies of Some Substituted 2-butylbenzimidazoles Angiotensin II Receptor Antagonists as Antihypertensive Agents. *Digest J Nanomat Biestruct*, **4** (4), 843 (2009).
22. M. C. SHARMA, D. V. KOHLI: 3D QSAR Studies on Series of 2, 3-dihydro-4(1H)-quinazolinone Derivatives Angiotensin II Receptor Antagonists: *k*NNMFA Approach. *Am-Euras J Sci Res*, **6** (2), 85 (2011).
23. M. C. SHARMA, D. V. KOHLI: 3D QSAR *k*NNMFA Approach Studies on Series of Substituted Piperidin-2-one Biphenyl Tetrazoles as Angiotensin II Receptor Antagonists. *Am-Euras Toxicol Sci*, **3** (2), 75(2011).
24. M. C. SHARMA, D. V. KOHLI: QSAR Study on Sulfonylcarbamate Derivatives: An Insight into the Structural Requirement for the Angiotensin II Receptor Antagonist. *Eur J Appl Sci*, **3** (1), 9 (2011).
25. M. C. SHARMA, D. V. KOHLI: 3D-QSAR Studies of Some Substituted Imidazolinones Angiotensin II Receptor Antagonists. *World Appl Sci J*, **12** (11), 2129 (2011).
26. M. C. SHARMA, D. V. KOHLI: (2011e) 3D QSAR Studies on a Series of-[(1- benzyl-1H-imidazol-5-yl)-alkyl]-amino Derivatives as Angiotensin II AT<sub>1</sub> Antagonists. *Am-Euras J Sci Res*, **6** (2), 79 (2011).
27. M. C. SHARMA, D. V. KOHLI: 3D QSAR Approach on Substituted Isoxazolidines Derivatives as Angiotensin II Receptor Antagonist. *Am-Euras Toxicol Sci*, **3** (2), 85 (2011).
28. M. C. SHARMA, D. V. KOHLI: 3D QSAR Studies of Substituted- 4(3H) Quinazolinones Derivatives as Angiotensin II Receptor Antagonists. *Eur J Appl Sci*, **3** (1), 15 (2011).
29. M. C. SHARMA, D. V. KOHLI: Predicting Alkylbenzimidazole Derivatives as Angiotensin II Receptor Antagonists: 3D QSAR by *k*NNMFA Approach. *Adv Biol Res*, **5** (3), 161 (2011).
30. M. C. SHARMA, D. V. KOHLI: 3D QSAR Studies on a Series of Sulfonylcarbamate Isostere Derivatives as Non-peptide Angiotensin II Receptor Antagonists: *k*NNMFA Method. *Am-Euras J Sci Res*, **6** (2), 64 (2011).
31. M. C. SHARMA, D. V. KOHLI: Exploration of Quantitative Structure–Activity Relationship Studies on a Series of Substituted Quinazolinones as Angiotensin II AT<sub>1</sub> Receptor Antagonists. *World Appl Sci J*, **12** (11), 2111 (2011).
32. M. C. SHARMA, D. V. KOHLI : 2D- and 3D-QSAR Studies of Substituted 4H-pyrido [1, 2-a] pyrimidin-4-ones Angiotensin II Receptor Antagonists. *Am-Euras Toxicol Sci*, **3** (2) 92 (2011).
33. M. C. SHARMA, D. V. KOHLI: An Insight into the Structural Requirement QSAR Approach on Substituted Isoxazolidines Derivatives as Angiotensin II Receptor Antagonist. *Am-Euras J Sci Res*, **6** (2), 71 (2011).

34. M. C. SHARMA, D. V. KOHLI: QSAR Studies on Substituted Benzimidazoles as Angiotensin II Receptor Antagonists: *k*NNMFA Approach. Arab J Chem, 2011 (in press).
35. M. C. SHARMA, D. V. KOHLI: An Approach to Design Antihypertensive Agents by 2D QSAR Studies on Series of Substituted Benzimidazoles Derivatives as Angiotensin II Receptor Antagonists. Arab J Chem, 2011 (in press).
36. M. C. SHARMA, D. V. KOHLI: QSAR Analysis and 3D QSAR *k*NNMFA Approach on a Series of Substituted Quinolines Derivatives as Angiotensin II Receptor Antagonists. Arab J Chem, 2011 (in press).
37. M. C. SHARMA, D. V. KOHLI: Quantitative Structure–Activity Analysis Studies on Triazolinone Aryl and Nonaryl Substituents as Angiotensin II Receptor Antagonists. J Saudi Chem Soc, 2011 (in press).
38. M. C. SHARMA, D. V. KOHLI: Two Dimensional and *k*-nearest-neighbor Molecular Field Analysis Approach on Substituted Triazolone Derivatives: An Insight into the Structural Requirement for the Angiotensin II Receptor Antagonist. J Saudi Chem Soc, 2011(in press).
39. M. C. SHARMA, D. V. KOHLI: Insight into the Structural Requirement of Substituted Quinazolinone Biphenyl Acylsulfonamides Derivatives as Angiotensin II Receptor Antagonists: 2D and 3D QSAR Approach. J Saudi Chem Soc, 2011 (in press).
40. M. C. SHARMA, D. V. KOHLI: QSAR Analysis of Imidazo[4,5-*b*]pyridine Substituted  $\alpha$ -phenoxyphenylacetic Acids as Angiotensin II AT<sub>1</sub> Receptor Antagonists. J Saudi Chem Soc, 2011 (in press).
41. M. C. SHARMA, D. V. KOHLI: Predicting Substituted 2-butylbenzimidazoles Derivatives as Angiotensin II Receptor Antagonists: Three-dimensional QSAR and Pharmacophore Mapping. J Saudi Chem Soc, 2011 (in press).
42. M. C. SHARMA, D. V. KOHLI: QSAR Studies of a Series of Angiotensin II Receptor Substituted Benzimidazole Bearing Acidic Heterocycles Derivatives. J Saudi Chem Soc, 2011 (in press).
43. M. C. SHARMA, S. SHARMA, N. K. SAHU, D. V. KOHLI: 3D QSAR *k*NNMFA Studies on 6-substituted Benzimidazoles Derivatives as Nonpeptide Angiotensin II Receptor Antagonists: A Rational Approach to Antihypertensive Agents. J Saudi Chem Soc, 2011 (in press).
44. M. C. SHARMA, S. SHARMA, N. K. SAHU, D. V. KOHLI: QSAR Studies of Some Substituted Imidazolinones Derivatives Angiotensin II Receptor Antagonists Using Partial Least Squares Regression (PLSR) Based Feature Selection. J Saudi Chem Soc, 2011 (in press).
45. M. C. SHARMA, D. V. KOHLI: Insight into the Structural Requirement of Aryltriazaolone Derivatives as Angiotensin II AT<sub>1</sub> Receptor: 2D- and 3D-QSAR *k*-nearest-neighbor Molecular Field Analysis Approach. Med Chem Res, **21**, 2837 (2012).
46. M. C. SHARMA, D. V. KOHLI: A Comprehensive Structure–Activity Analysis of 2, 3,5-trisubstituted 4,5-dihydro-4-oxo-3H-imidazo [4,5-*c*] Pyridine Derivatives as Angiotensin II Receptor Antagonists: Using 2D- and 3D-QSAR Approach. Med Chem Res, 2012 (in press).
47. M. C. SHARMA, D. V. KOHLI: Comprehensive Two- and Three-dimensional QSAR Studies of 3-substituted 6-butyl-1,2-dihydropyridin-2-ones Derivatives as Angiotensin II Receptor Antagonists. Med Chem Res, 2012 (in press).
48. M. C. SHARMA, D. V. KOHLI: Comprehensive Structure–Activity Relationship Analysis of Isoxazolinyl and Isoxazolidinyl Substituted Quinazolinone Derivatives as Angiotensin II Receptor Antagonists. J Saudi Chem Soc, 2012 (in press).
49. M. C. SHARMA, S. SHARMA, D. V. KOHLI: Structural Insights for 5- $\beta$  Ketosulfoxide Imidazolyl Biphenyl Sulfonylureas Derivatives as Angiotensin II AT<sub>1</sub> Receptor Antagonists Using *k*NN-MFA with Genetic Algorithm. J Saudi Chem Soc, 2012 (in press).
50. M. C. SHARMA, D. V. KOHLI: A Comprehensive Structure–Activity Analysis of 5-carboxyl Imidazolyl Biphenyl Sulfonylureas Derivatives Angiotensin AT<sub>1</sub> Receptor Antagonists: 2D- and 3D-QSAR Approach. Arab J Chem, 2012 (in press).

51. M. C. SHARMA: Structural Insight for (6-oxo-3-pyridazinyl)-benzimidazoles Derivatives as Angiotensin II Receptor Antagonists: QSAR, Pharmacophore Identification and *k*NNMFA Approach. *J Saudi Chem Soc*, 2012 (in press).
52. M. C. SHARMA, D. V. KOHLI: Comprehensive Structure–Activity Relationship Analysis of Substituted 5-(biphenyl-4-ylmethyl) Pyrazoles Derivatives as AT<sub>1</sub> Selective Angiotensin II Receptor Antagonists: 2D and *k*NNMFA QSAR Approach. *Med Chem Res*, 2012 (in press).
53. M. C. SHARMA, S. SHARMA, D. V. KOHLI: QSAR Approach Insight the Structural Requirement of Substituted Quinazolinones Derivatives as Angiotensin II Receptor Antagonists. *Oxid Commun*, **35** (3), 694 (2012).
54. M. C. SHARMA, S. SHARMA, D. V. KOHLI: QSAR Studies of 2-alkylbenzimidazole Derivatives as Angiotensin II Receptor Antagonists. *Oxid Commun*, **35** (3), 708 (2012).
55. M. C. SHARMA, D. V. KOHLI: Predicting 2, 3-dihydroquinazolinones Derivatives as Angiotensin II Receptor Antagonists: 2D QSAR Approach. *Oxid Commun*, **35** (3), 721 (2012).
56. K. S. BHADORIYA, M. C. SHARMA, S. V. JAIN, G. S. RAUT, J. R. RANANAWARE: Three-dimensional Quantitative Structure–Activity Relationship (3D-QSAR) Analysis and Molecular Docking-based Combined in Silico Rational Approach to Design Potent and Novel TRPV1 Antagonists. *Med Chem Res*, 2012 (in press).
57. K. S. BHADORIYA, M. C. SHARMA, S. V. JAIN, S. A. KAD, D. RAGHUVANSHI: QSAR Studies of Fused 5,6-bicyclic Heterocycles as  $\gamma$ -secretase Modulators. *J Pharm Res*, **5** (8), 4127 (2012).
58. N. K. SAHU, SADHANA SHAHI, M. C. SHARMA, D. V. KOHLI: QSAR Studies on Imidazopyridazine Derivatives as Pfk7 Inhibitors. *Mol Simul*, **37** (9), 752 (2011).
59. M. C. SHARMA, D. V. KOHLI, S. SHARMA: Synthesis and Biological Activity of Some Antihypertensive Activity: [(2-substituted 5-nitro-benzoimidazol-1-ylmethyl)]-biphenyl-2-carboxylic Acid. *Int J Pure Appl Chem*, **7** (1), 37 (2012).
60. M. C. SHARMA, D. V. KOHLI, S. SHARMA: Insight into the Structural Requirement D and L-N-[(1-benzyl-1H-imidazol-5-yl)-alkyl]-amino Acids as Angiotensin II AT<sub>1</sub> Antagonists: 2D QSAR Approach. *Int J Pure Appl Chem*, **7** (1), 15 (2012).
61. M. C. SHARMA, S. SHARMA: Prediction of Angiotensin II AT<sub>1</sub> Receptor Antagonists Activity of 2-alkylbenzimidazoles Bearing a N-phenyl Pyrrole Moiety as Novel – A *k*NNMFA Approach. *Int J Pure Appl Chem*, **7** (1), 25 (2012).
62. M. C. SHARMA, S. SHARMA, K. S. BHADORIYA: QSAR Analyses and Pharmacophore Studies of Tetrazole and Sulfonamide Analogs of Imidazo[4,5-b]pyridine Using Simulated Annealing Based Feature Selection. *J Saudi Chem Soc*, <http://dx.doi.org/10.1016/j.jscs.2012.10.001>.
63. W. V. MURRAY, P. LALAN, A. GILL, M. F. ADDO, J. M. LEWIS, D. K. H. LEE, R. RAMPULLA, M. P. WACHTER, J. D. HSI, D. C. UNDERWOOD: Substituted Piperidin-2-one Biphenyl Tetrazoles Angiotensin II Antagonists. *Bioorg Med Chem Lett*, **2** (12), 1775 (1992).
64. VLIFE MDS Software Package, Version 3.5, Supplied by Vliffe Science Technologies Pvt. Ltd, 1, Akshay 50, Anand park, Aundh, Pune, India 411007.
65. T. A. HALGREN: Merck Molecular Force Field: I. Basis, Form, Scope, Parameterization and Performance of MMFF94. *J Comput Chem*, **17**, 490 (1996).
66. K. BAUMANN: An Alignment-independent Versatile Structure Descriptor for QSAR and QSPR Based on the Distribution of Molecular Features. *J Chem Inf Comp Sci*, **42**, 26 (2002).
67. A. GOLBRAIKH, A. TROPSHA: Predictive QSAR Modeling Based on Diversity Sampling of Experimental Datasets for the Training and Test Set Selection. *J Comput Aid Mol Des*, **16**, 357 (2002).
68. R. D. CRAMER, D. E. PATTERSON, J. D. BUNCE: Comparative Molecular Field Analysis (CoMFA) 1. Effect of Shape on Binding of Steroids to Carrier Proteins. *J Am Chem Soc*, **110**, 5959 (1988).
69. W. ZHENG, A. TROPSHA: Novel Variable Selection Quantitative Structure–Property Relationship Approach Based on the *k*-nearest-neighbor Principle. *J Chem Inf Comp Sci*, **40**, 185 (2000).

Received 15 December 2010

Revised 1 February 2011

## **RATIONALISATION OF 2-ALKYLBENZIMIDAZOLES BEARING N-PHENYLPYRROLE MOIETY AS NOVEL ANGIOTENSIN II AT<sub>1</sub> RECEPTOR ANTAGONISTS – A QSAR APPROACH**

M. C. SHARMA\*, D. V. KOHLI

*Department of Pharmaceutical Sciences, Dr. Hari Singh Gaur University,  
470 003 Sagar (M.P.), India*

*E-mail: mukeshcsharma@yahoo.com*

### **ABSTRACT**

The output of present research work is interesting; the 2D QSAR studies indicated contribution of different physicochemical descriptors. The compounds in the selected series were characterised by physicochemical and fragmental descriptors calculated using 2D-QSAR module of VLife MDS software. Correlations between different inhibitory activities and calculated predictor variables were established through employing the multiple regressions analysis. Quantitative structure–activity relationship (QSAR) study revealed that steric, electrostatic interactions, electro-topological parameters, estate numbers and alignment independent descriptors are primarily responsible for angiotensin II AT<sub>1</sub> receptor antagonists. QSAR model demonstrated that anticancer activity is correlated with some of the parameters, viz. T\_T\_O\_1, polar surface area including P and S, MomInertiaZ, SsssCHE, and SssCH<sub>3</sub>count, etc. The best model showed  $r^2$  value = 0.8305 and this model was obtained by multiple regression method with good predictive ability. These results should provide guidelines for design of more potent and selective angiotensin II AT<sub>1</sub> receptor antagonist as antihypertensive activity.

*Keywords:* angiotensin II, antagonist AT<sub>1</sub> receptor, 2-alkylbenzimidazole, QSAR, hypertension.

### **AIMS AND BACKGROUND**

The octapeptide angiotensin II (Ang II, Asp-Arg-Val-Tyr-Ile-His-Pro-Phe) acts on 2 receptors in the rennin–angiotensin system (RAS), the AT<sub>1</sub> and the AT<sub>2</sub> receptors. The AT<sub>1</sub> receptor mediates the well-known effects of Ang II, such as regulation of blood pressure and electrolyte and water retention. The physiological role of the AT<sub>2</sub> receptor

---

\* For correspondence.

is still under investigation and has been linked to processes such as apoptosis, tissue repair, and fetal development<sup>1,2</sup>. Angiotensin II (Ang II), a potent vasoconstrictive hormone formed within the RAS cascade, is implicated in the increase of the arterial blood pressure. Drug design for developing novel synthetic antihypertensive drugs was targeted either to the inhibition of Ang II biosynthesis (renin or angiotensin converting enzyme (ACE) inhibitors) or to the antagonism of Ang II binding to angiotensin II (AT<sub>1</sub>) receptors. Angiotensin II receptor blockers (ARBs) have been developed to produce a more complete blockade of the action of Ang II compared to other drug classes as well as an improved side effect profile<sup>3</sup>. Many topological descriptors can be used to describe organic molecular structure with QSAR aims. The quantitative structure–activity relationship approach pioneered by Hansch et al.<sup>4</sup> helps to correlate the specific biological activities or physical properties of a series of compounds with the measured or computed molecular properties of the compounds, in terms of descriptors. QSAR methodologies save resources and expedite the process of the development of new molecules and drugs<sup>5–9</sup>. The author of the article and his research team has developed a few QSAR models to predict biological activity of different group of compounds<sup>10–61</sup>. Herein we discussed 2D-QSAR analysis of some 2-alkylbenzimidazoles bearing an N-phenylpyrrole moiety as novel angiotensin II AT<sub>1</sub> receptor antagonists activity. The relevance of the model used for the design of novel derivatives should be assessed not only in terms of predictivity, either internal or external, but also in terms of their ability to provide a chemical and structural explanation of their binding interaction.

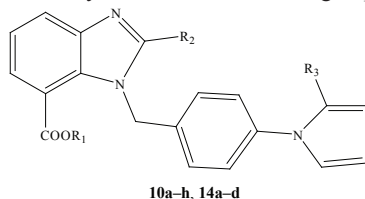
## EXPERIMENTAL

### DATA SET

The Ang II receptor antagonistic activity data of their 2-alkylbenzimidazoles bearing N-phenylpyrrole moiety as novel angiotensin II AT<sub>1</sub> receptor antagonists were taken from the reported work of Xiao Ming Wu et al.<sup>62</sup> (Table 1). Molecular modelling studies (2D) were performed using the Molecular Design Suite (VLife MDS software package, version 3.5; from VLife Sciences<sup>63</sup>, Pune, India), conformational analysis was carried out using molecular modelling user interface implemented on Acer PC with a Pentium IV processor and Windows XP operating system. All the structures were constructed using the 2D draw application provided as a tool of main MDS window. All compounds were built on molecular design suite window provided in the VLife MDS 3.5 software (VLife Sciences Technologies Pvt. Ltd., Pune, India). Energy minimisation was done by geometry optimisation of molecules using molecular mechanics force field (MMFF) by using root mean square gradient of 1. Most stable structure for each compound was generated and used for calculating various physicochemical descriptors such as thermodynamic, steric, and electronic values of descriptors. The 2D structures were converted to 3D structures by sending them to MDS. Energy minimisation and geometry optimisation was conducted using the Merck molecular force field (MMFF) method with root mean square (RMS) gradient set to

0.01 kcal/mol Å and iteration limit to 10 000. The 2D descriptors (physicochemical and alignment independent) were calculated for the optimised compounds on QSAR plus work sheet. The invariable descriptors (the descriptors that are constant for all the molecules) were removed as they do not contribute to QSAR.

**Table 1.** Structure and activities of 2-alkylbenzimidazoles bearing N-phenylpyrrole moiety



Compd.	R <sub>1</sub>	R <sub>2</sub>	R <sub>3</sub>	IC <sub>50</sub> (nM) ± SEM	pIC <sub>50</sub>
<b>1a</b>	Me	Bu	CN <sub>4</sub> H	9.8 ± 0.2	0.99123
<b>2b*</b>	Me	Pr	CN <sub>4</sub> H	32 ± 1.5	1.50515
<b>3c</b>	Me	Et	CN <sub>4</sub> H	140 ± 8.6	2.14613
<b>4d</b>	Me	Me	CN <sub>4</sub> H	200 ± 14	2.30103
<b>5e*</b>	Et	Bu	CN <sub>4</sub> H	19 ± 3.1	1.27875
<b>6f</b>	Et	Pr	CN <sub>4</sub> H	41 ± 5.2	1.61278
<b>7g*</b>	H	Bu	CN <sub>4</sub> H	6.9 ± 0.1	0.83885
<b>8h</b>	H	Pr	CN <sub>4</sub> H	16 ± 1.8	1.20412
<b>9a</b>	H	Bu	CO <sub>2</sub> H	33 ± 2.4	1.51851
<b>10b</b>	H	Pr	CO <sub>2</sub> H	92 ± 4.6	1.96379
<b>11c*</b>	H	Et	CO <sub>2</sub> H	160 ± 38	2.20412
<b>12d</b>	H	Me	CO <sub>2</sub> H	250 ± 47	2.39794

pIC<sub>50</sub> = -lg IC<sub>50</sub> to generate equation; \* indicates the compounds considered in the test set in 2D QSAR.

#### DESCRIPTORS CALCULATION

The physicochemical properties (231 descriptors) were calculated on worksheet provided in VLife MDS 3.5 software (complete descriptors data set of all compounds can be provided on demand) and were considered as independent variable, with biological activity as dependent variable (Table 2). The software is also used to obtain a correlation matrix for the selection of the parameters having minimum inter-correlation among them and having maximum correlation with biological activity. This was followed by stepwise multiple linear regression analysis to achieve the best QSAR model. The plus/minus data within parentheses are the error of regression coefficients associated with the corresponding regression coefficients in the regression equation.

The MDS 3.5 program was employed for the calculation of different quantum chemical descriptors including heat of formation, dipole moment, local charges, and different topological, elemental count including bromine count, fluorine count, path count and constitutional descriptors for each molecule. Chemical parameters including



**Table 2.** Physicochemical properties of 2-alkylbenzimidazoles derivatives

SsssCHE	Mom InertiaZ	T_O_Cl_5	T_C_O_3	T_2_N_4	SsCH <sub>3</sub> count
16.6902	19.1017	3	4	2	4.59000
16.1902	18.3946	3	4	2	4.56324
15.6902	17.6875	3	4	2	4.41869
15.1522	16.9804	3	4	2	4.26311
17.1902	19.8088	3	4	2	4.77342
16.6902	19.1017	3	4	2	4.66213
16.1522	18.1407	3	4	2	4.57568
15.6522	17.4336	3	4	2	4.46439
14.9904	17.1545	0	1	0	4.28167
14.4904	16.4474	0	1	0	4.17038
13.9904	15.7403	0	1	0	4.02583
13.4524	15.0332	0	1	0	3.87025

molar volume (V), molecular surface area (SA), hydrophobicity ( $\lg P$ ), hydrogen acceptor count (HAC), hydration energy (HE) and molecular polarisability (MP) were also calculated by using software. The various descriptors selected for 2D QSAR were vdWSurfaceArea (the van der Waals surface area of the molecule), -vePotentialSurfaceArea (total van der Waals surface area with negative electrostatic potential of the molecule), +vePotentialSurfaceArea (total van der Waals surface area with positive electrostatic potential of the molecule) dipole moment, YcompDipole ( $y$ -component of the dipole moment), element count, path count, cluster, distance-based topological indices, connectivity index, hydrophobic and hydrophilic areas like SAMostHydrophilic (most hydrophilic value on the vdW surface by the Audry method using  $\text{Slg}p$ ), SAMostHydrophobicHydrophilic Distance (distance between most hydrophobic and hydrophilic point on the vdW surface by the Audry method using  $\text{Slg}p$ ), SAHydrophilicArea (vdW surface descriptor showing hydrophilic surface area by the Audry method using  $\text{Slg}P$ ) and SKMostHydrophilic (most hydrophilic value on the vdW surface by the Kellog method using  $\text{Slg}p$ ), radius of gyration, the Wiener index, moment of inertia, semi-empirical descriptors, HOMO (highest occupied molecular orbital), LUMO (lowest unoccupied molecular orbital), heat of formation and ionisation potential. Alignment independent descriptors (AI) are calculated as discussed in the Baumann paper<sup>64</sup>. For calculation of AI descriptors every atom in the molecule was assigned at least one and at most three attributes. The first attribute is 'T-attribute' to thoroughly characterise the topology of the molecule. The second attribute is the atom type. The atom symbol is used here. The third attribute is assigned to atoms taking part in a double or triple bond. After all atoms have been assigned their respective attributes, selective distance count statistics for all combinations of different attributes are computed. In this study to calculate AI descriptors, we have used the following attributes, 2 (double-bonded atom), 3 (triple-bonded atom), C, N, O, S, H, F, Cl, Br and I and the distance range of 0–7.

Dataset of 12 molecules (Table 1) was divided into training (9) and test (3) set compounds. Selection of the training set and the test set molecules was done manually by considering the fact that test set molecules represent a range of biological activity similar to that of the training set<sup>65</sup>. Thus, the test set was a true representative of the training set. This was achieved by arbitrarily setting aside 4 compounds as a test set with a regularly distributed biological data. Sphere exclusion method was adopted for division of training and test set and for their creation from the data. This is a rational selection method which takes into consideration both biological and chemical space for division of dataset. Dissimilarity value provides handle to vary train/test set size. It needs to be adjusted by trial and error until a desired division of train and test set is achieved. As a rule, increase in dissimilarity value will lead to increase in number of molecules in the test set.

In 2D QSAR techniques the cross-validation analysis was performed using leave-one-out method. In the selected equations, the cross-correlation limit was set as 0.5, number of variables as 10, and term selection criteria as  $r^2$ .  $F$ -value specified to evaluate the significance of a variable. The higher the  $F$ -value, the more stringent is the significance level  $F$ -test 'in' as 4 and  $F$ -test 'out' as 3.99. Variance cut-off was set to 0 and scaling as auto-scaling where number of random iteration was set to 100. Following statistical parameters were considered to compare the generated QSAR models, correlation coefficient ( $r$ ), squared correlation coefficient ( $r^2$ ), predictive  $r^2$  for external test set (pred\_  $r^2$ ) for external validation, and the Fischer value ( $F$ ).

*Validation of QSAR models.* The cross-validated  $r^2$  ( $q^2$ ) value was calculated using:

$$q^2 = 1 - \frac{\sum(y_i - \hat{y}_i)^2}{\sum(y_i - y_{\text{mean}})^2},$$

where  $y_i$  and  $\hat{y}_i$  are the actual and predicted activities of the  $i$ -th molecule, respectively, and  $y_{\text{mean}}$  is the average  $k$ -nearest-neighbour activity of all molecules in the training set<sup>66</sup>. Both summations are over all molecules in the training set. Since the calculation of the pair wise molecular similarities, and hence the predictions, were based on the current trial solution, the  $q^2$  obtained is indicative of the predictive power of the current  $k$ -nearest-neighbour MFA model.

The predicted  $r^2$  (pred\_  $r^2$ ) value was calculated using,

$$\text{pred\_}r^2 = 1 - \frac{\sum(y_i - \hat{y}_i)^2}{\sum(y_i - y_{\text{mean}})^2},$$

where  $y_i$  and  $\hat{y}_i$  are the actual and predicted activities of the  $i$ -th molecule in test set, respectively, and  $y_{\text{mean}}$  is the average activity of all molecules in the training set. Both summations are over all molecules in the test set. The pred\_  $r^2$  value is indicative of the predictive power of the current model for external test set.

To evaluate the statistical significance of the QSAR model for an actual data set, we have employed one-tail hypothesis testing. The robustness of the QSAR models

for experimental training sets was examined by comparing these models to those derived for random data sets. Random sets were generated by re-arranging biological activities of the training set molecules. The significance of the models obtained was derived based on the calculated  $Z_{\text{score}}$  (Ref. 67).

$$Z_{\text{score}} = \frac{h - \mu}{\sigma},$$

where  $h$  is the  $q^2$  value calculated for the actual dataset;  $\mu$  – the average  $q^2$ , and  $\sigma$  – its standard deviation calculated for various iterations using models build by different random data sets. The probability ( $\alpha$ ) of significance of randomisation test is derived by comparing  $Z_{\text{score}}$  value with  $Z_{\text{score}}$  critical value, if  $Z_{\text{score}}$  value is less than 4.0; otherwise it is calculated by the formula as given in literature. For example, a  $Z_{\text{score}}$  value greater than 5.30 indicates that there is a probability ( $\alpha$ ) of less than 0.001 that the QSAR model constructed for the real dataset is random.

#### MULTIPLE LINEAR REGRESSION (MLR) ANALYSIS

The statistical models were developed using multiple linear regression. The equations were found to derive QSAR equation from model building method (MLR) coupled with stepwise method for assuming the biological activity with the help of physicochemical descriptor values. Multiple regressions are the standard method for multivariate data analysis. It is also called as ordinary least square regression (OLS). This method of regression estimates the values of the regression coefficients by applying least square curve fitting method. For getting reliable results, dataset having typically 5 times as many data points (molecules) as independent variables (descriptors) is required. The regression equation takes the form

$$Y = b_1x_1 + b_2x_2 + b_3x_3 + c,$$

where  $Y$  is dependent variable;  $b$  – regression coefficients for the corresponding  $x$  (independent variable);  $c$  – a regression constant, or intercept<sup>68, 69</sup>. This method consists of ranking the molecules according to their dependent-variable value and then populating the training and prediction sets such that the range of the dependent variable is represented within each set.

#### RESULTS AND DISCUSSION

All 12 molecules were subjected to regression analysis using multiple linear regressions, as model building method coupled with stepwise variable selection. QSAR equations were generated using  $\lg IC_{50}$  values as the variable and various parameter values as independent variables. Regression analysis was carried out for Ang II inhibitory activity and the best model was cross-validated. The cross-correlation limit was set at 0.5, number of variables in the final equation at 5, and term selection criteria as  $r^2$ ,  $F$ -test 'in' at 4 and  $r^2$ ,  $F$ -test 'out' at 3.99. Variance cut-off was set at 0, scaling to

auto-scaling, and number of random iterations to 10. The following statistical parameters were considered to compare the generated QSAR models: correlation coefficient ( $r$ ), squared correlation coefficient ( $r^2$ ), predicted  $r^2$  (pred\_  $r^2$ ), and the Fischer value ( $F$ ). The statistical significance of these models was further supported by the ‘fitness plot’ obtained for each model; this is a plot of observed versus predicted activity of training- and test-set compounds and provides an idea about how well the model was trained and how well it predicts the activity of the external test set.

#### Model 1

$$\lg(\text{IC}_{50}) = +0.3963 (\pm 0.0188) \text{T\_C\_O\_3} - 0.2669 (\pm 0.0215) \text{SssCH}_3\text{count} \\ + 0.3297 (\pm 0.0510) \text{SsssCHE} + 0.0026$$

$$n = 12, \text{ degree of freedom} = 5, r^2 = 0.9826, q^2 = 0.9584, F\text{-test} = 94.3229, r^2 \text{ se} = 0.0851, \\ q^2 \text{ se} = 0.1317, \text{pred\_}r^2 = 0.7501, \text{pred\_}r^2 \text{ se} = 0.4787$$

The statistically significant model (Model 1) with coefficient of determination ( $r^2$ ) = 0.9826 (which corresponds to value of  $r=0.84$ ) was considered as a model for angiotensin II receptor antagonists. The model showed an internal predictive power ( $q^2=0.9584$ ) of 95% and predictivity for external test set (pred\_  $r^2$  =0.7501) about 75%. The overall statistical significance level was found to be better than 99.9% as it exceeded the tabulated  $F_{1,21\alpha 0.001} = 94.3229$ . The developed MLR model reveals that the descriptor T\_C\_O\_3 carbon atoms (single-, double- or triple-bonded) separated from any oxygen atom (single- or double-bonded) by bond distance in a molecule plays most important role (~20%) in determining activity. The next important descriptor is SssCH<sub>3</sub>count which is also directly proportional to the activity the descriptor implies the significance of number of carbon atoms –CH<sub>3</sub>-group connected with 2 single bonds. The other descriptor SsssCHE is a topological index, which signifies the total number of –CH-groups connected with 3 single bonds. A high positive correlation suggests that better Ang II inhibition can be achieved by increasing the saturated rings and saturated aliphatic chains. The above model is validated by predicting the biological activities of the test molecules as indicated in Table 3. The plot of observed versus predicted activities for the test compounds is represented in Fig. 1.

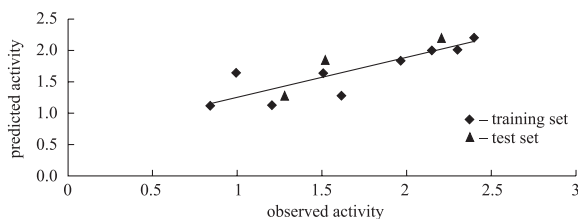


**Fig. 1.** Graph of observed and predicted activities of the training and test set QSAR Model 1

**Table 3.** Comparative observed and predicted activities (LOO) 2-alkylbenzimidazoles derivatives

pIC <sub>50</sub>	QSAR Model 1	QSAR Model 2	QSAR Model 3	QSAR Model 4	QSAR Model 5
0.991226	1.635700	1.189019	1.259086	1.306275	1.263130
1.50515	1.635700	1.586500	1.540758	1.549515	1.578706
2.146128	1.994055	1.983981	2.010210	2.030620	2.104666
2.30103	2.006696	2.381462	2.291882	2.282188	2.420242
1.278754	1.273197	1.189019	1.172692	1.053697	0.947554
1.612784	1.273197	1.586500	1.454363	1.296938	1.263130
0.838849	1.118598	0.838861	0.841041	0.836176	0.998880
1.20412	1.118598	1.236342	1.122712	1.079417	1.314456
1.518514	1.833581	1.498005	1.607157	1.573839	1.419648
1.963788	1.833581	1.895486	1.888828	1.817079	1.735224
2.20412	2.191936	2.292967	2.358281	2.298184	2.261184
2.39794	2.204577	2.690448	2.639952	2.549752	2.576760

### Model 2

$\lg(\text{IC}_{50}) = +0.5711(\pm 0.0836) T\_2\_N\_1 - 0.2548(\pm 0.0696) \text{Polar surface area excluding P and S} - 0.3968(\pm 0.1544) \text{SsCH}_3\text{E-index} + 0.0142$

$n = 12$ , degree of freedom = 5,  $r^2 = 0.7925$ ,  $q^2 = 0.6777$ ,  $F\text{-test} = 17.7204$ ,  $r^2\text{se} = 0.2873$ ,  $q^2\text{s} = 0.3870$ ,  $\text{pred}_r^2 = 0.7350$ ,  $\text{pred}_r^2\text{se} = 0.3447$

Model 2 generated using the multiple regression analysis method with 0.7925 as the coefficient of determination ( $r^2$ ) was considered using the same molecules in the test and training sets. The model can explain 79.7% of the variance in the observed activity values. The model shows an internal predictive power ( $q^2 = 0.6777$ ) of 68% and a predictivity for the external test set ( $\text{pred}_r^2 = 0.7350$ ) of about 73.5%. The  $F$ -test value of 17.7204 shows the overall statistical significance level for 99.99% of the model, which means the probability of failure for the model is 1 in 10 000. The developed MLR model reveals that the descriptor Polar surface area excluding P and S (i.e. phosphorus and sulphur) plays most important role (~85%) in determining activity. This suggests that substituents like  $-\text{OH}$ ,  $-\text{NH}_2$ ,  $-\text{NO}_2$  would increase the activity. The next important descriptor is  $T\_2\_N\_1$  which is also directly proportional to the activity the descriptor implies the significance of number of count of number of double-bonded atoms (i.e. any double-bonded atom,  $T\_2$ ) separated from nitrogen atom by 5 bonds. The descriptor explains the importance of primary, secondary or tertiary alkyl substitution at position. The descriptor  $\text{SsCH}_3\text{E-index}$  is electrotopological state indices for number of  $-\text{CH}_3$ -group connected with one single bond. This descriptor showed negative contribution in selected model (Model 2) and its contributions are approx ~25%. Negative contribution of this descriptor revealed the decrease of anti-hypertensive activity of alkyl benzimidazole with the presence of  $\text{CH}_3$ -group such as

compounds **1a**, **2b**, **3c**, **4d** and **12d**. The above model is validated by predicting the biological activities of the test molecules as indicated in Table 3. The plot of observed versus predicted activities for the test compounds is represented in Fig. 2.

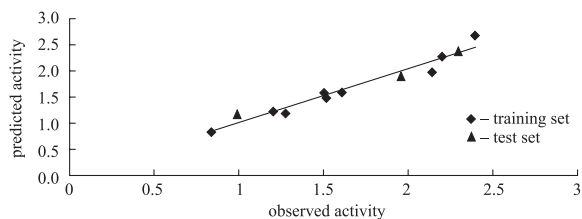


**Fig. 2.** Graph of observed versus predicted activities of the training and test set QSAR Model 2

### Model 3

$$\lg(\text{IC}_{50}) = +0.4621 (\pm 0.1056) \text{ T\_O\_Cl\_5} - 0.3383 (\pm 0.0716) \text{ SssCH}_3\text{count} \\ + 0.0720 (\pm 0.0278) \text{ XAAverageHydrophobicity} + 0.0008$$

$$n = 12, \text{ degree of freedom} = 4, r^2 = 0.7423, q^2 = 0.6386, F\text{-test} = 16.6404, r^2\text{se} = 0.1840, \\ q^2\text{se} = 0.4311, \text{ pred\_}r^2 = 0.6104, \text{ pred\_}r^2\text{se} = 0.2873$$

The descriptor was T\_O\_Cl\_5 which was a minor (~40%) contributor for biological activity. The descriptor means the count of number of bonded atoms separated from oxygen by 5 bonds in chlorine, which is having a positive impact on the biological activity. The next descriptor XAAverageHydrophobicity hydrophilic value on the vdW surface increase activity. The above model is validated by predicting the biological activities of the test molecules as indicated in Table 3. The plot of observed versus predicted activities for the test compounds is represented in Fig. 3. Model 3 generated using the multiple regression analysis method with 0.7423 as the coefficient of determination ( $r^2$ ) was considered using the same molecules in the test and training sets. The model can explain 74.23% of the variance in the observed activity values. The model shows an internal predictive power ( $q^2 = 0.6386$ ) of 64% and a predictivity for the external test set ( $\text{pred\_}r^2 = 0.6104$ ) of about 61%. The  $F$ -test value of 16.6404 shows the overall statistical significance level for 99.99% of the model.

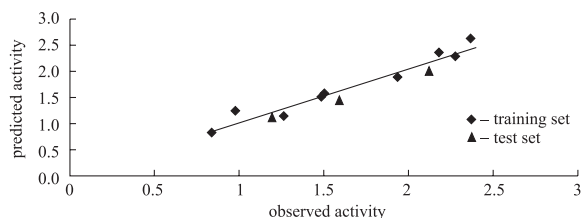


**Fig. 3.** Graph of observed versus predicted activities of the training and test set QSAR Model 3

#### Model 4

$$\lg(\text{IC}_{50}) = +0.4539(\pm 0.0664) \text{ T\_T\_O\_1} - 0.3323(\pm 0.0431) \text{ SssCH}_3\text{count} \\ + 0.0001(\pm 0.0000) \text{ MomInertiaZ} + 0.3849(\pm 1.5266) \text{ H-Donor Count} - 0.0004$$

$n = 12$ , degree of freedom = 4,  $r^2 = 0.7658$ ,  $q^2 = 0.9030$ ,  $F\text{-test} = 28.2280$ ,  $r^2 \text{ se} = 0.1365$ ,  
 $q^2 \text{ se} = 0.2298$ ,  $\text{pred}_r^2 = 0.6205$ ,  $\text{pred}_r^2 \text{ se} = 0.4702$

The statistically significant model (Model 4) with coefficient of determination ( $r^2$ ) = 0.7658 (which corresponds to value of  $\text{pred}_r^2 \text{ se} = 0.4702$ ) was considered as a model for angiotensin II receptor antagonists. The model showed an internal predictive power ( $q^2 = 0.9030$ ) of 90% and predictivity for external test set ( $\text{pred}_r^2 = 0.6205$ ) about 62%. The overall statistical significance level was found to be better than 99.9% as it exceeded the tabulated  $F_{1, 21, 0.001} = 28.2280$ . In this QSAR equation, the positive coefficient of T\_T\_O\_1, MomInertiaZ, and H-Donor Count showed that increase in the values of these descriptors are beneficial for the antihypertensive activity. The negative coefficient of SssCH<sub>3</sub>count showed that increase in the values of these descriptors is detrimental for the activity. The plot of observed versus predicted activities for the test compounds is represented in Fig. 4.

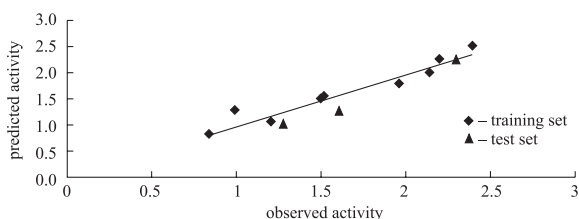


Fig. 4. Graph of observed versus predicted activities of the training and test set QSAR Model 4

#### Model 5

$$\lg(\text{IC}_{50}) = +0.1652 \text{ T\_T\_N\_3} - 1.3656 \text{ T\_2\_N\_4} + 0.3008 \text{ Hydrogens Count} - 0.1306$$

$n = 12$ , degree of freedom = 4,  $r^2 = 0.6818$ ,  $q^2 = 0.6385$ ,  $F\text{-test} = 29.8430$ ,  $r^2 \text{ se} = 0.1921$ ,  
 $q^2 \text{ se} = 0.2066$ ,  $\text{pred}_r^2 = 0.5891$ ,  $\text{pred}_r^2 \text{ se} = 0.2713$

Model 5 shows good squared correlation coefficient ( $r^2$ ) of 0.681 explains 68% variance in biological activity. Cross-validated squared correlation coefficient of this model was 0.6385, which shows the good internal prediction power of this model. In this QSAR Model 5, the positive coefficient of T\_T\_N\_3 and Hydrogens Count showed that increase in the values of these descriptors are beneficial for the activity. The negative coefficient of T\_2\_N\_4 showed that increase in the values of these descriptors is detrimental for the activity. Here, T\_T\_N\_3 (i.e. nitrogen molecule) which has major (~40%) contribution in the positive direction for the biological activity. The later descriptor was Hydrogens Count which was a minor (~30%) contributor for biological activity. The descriptor T\_2\_N\_4 (i.e. the number of double-bonded

atoms separated from the nitrogen atom by 4 bonds) indicates a negative contribution (~15%) to the biologic activity. It suggests that the mono substituents with a nitrogen atom in the *para*-position of the phenyl ring is detrimental to activity.

## CONCLUSIONS

In conclusion, the study presented here may play an important role in understanding the relationship of 2 dimensional descriptors with structure and biological activity of the present data set. By studying the significant models obtained through 2D QSAR study, one can choose the suitable substituent by taking into consideration various topological and physicochemical descriptors so as to get compounds with improved antihypertensive activities. The physicochemical and alignment-independent descriptors were found to have an important role in governing the change in activity. The good correlation between experimental and predicted biological activity for compounds in the test set further highlights the reliability of the constructed QSAR model. Thus the above QSAR study gives important information about the structural requirements of the substituted benzimidazole moiety and further helped in tailoring new analogs to find an active member.

## ACKNOWLEDGEMENT

The author wishes to express gratitude to V-life Science Technologies Pvt. Ltd. for providing the software for the study. Authors like to acknowledge Head, School of Pharmacy, Devi Ahilya Vishwavidyalaya Indore for providing facilities to carry out the study.

## REFERENCES

1. E. KASCHINA, T. UNGER: Angiotensin AT1/AT2 Receptors: Regulation, Signalling and Function. *Blood Press*, **12**, 70 (2003).
2. M. D. GASPARO, K. J. CATT, T. INAGAMI, J. W. WRIGHT, T. UNGER: International Union of Pharmacology. XXIII. The Angiotensin II Receptors. *Pharmacol Rev*, **52**, 415 (2000).
3. J. M. KRUM: Role of Valsartan and Other Angiotensin Receptor Blocking Agents in the Management of Cardiovascular Disease. *Pharmacol Res*, **46**, 203 (2002).
4. C. HANSCH, P. P. MALONEY, T. FUJITA, R. M. MUIR: Correlation of Biological Activity of Phenoxyacetic Acids with Hammett Substituent Constants and Partition Coefficients. *Nature*, **194**, 178 (1962).
5. J. SINGH, V. K. DUBEY, V. K. AGARWAL, P. V. KHADIKAR: QSAR Study on Octanol–Water Partitioning: Dominating Role of Equalised Electronegativity. *Oxid Commun*, **31** (1), 27 (2008).
6. J. SINGH, V. K. AGARWAL, S. SINGH, P. V. KHADIKAR: Use of Topological as well as Quantum Chemical Parameters in Modelling Antimalarial Activity of 2,4-diamino-6-quinazoline Sulphonamides. *Oxid Commun*, **31** (1), 17 (2008).
7. A. K. SRIVASTAVA, ARCHANA, M. JAISWAL: Quantitative Structure–Activity Relationship Studies of  $\rho$ -arylthiocinnamides as Antagonists of Biochemical ICAM-1/LFA-1 Interaction in Relation to Anti-inflammatory Activity. *Oxid Commun*, **31**, 44 (2008).



8. A. K. SRIVASTAVA, M. JAISWAL, ARCHANA, A. SRIVASTAVA: QSAR Modelling of Selective CC Chemokine Receptor 3 (CCR3) Antagonists Using Physicochemical Parameters. *Oxid Commun*, **32**, 55 (2009).
9. S. JOSHI, M. YADAV, L. PARADKAR, N. S. ANURAJ: A QSAR Study on Minimum Inhibitory Concentrations of Some Phenols: Predicting  $-\log$  MIC Using Topological Indices. *Oxid Commun*, **35** (3), 684 (2012).
10. M. C. SHARMA, N. K. SAHU, D. V. KOHLI, S. C. CHATURVEDI, S. SHARMA: QSAR, Synthesis and Biological Activity Studies of Some Thiazolidinones Derivatives. *Digest J Nanomat. Biostruct*, **4** (1), 223 (2009).
11. A. DHAKAD, M. C. SHARMA, S. C. CHATURVEDI, S. SHARMA: 3D-QSAR Studies, Biological Evaluation Studies on Some Substituted 3-chloro-1-[5-(5-chloro-2-phenyl-benzimidazole-1-ylmethyl)-[1,3,4] thiaziazole-2-yl]-azetidin-2-one as Potential Antimicrobial Activity. *Digest J Nanomat Biostruct*, **4** (2), 275 (2009).
12. M. C. SHARMA, D. V. KOHLI, S. SHARMA, S. C. CHATURVEDI: Two-dimensional Quantitative Structure Activity Relationships -2, 3 diarylthiophenes as Selective COX-1-2 Inhibitors. *Digest J Nanomat Biostruct*, **4** (3), 459 (2009).
13. M. C. SHARMA, D. V. KOHLI, N. K. SAHU, S. SHARMA, S. C. CHATURVEDI: 2D-QSAR Studies of Some 1, 3,4-thiaziazole-2yl azetidine 2-one as Antimicrobial Activity. *Digest J Nanomat Biostruct*, **4** (2), 339 (2009).
14. M. C. SHARMA, S. SHARMA, D. V. KOHLI, S. C. CHATURVEDI: Three Dimensional Quantitative Structural–Activity Relationship (3D-QSAR) Studies of Some 3-{4-[3-(2-aryl-phenoxy) butoxy]-phenyl} Propionic Acids as Novel PPAR  $\gamma/\delta$  Agonists. *Der Pharma Chemica*, **2** (1), 82 (2010).
15. M. C. SHARMA, S. SHARMA, D. V. KOHLI, S. C. CHATURVEDI: Molecular Modelling Studies Atom Based of 3-bromo-4-(1-H-3-indolyl)-2, 5-dihydro-1H-2, 5-pyrroledione Derivatives Antibacterial Activity against *Staphylococcus aureus*. *Der Pharmacia Lettre*, **2** (1), 1 (2010).
16. M. C. SHARMA, S. SHARMA: Quantitative Structural–Activity Relationship (QSAR) Study for Antimycobacterial Activities of Pyrazine Containing Thiazoline and Thiazolidinone Derivatives. *Optoelect Advan Mater – Rapid Commun*, **4** (3), 415 (2010).
17. M. C. SHARMA, S. SHARMA: Quantitative Structure–Activity Relationship Studies of a Novel Class of Dual PPAR  $\gamma/\delta$  Agonists. *Int J Pharm Tech Res*, **2** (2), 1376 (2010).
18. S. SHARMA, M. C. SHARMA, A. D. SHARMA: Quantitative Structure–Activity Relationship Analysis of a Series of Antibacterial 3-bromo-4-(1-H-3-indolyl)-2,5-dihydro-1H-2,5-pyrroledione Derivatives. *J Chem Pharma Res*, **2** (2), 421 (2010).
19. N. K. SAHU, M. C. SHARMA, V. K. MOURYA, D. V. KOHLI: QSAR Studies of Some Side Chain Modified 7-chloro-4-aminoquinolines as Antimalarial Agents. *Arab J Chem*, 2011 (in press).
20. M. C. SHARMA, D. V. KOHLI, S. C. CHATURVEDI, S. SHARMA: Molecular Modeling Studies of Some Substituted 2-butylbenzimidazoles Angiotensin II Receptor Antagonists as Antihypertensive Agents. *Digest J Nanomat Biostruct*, **4** (4), 843 (2009).
21. M. C. SHARMA, D. V. KOHLI: 3D QSAR Studies on Series of 2, 3-dihydro-4(1H)-quinazolinone Derivatives Angiotensin II Receptor Antagonists: *k*NNMFA Approach. *Am-Euras J Sci Res*, **6** (2), 85 (2011).
22. M. C. SHARMA, D. V. KOHLI: 3D QSAR *k*NNMFA Approach Studies on Series of Substituted Piperidin-2-one Biphenyl Tetrazoles as Angiotensin II Receptor Antagonists. *Am-Euras Toxicol Sci*, **3** (2), 75(2011).
23. M. C. SHARMA, D. V. KOHLI: QSAR Study on Sulfonylcarbamate Derivatives: An Insight into the Structural Requirement for the Angiotensin II Receptor Antagonist. *Eur J Appl Sci*, **3** (1), 9 (2011).
24. M. C. SHARMA, D. V. KOHLI: 3D-QSAR Studies of Some Substituted Imidazolinones Angiotensin II Receptor Antagonists. *World Appl Sci J*, **12** (11), 2129 (2011).
25. M. C. SHARMA, D. V. KOHLI: 3D QSAR Studies on a Series of-[1- benzyl-1H-imidazol-5-yl)-alkyl]-amino Derivatives as Angiotensin II AT<sub>1</sub> Antagonists. *Am-Euras J Sci Res*, **6** (2), 79 (2011).

26. M. C. SHARMA, D. V. KOHLI: 3D QSAR Approach on Substituted Isoxazolidines Derivatives as Angiotensin II Receptor Antagonist. *Am-Euras Toxicol Sci*, **3** (2), 85 (2011).
27. M. C. SHARMA, D. V. KOHLI: 3D QSAR Studies of Substituted- 4(3H) Quinazolinones Derivatives as Angiotensin II Receptor Antagonists. *Eur J Appl Sci*, **3** (1), 15 (2011).
28. M. C. SHARMA, D. V. KOHLI: Predicting Alkylbenzimidazole Derivatives as Angiotensin II Receptor Antagonists: 3D QSAR by *k*NNMFA Approach. *Adv Biol Res*, **5** (3), 161 (2011).
29. M. C. SHARMA, D. V. KOHLI: 3D QSAR Studies on a Series of Sulfonylcarbamate Isostere Derivatives as Non-peptide Angiotensin II Receptor Antagonists: *k*NNMFA Method. *Am-Euras J Sci Res*, **6** (2), 64 (2011).
30. M. C. SHARMA, D. V. KOHLI: Exploration of Quantitative Structure–Activity Relationship Studies on a Series of Substituted Quinazolinones as Angiotensin II AT<sub>1</sub> Receptor Antagonists. *World Appl Sci J*, **12** (11), 2111 (2011).
31. M. C. SHARMA, D. V. KOHLI : 2D- and 3D-QSAR Studies of Substituted 4H-pyrido [1, 2-a] pyrimidin-4-ones Angiotensin II Receptor Antagonists. *Am-Euras Toxicol Sci*, **3** (2) 92 (2011).
32. M. C. SHARMA, D. V. KOHLI: An Insight into the Structural Requirement QSAR Approach on Substituted Isoxazolidines Derivatives as Angiotensin II Receptor Antagonist. *Am-Euras J Sci Res*, **6** (2), 71 (2011).
33. M. C. SHARMA, D. V. KOHLI: QSAR Studies on Substituted Benzimidazoles as Angiotensin II Receptor Antagonists: *k*NNMFA Approach. *Arab J Chem*, 2011 (in press).
34. M. C. SHARMA, D. V. KOHLI: An Approach to Design Antihypertensive Agents by 2D QSAR Studies on Series of Substituted Benzimidazoles Derivatives as Angiotensin II Receptor Antagonists. *Arab J Chem*, 2011 (in press).
35. M. C. SHARMA, D. V. KOHLI: QSAR Analysis and 3D QSAR *k*NNMFA Approach on a Series of Substituted Quinolines Derivatives as Angiotensin II Receptor Antagonists. *Arab J Chem*, 2011 (in press).
36. M. C. SHARMA, D. V. KOHLI: Quantitative Structure–Activity Analysis Studies on Triazolinone Aryl and Nonaryl Substituents as Angiotensin II Receptor Antagonists. *J Saudi Chem Soc*, 2011 (in press).
37. M. C. SHARMA, D. V. KOHLI: Two Dimensional and *k*-nearest-neighbor Molecular Field Analysis Approach on Substituted Triazolone Derivatives: An Insight into the Structural Requirement for the Angiotensin II Receptor Antagonist. *J Saudi Chem Soc*, 2011 (in press).
38. M. C. SHARMA, D. V. KOHLI: Insight into the Structural Requirement of Substituted Quinazolinone Biphenyl Acylsulfonamides Derivatives as Angiotensin II Receptor Antagonists: 2D and 3D QSAR Approach. *J Saudi Chem Soc*, 2011 (in press).
39. M. C. SHARMA, D. V. KOHLI: QSAR Analysis of Imidazo[4,5-b] pyridine Substituted  $\alpha$ -phenoxyphenylacetic Acids as Angiotensin II AT<sub>1</sub> Receptor Antagonists. *J Saudi Chem Soc*, 2011 (in press).
40. M. C. SHARMA, D. V. KOHLI: Predicting Substituted 2-butylbenzimidazoles Derivatives as Angiotensin II Receptor Antagonists: Three-dimensional QSAR and Pharmacophore Mapping. *J Saudi Chem Soc*, 2011 (in press).
41. M. C. SHARMA, D. V. KOHLI: QSAR Studies of a Series of Angiotensin II Receptor Substituted Benzimidazole Bearing Acidic Heterocycles Derivatives. *J Saudi Chem Soc*, 2011 (in press).
42. M. C. SHARMA, S. SHARMA, N. K. SAHU, D. V. KOHLI: 3D QSAR *k*NNMFA Studies on 6-substituted Benzimidazoles Derivatives as Nonpeptide Angiotensin II Receptor Antagonists: A Rational Approach to Antihypertensive Agents. *J Saudi Chem Soc*, 2011 (in press).
43. M. C. SHARMA, S. SHARMA, N. K. SAHU, D. V. KOHLI: QSAR Studies of Some Substituted Imidazolinones Derivatives Angiotensin II Receptor Antagonists Using Partial Least Squares Regression (PLSR) Based Feature Selection. *J Saudi Chem Soc*, 2011 (in press).
44. M. C. SHARMA, D. V. KOHLI: Insight into the Structural Requirement of Aryltriaolinone Derivatives as Angiotensin II AT<sub>1</sub> Receptor: 2D and 3D-QSAR *k*-nearest-neighbor Molecular Field Analysis Approach. *Med Chem Res*, **21**, 2837 (2012).

45. M. C. SHARMA, D. V. KOHLI: A Comprehensive Structure–Activity Analysis of 2, 3,5-trisubstituted 4,5-dihydro-4-oxo-3H-imidazo [4,5-c] Pyridine Derivatives as Angiotensin II Receptor Antagonists: Using 2D- and 3D-QSAR Approach. *Med Chem Res*, 2012 (in press).
46. M. C. SHARMA, D. V. KOHLI: Comprehensive Two- and Three-dimensional QSAR Studies of 3-substituted 6-butyl-1,2-dihydropyridin-2-ones Derivatives as Angiotensin II Receptor Antagonists. *Med Chem Res*, 2012 (in press).
47. M. C. SHARMA, D. V. KOHLI: Comprehensive Structure–Activity Relationship Analysis of Isoxazoliny and Isoxazolidiny Substituted Quinazolinone Derivatives as Angiotensin II Receptor Antagonists. *J Saudi Chem Soc*, 2012 (in press).
48. M. C. SHARMA, S. SHARMA, D. V. KOHLI: Structural Insights for 5- $\beta$  Ketosulfoxide Imidazolyl Biphenyl Sulfonylureas Derivatives as Angiotensin II AT<sub>1</sub> Receptor Antagonists Using kNN-MFA with Genetic Algorithm. *J Saudi Chem Soc*, 2012 (in press).
49. M. C. SHARMA, D. V. KOHLI: A Comprehensive Structure–Activity Analysis of 5-Carboxyl Imidazolyl Biphenyl Sulfonylureas Derivatives Angiotensin AT<sub>1</sub> Receptor Antagonists: 2D- and 3D-QSAR Approach. *Arab J Chem*, 2012 (in press).
50. M. C. SHARMA: Structural Insight for (6-oxo-3-pyridaziny)-benzimidazoles Derivatives as Angiotensin II Receptor Antagonists: QSAR, Pharmacophore Identification and kNNMFA Approach. *J Saudi Chem Soc*, 2012 (in press).
51. M. C. SHARMA, D. V. KOHLI: Comprehensive Structure–Activity Relationship Analysis of Substituted 5-(biphenyl-4-ylmethyl) Pyrazoles Derivatives as AT<sub>1</sub> Selective Angiotensin II Receptor Antagonists: 2D and kNNMFA QSAR Approach. *Med Chem Res*, 2012 (in press).
52. M. C. SHARMA, S. SHARMA, D. V. KOHLI: QSAR Approach Insight the Structural Requirement of Substituted Quinazolinones Derivatives as Angiotensin II Receptor Antagonists. *Oxid Commun*, **35** (3), 694 (2012).
53. M. C. SHARMA, S. SHARMA, D. V. KOHLI: QSAR Studies of 2-alkylbenzimidazole Derivatives as Angiotensin II Receptor Antagonists. *Oxid Commun*, **35** (3), 708 (2012).
54. M. C. SHARMA, D. V. KOHLI: Predicting 2, 3-dihydroquinazolinones Derivatives as Angiotensin II Receptor Antagonists: 2D QSAR Approach. *Oxid Commun*, **35** (3), 721 (2012).
55. K. S. BHADORIYA, M. C. SHARMA, S. V. JAIN, G. S. RAUT, J. R. RANANAWARE: Three-dimensional Quantitative Structure–Activity Relationship (3D-QSAR) Analysis and Molecular Docking-based Combined in Silico Rational Approach to Design Potent and Novel TRPV1 Antagonists. *Med Chem Res*, 2012 (in press).
56. K. S. BHADORIYA, M. C. SHARMA, S. V. JAIN, S. A. KAD, D. RAGHUVANSHI: QSAR Studies of Fused 5,6-bicyclic Heterocycles as  $\gamma$ -secretase Modulators. *J Pharm Res*, **5** (8), 4127 (2012).
57. N. K. SAHU, SADHANA SHAHI, M. C. SHARMA, D. V. KOHLI: QSAR Studies on Imidazopyridazine Derivatives as Pfk7 Inhibitors. *Mol Simul*, **37** (9), 752 (2011).
58. M. C. SHARMA, D. V. KOHLI, S. SHARMA: Synthesis and Biological Activity of Some Antihypertensive Activity: [(2-substituted 5-nitro-benzoimidazol-1-ylmethyl)-biphenyl-2-carboxylic Acid. *Int J Pure Appl Chem*, **7** (1), 37 (2012).
59. M. C. SHARMA, D. V. KOHLI, S. SHARMA: Insight into the Structural Requirement D- and L-N-[(1-benzyl-1H-imidazol-5-yl)-alkyl]-amino Acids as Angiotensin II AT<sub>1</sub> Antagonists: 2D QSAR Approach. *Int J Pure Appl Chem*, **7** (1), 15 (2012).
60. M. C. SHARMA, S. SHARMA: Prediction of Angiotensin II AT<sub>1</sub> Receptor Antagonists Activity of 2-alkylbenzimidazoles Bearing a N-phenyl Pyrrole Moiety as Novel – A kNNMFA Approach. *Int J Pure Appl Chem*, **7** (1), 25 (2012).
61. M. C. SHARMA, S. SHARMA, K. S. BHADORIYA: QSAR Analyses and Pharmacophore Studies of Tetrazole and Sulfonamide Analogs of Imidazo[4,5-b]pyridine Using Simulated Annealing Based Feature Selection. *J Saudi Chem Soc*, .<http://dx.doi.org/10.1016/j.jscs.2012.10.001>.
62. JIN YI XU, YI ZENG, QIAN RAN, ZHEN WEI, YI BI, QIAN HUI HE, QIU JUAN WANG, SONG HU, JING ZHANG, MING YUE TANG, WEI YI HUAA, XIAO MING WUA: Synthesis and Bio-

- logical Activity of 2-alkylbenzimidazoles Bearing a N-phenylpyrrole Moiety as Novel Angiotensin II AT<sub>1</sub> Receptor Antagonists. *Bioorg Med Chem Lett*, **17**, 2921 (2007).
63. VLIFE MDS Software Package, Version 3.5, Supplied by Vlife Science Technologies Pvt. Ltd, 1, Akshay 50, Anand park, Aundh, Pune, India 411007.
  64. K. BAUMANN: An Alignment-independent Versatile Structure Descriptor for QSAR and QSPR Based on the Distribution of Molecular Features. *J Chem Inf Comp Sci*, **42**, 26 (2002).
  65. A. GOLBRAIKH, A. TROPSHA: Predictive QSAR Modeling Based on Diversity Sampling of Experimental Datasets for the Training and Test Set Selection. *J Comput Aid Mol Des*, **16**, 357 (2002).
  66. R. D. CRAMER, D. E. PATTERSON, J. D. BUNCE: Comparative Molecular Field Analysis (CoMFA) 1. Effect of Shape on Binding of Steroids to Carrier Proteins. *J Am Chem Soc*, **110**, 5959 (1988).
  67. W. ZHENG, A. TROPSHA: Novel Variable Selection Quantitative Structure–Property Relationship Approach Based on the *k*-nearest-neighbor Principle. *J Chem Inf Comp Sci*, **40**, 185 (2000).
  68. A. T. BALABAN: Highly Discriminating Distance-based Topological Index. *Chem Phys Lett*, **89**, 399 (1982).
  69. D. PLAUSIC, M. SOSKIC, N. LERS: On the Calculation of the Molecular Descriptor. *J Chem Inf Comp Sci*, **38**, 889 (1998).

*Received 15 December 2010*

*Revised 24 January 2011*

## MODELLING TOXICITY OF SOME AROMATIC COMPOUNDS TOWARDS *Tetrahymena pyriformis* USING SOME PHYSICOCHEMICAL PARAMETERS

B. SHAIK<sup>a</sup>, J. SINGH<sup>b</sup>, I. AHMAD<sup>a</sup>, VENKATESHWAR<sup>a</sup>, V. K. AGRAWAL<sup>a\*</sup>

<sup>a</sup>Department of Applied Sciences, National Institute of Technical Teachers Training and Research, Shamla Hills, 462 002 Bhopal, Madhya Pradesh, India

<sup>b</sup>Department of SHM, Amrapali Institute of Technology and Sciences, Shiksha Nagar, Lamachaur, 263 139 Haladwani, Uttara Khand, India  
E-mail: apsvka@yahoo.co.in; basheerulla.81@gmail.com; jyoti\_singh07@rediffmail.com

### ABSTRACT

The present study is based on 174 aromatic compounds containing phenols, nitrobenzenes and benzonitriles whose toxicity towards *Tetrahymena pyriformis* was modelled using physicochemical parameters. It has been found that MW, MR, MV, PC, IR, ST and density are the best suitable parameters for modelling the lg IGC<sup>-1</sup><sub>50</sub> toxicity.

*Keywords:* toxicity, nitrobenzenes, phenols, benzonitriles, regression analysis, QSTR, *Tetrahymena pyriformis*.

### AIMS AND BACKGROUND

The prediction and property toxicity determination through the structures of organic compounds is being constantly pursued by scientists and is a fascinating field<sup>1-3</sup>. Its experimental determination is a difficult, time-consuming and expensive job, especially in living systems and other biological compounds.

In this study a miscellaneous set of 174 aromatic compounds containing phenols, nitrobenzenes and benzonitriles are chosen from the work of Roy et al.<sup>4</sup> to verify their toxic potency to *Tetrahymena pyriformis*. They are divided in 2 groups on the basis of their properties. One showing electron-donor property comprising of 97 phenol derivatives and the other – with electron-acceptor property consisting of 77 nitrobenzenes and benzonitriles grouped together. In QSTR/QSAR study various dependent parameters including topological and electronic, quantum mechanical descriptors<sup>5-8</sup>

---

\* For correspondence (presently: Director, National Institute of Technical Teachers Training and Research, Shamla Hills, 462 002 Bhopal, India).

have been used to explain the toxic potency<sup>1-3</sup>. However, less efforts have been made in modelling the toxicity of such compounds using physicochemical parameters.

We, therefore, calculated various physicochemical properties and tried to obtain many significant models to predict the toxicity values towards *Tetrahymena pyriformis* using multivariate regression analysis<sup>9</sup>. We have also used cross-validation parameters for the validation of the obtained significant models.

## RESULTS AND DISCUSSION

The 174 compounds under present investigation are taken from the work of Roy et al.<sup>4</sup> and are reported in Table 1. Table 1 also reports the logarithm of toxicity values,  $IGC^{-1}_{50}$  (50% inhibitory growth concentration against *Tetrahymena pyriformis*) of the compounds and the calculated physicochemical parameters. These parameters (MW – molecular weight; MR – molar refractivity; MV – molar volume; PC – parachor; IR – index of refraction; ST – surface tension;  $d$  – density; Pol – polarisability) have been calculated using Chem Sketch program obtained from ACD Lab<sup>10</sup>. The correlation matrix showing inter-correlation among all the descriptors are calculated and summarised in Table 2. A close look at Table 2 reveals that the parameters with more than 0.8 values are highly linearly correlated and also indicates that MW and  $d$  have good correlation and, hence, they can be used for modelling the toxicity ( $IGC^{-1}_{50}$ ) of the present set of compounds.

As mentioned earlier, the data set has been classified according to their properties. The first 97 are aromatic compounds with electron-donor capacity. The second sets of 77 compounds are also aromatic in nature but are having electron acceptor properties. Hence, we have reported our results in three steps: first for 97 compounds, second for 77 compounds, and finally for the entire data set of 174 compounds. The data was subjected to regression analysis and the models obtained are summarised in Table 3.

**Table 1.** Molecules with their experimental  $\lg \text{IGC}_{50}^{-1}$  activity

Comp. No	Molecules	$\lg \text{IGC}_{50}^{-1}$	MW	MR	MV	PC	IR	ST	$d$	Pol
1	2	3	4	5	6	7	8	9	10	11
1	3-aminophenol	-0.520	109.126	32.370	90.100	248.100	1.637	57.400	1.210	12.830
2	salicylic acid	-0.510	138.121	35.080	100.300	284.400	1.165	64.400	1.375	13.900
3	2-methoxy phenol	-0.510	124.137	34.810	111.800	278.900	1.534	38.600	1.109	13.800
4	3-hydroxy acetophenone	-0.380	136.148	38.600	119.300	307.400	1.552	43.900	1.140	15.120
5	2-ethoxyphenol	-0.360	138.164	39.440	128.300	318.700	1.526	38.000	1.078	15.830
6	2-methoxyphenol	-0.330	124.137	34.810	111.800	278.900	1.534	38.600	1.109	13.800
7	2-methylphenol	-0.300	108.138	32.950	104.100	259.000	1.545	38.800	1.038	13.060
8	3-ethoxy-4-methoxyphenol	-0.300	188.190	46.120	152.300	375.400	1.517	36.800	1.103	18.280
9	4-hydroxyacetophenone	-0.300	136.148	38.160	119.300	307.400	1.552	43.900	1.140	15.120
10	salicylamide	-0.240	137.136	37.060	108.500	296.700	1.612	60.100	1.860	14.690
11	phenol	-0.210	94.111	28.130	87.800	222.200	1.553	40.900	1.071	11.150
12	4-cresol	-0.180	108.138	32.950	104.100	259.900	1.545	38.800	1.038	13.060
13	3-acetamidophenol	-0.160	151.183	42.400	120.900	326.000	1.618	52.800	1.249	16.810
14	4-methoxyphenol	-0.140	124.137	34.810	111.800	278.900	1.534	38.600	1.109	13.800
15	isovanillin	-0.140	152.147	41.560	123.500	324.000	1.587	47.300	1.231	16.470
16	3,5-dimethoxyphenol	-0.090	154.163	41.490	135.800	335.800	1.522	37.200	1.134	16.440
17	4-aminophenol	-0.080	109.126	32.370	90.100	248.100	1.637	57.400	1.210	12.830
18	3-methylphenol	-0.600	108.138	32.950	104.100	259.900	1.545	38.800	1.038	13.060
19	3-cyanophenol	-0.060	119.121	32.840	97.200	268.200	1.590	57.800	1.220	13.020
20	methyl-3-hydroxybenzoate	-0.050	152.147	39.900	125.700	327.100	1.547	45.700	1.209	15.820
21	3-methoxy-4-hydroxybenzaldehyde	-0.030	152.147	41.560	123.500	324.000	1.587	47.300	1.231	16.470
22	4-ethoxyphenol	0.010	138.164	39.440	128.300	318.700	1.526	38.000	1.076	15.630
23	3-ethoxy-4-hydroxybenzaldehyde	0.020	166.174	46.190	140.000	383.700	1.573	45.500	1.186	18.310
24	4-fluorophenol	0.020	112.102	28.120	92.000	229.400	1.523	38.500	1.217	11.150

to be continued

1	2	3	4	5	6	7	8	9	10	11
25	2-cyanophenol	0.030	119.121	32.840	97.200	268.200	1.590	57.800	1.220	13.020
26	4-hydroxypropiophenone	0.050	150.175	42.790	135.900	347.200	1.542	42.600	1.104	16.960
27	2,4-dimethylphenol	0.070	122.164	37.780	120.400	287.500	1.540	37.200	1.014	14.970
28	2,5-dimethylphenol	0.080	122.164	37.780	120.400	297.500	1.540	37.200	1.014	14.970
29	2-hydroxyacetophenone	0.080	136.148	38.160	120.400	297.500	1.540	37.200	1.014	15.120
30	methyl-4-hydroxybenzoate	0.080	152.147	39.900	125.700	327.100	1.547	45.700	1.208	15.820
31	3-hydroxybenzaldehyde	0.090	122.121	34.880	99.500	287.300	1.618	52.200	1.226	13.830
32	3,5-dimethylphenol	0.110	122.164	37.780	120.400	297.500	1.540	37.200	1.014	14.970
33	3,4-dimethylphenol	0.120	122.164	37.780	120.400	297.500	1.540	37.200	1.014	14.970
34	2,3-dimethylphenol	0.120	122.164	37.780	120.400	297.500	1.540	37.200	1.014	14.970
35	2,4-diaminophenol	0.130	124.141	36.600	92.400	273.900	1.722	77.100	1.343	14.510
36	2-ethylphenol	0.160	122.164	37.680	120.800	298.800	1.536	37.600	1.012	14.930
37	syringaldehyde	0.170	182.173	48.240	147.500	380.600	1.567	44.300	1.234	19.120
38	2-chlorophenol	0.180	128.556	33.020	99.800	258.100	1.575	44.700	1.287	13.090
39	2-fluorophenol	0.190	112.102	28.120	92.000	229.400	1.523	38.500	1.217	11.150
40	4-ethylphenol	0.210	122.164	37.680	120.600	298.800	1.536	37.600	1.012	14.930
41	3-ethylphenol	0.230	122.164	37.680	120.600	298.800	1.536	37.600	1.012	14.930
42	salicylaldehyde	0.250	137.136	37.010	115.800	300.800	1.552	45.500	1.180	14.670
43	4-hydroxybenzaldehyde	0.270	122.121	34.880	99.500	267.300	1.618	52.000	1.226	13.830
44	3,4-dinitrophenol	0.270	184.106	41.220	111.500	333.200	1.660	79.600	1.650	16.340
45	2,3,6-trimethylphenol	0.280	136.191	42.600	136.600	335.200	1.535	36.100	0.996	16.880
46	2,4,6-trimethylphenol	0.280	136.191	42.800	136.600	335.200	1.535	38.100	0.998	16.890
47	2-allylphenol	0.330	134.175	42.020	132.200	327.800	1.548	37.600	1.014	16.660
48	2,3,5-trimethylphenol	0.360	136.191	42.600	138.600	335.200	1.535	36.100	0.996	16.890
49	2-amino-4- <i>tert</i> -butylphenol	0.370	185.232	50.750	158.800	398.100	1.560	40.700	1.053	20.120
50	3-methoxysalicylaldehyde	0.380	152.147	41.560	123.500	324.000	1.587	47.300	1.231	16.470

to be continued



Continuation of Table 1

1	2	3	4	5	6	7	8	9	10	11
51	salicylhydroxamic acid	0.380	153.135	38.850	109.200	312.300	1.626	66.900	1.402	15.320
52	3-fluorophenol	0.380	112.102	28.120	92.000	229.400	1.523	38.500	1.127	11.150
53	2-chloro-5-methylphenol	0.390	142.583	37.850	118.000	295.800	1.585	42.100	1.228	15.000
54	salicylaldehyde	0.420	122.121	34.880	99.500	267.300	1.618	52.000	1.226	13.830
55	5-amino-2-methoxyphenol	0.450	139.152	39.040	114.100	304.700	1.599	50.800	1.219	15.480
56	2,3-dinitrophenol	0.460	184.106	41.220	111.500	333.200	1.660	79.600	1.650	16.340
57	2,6-difluorophenol	0.470	130.092	28.120	96.200	238.500	1.495	36.400	1.351	11.140
58	4-isopropylphenol	0.470	136.191	42.310	137.900	337.300	1.525	35.700	0.987	16.770
59	ethyl-3-hydroxybenzoate	0.480	166.174	44.540	142.200	366.900	1.538	44.200	1.168	17.650
60	2-amino-4-nitrophenol	0.480	154.123	38.910	101.900	303.600	1.888	78.500	1.511	15.420
61	3-nitrophenol	0.510	139.109	34.690	99.700	277.700	1.612	60.200	1.395	13.740
62	2,6-dinitrophenol	0.540	184.106	41.220	111.500	333.200	1.660	79.600	1.650	16.340
63	4-chlorophenol	0.550	128.556	33.020	99.800	258.100	1.575	44.700	1.287	13.090
64	ethyl-4-hydroxybenzoate	0.570	166.174	44.540	142.200	366.900	1.538	44.200	1.168	17.650
65	4-methyl-2-nitrophenol	0.570	153.135	39.500	115.900	315.400	1.596	54.700	1.320	15.660
66	2,4-difluorophenol	0.600	130.092	28.120	98.200	236.500	1.495	36.400	1.351	11.140
67	$\alpha$ , $\alpha$ , $\alpha$ -trifluoro-4-cresol	0.620	162.109	33.110	121.300	279.400	1.457	28.100	1.335	13.120
68	4-propylphenol	0.640	136.191	42.310	137.100	338.600	1.529	37.100	0.992	16.770
69	4-nitrosophenol	0.350	123.109	32.400	99.800	282.200	1.584	48.000	1.230	12.840
70	2-nitrophenol	0.670	139.109	34.670	99.700	277.700	1.612	60.200	1.395	13.950
71	2-chloro-4,5-dimethylphenol	0.690	156.609	42.670	132.300	333.400	1.558	40.200	1.183	16.910
72	4-chloro-2-methylphenol	0.700	142.583	37.850	160.000	295.800	1.585	42.100	1.228	15.000
73	4-butoxyphenol	0.700	166.217	48.710	161.300	398.300	1.515	37.100	1.029	19.310
74	2-hydroxy-4,5-dimethylacetophe- none	0.710	164.201	47.810	151.900	382.700	1.541	40.200	1.080	18.950
75	2,6-dichlorophenol	0.740	163.001	37.920	111.700	294.000	1.593	47.800	1.458	15.030

to be continued

1	2	3	4	5	6	7	8	9	10	11
76	2-chloromethyl-4-nitrophenol	0.750	187.580	44.440	127.400	353.000	1.614	58.900	1.472	17.610
77	3-chloro-5-methoxyphenol	0.760	158.582	39.700	123.800	314.800	1.554	41.700	1.280	15.740
78	2-amino-4-chlorophenol	0.780	143.571	37.260	102.000	283.900	1.650	59.800	1.406	14.770
79	4-chloro-3-methylphenol	0.800	142.583	37.850	118.000	295.800	1.565	42.100	1.228	15.000
80	3-chlorophenol	0.870	128.558	33.020	99.800	258.100	1.575	44.700	1.287	13.090
81	4-amino-2-nitrophenol	0.880	154.123	38.910	101.900	303.800	1.688	78.500	1.511	15.420
82	2,5-dinitrophenol	0.950	184.106	41.220	111.500	333.200	1.660	79.600	1.650	16.340
83	2,4-dichlorophenol	1.040	163.001	37.920	111.700	294.000	1.593	47.800	1.458	15.030
84	3-chloro-4-fluorophenol	1.130	146.547	33.020	104.000	285.200	1.547	42.200	1.408	13.090
85	2,5-dichlorophenol	1.130	163.001	37.920	111.700	294.000	1.593	47.800	1.458	15.030
86	2-amino-4-chloro-5-nitrophenol	1.170	188.569	43.810	113.900	339.400	1.695	78.800	1.655	17.360
87	2,3-dichlorophenol	1.280	163.001	37.920	111.700	294.000	1.593	47.800	1.458	15.030
88	2,4,6-trichlorophenol	1.410	197.446	42.810	123.700	329.800	1.608	50.500	1.596	16.970
89	3,5-dichlorophenol	1.570	163.001	37.920	111.700	194.000	1.593	47.800	1.458	15.030
90	4-chloro-6-nitroresol	1.640	187.580	44.390	127.900	351.200	1.610	56.800	1.466	17.600
91	2,4-chloro-6-nitrophenol	1.750	207.999	44.470	123.600	349.500	1.638	63.900	1.838	17.620
92	3,4-dichlorophenol	1.750	163.001	37.920	111.700	294.000	1.593	47.800	1.458	15.030
93	4-chloro-2-nitrophenol	1.050	173.554	39.570	111.600	313.600	1.626	62.200	1.554	15.680
94	2,4,5-trichlorophenol	1.100	197.446	42.810	123.700	329.800	1.608	50.500	1.596	16.970
95	2,3,5,6-tetrachlorophenol	1.220	231.891	47.710	135.600	385.700	1.620	52.800	1.709	18.910
96	2,3,5-trichlorophenol	1.370	197.446	42.810	123.700	329.800	1.608	50.500	1.596	16.970
97	2,3,4,5-tetrachlorophenol	1.710	231.891	47.710	135.600	365.700	1.620	52.800	1.709	18.910
98	2-nitrobenzoic acid	-1.640	167.119	39.720	113.800	324.800	1.615	66.400	1.468	15.740
99	3-nitrobenzamide	-0.190	166.134	41.720	119.900	337.100	1.612	62.300	1.384	16.540
100	2-nitrobenzylalcohol	-0.160	153.135	39.240	115.000	316.200	1.597	57.000	1.330	15.550
101	3-nitroaniline	0.030	138.124	37.030	103.500	288.500	1.634	60.300	1.333	14.680

to be continued

Continuation of Table 1

1	2	3	4	5	6	7	8	9	10	11
102	2-nitrotoluene	0.050	137.136	37.620	117.500	300.400	1.553	42.600	1.166	14.910
103	3-nitrotoluene	0.050	137.136	37.620	117.500	300.400	1.166	42.600	1.166	14.910
104	2-nitroaniline	0.080	138.124	37.030	103.500	288.500	1.634	60.300	1.333	14.680
105	4-nitrobenzylalcohol	0.100	153.135	39.240	115.000	316.200	1.597	57.000	1.330	15.550
106	3-nitrobenzaldehyde	0.140	151.120	39.550	112.000	307.800	1.617	55.100	1.338	15.670
107	nitrobenzene	0.140	123.109	32.790	101.200	262.700	1.561	45.300	1.215	13.000
108	2-nitrobenzaldehyde	0.170	151.120	39.550	112.900	307.800	1.617	55.100	1.338	15.670
109	4-nitrotoluene	0.170	137.136	37.620	117.500	300.400	1.553	42.600	1.166	14.910
110	4-nitrobenzamide	0.180	166.134	41.720	119.900	337.100	1.612	62.300	1.384	16.540
111	4-nitrobenzaldehyde	0.200	151.120	39.550	112.900	307.800	1.617	55.100	1.338	15.670
112	4-fluoronitrobenzene	0.250	141.100	32.790	105.400	269.800	1.534	42.800	1.337	12.990
113	1,3-dimethyl-2-nitrobenzene	0.300	151.163	42.440	133.800	338.000	1.547	40.700	1.129	16.820
114	3-nitroacetophenone	0.320	165.146	42.820	132.800	347.900	1.558	47.100	1.243	16.970
115	5-hydroxy-2-nitrobenzaldehyde	0.330	167.119	41.430	111.300	322.800	1.666	70.500	1.500	16.420
116	methyl-4-nitrobenzoate	0.400	181.145	44.570	139.100	367.600	1.553	48.600	1.301	17.660
117	3,5-dinitrobenzylalcohol	0.530	198.133	45.790	128.900	371.700	1.641	73.500	1.560	18.150
118	4-nitroanisole	0.540	153.135	39.470	125.200	319.400	1.542	42.200	1.222	15.640
119	2,3-dimethylnitrobenzene	0.560	151.163	42.440	133.800	338.000	1.547	40.700	1.129	16.820
120	3-nitroanisole	0.670	153.135	39.470	125.200	319.400	1.542	42.200	1.222	15.640
121	2-chloro-6-nitrotoluene	0.680	171.581	42.510	129.600	336.200	1.570	45.400	1.324	16.850
122	2-chloronitrobenzene	0.680	157.554	37.690	113.200	298.600	1.580	48.300	1.391	14.940
123	ethyl-4-nitrobenzoate	0.710	195.172	49.020	155.600	407.300	1.544	46.900	1.253	19.500
124	3-chloronitrobenzene	0.730	157.554	37.690	113.200	298.600	1.580	48.300	1.301	14.940
125	4-ethylnitrobenzene	0.800	151.163	42.340	134.000	339.300	1.544	41.000	1.127	16.780
126	4-chloro-2-nitrotoluene	0.820	171.581	42.510	129.500	336.200	1.570	45.400	1.324	16.850
127	4-nitrophenetole	0.830	169.135	41.220	131.600	339.000	1.538	44.000	1.284	16.340

to be continued

1	2	3	4	5	6	7	8	9	10	11
128	6-methyl-1,3-dinitrobenzene	0.870	182.134	44.160	129.300	355.800	1.598	57.200	1.407	17.500
129	1,3-dinitrobenzene	0.890	168.107	39.340	113.100	318.200	1.612	62.600	1.486	45.590
130	2,4-dichloronitrobenzene	0.990	192.000	42.580	125.100	334.400	1.595	50.900	1.533	16.880
131	2,3-dichloronitrobenzene	1.070	192.000	42.580	125.100	334.400	1.595	50.900	1.533	16.880
131	3,4-dinitrobenzyl alcohol	1.090	198.133	45.790	126.900	371.700	1.641	73.500	1.560	18.150
133	2,5-dichloronitrobenzene	1.130	192.000	42.580	125.100	334.400	1.595	50.900	1.533	18.880
134	3,5-dichloronitrobenzene	1.130	192.000	42.580	125.100	334.400	1.595	50.900	1.533	16.880
135	3,4-dichloronitrobenzene	1.160	192.000	42.580	125.100	334.400	1.595	50.900	1.533	16.880
136	4-nitrobenzylchloride	1.180	171.581	42.560	128.900	338.000	1.574	47.100	1.330	16.870
137	1,2-dinitrobenzene	1.250	168.107	39.340	113.100	318.200	1.612	62.600	1.486	15.590
138	1,4-dinitrobenzene	1.300	168.107	39.340	113.100	318.200	1.612	62.600	1.486	15.590
139	2,4,6-trichloronitrobenzene	1.430	226.445	47.480	137.100	370.300	1.609	53.200	1.651	18.820
140	2,3,4,-trichloronitrobenzene	1.510	226.445	47.480	137.100	370.300	1.609	53.200	1.651	18.820
141	2,4,5-trichloronitrobenzene	1.530	226.445	47.480	137.100	370.300	1.609	53.200	1.651	18.820
141	2,3,4,5-tetrachloronitrobenzene	1.780	260.890	52.370	149.000	406.200	1.620	55.100	1.750	20.760
143	2,3,5,6-tetrachloronitrobenzene	1.820	260.890	52.370	149.000	406.200	1.620	55.100	1.750	20.760
144	2,4,6-trichloro-1,3-dinitrobenzene	2.190	271.442	54.020	148.900	425.800	1.645	66.700	1.822	21.410
145	1,2-dinitro-4,5-dichlorobenzene	2.210	236.997	49.130	137.000	389.900	1.636	65.600	1.729	19.470
146	4,6-dichloro-1,2-dinitrobenzene	2.420	236.997	49.130	137.000	389.900	1.636	65.600	1.729	19.470
147	2,4,5-trichloro-1,3-dinitrobenzene	2.590	271.442	54.020	148.900	425.800	1.645	66.700	1.822	21.410
148	2,3,5,6-tetrachloro-1,4-dinitrobenzene	2.740	305.887	58.920	160.900	461.700	1.653	67.700	1.900	23.350
149	4-cyanopyridine	-0.820	104.109	19.110	92.800	248.500	1.538	51.400	1.120	11.540
150	2-cyanopyridine	-0.790	104.109	29.110	92.800	248.500	1.539	51.400	1.120	11.540
151	3-cyanopyridine	-0.740	104.109	29.110	92.800	248.500	1.539	51.400	1.120	11.540

to be continued

Continuation of Table 1

1	2	3	4	5	6	7	8	9	10	11
152	3-cyano-4,6-dimethyl-2-hydroxypropidine	-0.700	148.162	39.890	122.300	340.300	1.565	59.900	1.210	15.810
153	benzonitrile	-0.520	103.121	31.320	99.900	253.000	1.539	41.000	1.030	12.410
154	2-aminobenzonitrile	-0.500	118.136	34.930	103.400	280.900	1.590	54.300	1.140	13.850
155	3-aminobenzonitrile	-0.470	118.136	34.930	103.400	280.900	1.590	54.300	1.140	13.850
156	4-cyanobenzamide	-0.380	148.162	41.080	118.300	336.000	1.611	65.000	1.250	16.280
157	1,2-dicyanobenzene	-0.340	128.131	35.880	110.000	300.600	1.565	55.600	1.160	14.220
158	4-fluorobenzonitrile	-0.260	121.112	31.430	104.900	260.300	1.511	37.900	1.150	12.460
159	3-tolunitrile	-0.250	117.148	35.940	110.100	291.100	1.531	39.600	1.000	14.420
160	2-tolunitrile	-0.240	117.148	35.940	116.100	291.200	1.531	39.600	1.000	14.240
161	4-tolunitrile	-0.100	117.148	35.940	116.100	291.200	1.531	39.600	1.000	14.240
162	3-chlorobenzonitrile	-0.060	137.566	36.140	111.200	290.100	1.563	46.200	1.230	14.330
163	methyl-4-cyanobenzoate	-0.060	117.148	35.940	116.100	291.200	1.531	39.600	1.000	14.240
164	3-cyanobenzaldehyde	-0.020	131.131	36.280	113.500	300.200	1.552	48.900	1.150	14.380
165	4-chlorobenzonitrile	0.000	137.560	36.140	111.200	290.100	1.583	46.200	1.230	14.330
166	4-cyanobenzaldehyde	0.040	131.131	36.280	113.500	300.200	1.552	48.900	1.150	14.380
167	3-methoxybenzonitrile	0.050	133.147	37.680	122.500	311.600	1.527	41.800	1.080	14.930
168	4-methoxybenzonitrile	0.100	133.147	37.880	122.500	311.600	1.527	41.800	1.080	14.930
169	4-aminobenzonitrile	0.250	118.136	34.930	103.400	280.900	1.580	54.300	1.140	13.850
170	2-chlorobenzonitrile	0.280	137.568	38.140	111.200	290.100	1.563	48.200	1.230	14.330
171	ethyl-4-cyanobenzoate	0.370	175.180	47.060	152.800	396.900	1.528	45.700	1.140	18.650
172	2-amino-5-chlorobenzonitrile	0.440	152.581	39.780	114.700	318.100	1.609	59.100	1.330	15.760
173	3-nitrobenzonitrile	0.450	148.110	37.350	112.200	310.000	1.579	58.200	1.310	14.800
174	3-nitrobenzonitrile	0.570	148.119	37.350	112.200	310.000	1.579	58.200	1.310	14.800

Table 2. Correlation matrix

	lg IGC <sup>-1</sup> <sub>50</sub>	MW	MR	MV	PC	IR	ST	<i>d</i>	Pol
lg IGC <sup>-1</sup> <sub>50</sub>	1								
MW	0.788	1							
MR	0.601	0.857	1						
MV	0.434	0.655	0.864	1					
PC	0.517	0.826	0.952	0.877	1				
IR	0.335	0.347	0.259	-0.042	0.193	1			
ST	0.288	0.443	0.280	-0.136	0.259	0.617	1		
<i>d</i>	0.700	0.792	0.463	0.120	0.406	0.513	0.711	1	
Pol	0.459	0.625	0.690	0.592	0.677	0.208	0.246	0.371	1

Table 3. Quality of statistical parameters along with their cross-validated parameters

Model No	Parameters used	$A_1=(1\dots\dots 9)$	<i>B</i>	SE	<i>R</i>	$R^2_A$	<i>F</i> -ratio	$Q=R/SE$	PRESS/SSY	$R^2_{cv}$	$S_{press}$	PSE
1	2	3	4	5	6	7	8	9	10	11	12	13
1	MW	0.0170(±0.0016)	-2.0420	0.9590	0.7365	-	110.2941	0.7680	0.8432	0.1567	0.4330	0.4284
2	MW	0.0246(±0.0019)	-0.9172	0.8349	0.8106	0.6496	88.1335	0.9708	0.5219	0.4780	0.3769	0.3709
	PC	-0.0073(±0.0013)										
3	MW	0.0274(±0.0021)	-0.5324	0.8018	0.8289	0.6768	66.6081	1.0338	0.4554	0.5445	0.3602	0.3543
	PC	-0.0083(±0.0013)										
	ST	-0.0101(±0.0034)										
4	MW	0.0270(±0.0020)	-3.2811	0.7670	0.8466	0.7043	56.9597	1.1037	0.3950	0.6049	0.3462	0.3370
	PC	-0.0083(±0.0012)										
	IR	1.9736(±0.6419)										
	ST	-0.0169(±0.0039)										
5	MW	0.0168(±0.0080)	-2.2596	0.6150	0.9267	-	438.1383	1.5069	0.1643	0.8356	0.3003	0.2963
6	MW	0.0177(±0.0009)	-1.9797	0.6027	0.9308	0.8626	230.1276	1.5443	0.1542	0.8458	0.2943	0.2883
	ST	-0.0083(±0.0041)										

to be continued

Continuation of Table 3

1	2	3	4	5	6	7	8	9	10	11	12	13
7	MW	0.0234(±0.0020)	-1.6326	0.5622	0.9409	0.8804	180.1664	1.6736	0.1295	0.8705	0.2745	0.2670
	MV	0.0243(±0.0073)										
	PC	-0.0142(±0.0035)										
8	MW	0.0238(±0.0020)	-2.9930	0.5419	0.9460	0.8859	147.0510	1.7457	0.1173	0.8827	0.2646	0.2555
	MV	0.0751(±0.0213)										
	PC	-0.0339(±0.0085)										
	ST	0.0285(±0.0113)										
9	MW	0.0226(±0.0021)	-2.9870	0.5345	0.9483	0.8919	121.4615	1.7742	0.1119	0.8881	0.2610	0.2502
	MR	0.0345(±0.0202)										
	MV	0.0733(±0.0211)										
	PC	-0.0368(±0.0085)										
	ST	0.0284(±0.0111)										
10	MW	0.0223(±0.0021)	-3.0268	0.5294	0.9501	0.8940	103.5636	1.7946	0.1078	0.8921	0.2585	0.2460
	MR	0.0332(±0.0200)										
	MV	0.0738(±0.0209)										
	PC	-0.0372(±0.0085)										
	ST	0.0280(±0.0110)										
	Pol	0.0134(±0.0088)										
11	MW	0.0156(±0.0008)	-1.9430	0.8404	0.8293	-	363.7580	0.9869	0.4535	0.5464	0.3788	0.3765
12	MW	0.0220(±0.0013)	-0.8870	0.7609	0.8635	0.7426	240.4544	1.1348	0.3410	0.6590	0.3430	0.3399
	PC	-0.0065(±0.0010)										
13	MW	0.0243(±0.0013)	-0.4711	0.7326	0.8750	0.7614	177.5761	1.1944	0.3059	0.6941	0.3302	0.3262
	PC	-0.0074(±0.0010)										
	ST	-0.0097(±0.0026)										

to be continued

Continuation of Table 3

1	2	3	4	5	6	7	8	9	10	11	12	13
14	MW	0.0238(±0.0013)	-2.5742	0.7132	0.8827	0.7739	143.0207	1.2377	0.2831	0.7169	0.3215	0.3166
	PC	-0.0072(±0.0010)										
	IR	1.5036(±0.4758)										
	ST	-0.0148(±0.0030)										
15	MW	0.0228(±0.0014)	-2.3970	0.7086	0.8851	0.7768	116.5406	1.2491	0.2762	0.7238	0.3194	0.3136
	MR	0.0284(±0.0161)										
	PC	-0.0100(±0.0019)										
	IR	1.3090(±0.4854)										
	ST	-0.0136(±0.0030)										
16	MR	0.0525(±0.0166)	-5.0571	0.6788	0.8958	0.7951	108.3345	1.3197	0.2460	0.7540	0.3060	0.2995
	MV	0.0061(±0.0056)										
	PC	-0.0046(±0.0021)										
	IR	1.1157(±0.4662)										
	ST	-0.0287(±0.0044)										
	<i>d</i>	2.9902(±0.1794)										



**Table 4.** Observed and predicted values of  $\log \text{IGC}^{-1}_{50}$  using model 16 and their residuals

Comp. No	Obs. $\lg \text{IGC}^{-1}_{50}$	Est. $\lg \text{IGC}^{-1}_{50}$	Residual	Comp. No	Obs. $\lg \text{IGC}^{-1}_{50}$	Est. $\lg \text{IGC}^{-1}_{50}$	Residual
1	2	3	4	5	6	7	8
<b>1</b>	-0.520	-0.161	-0.359	<b>43</b>	0.270	0.122	0.148
<b>2</b>	-0.510	-0.359	-0.151	<b>44</b>	0.270	0.743	-0.473
<b>3</b>	-0.510	0.081	-0.591	<b>45</b>	0.280	0.117	0.163
<b>4</b>	-0.380	0.154	-0.534	<b>46</b>	0.280	0.076	0.204
<b>5</b>	-0.360	0.157	-0.517	<b>47</b>	0.330	0.119	0.211
<b>6</b>	-0.330	0.081	-0.411	<b>48</b>	0.360	0.129	0.231
<b>7</b>	-0.300	-0.177	-0.123	<b>49</b>	0.370	0.455	-0.085
<b>8</b>	-0.300	-	-	<b>50</b>	0.380	0.472	-0.092
<b>9</b>	-0.300	0.131	-0.431	<b>51</b>	0.380	0.287	0.093
<b>10</b>	-0.240	-	-	<b>52</b>	0.380	-0.118	0.498
<b>11</b>	-0.210	-0.312	0.102	<b>53</b>	0.390	0.513	-0.123
<b>12</b>	-0.180	-0.181	0.001	<b>54</b>	0.420	0.122	0.298
<b>13</b>	-0.160	0.421	-0.581	<b>55</b>	0.450	0.248	0.202
<b>14</b>	-0.140	0.081	-0.221	<b>56</b>	0.460	0.743	-0.283
<b>15</b>	-0.140	0.472	-0.612	<b>57</b>	0.470	0.565	-0.095
<b>16</b>	-0.090	0.417	-0.507	<b>58</b>	0.470	0.073	0.397
<b>17</b>	-0.080	-0.161	0.081	<b>59</b>	0.480	0.390	0.090
<b>18</b>	-0.060	-0.181	0.121	<b>60</b>	0.480	0.571	-0.091
<b>19</b>	-0.060	-0.220	0.160	<b>61</b>	0.510	0.327	0.183
<b>20</b>	-0.050	0.320	-0.370	<b>62</b>	0.540	0.743	-0.203
<b>21</b>	-0.030	0.472	-0.502	<b>63</b>	0.550	0.413	0.137
<b>22</b>	0.010	0.151	-0.141	<b>64</b>	0.570	0.390	0.180
<b>23</b>	0.020	0.441	-0.421	<b>65</b>	0.570	0.420	0.150
<b>24</b>	0.020	0.152	-0.132	<b>66</b>	0.600	0.587	0.013
<b>25</b>	0.030	-0.220	0.250	<b>67</b>	0.620	0.940	-0.320
<b>26</b>	0.050	0.210	-0.160	<b>68</b>	0.640	0.041	0.599
<b>27</b>	0.070	0.013	0.057	<b>69</b>	0.350	0.013	0.337
<b>28</b>	0.080	-0.033	0.113	<b>70</b>	0.670	0.326	0.344
<b>29</b>	0.080	-0.013	0.093	<b>71</b>	0.690	0.569	0.121
<b>30</b>	0.080	0.317	-0.237	<b>72</b>	0.700	0.771	-0.071
<b>31</b>	0.090	0.023	0.067	<b>73</b>	0.700	0.344	0.356
<b>32</b>	0.110	-0.033	0.143	<b>74</b>	0.710	0.404	0.306
<b>33</b>	0.120	-0.033	0.153	<b>75</b>	0.740	1.019	-0.279
<b>34</b>	0.120	-0.033	0.153	<b>76</b>	0.750	0.930	-0.180
<b>35</b>	0.130	-0.118	0.248	<b>77</b>	0.760	0.690	0.070
<b>36</b>	0.160	-0.064	0.224	<b>78</b>	0.780	0.534	0.246
<b>37</b>	0.170	0.781	-0.611	<b>79</b>	0.800	0.490	0.310
<b>38</b>	0.180	0.413	-0.233	<b>80</b>	0.870	0.413	0.457
<b>39</b>	0.190	0.152	0.038	<b>81</b>	0.880	0.347	0.533
<b>40</b>	0.210	-0.065	0.275	<b>82</b>	0.950	0.743	0.207
<b>41</b>	0.230	-0.065	0.295	<b>83</b>	1.040	1.019	0.021
<b>42</b>	0.250	0.154	0.096	<b>84</b>	1.130	0.715	0.415

to be continued

Continuation of Table 4

1	2	3	4	5	6	7	8
<b>85</b>	1.130	1.019	0.111	<b>130</b>	0.990	1.296	-0.306
<b>86</b>	1.170	0.942	0.228	<b>131</b>	1.070	1.296	-0.226
<b>87</b>	1.280	1.019	0.261	<b>131</b>	1.090	0.784	0.306
<b>88</b>	1.410	1.535	-0.125	<b>133</b>	1.130	1.296	-0.166
<b>89</b>	1.570	1.485	0.085	<b>134</b>	1.130	1.296	-0.166
<b>90</b>	1.640	0.977	0.663	<b>135</b>	1.160	1.296	-0.136
<b>91</b>	1.750	1.902	-0.152	<b>136</b>	1.180	0.780	0.400
<b>92</b>	1.750	-	-	<b>137</b>	1.250	0.669	0.581
<b>93</b>	2.050	-	-	<b>138</b>	1.300	0.669	0.631
<b>94</b>	2.100	1.535	0.565	<b>139</b>	1.430	1.762	-0.332
<b>95</b>	2.220	1.891	0.329	<b>140</b>	1.510	1.762	-0.252
<b>96</b>	2.370	-	-	<b>141</b>	1.530	1.762	-0.232
<b>97</b>	2.710	1.984	0.726	<b>142</b>	1.780	2.179	-0.399
<b>98</b>	-1.640	-	-	<b>143</b>	1.820	2.179	-0.359
<b>99</b>	-0.190	0.451	-0.641	<b>144</b>	2.190	2.084	0.106
<b>100</b>	-0.160	0.362	-0.522	<b>145</b>	2.210	1.664	0.546
<b>101</b>	0.030	0.260	-0.230	<b>146</b>	2.420	-	-
<b>101</b>	0.050	0.241	-0.191	<b>147</b>	2.590	2.084	0.506
<b>103</b>	0.050	-0.191	0.241	<b>148</b>	2.740	2.462	0.278
<b>104</b>	0.080	0.260	-0.180	<b>149</b>	-0.820	-1.051	0.231
<b>105</b>	0.100	0.362	-0.262	<b>150</b>	-0.790	-0.524	-0.266
<b>106</b>	0.140	0.500	-0.360	<b>151</b>	-0.740	-0.524	-0.216
<b>107</b>	0.140	0.140	0.000	<b>151</b>	-0.700	-0.149	-0.551
<b>108</b>	0.170	0.506	-0.336	<b>153</b>	-0.520	-0.355	-0.165
<b>109</b>	0.170	0.241	-0.071	<b>154</b>	-0.500	-0.270	-0.230
<b>110</b>	0.180	0.451	-0.271	<b>155</b>	-0.470	-0.270	-0.200
<b>111</b>	0.200	0.506	-0.306	<b>156</b>	-0.380	-0.066	-0.314
<b>111</b>	0.250	0.539	-0.289	<b>157</b>	-0.340	-0.276	-0.064
<b>113</b>	0.300	0.357	-0.057	<b>158</b>	-0.260	0.065	-0.325
<b>114</b>	0.320	0.494	-0.174	<b>159</b>	-0.250	-0.285	0.035
<b>115</b>	0.330	0.621	-0.291	<b>160</b>	-0.240	-0.248	0.008
<b>116</b>	0.400	0.657	-0.257	<b>161</b>	-0.100	-0.248	0.148
<b>117</b>	0.530	0.796	-0.266	<b>161</b>	-0.060	0.271	-0.331
<b>118</b>	0.540	0.464	0.076	<b>163</b>	-0.060	-0.248	0.188
<b>119</b>	0.560	0.357	0.203	<b>164</b>	-0.020	-0.084	0.064
<b>120</b>	0.670	0.464	0.206	<b>165</b>	0.000	0.293	-0.293
<b>121</b>	0.680	0.817	-0.137	<b>166</b>	0.040	-0.084	0.124
<b>122</b>	0.680	0.765	-0.085	<b>167</b>	0.050	-0.041	0.091
<b>123</b>	0.710	0.704	0.006	<b>168</b>	0.100	-0.030	0.130
<b>124</b>	0.730	0.496	0.234	<b>169</b>	0.250	-0.281	0.531
<b>125</b>	0.800	0.329	0.471	<b>170</b>	0.280	0.319	-0.039
<b>126</b>	0.820	0.816	0.004	<b>171</b>	0.370	0.310	0.060
<b>127</b>	0.830	0.633	0.197	<b>172</b>	0.440	0.333	0.107
<b>128</b>	0.870	0.750	0.120	<b>173</b>	0.450	0.160	0.290
<b>129</b>	0.890	0.669	0.221	<b>174</b>	0.570	0.160	0.410

It has been observed that 2 compounds **8** and **93** are serious outliers and hence they were excluded from the analysis. After deletion of compounds **8** and **93** we obtained the following models:

*One-parametric.* Only one significant model has been obtained in which MW is present as correlating parameter. The model is as follows:

$$\lg \text{IGC}^{-1}_{50} = 0.0170 (\pm 0.0016) \text{MW} - 2.0420 \quad (1)$$

$N = 95, \text{SE} = 0.9590, R = 0.7365, F\text{-ratio} = 110.2941, Q = 0.7680.$

*Two-parametric.* To improve the quality of the model we tried for bi-parametric models and one such model with better statistics is obtained in which PC has been found as one of the correlating parameters along with MW.

$$\lg \text{IGC}^{-1}_{50} = 0.0246 (\pm 0.0019) \text{MW} - 0.0073 (\pm 0.0013) \text{PC} - 0.9172 \quad (2)$$

$N = 95, \text{SE} = 0.8349, R = 0.8106, F\text{-ratio} = 88.1335, Q = 0.9708.$

The negative coefficient of PC suggests that this parameter has a negative role towards  $\lg \text{IGC}^{-1}_{50}$  activity.

*Three-parametric.* When ST, PC and MW were taken together then we obtained a three-parametric model with improved statistics.

$$\begin{aligned} \lg \text{IGC}^{-1}_{50} = & 0.0274 (\pm 0.0021) \text{MW} - 0.0083 (\pm 0.0013) \text{PC} \\ & - 0.0101 (\pm 0.0034) \text{ST} - 0.5324 \end{aligned} \quad (3)$$

$N = 95, \text{SE} = 0.8018, R = 0.8289, F\text{-ratio} = 66.6081, Q = 1.0338.$

The negative sign associated with ST clearly shows that the surface tension has a retarding effect towards  $\lg \text{IGC}^{-1}_{50}$ .

*Four-parametric.*

$$\begin{aligned} \lg \text{IGC}^{-1}_{50} = & 0.0270 (\pm 0.0020) \text{MW} - 0.0083 (\pm 0.0012) \text{PC} + 1.9736 (\pm 0.6419) \text{IR} \\ & - 0.0169 (\pm 0.0039) \text{ST} - 3.2811 \end{aligned} \quad (4)$$

$N = 95, \text{SE} = 0.7670, R = 0.8466, F\text{-ratio} = 56.9597, Q = 1.1038.$

The best four-parametric model contains MW, PC, IR and ST as correlating parameters. On the basis of  $R$  and the Pogliani quality actor ( $Q$ ) (Refs 11–13) values we can infer that this is the most appropriate model for modelling the toxicity of 97 aromatic compounds used in the present study. The negative coefficients of parachor (PC), surface tension (ST) and index of refraction (IR) indicate that they have negative roles towards the toxicity ( $\lg \text{IGC}^{-1}_{50}$ ). This model shows a variance of about 71% variance. The predictive power of the model has been shown by plotting a graph of observed and estimated values and is demonstrated in Fig. 1.

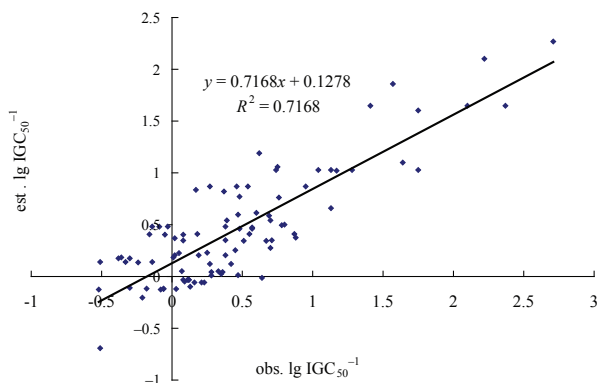


**Fig. 1.** Correlation between observed and estimated  $\lg \text{IGC}_{50}^{-1}$  using model 4

#### MODELLING OF $\lg \text{IGC}_{50}^{-1}$ FOR 77 COMPOUNDS

As discussed before the second set contains those compounds which are aromatic in nature and have a tendency to accept electrons. We have tried to model the  $\lg \text{IGC}_{50}^{-1}$  using physicochemical parameters and found that they are suitable for such studies.

While performing stepwise regression analysis it has been observed that compounds **98**, **137** and **138** are serious outliers hence they were deleted from the data set. Their exceptional behaviour needs explanation. All these compounds are having nitro-groups present in their structure which may be attributed for this behaviour. We have again tried to obtain the models for remaining 74 compounds and models which are statistically significant are given below.

##### *One-parametric*

$$\lg \text{IGC}_{50}^{-1} = 0.0168 (\pm 0.0008) \text{ MW} - 2.2596 \quad (5)$$

$$N = 74, \text{ SE} = 0.6150, R = 0.9267, F\text{-ratio} = 438.1383, Q = 1.5069.$$

##### *Two-parametric*

$$\lg \text{IGC}_{50}^{-1} = 0.0177 (\pm 0.0009) \text{ MW} - 0.0083 (\pm 0.0041) \text{ ST} - 1.9797 \quad (6)$$

$$N = 74, \text{ SE} = 0.6027, R = 0.9308, F\text{-ratio} = 230.1276, Q = 1.5443.$$

##### *Three-parametric*

$$\lg \text{IGC}_{50}^{-1} = 0.0234 (\pm 0.0020) \text{ MW} + 0.0243 (\pm 0.0073) \text{ MV} - 0.0142 (\pm 0.0035) \text{ PC} - 1.6326 \quad (7)$$

$$N = 74, \text{ SE} = 0.5622, R = 0.9409, F\text{-ratio} = 180.1664, Q = 1.6736.$$

### Four-parametric

$$\lg \text{IGC}_{50}^{-1} = 0.0238 (\pm 0.0020) \text{ MW} + 0.0751 (\pm 0.0213) \text{ MV} - 0.0339 (\pm 0.0085) \text{ PC} + 0.0285 (\pm 0.0113) \text{ ST} - 2.9930 \quad (8)$$

$$N = 74, \text{ SE} = 0.5419, R = 0.9460, F\text{-ratio} = 147.0510, Q = 1.7457.$$

### Five-parametric

$$\lg \text{IGC}_{50}^{-1} = 0.0226 (\pm 0.0021) \text{ MW} + 0.0345 (\pm 0.0202) \text{ MR} + 0.0733 (\pm 0.0211) \text{ MV} - 0.0368 (\pm 0.0085) \text{ PC} + 0.0284 (\pm 0.0111) \text{ ST} - 2.9870 \quad (9)$$

$$N = 74, \text{ SE} = 0.5345, R = 0.9483, F\text{-ratio} = 121.4615, Q = 1.7742.$$

### Six-parametric

$$\lg \text{IGC}_{50}^{-1} = 0.0223 (\pm 0.0021) \text{ MW} + 0.0332 (\pm 0.0200) \text{ MR} + 0.0738 (\pm 0.0209) \text{ MV} - 0.0372 (\pm 0.0085) \text{ PC} + 0.0280 (\pm 0.0110) \text{ ST} + 0.0134 (\pm 0.0088) \text{ Pol} - 3.0268 \quad (10)$$

$$N = 74, \text{ SE} = 0.5294, R = 0.9501, F\text{-ratio} = 103.5636, Q = 1.7946.$$

The  $R$  value for the six-parametric models has been found to be 0.9510 which is highest among all the models. Similarly the  $Q$  value is also highest in this case. Hence, it is clear that this model is the best for modelling the toxicity of present set of compounds having electron-acceptor properties. The descriptors which are found effective include MW, MR, MV, PC, ST, Pol out of which only PC has a negative role towards  $\lg \text{IGC}_{50}^{-1}$ . The predictive power of the model is demonstrated in Fig. 2.

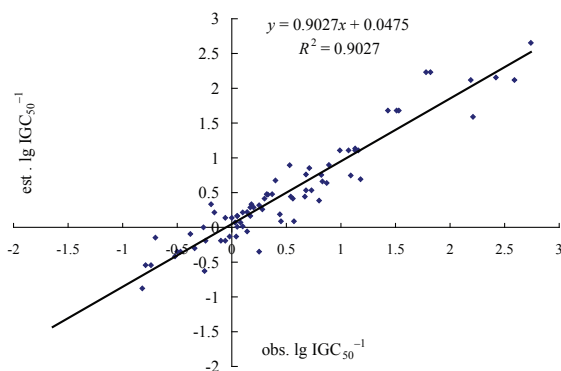


Fig. 2. Correlation between observed and estimated  $\lg \text{IGC}_{50}^{-1}$  using model 10

### MODELLING OF $\lg \text{IGC}_{50}^{-1}$ FOR 174 COMPOUNDS

When we have taken the entire data set of 174 compounds and tried to model toxicity ( $\lg \text{IGC}_{50}^{-1}$ ) we have obtained numerous statistically significant models but during the analysis compounds **8**, **10**, **92**, **93**, **96**, **98** and **146** were found to be serious outliers hence they were deleted from further analysis. Again the data was subjected to

regression analysis and the step wise regression resulted into following statistically significant models.

*One-parametric*

$$\lg \text{IGC}^{-1}_{50} = 0.0156 (\pm 0.0008) \text{MW} - 1.9430 \quad (11)$$

$N = 167, \text{SE} = 0.8404, R = 0.8293, F\text{-ratio} = 363.7580, Q = 0.9869.$

*Two-parametric*

$$\lg \text{IGC}^{-1}_{50} = 0.0220 (\pm 0.0013) \text{MW} - 0.0065 (\pm 0.0010) \text{PC} - 0.8870 \quad (12)$$

$N = 167, \text{SE} = 0.7609, R = 0.8635, F\text{-ratio} = 240.4544, Q = 1.1348.$

*Three-parametric*

$$\lg \text{IGC}^{-1}_{50} = 0.0243 (\pm 0.0013) \text{MW} - 0.0074 (\pm 0.0010) \text{PC} - 0.0097 (\pm 0.0026) \text{ST} - 0.4711 \quad (13)$$

$N = 167, \text{SE} = 0.7326, R = 0.8750, F\text{-ratio} = 177.5761, Q = 1.1944.$

*Four-parametric*

$$\lg \text{IGC}^{-1}_{50} = 0.0238 (\pm 0.0013) \text{MW} - 0.0072 (\pm 0.0010) \text{PC} + 1.5036 (\pm 0.4758) \text{IR} - 0.0148 (\pm 0.0030) \text{ST} - 2.5742 \quad (14)$$

$N = 167, \text{SE} = 0.7132, R = 0.8827, F\text{-ratio} = 143.0207, Q = 1.2377.$

*Five-parametric*

$$\lg \text{IGC}^{-1}_{50} = 0.0228 (\pm 0.0014) \text{MW} + 0.0284 (\pm 0.0161) \text{MR} - 0.0100 (\pm 0.0019) \text{PC} + 1.3090 (\pm 0.4854) \text{IR} - 0.0136 (\pm 0.0030) \text{ST} - 2.3970 \quad (15)$$

$N = 167, \text{SE} = 0.7086, R = 0.8851, F\text{-ratio} = 116.5406, Q = 1.2491.$

*Six-parametric*

$$\lg \text{IGC}^{-1}_{50} = 0.0525 (\pm 0.0166) \text{MR} + 0.0061 (\pm 0.0056) \text{MV} - 0.0046 (\pm 0.0021) \text{PC} + 1.1157 (\pm 0.4662) \text{IR} - 0.0287 (\pm 0.0044) \text{ST} + 2.9902 (\pm 0.1794) d - 5.0571 \quad (16)$$

$N = 167, \text{SE} = 0.6788, R = 0.8958, F\text{-ratio} = 108.3345, Q = 1.3197.$

The six-parametric model is the best for modelling in which MR, MV, PC, IR, ST and  $d$  are correlating parameters. Also PC and ST have negative roles towards  $\lg \text{IGC}^{-1}_{50}$ . The  $R$  value for this model comes out to be 0.8959 which accounts for approximately 81% variance. Also the highest  $Q$ -value for this model suggests that this is the most appropriate model for modelling the  $\lg \text{IGC}^{-1}_{50}$  value of the present set of compounds.

We have also calculated the toxicity ( $\lg \text{IGC}^{-1}_{50}$ ) of the compounds used in the present study by most appropriate models. The estimated values are found to be very close to the observed ones (Table 4). A comparison of observed versus estimated

values have been demonstrated in Fig. 3 (Table 4). The predictive power of the model has been found to be 0.8025.

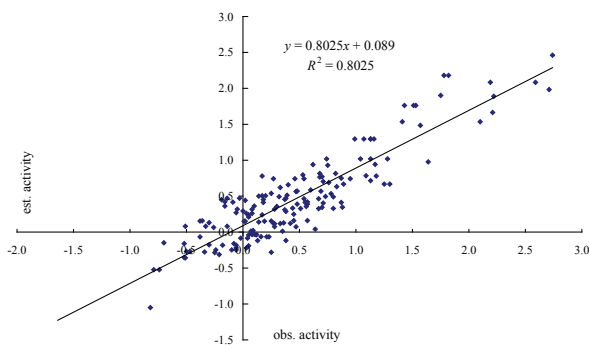


Fig. 3. Correlation between observed and estimated  $\lg \text{IGC}^{-1}_{50}$  using model 16

## CONCLUSIONS

On the basis of the above results and discussion following conclusion may be drawn:

1. The physicochemical parameters are good parameters for modelling the  $\lg \text{IGC}^{-1}_{50}$  values of present set of compounds.
2. The ST and PC have negative roles towards  $\lg \text{IGC}^{-1}_{50}$  activity. Therefore those compounds having higher value of surface tension and parachor will show lower inhibitory activity.
3. Similarly compounds with high density, molecular weight, molar refractivity and index of refraction will have higher  $\text{IGC}^{-1}_{50}$  activity.

## REFERENCES

1. M. NENDZA, J. VOLMER, W. KLEIN: Risk Assessment Based on QSAR Estimate. In: Practical Applications of Qualitative Structure–Activity Relationships in Environmental Chemistry and Toxicology (Eds N. Kalcher, J. Devillers). Kluwer Academic Publishers. Dordrecht, The Netherlands, 1990, p. 213.
2. T. W. SCHULTZ: *Tetrahymena pyriformis* Population Growth Impairment Endpoint: A Surrogate for Fish Lethality. Toxicol Method, **7**, 289 (1997).
3. S. D. DIMITROV, O. G. MEKENYAN, T. W. SCHULTZ: Interspecies Modeling of Narcotics Toxicity to Aquatic Animals. B Environ Contam Tox, **65**, 399 (2000).
4. D. R. ROY, R. PARTHASARATHI, V. SUBRAMANIAN, P. K. CHATTARAJ: An Electrophilicity Based Analysis of Toxicity of Aromatic Compounds towards *Tetrahymena pyriformis* QSAR. Comb Sci, **25**, 114 (2006).
5. J. SINGH, B. SHAIK, S. SINGH, V. K. AGRAWAL, P. V. KHADIKAR, C. T. SUPURAN: Comparative QSAR Study on Para-substituted Aromatic Sulphonamides as CAII Inhibitors : Information vs Topological (distance-based and connectivity) Indices. Chem Biol Drug Des, **71**, 244 (2008).

6. J. SINGH, S. SINGH, B. SHAIK N. SOHANI, V. K. AGRAWAL, P. V. KHADIKAR: Mutagenicity of Nitrated Polycyclic Aromatic Hydrocarbons: A QSAR Investigation. *Chem Biol Drug Des*, **71**, 230 (2008).
7. V. K. AGRAWAL, J. SINGH, S. SINGH, P. V. KHADIKAR: Use of Topological as Well as Quantum Chemical Parameters in Modeling Antimalarial Activity of 2,4-diamino-6-quinazoline Sulfonamides. *Oxid Commun*, **1**, 2 (2008).
8. P. V. KHADIKAR, J. SINGH, V. K. AGRAWAL: QSAR Study on Modeling of the Rate of Glycine Conjugation of Some Benzoic Acid Derivatives: A Topological Approach. *Oxid Commun*, **32**, 40 (2009).
9. S. CHATTERJEE, A. S. HADI, B. PRICE: *Regression Analysis by Examples*. 3rd ed. Wiley Vch., New York, 2000.
10. Chem Sketch Software for the Calculation of Referred Physicochemical Parameters: [www.acdlabs.com](http://www.acdlabs.com)
11. L. POGLIANI: Structure–Property Relationships of Amino Acids and Some Peptides. *Amino Acids*, **6**, 141 (1994).
12. L. POGLIANI: Modeling with Special Descriptors Derived from a Medium Size Set of Connectivity Indices. *J Phys Chem*, **100**, 18065(1996).
13. L. POGLIANI: From Molecular Connectivity Indices to Semi-empirical Connectivity Terms: Recent Trend in Graph Theoretical Descriptors. *Chem Rev*, **100**, 3827 (2000).

*Received 12 January 2010*

*Revised 14 February 2010*



## **ENVIRONMENTAL RISK ASSESSMENT OF BISPHENOL A AND ITS METABOLITES AS ENDOCRINE DISRUPTORS**

Y. KOLEVA<sup>a\*</sup>, S. GEORGIEVA<sup>b</sup>

<sup>a</sup>*Department of Organic Chemistry, 'Prof. Assen Zlatarov' University–Bourgas, 1 'Prof. Yakimov' Street, 8010 Bourgas, Bulgaria*

*E-mail: yanuriana@abv.bg*

<sup>b</sup>*Department of Pharmacy, Medical College, 'Prof. Assen Zlatarov' University–Bourgas, 69 'St. Stambolov' Street, 8000 Bourgas, Bulgaria*

*E-mail: fotkova@abv.bg*

### **ABSTRACT**

One of chemical found ubiquitously in our environment, bisphenol A (BPA), has received a tremendous amount of attention from research scientists, government panels, and the popular press. Understanding this topic is essential for educating the public professionals about potential risks associated with developmental exposure to BPA and other endocrine disruptors, the design of rigorously researched programs using both epidemiological and animal studies, and ultimately the development of a public health policy. The aim of this work was to predict risk assessment (persistence, bioaccumulation and chronic toxicity) of bisphenol A (parent structure) and its microbial metabolites (observed and predicted) using the QSAR models in the PBT Profiler and in addition to predict the estrogenic activity of the parent structure and metabolites of bisphenol A by the OECD (Q)SAR Application Toolbox. The estrogenic activity of the parent structure (bisphenol A) was predicted to be very strong binder by the OECD (Q)SAR Application Toolbox and the PBT Profiler has estimated that bisphenol A is persistent in the environment, is not expected to bioaccumulate in the food chain, and is chronic toxic (moderate concern). Analysis of the data reveals that the estrogenic activity of observed metabolites of bisphenol A is varied (non-cyclic structure, weak, strong and very strong binder) and for predicted metabolites of bisphenol A is non-cyclic structure and weak binder. All observed and predicted (with few exceptions) metabolites are persistent in the environment but they are not bioaccumulative. More observed metabolites are chronically toxic (high, moderate and low concern) and the toxic behaviour of predicted metabolites of bisphenol A is varied (high, moderate and low concern).

*Keywords:* bisphenol A, persistence, bioaccumulation, toxicity, environment.

---

\* For correspondence.

## AIMS AND BACKGROUND

Bisphenol A (BPA) is an industrial chemical, used to manufacture polycarbonate and numerous plastic articles. However, recent studies have shown that it can leach out of certain products, including the plastic lining of cans used for food, polycarbonate babies bottles and tableware, and white dental fillings and sealants. Low levels of BPA have also been found to cause biological effects, and its mode of action appears to mimic that of the female hormone, oestrogen. BPA, therefore, belongs to a group of chemicals termed 'hormone disruptors' or 'endocrine disruptors', that are able to disrupt the chemical messenger system in the body. There is growing international concern about man-made endocrine disrupting chemicals (EDCs), because they can derail the development of offspring exposed in the womb. It is feared that they may be partly responsible for the decline in sperm counts, and the increased rates of hormone related cancers, such as cancers of the breast, testes and prostate. They are also suspected of causing birth defects of the reproductive tract (including un-descended testes), and other hormone-related effects, such as earlier puberty in girls<sup>1</sup>.

World Wildlife Fund for Nature (WWF) is particularly concerned because the reproduction and development of many wildlife species have already been affected by EDCs released into the environment. WWF is, therefore, working to ensure that these substances are adequately controlled, which in many circumstances will include phasing them out of use. Even at very low levels, recent studies have shown that BPA can affect the sex ratio of frogs<sup>2</sup>, and can cause the sterilisation of water snails<sup>3</sup>. Given the intricate nature of ecosystems, and the lack of knowledge of the effects on many other species, this is a major concern.

Behind our backs we have the growing mountain of man-produced chemicals. It has been estimated that about 100 000 chemicals are traded commercially, plus thousands more are formed and released as by-product of chemical production, use, and combustion. Some of them are high production volume chemicals, produced or imported in quantities over 1000 t per year in the European Union<sup>4,5</sup>. Most of these chemicals lack adequate toxicological and ecotoxicological data and new chemicals are continuously being produced. Risk assessment of xenobiotics should be looked on from different views including molecular biology, cell toxicology, toxicology, ecology, chemistry and computer modelling (e.g. quantitative structure–activity relationship (QSAR) considerations). A successful risk assessment requires an approach that integrates data and knowledge from all the separate components.

The aim of this work was to predict risk assessment of bisphenol A and its microbial metabolites using the QSAR models in the PBT Profiler. In addition to predict the estrogenic activity of metabolites of bisphenol A by the OECD (Q)SAR Application Toolbox.

## EXPERIMENTAL

*Compound data.* Bisphenol A as an endocrine disruptor and its observed and predicted metabolites are presented in Tables 1–3.

*Criteria used by the PBT profiler.* The PBT profiler is a screening-level tool that provides estimates of the persistence, bioaccumulation, and chronic fish toxicity potential of chemical compounds. It is designed to be used when data are not available. In order to help interested parties make informed decision on a chemical PBT characteristics, the PBT profiler automatically identifies chemicals that may persistent in the environment and bioaccumulate in the food chain. These chemicals are identified using thresholds published by the Environmental Protection Agency (EPA) (Ref. 6).

*Persistence criteria.* The PBT profiler combines the persistence criteria for water, soil, and sediment and highlights chemicals with an estimated half-life  $\geq 2$  months and  $< 6$  months as persistent and those with an estimated half-life  $\geq 6$  months as very persistent. The half-life in air is not used in the PBT profiler Persistence summary (chemicals with an estimated half-life  $> 2$  days are considered as persistent). The PBT profiler uses 30 days in a month for its comparisons.

*Bioaccumulation criteria.* The PBT profiler combines the bioaccumulation criteria and highlights chemicals with a BCF  $\geq 1000$  and  $< 5000$  as bioaccumulative and those with a BCF  $\geq 5000$  as very bioaccumulative.

*Toxicity criteria.* To highlight a chemical that may be chronically toxic to fish, the PBT profiler uses the following criteria: Fish ChV (chronic value)  $> 10$  mg/l (low concern), fish ChV = 0.1–10 mg/l (moderate concern) and fish ChV  $< 0.1$  mg/l (high concern).

*OECD (Q)SAR application toolbox.* The OECD (Q)SAR Application Toolbox is software tool used in regulatory toxicology to fill gaps in (eco)toxicity data. They include different SAR and QSAR models for estimating (eco)toxicological endpoints. (Quantitative) Structure–Activity Relationships [(Q)SARs] are methods for estimating properties of a chemical from its molecular structure and have the potential to provide information on hazards of chemicals, while reducing time, monetary cost and animal testing currently needed<sup>7</sup>.

*Observed microbial metabolism.* Degradation pathways used by microorganism to obtain carbon and energy from 200 chemicals are stored in a special file format that allows easy computer access to catabolic information. Most of pathways are related to aerobic conditions. Different sources including monographs, scientific articles and public web sites such as the UM-BBD (Ref. 8) were used to compile the database.

*Microbial metabolism simulator.* The original CATABOL simulator of microbial metabolism is implemented in the system<sup>9–11</sup>.

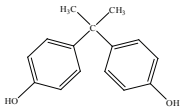
## RESULTS AND DISCUSSION

The PBT profiler uses a well-defined set of procedures to predict the persistence, bioaccumulation, and toxicity of chemical compounds when experimental data are not available. The persistence, bioaccumulation, and fish chronic toxicity values estimated by the PBT profiler are automatically compared to criteria published by EPA.

Moreover, prediction of chemical binding to the ER is important for regulatory purposes. The present work showed that the QSAR approach in the OECD (Q)SAR Toolbox has been used for identifying interaction mechanisms for bisphenol A and its microbial metabolites in Tables 1–3.

The results of the estimation of the parent structure of bisphenol A for persistence, bioaccumulation, toxicity as well as estrogenic activity are presented in Table 1.

**Table 1.** PBT profiler estimate of bisphenol A

No	CAS number, name of compound and structure	Persistence		Bio-accumulation BCF	Toxicity fish ChV (mg/l)	Predicted ER binding
		media (water, soil, sediment, air) half-life (days)	percent in each medium (%)			
1	80-05-7; bisphenol A 	38; 75; 340; 0.2	12; 88; 1; 0	72	0.55	very strong binder, OH

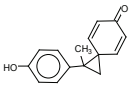
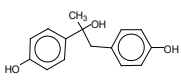
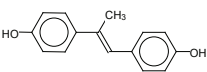
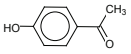
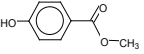
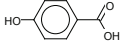
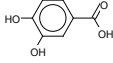
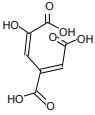
ER binding of bisphenol A was predicted to be very strong binder by the OECD (Q)SAR Application Toolbox. The PBT profiler has estimated that bisphenol A is expected to be found predominantly in soil and its persistence estimate is based on its transformation in this medium. Its half-life in soil, 75 days, exceeds the EPA criteria of  $\geq 2$  months (and  $\leq 6$  months). Therefore, bisphenol A is estimated to be persistent in the environment. Also, the PBT profiler estimates that bisphenol A is not expected to bioaccumulate in the food chain because it does not exceed the BCF criteria.

PBT chemicals are those that persist in the environment, bioconcentrate in aquatic organisms, and may bioaccumulate in humans, birds, and wild mammals. Exposure to PBT chemicals will result in chronic exposures which, in turn, leads to chronic toxicity. It is estimated that bisphenol A is chronically toxic to fish. It is important to note that bisphenol A may also be toxic to other aquatic organisms. Some aquatic organisms, such as daphnids, may be more sensitive both to acute and chronic exposures to bisphenol A.

Then, analysis of data in Table 1 reveals that bisphenol A is persistent and toxic (Fish ChV(chronic value)) but is not bioaccumulative. The toxicity of bisphenol A is with moderate value (0.1–10 mg/l).

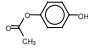
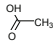
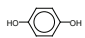
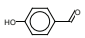
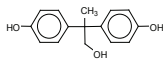
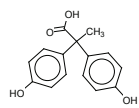
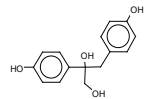
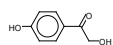
The results of the estimation of the observed metabolites of bisphenol A for persistence, bioaccumulation, toxicity as well as estrogenic activity are presented in Table 2.

**Table 2.** PBT profiler estimate of observed metabolites for bisphenol A

No	CAS number, name of metabolite and structure	Persistence		Bio- accumu- lation BCF	Toxicity fish ChV (mg/l)	Predicted ER binding
		media (water, soil, sediment, air) half-life (days)	percent in each medium (%)			
1	2	3	4	5	6	7
1		38; 75; 340; 0.24	12; 88; 1; 0	75	0.007	strong binder, OH
2		38; 75; 340; 0.19	14; 85; 0; 0	28	1.3	very strong binder, OH
3		15; 30; 140; 0.0067	16; 82; 3; 0	240	0.26	very strong binder, OH
4	99-93-4; 4-hydroxyaceto phenone 	15; 30; 140; 0.54	31; 69; 0; 0	0.94	0.004	weak binder, OH
5	99-76-3; methyl 4-hydroxy- benzoate 	15; 30; 140; 1.5	23; 76; 0; 0	9.1	0.005	weak binder, OH
6	99-96-7; 4-hydroxybenzoic acid 	15; 30; 140; 1.2	28; 72; 0; 0	3.2	0.042	weak binder, OH
7	99-50-3; 3,4-dihydroxyben- zoic acid 	15; 30; 140; 1.7	36; 64; 0; 0	3.2	96	weak binder, OH
8		2.3; 4.7; 21; 0.67	27; 73; 0; 0	3.2	13	non-cyclic structure

to be continued

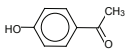
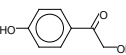
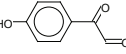
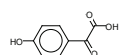
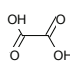
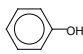
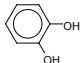
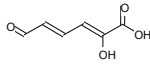
Continuation of Table 2

1	2	3	4	5	6	7
9	50-00-0; formaldehyde  <chem>H2C=O</chem>	15; 30; 140; 2	43; 54; 0; 3	3.2	3.9	non-cyclic structure
10	3233-32-7; 4-hydroxyphenyl acetate  	15; 30; 140; 0.67	34; 65; 0; 0	2.5	0.005	weak binder, OH
11	62-54-4; acetic acid, calcium salt  	8.7; 17; 78; 26	36; 62; 0; 3	3.2	2000	non-cyclic structure
12	123-31-9; hydroquinone  	15; 30; 140; 0.71	37; 63; 0; 0	3.2	0.007	weak binder, OH
13	123-08-0; 4-hydroxybenzal- dehyde  	15; 30; 140; 0.58	31; 69; 0; 0	3.6	0.004	weak binder, OH
14		38; 75; 340; 0.19	20; 80; 0; 0	7.1	5.5	very strong binder, OH
15		15; 30; 140; 0.2	18; 81; 0; 0	3.2	6.3	very strong binder, OH
16		38; 75; 340; 0.17	30; 70; 0; 0	3.1	8.6	very strong binder, OH
17		15; 30; 140; 0.5	39; 61; 0; 0	3.2	0.005	weak binder, OH

Analysis of data in Table 2 reveals that the estrogenic activity of observed metabolites of bisphenol A is varied (non-cyclic structure, weak, strong and very strong binder). As all observed metabolites are persistent in the environment but they are not bioaccumulative. More observed metabolites are chronically toxic (high, moderate and low concern).

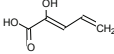
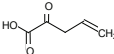
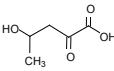
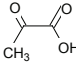
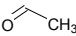
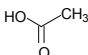
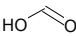
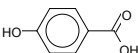
The results of the estimation of predicted metabolites of bisphenol A for persistence, bioaccumulation, toxicity as well as estrogenic activity are presented in Table 3.

**Table 3.** PBT profiler estimate of predicted metabolites for bisphenol A

No	CAS number, name of compound and structure	Persistence		Bio-accu- mulation BCF	Toxicity fish ChV (mg/l)	Predicted ER binding
		media (water, soil, sediment, air) half-life (days)	percent in each medium (%)			
1	2	3	4	5	6	7
1	99-93-4; 4-hydroxyaceto phenone 	15; 30; 140; 0.54	31; 69; 0; 0	0.94	0.004	weak binder, OH
2		15; 30; 140; 0.5	39; 61; 0; 0	3.2	0.005	weak binder, OH
3	24645-80-5; 4-hydroxyphenyl- glyoxal 	15; 30; 140; 0.18	37; 63; 0; 0	3.2	0.005	weak binder, OH
4	15573-67-8; 4-hydroxyphenyl- glyoxylic acid 	8.7; 17; 78; 0.5	32; 67; 0; 0	3.2	0.005	weak binder, OH
5	62-76-0; disodium oxalate 	15; 30; 140; 180	39; 61; 0; 0	3.2	490000000	non-cyclic structure
6	100-67-4; phenol, potassium salt 	15; 30; 140; 0.75	39; 61; 0; 0	4.3	5.300	weak binder, OH
7	120-80-9; 1,2-benzenediol 	15; 30; 140; 0.71	36; 64; 0; 0	3.2	14	weak binder, OH
8	3270-98-2; hydroxymuconic semialdehyde 	8.7; 17; 78; 0.38	34; 66; 0; 0	3.2	0.46	non-cyclic structure

to be continued

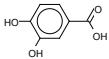
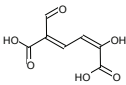
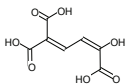
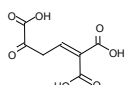
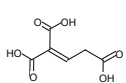
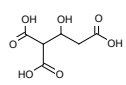
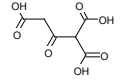
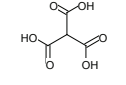
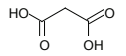
Continuation of Table 3

1	2	3	4	5	6	7
9	50480-68-7; 2-hydroxy-2,4- pentadienoic acid 	8.7; 17; 78; 0.26	42; 57; 0; 1	3.2	2.2	non-cyclic structure
10	20406-62-6; 2-oxopentenoic acid 	8.7; 17; 78; 0.36	35; 65; 0; 0	3.2	1000	non-cyclic structure
11	3318-73-8; 4-hydroxy-2-oxo- pentanoic acid 	8.7; 17; 78; 0.58	34; 65; 0; 0	3.2	18000	non-cyclic structure
12	113-24-6; sodium pyruvate 	15; 30; 140; 160	39; 61; 0; 0	3.2	8900000	non-cyclic structure
13	75-07-0; acetaldehyde 	15; 30; 140; 0.96	49; 46; 0; 5	3.2	13	non-cyclic structure
14	62-54-4; calcium acetate 	8.7; 17; 78; 26	36; 62; 0; 3	3.2	2000	non-cyclic structure
15	50-00-0; formaldehyde $H_2C=O$	15; 30; 140; 2	43; 54; 0; 3	3.2	3.9	non-cyclic structure
16	64-18-6; formic acid 	8.7; 17; 78; 31	36; 60; 0; 4	3.2	460	non-cyclic structure
17	99-96-7; 4-hydroxybenzoic acid 	15; 30; 140; 1.2	28; 72; 0; 0	3.2	0.042	weak binder, OH

to be continued



Continuation of Table 3

1	2	3	4	5	6	7
18	99-50-3; 3,4-dihydroxyben- zoic acid 	15; 30; 140; 1.7	36; 64; 0; 0	3.2	96	weak binder, OH
19		8.7; 17; 78; 0.54	34; 65; 0; 0	3.2	1.6	non-cyclic structure
20		2.3; 4.7; 21; 0.67	27; 73; 0; 0	3.2	40	non-cyclic structure
21		2.3; 4.7; 21; 0.54	27; 73; 0; 0	3.2	1100000	non-cyclic structure
22		2.3; 4.7; 21; 0.54	27; 73; 0; 0	3.2	69000	non-cyclic structure
23		2.3; 4.7; 21; 1.1	27; 73; 0; 0	3.2	1300000	non-cyclic structure
24		2.3; 4.7; 21; 5.4	27; 73; 0; 0	3.2	3600000	non-cyclic structure
25		2.3; 4.7; 21; 6.7	27; 73; 0; 0	3.2	340000	non-cyclic structure
26	141-82-2; malonic acid 	8.7; 17; 78; 10	34; 66; 0; 0	3.2	48000	non-cyclic structure

Analysis of data in Table 3 reveals that the estrogenic activity of predicted metabolites of bisphenol A is varied (non-cyclic structure and weak binder). With few exceptions, predicted metabolites are persistent in the environment but they are not bioaccumulative. The toxic behaviour of predicted metabolites of bisphenol A is varied (high, moderate and low concern).

## CONCLUSIONS

Quantitative structure–activity relationships (QSAR) methods can be applied to estimate the behaviour of bisphenol A and its metabolites (observed and predicted) in the environment and to predict their estrogenic activity. The analyses of results of this work on bisphenol A and its metabolites (observed and predicted) show that the

parent structure and its metabolites are largely persistent in the environment but they are not bioaccumulative. Bisphenol A and most metabolites (observed and predicted) are chronically toxic. Moreover, the estrogenic activity of bisphenol A shows that it is very strong binder, its observed metabolites have different estrogenic activity and predicted metabolites have no estrogenic activity or are weak binders.

## REFERENCES

1. G. LYONS: Bisphenol A. A Known Endocrine Disruptor. A WWF European Toxics Programme Report, 2000.
2. W. KLOAS, R. EINSPANIER, I. LUTZ: Amphibians as a Model to Study Endocrine Disruptors: II. Estrogenic Activity of Environmental Chemicals *in vitro* and *in vivo*. *Sci Total Environ*, **225**, 59 (1999).
3. J. OEHLMANN, U. SCHULTE-OEHLMANN, W. KLOAS, O. JAGNYTSCH, I. LUTZ, K. O. KUSK, L. WOLLENBERGER, E. M. SANTOS, G. C. PAULL, K. J. W. van LOOK, C. R. TYLER: A Critical Analysis of the Biological Impacts of Plasticizers on Wildlife. *Ecotoxicology*, **9**, 383 (2000).
4. D. STANNERS, P. BOURDEAU: Europe's Environment – the Debris Assessment. Office for Official Publications of the European Communities, Luxembourg, 1995.
5. J. W. THORNTON: Nonmammalian Nuclear Receptors: Evolution and Endocrine Disruption. *Pure Appl Chem*, **75** (11–12), 1827 (2003).
6. Criteria Used by the PBT Profiler: <http://www.pbtprofiler.net/criteria.asp>; J. E. GIRARD: In: Principles of Environmental Chemistry. Ch. 14. Organic Chemicals in the Environment. 2nd ed. Jones & Bartlett Publishers, LLC, 2010, 402–439.
7. OECD (Q)SARs Application Toolbox: [http://www.oecd.org/document/23/0,3343,en\\_2649\\_34379\\_33957015\\_1\\_1\\_1\\_1,00.html](http://www.oecd.org/document/23/0,3343,en_2649_34379_33957015_1_1_1_1,00.html)
8. L. B. M. ELLIS, D. ROE, L. P. WACKETT: The University of Minnesota Biocatalysis/Biodegradation Database: the First Decade. *Nucleic Acids Res*, **34**, D517 (2006).
9. J. JAWORSKA, S. DIMITROV, N. NIKOLOVA, O. MEKENYAN: Probabilistic Assessment of Biodegradability Based on Metabolic Pathways: CATABOL System. *SAR QSAR Environ Res*, **13**, 307 (2002).
10. S. DIMITROV, R. BRETON, D. MACKDONALD, J. WALKER, O. MEKENYAN: Quantitative Prediction of Biodegradability, Metabolite Distribution and Toxicity of Stable Metabolites. *SAR QSAR Environ Res*, **13**, 445 (2002).
11. S. DIMITROV, V. KAMENSKA, J. D. WALKER, W. WINDLE, R. PURDY, M. LEWIS, O. MEKENYAN: Predicting the Biodegradation Products of Perfluorinated Chemicals Using CATABOL. *SAR QSAR Environ Res*, **15**, 69 (2004).

*Received 16 April 2012*

*Revised 21 July 2012*

## **EVALUATION OF OXIDATIVE STRESS MARKERS AND ANTIOXIDANT STATUS IN THE ALZHEIMER DISEASE, VASCULAR DEMENTIA AND THE PARKINSON DISEASE**

A. GONENC<sup>a\*</sup>, A. HACISEVKI<sup>a</sup>, A. K. ERDEMOGLU<sup>b</sup>, M. E. DAGKIRAN<sup>a</sup>, M. TORUN<sup>a</sup>

<sup>a</sup>*Department of Biochemistry, Faculty of Pharmacy, Gazi University, Ankara, Turkey*

*E-mail: aymelek@gazi.edu.tr*

<sup>b</sup>*Department of Neurology, Faculty of Medicine, Kirikkale University, Kirikkale, Turkey*

### **ABSTRACT**

Oxidative stress may be involved in pathogenesis of neurodegenerative diseases. We aimed to measure MDA, NO, 8-OHdG and TAC, SOD and CAT levels in the Alzheimer disease, Parkinson disease and vascular dementia, and evaluate oxidant and antioxidant status in these diseases. Oxidative stress parameters were measured in 20 patients with vascular dementia, 20 patients with the Alzheimer disease, 20 patients with the Parkinson disease and 20 matching controls. MDA, NO and TAC were assayed with spectrophotometric methods. 8-OHdG was quantitated by the Elisa method. SOD and CAT were assayed with colorimetric methods. MDA, NO, 8-OHdG and SOD levels in total patient group were higher ( $p = 0.039$ ,  $0.041$ ,  $0.021$  and  $0.045$ , respectively), while TAC levels were lower ( $p = 0.010$ ) as compared with controls. When compared to controls, the following were higher: MDA in the Parkinson disease ( $p = 0.036$ ); NO in the Alzheimer disease ( $p = 0.028$ ). However, TAC in the Alzheimer disease ( $p = 0.024$ ) were lower. We observed negative correlations between TAC and MDA in the Parkinson disease ( $r = -0.496$ ,  $p = 0.026$ ); between SOD and 8-OHdG in the Alzheimer disease ( $r = 0.526$ ,  $p = 0.017$ ).

These findings support the idea that the oxidative stress may play an important role in the pathogenesis of neurodegenerative diseases. This preliminary study shows an increase in free radical production in the Alzheimer disease and Parkinson disease. Also, there is a defect in the antioxidant defense system, which may lead to oxidative damage in patients with the Alzheimer disease.

**Keywords:** oxidative stress, lipid peroxidation, dementia, the Parkinson disease, DNA damage, antioxidant capacity.

---

\* For correspondence.

## AIMS AND BACKGROUND

There is increasing evidence that oxidative stress is involved in the pathogenesis of various neurodegenerative disorders, including the Parkinson disease, vascular dementia and the Alzheimer disease<sup>1-4</sup>. Oxidative stress is a general term which used to describe the steady state level of oxidative damage in a cell, tissue, or organ, caused by the reactive oxygen and nitrogen species and imbalance between the formation of cellular oxidants and the antioxidative processes. Free radicals, DNA, lipid and protein oxidation products, antioxidant enzymes, and antioxidant molecules are used for evaluation of oxidative stress in dementia and the Parkinson disease<sup>5-7</sup>. Nitric oxide is a free radical produced by a family of nitric oxide synthases. The sum of nitrates and nitrites was used as the measurement of nitric oxide synthase activity and biosynthesis. Higher production of nitric oxide has been observed in patients with neurodegenerative and psychiatric diseases<sup>8,9</sup>. Taking into account that the brain is rich in polyunsaturated fatty acids, free radicals are expected to initiate lipid peroxidation. Malondialdehyde represent one of the major products of lipid peroxidation. Occurrence of lipid peroxidation in the brain in dementia and Parkinson disease has been confirmed by several studies<sup>10,11</sup>.

Reactive oxygen species can also cause oxidative damage to DNA. It includes base modification, deoxyribose oxidation, strand breakage and DNA cross-linking. The most investigated DNA adduct is 8-OHdG which derives from guanine which, being the DNA base with the lowest oxidation potential, is readily oxidised<sup>12</sup>. Several studies have reported that the levels of 8-OHdG in the serum, leukocyte or cerebrospinal fluid were higher in dementia and the Parkinson disease than in age-matched controls<sup>13-15</sup>. Under normal circumstances, the brain is protected from free radical damage by a careful balance between prooxidant and antioxidant mechanisms which include antioxidant enzymes and free radical scavenging molecules<sup>16</sup>. Superoxide dismutase, catalase and glutathione peroxidase are 3 main enzymes involved in cellular protection against damage due to oxygen-derived free radicals. Non-enzymatic antioxidants include glutathione, uric acid,  $\alpha$ -tocopherol, ascorbic acid,  $\beta$ -carotene and coenzyme Q10. Many studies have shown reductions of antioxidant molecules in neurogenerative diseases when compared to the healthy controls<sup>17,18</sup>. But, studies of antioxidant enzymes in dementia and the Parkinson disease have not shown a consistent pattern<sup>19,20</sup>.

The aim of this study is to measure malondialdehyde (MDA), nitric oxide (NO), 8-hydroxy-2-deoxyguanosine (8-OHdG) and total antioxidant capacity (TAC) levels and superoxide dismutase (SOD), catalase (CAT) activities in the Alzheimer disease, vascular dementia, the Parkinson disease, and evaluate oxidant and antioxidant status in these diseases.

## EXPERIMENTAL

*Patients.* The study included 20 patients diagnosed with the Alzheimer disease (11 female, 9 male; age 78 (70–82) years), 20 patients diagnosed with the Parkinson disease (7 female, 13 male; age 68 (49–80) years), 20 patients diagnosed with vascular dementia (10 female, 10 male; age 69 (54–81) years). Control group consisted of 20 individuals (10 female, 10 male; age 62 (54–82) years with age-appropriate cognitive status. Controls have no clinical evidence of metabolic, neurological, or psychiatric disorders. Newly diagnosed patients and healthy volunteers were recruited from Kiriikkale University Hospital, Neurology Department. Neurologist trained in dementia as well as cognitive tests used to define for the status of patients. Diagnosis of dementia were made according to the DSM-IV and NINDS-AIREN criteria. The neurological state of patients with the Parkinson disease was estimated using the Unified Parkinson Disease Rating Scale. Among them were no patients with chronic systemic diseases such as diabetes, renal disease, hepatic disease, brain chronic ischemia, or malignancy. Written informed consent was obtained from all subjects before in this observational study. The study was performed in accordance with the ethical standards set by the Declaration of Helsinki and was approved by the Hospital Ethical Committee.

*Methods.* Venous blood samples were taken from overnight fasting subjects. 5 ml blood were collected into untreated tube for serum malondialdehyde, total antioxidant capacity, superoxide dismutase, catalase and 8-OHdG analyses, were collected in separate tube with EDTA for plasma NO analysis. The tubes were stored at room temperature for 30 min and then they were centrifuged at 837 g for 10 min to separate the serum/plasma. These specimens were frozen immediately at  $-60^{\circ}\text{C}$  for 2 months until analysis.

Serum MDA levels were determined with the spectrophotometric method<sup>21</sup>. Serum (100  $\mu\text{l}$ ) was mixed with 1000  $\mu\text{l}$  0.67% TBA and 500  $\mu\text{l}$  of 20% trichloroacetic acid. The mixture was incubated at  $100^{\circ}\text{C}$  for 20 min. After cooling, the mixture was centrifuged at 12 000 g for 5 min and the absorbance was measured at 530 nm using a Beckman DU 650 spectrophotometer (Beckman Instruments Ltd., High Wycombe, Buckinghamshire, UK).

Plasma NO was measured with a nitrate/nitrite assay kit (Cayman, Ann Arbor, MI, USA). This assay determines nitric oxide concentrations based on the enzymatic conversion of nitrate to nitrite by nitrate reductase. The inter-assay coefficient of variation (CV) is 4.4%.

Serum total antioxidant capacity (TAC) levels were determined according to 2,2'-azino-bis(3-ethylbenzothiazoline-6-sulphonic acid) (ABTS) radical cation (ABTS<sup>+</sup>) decolourisation assay described by Re et al.<sup>22</sup> In this method, when the aliquot of serum is added to the ABTS<sup>+</sup> solution, decolourisation as a result of the presence of serum antioxidants which reverse the formation of ABTS<sup>+</sup> is observed. Percentage inhibition values of samples and standards and total antioxidant capacity levels were calculated from a calibration curve.

SOD activity was assayed following the procedure of the Cayman SOD kit (Ann Arbor, MI, USA), which utilises a tetrazolium salt for detection of superoxide radicals. The enzyme activity is expressed as unit/ml and 1 unit of enzyme is defined as amount of enzyme needed to exhibit 50% dismutation of the superoxide radical. It has a 3.0% CV inter-assay precision.

CAT activity in the serum was assayed following the procedure of the Cayman Catalase assay kit (Ann Arbor, MI, USA), which utilises the peroxidatic function of catalase for determination of enzyme activity. One unit defined as the amount of enzyme that will caused the formation of 1.0 nmol of formaldehyde per min at 25°C. The inter-assay CV is 3.6%.

Serum 8-OHdG was measured with a competitive ELISA kit (DNA Damage ELISA kit; Assay Designs, Ann Arbor, MI, USA). Absorbance was measured by a Versamax microplate reader (Molecular Devices, Sunnyvale, CA, USA) at 450 nm. Results are expressed in nanograms per millilitre. The inter-assay coefficient of variation of the DNA damage is 5.7.

Serum total cholesterol, HDL-cholesterol and triglycerides were measured spectrophotometrically on a Hitachi P-800 autoanalyser (Roche, Almere, The Netherlands) by using a commercial kit (Roche, Mannheim, Germany). Serum high sensitive C-reactive protein (hs-CRP) was determined by automated particle-enhanced immunoturbidimetric assay performed on a Hitachi P-800 autoanalyser.

Statistical analyses were performed by using SPSS packed programme (version 10 software, SPSS Inc. Chicago, Illinois, USA). In normally distributed groups the results were presented with mean and SE, otherwise with medians and interquartile range. Data on age are presented as median and interquartile range. The significance of the differences between groups was determined by one-way analysis of variance (ANOVA) and Tukey test for normal distributions, and by the Kruskal-Wallis and Mann–Whitney U-test in abnormal distributions. Pearson correlation coefficient was used to test the strength of any associations between different variables.

## RESULTS AND DISCUSSION

The clinical characteristics and laboratory data from patient and control groups are summarised in Table 1. The levels of LDL-cholesterol in vascular dementia group were statistically higher than those of the Parkinson disease, Alzheimer disease and control groups ( $p = 0.001$ ,  $0.001$ , and  $0.046$ , respectively). No significant differences were determined in the comparison of total cholesterol, triglycerides, HDL-cholesterol and hs-CRP levels between diseased groups and controls ( $p > 0.05$ ).

MDA, NO, 8-OHdG levels and SOD activity were significantly higher in total patients when compared to the control group ( $p=0.039$ ,  $0.041$ ,  $0.021$  and  $0.045$ , respectively) (Table 2). Serum TAC levels were significantly lower in total patient group than the control group ( $p=0.010$ ). No statistical difference was determined in the comparison of CAT activity between total patients and controls ( $p=0.653$ ).

**Table 1.** Clinical characteristics and laboratory data from patient and control groups

General characteristics	PD	AD	VaD	Controls
Total number of subjects	20	20	20	20
Age (years)	68 (49–80)	78 (57–86)	69 (54–81)	62 (54–82)
BMI (kg/m <sup>2</sup> )	24.95±0.54	24.39±0.55	24.84±0.50	24.78±0.62
Gender (F/M)	7/13	11/9	10/10	10/10
Biochemical parameters				
Total cholesterol (mg/dl)	5.61±0.26	5.89±0.30	6.15±0.43	5.93±0.33
Triglycerides (mg/dl)	1.89±0.11	2.01±0.13	2.12±0.19	2.03±0.14
LDL-cholesterol (mg/dl)	3.72±0.15*	3.79±0.15*	4.66±0.17	4.06±0.17**
HDL-cholesterol (mg/dl)	1.13±0.04	1.13±0.04	1.16±0.02	1.20±0.03
hs-CRP (mg/dl)	0.20±0.02	0.16±0.02	0.19±0.02	0.15±0.02

Abbreviations: PD – the Parkinson disease, AD – the Alzheimer disease, VaD – vascular dementia; Values are represented as median (IQR); \*as compared to VaD group,  $p=0.001$ ; \*\* as compared to VaD group,  $p = 0.046$ .

**Table 2.** MDA, NO, TAC and 8-OHdG levels and SOD, CAT activities in total patients and controls

	Total patients (N=60)	Controls (N=20)	<i>p</i>
MDA (μmol/l)	2.41 (1.88–3.58)	2.03 (1.78–2.48)	0.039
NO (μmol/l)	39.08 (30.51–51.63)	32.38 (28.86–40.30)	0.041
TAC (mmol/l)	1.87 (1.68–1.96)	1.97 (1.85–2.05)	0.010
SOD (U/ml)	5.44 (4.05–7.29)	4.71 (3.53–5.63)	0.045
CAT (nmol/min/ml)	49.37 (30.16–70.37)	43.57 (36.99–55.10)	0.653
8-OHdG (ng/ml)	8.65 (6.88–10.44)	7.24 (5.35–8.66)	0.021

Abbreviations: MDA – malondialdehyde; NO – nitric oxide; TAC – total antioxidant capacity; SOD – superoxide dismutase; CAT – catalase; 8-OHdG=8-hydroxy-2-deoxyguanosine; values are represented as median (IQR).

A significant increase of serum MDA levels was found in patients with the Parkinson disease ( $3.09±0.37$ ) as compared with controls ( $2.05±0.12$ ) ( $p=0.036$ ) (Fig. 1a). NO levels in the Alzheimer disease group ( $46.63±3.52$ ) were found higher than those of control group ( $34.27±1.71$ ) ( $p=0.028$ ) (Fig. 1b). A significant decrease of serum TAC levels was observed in patients with the Alzheimer disease ( $1.77±0.05$ ) when compared to controls ( $1.96±0.03$ ) ( $p=0.024$ ) (Fig. 1a). No significant differences were determined in the comparison of SOD and CAT activities and 8-OHdG levels between patient and control groups.

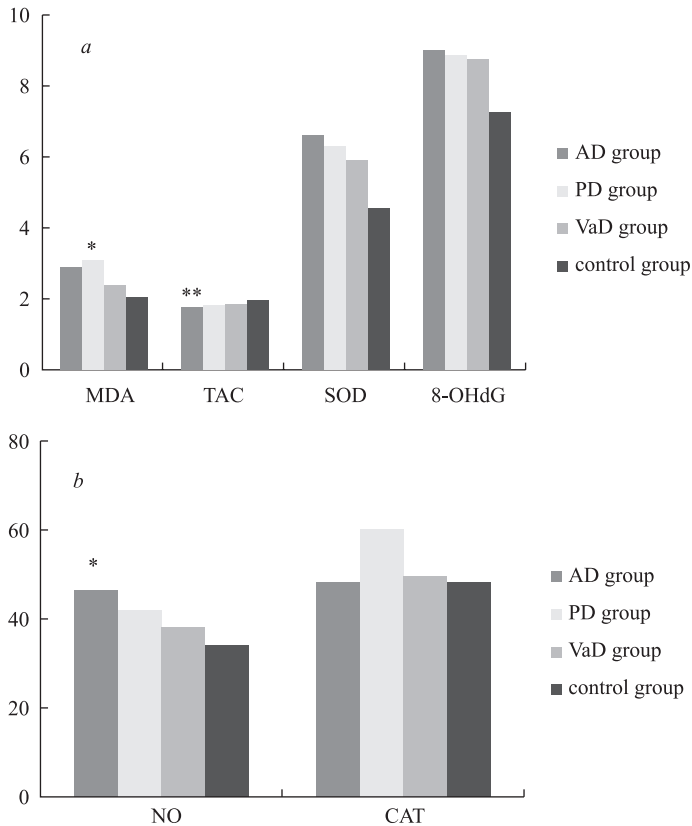


**Fig. 1.** *a* – Comparison of MDA, TAC, SOD and 8-OHdG levels between AD, PD, VaD and control groups (\* significant difference from control group ( $p=0.036$ ); \*\* significant difference from control group ( $p=0.028$ )); *b* – comparison of NO and CAT levels between AD, PD, VaD and control groups (\* significant difference from control group ( $p=0.024$ ))

Using bivariate correlation analysis of the measured parameters, serum TAC values in patients with the Parkinson disease showed negative correlation with MDA ( $r = -0.496$ ,  $p=0.026$ ) (Table 3). There was inverse correlation between SOD and 8-OHdG ( $r = -0.526$ ,  $p=0.017$ ) in patients with the Alzheimer disease.

**Table 3.** The Pearson correlation coefficients between measured parameters in patient groups

		MDA	8-OHdG
PD ( $N=20$ ) $p=0.026$	TAC	$r = -0.496$	–
AD ( $N=20$ ) $p=0.017$	SOD	–	$r = -0.526$

Oxidative stress has been implicated in a wide variety of pathological processes<sup>23–25</sup>. In the present study, we measured the MDA, NO, 8-OHdG, TAC levels and activi-



ties of some enzymatic antioxidant systems (SOD and CAT) as an oxidative stress biomarkers in the blood of patients with dementia and the Parkinson disease, compared to aged-match control group. Our data show that oxidative stress is found in these neurodegenerative diseases. The most important findings of our study were higher concentrations of MDA, indicating increased lipid peroxidation in the Parkinson disease; higher concentrations of NO and lower levels of TAC in the Alzheimer disease.

The free radical reaction of these lipids with molecular oxygen is a process known as lipid peroxidation, a process that involves intermediate oxygen containing free radicals that attack and abstract hydrogen atoms from lipids, particularly polyunsaturated lipids. Brain membrane phospholipids are composed of polyunsaturated fatty acids, which are especially vulnerable to free radical attack because their double bonds allow easy removal of hydrogen ions. Several studies have demonstrated raised malondialdehyde levels in dementia and the Parkinson patients compared with age-matched controls<sup>26,27</sup>. In this study, we have found higher MDA concentrations in total neurodegenerative patients compared to those of control subjects. Malondialdehyde levels were highest in the Parkinson disease group, and a significant difference was found only in this patient group compared to controls. These finding is in agreement with other study about the Parkinson disease, showing increases in systemic oxidative stress, measured in serum as lipid peroxidation levels<sup>28</sup>. On the contrary, other study reported no significant changes in serum level of malondialdehyde in the Parkinson disease patients<sup>29</sup>.

Oxidative stress and vascular dysfunction have been recognised as contributing factors in the pathogenesis of the Alzheimer disease and vascular dementia<sup>30,31</sup>. In the previous study decrease of serum NO levels in patients with the Alzheimer disease as compared with controls had been reported<sup>32</sup>. This evidence has been recently documented by Corzo et al.<sup>33</sup> who found lower serum NO concentrations in vascular dementia and the Alzheimer groups, as compared with controls. Lepara et al.<sup>34</sup> did not find significant differences in plasma NO levels between 2 dementia groups and controls. Our data show significant higher levels of NO in total neurodegenerative patient group compare with healthy subjects. In this study, the highest NO plasma levels were observed in the Alzheimer disease patients, and a significant difference was found only in this patient group compared to controls. The excess of NO observed in the Alzheimer disease group may reflect overproduction of nitric oxide by astrocytes and microglia which could be neurotoxic and may play a role in neurodegeneration.

Oxidative damage to DNA may play an important role in neurodegenerative diseases. Several studies demonstrate an increase in oxidative DNA damage in the brains of subjects with the Alzheimer and Parkinson diseases<sup>35,36</sup>. The most pronounced DNA adduct described is 8-OHdG is increased in nuclear and mitochondrial brain fractions in the Alzheimer disease. Migliore et al.<sup>37</sup> reported a statistically significant increase in the amounts of 8-OHdG in peripheral blood cells of patients with the Alzheimer disease compared with controls. Higher 8-OHdG has also been reported in the leukocytes and urine of the Parkinson disease patients compared to controls<sup>14,38</sup>. Our data show

significant higher concentrations of 8-OHdG in the serum of total neurodegenerative patient group. However, any significant difference was not found between dementia or the Parkinson disease groups compared to healthy controls.

The results for enzymes providing protection against free radical-induced cellular damage are equivocal. Reduced activities of antioxidant enzymes in dementia support a role for oxidative stress in the neurodegeneration of dementia and the Parkinson disease<sup>12,19,28,39</sup>. However, some studies have reported that SOD activity to be increased in the Alzheimer disease<sup>20,40</sup>. In this study SOD activity in total neurodegenerative patients was significantly higher than in the control group. The high level of SOD enzyme activity in these patients may be associated with accumulation of H<sub>2</sub>O<sub>2</sub> and excessive free radicals. However, any significant difference was not found between dementia or the Parkinson disease groups compared to healthy controls.

The brain contains only small amounts of CAT. It has been reported that lower in CAT activity in patients with the Parkinson disease as well as in dementias<sup>19,40,41</sup>. However, it has been reported similar erythrocyte CAT activity of subjects with the Alzheimer compared to the controls<sup>28</sup>. In this study, we found that CAT activity is higher in total patient group compared with age-matched control subjects, but statistically significant difference were not found between the Alzheimer disease, vascular dementia, the Parkinson disease and controls.

Foy et al.<sup>18</sup> have found significant reductions in antioxidants in dementia and the Parkinson disease patients when they are compared to the controls. Vaisi-Raygani et al.<sup>40</sup> and Gackowski et al.<sup>42</sup> have also found diminished total antioxidant levels in patients with dementia. Our study has shown that totally neurodegenerative patient group had a lower level of TAC in comparison to controls. TAC levels in the Alzheimer disease group was the lowest compared to controls. This indicates that non-enzymatic antioxidant defense was lower in the Alzheimer disease. Our finding is in accordance with previous studies<sup>18,40,42</sup>.

## CONCLUSIONS

In conclusion, these findings support the idea that the oxidative stress may play an important role in the pathogenesis of neurodegenerative diseases. Our study shows an increase in nitric oxide production in the Alzheimer disease and lipid peroxidation in the Parkinson disease. Also, there is a defect in the antioxidant defense system, which may lead to oxidative damage in patients with the Alzheimer disease. In spite of small number of participants, the present study is one of the limited number of studies evaluating many oxidative stress biomarkers in both dementia and the Parkinson disease. Larger studies are required to establish oxidant-antioxidant status these diseases.

## REFERENCES

1. A. KIKUCHI, A. TAKEDA, H. ONODERA, T. KIMPARA, K. HISANAGA, N. SATO, A. NUNOMURA, R.J. CASTELLANI, G. PERRY, M. A. SMITH, Y. ITOYAMA: Systemic Increase of

- Oxidative Nucleic Acid Damage in Parkinson's Disease and Multiple System Atrophy. *Neurobiol Dis*, **9**, 244 (2002).
2. A. AGIL, R. DURÁN, F. BARRERO, B. MORALES, M. ARAÚZO, F. ALBA, M.T. MIRANDA, I. PRIETO, M. RAMÍREZ, F. VI: Plasma Lipid Peroxidation in Sporadic Parkinson Disease: Role of the L-dopa. *J Neurol Sci*, **31**, 240 (2006).
  3. M. F. BEAL: Oxidative Damage as an Early Marker of Alzheimer's Disease and Mild Cognitive Impairment. *Neurobiol Ageing*, **26**, 585 (2005).
  4. F. MANGIALASCHE, M. C. POLIDORI, R. MONASTERO, S. ERCOLANI, C. CAMARDA, R. CECCHETTI, P. MECOCCI: Biomarkers of Oxidative and Nitrosative Damage in Alzheimer's Disease and Mild Cognitive Impairment. *Ageing Res Rev*, **8**, 285 (2009).
  5. S. YOUNES-MHENNI, M. FRIH-AYED, A. KERKENI, M. BOST, G. CHAZOT: Peripheral Blood Markers of Oxidative Stress in Parkinson's Disease. *Eur Neurol*, **58**, 78 (2007).
  6. C. ISOBE, T. ABE, Y. TERAYAMA: Levels of Reduced and Oxidized Coenzyme Q-10 and 8-hydroxy-2'-deoxyguanosine in the Cerebrospinal Fluid of Patients with Living Parkinson's Disease Demonstrate that Mitochondrial Oxidative Damage and/or Oxidative DNA Damage Contributes to the Neurodegenerative Process. *Neurosci Lett*, **469**, 159 (2009).
  7. J. GREILBERGER, C. KOIDL, M. GREILBERGER, M. LAMPRECHT, K. SCHROECKSNADEL, F. LEBLHUBER, D. FUCHS, K. OETTL: Malondialdehyde, Carbonyl Proteins and Albumindisulphide as Useful Oxidative Markers in Mild Cognitive Impairment and Alzheimer's Disease. *Free Radic Res*, **42**, 633 (2008).
  8. M. VALKO, D. LEIBFRITZ, J. MONCOL, M.T. CRONIN, M. MAZUR, J. TELSER: Free Radicals and Antioxidants in Normal Physiological Functions and Human Disease. *Int J Biochem Cell Biol*, **1**, 44 (2007).
  9. E. MARIANI, M. C. POLIDORI, A. CHERUBINI, P. MECOCCI: Oxidative Stress in Brain Aging, Neurodegenerative and Vascular Diseases: An Overview. *J Chromatogr B: Analyt Technol Biomed Life Sci*, **1**, 65 (2005).
  10. M. SHAMOTO-NAGAI, W. MARUYAMA, Y. HASHIZUME, M. YOSHIDA, T. OSAWA, P. RIEDERER, M. NAOI: In Parkinsonian Substantia Nigra, Alpha-Synuclein Is Modified by Acrolein, a Lipid-peroxidation Product, and Accumulates in the Dopamine Neurons with Inhibition of Proteasome Activity. *J Neural Transm*, **114**, 1559 (2007).
  11. M. PADURARIU, A. CIOBICA, L. HRITCU, B. STOICA, W. BILD, C. STEFANESCU: Changes of Some Oxidative Stress Markers in the Serum of Patients with Mild Cognitive Impairment and Alzheimer's Disease. *Neurosci Lett*, **469**, 6 (2010).
  12. M. A. LOVELL, W. R. MARKESBERY: Oxidative DNA Damage in Mild Cognitive Impairment and Late-stage Alzheimer's Disease. *Nucleic Acids Res*, **22**, 7497 (2007).
  13. T. ABE, C. ISOBE, T. MURATA, C. SATO, H. TOHGI: Alteration of 8-hydroxyguanosine Concentrations in the Cerebrospinal Fluid and Serum from Patients with Parkinson's Disease. *Neurosci Lett*, **336**, 105 (2003).
  14. C. M. CHEN, J. L. LIU, Y. R. WU, Y. C. CHEN, H. S. CHENG, M. L. CHENG, D. T. Y. CHIU: Increased Oxidative Damage in Peripheral Blood Correlates with Severity of Parkinson's Disease. *Neurobiology of Disease*, **33**, 429 (2009).
  15. K. GMITTEROVA, U. HEINEMANN, J. GAWINECKA, D. VARGES, B. CIESIELCZYK, P. VALKOVIC, J. BENETIN, I. ZERR: 8-OHdG in Cerebrospinal Fluid as a Marker of Oxidative Stress in Various Neurodegenerative Diseases. *Neurodegenerative Dis*, **6**, 263 (2009).
  16. W. LOPACZYNSKI, S. H. ZEISEL: Antioxidants Programmed Cell Death and Cancer. *Nutr Res*, **21**, 295 (2001).
  17. I. GUIDI, D. GALIMBERTI, S. LONATI, C. NOVEMBRINO, F. BAMONTI, M. TIRITICCO, C. FENOGLIO, E. VENTURELLI, P. BARON, N. BRESOLIN, E. SCARPINI: Oxidative Imbalance in Patients with Mild Cognitive Impairment and Alzheimer's Disease. *Neurobiol Ageing*, **27**, 262 (2006).

18. C. J. FOY, A. P. PASSMORE, M. D. VAHIDASSR, I. S. YOUNG, J. T. LAWSON: Plasma Chain-breaking Antioxidants in Alzheimer's Disease Vascular Dementia and Parkinson's Disease. *QJM*, **92**, 39 (1999).
19. Á. CASADO, E. LÓPEZ-FERNÁNDEZ, C. CONCEPCIÓN, R. de la TORRE: Lipid Peroxidation and Antioxidant Enzyme Activities in Vascular and Alzheimer Dementias. *Neurochem Res*, **33**, 450 (2008).
20. L. ROSSI, R. SQUITTI, P. PASQUALETTI, E. MARCHESE, E. CASSETTA, E. FORASTIERE, G. ROTILIO, P.M. ROSSINI, A. FINAZZI-AGRÓ: Red Blood Cell Copper Zinc Superoxide Dismutase Activity Is Higher in Alzheimer's Disease and Is Decreased by D-penicillamine. *Neurosci Lett*, **329**, 137 (2002).
21. T. F. SLATER, B. C. SAWYER: The Stimulatory Effects of Carbon Tetrachloride and Other Halogenoalkanes on Peroxidative Reactions in Rat Liver Fractions *in vitro*: General Features of the Systems Used. *Biochem J*, **123**, 805 (1971).
22. R. RE, N. PELLEGRINI, A. PROTEGGENTE, A. PANNALA, M. YANG, C. RICE-EVANS: Antioxidant Activity Applying an Improved ABTS Radical Cation Decolorization Assay. *Free Radic Biol Med*, **26**, 1231 (1999).
23. A. GONENC, D. ERTEN, S. ASLAN, M. AKINCI, B. SIMSEK, M. TORUN: Lipid Peroxidation and Antioxidant Status in Blood and Tissue of Malignant Breast Tumor and Benign Breast Disease. *Cell Biol Int*, **30**, 376 (2006).
24. S. KASAP, A. GONENC, D. ERTEN SENER, I. HISAR: Serum Cardiac Markers in Patients with Acute Myocardial Infarction: Oxidative Stress, C-reactive Protein and N-terminal Probrain Natriuretic Peptide. *J Clin Biochem Nutr*, **41**, 50 (2007).
25. T. F. SUBHANI, M. A. NASAR, A. JARRARI, V. D'SOUZA, M. A. NASEER, F. SHAKEEL: 5'-nucleotidase, Oxidative Stress and Antioxidant Status in Alcohol Consumers and Cirrhotic Patient. *Biochem Med*, **19**, 277 (2009).
26. R. DEI, A. TAKEDA, H. NIWA, M. LI, Y. NAKAGOMI, M. WATANABE: Lipid Peroxidation and Advanced Glycation End Products in the Brain in Normal Aging and in Alzheimer's Disease. *Acta Neuropathol*, **104**, 113 (2002).
27. H. AYBEK, F. ERCAN, D. ASLAN, T. SAHINER: Determination of Malondialdehyde, Reduced Glutathione Levels and APOE4 Allele Frequency in Late-onset Alzheimer's Disease in Denizli, Turkey. *Clin Biochem*, **3-4**, 172 (2007).
28. S. NIKAM, P. NIKAM, S. K. AHALEY, A. V. SONTAKKE: Oxidative Stress in Parkinson's Disease. *Indian J Clin Biochem*, **24**, 98 (2009).
29. J. E. AHLKOG, R. J. UTTI, P. A. LW, G. M. TYCE, K. K. NICKANDER, R. C. PETERSEN, E. KOKMEN: No Evidence for Systemic Oxidant Stress in Parkinson's or Alzheimer's Disease. *Mov Disord*, **10**, 566 (1995).
30. G. PERRY, A. NUNOMURA, P. K. JONES, C. A. ROTTKAMP, X. ZHU, G. ALIEV, A. CASH, M. A. SMITH: Oxidative Imbalance Is a Major Feature of Alzheimer Disease. *Curr Topics Biochem Res*, **3**, 151 (2000).
31. J. C. de la TORRE, G. B. STEFANO: Evidence that Alzheimer's Disease Is a Microvascular Disorder: The Role of Constitutive Nitric Oxide. *Brain Res Rev*, **34**, 119 (2000).
32. R. CACABELOS, L. FERNÁNDEZ-NOVOA, V. LOMBARDI, L. CORZO, V. PICHEL, Y. KUBOTA: Cerebrovascular Risk Factors in Alzheimer's Disease: Brain Hemodynamics and Pharmacogenomic Implications. *Neurol Res*, **25**, 567 (2003).
33. L. CORZO, R. ZAS, S. RODRIGUEZ, L. FERNÁNDEZ-NOVOA, R. CACABELOS: Decreased Levels of Serum Nitric Oxide in Different Forms of Dementia. *Neurosci Lett*, **420**, 263 (2007).
34. O. LEPARA, N. AVDAGIC, A. VALJEVAC, A. ZACIRAGIC, A. HADZOVIC-DZUVO, D. LEPARA, I. TAHIROVIC, E. SOFIC: Serum Nitric Oxide Levels in Patients with Probable Alzheimer Disease and Vascular Dementia. *Turk J Biochem*, **35**, 363 (2010).
35. S. P. GABBITA, M. A. LOVELL, W. R. MARKESBER: Increased Nuclear DNA Oxidation in the Brain in Alzheimer's Disease. *J Neurochem*, **71**, 2034 (1998).

36. J. ZHANG, G. PERRY, M. A. SMITH, D. ROBERTSON, S. J. OLSON, D. G. GRAHAM, T. J. MONTINE: Parkinson's Disease Is Associated with Oxidative Damage to Cytoplasmic DNA and RNA in Substantia Nigra Neurons. *Am J Pathol*, **154**, 1423 (1999).
37. L. MIGLIORE, I. FONTANA, F. TRIPPI, R. COLOGNATO, F. COPPEDE, G. TOGNONI, B. NUCCIARONE, G. SICILIANO: Oxidative DNA Damage in Peripheral Leukocytes of Mild Cognitive Impairment and AD Patients. *Neurobiol Ageing*, **5**, 567 (2005).
38. R. C. S. SEET, C. Y. LEE, E. C. H. LIM, J. J. H. TAN, A. M. L. QUEK, W. L. CHONG, W. F. LOOI, S. H. HUANG, H. WANG, Y. H. CHAN, B. HALLIWELL: Oxidative Damage in Parkinson Disease: Measurement Using Accurate Biomarkers. *Free Rad Biol Med*, **48**, 560 (2010).
39. N. TABET, Z. WALKER, D. MANTLE, D. COSTA, M. ORRELL: *In vivo* Dopamine Pre-synaptic Receptors and Antioxidant Activities in Patients with Alzheimer's Disease Dementia with Lewy Bodies and in Controls: A Preliminary Report. *Dement Geriatr Cogn Disord*, **16**, 46 (2003).
40. A. VAISI-RAYGANI, Z. RAHIMI, M. ZAHRAIE, M. NOROOZIAN, A. POURMOTABBED: Enzymatic and Non-enzymatic Antioxidant Defense in Alzheimer's Disease. *Acta Medica Iranica*, **45**, 271 (2007).
41. S. ABRAHAM, C. C. SOUNDARARAJAN, S. VIVEKANANDHAN, M. BEHARI: Erythrocyte Antioxidant Enzymes in Parkinson's Disease. *Indian J Med Res*, **121**, 111 (2005).
42. D. GACKOWSKI, R. ROZALSKI, A. SIOMEK, T. DZIAMAN, K. NICPON, M. KLIMARCZYK: Oxidative Stress and Oxidative DNA Damage Is Characteristic for Mixed Alzheimer Disease/Vascular Dementia. *J Neurol Sci*, **266**, 57 (2008).

*Received 9 November 2012*

*Revised 22 December 2012*

## **INCREASED KYNURENINE/TRYPHTOPHAN AND NEOPTERIN LEVELS IN HEMODIALYSIS**

A. HACISEVKI<sup>a\*</sup>, B. BABA<sup>a</sup>, S. SEZER<sup>b</sup>, Y. OZKAN<sup>a</sup>

<sup>a</sup>*Department of Biochemistry, Faculty of Pharmacy, Gazi University, 06 330 Etiler, Ankara, Turkey*

*E-mail: abozkir @ gazi.edu.tr*

<sup>b</sup>*Department of Nephrology, Faculty of Medicine, Baskent University, Ankara, Turkey*

### **ABSTRACT**

In our study, the tryptophan degradation via the kynurenine pathway and neopterin levels as markers of cellular immune activity were evaluated in hemodialysis (HD) patients in order to confirm the data of previous studies. In this case-control study, serum tryptophan and kynurenine concentrations were determined by HPLC, neopterin levels were measured with ELISA in 54 hemodialysis patients and 33 healthy controls. There were significantly increased kynurenine, kynurenine/tryptophan ratio and neopterin levels, and decreased tryptophan levels in hemodialysis patients compared with the healthy controls ( $p=0.0001$ ). In our study, tryptophan degradation and neopterin levels are increased in HD patients. These changes may result from impaired excretion of the compounds or neopterin production and tryptophan degradation in the course of inflammation and immune activation during hemodialysis.

*Keywords:* hemodialysis, kynurenine, kynurenine/tryptophan, neopterin, tryptophan.

### **AIMS AND BACKGROUND**

End-stage renal disease (ESRD) is growing health problem in the world. The prevalence of end-stage renal disease was 819 per million populations in the reports of Turkish Society of Nephrology in 2009 (Ref. 1). Despite significant improvements in hemodialysis technics, incidence of ESRD is increasing and cardiovascular and infectious diseases are the most common cause of morbidity and mortality in hemodialysis (HD) patients. These two complications are linked to alteration in the immune system in ESRD. Immune dysfunction in which immune activation and immune sup-

---

\* For correspondence.

pression coexist is a complex interaction between the innate and adaptive systems<sup>2</sup>. Many clinical and experimental studies indicate that acquired immunity is impaired in hemodialysis patients. The immunodeficiency of uremic patients is related to multiple and complex alterations of the cytokine network and of its target cells such as T- or B-lymphocytes and monocytes. Inflammation and increased oxidative stress are also common features in uremic patients specially those on maintenance HD. The concept that HD evokes an inflammatory response is based on the observation that dialysis causes the release in blood of inflammatory cytokines, such as TNF- $\alpha$  (Ref. 3).

Neopterin (NP) belongs to the group of compounds known as pteridines and observation of NP level is helpful to monitor the body status of cellular immunity and inflammatory response. NP, a 2-amino-4-hydroxy-(1,2,3-trihydroxy-propyl)-pteridine with low molecular mass, produced by activated monocytes/macrophages from GTP which is converted to 7,8-dihydroneopterintriphosphate by GTP cyclohydrolase I (Refs 4 and 5). The activity of this enzyme is greatly enhanced by interferon-gamma (IFN- $\gamma$ ). Although IFN- $\gamma$  is the most potent inducer of NP synthesis in human cells, the production of NP is co-stimulated by tumor necrosis factor-alpha (TNF- $\alpha$ ). On the other hand, NP stimulates TNF- $\alpha$  gene expression, which enhances TNF- $\alpha$  synthesis<sup>4</sup>. IFN- $\gamma$  also stimulates the release of reactive oxygen species (ROS) from immunocompetent cells, the amount of neopterin produced also serves as an indirect estimate of oxidative stress<sup>5,6</sup>. Therefore, NP is an early and sensitive marker used for reflection of cellular immune activation status induced by the lymphocyte-macrophage system<sup>7</sup>.

Tryptophan (Trp) is the least abundant of all essential amino acids and has 3 fates in the body: (i) general protein synthesis; (ii) serotonin biosynthesis, and (iii) catabolism through the kynurenine pathway which is the major route for Trp metabolism in mammals<sup>8</sup>. In the first step of kynurenine metabolic way, Trp is transformed into Kyn in reaction catalysed by 2 dioxygenases: tryptophan 2,3-dioxygenase (TDO, EC 1.13.11.11) expressed primarily in liver, and indoleamine 2,3-dioxygenase (IDO, EC 1.13.11.17) expressed in a wider range of tissues. Unlike TDO, IDO is highly up-regulated locally or systemically by immune activation and inflammation, mainly by IFN- $\gamma$ , but also by IFNs type I, TNF- $\alpha$  and lipopolysaccharide (LPS) (Refs 9–12). Therefore, like increased neopterin formation, enhanced Trp degradation is observed in diseases concomitant with cellular immune activation. Increased Kyn/Trp has been demonstrated as a key player in immunologic processes including infection, autoimmunity, allergic reaction, chronic inflammation and renal injury<sup>13,14</sup>. Toxic catabolites of kynurenine pathway have been demonstrated to be involved in the development of key uremic symptoms in the rat experimental chronic renal insufficiency<sup>15–17</sup>.

In previous studies, abnormalities in Trp metabolism have been reported in patients receiving dialysis on continuous ambulatory peritoneal dialysis (CAPD) (Refs 18 and 19) and on maintenance hemodialysis<sup>13,20–22</sup>. However, there are few studies evaluating Kyn/Trp ratio<sup>13,18,22</sup> in chronic kidney disease. Recently, in a study, Koenig et al.<sup>23</sup> evaluated the Kyn/Trp and immuno inflammatory marker neopterin levels in uremic patients in terms of patients psychological performance. Imbalance between

immunoactivation and immunosuppression lead to increased susceptibility to infection and inflammatory response which is major problems in HD. Because of broad, incompletely understood disturbances in metabolism that are linked to adverse outcome, new markers or effectors of aberrant inflammation in renal diseases are needed to identify. This study was performed to evaluate the tryptophan degradation via the kynurenine pathway and neopterin levels as markers of cellular immune activity in hemodialysis patients.

## EXPERIMENTAL

*Study population.* 33 healthy individuals (16 male, 17 female,  $48.70 \pm 2.91$  years of age) with no clinical symptoms of any disease and 54 HD patients (28 male, 26 female,  $46.92 \pm 1.84$  years of age) participated in the study. All participants rights were protected, and informed consent was obtained according to the Helsinki Declaration. The study protocol was approved by the Ethics Committee of Baskent University Hospital Medical Ethics Committee. The weekly duration of dialysis was 12 h in 3–4 h sessions. In the ESRD patients, renal failure was due to type 2 diabetes in 8 cases, glomerulonephritis in 13 cases, hypertension in 10 cases, tubulointerstitial disease (stone, pyelonephritis, polycystic kidney disease) in 11 cases and was unknown in 12 cases. All the subjects including controls filled out a questionnaire containing questions on the following: age, sex, body weight, history of family, smoking habit, alcohol intake, physical exercise and diet.

*Blood collection.* Fasting peripheral venous blood samples were collected and centrifuged at 3000 g for 10 min for serum and plasma separation, thereafter stored at  $-80^{\circ}\text{C}$  until analysed.

*Measurement of tryptophan and kynurenin levels.* Serum Trp and Kyn levels were measured by HPLC with UV detection<sup>24</sup>. Briefly, 200  $\mu\text{l}$  of the serum sample were mixed with 26  $\mu\text{l}$  40% perchloric acid for protein precipitation, followed by vortex-mixing for 1 min and centrifuged at 15 000 g for 10 min at  $4^{\circ}\text{C}$ . 20  $\mu\text{l}$  of the supernate were injected into the HPLC system (ThermoFinnigan Surveyor) for analysis. The chromatographic separation was carried out using the mobile phase consisting of 15 mmol/l acetate buffer (pH 4.0) and acetonitrile (92:8, v/v) at a flow rate of 0.8 ml/min. A Supelco LC-18<sub>DB</sub> analytical column (150 mm  $\times$  4 mm ID, 3  $\mu\text{m}$ ) (Sigma) was used for the analysis. The eluate was monitored by the programmed wavelength detection setting at 360 nm for Kyn and at 278 nm for Trp.

*Measurement of neopterin levels.* Serum NP levels were determined by ELISA (DRG Diagnostic EIA-1476) according to the manufacturer instructions.

*Statistical analysis.* The distribution of data was evaluated with the Kolmogorov–Smirnov test. Because some of data sets were not normally distributed, statistical comparisons between groups were performed using non-parametric Mann Whitney



*U*-test. Values were expressed as median and interquartile range (IQR). *p*-Values less than 0.05 were considered to indicate statistical significance. Analyses were performed with SPSS statistical package program (SPSS 10.0 version, USA).

## RESULTS AND DISCUSSION

In the present study, 54 patients (26 female, 28 male) with a mean age of 46.9±1.8 years, and 33 healthy controls (16 male, 17 female) with mean age of 48.7±2.9 years were included in this study. Both groups had similar age range and there was no significant difference between groups with respect to age (*p* = 0.433). As expected, HD patients had significantly higher urea and creatinine levels compared with healthy controls (*p* = 0.0001). Results for Trp, Kyn, Kyn/Trp and neopterin levels are given in Table 1. Increased kynurenine and neopterin levels were found in HD group as compared with levels found in control group (*p* = 0.0001 for both parameters). HD patients had significantly lower Trp levels, and Kyn/Trp ratio showed significant increase in this group.

**Table 1.** Levels of tryptophan, kynurenine, Kyn/Trp, neopterin, urea and creatinine in patients and healthy controls

Parameters	Patients, <i>n</i> =54	Healthy controls, <i>n</i> =33	<i>p</i>
Tryptophan (µmol/l)	13.30 (8.74–19.32)	33.87 (28.23–38.77)	0.0001
Kynurenine (µmol/l)	2.85 (2.16–3.64)	1.35 (1.24–1.81)	0.0001
Kynurenine/tryptophan ((Kyn/Trp)×10 <sup>3</sup> )	212.15 (166.42–273.68)	43.55 (35.15–50.77)	0.0001
Neopterin (ng/ml)	34.79 (29.59–44.43)	3.40 (2.13–5.02)	0.0001
Urea (mg/dl)	77.50 (65.50–90.00)	15.00 (11.00–16.00)	0.0001
Creatinine (mg/dl)	10.27 (8.85–11.88)	0.95 (0.77–0.99)	0.0001

Note: values are represented as median (IQR).

Patients undergoing chronic hemodialysis have an impaired immune system and frequently show clinical and/or laboratory signs of systemic inflammation. Also, microinflammation is recognised as principle causes of dialysis-related illnesses<sup>2,3</sup>. Dialysis has been associated with acute changes in complement activation, macrophage function, T-cell activation and the release of various proinflammatory cytokines. Bioincompatibility of dialysis techniques probably induces an inappropriate monocyte activation, cytokine production and enhances the generation of other uraemic toxins<sup>25,26</sup>. Activation of the immune system which occurs in inflammatory diseases leads to parallel increases in pterin synthesis and increased production of neuroactive L-tryptophan metabolites<sup>27</sup>. The amino acid metabolite level is a key index of the disease condition in chronic renal failure and among these metabolites tryptophan is especially noteworthy<sup>20</sup>.

Kynurenine pathway is the major route for tryptophan metabolism in mammals. Kynurenine (Kyn) is the first stable intermediate formed from kynurenine pathway

of tryptophan (Trp) degradation. This pathway initiated either by tryptophan 2,3-dioxygenase (TDO), its expression restricted with liver, or indolamine 2,3-dioxygenase (IDO). Unlike TDO, IDO is widely expressed in most of dendritic cells, monocytes, macrophages, tumor cells and endothelial cells. IDO enzyme activity is relatively low during normal non-pathological conditions and highly up-regulated locally or systemically by immune activation and inflammation, particularly by IFN- $\gamma$  and TNF- $\alpha$  (Ref. 10). Kynurenine itself can be further metabolised along two distinctive pathways to form metabolites of the kynurenine pathway. Among these metabolites kynurenic acid and quinolinic acid are known to have certain physiological as well as pathological effects depending on their concentration<sup>28</sup>. In the end stages of chronic renal failure endogenous metabolites which are normally excreted in the urine accumulate in the blood of such patients<sup>21,29</sup>. Disturbances in the tryptophan metabolism and accumulation of the toxic tryptophan metabolites are thus of concern in ureamic patients, particularly those undergoing dialysis.

In rat model, it was shown that acceleration of peripheral kynurenine pathway metabolism occurs in rats with renal insufficiency and runs parallel with the severity of case<sup>15,24,25</sup>. Pawlak et al.<sup>18,19</sup> reported that plasma levels of Trp were significantly lower in HD patients compared to controls while Kyn and Kyn/Trp ratio were elevated. In spite of the fact that Schefold et al.<sup>13</sup> reported unchanged Trp increased Kyn levels in chronic kidney disease, lower plasma Trp and higher Kyn levels in HD patients compared with healthy subjects were reported in other studies<sup>21,29</sup>. In these studies, IDO activity was estimated indirectly by the Kyn/Trp ratio. Recently, Eleftheriadis et al.<sup>30</sup> showed markedly increased IDO enzyme concentration in HD patients compared with controls. Same groups also showed that IDO levels were twice higher in HD patients compared to healthy volunteers, and TNF- $\alpha$  levels were also much higher in HD patients<sup>31</sup>. They suggested that chronic inflammation up-regulate the IDO activity and therefore increase tryptophan degradation. As a different from these studies, we evaluated neopterin levels apart from Kyn, Trp and Kyn/Trp in HD patients. We observed decreased serum Trp levels while increased Kyn, Kyn/Trp and NP in HD patients with respect to healthy subjects. Our results are consistent with the finding of study recently reported by Koenig et al. However, their study group consists of hemodialysis patients having sleep disturbance, depression and under antidepressant therapy. In our study, the tryptophan degradation via the kynurenine pathway and neopterin levels as markers of cellular immune activity were evaluated in hemodialysis patients in order to confirm the data of previous studies.

In parallel to IDO, IFN- $\gamma$  induces the enzyme GTP-cyclohydrolase I in monocyte-derived macrophages and dendritic cells, which forms neopterin during immune responses<sup>32</sup>. It has been demonstrated that the production of NP is induced mainly by IFN- $\gamma$  and, to lesser degree, by IFN- $\alpha$ , endotoxins, TNF- $\alpha$ , lipopolysaccharides. NP is found in considerably high concentrations in human body fluids when the cellular immune system is activated<sup>4</sup>. Therefore, neopterin formation coincides with increased

IDO activity in various human diseases<sup>32</sup>. TNF- $\alpha$  and NP levels were generally elevated in HD patients compared to controls in literature<sup>33-35</sup>.

In summary, patients treated with hemodialysis have increased neopterin levels and tryptophan degradation; these changes may result from impaired excretion of the compound or result from neopterin production and tryptophan degradation in the course of inflammation and immune activation during hemodialysis. Microinflammation is suggested to be undergoing during the chronic uremic state and many metabolic alterations are influenced that causes increased morbidity and mortality in dialysis patients. These data additionally suggest that activation kynurenine pathway and decrease in Trp levels occur before the evidence of clinical inflammation in uremic state. It is not possible to assess which is the main triggering factor for these changes but combining the uremic process with microinflammation that starts in tissues and assuming that these changes occur in parallel before the signs of clinically evident inflammation seems logical. A comparison of dialysis patients with various degrees of inflammation in terms of Trp, Kyn, Kyn/Trp and NP and or a prospective follow up study that searches for the alterations of these parameters during states of inflammation will be able to answer this question.

## CONCLUSIONS

In conclusion, our results which show decreased serum Trp levels while increased Kyn and NP in HD patients with respect to healthy subjects, are consistent with the findings of previous studies. Our data confirmed that tryptophan degradation and levels of neopterin increase in HD patients. These changes may result from impaired excretion of the compounds or neopterin production and tryptophan degradation in the course of inflammation and immune activation during hemodialysis. The result of this study might lead to further studies to elucidate exact role of IDO enzyme in HD and, also to evaluate Trp degradation, NP as a potential predictive markers in HD.

## REFERENCES

1. Turkish Society of Nephrology, Chronic Renal Disease in Turkey. [http://tsn.org.tr/folders/file/CREDIT\\_Slayt\\_Seti.ppt](http://tsn.org.tr/folders/file/CREDIT_Slayt_Seti.ppt), (Last accessed: July 2012).
2. S. KATO, M. CHMIELEWSKI, H. HONDA, R. PECOITS-FILHO, S. MATSUO: Aspects of Immune Dysfunction in End-stage Renal Disease. *Clin J Am Soc Nephrol*, **3**, 1526 (2008).
3. C. LIBETTA, V. SEPE, P. ESPOSITO, F. GALLI, A. CANTON: Oxidative Stress and Inflammation: Implications in Uremia and Hemodialysis. *Clin Biochem*, **44**, 1189 (2011).
4. A. BERDOWSKA, K. ZWIRSKA-KORCZALA: Neopterin Measurement in Clinical Diagnosis. *J Clin Pharm Therap*, **26**, 319 (2001).
5. F. V. HAMERLINCK: Neopterin: A Review. *Exp Dermatol*, **8**, 167 (1999).
6. B. WIDNER, B. WIRLEITNER, G. BAIER-BITTERLICH, G. WEISS, D. FUCHS: Cellular Immune Activation, Neopterin Production, Tryptophan Degradation and the Development of Immunodeficiency. *Arch Immunol Ther Exp (Warsz)*, **48** (4), 251 (2000).
7. L. YANCHUN, H. ZHIDONG: Significance of Humoral Neopterin in Clinical Diagnostics and Prognosis. *J Med Coll PLA*, **26**, 45 (2011).

8. D. M. RICHARD, M. A. DAWES, C. W. MATHIAS, A. ACHESON, N. HILL-KAPTURCZAK: L-Tryptophan: Basic Metabolic Functions, Behavioral Research and Therapeutic Indications. *Int J Tryptophan Res*, **2**, 45 (2009).
9. O. TAKIKAWA: Biochemical and Medical Aspects of the Indoleamine 2,3-dioxygenase-initiated L-tryptophan Metabolism. *BBRC*, **338**, 12 (2005).
10. J. R. MOFFET, M. A. NAMBOODIRI: Tryptophan and the Immune Response. *Immunol Cell Biol*, **81**, 247 (2003).
11. A. MELLOR: Indoleamine 2,3-dioxygenase and Regulation of T Cell Immunity. *BBRC*, **338**, 20 (2005).
12. K. SCHROCKSNADEL, B. WIRLEITNER, C. WINKLER, D. FUCHS: Monitoring Tryptophan Metabolism in Chronic Immune Activation. *Clin Chim Acta*, **364**, 82 (2006).
13. J. C. SCHEFOLD, J. P. ZEDEN, C. FOTOPOULOU, S. HAEHLING, R. PSCHOWSKI, D. HASPER, H. D. VOLK, C. SCHUETT, P. REINKE: Increased Indoleamine 2,3-dioxygenase (IDO) Activity and Elevated Serum Levels of Tryptophan Catabolites in Patients with Chronic Kidney Disease: A Possible Link between Chronic Inflammation and Uraemic Symptoms. *Nephrol Dial Transplant*, **24**, 1901 (2009).
14. Y. OZKAN, G. METE, A. SEPICI-DINCEL, V. SEPICI, B. SIMSEK: Tryptophan Degradation and Neopterin Levels in Treated Rheumatoid Arthritis Patients. *Clin Rheumatol*, **31**, 29 (2012).
15. D. PAWLAK, A. TANKIEWICZ, W. BUCZKO: Kynurenine and Its Metabolites in the Rat with Experimental Renal Insufficiency. *J Physiol Pharmacol*, **52** (4), 755 (2001).
16. D. PAWLAK, A. TANKIEWICZ, T. MATYS, W. BUCZKO: Peripheral Distribution of Kynurenine Metabolites and Activity of Kynurenine Pathway Enzymes in Renal Failure. *J Physiol Pharmacol*, **54** (2), 175 (2003).
17. D. PAWLAK, A. TANKIEWICZ, P. MYSLIWIEC, W. BUCZKO: Tryptophan Metabolism via the Kynurenine Pathway in Experimental Chronic Renal Failure. *Nephron*, **90** (3), 328 (2002).
18. K. PAWLAK, T. DOMANIEWSKI, M. MYSLIWIEC, D. PAWLAK: The Kynurenines Are Associated with Oxidative Stress, Inflammation and the Prevalence of Cardiovascular Disease in Patients with End-stage Renal Disease. *Atherosclerosis*, **204**, 309 (2009).
19. K. PAWLAK, S. BRZOSKO, M. MYSLIWIEC, D. PAWLAK: Kynurenine, Quinolinic Acid – the New Factors Linked to Carotid Atherosclerosis in Patients with End-stage Renal Disease. *Atherosclerosis*, **204**, 561 (2009).
20. A. SAITO, T. NIWA, K. MAEDA, K. KOBAYASHI, Y. YAMAMOTO: Tryptophan and Indolic Tryptophan Metabolites in Chronic Renal Failure. *Am J Clin Nutr*, **33**, 1402 (1980).
21. D. PAWLAK, K. PAWLAK, J. MALYSZKO, M. MYSLIWIEC, W. BUCZKO: Accumulation of Toxic Products Degradation of Kynurenine in Hemodialyzed Patients. *Int Urol Nephrol*, **33**, 399, (2001).
22. A. KATO, Y. SUZUKI, T. SUDA, M. SUZUKI, M. FUJIE: Relationship between an Increased Serum Kynurenine/Tryptophan Ratio and Atherosclerotic Parameters in Hemodialysis Patients. *Hemodialysis Int*, **14**, 418, (2010).
23. P. KOENIG, C. NAGL, G. NEURAUTER, H. SCHENNACH, G. BRANDACHER: Enhanced Degradation of Tryptophan in Patients on Hemodialysis. *Clin Nephrol*, **74** (6), 465, (2010).
24. X. ZHANG, Y. HE, M. DING: Simultaneous Determination of Tryptophan and Kynurenine in Plasma Samples of Children Patients with Kawasaki Disease by High-performance Liquid Chromatography with Programmed Wavelength Ultraviolet Detection. *J Chromatogr B*, **877**, 1678 (2009).
25. P. JACOBS, G. GLORIEUX, R. VANHOLDER: Interleukin/Cytokine Profiles in Hemodialysis and in Continuous Peritoneal Dialysis. *Neophrol Dial Transplant*, **19**, 41, (2004).
26. G. PERTOSA, G. GRANDALIANO, L. GESUALDO, F. P. SCHENA: Clinical Relevance of Cytokine Production in Hemodialysis. *Kidney Int Suppl*, **76**, 104, (2000).
27. N. SAKAI, K. SAITO, S. KAUFMAN, M. P. HEYES, S. MILSTEIN: Induction of Pterin Synthesis Is Not Required for Cytokine-stimulated Tryptophan Metabolism. *Biochem J*, **295**, 543, (1993).

28. Y. CHEN, GJ. GUILLEMIN: Kynurenine Pathway Metabolites in Humans: Disease and Healthy States. *Int J Tryptophan Res*, **2**, 1, (2009).
29. K. SAITO, S. FUJIGAKI, M. P. HEYES, K. SHIBATA, M. TAKEMURA: Mechanism of Increases in L-kynurenine and Quinolinic Acid in Renal Insufficiency. *Am J Physiol Renal Physiol*, **279**, 565, (2000).
30. T. ELEFThERIADIS, G. ANTONIADI, V. LIAKOPOULOS, I. STEFANIDIS, G. GALAKTIDOU: Plasma Indoleamine 2,3-dioxygenase Concentration Is Increased in Hemodialysis Patients and May Contribute to the Pathogenesis of Coronary Heart Disease. *Ren Fail*, **34** (1), 68, (2012).
31. T. ELEFThERIADIS, V. LIAKOPOULOS, G. ANTONIADI, I. STEFANIDIS, G. GALAKTIDOU: Indoleamine 2,3-dioxygenase Is Increased in Hemodialysis Patients and Affects Immune Response to Hepatitis B Vaccination. *Vaccine*, **29**, 2242, (2011).
32. S. SCHROECKSNADEL, R. SUCHER, K. KURZ, D. FUCHS, G. BRANDACHER: Influence of Immunosuppressive Agents on Tryptophan Degradation and Neopterin Production in Human Peripheral Blood Mononuclear Cells. *Transplant Immunol*, **25**, 119, (2011).
33. L. AIRAGHI, L. GAROFALO, M. G. CUTULI, R. DELGADO, A. CARLIN: Plasma Concentrations of  $\alpha$ -melanocyte-stimulating Hormone Are Elevated in Patients on Chronic Hemodialysis. *Nephrol Dial Transplant*, **15**, 1212, (2000).
34. A. ASCI, T. BAYDAR, R. CETINKAYA, A. DOLGUN, A. SAHIN: Evaluation of Neopterin Levels in Patients Undergoing Hemodialysis. *Hemodialysis Int*, **14**, 240, (2010).
35. A. DOGUKAN, H. H. AKBULUT, V. BULUT: Neopterin Levels in Patients Undergoing Chronic Hemodialysis. *Official J Turkish Soc Nephrol*, **11** (1), 18, (2002).

*Received 5 December 2012*

*Revised 12 January 2013*

**SYNTHESIS AND PESTICIDAL ACTIVITIES OF SOME  
2,5-DISUBSTITUTED-6-THIO-1,2,4-TRIAZOLO-[3,2-b]-  
1,3,4-THIADIAZOLES AND 5-SUBSTITUTED ARYL/  
ARYLOXYMETHYL-2-(PHTHALOMIDOMETHYLAMINO)-  
1,3,4-THIADIAZOLES**

SH. TIWARI

*Department of Chemistry, University of Allahabad, Allahabad, India  
E-mail: drshailendertiwariau@gmail.com*

ABSTRACT

Some 2,5-disubstituted-6-thio-1,2,4-triazolo-[3,2-b]-1,3,4-thiadiazoles have been synthesised by cyclisation of 5-aryloxymethyl-2-(N-phenyl thiocarbanilido)-1,3,4-thiadiazoles with bromine in carbon tetrachloride, and 5-substituted aryl/aryloxymethyl-2-(phthalomidomethylamino)-1,3,4-thiadiazoles have been synthesised by refluxing a mixture of 2-amino-5-substituted aryl/aryloxymethyl-1,3,4-thiadiazoles with phthalimide and formaldehyde in ethanol. All these compounds have been assayed for their herbicidal activities against *Echinochloa oryzicola*, *Echinochloa crusgalli*, *Oryza sativa*, *Glycine max* and antifungal activities against *Aspergillus niger* and *Pyricularia oryzae*.

*Keywords:* 1,3,4-thiadiazoles, 1,2,4-triazoles, herbicidal activity, fungicidal activity.

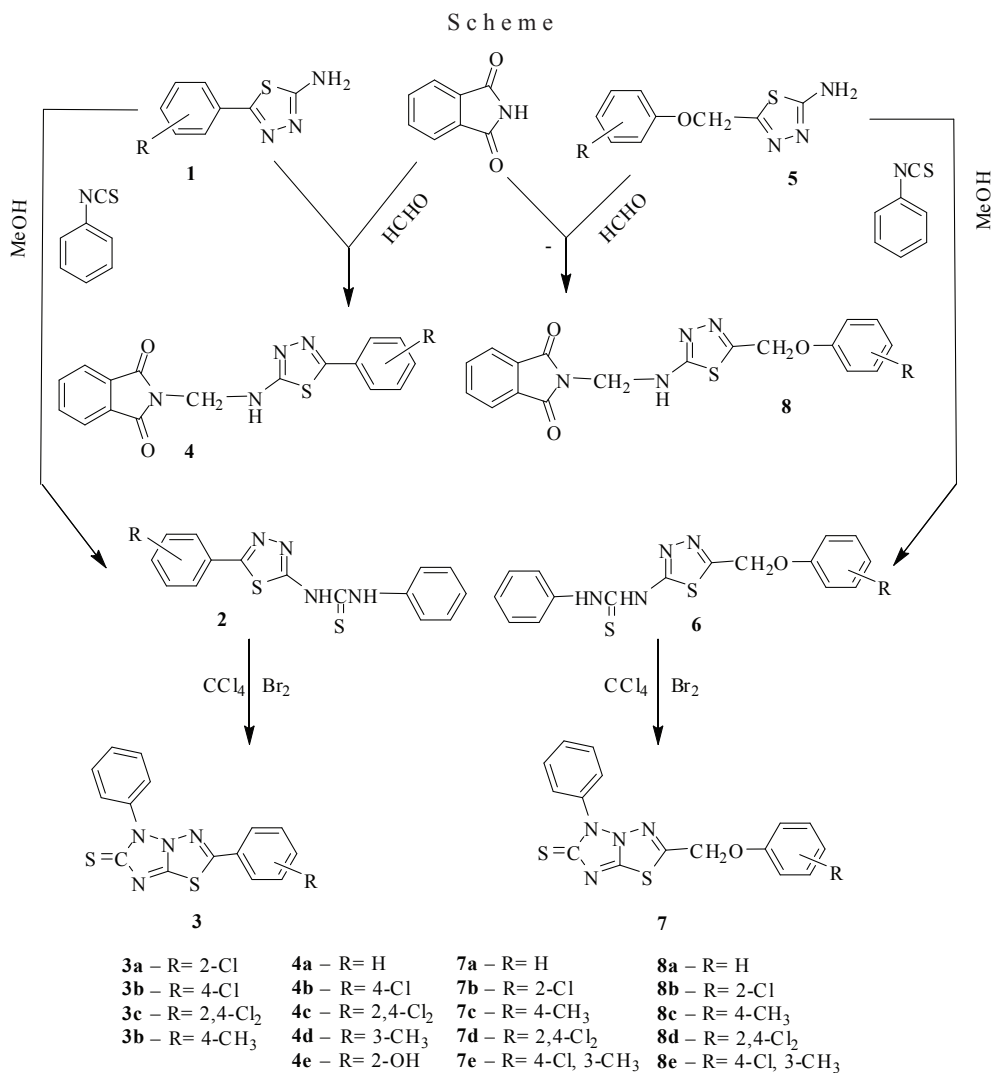
AIMS AND BACKGROUND

1,3,4-thiadiazole nucleus is associated with broad spectrum of biocidal activities possibly by virtue of incorporating the toxophoric >N-C-S-moiety<sup>1</sup>, further 2-amino-1,3,4-thiadiazole may be viewed as a cyclic analogue of thiosemicarbazone, the physiological properties of which have been well established<sup>2,3</sup>. Likewise, 1,2,4-triazoles and related compounds have been known as biologically active agents<sup>4-6</sup>.

The above observations coupled with the view that planarity and compactness of a molecule might augment its other biological activities, as it does with herbicidal activities<sup>7</sup>, led us to study a molecule which combines these 2 biolabile rings together to give a compact and planar system. With this objective in mind and in continuation of our work on fused heterocycles<sup>8,9</sup> of pesticidal interest, we report herein the synthesis and pesticidal activity of the title compounds.

## EXPERIMENTAL

*Initial reagents.* The required starting materials, 2-amino-5-substituted aryl-1,3,4-thiadiazoles **1** and 2-amino-5-substituted arylozymethyl-1,3,4-thiadiazoles **5** were prepared according to the reported methods<sup>10</sup>. The synthons **1** and **5** refluxing with phenyl isothiocyanate for 2 h in methanol furnished **2** and **6**, respectively, which on cyclisation with bromine in CCl<sub>4</sub> furnished the title compounds **3** and **7**, respectively. Further, when the synthons **1** and **5** were refluxed with phthalimide and formaldehyde in ethanol for 3 h furnishing the title compounds **4** and **8**, respectively (Scheme). The structures of these compounds were established by elemental analysis, IR and PMR spectral data.



Melting points were taken in open capillary tubes and are uncorrected. IR spectra were recorded in KBr on a Perkin–Elmer-881 spectrophotometer and PMR spectra on a Perkin–Elmer R-32 spectrometer at 60 MHz. The procedure for one typical case for each step is described.

*2-Amino-5(substituted aryl/aryloxymethyl)-1,3,4-thiadiazoles.* The thiadiazoles were prepared according to the known method<sup>10</sup>. Thus appropriate thiosemicarbazide (4.4 g, 0.02 mol) was treated with concentrated H<sub>2</sub>SO<sub>4</sub> (4 ml) dropwise. The resultant paste-like mass so obtained was cooled and poured into cold water. In neutralisation with ammonia, solid product was obtained, which was filtered, washed and recrystallised from aqueous ethanol.

*5-Substituted aryl-2-(N-phenylthiocarbanilido)-1,3,4-thiadiazoles (2c):* A mixture of 2-amino-5-(2,4-dichlorophenyl)-1,3,4-thiadiazole (4.8 g, 0.02 mol) and phenyl isothiocyanate (2.4 ml, 0.02 mol) was refluxed in methanol for 2 h. It was then poured into water and the compound thus obtained was filtered, dried and recrystallised from aqueous ethanol. m. p. 152°C. IR (KBr): 3230 (NH), 1620 (C=N), 1600, 1500 and 1490 cm<sup>-1</sup> (aromatic), 1220 (C=S), 1230, 1060 (C–S–C), PMR (DMSO-*d*<sub>6</sub>); δ 6.2–7.8 (m, 8H, Ar~H), 8.2–8.6 (b, 2H, NH). Compound 6C: IR (KBr): 3230 (NH), 2910 (OCH<sub>2</sub>), 1620 (C=N), 1590 and 1490 cm<sup>-1</sup> (aromatic) 1215 (c=s); 1230, 1060 (C–S–C) PMR (DMSO-*d*<sub>6</sub>): δ 8.2 (b, 2H, NH), 6.2–7.8 (m, 8H, Ar~H), 5.1 (s, 2H–OCH<sub>2</sub>), 1.7 (s, 3H, CH<sub>3</sub>);

*2,5-Disubstituted-6-thio-1,2,4-triazolo-[3,2-b]-1,3,4-thiadiazoles (3c):* A mixture of 5-(2,4-dichlorophenyl)-2-(N-phenyl-thiocarbanilido)-1,3,4-thiadiazole (3.2 g, 0.01 mol) was cyclised with bromine (0.5 ml, 0.01 mol) in carbotetrachloride. Excess of solvent was removed by evaporation and residue poured into water. The precipitated product was recrystallised from aqueous ethanol. m. p. 158°C. IR (KBr): 1610 (C=N), 1580, 1530, 1500 (aromatic ring), 1220 (C=S), 1230, 1060 (C–S–C) and 740 cm<sup>-1</sup> (C–Cl); PMR (DMSO-*d*<sub>6</sub>): δ 6.9–7.7 (m, 8H, Ar~H).

*Compound 7c:* IR (KBr): 1620 (C=N), 1590, 1570, 1510 (aromatic ring), 1220 (C=N), 1230 and 1050 cm<sup>-1</sup> (C–S–C); PMR (DMSO-*d*<sub>6</sub>): δ 5.2 (s, 2H–OCH<sub>2</sub>), 6.8–7.7 (m, 8H, Ar~H).

*5-Substituted aryl-2-(phthalamidomethyl amino)-1,3,4-thiadiazoles (4c):* A mixture of 2-amino-5-(2,4-dichlorophenyl)-1,3,4-thiadiazole (4.8 g, 0.02 mol), phthalimide (3.0 g, 0.02 mol) and formaldehyde (2.0 ml) was refluxed in ethanol for 3 h. The solvent was removed and the residue poured into water. The solid compound, thus obtained was filtered, washed, dried and recrystallised from aqueous ethanol to get 4c, m.p. 194°C, IR (KBr): 3220 (NH), 2840 (–CH<sub>2</sub>), 1690 (C=O), 1610 (C=N), 1560, 1540, 1420 (aromatic ring), 1230, 1060 (C–S–C) and 740 cm<sup>-1</sup> (C–Cl). PMR (DMSO-*d*<sub>6</sub>): δ 4.2 (S, 2H–N–CH<sub>2</sub>–N), 6.8–7.6 (m, QH, Ar~H).



**Compound 8c:** IR (KBr): 3210 (NH), 1690 (C=O), 1610 (C=N), 1590, 1560, and 1480  $\text{cm}^{-1}$  (aromatic ring) PMR (DMSO- $d_6$ ): & 1.8 (3, 3H-CH<sub>3</sub>), 4.2 (s, 2H-N-CH<sub>3</sub>N), 4.8 (d, 2H, -OCH<sub>2</sub>), 6.8–7.6 (m, 8H, Ar~H).

**Table 1.** Characterisation data of compounds **3a-d**, **4a-e**, **7a-e** and **8a-e**

Compd.	m.p. (°C)	Yield (%)	Mol. formula	Found (%) (calc.)		
				C	H	N
<b>3a</b>	128	63	C <sub>15</sub> H <sub>10</sub> N <sub>4</sub> S <sub>2</sub> Cl	52.10	2.89	16.21
				52.40	2.41	16.60
<b>3b</b>	146	62	C <sub>15</sub> H <sub>10</sub> N <sub>4</sub> S <sub>2</sub> Cl	52.10	2.89	16.21
				52.39	2.40	16.62
<b>3c</b>	158	68	C <sub>15</sub> H <sub>9</sub> N <sub>4</sub> S <sub>2</sub> Cl <sub>2</sub>	47.37	2.37	14.74
				47.57	2.57	14.94
<b>3d</b>	173	72	C <sub>16</sub> H <sub>13</sub> N <sub>4</sub> S <sub>2</sub>	59.08	4.00	17.23
				59.40	4.30	17.66
<b>4a</b>	149	62	C <sub>17</sub> H <sub>12</sub> N <sub>4</sub> SO <sub>2</sub>	60.71	3.57	16.67
				60.29	3.27	16.32
<b>4b</b>	185	72	C <sub>17</sub> H <sub>11</sub> N <sub>4</sub> SO <sub>2</sub> Cl	56.06	2.97	15.11
				56.90	2.69	15.40
<b>4c</b>	194	68	C <sub>17</sub> H <sub>10</sub> N <sub>4</sub> SO <sub>2</sub> Cl <sub>2</sub>	50.37	2.47	13.83
				50.57	2.67	14.03
<b>4d</b>	160	77	C <sub>18</sub> H <sub>14</sub> N <sub>4</sub> SO <sub>2</sub>	61.71	4.00	16.00
				61.25	3.89	16.30
<b>4e</b>	160	76	C <sub>17</sub> H <sub>12</sub> N <sub>4</sub> SO <sub>3</sub>	57.95	3.41	15.91
				57.79	3.58	15.60
<b>7a</b>	144	65	C <sub>16</sub> H <sub>12</sub> N <sub>4</sub> S <sub>2</sub> O	56.47	3.53	16.47
				56.07	3.63	16.67
<b>7b</b>	162	71	C <sub>16</sub> H <sub>11</sub> N <sub>4</sub> S <sub>2</sub> OCl	51.27	2.94	14.95
				51.49	3.64	14.67
<b>7c</b>	124	72	C <sub>17</sub> H <sub>14</sub> N <sub>4</sub> S <sub>2</sub> O	57.63	3.96	15.82
				57.93	4.26	16.12
<b>7d</b>	154	73	C <sub>16</sub> H <sub>10</sub> N <sub>4</sub> S <sub>2</sub> OCl <sub>2</sub>	46.94	2.45	13.69
				46.61	2.65	13.34
<b>7e</b>	119	64	C <sub>17</sub> H <sub>13</sub> N <sub>4</sub> S <sub>2</sub> OCl	52.50	3.34	14.41
				52.62	3.66	14.33
<b>8a</b>	145	68	C <sub>18</sub> H <sub>14</sub> N <sub>4</sub> SO <sub>3</sub>	59.02	3.83	15.30
				59.32	3.83	14.74
<b>8b</b>	140	74	C <sub>18</sub> H <sub>13</sub> N <sub>4</sub> S <sub>3</sub> Cl	53.93	3.25	13.98
				53.43	3.65	15.59
<b>8c</b>	168	72	C <sub>19</sub> H <sub>16</sub> N <sub>4</sub> SO <sub>3</sub>	60.00	4.21	14.74
				60.20	4.41	14.94
<b>8d</b>	115	78	C <sub>18</sub> H <sub>12</sub> N <sub>4</sub> SO <sub>3</sub> Cl <sub>2</sub>	49.66	2.76	12.87
				49.39	2.29	12.39
<b>8e</b>	157	81	C <sub>19</sub> H <sub>15</sub> N <sub>4</sub> SO <sub>3</sub> Cl	55.01	3.62	13.51
				55.41	13.59	13.28

Other such compounds were also prepared in a similar way and their characterisation data are given in Table 1.

## RESULTS AND DISCUSSION

### HERBICIDAL ACTIVITY

All the compounds were subjected to primary post- and pre-emergent herbicidal evaluation at a rate of 8.0, 4.0, 1.0 and 0.5 kg/ha. The test species are *Echinochloa oryzicota*, *Echinochloa crusgalli*, *Oryza sativa* and *Glycine max*.

Test plants were grown and maintained in clay loam under green house condition throughout the experiment. In case of post-emergent evaluation, the test compound solution was directly sprayed over 10-day old plants growing in 100 cm<sup>2</sup> pots. In case of pre-emergent evaluation the test compound solution was dripped uniformly onto the soil surface in a 100 cm<sup>2</sup> pots where the test plants were just sown and covered with a thin layer of soil. Visual observation was made in each case 20 days after the treatment using the following scores: 5 (100%), 4 (99–75%), 3 (74–35%), 2 (34–5%) and 1 (4–0%). The most active compounds was found to be **3c** and **7c** (100% at 8.0 kg/ha and 75% at 0.5 kg/ha). Their activity is probably due to the presence of a 2,4-dichloro group on phenyl and a 4-methyl group on phenoxy ring. The detailed data on compounds **3c**, **4c**, **7c** and **8c** having promising herbicidal activity are given in Table 2.

**Table 2.** Herbicidal activity of compounds **3c**, **4c**, **7c** and **8c**

Compd.	Applica- tion rate (kg/ha)	Post-emergence species				Pre-emergence species			
		<i>Echino- chloa oryzi- cota</i>	<i>Echino- chloa crusgalli</i>	<i>Oryza sativa</i>	<i>Glycine max</i>	<i>Echino- chloa oryzi- cota</i>	<i>Echino- chloa crusgalli</i>	<i>Oryza sativa</i>	<i>Glycine max</i>
<b>3c</b>	8.0	5	5	4	4	5	5	4	5
	4.0	5	4	4	4	4	5	5	4
	1.0	3	2	2	2	3	3	2	3
	0.5	2	1	1	1	2	2	1	1
<b>4c</b>	8.0	5	5	4	4	5	5	5	5
	4.0	4	5	5	4	5	4	4	4
	1.0	4	4	3	4	4	4	4	4
	0.5	3	3	3	3	4	3	3	4
<b>7c</b>	8.0	5	5	5	5	5	5	5	4
	4.0	4	4	4	4	4	4	4	4
	1.0	4	3	2	1	3	2	2	2
	0.5	1	1	1	1	1	1	1	1
<b>8c</b>	8.0	5	5	4	5	5	5	4	5
	4.0	4	5	5	4	4	4	5	4
	1.0	3	2	2	2	3	3	2	3
	0.5	2	1	1	1	2	2	1	1

## FUNGICIDAL ACTIVITY

Nineteen compounds were screened for their antifungal activity by agar growth technique<sup>11</sup> against *Aspergillus niger* and *Pyricularia oryzae* at 1000, 100 and 10 ppm concentrations.

**Table 3.** Fungicidal activity of compounds **5a-e**, **6a-d**, **7a-e** and **8a-d** (mean% inhibition after 7 days)

Compound	<i>Pyricularia oryzae</i> (ppm)			<i>Aspergillus niger</i> (ppm)		
	1000	100	10	1000	100	10
<b>3c</b>	88	46	24	85	46	22
<b>4c</b>	91	43	26	92	44	28
<b>7c</b>	87	51	31	85	39	29
<b>8c</b>	83	31	14	86	39	23
Carbendazim	100	97	84	100	94	80

The results were compared with that of commercial fungicide carbendazim tested under similar conditions. Amongst these, **3c**, **4c**, **7c** and **8c** showed activity nearly comparable (89–96% at 1000 ppm) to that of carbendazim (100% at 1000 ppm) as shown in Table 3.

## CONCLUSIONS

In conclusion, we have synthesised 2,5-disubstituted-6-thio-1,2,4-triazolo-[3,2-b]-1,3,4-thiadiazole and 5-substituted aryl/aryloxymethyl-2-(phthalomidomethylamino)-1,3,4-thiadiazole derivatives. All these compounds have been assayed for their herbicidal activities against *Echinochloa oryzicola*, *Echinochloa crusgalli*, *Oryza sativa*, *Glycine max* and antifungal activities against *Aspergillus niger*, *Pyricularia oryzae*. Some of them have shown excellent herbicidal and fungicidal activity.

## ACKNOWLEDGEMENT

The authors are thankful to the Prof. Nizamuddin, Chemistry Department, D.D.U. Gorakhpur University, for his valuable suggestions and guidance during the whole work, and to the Director, (RSIC) CDRI, Lucknow for recording spectra and carrying out elemental analyses.

## REFERENCES

1. A-MOHSEN OMAR, M. E. OMAIMA, M. ABOULWafa: Synthesis and *in vitro* Antimicrobial and Antifungal Properties of Some Novel 1,3,4-thiadiazole and s-triazolo[3,4,-b][1,3,4]thiadiazole Derivatives. *J Heterocyclic Chem*, **23**, 1339 (1986).
2. J. SANDSTROM: Recent Advances in Chemistry of 1,3,4-thiadiazoles. In: *Advances in Heterocyclic Chemistry* (Eds A. R. Katritzky, A. J. Boulton). Academic Press, New York, 1968, p. 165.
3. N. GÜLERMAN, S. ROLLAS, M. ÜLGEN, J. W. GORROD: Synthesis and Evaluation of Some Substituted 1,3,4-thiadiazole Derivatives. *Bol Chim Farm*, **134** (8), 461 (1995).

4. A. AL-MASOUDI, Y. A. AL-SOUD, N. J. AL-SALIHI, N. A. AL-MASOUDI: 1,2,4-triazoles: Synthetic Approaches and Pharmacological Importance. *Chem Heterocyc Compd*, **42**, 1377 (2006).
5. K. T. POTTS: The Chemistry of 1,2,4-triazoles. *Chem Rev*, **61**, 87 (1961).
6. H. N. DOGAN, S. ROLLAS, H. ERDENIZ: Synthesis, Structure Elucidation and Antimicrobial Activity of Some 3-hydroxy-2-naphthoic Acid Hydrazone Derivatives. II *Farmaco*, **53**, 46247(1998).
7. N. TIWARI, B. CHATURVEDI, NIZAMUDDIN: Synthesis of Some 2-aryloxymethyl-1,3,4-thiadiazolo[2, 3-b]-quinazolin-4-ones and 2-aryloxymethyl-5-substituted-1,3,4-thiadiazolo[3,2-a]-s-triazin-7-thiones as Potential Biocides. *J Pestic Sci*, **15**, 357 (1990).
8. S. TIWARI, N. TIWARI, T. AGRAWAL, M. H. KHAN, NIZAMUDDIN: Synthesis of Some 2-substituted-1,3,4-thiadiazolo(2,3-c)1,2,4-triazino(5,6-b)indoles as Fungicides. *Indian J Chem*, **34B**, 1810 (1995).
9. M. H. KHAN, S. TEWARI, K. BEGUM, NIZAMUDDIN: Synthesis of Some 3'-(5-substituted-3-mercapto-1,2,4-triazol-4-yl)sipro[indole-3,2'-thiazolidine]-2,4'-diones and 3-substituted-1,2,4-triazole[3,4-b]indolo-[3,2-e][1,3,4]thiadiazoles as Fungicides. *Indian J Chem*, **34B**, 1075 (1998).
10. S. S. SHUKUROV, M. A. KUKANIEV, B. M. BOBOGARIBOV, S. S. SABIRO: Synthesis of 2-amino-5-aryl-1,3,4-thiadiazoles And Their Condensed Analogs with the Use of Aromatic Nitrites. *Russ Chem B*, **44** (10), 1955 (1995).
11. M. H. KHAN, Q. BANO: Synthesis and Biological Activities of Some 2-aryloxymethyl-4-(2-hydroxyphenyl)-1,5-benzodiazepines. *Indian J Pharm Sci*, **57**, 49 (1995).

*Received 18 September 2010*

*Revised 2 October 2010*

## **REPORT ON SELECTIVE ACYLATION OF BENZYLIC ALCOHOL TO BENZYL ACETATE WITH CATALYTIC SYSTEM Ni/SiO<sub>2</sub>: AN ENVIRONMENTALLY BENEVOLENT APPROACH**

M. ALAM<sup>a</sup>, A. RAHMAN<sup>b</sup>, N. M. ALANDIS<sup>c</sup>, M. R. SHAIK<sup>c\*</sup>

<sup>a</sup>*Research Center – College of Science, King Saud University, 11 451 Riyadh, Kingdom of Saudi Arabia*

<sup>b</sup>*Department of Chemistry, Vidya Vikas College of Engineering Chevella, RR District, Hyderabad, Andhra Pradesh, India*

<sup>c</sup>*Department of Chemistry, College of Science, King Saud University, P. O. Box 2455, 11 451 Riyadh, Kingdom of Saudi Arabia*  
*E-mail: rafiskm@gmail.com*

### **ABSTRACT**

An efficient and selective method was developed for the first time with 10% Ni/SiO<sub>2</sub> catalytic system for acylation of benzyl alcohol to benzyl acetate with 98% conversion using acetonitrile solvent under reflux with acetic anhydride. In this method we used aromatic alcohols like 4-chlorobenzyl alcohol and 4-nitrobenzyl alcohol, respectively. Ni species formed on silica surface demonstrates that Ni silica catalyst is active, while the calcined 2, 5 and 10% Ni/SiO<sub>2</sub> were less active compared with uncalcined 2, 5 and 10% Ni/SiO<sub>2</sub> catalysts, which were active for the title reaction. 10% Ni/SiO<sub>2</sub> catalysts were characterised by XRD, IR, BET, SEM, and UVDRS analyses. The catalysts showed remarkable reusability of 3 cycles, there is no leaching of catalysts, and finally blank reaction was also tested. The method of acylation is superactive, economic, and environmentally benevolent.

*Keywords:* acylation, benzyl alcohol, acetic anhydride, benzyl acetate.

### **AIMS AND BACKGROUND**

The acylation of aliphatic and aromatic alcohols is one of the most important processes in organic synthesis<sup>1</sup>. Acylation using acid anhydrides provides a cheap and an efficient method for protecting OH-groups during oxidation, and coupling reactions<sup>1,2</sup> or synthesis of esters with high potential applications as fragrances, flavours, surfactants and solvents<sup>3,4</sup>. On the other hand, the aromatic ketones resulting from the Friedel–Crafts

---

\* For correspondence.

acylation of aromatic compounds are valuable intermediates for the preparation of fine chemicals pharmaceuticals, agrochemicals and cosmetics<sup>2</sup>. Generally, acylation reactions are environmentally unfriendly due to using homogeneous catalysts such as organic bases (pyridine in triethylamine or pyridine with 4-(dimethylamine)pyridine), homogeneous Lewis acid catalysts ( $\text{AlCl}_3$ ,  $\text{BF}_3$ ,  $\text{TaCl}_5$ ), or inorganic acids<sup>1,2</sup>, which generate large amounts of toxic waste products, from which the catalysts are very difficult to recover, and reusability is also difficult. They also often necessitate the presence of environmentally unfriendly solvents like dichloromethane<sup>5</sup>. In order to overcome these problems, the attention was focused on the use of reusable, economic and ecofriendly heterogeneous catalysis. Some solid acid catalysts including zeolites<sup>6,7</sup>, exchanged clays<sup>8</sup>, oxides<sup>9</sup>, K-10 montmorillonite<sup>10</sup>, Al-MCM-4 (Ref. 11), or supported reagents<sup>11-14</sup> were used in these reactions, but they require high reaction temperatures or the use of environmentally unfriendly solvents. Other types of catalysts which exhibit a high activity in these reactions are metal triflate derivatives<sup>15-21</sup> but which are mostly used as homogeneous catalysts. These triflates possess strong Lewis acid and, in contrast to metal halides, they exhibit a very high tolerance towards water and more environmentally friendly catalysts<sup>22,23</sup>. Since 1980, the amorphous metal-metalloid alloys received special attention for their excellent catalytic activity properties and selectivity. Since the past 50 years nickel-based catalysts are attracting much attention for use in various industrially important reactions such as hydrodesulphurisation, reduction of nitriles, nitro, dealkylation, etc. Ni- and Co-containing amorphous alloys have properties that are of interest in catalysis, such as the presence of a large number of surface coordinating unsaturated sites and the lack of crystal defects. Jonnalagadda et al.<sup>24-26</sup> earlier reported on nitro-reduction, alcohol oxidation, the Knoevenagel reaction and aldehydes reduction with Ni/SiO<sub>2</sub>-supported system with excellent conversion and selectivity. In view of the above encouraging results the research project was further extended to examine the efficiency of 10% Ni/SiO<sub>2</sub> catalyst for acylation reaction of benzyl alcohol to benzyl acetate using acetic anhydride as acylating agent. The main objective of the present work is to evaluate the superactive 2, 5 and 10% Ni/SiO<sub>2</sub> catalysts for selective acylation of benzyl alcohol to the corresponding benzyl acetate at 65°C, and to study the effect of Ni species on silica surface in order to assess its catalytic aptitude for a potential use of the reaction for industrial purposes.

The object of the present study was to carry out acylation of benzylic alcohols to benzyl acetates with Ni/SiO<sub>2</sub> catalysts system, which Ni species are associated with silica. The aim of the manuscript addresses avoiding the use of high temperature to minimise the thermal risks during industrial production. The second question addressed is the achievement of high conversion and selectivity using acylating agent, to produce the desired chemical reliability in the required quality, reusability of the catalysts, economic and ecofriendly methodology. Additional features looked for are the operational simplicity, safe and energy efficient procedure.

## EXPERIMENTAL

*Materials.* All chemicals were synthesis grade reagents purchased from Merck, Germany.

*Preparation of catalysts.* The catalysts were prepared by impregnation method by dissolving nickel nitrate nonahydrate (2.5 g) in distilled water (20.0 ml) and adding to it silica gel (5.0 g) and stirring for 2 h using a magnetic stirrer at room temperature ( $20\pm 1^\circ\text{C}$ ) and ageing at room temperature for overnight. The excess water was removed by heating the mixture on water bath and using a rotavapour under vacuum to evaporate the water. The catalyst material was dried in an oven at  $100^\circ\text{C}$  for 12 h (Ref. 18).

*Typical reaction procedure.* A solution of 1.0 mmol benzyl alcohol with 10.0 ml acetonitrile as solvent and 0.5 g catalyst was prepared followed by slow addition of 1.5 mmol acetic anhydride at  $65^\circ\text{C}$ . In case of silica-supported catalysts, acetic anhydride was added for a 5-min period. The reaction mixture was magnetically stirred continuously. Then the reaction mixture was quenched with deionised water and extracted with ethyl acetate. The organic layer was dried on anhydrous sodium sulphate and the solvent was evaporated on rotavapour to give crude product of benzyl acetate, which was further subjected to column chromatography to afford pure benzyl acetate. The product was characterised by IR (Nicolet 460 spectrometer) and  $^1\text{H-NMR}$  (Bruker-S-300) spectroscopy. The IR spectrum shows the characteristic ester peaks at: 1742.75, 1229.23, 1027.17 ( $\text{cm}^{-1}$ ). The  $^1\text{H-NMR}$  shows:  $\delta = 2.09$  [3H, s], 2.16 [1H, s], 4.7 [2H, s], 7.2–7.5 [5H, aromatic] in the middle of the reaction. At the end of the reaction, the singlet at 2.16 [hydroxylic proton of benzyl alcohol] disappears showing the 100% conversion to benzyl acetate.

## RESULTS AND DISCUSSION

Acylation of benzyl alcohol to benzyl acetate was carried out with 10% Ni/SiO<sub>2</sub> (uncalcined) at  $65^\circ\text{C}$  and the reaction was completed in 3 h. It resulted in 97% conversion with 100% selectivity. The positive results lead the authors to investigate the catalytic activity of 2, 5 and 10%-loaded Ni/SiO<sub>2</sub> catalytic system under similar conditions (Table 1).

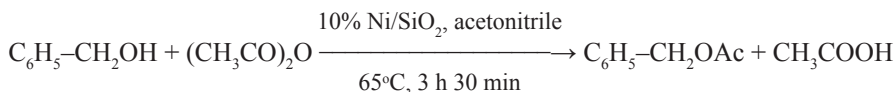
**Table 1.** Selective acylation of benzyl alcohol to benzyl acetate with acetic anhydride  
Benzyl alcohol = 1.0 mmol, acetic anhydride = 1.5 mmol, catalyst = 0.5 g

Support	Ni loading (%)	Reaction time	Conversion (%)	Selectivity (%)
SiO <sub>2</sub>	2	10 h	70	100
	5	3 h 30 min	80	100
	10	3 h	97	100

Note: mean of duplicate runs.

For operational convenience, for most of the reactions, it is attempted to monitor the time required for 100% conversion, where the starting material is completely consumed rather than half-reaction time. With 2% Ni-loading the conversion was 70% and the time of duration 4 h and with 5% Ni-loaded the conversion was 80%, which takes 3 h and 30 min. All catalysts exhibited 100% selectivity. Thus, the order of reactivity of Ni catalyst is: 2% Ni/SiO<sub>2</sub> < 5% Ni/SiO<sub>2</sub> < 10% Ni/SiO<sub>2</sub>. Identifying 10%Ni/SiO<sub>2</sub> as the ideal catalyst under the optimum conditions, all the reactions were studied in duplicate and the results were reproducible.

#### S c h e m e



Triflates are incorporated on the silica after the formation of the sol. For embedding *tert*-butyldimethylsilyltrifluoro-methanesulphonate (BDMST) an adapted route for the synthesis of the silica gel was used, which takes 6 days for the formation of catalysts due to the limitations of the above process. Authors designed simple method of preparation of Ni/SiO<sub>2</sub> catalysts in order to obtain the same active species. The influence of the operation parameters such as order of reactants, speed of agitation, time of ageing is important during the impregnation process for the development of the catalytic process.

The presence of weak interaction between metal and support is due to the little impregnation<sup>26</sup>. During the acylation of benzyl alcohol to benzyl acetate, the activity of the catalysts is credited to the presence of Ni uniformly distributed on the surface of the silica. All the results and the characterisation of Ni/SiO<sub>2</sub> identify that Ni in association with silica the active species and has major role to maximise the activation of acetic anhydride to form benzyl acetate. The observed generation of benzyl acetate with nickel on silica compared with 2, 5 and 10% Ni-loaded is noticeable for lower activity of 2 and 5% Ni/SiO<sub>2</sub> reinforcing the above inference. The low metallic surface of nickel on the silica support encourages the nickel oxide crystallised formation. Practically for Ni/SiO<sub>2</sub> inactive catalytic system reactivity with 2 and 5% Ni-loaded material is decreased possibly due to the formation of nickel basic sites. The weaker interaction between metal and support due to multilayer nickel on the support or the formation of the thick Ni particles could have contributed to the decrease of the catalytic activity. A similar observation was reported in literature, while studying the oxidation of alcohols using Ni-loaded hydrotalcites as catalysts in the presence of oxygen<sup>27</sup>. Duration of time was also examined for 2, 5 and 10% Ni/SiO<sub>2</sub> and the data are given in Table 1. It is evident that 10% Ni/SiO<sub>2</sub> catalysts is suitable for acylation of benzyl alcohol to benzyl acetate with acetic anhydride as acylating reagent. Acylation reaction was tested with calcined NiO, which resulted in only 50%



conversion with 100% selectivity and shows that the bulk catalysts exhibited some catalytic activity. In view of these results the authors further evaluated the catalytic aptitude of calcined 2, 5 and 10% Ni/SiO<sub>2</sub> catalysts. The results showed that calcined 10%Ni/SiO<sub>2</sub> resulted in 60% conversions, 2, 5, and 10% Ni/SiO<sub>2</sub> with only 15% conversion but retained 100% selectivity in 12 h duration of time. The reactions were tested for further 24 h duration of time and it was observed that there was no change in conversion and selectivity. This specifies that the catalysts are active only for 12 h and the 10%Ni/SiO<sub>2</sub> uncalcined is the superactive catalysts for the reaction. Blank (without catalyst) reaction was run for benzyl alcohol with acetic anhydride in similar conditions. It is concluded that catalyst is required for this reaction. Leaching test was conducted, i.e. the Ni/SiO<sub>2</sub> catalysts were washed with water and acetonitrile and then the substrate and acetic anhydride were added. The reaction was run under similar conditions for a specified period of time. It was observed that the reaction did not occur which shows that the Ni metal is well adhered to the silica surface as confirmed by SEM analysis.

The selective acylation of benzyl alcohol to benzyl acetate is important and interesting area of research. Particularly, the nitro-group which is electron-withdrawing enhances the reaction when interacted on the surface of the catalysts. Using 10% Ni/SiO<sub>2</sub> as appropriate catalyst that facilitates the adsorption of benzyl alcohol and acetic anhydride will enhance the catalytic efficiency with high conversion and selectivity for the acylation reaction. The rate of acylation is determined by the rate of initial adsorption of the substrate on the active sites of the catalytic surface.

The efficiency of the catalytic system comprising of 10% Ni/SiO<sub>2</sub> for acylation of various substituted benzyl alcohols was investigated. Table 2 summarises the results obtained using 10% Ni/SiO<sub>2</sub> system in acetonitrile as a solvent. The best results were obtained for acylation of benzyl alcohol with 97% conversion, 4-chloro benzyl alcohol with 75% conversion, 4-nitro benzyl alcohol with 80% conversion, *p*-methoxy benzyl alcohol gave 70% conversion, 4-methyl benzyl alcohol with 76% conversion, 3-methyl benzyl alcohol with 65% conversion, 2-methyl benzyl alcohol with 60% conversion. All these substrates containing electron-withdrawing groups and electron-activating groups resulted in more than 60% conversion and 100% selectivity. The reusability of 10% Ni/SiO<sub>2</sub> catalysts with benzyl alcohol as model substrate is repeated. S. No 1 in Table 2 was tested after the reaction the catalysts was washed with water, acetonitrile and dried in oven at 80°C for 4 h and then the temperature was raised to remove water. The dried catalysts was ready to check reusability. It was observed that in the 1st reusability test resulted in 97% conversion. The catalyst was washed with water, acetonitrile and dried in oven at 80°C for 4 h to remove the moisture. The dried catalyst was ready to check reusability. It was observed that in the 1st reusability test 97% conversion was achieved. The same procedure was followed for other 2nd and 3rd runs with conversion 80 and 60%, respectively. It was observed that the decrease in the catalytic activity is due to the uneven distribution of nickel species on silica surface<sup>24-27</sup>.

**Table 2.** Selective acylation of various aromatic alcohols to aromatic esters with 10% Ni/silica catalysts

Substrate – 2.0 mmol, acetic anhydride 1.5 mmol, catalyst – 0.5 g, duration time – 3h 30 min

S. No	Carbonyl + acetic anhydride	Product	Conversion (%)	Selectivity (%)
1	Ph-CH <sub>2</sub> OH + (CH <sub>3</sub> CO) <sub>2</sub> O	PhCH <sub>2</sub> OAc	97	100
2	4-Cl-C <sub>6</sub> H <sub>4</sub> CH <sub>2</sub> OH + (CH <sub>3</sub> CO) <sub>2</sub> O	4-Cl-C <sub>6</sub> H <sub>4</sub> CH <sub>2</sub> OAc	75	100
3	4-MeO-C <sub>6</sub> H <sub>4</sub> CH <sub>2</sub> OH + (CH <sub>3</sub> CO) <sub>2</sub> O	4-MeO-C <sub>6</sub> H <sub>4</sub> CH <sub>2</sub> OAc	70	100
4	4-NO <sub>2</sub> -C <sub>6</sub> H <sub>4</sub> CH <sub>2</sub> OH + (CH <sub>3</sub> CO) <sub>2</sub> O	4-NO <sub>2</sub> -C <sub>6</sub> H <sub>4</sub> CH <sub>2</sub> OAc	80	100
5	4-Me-C <sub>6</sub> H <sub>4</sub> CH <sub>2</sub> OH + (CH <sub>3</sub> CO) <sub>2</sub> O	4-Me-C <sub>6</sub> H <sub>4</sub> CH <sub>2</sub> OAc	76	100
6	3-Me-C <sub>6</sub> H <sub>4</sub> CH <sub>2</sub> OH + (CH <sub>3</sub> CO) <sub>2</sub> O	3-Me-C <sub>6</sub> H <sub>4</sub> CH <sub>2</sub> OAc	65	100
7	2-Me-C <sub>6</sub> H <sub>4</sub> CH <sub>2</sub> OH + (CH <sub>3</sub> CO) <sub>2</sub> O	3-Me-C <sub>6</sub> H <sub>4</sub> CH <sub>2</sub> OAc	60	100

*Effect of temperature.* The effect of temperature increase on the catalytic activity was tested at 120°C with 10% Ni/SiO<sub>2</sub> catalysts system and resulted in very little conversion of benzyl alcohol to benzyl acetate. Gosh et al.<sup>5</sup> reported that the acylation of phenol and alcohols with La(OTf)<sub>3</sub> at 120°C proceeded with 99% conversion in 3 min. Thus, using 10% Ni/SiO<sub>2</sub>, the conversion of benzyl alcohol was 85% after 2 h. It was demonstrated that the 10% Ni/SiO<sub>2</sub> catalyst was particularly superactive at 65°C compared to La(OTf)<sub>3</sub> (Ref. 5) and the authors avoid the use of high temperatures due for the formation of side products and the use of specialised equipment.

*Mechanism.* Acylation of alcohols generally proceeds via an acyl-oxygen cleavage bimolecular mechanism; it can be expected that the rate of esterification could be affected due to the transient complex of the metal ion with the carbonyl group. According to the reaction mechanism, the density of the Bronsted acid sites, i.e. hydroxyl group present on silica surface facilitates the formation of Ni-acylium ion, which rapidly leads to the product formation (Table 2).

*Catalysts characterisation.* 10% Ni/SiO<sub>2</sub> catalysts were characterised by BET surface area, XRD, IR, SEM, and UV-DRS techniques.

*XRD characterisation of 10% Ni/SiO<sub>2</sub>.* The XRD spectra (a Phillips-PW 1830XRD diffraction spectrometer) represented characteristic diffraction lines of the nickel phase and support, and no mixed nickel oxide support phases were identified. The pattern for the supports were of crystallised materials with the well-defined broad diffraction lines bands of amorphous SiO<sub>2</sub> support around 2θ = 45.

*BET data for 10% Ni/SiO<sub>2</sub>.* The specific area, i.e. the BET surface area of the catalysts, is 180 mg<sup>-1</sup>. During the impregnation stage of the preparation, the surface hydroxyl groups of the support are consumed by the reaction with the active phase precursor.

*FT-IR spectra of 10% Ni/SiO<sub>2</sub>.* The inspection of IR spectra (a Perkin-Elmer FT-IR spectrometer) of 10% Ni/SiO<sub>2</sub> fresh catalysts shows that the band at 1100 cm<sup>-1</sup> (asymmetrical Si-O-Si) is very perceptible to the formation of silicates<sup>24-26</sup>. SiO<sub>2</sub> does not

have free hydroxyl groups on the surface and confirms that nickel species are formed *in situ* during the reaction of selective acylation of benzyl alcohol. In the IR spectra of 10% Ni/SiO<sub>2</sub>, the strong and intense absorption band between 1078–1050 cm<sup>-1</sup> shows the presence of Si–O–Ni bonds<sup>26</sup>. Silica do not have free OH group on the surface. These results confirm that the aromatic alcohol obtained probably anchored to the support. This attributes to the Ni active species in association with silica for the activation of acetic anhydride for the formation of final product. The IR studies confirmed that Ni species of 10% Ni/SiO<sub>2</sub> catalyst is superactive for selective acylation of benzylic alcohols to benzyl acetate with good conversion and high selectivity.

*SEM study of Ni/SiO<sub>2</sub>.* SEM characterisation morphology and location of Ni species on the surface of the catalyst were examined by scanning electron microscopy (SEM) using a JEOL JSM-6100 microscope equipped with an energy-dispersive X-ray analyser (EDX). The images were taken with an emission current = 100 IA by a tungsten (W) filament and an accelerator voltage = 12 kV. The SEM figures of the 2, 5 and 10% Ni-loaded silica are shown in Fig. 1*a, b* and *c*, respectively.

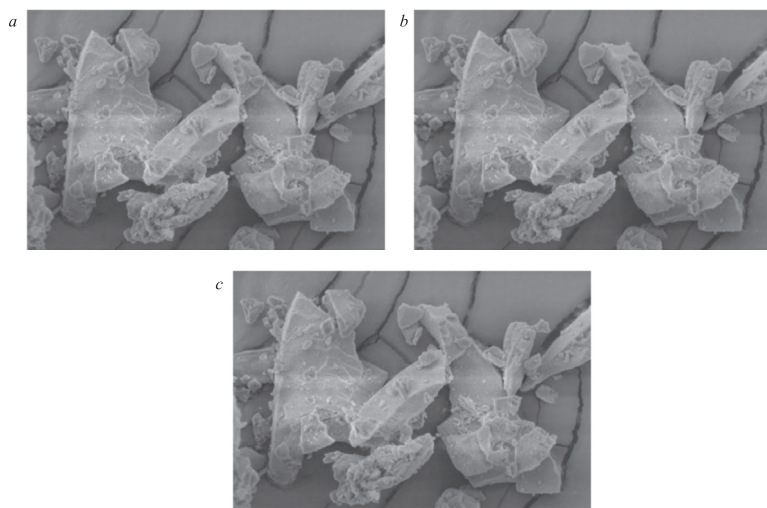


**Fig. 1.** SEM micrographs of: 2% Ni in silica (*a*); 5% Ni in silica (*b*), and 10% Ni in silica (*c*)

The morphology exhibited crystalline Ni of 2–4 nm which is well distributed over the silica surface of 10%-Ni loaded silica, which indicates that the distribution of Ni on support is either in conglomerates or in layers, thus hindering the participation both of Ni and silica active sites in the reaction. SiO<sub>2</sub> individually had no catalytic effect on the reaction. The observed reactivity of Ni-supported on silica material can be possibly attributed to the metal and support interactions, and the resultant changes in surface properties of the reactive sites. Earlier studies by Urbano et al. have revealed that supported Ni catalysts prepared from Ni(NO<sub>3</sub>)<sub>2</sub> by impregnation exhibit wide size distribution when compared with the prepared by more controlled and deposi-

tion method precipitation route, which generates low metallic Ni particles. The low metallic surface of nickel on the silica support encourages the crystallised nickel oxide formation. The presence of weak interaction between metal and support, due to little distribution of Ni entailing the formation of the layer of impregnated Ni, probably contributes to the increase of catalytic activity<sup>24,25</sup>. The observed non-reactivity with 2 and 5% Ni-loaded material could be possibly due to the multilayer of Ni loading on the support resulting in loss of activity as suggested by Choudary et al.<sup>27</sup> This is also supported by the SEM figures of the different amounts of Ni-loaded silica in the current study. An examination of SEM figures show that Ni particles are well distributed in 2 and 5% Ni loaded material with fine particles and the 10%-loaded material shows Ni multilayers and conglomeration of Ni particles on the silica surface. Further, the broadened silica peak with the 10% Ni loading relative to lower Ni-loaded surfaces in the XRD patterns also supports the surface characteristics illustrated by SEM figures. Houi et al. have reported that the activity of Ni on silica surface depends on the particle size of the metal and lower catalytic activity is observed with increased Ni particle size. Authors observed that the surface of 10% Ni-loaded silica is almost completely covered by nickel particles<sup>24-26</sup> and even suggesting that the Ni could be unevenly distributed, this has contributed to the low activity of 2 and 5% Ni-loaded silica.

*UVDRS characterisation.* Spectra of the supported materials, after initial drying, but before calcinations and reduction, were measured by diffuse reflectance UV diffusion spectroscopy and their absorption maxima and assignments were recorded. 10% Ni/SiO<sub>2</sub> of all percentages showed 740 nm<sup>-1</sup> range during UV diffusion analysis when compared with nickel nitrate aqueous solution and nickel nitrate, which showed UV range of 728 and 707 nm<sup>-1</sup>. Ni silica catalysts of all samples showed particle size in the range of 20–250 Å and the moisture content observed was 7%.

## CONCLUSIONS

The present study confirms that acetic anhydride silica system is superior to the other acylating agents systems for selective acylation of aromatic alcohols to aromatic acetates. Acylating species generated *in situ* by the decomposition acetic anhydride on nickel silica, which leads to the final product of acylation reaction for substituted benzylic alcohols to benzyl acetates with > 65% conversions and 100% selectivity is achieved at 65°C in 3 h 30 min duration of time (Table 2). In most cases more than 70% conversions were achieved. This system applies even to electron-withdrawing groups such as nitro, methoxy attached to 4-position of benzylic group. It is a well equipped system with no need for any specialised facilities. The catalyst is loaded without pre-addition of acetic anhydride reagent. The catalyst is reusable for 3 consecutive cycles and there is no leaching of catalysts. The NiO and 2, 5 and 10% Ni/SiO<sub>2</sub> calcined catalysts exhibited less activity. Finally it was concluded that 10% uncalcined Ni/SiO<sub>2</sub> catalysts is superactive for the reaction. Further, this process is economically viable

and can be upgraded to large-scale reactions. This forms a new alternative methodology at 65°C, which excludes the use of harsh reaction conditions.

## ACKNOWLEDGEMENTS

The project was supported by King Saud University, Deanship of Scientific Research, College of Science-Research Center.

## REFERENCES

1. A. N. PARVULESCU, B. C. GAGEA, G. PONCELET, V. I. PARVULESCU: Acylation of Alcohols and Activated Aromatic Compounds on Silica-embedded Triflate Catalysts. *Appl Catal A: Gen*, **301**, 133 (2006).
2. A. N. PARVULESCU, B. C. GAGEA, V. I. PARVULESCU, D. DE VOS, P. A. JACOBS: Acylation of 2-methoxynaphthalene with Acetic Anhydride over Silica-embedded Triflate Catalysts. *Appl Catal A: Gen*, **306**, 159 (2006).
3. G. BOND, J. A. GARDNER, R. W. McCABE, D. J. SHORROCK: Friedel–Crafts Acylation Reactions Using Heterogeneous Catalysts Stimulated by Conventional and Microwave Heating. *J Mol Catal A: Chem*, **278**, 1 (2007).
4. B. SREEDHAR, R. ARUNDHATHI, M. AMARNATH REDDY, G. PARTHASARATHY: Highly Efficient Heterogeneous Catalyst for Acylation of Alcohols and Amines Using Natural Ferrous Chamosite. *Appl Clay Science*, **43**, 425 (2009).
5. R. GOSH, S. MAITI, A. CHAKRABORTY: Facile Catalyzed Acylation of Alcohols, Phenols, Amines and Thiols Based on  $ZrOCl_2 \cdot 8H_2O$  and Acetyl Chloride in Solution and in Solvent-free Conditions. *Tetrahedron Lett*, **46**, 147 (2005).
6. R. BALLINI, G. BOSICA, S. CARLONI, L. CIARALLI, R. MAGGI, G. SARTORI: Zeolite HSZ-360 as a New Reusable Catalyst for the Direct Acetylation of Alcohols and Phenols under Solventless Conditions. *Tetrahedron Lett*, **39**, 6049 (1998).
7. C. P. BEZOUHANOVA: Synthesis of Aromatic Ketones in the Presence of Zeolite Catalysts. *Appl Catal A: Gen*, **229**, 127 (2002).
8. J. FARKAS, S. BEKASSY, B. AGAI, M. HEGEDUS, F. FIGUERAS: Acylation of Resorcinol on Clay Catalysts. *Synth Commun*, **30**, 2479 (2000).
9. M. SARVARI, H. SHARGHI: Reactions on a Solid Surface. A Simple, Economical and Efficient Friedel–Crafts Acylation Reaction over Zinc Oxide (ZnO) as a New Catalyst. *J Org Chem*, **69**, 6953 (2004).
10. S. G. PAI, A. R. BAJPAI, A. B. DESHPANDE, S. D. SAMANT: Friedel–Crafts Benzoylation of Arenes Using  $FeCl_3$  Impregnated Montmorillonite K10. *Synth Commun*, **27**, 2267 (1997).
11. K.G. BHATTACHARYYA, A. K. TALUKDAR, P. DAS, S. SIVASANKER: Acetylation of Phenol with Al-MCM-41. *Catal Commun*, **2**, 105 (2001).
12. C. CASTRO, A. CORMA, J. PRIO: On the Acylation Reactions of Anisole Using  $\alpha$ ,  $\beta$ -unsaturated Organic Acids as Acylating Agents and Solid Acids as Catalysts: A Mechanistic Overview. *J Mol Catal A: Chem*, **177**, 273 (2002).
13. V. R. CHOUDHARY, S. K. JANA, N. S. PATIL: Acylation of Aromatic Compounds Using Moisture Insensitive  $InCl_3$  Impregnated Mesoporous Si-MCM-41 Catalyst. *Tetrahedron Lett*, **43**, 1105 (2002).
14. J. A. MELERO, R. van GRIEKEN, G. MORALES, V. NUNO: Friedel–Crafts Acylation of Aromatic Compounds over Arenesulfonic Containing Mesostructured SBA-15 Materials. *Catal Commun*, **5**, 131 (2004).

15. R. DALPOZZO, A. de NINO, L. MAIUOLO, A. PEROCOPIO, M. NARDI, G. BARTOLI, R. ROMEO: Highly Efficient and Versatile Acetylation of Alcohols Catalysed by Cerium(III) Triflate. *Tetrahedron Lett*, **44**, 5621 (2003).
16. A. G. M. BARRET, D. C. BRADDOCK: Scandium(III) or Lanthanide(III) Triflates as Recyclable Catalysts for the Direct Acetylation of Alcohols with Acetic Acid. *Chem Commun*, 351 (1997).
17. R. ALLETTI, M. PERAMBUDURU, S. SAMANTHA, V. R. REDDY: Gadolinium Triflate: An Efficient and Convenient Catalyst for Acetylation of Alcohols and Amines. *J Mol Catal A: Chem*, **226**, 57 (2005).
18. K. ISHIHARA, M. KUBOTA, H. YAMAMOTO: A New Scandium Complex as an Extremely Active Acylation Catalyst. *Synlett*, 265 (1996).
19. K. ISHIHARA, M. KUBOTA, H. KUNIHARA, H. YAMAMOTO: Scandium Trifluoromethanesulfonate as an Extremely Active Lewis Acid Catalyst in Acylation of Alcohols with Acid Anhydrides and Mixed Anhydrides. *J Org Chem*, **61**, 4560 (1996).
20. K. K. CHAUHAN, C. G. FROST, I. LOVE, D. WAITI: Indium Triflate: An Efficient Catalyst for Acylation Reactions. *Synlett*, **22**, 1743 (1999).
21. B. KARIMI, J. MAKEKI: Lithium Trifluoromethanesulfonate (LiOTf) as a Recyclable Catalyst for Highly Efficient Acetylation of Alcohols and Diacetylation of Aldehydes under Mild and Neutral Reaction Conditions. *J Org Chem*, **68**, 4951 (2003).
22. B. C. GAGEA, A. N. PARVULESCU, V. I. PARVULESCU, A. AUROUX, P. GRANGE, G. PONCELET: Alkylation of Phenols and Naphthols on Silica-immobilized Triflate Derivatives. *Catal Lett*, **91**, 141 (2003).
23. A. N. PARVULESCU, B. C. GAGEA, V. PARVULESCU, V. I. PARVULESCU, G. PONCELET, P. GRANGE: Comparative Behavior of Silica-embedded *tert*-butyldimethylsilyltrifluoro-methanesulfonate and Lanthanum Triflate Catalysts. *Catal Today*, **73**, 177 (2003).
24. A. RAHMAN, S. B. JONNALAGADDA: Swift and Selective Reduction of Nitroaromatics to Aromatic Amines with Ni–Boride–Silica Catalysts System at Low Temperature. *Catal Lett*, **123**, 264 (2008).
25. A. RAHMAN, S. B. JONNALAGADDA: Rapid and Selective Reduction of Aldehydes, Ketones, Phenol, and Alkenes with Ni–Boride–Silica Catalysts System at Low Temperature. *J Mol Catal A*, **299**, 98 (2009).
26. V. S. R. RAJASEKHAR, A. RAHMAN, S. B. JONNALAGADDA: Selective Catalytic Knoevenagel Condensation by Ni–SiO<sub>2</sub> Supported Heterogeneous Catalysts: An Environmentally Benign Approach. *Catalysis Commun*, **10**, 365 (2009).
27. B. M. CHOUDARY, M. L. KANTAM, A. RAHMAN, Ch. VENKAT REDDY, K. KOTESHWAR RAO: The First Example of Activation of Molecular Oxygen by Nickel in Ni–Al Hydrotalcite: A Novel Protocol for the Selective Oxidation of Alcohols. *Angew Chem Int*, 785 (2001).

*Received 17 February 2012*

*Revised 24 March 2012*

## **ERRATA**

Due to some misunderstandings between the Editors and authors, the article entitled ‘Antioxidant, Antimicrobial Activity and GC-MS Analysis of *Russelia equisetiformis* Essential Oils’ by M. RIAZ, N. RASOOL, I. H. BUKHARI, K. RIZWAN, M. ZUBAIR, F. JAVED, A. A. ALTAF, H. M. A. QAYYUM, published in **35** (4), 1027 (2012), is re-published in **36** (1), (2013).

## ANTIOXIDANT, ANTIMICROBIAL ACTIVITY AND GC-MS ANALYSIS OF *Russelia equisetiformis* ESSENTIAL OILS

M. RIAZ<sup>a</sup>, N. RASOOL<sup>a\*</sup>, I. H. BUKHARI<sup>a</sup>, K. RIZWAN<sup>a</sup>, M. ZUBAIR<sup>a</sup>,  
F. JAVED<sup>b</sup>, A. A. ALTAF<sup>b,c</sup>, H. M. A. QAYYUM<sup>b</sup>

<sup>a</sup>Department of Chemistry, Government College University, 38 000 Faisalabad, Pakistan

<sup>b</sup>Department of Chemistry, Quaid-i-Azam University, 45 320 Islamabad, Pakistan

<sup>c</sup>Department of Chemistry, University of Malakand, Chakdara, Dir (lower), Pakistan

E-mail: nasirhej@yahoo.co.uk

### ABSTRACT

In this research work the chemical composition by GC-MS, antioxidant and antimicrobial studies of *Russelia equisetiformis* (Fire cracker) flowers, leaves and stems essential oils were carried out. The essential oils were obtained by hydro-distillation and analysed by GC-MS for their chemical composition. The GC-MS analysis showed hexadecanoic acid methyl ester as the major constituent of *R. equisetiformis* essential oils in amounts of 11.036, 10.951 and 13.212% for the leaves, stems and flowers, respectively, followed by  $\alpha$ -pinene 7.256, 9.595, 13.256% for leaves stems and flowers, respectively. The stearic acid was found to be 9.291 and 7.028 in flowers and leaves, respectively. The antioxidant activity of the essential oils was determined by DPPH radical scavenging assay and inhibition in linoleic acid oxidation and it was found to be in the range of 9.96–25.31 and 65.32–89.21  $\mu\text{g/ml}$ , respectively. The potential of the essential oils against the selected fungal and bacterial strains was evaluated in present studies by disc diffusion and minimum inhibitory concentration (MIC) assays.

**Keywords:** *Russelia equisetiformis*, antimicrobial and antioxidant activity, GC-MS, essential oil.

### AIMS AND BACKGROUND

The use of essential oils as functional ingredients in foods, drinks and cosmetics has been gaining greater concern, because the synthetic additives used as antioxidant were harmful<sup>1</sup>. The natural antioxidants have been considered to be valuable constituents

---

\* For correspondence.



for the prevention of human diseases<sup>2-4</sup>. The medicinal plant offers a broad variety of natural plants which are rich sources of phytochemicals such as antioxidants, vitamin E, vitamin C and carotenoids<sup>5-9</sup>.

The natural extracts with a pleasant smell combined with a preservative action have properties to avoid lipid deterioration and spoilage by microorganisms. The oxidation of food causes the development of undesirable smell, creates toxicity and greatly affects the shelf-life of food products<sup>10,11</sup>. The essential oils and their chemical constituents are gaining great interest due to their comparatively safe status, their wide acceptance by the consumers and multipurpose functional uses<sup>12</sup>. In recent years, the herbal extracts and essential oils have paved a path to the scientific research due to the reason that they are naturally occurring as well as biologically active<sup>13,14</sup>. Various authors have evaluated the nutritional, antioxidant and biological properties of various plant species in Pakistan<sup>6,7,11,15-19</sup>

The essential oil is considered beneficial in folk medicine to treat respiratory disorders, allergies, diabetes, impotence, anxiety, stomach cramps, constipation, infertility, headaches and vomiting. Furthermore, scientific data have proven that the antioxidative power of the volatile oils in basil makes it a healthy stimulant of the immune system<sup>20</sup>.

Essential oils from medicinal plants can be used for microbial resistance development in food items. The use of natural preservatives is more safe than synthetic antioxidants. Essential oils are terpene hydrocarbons as well as their oxygenated derivatives such as acids, alcohols, ketones, aldehydes and esters. The essential oils have been extracted from different plants parts<sup>21</sup>.

The medicinal significances of *R.* (Badami, Vaijanathappa & Bhojraj, 2008) *equisetiformis* plant lies in fact that it was used as an aperient, emmenagogue, febrifuge, tonic against diseases such as used in the treatment of typhoid mentioned in the literature available<sup>22</sup>. Presently the essential oils are also studied for the flavouring foods. To best of our knowledge there was no any detailed report available in the literature on the, antioxidant and antimicrobial activities and GC-MS analysis of the *Russelia equisetiformis* essential oils. So in the present study, we analysed the chemical composition of the essential oil extracted from the flowers, leaves and stems of *Russelia equisetiformis* native to Pakistan.

## EXPERIMENTAL

The *R. equisetiformis* (scrophulariaceae) flowers, stems and leaves were collected from Faisalabad, Pakistan. The plant was further identified and authenticated by the Dr. Mansoor Hameed (Taxonomist), Department of Botany, University of Agriculture, Faisalabad Pakistan. A voucher specimen (4203) has been deposited in collection/herbarium Department of Botany University of Agriculture Faisalabad. After collection plant leaves were washed, shade dried and grinded.

*Isolation of the essential oils.* The air-dried and ground flowers, leaves and stems of *Russelia equisetiformis* were hydro-distilled for 4 hours by using a clevenger-type apparatus as earlier method described<sup>17,23</sup>. The essential oils were collected and dried over anhydrous sodium sulphate, filtered and stored at 4°C until provided for analysis.

Physical parameters of essential oils. The physical parameters of the isolated essential oils such as density and refractive index were determined using earlier described standard protocol<sup>24</sup>.

*Gas chromatography mass spectrometry (GC-MS) analysis.* The samples were analysed using GCMS-QP2010 (SHIMADZU, Japan) under the following conditions: 1 µl sample solution was injected manually in split-less mode (sampling time 1 min) and injection-port set at 200°C. Gas chromatography was equipped with capillary column (DB-5), 30 m long, 0.25 mm internal diameter and 0.25 µm film thickness. Oven temperature was programmed in a 3-step gradient: initial temp. set at 40°C (held for 5 min), stopped till 160°C at 10°C rise per min, followed by 5°C/min rise till 270°C and lastly reached 330°C at a 15°C /min rise where it was held for 5 min. Helium gas flow rate was 1.1 ml/min (pressure 60 kPa and linear velocity 38.2 cm/s). Ions/fragments were monitored in scanning mode through 40–550 *m/z*. The identification of the compounds was based on comparison of their mass spectra with those of their NIST 05 mass spectral library<sup>25</sup>.

*Free radical scavenging assay.* For the determination of IC<sub>50</sub> by DPPH free radical scavenging assay method described by Iqbal et al. was used<sup>26</sup>. The IC<sub>50</sub> values were calculated from the plot of percentage scavenging against concentration of the essential oils. Three replicates were recorded for each sample.

*Percentage inhibition of linoleic acid oxidation.* The antioxidant activities of essential oils were also calculated in terms of measurement of percentage inhibition of per oxidation in the linoleic acid system as earlier method described<sup>26</sup>. The sample that has not any antioxidant component was used as a blank. Percentage inhibition of linoleic acid oxidation was determined by the following equation:

$$\text{inhibition (\%)} = 100 - \left( \frac{\text{absorbance increase of sample at 360 h}}{\text{absorbance increase of control at 360 h}} \times 100 \right)$$

*Bleachability of β-carotene in linoleic acid system.* Antioxidant activity of the *R. equisetiformis* essential oil was also analysed by bleaching of β-carotene/linoleic acid emulsion system as method described<sup>27</sup>. The solution of β-carotene and linoleic acid mixture was prepared by dissolving 0.1 mg β-carotene, 20 mg linoleic acid and 100 mg Tween 40 in 1.0 ml of chloroform. The chloroform was removed under vacuum in rotary evaporator at 50°C. 5.0 ml of this reaction mixture were added to test tubes containing 200 µl of the essential, prepared at 4.0 g/l concentrations and the absorbance at the zero time was measured at 490 nm against a blank, consisting of an emulsion without β-carotene. Then emulsion was incubated for 50 h at room temperature and

the absorbance was recorded at different time intervals. For butylated hydroxytoluene (BHT) used as standard and blank the same procedure was applied.

**Antimicrobial assay.** In order to evaluate the antimicrobial activity of selected bacterial, i.e. *Escherichia coli*, *Pasturella multocida*, and *Staphylococcus aureus*, *Bacillus subtilis* and fungal strains, i.e. *Aspergillus flavus*, *Alternaria alternata*, *Aspergillus niger* and *Rhizopus solani* by using plant essential oils analysed by disc diffusion method<sup>28</sup>, minimum inhibitory concentration (MIC) was determined by using the modified method described by Sarker and co-workers<sup>29</sup>. For the evaluation of minimum inhibitory concentration (MIC) different concentrations of plant essential oils ranging from 0.1 to 10000 µg/ml were used by serial dilution. The range of dilution was carried out by keeping in mind the antimicrobial activity in zone of inhibition assay. The plant samples of essential oils show better activity in zone of inhibition, the serial dilution for MIC was carried at smaller concentration and for samples showing less activity, higher concentration was used for serial dilution

**Statistical analysis.** The experiments were carried out in triplicate and statistical analysis of the data was performed by analysis of variance, using the Costat software. The probability value  $p \leq 0.05$  considered to denote a statistically significance evaluation. All data were presented as mean values and standard deviation (SD).

## RESULTS AND DISCUSSION

Table 1 shows the percentage yield and some other physical properties of the *R. equisetiformis* essential oils. The highest amount of the essential oils in the *R. equisetiformis* was obtained (0.61%) from the flowers of the plant. The essential oils parentage yield was found to be in the range of 0.42–0.61% for *R. equisetiformis* leaves, stems and flowers. The values of refractive index and density of the *R. equisetiformis* essential oils were determined. No literature has been found for the comparison of essential oils results of this plant.

**Table 1.** Yield (percent), physical properties and antioxidant studies of *R. equisetiformis* essential oils

Plant parts	Yield (%)	Density (g/ml)	Refractive index (25°C)	DPPH (IC <sub>50</sub> µg/ml)	Inhibition in linoleic acid oxidation
Flowers	0.61±0.02 <sup>a</sup>	0.96±0.05 <sup>a</sup>	1.5043±0.002 <sup>a</sup>	12.25±0.19 <sup>c</sup>	76.25±0.61 <sup>b</sup>
Leaves	0.42±0.01 <sup>c</sup>	0.94±0.03 <sup>a</sup>	1.4804±0.001 <sup>a</sup>	19.36±0.15 <sup>b</sup>	69.36±0.68 <sup>c</sup>
Stems	0.49±0.05 <sup>b</sup>	0.97±0.04 <sup>a</sup>	1.5001±0.003 <sup>a</sup>	25.31±0.21 <sup>a</sup>	65.32±0.56 <sup>d</sup>
BHT	–	–	–	9.69±0.12 <sup>d</sup>	89.21±0.78 <sup>a</sup>

The results are means ±standard deviation of 3 separate experiments; different alphabetical letters in superscript indicate significant differences within the samples.

The refractive index (25°C) and density (g/ml) of *R. equisetiformis* essential oils were not significantly differed ( $p > 0.05$ ) among the different parts (Table 1). No literature has been available regarding the essential oil of this plant, however, the yield

of essential oils in the plant under study was found to be (0.42–0.61% comparable to earlier reports by Politeo et al.<sup>30</sup>, who found the yield of the essential oils from aerial parts of the plant by hydro-distillation to be 0.62%.

*Chemical composition of the essential oils analysed by GC-MS.* The chemical composition of *R. equisetiformis* essential oils was presented in Table 2. The analysed essential oils mainly contained hexadecanoic acid methyl ester as the major constituent of *R. equisetiformis* essential oil in amounts of 11.036, 10.951 and 13.212% for the leaves, stems and flowers, respectively, followed by  $\alpha$ -pinene – 7.256, 9.595, 13.256% for leaves, stems and flowers.

**Table 2.** Compounds identified in the essential oil of *R. equisetiformis* and their percentage area

RI	Components	Percentage area		
		flowers	stems	leaves
940	$\alpha$ -pinene	13.256	9.595	7.256
953	camphene	0.256	nd	0.153
970	$\beta$ -pinene	7.742	6.253	4.595
1049	$\beta$ -ocimene	0.568	0.235	3.596
1058	$\gamma$ -terpinene	1.232	5.261	3.253
1204	verbenone	0.221	3.499	3.271
1365	geranic acid	6.235	t	5.597
1411	methyl eugenol	5.87	4.865	t
1654	$\alpha$ -cadinol	1.004	3.263	nd
1719	methyl tetradecanoate	nd	6.259	5.265
1756	aristol-9-en-8-one	1.744	0.761	4.451
1793	1-octadecene	0.753	3.569	nd
1962	hexadecanoic acid, methyl ester	13.212	10.951	11.036
2000	eicosane	nd	8.035	4.56
2124	octadecanoic acid, methyl ester	6.348	5.256	6.368
2173	3-methylheicosane	1.236	6.369	nd
2194	octadecanoic acid, ethyl ester	7.343	nd	5.689
2200	stearic acid	9.291	t	7.023
2288	<i>n</i> -docosane	3.257	8.197	7.663
2327	eicosanoic acid, methyl ester	0.299	nd	6.161
2435	11-methyltetracosane	10.889	9.025	8.437
2527	docosanoic acid, methyl ester	5.974	4.263	nd
2733	3-Methylheptacosane	0.949	t	t
2934	hexacosanoic acid, methyl ester	2.309	3.286	3.789

t – traces; \* nd – not identified; mode of identification= RI and GC-MS.

The stearic acid was found to be 9.291 and 7.023% in flowers and leaves, respectively. The stearic acid was found to be in traces in the essential oil of stems. Some of the chemical constituents were found in traces and some were not detected in *R. equi-*

*setiformis* parts. Therefore, the chemical constituents found in *Russelia equisetiformis* may play major roles in the biological activity and pharmacological properties.

**Antioxidant activity.** The antioxidant activity of the *R. equisetiformis* essential oils was analysed by different *in vitro* assays. The free radical scavenging ability of the essential oils was measured by the DPPH assay (Table 1). The *R. equisetiformis* essential oils were able to reduce the stable, purple-coloured radical DPPH into yellow-coloured DPPH-H. *R. equisetiformis* essential oil obtained from flowers showed greater radical scavenging activity than those from leaves and stems, exhibiting IC<sub>50</sub> values of 12.25, 19.36 and 25.31 µg/ml for flowers, leaves and stems, respectively. When the DPPH scavenging capacity of essential oils was compared with BHT, it showed some less radical scavenging capacity with IC<sub>50</sub> values of 9.69 µg/ml. The smaller were the IC<sub>50</sub> values better is the antioxidant activity and *vice versa*. The percentage inhibition of linoleic acid oxidation as exhibited by *R. equisetiformis* essential oils is shown in Table 1. The evaluated *R. equisetiformis* essential oils inhibited the oxidation of linoleic acid showing an antioxidant activity of essential oils to be in the range of 65.32, 69.36, 76.25, and 89.21% for flowers, leaves, stems and BHT, respectively. The antioxidant potential of *R. equisetiformis* essential oils might be attributed to the presence of some phytochemicals<sup>31</sup>. The antioxidant activity of the essential oils of *R. equisetiformis* by bleaching of β-carotene with linoleic acid system was studied (Fig. 1). The decrease in absorbance of β-carotene showed a lower rate of oxidation of linoleic acid and higher antioxidant activity in the presence of essential oils from *R. equisetiformis*. Essential oils of *R. equisetiformis* flowers exhibited better antioxidant activity than leaves and stems. Based on these results, order of antioxidant activity of *R. equisetiformis* essential oils was as follows: BHT > flowers > leaves > stems. The antioxidant activity of essential oils has formed the basis of many uses including pharmaceuticals, natural therapies, preservation of fresh and processed food and alternative medicine<sup>13</sup>. As per literature survey, the antioxidant properties of essential oils have probably imparted due to the presence of monoterpenes and oxygenated terpenes. On the other hand, the antioxidant activity of 98 pure essential oils chemical components and showed that monoterpene hydrocarbons had a significant biological activity<sup>32</sup>. Furthermore, some researchers showed that some essential oils rich in non-phenolic compounds such as terpenoids, fatty acid/methyl esters also have antioxidant potentials<sup>33</sup> previously reported as potent radical scavengers, because of the phenylpropanoid moiety<sup>13</sup>. During literature review it was also found that the biological activities such as antioxidant potential of essential oils is due to some phyto-components such as palmitic acid (hexadecanoic acid, ethyl ester and *n*-hexadecaonic acid), unsaturated fatty acid, docosatetraenoic acid and octadecatrienoic acid<sup>16,34</sup>.

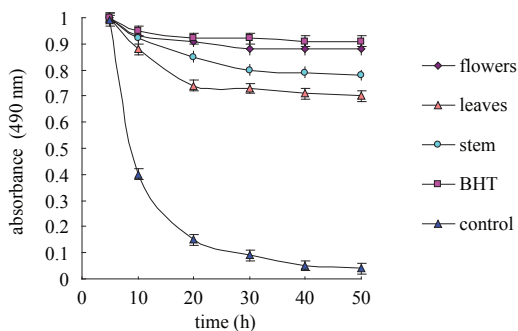


**Fig. 1.** Antioxidant activity of *R. equisetiformis* essential oils analysed by bleaching of  $\beta$ -carotene-linoleic acid emulsion

*Antimicrobial activity of essential oils.* The selected microorganisms were studied for antimicrobial assay by the essential oils of *R. equisetiformis* (Table 2). The essential oils of the plant showed antimicrobial potential against the bacterial and fungal strains. The results obtained from the disc diffusion method measured in inhibition zone (IZ) in millimeter and by measurement of minimum inhibitory concentration (MIC) in  $\mu\text{g/ml}$  showed that essential oil of flowers showed good inhibitory activity against *S. aureus* (21.9 mm; 250.0  $\mu\text{g/ml}$ ) and against *B. subtilis*, (20.1 mm; 312.0  $\mu\text{g/ml}$ ), respectively by the essential oil of flowers; the less inhibitory activity was observed against *A. flavus* with smallest inhibition zone = 10.1 mm and the highest MIC = 937.0  $\mu\text{g/ml}$ . The antimicrobial activity of essential oil of flowers against the *E. coli* was found to be 11.3 mm and MIC = 750.0  $\mu\text{g/ml}$ , respectively.

The antimicrobial activity of the flowers, stems and leaves follows the sequence: flowers > leaves > stems. The essential oil of leaves showed good potential against all the tested bacterial and fungal stains. The essential oil of stems showed poor activity as compared with the essential oil of flowers. For the comparison of results rifampicin and fluconazole were used as positive control for bacterial and fungal strains, respectively. The standard drugs showed higher activity on the microbes than the tested essential oils (Table 3). The standard antibiotics were highly purified chemical compounds so their activity was higher as compared to the essential oils of flowers, leaves and stems.

So the *R. equisetiformis* plant may be used in future to cure the diseases caused by the tested microbes. The antimicrobial activity may be due to the presence of phytochemicals some of which are reported to have antimicrobial activity<sup>35,36</sup>. As per literature review, the antimicrobial potential of essential oils is difficult to correlate to a specific compound.

**Table 3.** Antimicrobial studies by inhibition zone and minimum inhibitory concentration ( $\mu\text{g/ml}$ ) of *Russelia equisetiformis* essential oils

Tested micro organisms	Zone of inhibition (mm)			Rifampicin	Fluconazole
	Flowers	Leaves	Stems		
<i>E. coli</i>	11.3 $\pm$ 0.12 <sup>g</sup>	9.9 $\pm$ 0.08 <sup>g</sup>	8.4 $\pm$ 0.09 <sup>g</sup>	22.71 $\pm$ 0.15 <sup>d</sup>	–
<i>P. multocida</i>	15.4 $\pm$ 0.09 <sup>e</sup>	13.2 $\pm$ 0.12 <sup>e</sup>	16.32 $\pm$ 0.15 <sup>a</sup>	31.21 $\pm$ 0.35 <sup>a</sup>	–
<i>S. aureus</i>	21.9 $\pm$ 0.24 <sup>a</sup>	19.2 $\pm$ 0.28 <sup>a</sup>	14.2 $\pm$ 0.12 <sup>b</sup>	29.01 $\pm$ 0.24 <sup>c</sup>	–
<i>B. subtilis</i>	20.1 $\pm$ 0.18 <sup>b</sup>	17.9 $\pm$ 0.18 <sup>b</sup>	11.6 $\pm$ 0.14 <sup>d</sup>	30.05 $\pm$ 0.09 <sup>b</sup>	–
<i>A. flavus</i>	10.1 $\pm$ 0.09 <sup>h</sup>	8.5 $\pm$ 0.07 <sup>h</sup>	7.4 $\pm$ 0.05 <sup>h</sup>	–	28.04 $\pm$ 0.06 <sup>b</sup>
<i>A. alternata</i>	17.2 $\pm$ 0.15 <sup>d</sup>	14.7 $\pm$ 0.13 <sup>d</sup>	9.8 $\pm$ 0.08 <sup>e</sup>	–	27.55 $\pm$ 0.23 <sup>c</sup>
<i>R. solani</i>	12.4 $\pm$ 0.12 <sup>f</sup>	10.8 $\pm$ 0.11 <sup>f</sup>	8.9 $\pm$ 0.09 <sup>f</sup>	–	25.04 $\pm$ 0.29 <sup>d</sup>
<i>A. niger</i>	19.3 $\pm$ 0.17 <sup>c</sup>	17.3 $\pm$ 0.15 <sup>c</sup>	12.8 $\pm$ 0.13 <sup>c</sup>	–	29.09 $\pm$ 0.19 <sup>a</sup>
Minimum inhibitory concentration ( $\mu\text{g/ml}$ )					
<i>E. coli</i>	750.0 $\pm$ 5.07 <sup>b</sup>	1500.0 $\pm$ 7.08 <sup>a</sup>	1850.0 $\pm$ 9.09 <sup>a</sup>	93.0 $\pm$ 0.82 <sup>b</sup>	–
<i>P. multocida</i>	625.0 $\pm$ 4.09 <sup>d</sup>	937.0 $\pm$ 6.12 <sup>d</sup>	1250.0 $\pm$ 8.15 <sup>c</sup>	183.5 $\pm$ 1.21 <sup>a</sup>	–
<i>S. aureus</i>	250.0 $\pm$ 1.24 <sup>h</sup>	312.0 $\pm$ 2.28 <sup>h</sup>	500.0 $\pm$ 4.04 <sup>h</sup>	31.25 $\pm$ 0.32 <sup>d</sup>	–
<i>B. subtilis</i>	312.0 $\pm$ 2.18 <sup>g</sup>	468.0 $\pm$ 3.18 <sup>g</sup>	625.0 $\pm$ 5.14 <sup>g</sup>	62.5 $\pm$ 0.52 <sup>c</sup>	–
<i>A. flavus</i>	937.0 $\pm$ 6.09 <sup>a</sup>	1000.0 $\pm$ 7.07 <sup>c</sup>	1000.0 $\pm$ 6.05 <sup>d</sup>	–	125.0 $\pm$ 1.06 <sup>a</sup>
<i>A. alternata</i>	468.0 $\pm$ 3.15 <sup>e</sup>	750.0 $\pm$ 5.13 <sup>e</sup>	937.0 $\pm$ 7.08 <sup>e</sup>	–	93.5 $\pm$ 0.85 <sup>b</sup>
<i>R. solani</i>	500.0 $\pm$ 0.12 <sup>c</sup>	1250.0 $\pm$ 6.11 <sup>b</sup>	1500.0 $\pm$ 9.09 <sup>b</sup>	–	23.5 $\pm$ 0.23 <sup>d</sup>
<i>A. niger</i>	375.0 $\pm$ 217 <sup>f</sup>	500.0 $\pm$ 3.15 <sup>f</sup>	750.0 $\pm$ 6.13 <sup>f</sup>	–	62.5 $\pm$ 0.62 <sup>c</sup>

The values are the average of triplicate  $\pm$ SD ( $p < 0.05$ ); different alphabetical letters in superscript indicate significant differences within the samples.

In general, the antimicrobial potential has been mainly explained by the presence of terpenes with aromatic rings and phenolic hydroxyl groups able to form hydrogen bonds with the active sites of the target enzymes. On the other hand, other terpenes, alcohols, aldehydes and esters can contribute to the overall antimicrobial potential of essential oils<sup>37</sup>. As per earlier reports the enantiomers of  $\alpha$ -pinene and  $\beta$ -pinene have a good antibacterial activity<sup>38</sup>. These chemical components exert their toxic effects against these microorganisms through the disruption of bacterial and fungal membrane integrity<sup>39</sup>. It might be said that  $\alpha$ -pinene and  $\beta$ -pinene are able to inhibit respiration, destroy cellular integrity and ion transport mechanism<sup>40</sup>. The essential oils might have some fatty acids/methyl esters which have been implicated in plant antimicrobial activities<sup>41</sup>. The hydrophilic nature of terpenes functional groups and lipophilic nature of their hydrocarbon skeleton are of main significance in the antimicrobial properties of the chemical components in essential oils<sup>42</sup>. As per earlier reports in several essential oils, the antimicrobial property might be due to the presence of related alcohols, phenols and terpenoids. The antimicrobial potential of essential oils of this plant might probably be due to the presence of isoprenes identified by GC-MS, which also supports our findings.

## CONCLUSIONS

This study was focused on determining the chemical composition, antioxidant activity and antimicrobial properties of essential oils extracted from the *Russelia equisetiformis* flowers, leaves and stems. The chemical analysis by GC-MS showed the presence of chemical constituents. In addition the essential oils reveal a very important *in vitro* antioxidant activity, confirmed by the results of radical scavenging activity, inhibition of linoleic acid and bleaching of  $\beta$ -carotene with linoleic acid system. It is important to note that the antioxidant activities of the studied essential oils might be due essentially to the abundance of hexadecanoic acid, methyl ester,  $\alpha$ -pinene and also to the overall chemical constituents contained in these essential oils. So in future plant may be used as a potential source to cure diseases caused by oxidants and microbes.

## ACKNOWLEDGEMENTS

Authors are highly thankful to the Higher Education Commission Islamabad, Pakistan for providing funds (HEC Indigenous Scholarship) for the purchase of chemicals and other research-related materials

## REFERENCES

1. D. W. REISCHE, D. A. LILLARD, R. R. EITENMILLER: Antioxidants in Food Lipids. Marcel Dekker, New York, USA, 1998.
2. M. N. BARI, M. ZUBAIR, K. RIZWAN, N. RASOOL, I. H. BUKHARI, S. AKRAM, T. H. BOKHARI, M. SHAHID, M. HAMEED, V. U. AHMAD: Biological Activities of *Opuntia Monacantha* Cladodes. J Chem Soc Pakistan, **34**, 990 (2012).
3. A. OZKAN, A. ERDOGAN: A Comparative Evaluation of Antioxidant and Anticancer Activity of Essential Oil from *Origanum onites* (Lamiaceae) and Its Two Major Phenolic Components. Turk J Biol, **35**, 735 (2011).
4. A. A. HAMID, O. O. AIYELAAGBE: Pharmacological Investigation of *Asystasia calyciana* for Its Antibacterial and Antifungal Properties. Int J Chem Biochem Sci, **1**, 99 (2012).
5. M. A. HANIF, A. Y. AL-MASKRI, Z. M. H. AL-MAHRUQI, J. N. AL-SABAHI, A. AL-AZKAWI, M. Y. AL-MASKARI: Analytical Evaluation of Three Wild Growing Omani Medicinal Plants. Nat Prod Commun, **6**, 1451 (2011).
6. M. ZIA-UL-HAQ, A. SHAKEEL, A. MANSOOR, I. SHAHID, M. KHALID: Effects of Cultivar and Row Spacing on Tocopherol and Sterol Composition of Chickpea (*Cicer arietinum* L.) Seed Oil. J Agric Sci (Tarim Bilimberber Dergisi), **15**, 25 (2009).
7. M. ZIA-UL-HAQ, S. AHMAD, S. IQBAL, D.L. LUTHRIA, R. AMAROWICZ: Antioxidant Potential of Lentil Cultivars Commonly Consumed in Pakistan. Oxid Commun, **34**, 820 (2011).
8. M. ZIA-UL-HAQ, K. AYESHA, A. SHAKIR, Q. MUGHAL, A. SHAKEEL, K. INAMULLAH: Phytopharmacological Profile of *Gratiola officinalis* L i n n, A Review. J Med Plants Res, **6**, 3087 (2012).
9. K. RIZWAN, M. ZUBAIR, N. RASOOL, M. RIAZ, M. ZIA-UL-HAQ, D. V. FEO: Phytochemical and Biological Studies of *Agave attenuata*. Int J Mol Sci, **13**, 6440 (2012).
10. R. S. FARAG, M. N. ALI, S. H. TAHA: Use of some Essential Oils as Natural Preservatives for Butter. J Am Oil Chem Soc, **67**, 188 (1990).



11. M. ZIA-UL-HAQ, S. IQBAL, S. AHMAD, M. BHANGER, W. WICZKOWSKI, R. AMAROWICZ: Antioxidant Potential of Desi Chickpea Varieties Commonly Consumed in Pakistan. *J Food Lipids*, **15**, 326 (2008).
12. X. ORMANCEY, S. SISALLI, P. COUTIERE: Formulation of Essential Oils in Functional Perfumery. *Parfums, Cosmetiques and Actualites*, **157**, 30 (2001).
13. B. BOZIN, D. MICICA, N. SIMIN, G. ANACKOV: Characterization of the Volatile Composition of Essential Oil of Some Lamiaceae Species and the Antimicrobial and Antioxidant Activities of the Entire Oils. *J Agr Food Chem*. **54**, 1822 (2006).
14. M. NISAR, M. SHAH, W. KALEEM, I. ALI, M. ZIA-UL-HAQ: Antimicrobial Screening of *Impatiens Bicolor* Royle. *Pak J Bot*, **42**, 523 (2010).
15. E. M. ABDALLAH, A. E. KHALID: A Preliminary Evaluation of the Antibacterial Effects of *Commiphora molmol* and *Boswellia papyrifera* Oleo-gum Resins Vapor. *Int J Chem Biochem Sci*, **1**, 1 (2012).
16. F. ASLAM, N. RASOOL, M. RIAZ, M. ZUBAIR, K. RIZWAN, M. ABBAS, T. BUKHARI, I. BUKHARI: Antioxidant, Haemolytic Activities and GC-MS Profiling of *Carissa carandas*. *Int J Phytomed*, **3**, 567 (2011).
17. M. A. HANIF, M. Y. AI-MASKARI, A. AI-MASKARI, A. AI-SHUKAILI, A. Y. AI-MASKARI, J. N. AI-SABAHI: Essential Oil Composition, Antimicrobial and Antioxidant Activities of Unexplored Omani Basil. *J Med Plants Res*, **5**, 751 (2011).
18. M. ZUBAIR, K. RIZWAN, N. RASOOL, N. AFSHAN, M. SHAHID: Antimicrobial Potential of Various Extract and Fractions of Leaves of *Solanum nigrum*. *Int J Phytomed*, **3**, 63 (2011).
19. MEHJABEEN, M. AHMAD, N. JAHAN, M. ZIA-UL-HAQ, S. M. ALAM, A. WAZIR, H. SAEEDUL: Antimicrobial Screening of Some Plants of Medicinal Importance. *Pak J Bot*, **43**, 1773 (2011).
20. A. Y. AI-MASKARIA, M. A. HANIF, M. Y. AI-MASKARI, A. S. ABRAHAM, J. N. AI-SABAHI, O. AI-MANTHERI: Essential Oil from *Ocimum basilicum* (Omani Basil): A Desert Crop. *Nat Prod Commun*, **6**, 1487 (2011).
21. M. A. HANIF, H. N. BHATTI, M. S. JAMIL, R. S. ANJUM, A. JAMIL, M. M. KHAN: Antibacterial and Antifungal Activities of Essential Oils Extracted from Medicinal Plants Using CO<sub>2</sub> Supercritical Fluid Extraction Technology. *Asian J Chem*, **22**, 7787 (2010).
22. E. O. AWE, A. ADELOYE, T. IDOWU, O. A. OLAJIDE, J. MAKINDE: Antinociceptive Effect of *Russelia equisetiformis* Leave Extracts: Identification of Its Active Constituents. *Phytomedicine*, **15**, 301 (2008).
23. A. I. HUSSAIN, F. ANWAR, S. TUFAIL, H. SHERAZI, R. PRZYBYLSKI: Chemical composition, Antioxidant and Antimicrobial Activities of Basil (*Ocimum basilicum*) Essential Oils Depends on Seasonal Variations. *Food Chem.*, **108**, 986 (2008).
24. E. GUENTHER: Determination of Physical and Chemical Properties: The Essential Oils. D. Van Nostrand Company Inc., Washington, 1960.
25. R. P. ADAMS: Identification of Essential Oil Components by Gas Chromatography/Mass Spectroscopy. Allured Publishing Corporation, Carol Stream IL, 2001.
26. S. IQBAL, M. I. BHANGER, F. ANWAR: Antioxidant Properties and Components of Some Commercially Available Varieties of Rice Bran in Pakistan. *Food Chem*, **93**, 265 (2005).
27. T. KULISIC, A. RADONIC, V. KATALINIC, M. MILOS: Use of different Methods for Testing Antioxidant Activity of Oregano Essential Oil. *Food Chem*, **85**, 633 (2004).
28. NCCLS: Performance Standards for Antimicrobial Disk Susceptibility Test by National Committee for Clinical Laboratory Standards (NCCLS) Wayne PA, M2-A6, 1997.
29. S. D. SARKER, L. NAHAR, Y. KUMARASAMY: Microtitre Plate Based Antibacterial Assay Incorporating Resazurium as an Indicator of Cell Growth, and Its Application in the *in vitro* Antibacterial Screening of Phytochemicals. *Methods*, **42**, 321 (2007).

30. O. POLITEO, M. JUKIC, M. MILOS: Chemical Composition and Antioxidant Capacity of Free Volatile Aglycones from Basil (*Ocimum basilicum* L.) Compared with Its Essential Oil. *Food Chem*, **101**, 379 (2007).
31. F. LU, L.Y. FOO: Antioxidant Activities of Polyphenols from Sage (*Salvia officinalis*). *Food Chem*, **75**, 197 (2001).
32. G. RUBERTO, M. T. BARATTA: Antioxidant Activity of Selected Essential Oil Components in Two Lipid Model Systems. *Food Chem*, **69**, 167 (2000).
33. K. F. EL-MASSRY, A. H. EL-GHORAB, A. FAROUK: Antioxidant Activity and Volatile Components of Egyptian *Artemisia judaica* L. *Food Chem*, **79**, 331 (2002).
34. P. KUMAR, S. KUMARAVEL, C. LALITHA: Screening of Antioxidant Activity, Total Phenolics and GC-MS Study of *Vitex negundo*. *Afr J Biochem Res*, **4**, 191(2010).
35. J. A. FIELD, G. LETTINGA: Toxicity of Tannic Compounds to Microorganisms. *Plants Polyphenols: Synthesis, Properties, Significance*. *Basic Life Sci*, **59**, 673 (1992).
36. A. SCALBERT: Antimicrobial Properties Of Tannins. *Phytochem*, **30**, 3875 (1991).
37. N. BELLETTI, M. NDAGIHMANA, C. SISTO, M.E. GUERZONI, R. LANCIOTTI, F. GARDINI: Evaluation of the Antimicrobial Activity of Citrus Essences on *Saccharomyces cerevisiae*. *Agr Food Chem*, **52**, 6932 (2004).
38. P. MAGIATIS, E. MELLIU, A. L. SKALTSOUNIS, I. B. CHINOU, S. MITAKU: Chemical Composition and Antimicrobial Activity of the Essential Oils of *Pistacia lentiscus* Var. *Planta Med*, **65**, 749 (1999).
39. K. KNOBLOCK, A. PAULI, B. LBERL, N. WEIS, H. WEIGAND: Antibacterial Activity and Antifungal Properties of Essential Oil Components. *J Essent Oil Res*, **1**, 119 (1988).
40. A. ULUBELEN, G. TOPCU, C. ERIS, U. SONMEZ, M. KARTAL, S. KURUCU, C. BOZOK-JOHANSSON: Terpenoids from *Salvia sclarea*. *Phytochem*, **36**, 971 (1994).
41. A. T. ORISHADIPE, J. I. OKOGUN, E. MISHELIA: Gas Chromatography-mass Spectrometry Analysis of the Hexane Extract of *Calliandra portoricensis* and Its Antimicrobial Activity. *Afr J Pure Appl Chem*, **4**, 131 (2010).
42. T. KILIC: Analysis of Essential Oil Composition of *Thymbra spicata* var. *spicata*: Antifungal, Antibacterial and Antimycobacterial Activities. *J Biosciences*, **61**, 324 (2006).

*Received 6 June 2012*

*Revised 14 July 2012*

## INSTRUCTION FOR AUTHORS

**Starting from 2011, the authors can publish their manuscripts as rapid publication (6 months after the receipt of positive referees comments and the revised version) after they pay a fee of 100 Euro. The articles intended to be published as rapid publication should follow the requirements for contribution length as pointed below. Authors from Universities and Organisations, which have a subscription or sponsorship to the Journal publish their papers free of charge. The authors receive a hard copy of the Journal issue containing their published article free of charge. Some figures, according to authors decision, can be published coloured in order to make them more understandable to the reader. The additional payment is 75 Euro per printed page.**

The authors are kindly requested to send a declaration on copyright transfer simultaneously with the manuscript submission to the editorial board of *Oxidation Communications*.

All authors must agree to be so listed and must have seen and approved the manuscript, its content, and its submission to *Oxidation Communications*. Submission of a paper that has not been approved by all authors will not be forwarded for evaluation and publication. Any changes in authorship must be approved in writing by all the original authors.

Manuscripts should present original results not previously published and not considered for publication elsewhere. Authors declare this in the notification letter. Only relevant experimental data that are discussed in the manuscript should be described. Authors are encouraged to present the experimental data in the form of tables. The duplication of experimental data in tables and figures should be avoided.

### MANUSCRIPTS TYPE

*Short communications* – up to 4 printed pages (about 14 000 characters) including text, all illustrative materials (tables, figures, etc.) and references.

*Research articles* – up to 8 printed pages (without figures – about 28 100 characters) and 10 printed pages with figures ( up to 35 260 characters) including main text, tables, figures, schemes and references.

*Reviews* – up to 15 printed pages (52 890 characters) including main text, tables, figures, schemes and references.

The Editorial Board will strictly follow the requirement for contribution length in view of the over-accumulation of scientific papers, submitted for publication in the Journal and the restricted volume of each book. Contributions within the stated lengths will be published free of page charges. Depending on the exceeding length are introduced page charges (up to 100 Euro).

Receipt of a contribution for consideration will be acknowledged immediately by the Editorial Office. The acknowledgement will indicate the paper reference number assigned to the contribution. Authors are particularly asked to quote this number on all subsequent correspondence.

### ORGANISATION

**The title page** should include the title, authors and their affiliations, complete address of the author to whom correspondence should be sent and an Abstract.

**Abstract** – should not exceed 200 words and should give the subjects and conclusions of the article and all results of general interest. References, compound numbers and abbreviations should be avoided.. A maximum of five keywords should follow the Abstract.

**Aims and Background** – should include brief and clear remarks outlining the specific purpose of the work and a short summary of the background material including numbered references.

**Experimental** – should be sufficiently detailed (but concise) to guarantee reproducibility.

**Results and Discussion** – should indicate the logic used for the interpretation of data without lengthy speculations. Authors submitting material on purely theoretical problems or on a new experimental technique might unite the sections Experimental, Results and Discussion into one section under the heading Discussion. Authors should avoid doubling of results in the form of Tables and Figures.

**Conclusions** – short summary of the main achievements of the research.

**References** – should be typed at the end of the manuscript and numbered in the order as first cited in the text as superscript Arabic numerals. In the list of references the original papers should be given with their titles. Abbreviations of journal titles should follow the style used in ISI Journal Title Abbreviations. Sequence and punctuation of references should be:

1. E. SZABÓ, G. L. ZÜGNER, M. FARKAS, I. SZILÁGYI, S. DÓBÉ: Direct Kinetic Study of the OH-radical Initiated Oxidation of Pivalaldehyde, (CH<sub>3</sub>)<sub>3</sub>CC(O)H, in the Gas Phase. *Oxid Commun*, **35** (3), 538 (2012).
  2. M. B. NEIMAN, D. GAL: *The Kinetic Isotope Method*. Akademiai Kiado, Budapest, 1971.
  3. J. A. HOWARD: In: *Advances in Free Radical Chemistry*. Vol. 4 (Ed. G. H. Williams). Lagos Press, London, 1972, 49–69.
  4. C. HANSCH (Ed.): *Comprehensive Drug Design*. Pergamon Press, New York, 1990, p. 19.
- In preparing the list of References attention must be drawn to the following points:
- (a) Names of all authors of cited publications should be given. Use of ‘et al.’ in the list of references is not acceptable;
  - (b) Only the initials of first and middle names should be given.

**Tables** – each bearing a brief title and numbered in Arabic numerals. The tables should be placed in the text as first cited.

**Figures and captions** – should be numbered consecutively with captions and must be placed at their first mentioning in the text.

Particular attention is drawn to the use of SI Units, IUPAC nomenclature for compounds and standard methods of literature citation.

## ELECTRONIC SUBMISSION OF MANUSCRIPTS

Manuscripts should be submitted in electronic form. Submission not in electronic form may face a delay in publication. All text (including the title page, abstract, keywords, all sections of the manuscript, figure captions, and references) and tabular material should be in one file. The manuscript must be prepared using MS Word 6.0 and above. Manuscripts in PDF format are not accepted.

Chemical equations must be supplied using equation editor. Tables must be created using table format feature.

Graphics, i.e. figures, schemes, etc. should be in a separate file. The file name should be descriptive for the graphic. Structures and schemes may be supplied in ChemWindow format and other graphics in Microsoft Excel or Microsoft PowerPoint format.

## SUBMISSION OF MANUSCRIPTS

Manuscripts should be sent to the following address:

Prof. Dr. **Slavi K. Ivanov**

SciBulCom Ltd., P. O. Box 249, 7 Nezabravka Str., 1113 Sofia, Bulgaria

Phone/Fax: +359 2 872 42 65, +359 2 978 72 12

E-mail: scibulcom2@abv.bg

All manuscripts are subject to critical review and the names of referees will not be disclosed to the authors. The manuscript sent back to the author for revision should be returned within 2 months by e-mail. Otherwise it will be considered withdrawn. Revised manuscripts are generally sent back to the original referees for comments, unless (in case of minor revisions) the editors accept them without seeking further opinions. Proofs should be corrected and returned as soon as possible. The authors receive CD-ROM containing copy of the book.